The feasibility of natural ventilation in healthcare buildings

By

Zulfikar Aliyu Adamu

A doctoral thesis submitted in partial fulfilment of the requirements for the award of Doctor of Philosophy of Loughborough University

June 2013

Abstract

Wards occupy significant proportions of hospital floor areas and due to their constant use, represent a worthwhile focus of study. Single-bed wards are specifically of interest owing to the isolation aspect they bring to infection control, including airborne pathogens, but threats posed by airborne pandemics and family-involvement in hospital care means cross-infection is still a potential problem. In its natural mode, ventilation driven by combined wind and buoyancy forces can lead to energy savings and achieve thermal comfort and high air change rates through secure openings. These are advantageous for controlling indoor airborne pathogens and external air and noise pollution. However, there is lack of detailed evidence and guidance is needed to gain optimum performance from available natural ventilation systems. This research is a proof of concept investigation into the feasibility and impact of natural ventilation systems targeting airflow rates, thermal comfort, heating energy and control of pathogenic bio-aerosols in hospital wards. In particular, it provides insights into the optimal areas of vent openings which could satisfy the complex three-pronged criteria of contaminant dilution, low heating energy and acceptable thermal comfort for occupants in a naturally ventilated single bed ward.

The main aim of this thesis is the structured study of four systems categorised into three groups: Simple Natural Ventilation (SNV) in which single and dual-openings are used on the same external wall; Advanced Natural Ventilation (ANV) which is an emerging concept; and finally Natural Personalised Ventilation (NPV) which is an entirely new concept borne out of the limitations of previous systems and gaps in literature. The focus of this research is in the exploratory study of the weaknesses and potentials of the four systems, based on multi-criteria performances metrics within three architecturally distinct single-bed ward designs. In contributing to the body of existing knowledge, this thesis provides a better understanding of the performances of three existing systems while presenting the new NPV system. The analysis is based on dynamic thermal modelling and computational fluid dynamics and in the case of the NPV system, salt-bath experiments for validation and visualisation of transient flows. In all cases, wards were assumed to be free of mechanical ventilation systems that might influence the natural flow of air.

The thesis meets three major objectives which have resulted in the following contributions to current knowledge:

- An understanding of the limitations and potentials of same-side openings, especially why and how dual-openings can be useful when retrofitted into existing wards.
- Detailed analysis of bulk airflow, thermal comfort, heating energy and room air distribution achievable from existing SNV and ANV systems, including insights to acceptable trickle ventilation rates, which will be particular useful in meeting minimum dilution and energy requirements in winter. This also includes qualitative predictions of the airflow pattern and direction obtainable from both systems.
- The innovation and study of a new natural ventilation system called Natural Personalised Ventilation (NPV) which provides fresh air directly over a patient's bed, creating a mixing regime in the space and evaluation of its comfort and energy performances.
- A low-energy solution for airborne infection control in clinical spaces is demonstrated by achieving buoyancy-driven mixing ventilation via the NPV system, and a derivative called ceiling-based natural ventilation (CBNV) is shown.
- A comparative analysis of four unique natural ventilation strategies including their performance rankings for airflow rates, thermal comfort, energy consumption and contaminant dilution or removal using an existing single-bed ward design as case study.
- Development of design and operational recommendations for future guidelines on utilising natural ventilation in single-bed wards either for refurbishment or for proposed designs.

These contributions can be extended to other clinical and non-clinical spaces which are suitable to be naturally ventilated including treatment rooms, office spaces and waiting areas. The findings signify that natural ventilation is not only feasible for ward spaces but that there is opportunity for innovation in its application through further research. Future work could focus on related aspects like: impacts of fan-assisted ventilation for a hybrid flow regime; pre-heating of supply air; integration with passive heat recovery systems as well the use of full-scale experiments to fine-tune and validate findings.

Table of Contents

List of Figures

List of Tables

Glossary of terms

ACH	Air changer per hour
ADB	Activity database
AIIR	Air infection and isolation room
ANV	Advanced natural ventilation
ASHRAE	American Society for Heating, Refrigeration and Air-Conditioning Engineers
ATT	Air turnover time
CBNV	Ceiling-based natural ventilation
CDC	Centre for disease control (US)
CFD	Computational Fluid Dynamics
CFM	Cubic feet per minute
CIBSE	Chartered Institute of Building Services Engineers
CICO	Centre-in, Centre-out
CIEO	Centre-in, Edge-out
CRE	Contaminant removal efficiency
DBT	Dry-bulb temperature
DH	Department of Health (UK)
DRT	Dry resultant temperature
DTM	Dynamic thermal modelling
DV	Displacement ventilation
EHR	Effectiveness of heat removal
EICO	Edge-in, Centre-out
EIEO	Edge-in, Edge-out
FOV	Field of view
GOSH	Great Ormond Street Hospital
HAI	Hospital-acquired infections
HBN	Health Building Notes
HCW	Healthcare worker
HTM	Health Technical Memorandum
IAQ	Indoor air quality
KERNG	k-ε Re-normalised Group
L/s	Litres per second
LACI	Local air change index
LES	Large-eddy simulations

LEV	Local exhaust ventilation
MACE	Mean air change efficiency
MDRTB	Multi-drug resistant tuberculosis
MRSA	Methicillin-resistant Staphylococcus aureus
MV	Mixing ventilation
MWh	Megawatts hours
NHS	National Health Service (UK)
NPL	Neutral pressure line
NPV	Natural personalised ventilation
PD/PPD	Percentage (of people) dissatisfied
PEI	Personal exposure index
PMV	Predicted mean vote
POI	Point of interest
PV	Personalised ventilation
RAD	Room air distribution
RANS	Reynolds Averaged Navier-Stokes
RICS	Royal Institute of Chartered Surveyors
S&A	Short and Associates
SARS	Severe acute respiratory syndrome
SNV	Simple natural ventilation
UVGI	Ultra-violet germicidal irradiation
VEF	Ventilation effectiveness factor
VOI	Volume of interest
WHO	World Health Organisation

List of variables and their meanings

A	*Area of (opening, floor) (m^2);*
A_m	*Effective area of opening (m^2)*
As	*Area of stack (m^2)*
b	*Breathing rate (m^3/s)*
B_f	*Buoyancy flux (m^4s^{-3})*
B_m	*Buoyancy of brine plume (m/s^2)*
C_c	*Volumetric heat capacity of air (1200 J/m^3 K)*
C_d	*Coefficient of discharge (-)*
C_e	*Concentration of pollutant at exhaust (-)*
C_m	*Mean concentration of pollutant in room (-)*
C_{mt}	*Morton's constant (0.158)*
C_p	*Concentration of pollutant at a given point, P (-)*
C	*Specific heat capacity of water ($Jkg^{-1}K^{-1}$)*
D	*Number of diseased persons in a space (-)*
F	*Fraction of floor area (%)*
$F_{o,m}$	*Flow rate of brine (m^3/s)*
g	*Gravitational force per unit mass (m/s^2)*
g'	*Reduced gravity (m/s^2)*
Gr	*Grashf number (-)*
g'_f	*Gravity at full scale (m/s^2)*
H	*Height of opening (m)*
H_m	*Height between inlet and outlet (m)*
I	*Number of infected persons in a space (-)*
j	*Quanta generation rate (quanta/s)*
K	*Normalising constant (-)*
n	*Ratio of depth to width (of a given space)*
Pi	*Probability of infection (-)*
Pr	*Prandtl number (-)*
Q	*Flow rare (l/s; m^3/s or cfm)*
q	*Heat gain (W/m^2)*
Re	*Reynolds number (-)*

S	*Number of susceptible persons in a space (-)*
T_e	*Temperature of air at exhaust (^oC or K)*
T_m	*Mean room temperature (^oC or K)*
T_{int}	*Internal temperature (^oC or K)*
T_{ext}	*External temperature (^oC or K)*
V	*Volume (of space) (m^3)*
$\dot{V}$	*Volumetric flow rate of air (m^3/s)*
V_f	*Volume flux of surrounding fresh water ($m^3 \cdot s^{-1}$)*
v	*Speed of air (m/s)*
α	*Thermal expansion coefficient (-)*
$\bar{\tau}$	*Mean age of air (s)*
τ_n	*Nominal time / air turnover time (s)*
τ_p	*Age of air at point, P (s)*
ΔT	*Change / rise in temperature (^oC or K)*
$\Delta\rho$	*Difference in density (kg/m^3)*
ρ	*Density (kg/m^3)*
ρ_m	*Density at model scale (kg/m^3)*
ρ'_f	*Density at full scale (kg/m^3)*

Acknowledgement

It has been a long journey so I would like start by thanking the Almighty for his guidance and blessings. In carrying out this PhD research, I am quite fortunate to have been supervised by two brilliant minds: Prof. Andrew Price and Prof Malcolm Cook. I remain immeasurably grateful for the time and effort they have spared in this regard. While it is not possible to list all others who have assisted one way or another in this making this research a most enjoyable endeavour, I am compelled to list some names that I can readily recall: Prof. Kevin Lomas; Dr Catherine Noakes, Prof. Hazim Awbi; Rosemary Glanville, Anne Noble; Kevin Hackett; Dr Jacqui Glass; Prof. Stephen Emmitt; Dr Francis Edum-Fotwe; Dr Grant Mills; Dr Giridharan Renganathan; Tom Carslake; Prof. Colin Gray; Prof. Nigel Klein and Dr Vanya Gant. I am also immeasurably grateful to Dr Ismail M. Budaiwi who has taught me and inspired me regarding ventilation and indoor air quality and Dr Adel M. Abdou, who is an outstanding professional in the academia. For Dr Baqer Ramadan, I remain eternally grateful for his support and friendship in the early years of my academic and research career at KFUPM.

The assistance of Stephen Todd in carrying out the salt-bath experiment is also appreciated.

Lastly but by no means the least in any way, I would like to express my appreciation to my entire family: my brothers (Dr Haroun, Anas and Muhammad, who were there when things began to get rather tough); and most especially my wife (Zainab) and the two most beautiful daughters any father could ever have (Alia and Amaani). I owe you for your patience and understanding.

The support of EPSRC and the School of Civil and Building Engineering (Loughborough University) in funding this research is appreciated.

CHAPTER 1: Introduction

1.1 Background

The energy crisis of the 1970s, its impact on air tightness of buildings and the consequent reduction in minimum fresh air rates from conditioning systems (Spengler, et al. 2001) are important heritages of the modern air-conditioned indoor environment. With the climate change concerns of the post-1990 era, there is a new impetus to deliver healthcare buildings that are not only energy efficient but which for healthcare purposes, also aid the therapeutic process of patients or the wellbeing of other occupants. However, there are drawbacks for existing buildings many of which are legacies of the tightly built and air-conditioned era. These drawbacks are linked to non-optimisation of designed facilities which persisted when 'the art of building' and not actual post-occupancy performances dictated design specifications (Hens, 2012). The UK Department of Health (DH) has thus acknowledged that over 40% of the energy consumed by existing hospitals goes into conditioning of spaces (DH, 2006). Modern healthcare buildings not only tend to be sophisticated, they also contain various sources of indoor air pollutants. Having inherited design features that are not favourable for preventing the spread of airborne contaminants, many contemporary hospitals are therefore primary examples of facilities caught in the indoor air quality crisis (Spengler, et al. 2001, p. 57.3).

The wards of typical hospitals are one of few spaces that truly enjoy constant occupancy all year round. In temperate countries, the need to keep such spaces thermally comfortable without compromising on fresh air provision, has always been an important challenge (Levy, 1996; Seppanen and Tarvainen, 1996;). This challenge has been complicated by the rise of drug-resistant strains of airborne diseases, e.g. tuberculosis (Gammage, 1996) and the hazards of global airborne pandemics (e.g. swine flu) in recent years. These airborne hazards have not only stressed the design and operation of hospital ventilation systems, but have also called into question the architectural design of wards where the most vulnerable of hospital occupants are found (ANA, 2003). This has led to increasing research and the adoption of single-bed wards as evident in many studies (Ulrich et al. 2004; Lawson and Phiri, 2004 and Dowdeswell, et al. 2004; van de Glind, et al. 2007; Policy+ 2009 and Florey et al. 2009).

There have also been studies which have focused on non-infection performances of single-bed wards including patient preference for shared accommodation especially among the elderly (Florey, et al. 2009) as well as for general psychological impacts of being isolated which, after extensive reviews, were shown by Abad et al. (2010) to have several adverse effects. This mixture of health and psychological/social factors make the subject of single bed hospital wards interesting and worthwhile.

The benefits of natural ventilation are nevertheless indisputable given the potential to save energy (Liddament, 1996; Awbi, 2003; Lomas and Ji, 2009) and deliver significant air change rates in hospitals (Qian, et a. 2010) using wind, buoyancy-induced airflows or a combination of both forces. Buoyancy-driven natural ventilation in particular has the advantage of being suitable for areas (e.g. urban locations) where wind may not be plentiful or reliable. In addition, when used with emerging concepts such as advanced natural ventilation (ANV), the drawbacks of urban air and noise pollution, as well as the safety concerns that have restricted the openable areas of traditional windows to 100mm (DH, 1998), can easily be overcome. Unfortunately, such new concepts of natural ventilation have only just been demonstrated (Lomas and Ji, 2009; Short and Al-Maiyah, 2009) as viable options for hospital ventilation and therefore are not yet in the mainstream.

Since wards also occupy significant proportions of hospital floor areas, their constant use pressured by the drive for optimum bed-space allocation or utilisation (NHS, 2010), means they represent an interesting and worthwhile focus of study. The desire to include family members in the care process according to Great Ormond Street Hospital (GOSH, 2011), also means that risk of cross-infection due to prolonged contact is not limited to patient-healthcare workers alone. The design of the new GOSH single-bed ward for instance has provision for a couch-bed upon which an overnight visitor is expected to sleep. This is an important issue that needs to be considered for ventilation and airborne infection, especially in view of the threats from airborne pandemic influenzas and similar health hazards. It is in the context of these multi-faceted factors that this research was conceived and executed.

In their study of the complex relationship between natural ventilation, heating energy and risk of airborne contaminants in Nightingale wards, Gilkeson, et al. (2013) provide evidence (through experiments and CFD modelling) that closing of windows to reduce heating energy (as often practiced in some UK hospitals) leads to quadrupling of the risks of airborne

infection. Hence, getting the right balance between airflow/dilution requirements and heating energy consequences will be important for systems which rely on windows for natural ventilation. However, as windows are just one type of natural ventilation systems, opportunity exists to explore the performances of other often under-utilised systems such as dual opening systems, advanced natural ventilation systems. Nevertheless, the question of what fraction of vent opening is safe or optimal to satisfy the contaminant dilution, thermal comfort and energy requirements of modern hospital wards, remains unanswered and this is a gap exploited in this research.

Although the achievable ventilation rates are higher than what can be obtained economically via mechanical ventilation, natural ventilation is beset by challenges such as the irregularity of airflow due to the driving forces being either unreliable (i.e. wind forces) or inadequate (e.g. buoyancy forces). Nonetheless, due to the constant presence of people and the reliance on assorted equipment in healthcare facilities, the latter challenge is of minimal consequence. This is because indoor heat sources can be estimated fairly accurate in terms of magnitude and period of availability; however, buoyancy-driven natural ventilation requires careful design of openings inclusive of their sizes, placement and operation. Furthermore, ventilation of wards where airborne infection is a potential risk, requires specific room air distribution and it has been shown (Beggs, et al, 2008; Li, et al. 2011) that mixing technique is much more effective than displacement technique. This adds to the challenge of using buoyancy to drive natural ventilation because mixing has been a feature of mechanical ventilation systems only.

The need to heat indoor spaces in temperate countries means that naturally ventilated buildings have to be designed to provide fresh air without excessive energy penalties. In healthcare facilities, this problem cannot be over-emphasized because it is critical to ensure specific ventilation rates are met for the well-being of patients and healthcare workers who inhabit hospitals (Atkinson, et al. 2009).

The potential of natural ventilation is enhanced and limited by a complex array of issues but for combined wind and buoyancy-driven flows, key variables include: the wind speed, external temperature and internal heat loads as well as appropriately sized and located openings to ensure that the system is both efficient and effective. The indoor temperature ranges suggested for hospital wards come from various authoritative sources such as: 18-

28°C by HTM 03-01 (DH 2007a); 19-24°C by (Carbon Trust, 2007) and 22-24°C (CIBSE, 2002). In this regards, the annual patterns of outdoor temperature in Birmingham and London (Fig. 1.1) for example, do not present a significant challenge for natural ventilation between the months of March and November, whereas in winter, the only challenge would be heating.

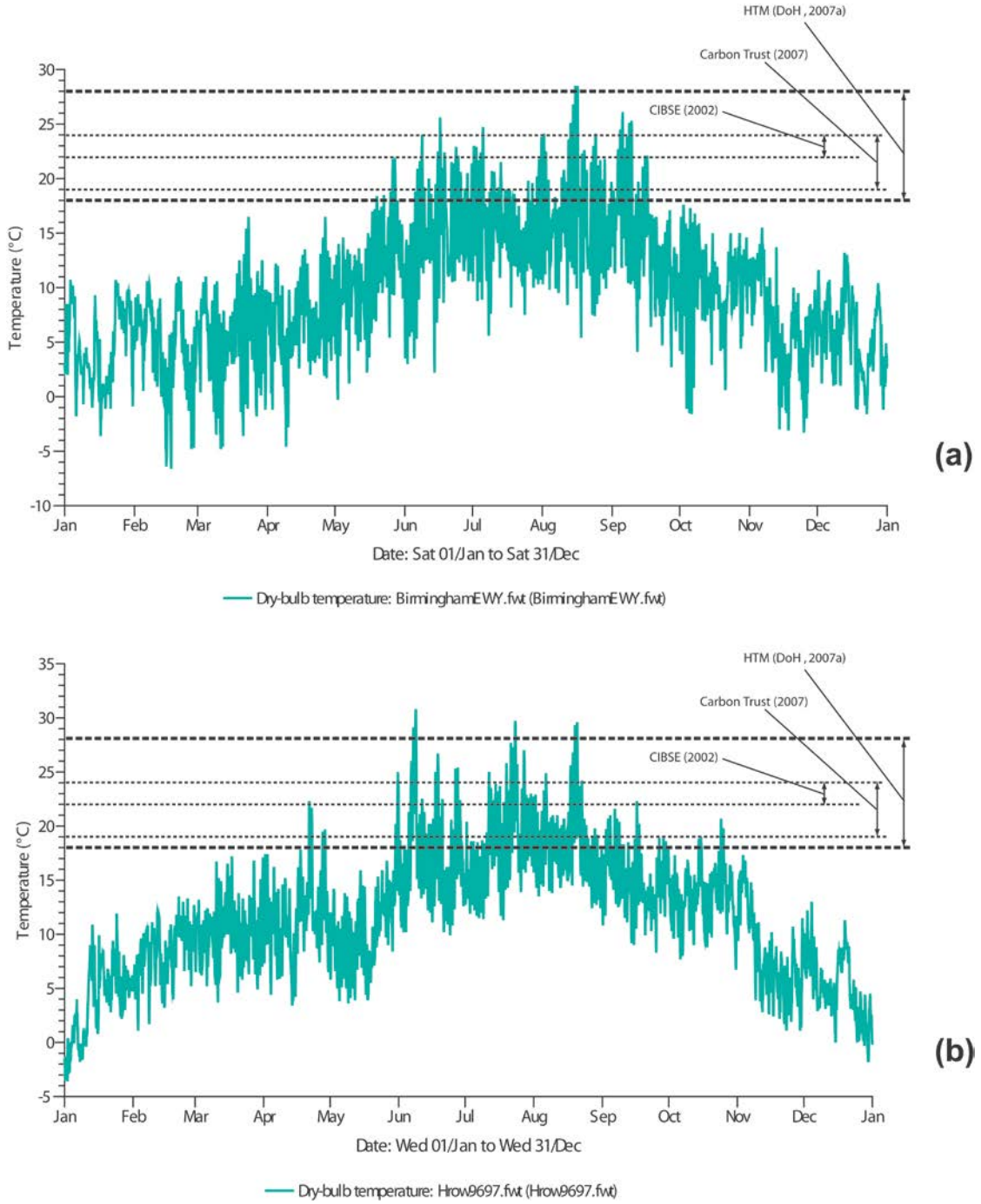

Figure 1:1: Fluctuations in suitability of external temperature for natural ventilation in (a) Birmingham and (b) London

1.2 Justification for the research

There were several rationales for this research. Despite clear evidence in existing literature produced within the last decade, that airflow pattern and direction are crucial for controlling pathogenic bio-aerosols (Li, et al. 2008; Atkinson, et al. 2009), current guidelines are lacking in utilising such evidence for the benefit of designers and facility operators. There is arguably an over-emphasis on quantitative aspects of ventilation (i.e. airflow rates), which have been questioned in origin and performance (Gammage, 1996; Lomas and Ji, 2009). Pattern and direction of airflow are qualitative features and should be considered along with quantitative requirements (airflow rates) in ventilation of clinical spaces where airborne infection is a potential hazard. With respect to single occupancy ward spaces, apart from airborne infection isolation rooms (AIIRs) there is lack of standard guidance on pattern and direction of airflow in standard wards especially those ventilated naturally. Examples of required pattern and direction can be found in CDC (2005). There is hence, a need to provide evidence-based qualitative guidance on naturally ventilated single-bed wards.

In their overview of how airflow and airborne contaminants were transported in spaces, Tang, et al. (2011) deduced that the problem is highly complex because it involves: ventilation rates; the buoyancy created by indoor heat sources; movement of occupants and the disturbances created by such movement; respiratory activities (e.g. talking, breathing and coughing); number of infectious persons; duration of exposure by susceptible co-occupants; and the dissimilar behaviour between aerosols and particulates. These factors, they argued make the subject so challenging that a small contribution to one aspect can have significant bearing on other aspects. The inadequacy or unavailability of specific and detailed design and operation guidelines or standards that will aid the conceptualisation, design and sizing of natural ventilation systems suitable for infection control makes this research necessary.

The Department of Health (DH) has outlined the statutory, clinical and functional needs of ventilation in healthcare facilities (DH, 2007) and understanding how these needs can be met is essential regardless of the mode of ventilation. Unfortunately, existing guidelines and documents on healthcare ventilation as published by the DH are biased towards mechanical ventilation. Although guidance on design of natural ventilation systems in the UK can be found in CIBSE's documentation (CIBSE, 2005 and CIBSE 2006), there are inadequate details about the clinical needs of hospital wards. The WHO on the other hand (Atkinson, et

al. 2009) has provided a guideline for use of natural ventilation in controlling airborne diseases but this document is lacking in terms of actual sizing of components or the energy needed for heating in the winter or cooler months in temperate countries.

The WHO guideline treats natural ventilation in terms of windows, which is a narrow view on the subject given the fact that specially designed inlets and outlets can function independently of glazed fenestrations. This aspect is very important since by decoupling airflow from the visual and daylighting needs of windows, natural ventilation can be used more creatively, as this study intends to demonstrate. In the DH, CIBSE and WHO documentation, there is also a lack of detailed information of the required trickle ventilation rates required to keep wards healthy and comfortable in winter periods. None of these guidelines offer any insight into how existing facilities can be refurbished to optimise natural ventilation.

Finally, state-of-the-art information on natural ventilation design for healthcare facilities can be found in peer-reviewed journals, in formats not ideal for instant consumption by designers and operators of such buildings. This research therefore also helps to synthesise, re-interpret, explore and evaluate these findings through critical review of literature prior to testing the limits and potentials of such natural ventilation designs using computational and experimental modelling techniques. There is currently a scarcity of research on the viability of natural ventilation for single-occupant hospital wards in temperate countries, which simultaneously take into account, four unique pre-requisites of performance: i.e. airflow rates; thermal comfort; heating energy and airborne contaminants.

This research is thus broadly a proof of concept aimed at exploring the feasibility of utilising natural ventilation in healthcare buildings, with a focus on single-bed ward spaces. The findings derived from the investigations carried out have in mind the refurbishment of existing healthcare buildings as well as the design of new facilities.

1.3 Aim and objectives

The aim of this research was to study the feasibility of various natural ventilation systems and their impacts on the indoor air quality, thermal comfort and energy performance of healthcare facilities; for the overall wellbeing of occupants. The following three objectives were used to achieve this objective.

I. To investigate the contemporary issues which influence natural ventilation systems and strategies, airborne infection control and overall indoor air quality (IAQ) of healthcare buildings with the goal of defining the areas of emphasis for the study based on contemporary research/practice and to identify knowledge gaps for potential exploitation.

II. To assess the performance and potential of existing, emerging or innovative natural ventilation systems in single-bed wards of hospitals to simultaneously meet the needs for:
    a) effective room air distribution in terms of airflow rates, pattern and direction;
    b) thermal comfort of occupants;
    c) airborne contaminant removal or dilution; and
    d) energy consumed for heating in winter periods.

III. To extract the outcomes from objectives (1) and (2) to develop recommendations for future guidelines on design and operation of natural ventilation of single-bed ward spaces.

1.4 Research Methodology

The approach to this research begins with an extensive and critical **review of literature**, which serves as a basis for understanding the issues at stake and their relative impacts on this subject. Additionally, a literature review is crucial for identifying the gaps in knowledge. Subsequently, this research utilised a combination of quantitative and qualitative methods, which include **dynamic thermal modelling** and **computational fluid dynamics** (CFD) modelling as well as flow visualisation through salt-bath experiment. These methods provide outputs which will serve as the core of the overall findings. The modelling work involved three types of wards: the Activity Database (ADB) ward, the Great Ormond Street Hospital

(GOSH) ward; and the advanced natural ventilation ward designed by Short and Associates (Short and Al-Maiyah, 2009). The modelling was based on tools whose underlying science are verified and validated by industry standards and they will be applied on existing or schematic design of hospital wards.

1.5 Scope and limitations

The multi-disciplinary nature of this research makes it necessary to define its scope and any limitations associated with the process and actual findings.

1.5.1 Scope of research

The underlying scope of this research is summarised as follows.

- **Driving forces:** The research focused on combined wind and buoyancy forces (for SNV systems) and wind-neutral or buoyancy-driven air flows (for inlet and stack / ANV systems).
- **Ward space:** The single-bed ward was selected as a clinical space of interest, even though the findings could be beneficial to other similar spaces such as treatment rooms and consulting offices.
- **Ventilation systems:** Four selected natural ventilation systems were adopted for detailed investigation as they represent techniques already in existence or with future potential. It is expected that the methodology (tools, methods and research design) used in this research can be applied in any future studies of similar objectives.

1.5.2 Limitations of research

The research is limited by several factors which are summarised below.

- **Passive scalar contaminants:** Airborne contaminants can be sub-divided into the truly airborne pathogens which are perpetually suspended in air and the particulates whose transportation depends on their size and density. However, from the ventilation point of view, the contaminants whose migration in space is wholly influenced by air currents are selected and modelled using generic passive scalar contaminants. This research therefore utilised only passive scalar contaminants.
- **Heat recovery:** This aspect is not considered due to the need to focus on techniques for delivering fresh air into single-bed wards and studying the room air distribution that occurs in the process. Although heating is considered for winter or cold periods, heat

recovery for natural airflow systems requires in-depth design and specification of materials. Considering this aspect will stretch the scope and will require different heat recovery techniques to be considered for the four selected ventilation systems.

- **Summer cooling:** This may be required in certain months of the year in some regions (e.g. Southern UK), but the temperate climate of the country favours heating as a more pressing issue. The cooling aspects of natural ventilation (e.g. use of labyrinths) will not be considered in this research.
- **Experimental facilities:** The research considered that experimentation work is beneficial for many reasons ranging from validation to practical observation of ventilation and contaminant transportation using smoke tests and tracer gasses. Due to constraints related to availability of suitable facilities, experimentation is limited to scaled salt-bath modelling for which resources are readily available.

1.6 Structure and content of thesis

The thesis is subdivided into 12 Chapters. There is an introductory chapter, three unique literature review chapters, a chapter on methodology, five independent study chapters, a discussion chapter and finally concluding chapter. Their contents are summarised below.

Chapter 1, ***Introduction:*** essentially introduces the research from a broad perspective with justification and clear outline of its aim and objectives.

Chapter 2, ***Review of ventilation and comfort in hospital wards***: is an overview of ventilation as a whole with emphasis on its natural mode, how its components are sized, with specific emphasis on room air distribution, the achievement of thermal comfort in wards and the consequent energy requirements.

Chapter 3, ***Review of infectious bio-aerosol control in hospital wards:*** covers the aspect of airborne contaminants, their sources and characteristics of dispersion in hospital wards and the historic and contemporary methods of controlling them.

Chapter 4, ***Review of modelling natural ventilation:*** is an appraisal of the modelling techniques available for studying natural ventilation, subdivided into computerised modelling

(zonal models, computational fluid dynamics) and physical models (large-scale mock-ups and scaled experiments).

Chapter 5, ***Research Methodology:*** Covers the nature and structure of research, the methods considered and adopted, the sources of data as well as the research design and modelling strategies.

Chapter 6, ***STUDY 1 – Single side single and dual opening systems:*** This describes the investigations conducted on two systems using two designs of single-bed wards (GOSH and ADB). The focus was on the different ventilation performances (airflow rates, thermal comfort, heating energy and airborne contaminant) offered by using either single or dual openings, as well as the impacts of size and elevation of openings of both ward types.

Chapter 7, ***STUDY 2 – Single-cell inlet and stack system:*** This study is an in-depth investigation of inlet and stack ventilation inclusive of advanced natural ventilation. The single bed ward designs from ADB and a schematic layout of a ward intended for mass adoption of the ANV as obtained from literature, were used.

Chapter 8, ***STUDY 3 - Natural Personalised Ventilation:*** This chapter presents and examines a new concept in buoyancy driven natural ventilation system, developed as a direct outcome of gaps identified in this research. The performances as well as the physical characteristics of the system are described using an iterative process of refinement and improvement of its features.

Chapter 9, ***STUDY 4 - Case studies and comparative analysis:*** The four separate systems investigated in Studies 1 to 3 are compared by fitting them into the design of the GOSH ward for evaluation purposes.

Chapter 10, ***STUDY 5 – Experimental validation:*** The natural personalised ventilation was validated using flow visualisation in a salt-bath experiment. This experimentation was mostly of qualitative benefit that allowed the transient nature of airflow through the NPV to be observed at a small and controllable scale.

Chapter 11, ***Discussion of results:*** This chapter is an abridgment and synthesis of the most critical findings obtained from the research with emphasis on the five studies.

Chapter 12, ***Conclusions and recommendations:*** This chapter contains two sections. The first section is a comprehensive summary of work conducted in the thesis and presents the conclusions drawn from the overall research. It also ascertains how the stated aims and objectives have been met. The second section is a summary of recommendations for the design and operation of natural ventilation systems with respect to hospital wards and other healthcare spaces which have similar clinical needs. This chapter also contains some recommendations for future research.

1.7 Summary of publication strategy and output

The outputs obtained from this research are listed below with reference to the objectives they met and the methodology applied (Fig. 1.2).

- Adamu, Z.A. Cook, M.J. and Price, A.D.F (2011) ***Natural Personalised Ventilation: A Novel Approach***; International Journal of Ventilation, Vol. 10, No. 3, pp 263-275. (Appendix A)

- Adamu, Z.A., Price, A.D.F and Cook, M.J. (2012) ***Performance evaluation of natural ventilation strategies for hospital wards – A case study of Great Ormond Street Hospital***, Building and Environment, Vol. 56, pp. 211-222; available at: http://dx.doi.org/10.1016/j.buildenv.2012.03.011. (Appendix B)

- Adamu, Z.A. Price, A.D.F and Cook, M.J. (2011) "**Single-sided ventilation strategies for healthcare buildings**", *ROOMVENT 2011, 12th International Conference on Air Distribution in Rooms, (Paper No. 134),* June 19 -22, Trondheim, Norway.

- Adamu, Z.A. Price, A.D.F and Cook, M.J. (2010) "**A framework for occupancy-responsive healthcare ventilation strategies**", *HaCIRIC 2010 Conference;* Edinburgh, UK.

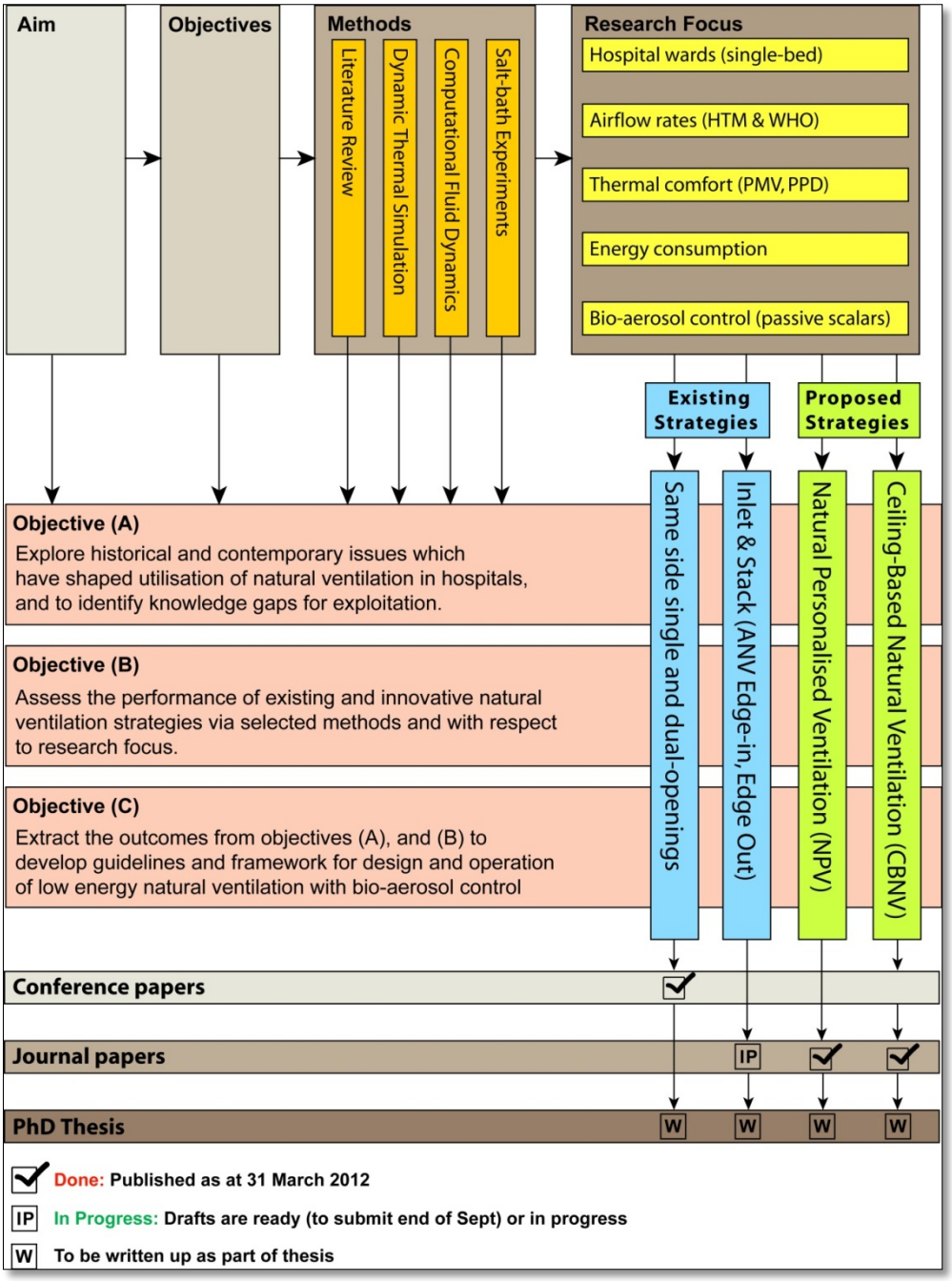

Figure 1:2: Framework for research publication

The schematic diagram shown in Fig. 1.2 describes the publication framework adopted which aligns the expected research outputs with research focus and gaps in existing ventilation strategies or the opportunities in proposed ventilation strategies.

CHAPTER 2: Review of natural ventilation and thermal comfort in wards

2.1 Introduction

The design features of natural ventilation systems determine their performance for the clinical and functional requirements of hospital spaces. Three important characteristics of a hospital ventilation system are identified as airflow rates, airflow pattern and airflow direction. The first is quantitative while the other two are qualitative components of room air distribution. These were reviewed to gain an understanding of why they are important and how they can be achieved, and importantly how they can be used as determinants for efficiency and effectiveness of a ventilation system. In addition to room air distribution strategies (mixing and displacement) natural ventilation is reviewed including the empirical and computerised models used for sizing the required openings. From the available natural ventilation systems in literature, four distinct types were identified as potential systems for exploration and exploitation including personalised ventilation. The benchmarks used in evaluating healthcare ventilation in terms of comfort and heating energy are also highlighted in this chapter.

2.2 Ventilation: role and performance

Ventilation is the process of replacing unwanted indoor air with fresh and clean air by distributing it in a room or building. The main purpose of ventilation is the provision of air of desirable quality for breathing and as such air brought in by any ventilation system is required to dilute airborne pollutants or induce their extraction or exhausting (Awbi, 2003). According to Schild (2006) there is a need for performance indicators and targets to be set for ventilation systems used in the built environment. Such indicators are required for assessing not only the performance of ventilation in rooms and buildings, but also for monitoring the evolution of the ventilation industry, as well as defining targets or objectives for future research. The performance indicators for ventilation were based on two major constraints (ibid) which are as follows.

1. Indoor environment indicators
    a. Air quality
    b. Thermal comfort

2. Energy consumption indicators of the systems.
    a. Heating energy
    b. Cooling energy

It is essential, therefore, that air quality and comfort constraints be considered while recognising or applying the energy constraints. Indeed, studies such as Khattar (2002) have shown that ventilation and thermal comfort can be decoupled such that wall and ceiling panels are used for cooling, leaving ventilation to address the airflow rate needs of occupants. With this approach, it could be easier to tackle the airflow needs of clinical spaces which have strict requirements for air changes. Ventilation systems are nevertheless designed to meet health, comfort and energy requirements, but unfortunately, a typical hospital in the UK allocates more than 40% of its energy for space conditioning (DH, 2006).

The problem of airborne hospital-acquired infections (HAIs) in particular, has led to the development of specific guidelines and standards for healthcare ventilation. In the UK, the Health Technical Memorandum (HTM) is a standard which covers ventilation and HTM 03-01 (parts A and B) clearly indicate that there are **statutory, functional and clinical** requirements for ventilation and IAQ of healthcare buildings (DH, 2007a). The **statutory** aspect is based on the Health and Safety at Work Act; the **functional** requirements deals with occupant comfort while the **clinical** requirements covers control of airborne contaminants. It is important to understand and appreciate the differences between ventilation for comfort and ventilation for infection control; (DH, 2007a; 2007b). The American Society for Heating, Refrigeration and Air-Conditioning Engineers (ASHRAE, 2004) also recognizes this disparity with its publication of Ventilation for Indoor Air Quality, as a distinct standard, separate from the thermal and comfort requirements of ventilation; in addition to the unique guidelines on ventilation of healthcare facilities as contained in ASHRAE 170-2008; (ASHRAE, 2008).

Schild (2006) implied that with respect to ventilation, specific indoor environmental indicators take precedent over energy indicators due to the health implications of undesirable performance of the entire system, which puts the individual at risk. This proposition led to the development of a hierarchy of constraints (Fig. 2.1), which orders the principles of ventilation, in a manner not dissimilar to Maslow's hierarchy of human needs (Maslow, 1943).

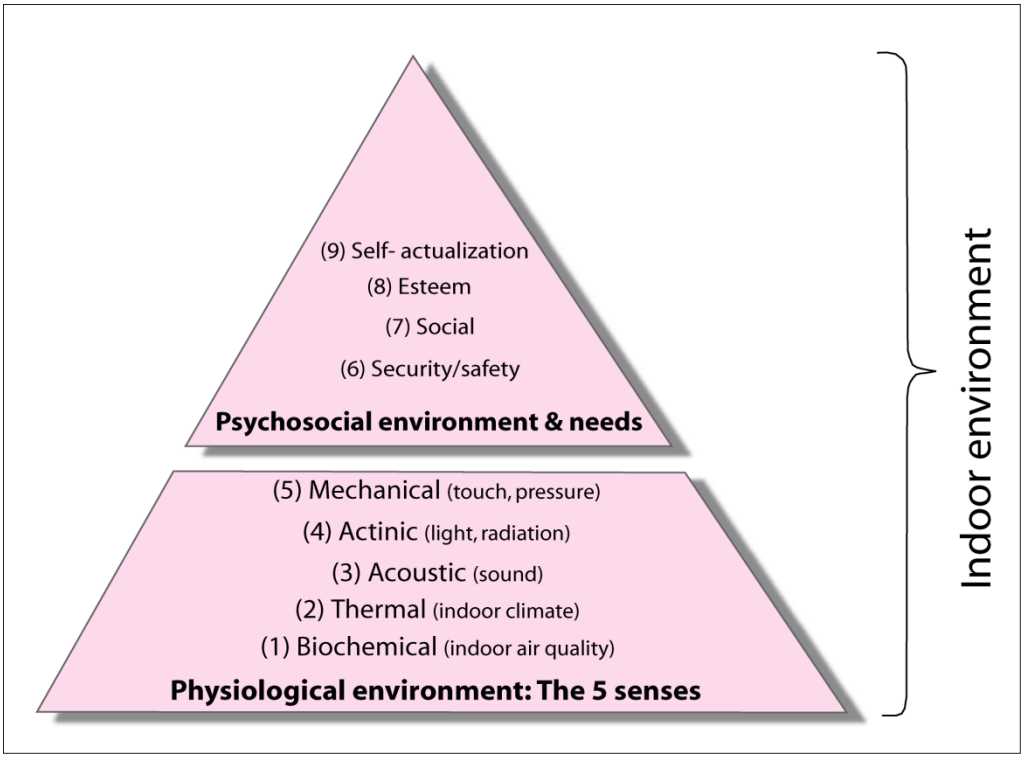

Figure 2:1: Hierarchy of constraints for ventilation systems (Schild, 2006)

From Fig. 2.1, the physiological needs of people (e.g. health and comfort) should be met first before psychosocial (e.g. aesthetics) can be addressed. How to meet these needs is not straight forward in multi-occupant buildings as Baker and Standeven, (1995; 1996), argued that very closely conditioned and controlled thermal environments (as offered by mechanical ventilation) are not really necessary because human beings derive pleasure in responding to and interacting with a stimulating and dynamic environment, such as those offered by naturally ventilated buildings.

2.3 Ventilation: Concepts and Classifications

Using the classification systems proposed by Etheridge and Sandberg (1996) and Linden (1999); ventilation air can either be from mechanical forces or from natural forces. Moreover, in contemporary literature, the tendency is for ventilation to be subdivided into three main systems or modes: natural; mechanical and hybrid ventilation systems (Liddament, 1996, Hieselberg, 2002; Awbi, 2003). Each of these modes/systems is designed with the same earlier mentioned purpose or function. With regards to healthcare buildings, Li, et al. (2008)

found that a ventilation system for airborne contaminant control would have three inherent features which include:

a) the ventilation rate;
b) the airflow direction; and
c) the air distribution or airflow pattern.

These features were identified by Li et al (2008) in their study on the effective ventilation of wards designed to cope with SARS-infected patients as has been supported by the world health organisation through its guidelines on natural ventilation for hospitals (Atkinson, et al. 2009).

These three parameters ought, therefore, to be central not only in the creation of guidelines but also for evaluating the performance of a ventilation system regarding effective removal of pathogenic bio-aerosols, but this has hardly been the case. The guidelines for ventilation of ward spaces i.e. HTM 03-01 of the UK (DH, 2007a) and AHSRAE 170-2008 of the US (ASHRAE, 2008) contain air change rates e.g. six air changes per hour (6 ACH) for general wards; which appear to have historically been selected arbitrarily (Gammage, 1996; Lomas and Ji, 2009) even if this selection was through a consensus process as was the case for ASHRAE's guidelines (Hammerling, 2009).

However, after reviewing evidence from literature, Beggs et al., (2008) concluded that studies on ward ventilation showed that the average residence time for particles at 6 ACH flow rate is 10 minutes as opposed to 30 minutes when 2 ACH is used, as was previously the standard. Yet, no direct link/inference was made to this particular (or a similar) study for the 6 ACH in both guidelines, even if it could be a sound justification. Apart from providing minimum relative ventilation rates, the HTM and ASHRAE guidelines provide no insight into how desirable airflow patterns and direction can be achieved in hospital spaces. In addition, guidance on the use of natural ventilation does not feature in any significant detail. The three key features of healthcare ventilation for bio-aerosol control are further explained below.

Ventilation Rate: This refers to the amount and quality of outdoor air ushered into a space with respect to time. This rate can either be an absolute rate; in which case, it is a flow rate in litres per second (l/s); cubic metres per second (m^3/s) and cubic feet per minute (CFM) – or it could be a relative rate, in which case the air flow rate is relative to the volume of the space,

which is regarded as an air change per hour (ACH). Given a volume of space, there is a relationship between its absolute airflow rate and its air change per hour as shown by Eqn. (2.1) below (Persily (2001) :

$$\text{ACH} = \frac{QK}{V} \tag{2.1}$$

Where:

Q = The absolute rate of airflow at inlets and outlets (in L/s; m^3/s; or CFM)

K = Normalizing Constant for time (i.e. 3600 for L/s or 60 for CFM)

V = Volume of space in litres (or cubic feet for CFM)

Thus, a typical calculation of ACH using metric variables would look like Eqn. (2.2) given by Atkinson, et al. (2009):

$$ACH = \frac{Ventilation\ rate\ (ls^{-1}) X\ 3600\ (shr^{-1}) X\ 0.001\ (m^3 s^{-1})}{Room\ volume(m^3)} \tag{2.2}$$

Unfortunately, relative ventilation does not appear to be well-understood based on perceptions of its applications in contemporary literature or by non-specialist practitioners as observed in interviews (Glanville, 2010; Noble, 2010). Perhaps the best definition comes from the first Nuffield studies (NPHT, 1955) where it was explained that 3 ACH (for instance) does not mean that in one hour, the whole air in a room has changed three times – as this would imply a highly effective ventilation regime. Rather, it means that in one hour, the volume of air that has entered the room is three times the volume of the room.

Airflow pattern: This covers the technique of delivery of external air to ensure an effective removal of pollutants in a given space. It is determined by use of either mixing or displacement strategies within the ventilation system design (Awbi, 2003).

Airflow direction: This deals with the net flow of air within a building, which (from IAQ perspective) should be from clean to dirty zones (Zang, 2005). This directionality can be extended to individual spaces as found in the design of negative pressure isolation rooms (CDC, 2005). Both airflow pattern and direction are also known as room air distribution (RAD).

It can be deduced, therefore, that it is possible for a ventilation system to be efficient but not effective, and this is acknowledged by Roulet and Vandaele, (1991) and by Seckar, et al. 2002). An efficient ventilation system can supply (and remove) the right amount of air into (and out of) a space, yet remain ineffective. Its ineffectiveness here implies it does not succeed in dilution or extraction of unwanted substances. Effectiveness of a ventilation system is therefore a function of its airflow pattern and direction. These qualities of a ventilation system have been elaborated further.

2.3.1 Efficiency and effectiveness of ventilation

Zang (2005) explains the two terms used to evaluate ventilation; which are its efficiency and its effectiveness. Ventilation efficiency deals with the amount (usually mass) of air that is delivered for every unit of power (usually kg/W) at a specific pressure. This implies that the more air is supplied per watt, the more efficient the ventilation is. Sometimes ventilation efficiency is expressed as ventilation efficiency ratio (VER), which is a non-dimensional term that has a value greater than zero. When ventilation is assessed in terms of its efficiency, its criterion relate to energy and performance of fans. It is thus not directly related to the effectiveness of the system or IAQ performance of the ventilation (this is described by the effectiveness of the system). An efficient ventilation system is therefore one that provides sufficient quantities of air as desired without prohibitive energy penalties.

Ventilation effectiveness on the other hand refers to the capacity of ventilation air with respect to pollutant removal in a given space. Methods used in quantifying the effectiveness of a ventilation system include air change efficiency, purging flow rate and purging time (Zang, 2005). Another indicator of ventilation effectiveness is contaminant removal efficiency (CRE) (Cheong and Phua, 2006) also known as personal exposure index (PEI) (Nielson, et al. 2007).

2.3.2 Ventilation performance metrics

To quantitatively describe the effectiveness of a ventilation system for controlling IAQ, a ventilation effectiveness factor (VEF) can be used (Zang, 2005). If the supply air does not contain any initial concentration of the pollutant of concern, the VEF for a room can be found as shown in Eqn. (2.3):

$$VEF\ (CRE) = \frac{C_e}{C_m} \qquad (2.3)$$

Where:

C_e *= concentration of pollutant at exhaust air.*

C_m *= mean concentration of pollutant in the airspace.*

NOTE: Equation 2.3 is applicable to an entire space. For specific points in a space; VEF becomes CRE, where C_m (in Eqn. 2.3) is replaced by C_p which is the concentration at the given point.

Other metrics applied in evaluating the performance of a ventilation system include: local air change index (LACI); the mean air exchange efficiency (MACE) as well as the effectiveness of heat removal (EHR). These metrics from Awbi, (2003) have also been applied in other studies (Karimipanah et al., 2007 and 2008) to demonstrate performance.

To compute LACI the nominal time or air turnover time τ_n and the local mean age of air have to be determined first. The nominal time or air turnover time τ_n is calculated as shown Eqn. (2.4):

$$\tau_n = \frac{\mathrm{V}}{\dot{V}} \qquad (2.4)$$

Where V is room volume (m^3) while $\dot{V}$ is volumetric flow rate (m^3/s). Upon deriving the air turnover time and obtaining the local age of air at a point, LACI (E_p) can then be calculated as follows in Eqn (2.5):

$$E_p = \frac{\tau_n}{\tau_p} \qquad (2.5)$$

Where τ_p represents the local age at a particular point in space. MACE (E_a), on the other hand is derived according to Karimipanah, et al. (2007) as shown in Eqn. (2.6) and also requires the use of τ_n as shown below.

$$E_a = \frac{\tau_n}{2\bar{\tau}_i} \text{ x } 100\ [\%] \qquad (2.6)$$

Where $\bar{\tau}_i$ = local age of air at a point in space (e.g. POI). Finally, EHR is derived as follows in Eqn. (2.7):

$$EHR = \frac{T_e}{T_m} \qquad (2.7)$$

In this case, T_e = Temperature at exhaust; T_m = Mean room temperature.

The time taken for for contaminants to be purged from a space is known as the air turnover time, ATT (Zang, 2005). Also referred to as the nominal time, ATT is measured in seconds unlike CRE which is non-dimensional and is shown in Eqn. (2.8):

$$ATT = \frac{Q}{V} \qquad (2.8)$$

Where Q is the airflow rate and V is the volume of space.

2.4 Room air distribution

The pattern and direction of air in a space are components of the room air distribution (RAD) strategy adopted for the ventilation system. Two common RAD strategies are mixing and displacement as explained below.

2.4.1 Mixing ventilation (MV) strategy

When mixing ventilation is used, the objective is to stimulate the mixing of indoor air by natural turbulence, and in the case of mechanical ventilation, this occurs with the aid of the design of supply diffusers. Perfect mixing is said to be achieved when the concentration of pollutants is uniform in the given space (Liddament, 1996); and this has led to its being also referred to as dilution ventilation. Achieving mixing requires the application of the momentum of supply jets and buoyancy forces and with good design; both ventilation and comfort (heating/cooling) can be achieved. Unlike displacement ventilation (DV); MV has been observed to cope well with large room loads (Awbi, 2003). Location of inlets and outlets vary but high level (ceiling and wall) supply of air above the occupied zone is common. Awbi, (2003) also reports that although overall efficiency and mean air change effectiveness of MV is less than one, - attributed to occasional presence of stagnation zones and short circuiting from inlets to outlets - design procedures exist for eliminating these problems.

2.4.2 Displacement ventilation (DV) strategy

The technique of displacement ventilation requires the spatial concentration of contaminants within a space to be non-uniform, such that at the upstream end of the pollutant, the air is uncontaminated while at the downstream end of the source, there is substantial contamination. In mechanized displacement ventilation, mixing is not allowed to occur since the supply air is

expected to displace the unwanted air. Displacement ventilation, therefore, uses gravitational and buoyancy forces to induce the stratified movement of air; and this could be upward or downward displacement (Liddament, 1996). The upward system is more widely used because it produces better overall IAQ. This happens because air is supplied at floor levels at a low velocity (e.g. between 0.25 and 0.5m/s) which then rises with the aid of momentum, assisted by buoyancy due to heat from people, equipment and surfaces. Displacement ventilation by itself is ineffective for space heating since any (pre-heated) outdoor air supplied into the space will quickly rise to the ceiling before filling the room. To counter this, it is mostly used only for fresh air supply (at/slightly below room temperature) with supplementary heating system (Awbi, 2003). Another limitation of this technique is that current floor (upward) displacement may not be able to handle cooling loads greater than 30-35 W/m2; meaning again that supplementary cooling would be required for higher loads, e.g. through chilled beams or chilled ceiling panels (Xing, et al. 2001). The relative efficiency of upward displacement is within the range of 1.4 to 1.7 as reported by Appleby (1989).

2.4.3 Other ventilation systems

Other room air distribution methods that hold promise include impinging jet ventilation (IJV) and the personalised ventilation (PV) techniques. The advantages of displacement and mixing have been exploited by Karimipinah and Awbi (2002) in producing the IJV system in which air at a certain momentum (lower than applied in MV systems but higher than applied in wall-based DV systems) is delivered downwards unto the floor. This creates a layer of air which is thin and travels considerable distances, even though the impingement forces the momentum to recede. PV can be traced to as far back as the Robins Aseptic Canopy described in Luciano (1977); as well as more advanced approaches described by Nielsen (2007a) including the use of retractable hoods and pillows as air terminals in Nielsen (2009). It is enlightening to note that all these strategies (with the exception of DV) are wholly dependent upon mechanical forces.

2.5 Natural ventilation: driving forces

The principles of natural ventilation are based primarily on either wind or thermal buoyancy (or both) as the driven forces which ensure that exchange of air occurs in a given space (Cook, et al 2003; Heiselberg, 2002). One of the main drawbacks of natural ventilation systems is the

uncertainty of its performance and this unreliability often leads to problems such as draught as well as undesirable thermal comfort conditions in winter and summer respectively (Heiselberg, 2002). If the definition of natural ventilation is liberalised (e.g. as contained in Qian, et al. 2010) and when new concepts such as advanced natural ventilation systems, (ANV) proposed by Lomas, (2007); and Lomas and Ji, (2009) are considered, the drawbacks of wind and buoyancy-induced ventilation can be rectified by technology, including computerised control, fan assistances and modern openings including the use of stacks, shafts and labyrinths.

Thus, whereas wind can hardly be relied upon or predicted accurately over a long time, buoyancy-driven flow depends on differentials in both indoor and outdoor temperature. As these two temperatures can more easily be predicted and because of the potential for negligible wind speeds in urban locations, buoyancy-driven ventilation becomes an attractive option. As demonstrated from experiments by Linden, et al. (1990) airflow rates in buoyancy-induced displacement systems are a direct function of the magnitude of internal heat sources. Lomas (2007) concludes that this relationship makes buoyancy-induced ventilation predictable and therefore reliable, especially when used in ANV systems, where wind is neither plentiful nor suitable.

ANV can best be described as a system that capitalises on stack effect to achieve natural air exchange using components like low level inlets, shafts and stacks (Fig. 2.2). The system is suited to buoyancy-driven airflow where fresh air comes from inlets or from a network of underground labyrinths as demonstrated in hospital ventilation by Short and Al-Maiyah (2009). There are four major types of stack-based ANV as elaborated in Lomas (2007) and in Lomas and Ji (2009). These include the Edge-in, Edge-out (E-E); the Edge-in, Centre-Out (E-C); the Centre-in, Edge-Out (C-E) and the Centre-in, Centre-Out (C-C). The edges and centres basically connote the location of inlets (openings or supply shafts) and outlets (exhaust stacks) respectively.

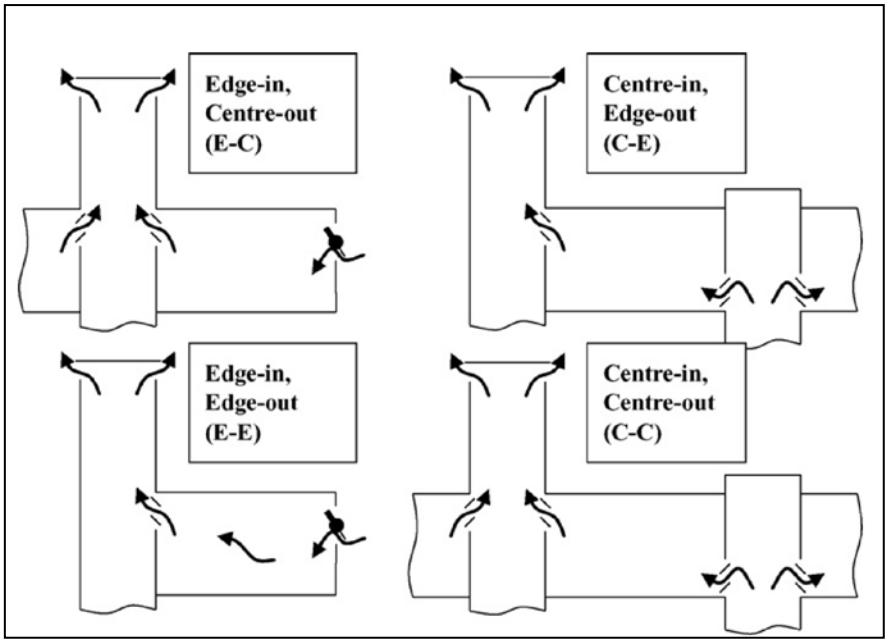

Figure 2:2: Types of stack-based ventilation used in ANV (Lomas, 2007)

One of the challenges facing ANV is the occasional need to have an auxiliary fan in stacks to supplement the desirable flow direction (outwards) when either internal buoyancy forces were 'sluggish' or when ambient temperatures had fallen below internal temperature. Without such fan assistance there would be reversal in the flow of air within stacks (Lomas and Ji, 2009). The UK's Department of Health acknowledges however, that naturally ventilated buildings can cope with systems failure and decaying infrastructure (NHS, 2007) and so in its guidelines for healthcare ventilation (DH, 2007a) it says this mode of ventilation should be the default and preferable option for ventilating healthcare spaces, as long as it meets consistency, quality and quantity criteria. The guideline is, however, lacking in terms of details of how these could be achieved, especially with respect to the six air changes per hour (ACH) recommended as minimum rate for wards, or the 10 l/s/person rate for diluting odours. It is plausible that this rate applies only to mechanical ventilation as the guideline is rather weak in its entirety, when it comes to the specifics for natural ventilation.

Based on the apparent need for specific guidelines for naturally ventilated hospitals, the World Health Organisation (WHO) has documented specific advice with emphasis on control of airborne infection in wards where it strongly recommends the rate of 60 l/s/patient (Atkinson, et al 2009). However, there are three major obstacles to this recommendation. Firstly, there are no design details (e.g. examples of techniques) through which this rate can be accomplished with acceptable climatic conditions or for that matter, what the rates should be during winter when trickle ventilation needs to be maintained in temperate countries.

Secondly, the recommended rate is apparently patient-centred, but it is not clear how such rates can be maintained consistently in single or multi-bed wards, using natural ventilation openings. Thirdly, achieving this rate steadily with natural ventilation is challenging because, unlike mechanical ventilation, the driving forces (i.e. wind and buoyancy) tend to fluctuate depending on climatic factors as well as occupancy and internal heat loads.

Interestingly, unlike the HTM and ASHRAE guidelines, the WHO guideline makes evidence-based recommendation based on two premises which are: (1) the effect that air change rate has on the decay of droplet nuclei; and (2) the risk of infection using the Wells-Riley model. At the heart of both premises is the assumed presence of an infected occupant as well as susceptible person(s). It can, therefore, be argued that for healthcare buildings, it is important to focus on occupants, for they are the primary beneficiaries or targets of ventilation and NOT the space. This is a crucial feature to be considered in this research. In fact, from Atkinson, et al (2009), the WHO's guideline is unique in the sense that it is probably the only existing guideline which specifically adopts and justifies absolute rates of ventilation from natural forces, for the purpose of infection control, and these rates are also centred on occupancy as evident in the recommended 60 l/s/patient.

2.5.1 Types of openings in natural ventilation

There are various taxonomies found in existing literature for natural ventilation systems (Allard, 1998; CIBSE, 2005; Lomas, 2007; Atkinson, et al. 2009). The British Standard method (Allard, 1998) for sizing openings recognises two major categories which are single-sided ventilation and cross ventilation. Both of these opening types can be computed based on wind as well as from wind and temperature differences with either one or two inlets/outlets in each case (Allard, 1998). These opening types are more elaborately covered by CIBSE (2005) and can be summarised as follows:

1. single-side, one vent system (single opening on one wall);
2. single-side, two vent system (dual openings on same wall);
3. cross-flow system (two openings on opposite walls); and
4. single-cell system (which use atria and stacks).

Single-side (single and dual openings) and cross-flow systems have also been classified as simple natural ventilation (SNV) by Lomas, (2007), Short and Lomas, (2007) as well as by Short and Al-Maiyah, (2009). Such systems tend to be used in spaces which are small in terms of geometry and internal heat gains. In CIBSE (2005) guidance on the length (L) to height (H) ratio for SNV systems can be found and for hospital wards, Atkinson, et al. (2009) suggest that this ranges from $H \leq 2.5$ for single openings applied in buoyancy-driven designs. In dual openings, the relationship is $H \leq 2.0$, however, in both instances; it has been argued that SNV are unsuitable for airborne infection control. Other openings that are found in literature are derivatives of single-cell system used in ANV stack configurations but with air supply coming from inlets or shafts with exhaust air escaping via stacks or atriums. These opening types can be applied in hospital facilities using different space configurations including single side corridor, central corridor, courtyard, wind tower, atrium and chimney and hybrid/mixed-mode arrangements (Atkinson, et al. 2009).

2.5.1.1 Single side single opening

Many other studies have been undertaken in the past on the performance of the single opening system including the prediction of achievable airflow rates by Dascalaki, et al. (1995); effect of room depth on travelling fresh air and the different impacts depth has on age of air and velocity/temperature in Gan, (2000); validation of two CFD models with experimental data on buoyancy-driven flows by Jiang and Chen (2003); and performance under both wind and buoyancy forces in Larsen and Heiselberg (2008). These studies have essentially focused on airflow aspect of this technique, with the exception of Alloca, et al. (2003) who analysed this system in terms of both airflow rates and interior temperature.

The WHO guideline (Atkinson, et al. 2009) does not recommend this system for natural ventilation of hospital wards, especially with regard to control of airborne contaminants. This is most likely due to restrictions in airflow rates/direction but nevertheless, there is need to understand in detail, its performance characteristics regarding comfort and energy in hospital wards specifically. This can be done using bulk annual airflow and CFD simultaneously so that this commonly found natural ventilation system can serve as a reference for other ventilation systems to be investigated within the confines of the stated PhD research objectives.

2.5.1.2 Single side dual openings

Single side dual openings have a drawback when applied to multi-floor spaces. From a study by Allocca et al. (2003), it was shown that in spaces which are ventilated with single side dual openings and vertically arranged atop each other, airflow through inlet of a higher floor could entrain the stale air exhausted from a lower floor. The situation leads to a temperature gradient which reveals a gradual rise in temperature as the floors increase. The potential implication of this fact with respect to migration of airborne contaminants can therefore be appreciated. However, while it is crucial to protect the fresh air from the exhausted air as far as ward ventilation is concerned, this system can still be beneficial for single-floor hospital wards. As such, the conclusion by the WHO (Atkinson, et al. 2009 p 44) that this system is ineffective for control of airborne contaminants is arguably hasty, especially with lack of dedicated studies in contemporary literature on airborne contaminants.

An extensive search of literature found no evidence that carefully designed single-side dual-openings have been thoroughly investigated in terms of rates, pattern and direction of airflow and their influence on indoor passive scalar contaminants in hospital wards. However, in Adamu, et al. (2011a) CFD was used to compare dual-openings in single-bed and four-bed wards regarding natural ventilation and passive scalar contaminants – with respect the sizes and vertical distances between the inlets and outlets. A previous study by Allocca et al. (2003) which was targeted at temperature and comfort and not passive contaminant control and was performed for a multi-floor building. The application and benefits of this system for hospital wards has therefore remained largely unanswered.

This line of reasoning presents an interesting avenue to exploit the potentials of this apparent over-looked but simple technique for ventilating hospital wards. Truly, both single and dual opening systems are going to be limited by design to spaces along the perimeters of hospitals (Short, et al. 2010). However, in the refurbishment of existing facilities which currently use single openings or for the possible design of new low rise facilities, it is necessary to provide evidence of performance for benefit-realisation. The lack of hard evidence in literature therefore encourages the investigation of this SNV system within the framework of this PhD research. Clearly, given the substantial number of existing facilities that rely on single openings/windows for natural ventilation of wards, there could be practical benefits for refurbishment and conversion into dual-opening systems.

2.5.1.3 Single cell inlet and stack (advanced natural ventilation)

Single cell inlet and stack systems are best exemplified by advanced natural ventilation, (ANV) as presented in Lomas, (2007). They comprise of low level air supply inlets/vents and exhaust stacks or can have air delivered from supply shafts which are sheltered from external noise/dust and whose air can be passively pre-cooled (Short and Al-Maiyah, 2009). In this study, the edge-in edge-out (EI-EO) and the edge-in centre-out (EI-CO) strategies of the ANV system are of particular interest. The performance of other techniques can easily be inferred from these two by simple reversal of the space orientation.

ANV in particular has been used in studying the performance of hospital wards in Lomas and Ji (2009) which investigated resilience of wards to climate change as well as in Short et al. (2010) where refurbishment of healthcare buildings was investigated. In addition, this system has the potential to eliminate the safety, security and acoustic concerns which limit SNV systems. In both studies of ANV however, only dynamic thermal modelling was used. The actual differences in airflow rates expected by the different heights of stacks for the three floor ward design from both studies or the control of pathogenic bio-aerosols were not considered in any detail, thereby presenting research gaps that can be filled via detailed CFD investigations.

2.5.1.4 Personalised ventilation (PV)

The importance of clean air around hospitalised patients has been aptly captured by Florence Nightingale, who promoted the first rule of nursing as being ‘to keep the air within as pure as the air without’. In her ‘Notes on Nursing’ she further emphasised that it was essential to ensure that without chilling a patient, the air he breathed was to be as pure as the external air (Nightingale, 1859). In the 19th Century, this was a straight forward matter of working with natural ventilation as a principal design element for hospitals, as evident in ‘Nightingale wards’. As hospital ventilation gradually became mechanised, it was still clear that there was a need to maintain air quality even with the recirculation and energy-saving measures that ensued (NPHT, 1955). Gradually, the need to have greater control with (and prioritisation of) patient ventilation saw the emergence of personalised ventilation (PV) as distinct airflow systems. A brief review of emergence of PV systems is given in the next subsection.

2.5.1.5 Contemporary personalised ventilation systems

PV has been 'defined' by Melikov (2004) as a system which delivers cooler and cleaner air directly to or over an occupant in such a manner that allows them to customise the flow characteristics (temperature, flow rate, direction) according to their needs. This system has developed as a ventilation technique which works independently of any supplementary/additional room ventilation system.

Recent developments in personalised ventilation systems are found in research and experimental studies where many concepts have been developed and tested. Notable studies from the last decade include Melikov et al (2002) and Melikov et al. (2003). Innovative approaches include the use of PV systems as parts of objects including: hospital beds (Nielsen, et al., 2007a and 2008); pillows (Nielsen, 2009) and chairs (Niu, et al., 2007). These studies also assessed risk to occupants from contaminants generated in such spaces using pollutant exposure models. So far, all PV systems have been mechanical, adding to energy and carbon concerns as outlined by the UK Department of Health (DH, 2006). There is hence a need to explore more energy efficient options for PV, and crucially, no evidence currently exists in literature suggesting that natural ventilation has been exploited for PV purposes.

In theory, it is possible to induce airflow through a horizontal duct situated close to a ceiling, with an air intake opening to the exterior and a discharge orifice in the interior. With the aid of an exhaust stack whose point of discharge is sufficiently higher than the horizontal duct, flow can be achieved with such a system with the aid of buoyancy forces, which if designed to deliver fresh air directly over a patient, can be described as a natural form of personalised ventilation or NPV. The theoretical background of the forces at work need to be considered in this regard, especially the drop distance of the incoming relatively cooler air, as well as the physical dimensions of the duct as implied in Awbi (2003).

2.5.2 Sizing of natural ventilation openings

It is desirable in any ventilation system to have flow of air at a rate which will ensure comfort and health. In natural ventilation, the rate of airflow through an opening can be determined through various rules of thumb and mathematical models. HTM 03-01; refers to CIBSE Guides for examples of such models. ASHRAE 170-2008 (ASHRAE, 2008) which specifically deals with ventilation of healthcare facilities makes no reference to natural

ventilation systems, but Standard 62.1 (ASHRAE, 2004) indicates prescriptive and performance-based approach to determining fresh air for natural ventilation. The prescriptive method suggests that for spaces directly ventilated from outdoors, the operable window area should be at least 4% of the net occupied floor area, with a depth not exceeding 8m.

There are many standardised mathematical models available for sizing natural ventilation openings, and although not all will be explored in this research, it is important to review them. The existing models for sizing natural ventilation openings include: empirical, network and zonal models. With respect to hospital buildings and airborne infection, the WHO guidelines, recognises two methodological approaches for sizing vents for natural ventilation. These are the direct methods and the indirect method. Direct sizing methods are used in basic cases where the fundamental parameters are used to determine required flow rates, as contained in Allard (1998) where up to five empirical models are summarised. In the indirect approach, network models are used to test different opening sizes in order to get the best fit for a given case, and an example is the loop method developed by Axley (1998). However, while the network model has capacity to consider contaminant sources for the well-mixed zone assumption, the direct empirical models contain no provisions for such.

2.5.2.1 Empirical models

Empirical models comprise sets of equations which govern ventilation due to wind velocity, temperature difference, number of openings and area of openings, with respect to building height and pressure coefficients. Two common examples of this model include the British Standard method (CIBSE, 2006) and the ASHRAE method as summarised in Allard (1998). Other examples of empirical models also outlined in Allard (1998) include: The Aynsley Method, The De Gidds and Phaff Method, Givonni's Method and The Florid Solar Energy Methods I & II. The drawback of these empirical models is that the variables considered (as evident in the equations) include wind speed and its coefficients, temperature (internal/external), area of opening, distance between openings, stack heights and stack coefficient. These models have no provisions for air pollutant variables. Examples of these models for single and double openings are given in Eqn. (2.9) and Eqn. (2.10) respectively as found in Allard, 1998.

- Ventilation due to temperature difference with one opening (British Standard method):

$$\mathrm{Q} = C_d A \left[\frac{\varepsilon\sqrt{2}}{(1+\varepsilon)(1+\varepsilon)^{1/2}}\right]\left(\frac{\Delta T g H_1}{\bar{T}}\right) \qquad (2.9)$$

$$\varepsilon = \frac{A1}{A2}; A = A1 + A2$$

- Ventilation due to temperature difference with two openings (CIBSE method):

$$A = \frac{Q}{C_d}\sqrt{\frac{T_{int}+273}{(T_{int}-T_{ext}) \times gH}} \quad (2.10)$$

Where:

A = area of (single) opening (m^2);

A1 = area of top opening (m^2);

A2 = area of bottom opening (m^2);

Q = desired ventilation rate (m^3/s);

C_d = Coefficient of discharge (-);

T_{int} = internal temperature (K);

T_{ext} = external temperature (K);

g = gravitational force per unit mass ($m.s^{-2}$);

H = height of opening (m).

These models are usually suitable for many natural ventilation applications but since they do not include contaminant concentrations, they are not suited to deal single-handedly, with analytic investigation of the performance of the healthcare ventilation from the IAQ point of view. IAQ in this case does not revolve only around indoor concentration of odours or CO_2 but covers the emission and transportation of bio-aerosols, as obtainable in hospital wards and similar clinical spaces. Nevertheless, it is possible to combine empirical models with computational fluid dynamics (CFD) for evaluation of ventilation systems.

2.5.2.2 The Loop Model (LoopDA)

A more intuitive approach to prediction, estimation and sizing of components for natural ventilation is the zonal model as exemplified by Axley (1998) through a tool called LoopDA. This model, based on a multi-zone network model allows natural ventilation components to be sized and analysed by establishing a first-order criteria for the design (i.e. an on objective for the ventilation system, e.g. a flow rate); afterwards, a continuous process of sizing flow components ensues, where each component must meet the established objective. The novelty of this approach lies in its ability to allow steady-state of transient simulations of the system to be conducted, in order to assess the performance of the design, or to set higher targets or

objectives, in order to review the appropriate size of components required to meet such targets.

Where the concentration of bio-aerosols becomes a key criterion (in addition to internal temperatures) for the quality of indoor air in a hospital environment, the Loop model can be a useful research and design tool. The minimum feasible size of each air flow component (opening, shafts, ducts, fans, etc.) is calculated by LoopDA through equations which evaluate the asymptotic limits of the equation for the specified internal and external design conditions. A key advantage of this model is that once components of natural ventilation have been sized, analysis of scenarios (i.e. what ifs) can be made through the multi-zone engine based on CONTAMW (Dols and Walton, 2000). This would allow investigation of the performance of the components under non-design conditions, the effect of indoor dispersal of airborne contaminants, as well as for reviewing the performance of fans and low-pressure ducts as used in hybrid modes of ventilation. The Loop model, however, is unable to compute energy consumed for heating of spaces and this is an important disadvantage as far as this research is concerned.

2.5.2.3 Sizing advanced natural ventilation systems

For sizing of ANV systems which require shafts and stacks, Lomas and Ji (2009) used 1% (i.e. 0.26m^2) of the floor area (i.e. 25.92 m^2) of a hospital ward to determine the size of the openings including shafts and stacks. The need to maintain free flow of air informed the decision to use the same cross-sectional area throughout the air flow path. Other mathematical models for calculating air flow and sizing natural ventilation components as used in Lomas (2007) are empirical and include Eqn. (2.11) for displacement and stack and Eqn. (2.12) for stacks and air outlets.

$$Q = \frac{qA}{C_c \Delta T} \left(\frac{m^3}{s}\right) \tag{2.11}$$

Where:

Q = volumetric flow of air (m^3/s)

q = heat gain (W/m^2)

A = floor area (m^2)

ΔT = permissible change/rise in temperature (K)

C_c =volumetric heat capacity of air (1200 J/m^3 K)

$$\frac{A_s}{A_f} = \frac{q_f}{v\, C_c \Delta T}\ x\ 100\ (\%) \qquad (2.12)$$

Where:

A_s = total area of stacks

A_f = floor area to be ventilated

v = speed of air

qf = heat load density of the space (W/m^2)

A simplified models for sizing the air inlets of ANV systems are discussed in detailed under the Methodology Chapter. Supporting equations for sizing air inlet plenum and air outlets from lightwells are obtainable from Lomas (2007).

2.6 Thermal comfort and energy in naturally ventilated hospital wards

The adoption of deep-plan design, the increase in utilisation of modern information technology-based equipment in healthcare as well as upsurge in patient activity due to increased demand for hospital care was identified in DH (2006) as being drivers for greater energy consumption in such facilities. Furthermore, there are some complications inherent in the UK's Department of Health guidelines on comfort and ventilation, HTM 03-01. As highlighted by Short and Al-Maiyah (2009), firstly, the use of dry-bulb temperatures (DBT) as opposed to dry resultant temperature makes the 28^{o}C maximum allowable temperature of wards rather demanding. Secondly, their findings also indicate that in a warmer future climate, existing hospitals in the southern portion of the UK will require more cooling.

2.6.1 Thermal comfort benchmark

Other than the metrics mentioned earlier, there are three other categories of performance metrics that can be used in evaluating the comfort in ventilation studies. With respect to thermal comfort in this particular research, the dry-resultant temperature (DRT) of the indoor environment will be used in conjunction with other metrics such as Fanger's Predictive Mean Vote (Fanger, 1967). The Predictive Mean Vote (PMV) is a popular metric developed and

widely applied in the prediction of thermal comfort especially in built human environments (Fanger, 1967). However, this model is not without observed shortcomings or criticisms as it has been found by many studies to over-predict the neutral temperature level (Oseland, 1995) by various proportions in many studies such as: by 2.2^{o}C (de Dear and Auliciens, 1985); by 2.4^{o}C (Schiller, 1990); by 3.6^{o}C (Oseland, 1996). Nevertheless, the PMV ranges specified for Class I buildings under the EN ISO 7730 standard (Olesen, 2007) are applicable to hospitals. The acceptable range is defined by this standard as being from: -0.2<PMV<+0.2. In the standardised and internationalised ratings, (ISO, 1994), the PMV scale is interpreted as: +3 (hot); +2 (warm); +1 (slightly warm); 0 (neutral); -1 (slightly cool); -2 (cool) and -3 (cold). Other related thermal comfort metrics applicable to this research are predicted percentage dissatisfied (PPD) and predicted percentage dissatisfied due to draught (PD) (Awbi, 2003).

2.6.1.1 Adaptive thermal comfort and warmer future climate

Adaptive thermal comfort was defined by de Dear and Brager (1998) based on the hypothesis that contextual circumstances of individuals and a given building's thermal history could influence their perception and reaction to thermal environment. This hypothesis has gained popularity and consideration over the years and many studies (Halawa and va Hoof, 2012; Lomas and Giridharan, 2012; McGilligan et al. 2011) have considered it with reference to or instead of the heat balance approach as defined by Fanger (1970) to defining thermal comfort. In particular, Nicol (2011) argued that the heat balance approach failed because of it could not explain why occupants in naturally ventilated buildings were able to tolerate and declare as comfortable, a wider range of temperatures that would have otherwise been declared uncomfortable in the 'chamber' approach.

In particular, studies by about adaptive thermal comfort in the UK such as: McGilligan et al (2011) which introduce the *Adaptive Comfort Degree-Day*; Lomas and Giridharan (2012), which looked at its implications for future thermal comfort in hospitals; and Barlow and Fiala (2007) who suggest that it can influence lower energy consumption for offices; reveal that it can be beneficial in meeting lower energy standards in future. Nevertheless, although this research will not utilise adaptive thermal comfort standards in evaluating the indoor climates of the hospital wards to be studied. The main obstacle to adopting adaptive comfort models for this research is the relative scarcity of knowledge on the extent to which sick or infirm occupants are able/allowed to personally and clinically to adapt to thermal environments. As

pointed by Lomas and Giridharan (2012) although the adaptive criteria lends itself to the advantage of sedentary occupants being able to adapt their clothing, there is bound to be conflict in some patients due to their clinical status or conditions.

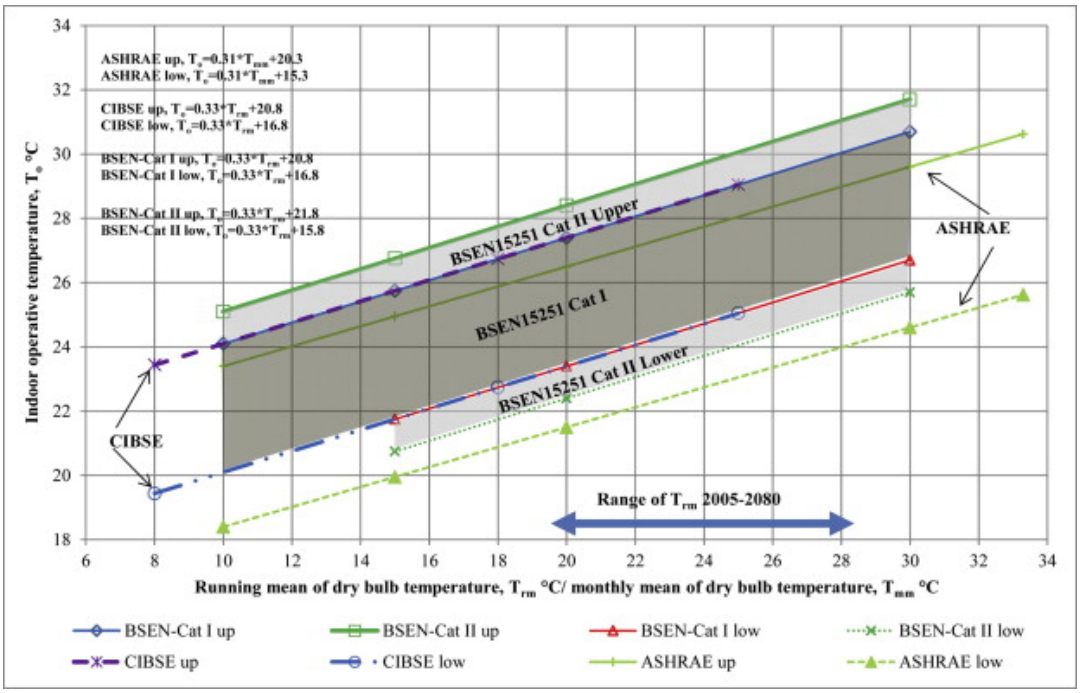

Figure 2:3: Adaptive thermal comfort standards compared with limits and boundaries (Lomas and Giridharan, 2012)

Furthermore, Lomas and Giridharan (2012) have illustrated how adaptive thermal comfort has been viewed with respect to many boundaries and limits of various standards including CIBSE, ASHRAE and BSEN for hospital buildings (Fig. 2.3). So while these variations further make it challenging to select a definitive 'standard' for adaptive thermal comfort, the unique advantage of adaptive comfort is that it is flexible, unlike other methods of measuring thermal comfort like the PMV. The role of adaptive comfort criteria in this research would therefore be best considered as a potential for some occupants only, and the results predicted (temperature and heating energy) can be viewed against its backdrop.

2.6.2 Energy benchmarks

For energy, the CIBSE energy benchmarks for Category 20 (hospitals) of 420kW.h/m^2 (fossil-thermal) can be used with respect to floor areas according to RICS gross internal area method (CIBSE, 2008). The original CIBSE benchmark for hospital will need to be adjusted to account for only space/air heating which according to DH (2006), is up to 44% of total

energy used by hospitals. These findings provide an indication of the energy performance that could be used in evaluating performance of hospital wards, in line with Objective II of this research, although focus will be on heating energy only.

2.7 Summary

Mechanical ventilation can achieve both mixing and displacement unlike combined wind and buoyancy-driven natural ventilation which relies on wind speeds and/or the upward movement of warm air in a space. However, buoyancy-driven flows have unique advantages since external and internal temperatures are more predictable than wind. Additionally, buoyancy-driven ventilation is suited to dense urban settings where wind can be minimal or negligible in many instances.

The existing healthcare ventilation guidelines utilise relative ventilation rates but for healthcare buildings, the WHO demonstrate that it is important to focus on occupants since they are the focus of ventilation and NOT the space. This indicates a paradigm shift whereby clinical requirements of ventilation are taking more prominence than functional needs as far as airborne infection control is concerned. However, the WHO's guideline on natural ventilation for this purpose is lacking in details or technical guidance that would empower designers and researchers with the qualitative and quantitative techniques to meet the occupancy-centred recommendation of 60 l/s/patient.

Although the Loop model is an empirical model that considers airborne contaminants, it is still unsuitable for detailed research where airflow pattern and direction are critical. Hence it is arguably better to use a combination of CIBSE/ASHRAE empirical models (as embedded in dynamic thermal modelling software) with CFD for a two-pronged modelling approach.

The available natural ventilation systems, reviewed for exploitation in this research, are uniquely studied in the context of single occupant hospital wards. There is an opportunity to further explore their potentials regarding airflow patterns and direction, which would be crucial to contaminant dilution and removal. This can be achieved through the use of computational fluid dynamics (CFD) to predict the steady-state variations of airborne pollutants in the wards. Another system that also presents opportunities for adoption in healthcare is personalised ventilation through natural airflow. This system is unique in

protecting occupants but has so far been based on mechanical airflow. Other approaches such as single side systems (single and dual openings), of which guidance (from CIBSE, 2005) exist for sizing openings, contain scarce evidence/guidance on their expected performance for control of airborne contaminant specifically or ward ventilation in general.

CHAPTER 3: Review of infectious bio-aerosols in hospital wards

3.1 Introduction

Pathogenic bio-aerosols and their role in hospital acquired infections (HAI) have become a source for concern in many hospitals. This chapter discusses the emission sources and the characteristics of airborne pathogenic droplets and particles from different pulmonary events, the forces acting upon these emissions and how ventilation is used to control their spread in the built environment. The ventilation rates, specific room air distribution strategies used to dilute or control the dispersal of such pathogens and the role of natural ventilation in this regard are also discussed. Personalised ventilation from a historic and contemporary perspective, and how it has been applied in protection of susceptible occupants from infectious bio-aerosols, the role of single bed wards in modern hospitals are also covered and the risk of infection from such spaces are also covered.

3.2 Characteristics of emitted airborne pathogens

When infectious droplets have been discharged via pulmonary activities such as breathing, coughing or sneezing; three forces immediately begin to act on each droplet with varying degrees of influence. These forces are airflow, gravity and drag (Xie et al. 2007). The relationship and influence of these forces on droplets occurs such that depending upon the speed of ejection the room's airflow influences the dispersal of the droplets and as they gradually fall due to gravitational force, their motion is resisted by drag forces. In the process, turbulence from the ventilation air in the room mixes and dilutes the infectious air containing the droplets. The largest of droplets fall quicker to the ground while the smallest remain suspended. Even after settlement of the large droplets, upon drying out, the infectious particles can be re-suspended during activities like bed-making, walking or cleaning as already shown by Hu, et al, (2005) and similarly by Roberts, et al. (2006).

A graphic representation of the mechanics of suspension of droplet nuclei produced by an infected patient (e.g. from coughing) under the effects of air friction and gravity is shown in Figure 3.1 derived from Tang, et al (2006) and also in Tang and Settles (2008). Understanding the forces at work, the potential travel distances as found in Xie et al (2007) as

well as how flow from a cough decays (Khan, et al., 2004) will benefit this research as these characteristics of bio-aerosols can influence the design of ventilation systems that are efficient and effective.

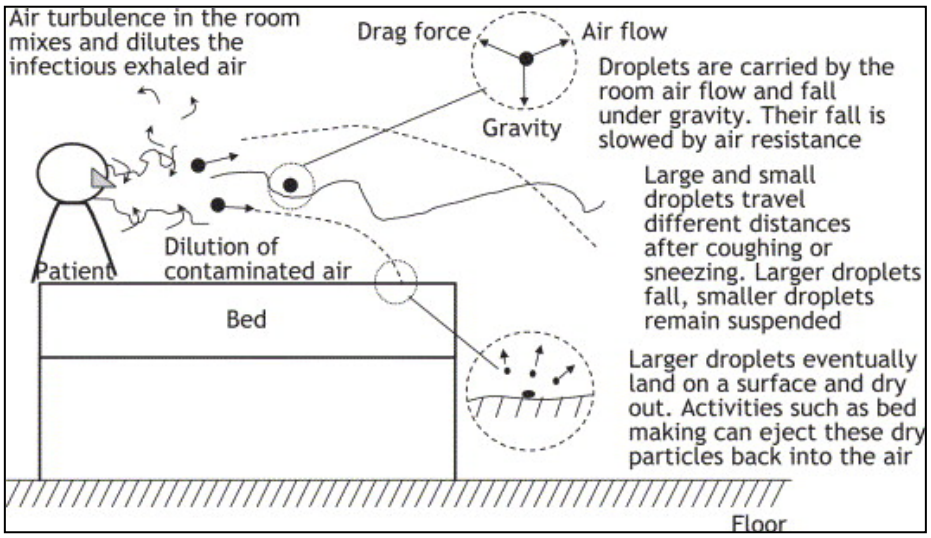

Figure 3:1: An illustration of the mechanics of suspension of droplet nuclei (Tang, et al. 2006)

In addition to the forces mentioned above, Cox and Wathes (1995) stated that the location, manner and amount of bioaerosols deposited on a landing site also depend on diffusion, temperature, electro-static forces and relative humidity. The density of bio-aerosols is yet another important factor that aids their migration in air. Compared to air which has a nominal density of 1.189 kg/m^3, the particulate density of many bioaerosols falls within the range of 0.9 to 1.3g/cm^3; which translates to 900 to 1300 kg/m^3 and a value of 1.1 g/cm^3 is widely used for computational applications (Cox and Wathes, 1995).

A decay profile from a single cough is given in Figure 3.2 from Khan, et al. (2004). This can for example aid the modelling of the emission and decay of bio-aerosols from source patients in CFD applications.

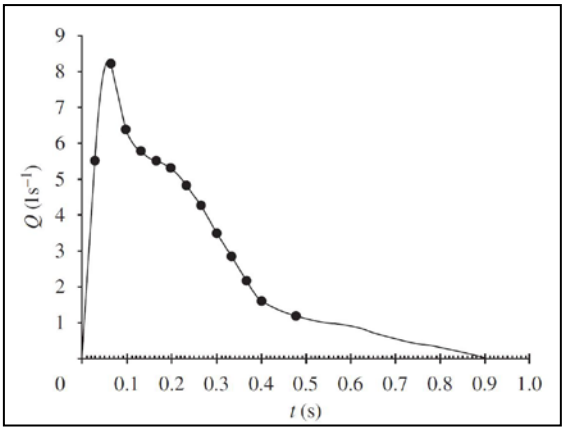

Figure 3:2: Profile of a single forced cough: airflow rate with time (Khan, et al. 2004)

3.3 Airborne contaminants in ventilated wards

3.3.1 Classification and emission of infectious aerosols

A classification of common exposures and sources of air contamination in hospitals has been made by Spengler, et al. (2001). This classification includes sensitizing and allergenic agents, irritants, direct toxins, mutagens, teratogens and latex. Other sources, include: surgical smoke; anaesthetic gases; and aerosolized medications (which are all non-biologic) as well as infectious aerosols/agents, which have biologic origins; a group of which are a centre of focus for this research. Tang et al, (2006) have provided an extensive list of pathogens that could migrate through air. Their list containing a total of 42 pathogens has been simplified and graphically summarized as shown in Figure 3.3. These pathogens have been grouped according to their proportions and biological natures. Clearly, pathogens of bacterial and viral origins should be of key interest for this research due to their constituting 81% of all airborne pathogens.

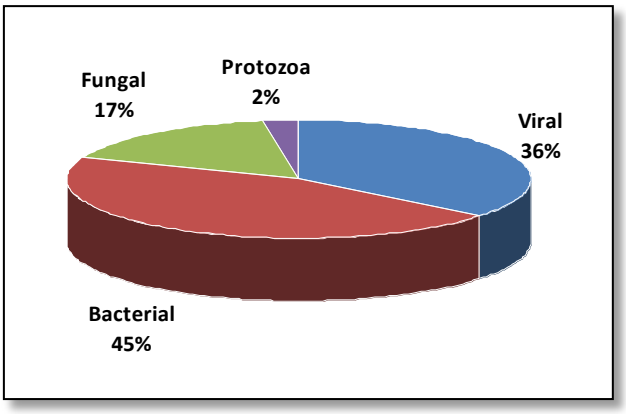

Figure 3:3: Breakdown of airborne pathogens according to their biological origins

3.3.2 Airborne pathogens causing healthcare-acquired infections

Eames, et al. (2009a) pointed out that airborne pathogens are primarily dispersed either as droplets or as particles. Droplets usually originate from pulmonary activities during which contagious moist substances (e.g. influenza viruses) are emitted from lower or upper parts of the human respiratory system. Other sources of contagious droplets could be dripping water, vomiting and diarrhoea, examples of which are the spores of Clostridium Deficille. Particles on the other hand tend to come from skin e.g. methicillin-resistant Staphylococcus aureus (MRSA).

From the airborne and ventilation perspective, the droplet nuclei or particles <1µm are of interest because they fall under passive scalar contaminants which are easily under the influence of ambient air flow (Morawska, 2006; and Jiang et al., 2009). The actual size of droplet nuclei emitted depends on the actual pulmonary event and since Loudon and Roberts (1967; 1968) it has been know that five minutes of talking can produce as much droplet nuclei as a single cough event. Xie et al. (2007) imply that up to 1 million droplets of up to 100 µm diameter size can be generated from a sneeze, in addition to thousands of saliva particles. In fact, infectious droplet nuclei are themselves dried-out remnants of larger <100 µm droplets and it is their small size allows them to remain suspended and influenced by ventilation. The Wells evaporation-falling curve for droplets as derived from Xie, et al (2007) shown in Fig. 3.4 below is instructive with regards to airborne transmission by droplets.

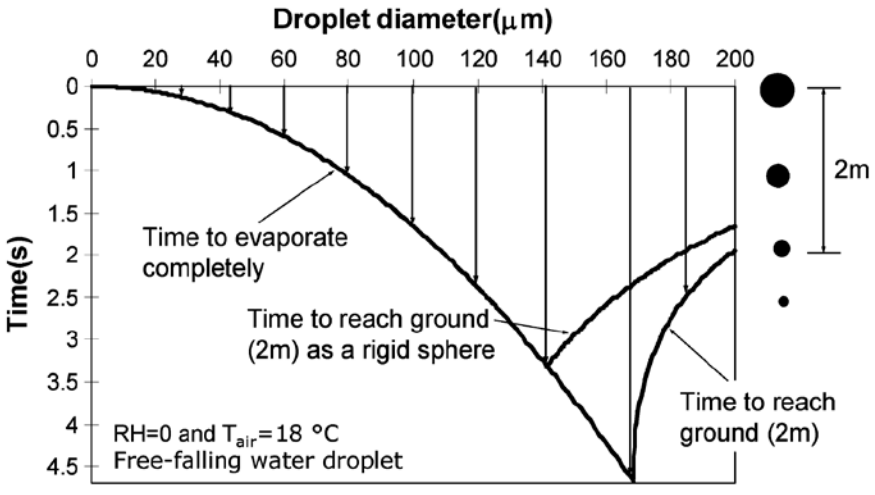

Figure 3:4: The Wells evaporation–falling curve of droplets (Xie, et al. 2007)

The validity and limitations related to the modelling of passive scalars as surrogates for airborne contaminants using CFD applications have been discussed in several studies

including Hathaway et al., (2011) and Mao and Celik, (2010). The limitations primarily concern the understanding of their size and mass as it relates to their perpetual suspension in the air.

3.4 Ventilation systems and bio-aerosols

3.4.1 Historical overview of hospital ventilation

Early in the new millennium, the UK Department of Health recognised the role of hospital space design and HAI when it commissioned a study on 'Reduction of Hospital Acquired Infection by Design' (ANA, 2003). This study was informed by many factors most prominently, the role of anti-microbial solutions leading to the rise of drug-resistant strains of infectious diseases; with a simultaneous decline in pre-antibiotic infection control measures. Such studies have precedents in Nightingale's recommendation of fresh air as a deterrent of cross infection by airborne pathogens. It can be deduced from literature, that the post-World War II era - which witnessed the emergence of mechanical ventilation modes that were adopted by hospitals across the UK – was an era of dramatic changes. Hospitals had hitherto relied primarily on natural ventilation as the 'tool of choice' in tackling airborne transmission within wards. Even then, the Nuffield studies (NPHT, 1955) which could be regarded as the first commissioned report on hospital buildings (Glanville, 2009); captures the reluctance to switch to fully mechanical ventilation systems, in the stead of natural ventilation, even though the latter had issues bordering on unreliability and thermal comfort in winter.

Interestingly, the Nuffield investigation suggested that hospital wards needed 'two rates of ventilation – a moderate continuous air-change and the means for a rapid blow-through when occasion demands it' and because mechanical ventilation systems are often fixed in terms of performance and thus lack flexibility (NPHT, 1955). This realisation of the need for dynamism in hospital ventilation is revealing as when contrasted by contemporary guidelines and standards which recommend single minimum rates of air change, the difference in both approaches is clear.

In achieving appropriate rates, pattern and direction of airflow (Li et al. 2008; Atkinson et al. 2009), two fundamental objectives that must be met by natural or mechanical ventilation as per airborne infection are dilution of contaminants and control of their migration within

contiguous spaces (Eames et al. 2009a). Dilution can be met with appropriate rates whereas migration can be checked by appropriate patterns/direction, as well as with assistance of pressurisation fans usually for exhaust purposes. These issues are explored further below.

3.4.2 Modern room air distribution and bio-aerosols

Using three case studies of naturally ventilated hospitals, Jiang et al. (2009) found that to protect susceptible occupants, the air emitted from a SARS-infected patient has to be diluted with fresh air 10,000 times the assumed pulmonary ventilation rate of 0.3m^3/h per person. If dilution is achieved with less than 1000 times of this breathing rate, it would be inadequate for protection and presents a high risk of infection. Relative to the assumed breathing rate, a safe dilution rate equates to 3000m^3/h, implying than a rate which is less than 300m^3/h is unsafe. However, this finding does not consider or apply to the equivalent safe rates when emissions are from cough or sneeze. According to Xie, et al (2007) exhaled droplets of between 60 – 100 μm can travel up to 6m away propelled by pulmonary air at sneezing velocities of up to 50m/s. A cough-induced exhalation would propel droplets at speeds up to 10m/s to be deposited over 2m away while breathing sends out droplets to a distance less than 1m away at speeds of about 1m/s. These parameters will be critical in modelling emission of contaminants in subsequent work.

In a related study focused on single-bed isolation rooms, Eames, et al (2009b), using water-based scaled models, investigated the dilution and mixing behaviours of passive contaminants and concluded that turbulence is important in order to achieve substantial homogeneity in the concentration of passive contaminants prior to (and in addition to) exhausting. Hence, a mixing strategy was shown by their experimental work (as with previous literature) to be an ideal technique for ventilating such spaces. In addition to these findings, the ingress of such airborne contaminants from adjacent spaces as shown in related studies (Tang et al., 2005, Eames, et al 2009a) needs to be kept in mind. Although the objectives of this study are aimed at single-bed wards not specifically designed as air infection isolation rooms (AIIRs) and the scope does not cover multiple spaces, the fact that airborne migration of contagious substances can occur within healthcare spaces points to the need for lessons to be learnt from design and operation of AIIRs. Thus, whereas the influence of contiguous spaces on a single-bed ward is neglected in this research, the dilution and mixing characteristics obtainable from

the four natural ventilation systems identified in Chapter 2 can provide insights into their capacity to deal with airborne pathogens.

According to Qian et al (2006), who experimented with exhaled infectious air from a person and how co-occupants could be at risk, airflow direction and proximity to source are primary factors to be considered. Their work which also used CFD modelling studied the risk of inhaling contaminated air from an infected person in a two-bed hospital ward, with the intention of understanding its impact on the respiratory performances of other occupants (i.e. a co-patient on a nearby bed and a standing healthcare worker (HCW) - as well as the performance of the ventilation system. They analysed three different strategies: mixing, downward and displacement and their results showed that locating air exhaust points at high locations was effective in removal of gaseous and fine particles exhaled from infected occupants, with such gases being at higher temperature than ambient air. They also deduced (as from previous CFD work in Qian, et al. 2004) that under displacement ventilation, concentration contours are primarily determined by the direction of exhaled air from a human source. What is not clear from this study is how much mixing of buoyant and contaminated exhaust air will occur with fresh air, if inlets are also located at high levels, as this scenario is not only common in mechanical mixing ventilation, but also a feature of high-level single opening windows in case of natural ventilation. This issue will be explored in this study.

Subsequent work by Qian et al (2006) supported the use of mixing and downward ventilation systems for hospitals with multiple beds and crucially, they did not recommend the use of displacement methods of ventilating hospital spaces, a position that was earlier taken by Friberg et al. (1996) for operating theatres and more recently by Beggs et al (2008) for wards.

Crucially, Yam, et al. (2011) noted that while the centre for disease control (CDC) in the US provides strict guidance on dilution via high ventilation rates as well as on the pattern/direction of airflow for isolation rooms – no such guidance exists for wards. However, Beggs, et al. (2008) also deduced that ward ventilation guidelines in both the United States and United Kingdom do not provide such details primarily because the ventilation design is assumed (or expected) to achieve mixing – which is typically possible via mechanical ventilation. It has also been shown by Noakes, et al. (2006a) through CFD studies that mixing ventilation is useful for the aseptic control of airborne contagion using ultraviolet germicidal irradiation (UVGI). However, the use of mechanical ventilation in achieving mixing is arguably an unattractive option from the energy perspective.

Furthermore, and with particular respect to wards, Beggs et al. (2008) established that due to the low velocities applicable to displacement strategies, this technique offers little benefit when the respiratory momentum of ejected contaminants (e.g. via coughing or sneezing) can significantly overcome the ascending airflow and the buoyancy-induced plumes around co-occupants. Also shown by Qian, et al. (2006) is the fact that under displacement ventilation, such forcefully emitted contaminants not only penetrate long distances, but can also get trapped in isolated pockets and require longer time to be dislodged or diluted. However, natural ventilation can potentially achieve higher air change rates than mechanical ventilation - up to 28 ACH in Escombe, et al. 2007; and between 18 and 24 ACH in Qian, et al. (2010); without inclement weather and consequent energy penalties. It is therefore necessary to cross-reference the 4 to 8 air changes used by Qian, et al. (2006) for their mechanical displacement, with the possible rates achievable with a natural mode of displacement ventilation. This is another important issue that will be investigated in this study.

Further support for the findings by Beggs et al (2008) is found in Eames et al. (2009b) and more recently by Li, et al. (2011) who demonstrated that a displacement ventilation strategy is indeed inferior in clinical settings where airborne contaminants are a potential hazard to occupants. Their findings show that in mechanical displacement ventilation systems, the emission characteristics of pulmonary activities like coughing and sneezing occur in the stratification zone whereas the mixing aspect (needed for diluting the airborne pathogens), occurs at the upper level (Fig. 3.5). Emitted puff would therefore be largely trapped in the lower stratified zone since the displacement momentum of air is not strong enough to allow mixing. These findings should logically be valid even for displacement in naturally ventilated spaces as well, regardless of the presence or absence of a mixing zone above the occupied zone.

This new knowledge presents obstacles for energy-saving and IAQ performance of healthcare facilities designed to use of buoyancy-driven natural ventilation which rely on displacement. Nevertheless, there is new evidence that this shortcoming can be eliminated as shown in Adamu et al. (2011b)[1].

[1] Adamu et al. (2011b) is a concurrent peer-reviewed finding from this thesis which showed that it is possible to achieve mixing via buoyancy-induced flows in a hospital ward through a top-down delivery of cooler outdoor air using a duct. The supplied air drops due to gravity and its density before rising (upon being warmed by indoor heat sources) and getting exhausted via a stack.

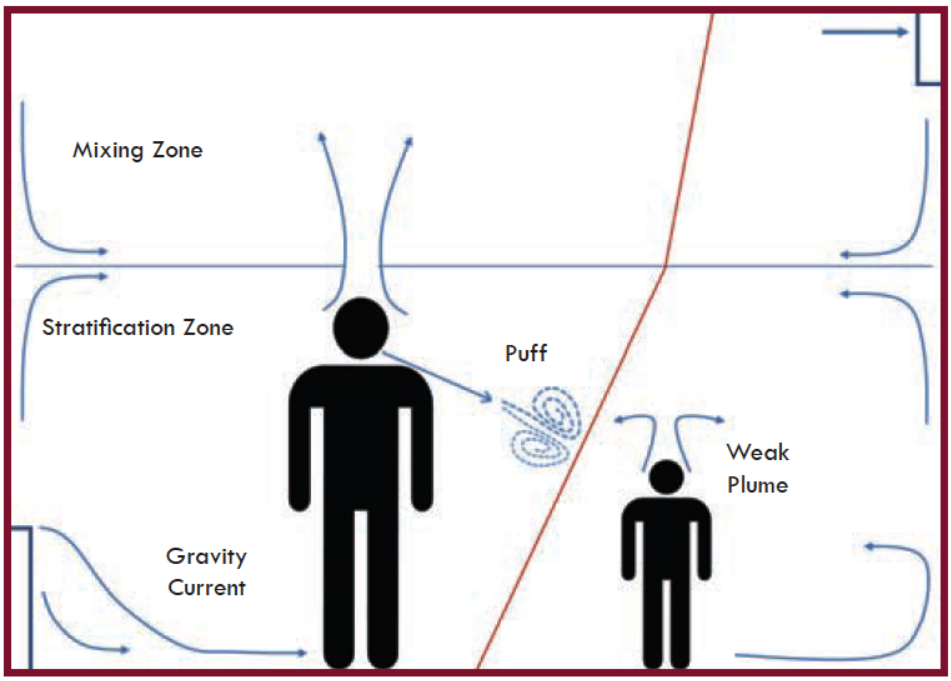

Figure 3:5: The trapping of exhaled puff in the stratified zone of displacement ventilation

(Source: Li, et al. 2011)

3.4.3 Adjacency and the hierarchy of cleanliness

It is impractical to expect a space within any healthcare building to exist or operate in total isolation to the rest of the facility. The movement of airborne pathogens is not only an intra-space problem, as inter-space migration is an issue as well. In this regard, the UK Department of Health (DH 2007a) suggested a hierarchy of cleanliness, which was a tabulated classification (Table 3.1) of rooms, their nominal pressure (in Pa), and the recommended airflow rates for diluting bacterial contaminants.

Hays et al (1995) suggested that pressure balance analyses should be conducted with preliminary layouts of ventilation systems over architectural floor plans. This would enable the pressure relationship that exists between all spaces, to be indicated on the plans, using symbols like (+) for positive pressure and (-) for areas of negative pressure; while (=) would indicate areas equal pressure. This procedure of assigning pressure symbols could be conducted in a flow that starts from core spaces, moving towards general areas like corridors and lobbies which connect with the external environment; or specifically in hospitals, it could be from sterile to clean to transitional and finally to the dirty zones. Where two spaces have the same class of cleanliness, no flow is required, (DH 2007a) and even if it did, it would hardly matter.

Such an exercise based on scientific evidence of inter-space cross contamination would provide insight into the overall flow of contaminants (usually from positive to negative pressure areas) if and when it occurs and can provide important input for facility designers and managers. As shown earlier, (Tang et al, 2005); doorways can fail to maintain the required pressure regimes on account of being opened by occupants, so it is necessary to understand the general flow of air (and contaminants) in light of potential consequences of pressure breakdowns.

Table 3.1: Hierarchy of cleanliness (as extracted from DH (2007a)

			Air-flow rate for bacterial contaminant dilution	
Class	Room	Nominal pressure (Pa)[a]	Flow in or supply (m^3/s)	Flow out or extract (m^3/s)
Sterile	Preparation room		See standard schemes in Appendix 7 for recommended design values	
	(a) lay-up	35		
	(b) sterile pack store	25		
	Operating room	25		
	Scrub bay[b]	25		
Clean	Sterile pack bulk store	+ve	6 AC/h	–
	Anaesthetic room[c]	14[c]	The greater of 15 AC/hr or 0.15	The greater of 15 AC/hr or 0.15
	Scrub room	14	–	0.10
Transitional	Recovery room	3	15 AC/hr[d]	15 AC/hr[d]
	Clean corridor	0	(See note e)	7 AC/hr
	General access corridor	0	(See note e)	7 AC/hr
	Changing rooms	3	7 AC/hr	7 AC/hr
	Plaster room	3	7 AC/hr	7 AC/hr
Dirty	Service corridor	0	–	(See note f)
	Disposal room	–5 or 0	–	0.41 or 0.10

The aspect of inter-space pressure relationship and the hierarchy of cleanliness will be important in naturally ventilated wards, where the pressure differential can be relatively small compared to any adjacent mechanically ventilated spaces.

3.5 Airborne contagion and natural ventilation

The study by Short and Al-Maiyah (2009) reviewed evidence from literature on the relationship between airborne infection and healthcare ventilation as part of a wider study on low-energy ventilation and cooling of hospitals. They deduced that there was lack of consensus on the scale of airborne transmission due in part to lack of evidence-based research,

which could be due to a paucity of reliable studies using advanced techniques like CFD modelling and full-scale tracer gas experiments (Li, et al. 2007). In producing the WHO guidelines for natural ventilation for infection control in healthcare settings, Atkinson, et al. (2009) produced more definitive conclusions. They found that not only does lack of ventilation or use of low ventilation rates link to a rise in outbreaks of airborne diseases, but that higher airflow rates could decrease the risk of infection. Additionally, Short and Al-Maiyah (2009) argued for defensive design which would deliver a system resilient enough to meet two important futuristic challenges: climate change and emerging pandemic airborne diseases (e.g. SARS).

Whereas Short and Al-Maiyah (2009) also imply that an ANV system (edge-in, edge out) can cope with the Department of Health policy on single-bed wards and reduction in healthcare-acquired infections (HCAI), the scope of their study does not cover bio-aerosol control, other than the presence of exhaust stacks supported by exhaust fans in the bathrooms. The performance of an edge-in edge-out ANV configuration needs therefore, to be evaluated from this perspective using CFD modelling and this fits within the objectives of this PhD research.

Interestingly, among the recommendations to policy makers made by Short and Al-Maiyah (2009) is that air supply and exhaust paths needed to be segregated in all individual spaces used for clinical purposes. However, it was apparent that this would come with additional cost due to inherent complexities. What is not clear from this recommendation is whether it applied to future buildings or for refurbishment of existing facilities. Additionally, it is not clear how specific natural ventilation systems would perform in bio-aerosol control using such segregated openings. It is plausible that variations not only in airflow rates but also in patterns and directions of airflow will be achieved by different systems. The question then becomes which system is best for clinical spaces like wards and why. These issues are undoubtedly important aspects of ventilation of hospital spaces that has remained unexplored at least with regards to natural ventilation.

Short and Al-Maiyah (2009) also recommended that mixing ventilation strategy should be restricted to non-clinical areas, even though it is economical and simple to achieve. Again, this recommendation is likely based on current knowledge where natural ventilation, especially when driven by buoyancy works via displacement. The need for a technique for achieving mixing ventilation through natural airflows becomes stronger, on the back of

findings by Beggs et al (2008) and Li et al, (2011) which argue that mixing ventilation is better for minimsing cross infection from airborne contaminants in clinical spaces.

In terms of effectiveness of ventilation in dealing with indoor air contaminants, Riley, et al. (1976) noted that using a 17 Watts ultraviolet germicidal irradiation (UVGI) fitting can deliver air cleansing benefits similar to ventilation using 10 ACH, Noakes, et al. (2006b) argued that air-conditioned ventilation may be expensive or infeasible. This deduction has not considered natural ventilation as a viable alternative, albeit with due regards to its limitations. Nevertheless, the existence of a guideline for controlling airborne infection in naturally ventilated hospitals attests to its feasibility. Examples of successful use of natural ventilation for this purpose can be found in many studies. Escombe et al (2007) showed with the aid of the Wells-Riley model that naturally ventilated wards had an infection rate of 11% as opposed to mechanically ventilated wards whose rate ranged from 33% to 39% depending on age of system.

In another study, Qian, et al. (2010) demonstrated that with ventilation rates of between 18 and 24 ACH, the risk of cross infection in wards of a naturally ventilated Hong Kong hospital were significantly reduced, and rates as high as 69 ACH were achieved as well. However, they also highlighted three main obstacles to use of natural ventilation for infection control. The first is the unreliability of natural forces at certain times leading to unpredictability of the system. Secondly, whereas it is often desirable to achieve negative pressurization of rooms for infection control, this is difficult when doorways are opened in naturally ventilated spaces, but this drawback is minimised if the quanta generated by infectious persons is low. The importance of adjacencies and hierarchies of cleanliness is apparent. Finally, they found that naturally ventilated spaces have difficulty maintaining stable thermal comfort conditions and when outdoor environment is extreme, similar conditions can be obtained indoors.

Qian et al (2010) did demonstrate, however, that with careful integration of exhaust fans, not only can natural airflow rates be increased but also, adequate pressure differential (and hence control of bio-aerosol migration) can be achieved between wards and adjacent spaces. In their investigations, they found that doubling or tripling the minimum ventilation rates (e.g. 12 ACH) as recommended by the Centre for Disease Control (CDC, 2005) would significantly reduce the risk of airborne infection in hospital wards. They used mechanical exhaust fans in a ward to create negative pressure, using tracer gas and mathematical modelling to study the

risk if cross-infection in a Hong Kong hospital. They deduced that it would take 20 minutes for the concentration of a contaminant to reduce to 1.8% with 12 ACH, whereas this level of reduction would only take 10 minutes with 24 ACH. Yet, the comfort and heating energy consequences of increasing air change are issues to be considered with such high ventilation rates. Kubica (1996) stated that such increment can bring discomfort to both staff and patients; and may be economically unfeasible in times of energy conservation; not to mention the air turbulence that could be generated by objects in the room under higher airflows. Such turbulent activity could interfere with desirable mixing and directionality of airflow.
Whereas it has been acknowledged in the WHO guidelines for natural ventilation that long term control of indoor pollutants should be tackled with absolute ventilation rates and not air change rates (Atkinson, et al. 2009), this provision nevertheless presents a challenge. It is not clear from this guideline, how designers (or facility operators) can determine/maintain absolute rates in the face of fluctuation in outdoor and indoor conditions, and crucially also, there are no suggested approaches to ensure or verify that the supplied rate meets the occupancy rate viz 60 l/s/patient. This is an important gap in knowledge that needs to be filled.

It is also insightful that Clark and de Calcina-Goff (2009) have argued that despite the wealth of historical and contemporary knowledge gathered on transmission of airborne pathogens in hospital, not much has been done to bring about fundamental changes for the issue to be at the vanguard of hospitals design. They also claimed that new facilities were often procured from architects who lack the requisite in-depth knowledge and skills in controlling airborne infection. Other challenges come in the form of lack of support for radical ideas as well as reluctance to implement concepts not covered by guidelines. This argument supports the need to explore existing systems like personalised ventilation, with a view of making innovative adaptations for low energy ventilation.

3.6 Personalised ventilation and occupant health

In healthcare, personalised ventilation has the capacity to provide dedicated and localised supply of fresh air around patients. This system is explored further from historical to contemporary applications.

3.6.1 Early PV systems: the pre-antibiotic era

Historical literature on the synergy between personal, architectural and mechanical subsystems in the post WWII years such as Trexler, (1975) and Luciano, (1977) reveal the considerable extent to which designers and infection control specialists went in order to make people and spaces as aseptic as possible. Examples of such systems include: the Trexler Surgical Isolator; the Trexler Life Island Unit; and the Robbins Aseptic Air Patient Isolation Canopy (Fig. 3.6) as described by Luciano (1977).

The Trexler Life Island Unit (Trexler, 1975) comprised a plastic sheet barrier around a patient's bed. This system was pioneered in the UK but was made more popular in the US, by PC Trexler, a hospital infection control engineer. Interestingly, his invention did not get the acceptance it deserved in the UK primarily because it was *'so very different from established methods'* (White, 1981).

Lessons to be learnt from revisiting these ventilation configurations are threefold. Firstly, they represent the peak of innovation in airborne infection control in the mid-20th century when active and passive preventive measures took precedent over treatment with antibiotics. Secondly, there are some contemporary airborne diseases which are resistant to drugs e.g. MRSA, MDRTB and pandemic influenzas and hence preventive (or defensive) ventilation-inspired design can be applied in dealing with their menace. Thirdly, contemporary findings (Nielsen, 2007a, 2009; Bolashikov and Melikov 2009) point towards the benefits of personalized ventilation (PV) systems for infection control purposes.

The Robbins Aseptic Air Patient Isolation Canopy (Luciano, 1977) is the first recorded use of PV in hospital wards. Nielsen (2007a, 2009) described some PV systems as 'radical' with their air supply coming from pillows and mattresses. Bolashikov and Melikov (2009) also called for new air distribution systems that would serves each occupant. They claimed that used appropriately, PV provides more benefits than total RAD with respect to occupant protection from airborne pathogens; and this performance can be optimized when PV is combined with mixing ventilation, than when mixing is used alone. The Robbins Aseptic Air Patient Isolation Canopy has been singled out for elaboration because of its simplicity in the personalisation of ventilated space.

3.6.1.1 The Robbins Aseptic Air Patient Isolation Canopy (1977)

The Robbins Aseptic Air Patient Isolation Canopy (Fig. 3.6) was developed in the US. This system came in two types, one of which comprised of a ceiling-mounted self-contained canopy that was suspended over a patient's bed in multi-bed wards. The supply air came from ductwork to the canopies. The air was diffused across four Robbins Aseptic Air UV cells through perforated ceilings in the canopy. To help minimize the vertical dispersal of supply and ensure its downward displacement, short (approximately 400 – 500mm long) curtains were suspended from the canopy. The canopy itself measured 4ft wide by 8ft long and supported a total airflow of 400 CFM which is approximately 120 ACH with respect to the canopy volume. Despite this high ventilation rate, it was reported that no movement of air was felt by the patient; that would otherwise have been experienced in the form of draft or turbulence (Luciano, 1977).

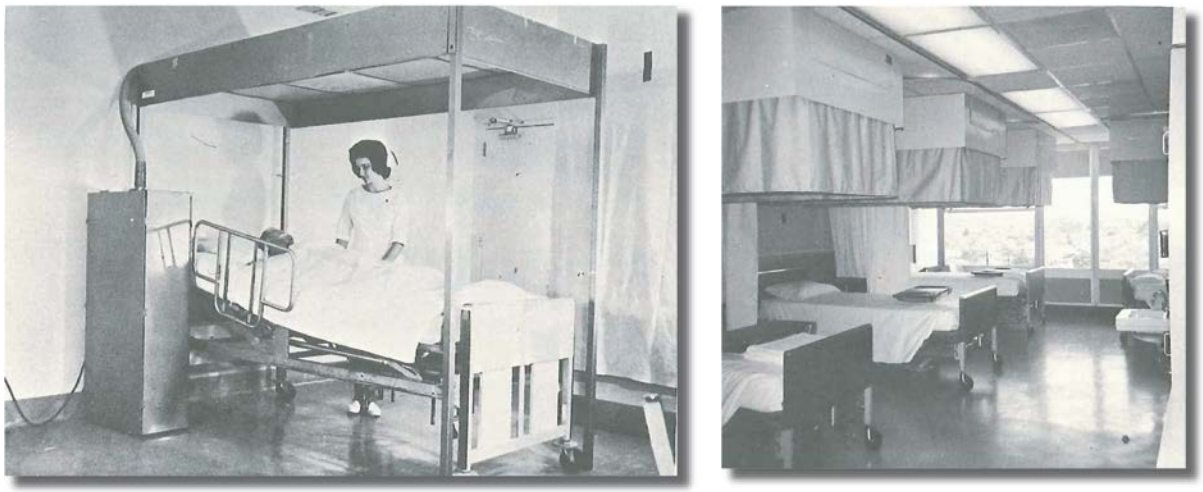

Figure 3:6: The Robbins Aseptic Air System in (a) the 1960 prototype (b) Improved version in a University of California Hospital ward

Microbial tests of the Robbins Aseptic Canopy were used to test the level of cross-infection from one bed to the next, on February 20 1969, on the 5th floor of the University of California Hospital. The tests involved aerosolising bacteriophage (i.e. naturally-occurring viruses that reside in bacteria) underneath one of the canopies at a rate of about 25,000 per minute, for 20 minutes. In this instance, the completely innocuous T_1 bacteriophage of E. coli was employed as the assumed airborne pathogen. Air sampling was simultaneously occurring under the adjacent canopies during this period. During the first test, measurements were taken from two adjacent beds while aerosols were generated under the canopy of the central bed. At bed

height, the number of bacteriophage or phage collected per cubic foot of air was 0.5 and 1.8; representing 99.2% and 97.1% reduction from the aerosol concentration in the middle canopy. In the opposite wall, the phage collected under the canopy was 0.25 per ft^3 of air, equating to 99.6% of the source concentration (Luciano, 1977).

As impressive as these results may seem, they should be considered within the context of technological capabilities of the 1970s. Nevertheless, the performance of this system is remarkable and provides clues to the way aseptic ventilation was conducted prior to the emergence of antibiotics. Lessons can be learned from such an approach in view of drug-resistant strains of airborne diseases and rise in occurrences of global airborne pandemics.

3.6.2 Modernised PV systems for bio-aerosol control

Modern personalised ventilation (PV) as defined in Melikov (2004) and applied in experiments for control of airborne diseases in studies such as Pantelic et al. (2009) have always relied on mechanised delivery of air. In another study (Nielsen, 2009), the objective and results obtained from a PV system include reduction in the concentrations of droplet nuclei and computing the personal exposure index from an experimental manikin. Further investigations on the effectiveness of PV can be found in Bolashikov and Melikov (2009).

The efficacy of airflow from PV systems in checking the ingress of contaminants into the breathing zone of occupants was also studied in detail by Pantelic, et al. (2009). They argued that rather than aiming for dilution of an entire space, focusing on clean air around an occupant can be useful in preventing the ingress of infectious droplet nuclei. Using a desktop PV system, they investigated the percentage reduction in risk at three travel distances from two common airborne diseases (i.e. influenza A and tuberculosis) emitted from a cough machine. The results (Table 3.2) indicate the reduction in risk based on distance, implied that at 1m, the momentum of cough was strong enough to counter airflow generated by the PV system, but some level of protection is still offered to the person at risk.

Table 3.2: Reduction in risk from Influenza A and Tuberculosis using PV systems

	Reduction (%)	
Distance (m)	**Influenza A**	**Tuberculosis**
1.0	51.3	63.0
1.75	27.7	41.4
3.0	54.5	64.6
Source: Pentelic, et al. (2009)		

At distance of 1.75m, the PV is able to re-assert its desired flow pattern after a given time but the momentum being generated from the cough machine's multi-phase flow is critical. Also, the interaction between cough momentum and the PV system's airflow is significant at this distance and leads to lower than expected protection. The PV system was found to be most effective at distances of up to 3m. The probabilities of being infected by either influenza or tuberculosis were also computed (Fig. 3.7) based on distance to PV system.

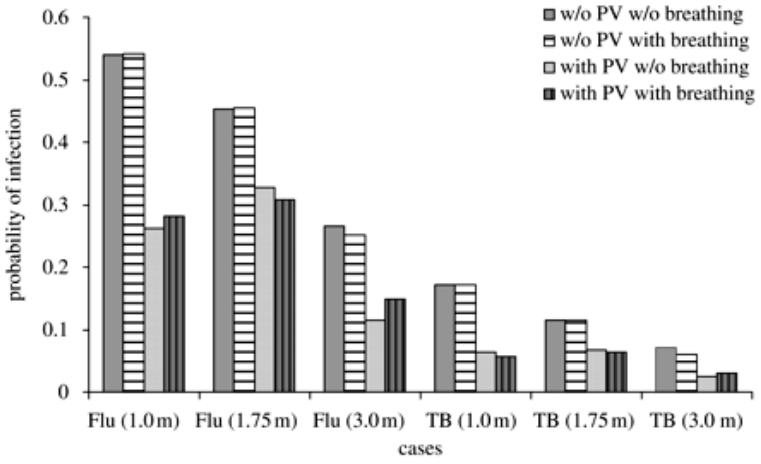

Figure 3:7: Probability of infection from Influenza A and Tuberculosis using PV systems (Pentelic, et al. 2009)

These results indicate the importance of proximity of infectious persons to susceptible persons in environments where PV systems are to be used.

3.7 Risk of infection in enclosed spaces

The Wells-Riley model provides a scientific basis for relating the risk of airborne infection to measurable variables such as total number of infected persons, the quantum of infection

generated by the diseased person(s), the breathing rate of each person and the rate of ventilation air supplied into the space. From Wells (1955) and application of this model by Rudnick and Milton (2003), it has been shown that with a constant number of susceptible and infectious persons in a space - and assuming there is a constant production of quanta - then the increase in numbers of infection will be inversely proportional to the ventilation rate. The Wells-Riley equation is given as shown in Eqn. (3.1).

$$Pi = \frac{D}{S} = 1 - \exp\left(-\frac{Ibjt}{Q}\right) \qquad (3.1)$$

Where: P is probability of infection by airborne pathogen; D is number of diseased persons in the space; S is number of susceptible/healthy persons in the space; I is the number of infectious people in space; b is the breathing rate per person (m^3/s); j is the quantum generation rate by infected person (quanta/s); t is the total exposure time (s); while Q is constant outdoor air supply flow rate (m^3/s).

This model, which has been of interest to infection control professionals, has been primarily applied to risk assessment studies, however, there is no evidence that it has been improved, modified or utilised as the determinant for required ventilation rate (i.e. air change per hour) for healthcare or other kinds of spaces. This is with the exception of Atkinson, et al. (2009), who recommended it as a rationale for determining minimum air change rates in healthcare settings. This model also has not been without criticism, for example Fisk (2008) argued that neglecting airborne pathogen removal processes other than via ventilation makes the model incomplete. Other drawbacks are that it considers each ventilated space as well-mixed; and it is based on steady state conditions meaning it does not account for changes with time. The latter disadvantage has been addressed by Rudnick and Milton (2003). As for the former, because studies such as those by Beggs et al. (2008) and Qian et al. (2006) recommended the use of mixing ventilation for hospital ward spaces (due to inherent problems associated with displacement strategies), therefore the well-mixed assumption of the Wells-Riley model is not such a disadvantage after all. From this model, Fig. 3.8 shows how the probability of infection increases (y-axis) as both the number of infectors (x-axis) and time spent in the same space (z-axis) with infector(s) increases.

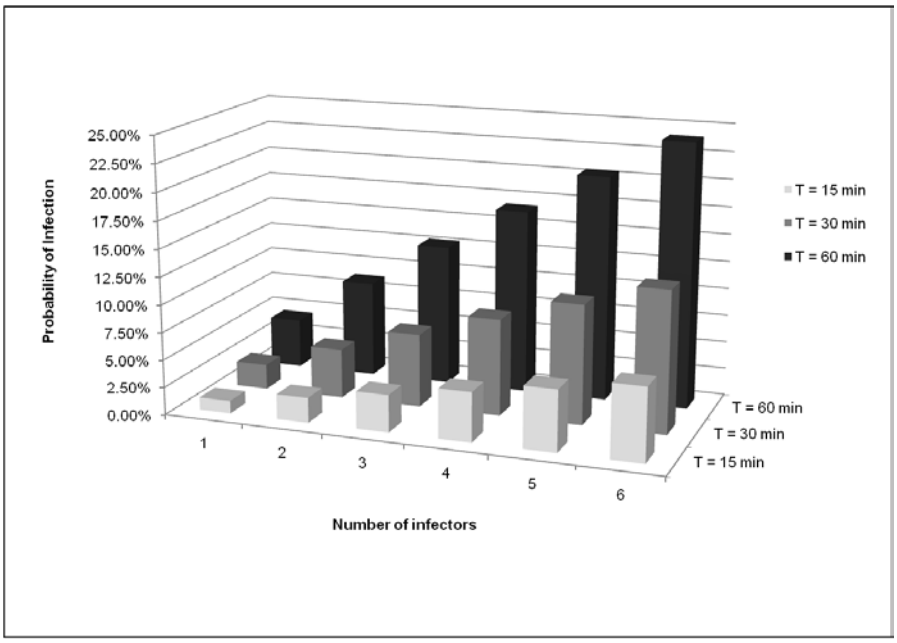

Figure 3:8: Probability of infection relative to number of infectors and time from Wells-Riley model

The existence of ADB space standards developed by the UK Department of Health (DH, 2010) has simplified the design of new buildings in terms of shape, volume and occupancies, but for engineering controls, only quantitative guidance (e.g. air change rates) is available. This research can therefore utilise the geometric standardisation from ADB single-bed ward spaces with the identified opportunities available for natural ventilation systems to fill the knowledge gaps regarding the clinical and functional performance of hospital wards.

3.8 The case for single-bed wards

The pros and cons of single-occupancy hospital wards as opposed to multi-bed wards has been the subject of debate and current policy directions towards single-occupancy in new hospitals. For example, a number of studies such as Ulrich et al. (2004) and Lawson and Phiri (2004), which according to Dowdeswell, et al. (2004) are not by themselves watertight, exist in support of single occupancy wards. The primary benefit of these wards include reduced transmission of airborne Healthcare acquired infection (HCAI). However, there are also some studies that present different conclusions, such as Vietri et al. (2004) who studied the transmission rates of MRSA in multi-bed wards and single/double bed wards, and concluded that single/double bed wards would not by themselves bring about reduced transmission rates compared to rates in open bay wards. This finding was supported by similar studies on MRSA transmission by Capeda et al. (2005). Similarly, van de Glind, et al. (2007) conducted

a literature review on studies concerning patient benefits in single wards and found that evidence is scarce and far between with inconclusive findings from existing studies. Concerning end-user (patient) preference, Florey et al. (2009) followed up with studies showing that claims for 100% single-room wards are not as overwhelming as being made.

From an airborne HCAI perspective, among the well-known determinants of contaminant migration include: the number of air changes per hour (ACH); the number of infectors (diseased persons); the volume of the shared space; as well as the number of susceptible people and their breathing rates (Rudnick and Milton, 2003). It is though tempting to consider that single-bed wards provide some level of isolation and protection as suggested by findings summarised by Policy+ (2009).

The adoption of single-bed wards will have consequences for energy consumption. According to the Department of Health (DH, 2005) the increased implementation of single-bed wards is among the factors leading to the increase in energy consumed by UK hospitals. According to the benchmarks set by CIBSE (2008) for hospitals (Category 20 buildings) the energy from fossil-thermal sources should not exceed 420kW.h/m^2. This benchmark is to be computed with respect to the gross internal area of a given floor areas as outlined by the Royal Institute of Chartered Surveyors (RICS). However, as not all the energy is allocated to space (or air) heating, a correction or adjustment has to be made. There is need to evaluate what these benchmarks imply practically for heating requirements of single-bed spaces which are naturally ventilated. This is an issue that will be considered in this research.

3.9 Summary

From evidence available in literature, droplet nuclei and pathogenic bio-aerosols of <1µm present an interesting and valid source of airborne contaminants in hospitals. The nature of their emission from either sneezing, coughing or breathing determines their travel distance. The time of exposure is clearly important as are the rates, patterns and direction of ventilation. The direction and pattern could be as effective as a flow rate, and the US centre for disease control has produced guidelines for mechanically ventilated isolation rooms which can help in the understanding and application of these principles, however, there is an obvious gap on how to achieve desirable rates under natural ventilation, and crucially, studies have demonstrated that mixing and dilution which are beneficial in controlling these contaminants,

have mostly been achieved by mechanical means of ventilation. An opportunity to explore these features through natural ventilation is therefore important as far as the objectives of this study are concerned because although higher rates are achievable in naturally ventilated wards, challenges exist in the form of actual effectiveness and protection of susceptible occupants. In this regard, there is a need to learn from specialised ventilation systems such as personalised ventilation and how it can be applied in the natural mode of ventilation for hospital wards, under both buoyancy and combined wind and buoyancy forces. The role of modern day single-bed wards is also an important factor to consider as it represents the future of healthcare ward spaces, especially from ADB guidelines.

Chapter 4: Review of modelling techniques for natural ventilation

4.1 Introduction

This chapter contains a review of the various approaches to modelling airflow and contaminants within buildings. It includes analytical, computer-based and experimental methods of investigating indoor air quality (IAQ) problems. Examples of experimental work and computational tools are given in order to capture the strengths, weaknesses and potentials of these methods.

4.2 Modelling airflow and indoor air quality

There are two basic types of model applicable to studies in ventilation and indoor air quality: (1) physical models, i.e. full-size or small scale laboratory representations of a phenomena such as found in wind tunnels or water tanks; and (2) mathematical models; i.e. a set of analytical or numerical algorithms which describe the physical and chemical nature of a problem (Zanetti, 1990). Mathematical models can be further sub-divided into:

- **Deterministic Models:** which are based on fundamental mathematical representations of a process; and
- **Statistical Models:** which are based on semi-empirical statistical relationships between measured values and available data.

Mathematical models are often applied through computational tools for studying airflow and contaminant transport in enclosed spaces. Two common methods are multi-zone and computational fluid dynamics (CFD) simulations. The recent growth in popularity of CFD modelling is probably due to its power and flexibility but also, the limitations of network air flow models and the constraints involved in setting up physical models. Table 4.1 summarizes the categories of air flow models, their primary purpose and examples.

Table 4.1: Categories of indoor air models, their specialties and examples

Type of Model	General Purpose of Model	Examples
Deterministic	Estimating population exposures	Wells-Riley (Wells, 1955)
Statistical	Estimating population exposures	SHAPE (Thomas, et al. 1984)
Mass Balance	Estimating Impact of Sources	Contamw, (Dols and Walton, 2000); SPARKS (Sparks, 1988)
Dynamic Thermal	Airflow and energy consumption	IES, (IES, 2011) EnergyPlus (Crawley, et al. 2000);
CFD	Estimating near-source individual exposures	PHOENICS, (Cham, 2011) Vortex, (Vortex, 2012) Flow3D (Flow3D, 2012)
Scaled	Flow visualisation and validation of other models	Salt-bath modelling, (Linden et al., 1990)

Airflow modelling has become an invaluable tool in ventilation and indoor air quality studies of healthcare buildings. With specific regards to healthcare-acquired infections, a state-of-the-art overview of common modelling techniques used in the observation and quantification of airflow and pathogenic bio-aerosols was performed by Tang, et al. (2011). This review provides an assessment of the materials, procedures and outputs obtainable from several techniques of modelling including: full-size mock-up models with the aid of humans or mannequins; visualisation through computational models such as CFD as well as reduced scaled models.

A demonstration of modelling for ventilation and IAQ studies can be found in Short and Al-Maiyah (2009), who reported on their investigation into low-energy ventilation and cooling design strategies for hospitals. They used dynamic thermal modelling (DTM) with water-based experiments. However, dispersal of airborne contaminants was not considered in that particular research. In other ventilation studies though not related to healthcare buildings, Short, et al. (2009) utilised a combination of DTM, CFD and water-bath experiments to investigate strategies for low-energy ventilation and cooling. Cook and Short (2005) also used DTM and CFD to explore the performance of low-energy ventilation in four large non-domestic buildings, one of which was a health and social care centre. These studies therefore provide good reference cases for the use of modelling in natural ventilation studies that can be of benefit to this research. Details of these modelling techniques, including their limitations, are reviewed here.

4.3 Computer-based Modelling

Unlike experimental methods, CFD, zonal and network air flow modelling programmes are very flexible with respect to the potential impacts of (and changes to) building geometry or thermal and fluid boundary conditions. These types of computational models handle geometry and architectural details in different ways, but their main advantage lies in their ability to idealize building geometry and the physical/chemical processes which occur within (Chen, 2009).

One of the main draw backs of the network method is that it works by assuming that a zone's air or contaminant distribution is well-mixed; whereas this is often not the case in reality, due to factors such as stratification, air turbulence and dynamics of air movement and contaminants distribution. DTM provides another zone-based modelling option which allows bulk annual airflow from natural, hybrid and mechanical systems as well as energy consumed from various sources (electricity, fossil fuels) to be computed (Heisleberg, 2002).

Unlike network modelling simulations, which are rather simple to run on an average desktop computer, most CFD simulations tend to require significant computational power. The results however, are usually detailed enough for most applications. CFD works by solving the differential equations which govern mass, momentum and energy transport on a fine grid; to provide a detailed picture of the flow pattern and temperature distribution. CFD is, therefore, widely used to calculate airflow patterns, distribution of air velocity, temperature of air and the concentrations of contaminants in enclosed spaces. It is used in identifying problematic areas of a space before construction begins and it is also helpful in determining issues such as the optimum locations and properties of supply air diffusers, return outlets and the overall amount of air needed to maintain acceptable indoor air quality. CFD calculations are either steady state or transient. The former refers to static conditions while the latter is applicable to studying time-varying processes. There are also many CFD techniques available and examples include direct numerical simulation (DNS), large-eddy simulation (LES), as well as the Reynolds Averaged Navier-Stokes (RANS) equations with turbulence models (Spengler and Chen, 2000). A summary of popular computational models used in ventilation research and by industry practitioners is provided in Table 4.2.

Table 4.2: Types and features of computerised ventilation modelling tools (Heisleberg, 2002).

	Simple analytical and empirical models	Zonal models	Multi-zone air flow models	Thermal models	CFD-models	Combined air flow and thermal models
Design phase	• Conceptual • Basic	• Detailed	• Detailed • Evaluation	• Basic • Detailed • Evaluation	• Detailed • Evaluation	• Detailed • Evaluation
Purpose	• Analysis of air flow rate, thermal comfort and energy use in discrete time steps or on yearly basis	• Analysis of airflow and temperature distribution in a single room.	• Analysis of air flow rate through the envelope on a yearly basis • Analysis of air flow rate between zones on a yearly basis • Analysis of IAQ in buildings	• Analysis of thermal conditions in zones on a yearly basis • Analysis of energy use on a yearly basis	• Analysis of airflow, IAQ and temperature distribution in a single room • Analysis of air flow around buildings • Analysis of surface pressure on envelope	• Optimization of building and system performance through combined analysis of air flow rates, temperature conditions and energy use
Available models	• Flow element models. • Spreadsheet programs • Vent sizing programs	• POMA	• COMIS • CONTAM	• TRNSYS • EnergyPlus • BSIM2000 • CAPSOL • ESP-r • IDA	• Fluent • Flovent • Vortex • CFX • PHOENICS	• TRNSYS + COMIS • Tas-Flows • CHEMIX • IDA-ICE
Outputs	• Mean indoor temperature • Peak temperatures • Draught risk • Heating & cooling load • Energy use	• Distribution of air flow • Distribution of pollutant concentration • Distribution of temperature	• Air flow rates through envelope opening • Air flow rates between zones • Average IAQ in each zone	• Hour by hour temperature variation in zones • Hour by hour heating and cooling loads • Hour by hour energy use	• Detailed distribution of airflow and temperature. • Study of design problems (trouble-shooting). • Mechanism of heat transfer and airflow in enclosures	• Hour by hour variation in temperature, air flow rate, IAQ and energy use • Optimized control strategy
Necessary equipment /computer	• Hand calculator • Personal computer, etc.	• Personal Computer	• Personal Computer	• Personal Computer	• Powerful personal computer • Workstation	• Powerful personal computer • Workstation
User	• Practitioner	• Expert	• Expert/ researcher	• Expert	• Expert/ researcher	• Researcher
Required time for application	• About half day per case to input data.	• About one day per case to input data.	• About two days per case to input data.	• About two days per case to input data.	• About 1 week per case to input data	• About 1 week per case to input data
CPU time	• A few minutes.	• 1-10 hours	• 1-10 hours	• < 1 hour	• 10-100 hours per case	• 10-100 hours per case

4.3.1 CFD and IAQ investigations

Most CFD tools as Laine, et al (2000) explained, require a high level of expertise and due to the time taken to run simulations, they are not always used by designers. Within the research community however, Li and Nielsen (2011) have reported that the application of CFD for airflow-related investigations has increased since 2002 and for validation purposes, the

concurrent use of experimental and theoretical models with CFD simulations has also become an important issue.

CFD tools work with a virtual 3D space, representing the physical dimensions (i.e. width, length and height). CFD software produces solutions by solving the equations which represent the physical phenomena in a space. It does this by dividing the space into grids or sub-volumes, and in each sub-volume, the conservation of mass, energy, momentum, and chemical/biological species are solved. The equations which govern these four phenomena involve physical parameters such as pressure, temperature, velocity and the chemical/biological concentrations within a sub-volume and its neighbours – all of which are solved simultaneously. However, the smaller the sub-volumes, the larger the number of equations that need to be solved and consequently, the more time that is required to arrive at a solution (Spengler and Chen, 2000).

A fast calculation would therefore have large grids/elements in which average temperature, velocity and concentrations of pollutants are calculated, but this may over-simplify the result and present solutions that do not represent actual conditions in a space. It is known that over-simplification can lead to significant errors in overall flow, and air can appear to move in the opposite direction of its actual flow (Spengler and Chen, 2000). It should always be borne in mind that CFD techniques are meant to be detailed studies and this primarily sets them apart from zone-based models.

The spread of gases, particles and bio-aerosols within ventilation air in a space is governed by the geometry of the space and the forces that influence the movement of these substances throughout the space. Tracking the movement of such contaminants in a CFD process can be done in one of two ways. The first method involves following each packet of gas or particles moving within the space, but due to the fact that the packets divide and mix (i.e. are constantly changing their location, velocity and concentration); this approach is largely impractical. A better approach is to subdivide the room into imaginary sub-volumes or elements, where each sub-volume does not have a solid boundary – thereby allowing gases (fluids) to flow across their boundaries. Each sub-volume has a single associated temperature, which is the average temperature of its constituents; as well as a single concentration of air and other contents. Additionally, each sub-volume has a single average velocity - vertical and horizontal (Chen and Glicksman, 2001).

At the start of the CFD simulation, the temperature, concentration and velocity of each sub-volume (and its constituents) are unknown at all sub-volumes; but the values at room (or domain) boundaries, air inlets or contaminant sources are known. The CFD algorithm then computes the temperatures, concentrations and velocities throughout the sub-volume based on either steady state or transient conditions, as specified in the global parameters of the investigation (Chen and Glicksman, 2001).

4.3.1.1 Turbulent flows in CFD simulations

Turbulent flows usually exist in most room flow investigations and it comprises of eddies which vary greatly in size. Modelling the behaviour of the smallest of eddies requires fine meshing of the domain space and solving such problems exactly requires direct numerical simulation, which computationally is large and impractical for the average computer. The presence of turbulent flows therefore tends to complicate the process of such CFD investigations and if not handled appropriately, they often become the leading cause of inaccurate predictions made by CFD software (Chen and Glicksman, 2001).

To overcome this, computational fluid dynamicists have devised several ways of approximating turbulent behaviour without recourse to fine sub-divisions. The drawback of such approximation is that while it makes computations cheaper in terms of hardware resources, there is a distinct lack of a single approximation technique for turbulent flows which is suitable for all scenarios. This has led to the development of several turbulence models (Chen and Glickman, 2001). Thus, the techniques utilized in studying high-speed turbulent flow over an aeroplane's wing would not necessarily be suitable for large rooms where buoyancy may be important. So eventually, whereas most commercially-driven CFD software will generate a solution to particular set of boundary conditions, it is by no means certain that the output is indeed the correct solution, and the selection of an appropriate turbulence model is essential (Spengler and Chen, 2000).

For healthcare buildings, Mendez, et al. (2008) implied that it is difficult to standardise ward design for ventilation performance via CFD. This is because the uniqueness of space geometry as well as the flexibility in furniture layout could lead to differences in airflow patterns, due to variations in local turbulence from case to case.

It is noteworthy also that the various CFD techniques mentioned earlier (i.e. DNS, LES and RANS equations with turbulence models) all handle turbulence in a different manner. Additionally, because there is no universal turbulence model available, CFD results can have uncertainties and experimental validation is usually required. Even when this is done, it becomes apparent that a validated CFD programme used in studying a particular type of flow, (e.g. natural convection) may not predict a different type of flow (e.g. forced convection) correctly, unless it has been configured and validated for both types of flows (Chen and Glicksman, 2001).

4.3.1.2 Documentation procedure for CFD simulations

Documentation of the CFD modelling process is important as it helps in the understanding of the engineering decisions taken including any assumptions or limitations. This is especially true for steady-state CFD investigations, where results are valid only for an instantaneous period of time, outside of which the results may cease to be valid. Additionally, many CFD simulations of buildings tend to simplify geometry and technical details of building components in order to optimise computational resources, without compromising the validity or applicability of the results. Versteeg and Malalasekera (2007) have provided a documentation procedure for undertaking CFD simulations as follows.

1. Problem description and purpose of simulation
2. Selection of code, justification and computer platform utilized
3. Schematic layout of space (with dimensions, flow inlets and outlets)
4. Boundary conditions (with justification of assumptions)
5. Properties of fluid and contaminants (with justification of assumptions and sources of data)
6. Turbulent models and justification
7. Grid sizes and definitions (coarse, medium fine)
8. Convergence criteria
9. Simulation design

The outputs from CFD simulations can vary, depending on the capability of the software, but for airflow purposes, these are usually in the form of:

- velocity vectors;
- streaklines/streamlines and particle paths;

- contour plots for flow variables; and
- profile plots.

4.3.1.3 Validation of CFD for natural ventilation

The importance and reliability of steady state CFD as a validated technique for investigating natural ventilation is found in Awbi (2003) with further validation and comparison using full-scale experiments conducted by Yang, et al. (2006). A validation study of three CFD model types useful for natural ventilation was conducted by Jiang, et al. (2004) where they evaluated RANS, unsteady RANS and LES models and compared their results with data obtained from experimental data from a scaled building in a wind tunnel. Their results showed that LES modelling results were closer to the experimental data than RANS, but the LES model took a significant amount of time and computational power to converge. Specific examples of buoyancy-driven ventilation studies can be found in: Cook, et al. (2006) and with combined with wind in Cook, et al. (2003) and Cook, et al. (2008). Heiselberg and Li (2009) is a study of flows through horizontal openings while Hunt and Syrios (2004) provides design criteria for enhancing buoyancy-driven flows using roof-mounted towers.

4.3.2 Dynamic Thermal Modelling

Dynamic thermal modelling (DTM) software are simulation engines which are able to calculate building thermal loads (e.g. heating cooling and plant loads) based on user-defined variables and time-steps. DTM software calculates the inter-zone or intra-zone movement of air using the well mixed zone assumption. The results are predictions of temperature, comfort, energy and airflow which enable users to size and evaluate the performances of the components and the space geometry. These tools are also capable of estimating the performance of energy-consuming devices used in air-conditioning systems such as pumps, fans, boilers and chillers. Users of DTM are able to define the geometry of the spaces or buildings being investigated and the automated control of the virtual environment according to expected user-requirements is possible as well (Crawley, et al. (2008). DTM models are typically run for predictions over an entire year.

Examples of dynamic thermal modelling software include: EnergyPlus (Crawley, et al. 2000); Apache (IES, 2011); TAS (2012) ESP-r (ESRU, 1997) DOE (LBNL, 1982) and TRYNSYS

(Klein, 1972). The choice of DTM application for a project is dependent on many factors including the technology of the ventilation system being designed, availability, cost and user-friendliness, but as implied by Crawley, et al. (2008). Many such tools allow users to import geometry from CAD software and while many users were found to rely on single software for their projects, having access and skills to a suite of tools would be the most productive way to work (Crawley, et al. 2008). Validation of DTM software was conducted by Lomas, et al (1997) while Attia, et al. (2012) demonstrated their use for zero-energy buildings.

4.4 Physical models

4.4.1 Large scale mock-up experiments

Flow visualisation in large scale experiments began with the use of tracer gases such as helium developed in 1936 (Zang, 2004) and with examples of hospital application in Whyte (1974). Other gases used include SF_6, CO_2 and N_2O (Prior, et al. 1983; Lagus and Persily, 1985; Tang, et al. 2011) with utilisation of tracer gas in studying airborne infectious diseases within ventilated spaces contained in Nielsen, (2009). A life-size mock-up of a hospital environment can be built specifically for testing its performance regarding airflow and contaminant transport. The working fluids in such experiments include the ambient air and smoke, whose movement provides qualitative and quantitative data about flow of air and contaminants (Tang, et al. (2011).

Examples of specific applications in healthcare buildings can be found for naturally ventilated wards in Escombe, et al. (2007) and Atkinson, et al. (2009); for isolation rooms in Rydock and Eian (2004) as well as for operating theatres in Andersson et al. (1983). In such experiments, quantitative data is collected either by measuring relative differences in concentration of tracer gasses at source, air supply and air exhaust points, or by measuring directly at specific points in space (Tang, et al. 2011).

Large scale experiments have also become invaluable techniques for validating other modelling methods such as CFD as found in various studies such as: Yang, et al. (2001); Yang, et al. (2006) and Li, et al. (2005). Large scale experimentation is strongly recommended by the UK's healthcare ventilation guideline (DH, 2007a). Tang, et al. (2011) revealed that this technique is not only popular with engineering services professionals, but it

is also approved in HTM 03-01 as a technique for validation of ventilation performance especially pressure differentials across isolation rooms and operation theatres. There are, however, some disadvantages related to this method as summarised below:

1. Cost and logistics of building a mock up facility.
2. Use of sophisticated equipment such as anemometers.
3. Cost and sophistication of equipment for laser Doppler anemometry (LDA) systems and 3D stereoscopic particle image velocimetry (SPIV).
4. High level of skill and expertise required to run experiments, including support personnel (Tang, et al. 2011).

4.4.2 Water-based experiments

Unlike most CFD airflow investigations of the built environment which tend to be steady-state simulations, water-based models provide dynamism and realism through visualisation of transient flows. Tang, et al. (2011) imply that the advantage of using water as a working fluid in such models is primarily due to its capacity to transport dye or tracer particles. The transportation which occurs in real-time can then be simultaneously visualised with the aid of advanced illumination and image-capturing techniques – from different angles and in different formats ranging from stills to video.

Tang, et al. (2011) stated that a Plexiglas model at a scale of 1:10 is commonly used for flow visualisation in hospitals and the working fluid for buoyancy-driven ventilation is usually water and the heat source is either electricity or salt-water. The heat source can either be a point source (Lin and Linden, 2002) or a distributed source (Gladstone and Woods, 2001; Fitzgerald and Woods, 2008) in which a coiled resistance wire is used to supply the heat. With the heated wire method, the temperature difference generated by the source drives the flow of fluid in the medium whereas in a salt-bath model, it is the density of brine that drives flow, albeit in an inverted orientation. The use of water-based experiments for studying the behaviour of contaminants is exemplified in Thatcher et al. (2004) and in Finlayson et al. (2004).

4.4.2.1 The salt-bath model

Salt-bath models allow the qualitative visualisation and quantitative measurements of fluid flow in a water tank, in which brine acts as the driver for buoyancy. Examples of salt-bath experiment used in evaluating ventilation in a scaled Plexiglass model include: mixing and displacement (Linden et al., 1990) and buoyancy-driven flows (Montero et al., 2001; Yang, et al. 2011). The principle of salt-bath modelling hinges on buoyancy being induced by two fluids of different known densities. In one approach, the fluid which represents the heat source i.e. buoyancy source (brine) is less dense than the 'ambient' fluid and it can be expressed as a reduced gravity, g'. Its relationship with actual gravity and difference between its density and that of the surrounding fluid can be computed as shown in Eqn (4.1):

$$g' = g\frac{\Delta\rho}{\rho_0} \qquad (4.1)$$

where g is acceleration due to gravity; $\Delta\rho$ is the difference in density between the buoyant fluid and ambient fluid while ρ_0 is a reference density. The momentum of the buoyancy source is determined by its flux B_f and is related to the volume flux V_f of surrounding fresh water which is of lesser density as shown in Eqn (4.2).

$$B_f = \frac{V_f\, g'\, \Delta\rho}{\rho_0} \qquad (4.2)$$

The relationship with actual heat sources e.g. from people can be expressed in Watts using Eqn (4.3)

$$W = \rho V_f C_p \Delta T \qquad (4.3)$$

where ρ is the reference density, C_p is the specific heat capacity and ΔT is the temperature differential resulting from the heat source.

4.4.2.2 Scale, geometry and similitude in water-based experiments

It is important for both full-scale building and the scaled model to be similar in many respects. Geometric similarity can be achieved by a simple scaling/conversion of the full-scale building into a size suitable to be built and visualised in a larger tank. There is no evidence in literature to suggest why any particular scale is ideal, but it can be inferred that the reduced scale model should be sufficient to allow adequate visualisation of flow when inserted in the water tank. In this regard, Yang, et al. (2011) state that a scale of between 1:20 and 1:100 can be used, while in Thatcher, et al. (2004) a scale of 1:30 was applied. The difference in temperature between the source and its surroundings as applied in studies such as Kaye, et al.

(2010) is usually about 10^{o}C, but there are other variables that need to be considered. Their magnitudes vary according to the physical dimensions of the adopted scaled model. The relationship between such variables used in water-based models of different scales (1:12 and 1:100) has been summarised in Table 4.3 as derived from Walker (2006). In Cook (1998), the relationship between heat sources, plumes and velocity and buoyancy in full-scale measurements and in salt-bath model can also be found.

Table 4.3: Example of input variables used in salt-bath modelling of two different scales (Walker, 2006)

Variable	**Water Model (1:12)**	**Water Model (1:100)**
ΔT (^{o}K)	6	6
β (1/ ^{o}K)	0.0002	0.0002
g (ms^{-2})	9.8	9.8
g' = g$\beta\Delta$T	0.0118	0.0118
α (m^{2}/s)	1.44 x 10^{-7}	1.44 x 10^{-7}
Pr	7.0	7.0
Re	1.10 x 10^{4}	1.70 x 10^{4}
Pe = PrRe	7.68 x 10^{4}	1.19 x 10^{5}
Gr	2.05 x 10^{8}	3.65 x 10^{9}
Ra = PrGr	1.43 x 10^{9}	2.55 x 10^{10}

Chapter 5: Research Methodology

5.1 Introduction

Methodology in research serves as a theoretical and conceptual framework for selecting specific methods and tools, as well as for adopting a particular research design or procedure for carrying out an investigation (Cousin, 2009). There are two broad methods available in scientific research and these are: quantitative methods and qualitative methods. In this research, quantitative methods are used through numerical techniques via computer simulations, while qualitative methods are applied through visualisation of flow in the scaled experiments performed. This chapter describes the procedural approach applied in this research with emphasis on the specific methods/tools used and their synthesis into an overall methodological framework. It contains the following sub-sections: a basic overview of the way gaps in literature have been exploited; the creation of a mind map that captures the link and opportunities inherent in these knowledge gaps; the structure and methodological considerations; selection of single-bed ward designs; the adopted methods; and finally the research strategy and design.

5.2 Strategy for exploiting knowledge gaps

The nature of this research is to explore the concept of natural ventilation as it applies to clinical spaces with wards being the emphasis. A central objective of the research is to investigate the feasibility of delivering airflow rates to control infectious bio-aerosols while achieving thermal comfort and low energy for heating from natural ventilation. Based on the gaps in current knowledge on the performance of buoyancy-driven ventilation systems and strategies that were identified in literature, this research works with the proposition that potential of natural ventilation has been under-utilised or misused. This presumption comes with support from the knowledge gaps found in literature (Fig. 5.1) which reveal that as far as hospital wards are concerned, natural ventilation has not been applied to achieve desirable room air distribution (pattern and direction); and that mixing is preferable to displacement. In addition, there is need for further investigation of expected healthcare performances of inlet and stack systems using CFD with respect to airborne contaminant dispersal in single bed wards. The knowledge gaps which serve as a platform for this research can be categorised

into three classes: ventilation performance; space and components designs as well as tools; and modelling approach.

Figure 5:1: Mapping knowledge gaps according to ventilation performance, space/component design and tools/modelling approach

5.3 Selection of ventilation systems for research

From the literature reviewed so far, four distinct ventilation systems have been selected for exploitation in this research. The criteria for their selection hinged on their simplicity, uniqueness, design flexibility and potential for improved performance. It is necessary to stress that healthcare professionals have been found (Short and Al-Maiyah, 2009) to aspire towards deep plans with sealed facades that would be safe, secure and prevent the acoustic problems inherent in urban settings. In addition to non-stop occupancy and use of modern heat-generating hospital equipment, these issues have been identified as features and constraints of contemporary hospitals (NHS, 2010). Hence, the selected systems will be sized and applied with these concerns in mind. These systems, three of which are originally unique to natural ventilation are highlighted below.

1. Single opening (vents/windows)
2. Same-side single and dual openings
3. Inlet and stack (ANV)
4. Personalised ventilation

The fourth system has so far been used only with mechanical ventilation-mode of ventilation. However, as part of the goal of this research is to explore how innovation can be achieved, this system is a candidate for exploitation using buoyancy-driven flows. Detailed clarification of these systems including their configuration and sizing follows in the next subsections.

5.3.1 The single opening (window)

Single openings, especially when used as windows, are a traditional and contemporary technique of natural ventilation in hospitals. Heiselberg, et al. (2001) had argued that the performance of windows was not well understood with regards to comfort and draught. By studying two window types, they concluded that bottom hung windows perform better in winter, when side hung windows are unsuitable. The situation is reverse in summer where side-hung windows are preferable for airflow and thermal comfort to be achieved. Guidance on how to size such openings using empirical techniques are found in CIBSE (2005) as shown in Eqn. (5.1), although it is doubtful that this model is utilised by hospital designers. Given a desirable airflow rate Q, as required by HTM 03-01 or the WHO, the required area of opening A, can be calculated as follows.

$$A = \frac{Q}{C_d}\sqrt{\frac{T_{int}+273}{(T_{int}-T_{ext}) \times gH}} \qquad (5.1)$$

Where:

A = area of opening (m^2);

Q = required ventilation rate (m^3/s);

C_d = discharge coefficient;

T_{int} = internal temperature (K);

T_{ext} = external temperature (K);

g = gravitational force per unit mass ($m.s^{-2}$);

H = height of opening (m).

In the application of this model for single vent, C_d typically takes a value of 0.25 (CIBSE, 2005).

5.3.2 Same side dual-openings

CIBSE (2005) also provides a single side concept which uses two openings of the same area, separated vertically. The areas of inlets and outlets for dual opening vents are also obtained from Eqn. (5.1) but in this instance, the value of C_d is typically 0.6. Additionally, *H* now becomes the height *between* the two openings. It is evident from Eqn. (5.1) that the required flow rate, *Q*, the temperature differential ΔT i.e. T_{int} - T_{ext} and the vertical distance between the two openings *H*, will all affect the size of opening, *A*. It is typical for values of C_d and *g* to be taken as 0.6 and 9.81m/s^2 respectively, while ΔT is assumed to be 1.

5.3.3 Single cell inlet and stack (advanced natural ventilation)

In this case, the stack sizes are based on the estimation techniques given by Lomas and Ji (2009) where the free opening area is assumed to be a fraction, *F*, of the gross floor area. Typical values of *F* range from 0.5 to 1.5% and the computed area should not be less than the area of the supply inlets so that flow is not restricted. Further, the authors indicated that even though the value of *F* may appear small, it is the length of shaft which then becomes a primary determining factor in the performance of the stack. The process used to derive the cross-sectional area of a stack (*As*) when a given space of width *w*, has a depth *n.w* (where n is the aspect ratio or depth/width) is given by (Lomas and Ji, 2009) as shown in Eqn. (5.2).

$$As = F.n.w^2\ (m^2) \qquad (5.2)$$

5.4 Structure and methodological considerations

5.4.1 Structure of research

An overview of the structure of research based on Hohmann (2006) is presented in Table 5.1 below. Essentially, the tasks in the research work can be sub-divided into literature review, methodology, investigations, results and finally discussions and conclusion.

Table 5.1: Structure of research (adapted from Hohmann, 2006)

Item of research	Component
Review of literature	Work done by others in the same field, subject matter or topic. It serves as a backbone to intended work
Methodology	Qualitative and/or quantitative methods including their integration into a research design.
Investigations/Studies	In-depth inquiry to generate data and new knowledge which will enable stated objectives to be met
Results	The findings made in the current investigation, including facts and figures derived from using specific methods.
Discussions and conclusions	Providing meanings and interpretation of findings against the backdrop of previous work by others.
Recommendations	Extraction of specific information from results in a format that will be useful for other researchers or industry practitioners.

5.4.2 Methodological considerations

Based on precedents set in literature, CFD, DTM and experimental work are valid approaches to the given aim and objectives of this research. Most of the data were used were from secondary sources (literature) as well as available libraries of material properties contained in DTM and CFD software. Due to the exploratory and conceptual nature of this research, there was no need to capture primary data or for any physical monitoring (with the exception of flow visualisation in the salt-bath experiment). The data collected and validated in many modelling and experimental studies reviewed in literature were deemed to suffice for the purpose of this thesis. Examples of the secondary data obtained from literature include:

- emission characteristics of pathogenic bio-aerosols;
- sizes of airborne viruses and bacteria;
- drawings of existing or proposed hospital wards;
- CFD modelling inputs from practices e.g. heat loads from human and miscellaneous indoor sources;
- CFD modelling inputs from vendor's technical support e.g. simulation relaxation factors, convergence and error margins; and
- weather files for dynamic thermal modelling (e.g. from CIBSE and ASHRAE databases).

5.4.3 The selected ward designs

Three types of single-bed ward spaces were used. Primarily, the automatically generated schematic design of a single-bed ward from the ADB software was utilised as an idealised ward layout, free of any preconceived natural ventilation openings (size or locations). In addition, the newly built great Ormond Street Hospital (GOSH) and the schematic single-bed ward proposed by Short and Associates (Short and Al-Maiyah, 2009) for ANV were considered. In the second ward type, the GOSH ward is representative of what a leading architectural firm (Llewellyn Davies Yeang Architects) have developed for an on-going hospital re-development project. The as-built case will be modelled and evaluated against proposed changes or improvements. In the third ward type, this concept represents a schematic design of a proposed ANV system which has featured in at least two research projects (Lomas and Ji, 2009; Short and Al-Maiyah, 2009). The aim of selecting this ward is to enable an ANV design (being a relatively new ventilation concept) to be evaluated in terms of room air distribution and other detailed specifics of ventilation performance. In all instances, similar occupancy (i.e. actual number of people and schedule of presence of people) are used in the ward spaces. Similar values of indoor heat sources are also applied in terms of lighting and equipment including their operational schedules for both DTM and CFD investigations. The taxonomy of the wards studied are therefore as follows:

- Activity Database ward = ADB Ward
- Great Ormond Street Hospital ward = GOSH Ward
- Short and Associate ward = S&A Ward

5.5 Adopted methods: Data, materials and methods

5.5.1 Dynamic thermal modelling data and assumptions

Two site locations were used in this research: London and Birmingham. The ward spaces are considered to be single storey except in the case of the Short and Al-Maiyah schematic design where three floors were modelled in the DTM application. All surfaces, with the exception of the facade walls were assumed to be adiabatic. The facade wall was assumed to be a composite 0.27m thick assembly of brick, insulation and concrete with internal plaster construction giving a collective U-value of 0.35 W/m^{2}K (Table 5.2). The shaft/stack construction material was assumed to be insulated and monolithic concrete of similar U-value to the facade wall. Three heating setpoints: 18^{o}C; 20^{o}C; and 24^{o}C were used in pairs for the simulations to account for heating needs especially in winter. These heating setpoints are based on the acceptable indoor temperature band as specified by various sources notably: 18-28^{o}C by HTM 03-01 (DH 2007a); 19-24^{o}C by (Carbon Trust, 2007) and 22-24^{o}C (CIBSE, 2002). The heating setpoint of 24^{o}C (from CIBSE 2002) is specifically applied to the SNV systems only.

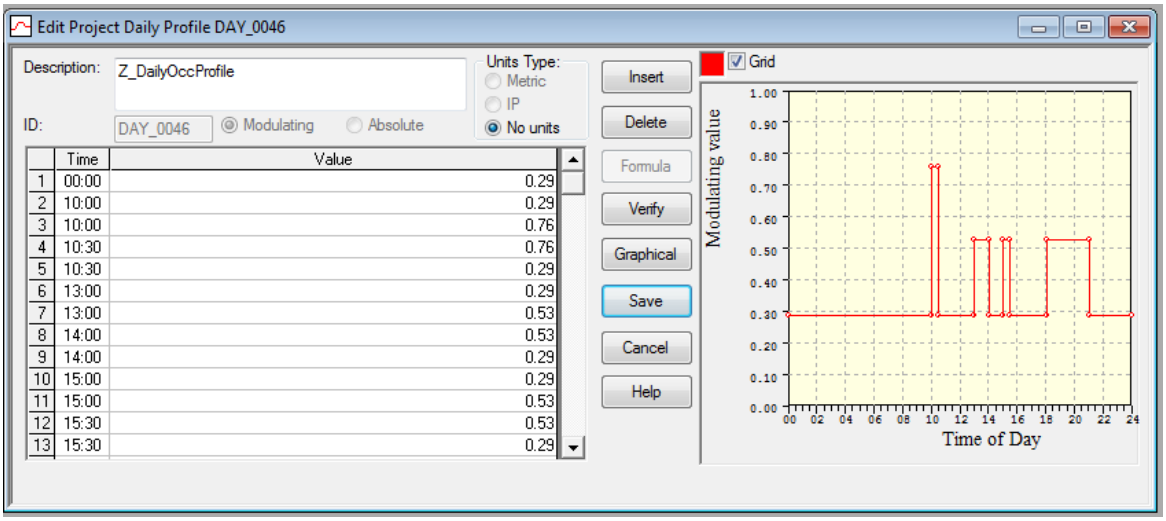

Figure 5:2: Scheduled profile of daily internal heat sources

Occupancy was scheduled as intermittent for a total of 120W at peak times from each occupant. Heat from lighting accounted for 70W, scheduled to be dimmed between 10:00pm and 06:00am. Heat from equipment was assumed to be 75W and constant. The schedule created for constant and intermittent indoor heat sources is shown by the profile in Fig. 5.2. With the exception of shafts, stacks and the NPV duct, all openings used were modelled as louvered inlets/outlets on a semi-exposed facade wall using a discharge coefficient, C_d of 0.6.

Where changes are made outside these general assumptions, they are stated for each case. An example is the size of openings which would be reduced from the maximum value by various fractions in order to estimate airflow rates for trickle ventilation. The opening fractions adopted are not always the same for all investigations. In summary, this research utilises the following boundary conditions and typical assumptions (Table 5.2) for all the wards:

Table 5.2: Components and variables of DTM and their assumed values

Components	Typical values assumed	Further notes
Site location	SNV = London Inlet/Stack = Birmingham	For London, weather file was for Heathrow, based on Test Reference Years (TRY) for South East England. Weather file for Birmingham was taken from ASHRAE data collected at Birmingham airport.
Floor area	GOSH = 23.55 m^2 ADB = 25 m^2 S&A = 25.9 m^2	Ceiling height for all spaces are assumed to be 3.6m unless stated as otherwise.
Height of wards ANV	Mid-floor, approximately 4m above ground level)	The absolute heights of three S&A Ward are replicated
Internally generated heat sources	120W per person (4 people); 75W Lighting; 70W (equipment)	The effective heat load is 20.6W/m^2 for the GOSH ward and 15 W/m^2 for the ADB ward[2].
Clo and Met values	Clo = 0.5 (summer) and 1.0 (winter); Met = 1.0 (sedentary)	
Schedule of occupancy and lighting/equipment	Occupant constantly present; healthcare workers presence depending specific schedule	See figure 5.2 for intermittent occupancy schedule
Schedule of lighting and equipment	Lighting dimmed from 10:00PM to 06:00AM	Equipment assumed to be in constant use.
Composite (0.27m thick) external wall	U-value 0.35 W/m^2K	Brickwork (outer leaf) Dense EPS slab insulation Concrete block (medium) Gypsum plastering (internal surface)
Windows	U-value = 3.1 W/m^2K. (all wards)	Assumed to be double glazed
Heating setpoints	18^{o}C and 20^{o}C	Additional setpoint of 24^{o}C to be used for SNV.
Discharge coefficient	0.6	
Wind pressure coefficient	SNV = 0.5	

The mechanical (extract) ventilation of bathrooms is ignored since the research aims at exploring the potentials of using natural airflow to satisfy thermal comfort requirements and to dilute or displace contaminants. In the GOSH ward however, a floor-level horizontal slit/grill in the doorway to the bathroom is created to allow cooler fresh air to enter and leave via a higher (ceiling level) slit.

[2] *The GOSH ward has an en-suite (mechanically ventilated) bathroom which is 5.33 m^2 in floor area, while the ADB ward does not. Mechanical extraction of air from the bathroom of the GOSH ward was therefore not considered, due to the focus of this research.*

It is often necessary to express the absolute area of opening as a percentage of the floor area and examples can be found in studies of ANV systems (Lomas and Ji, 2009; Short and Al-Maiyah, 2009). In this study therefore, the Inlet and Stack systems have adopted 1% of the floor area of the ADB Ward as the maximum area of opening as suggested by the sizing equation in Lomas and Ji (2009). The equivalent floor area for the S&A Ward also follows this 1% assumption which for the floor area of 25.92m^2 gives a maximum absolute opening area of 0.26m^2.

For consistency, the areas of opening in the SNV systems with single and dual openings to be investigated are also expressed (Table 5.3) relative to their optimum (full) size and as a fraction of floor areas for both ADB and GOSH wards, both of which are 25m^2:

Table 5.3: Openings for SNV systems expressed as absolute fractions and as fractions of floor area

Opening Fraction	**Equivalent proportion of floor area (%) for SINGLE openings**		**Equivalent proportion of floor area (%) for DUAL openings**	
	ADB Absolute/Floor	**GOSH Absolute/Floor**	**ADB Absolute/Floor**	**GOSH Absolute/Floor**
100%	0.69 (3.0%)	0.83 (3.3%)	1.38 (6.0%)	1.66 (6.6%)
75%	0.52 (2.1%)	0.62 (2.5%)	1.04 (4.2%)	1.24 (5.0%)
50%	0.35 (1.4%)	0.42 (1.2%)	0.7 (2.8%)	0.84 (2.4%)
25%	0.17 (0.69%)	0.21 (0.8%)	0.34 (1.4%)	0.42 (1.6%)
12.5%	0.09 (0.36%)	0.10 (0.4%)	0.18 (0.72%)	0.20 (0.8%)
6.25%	0.04 (0.16%)	0.05 (0.2%)	0.08 (0.32%)	0.10 (0.4%)

For simplicity, reference to area of openings will generally utilise the opening fraction, (first column in Table 5.3) where 100% indicates a fully open orifice, however, occasional reference to the percentage floor area of specific openings will be employed.

5.5.2 Boundary conditions for CFD simulations

In the steady-state CFD simulations using PHOENICS (Cham, 2011), adiabatic boundary conditions were also used for the walls. Occupants were modelled using digital manikins which emitted 90W of heat each, with the exception of the lying patient, modelled as a solid block and assumed to emit 50W only due to the assumed blanket cover. The positions of other occupants (healthcare workers and visitors) varied with each separate study. Based on

reasonable engineering judgement, equipment was assumed to emit 75W while lighting was modelled as a surface-open mounted luminaire emitting 70W of heat. This was rationed into 20-to-80 (source-to-floor) ratio, meaning the actual lighting fixtures were allocated 14W while the floor was allocated 56W of radiated heat. The turbulence model used was the renormalised group k-ε (KERNG) turbulence model (Yakhot and Orszag, 1986) in conjunction with the Boussinesq approximation for buoyancy. Ambient air temperature varied but was typically 20^{o}C for summer and 5^{o}C for winter. Whereas pre-warming of incoming fresh air is usual practice (and active heating was considered in DTM aspect of the research), the CFD investigations were aimed at exploring the potentials for optimising indoor heat for same purpose. This would be achieved through strategic location of openings and overall system design. This approach is intended to eliminate or minimise the need for active heating and to further demonstrate the potentials and weakness of selected natural ventilation systems in terms of meeting thermal comfort needs of occupants.

The source of airborne contamination was assumed to be a cough which was given off by the visitor(s) at a mass flow rate of 0.003kg/s. The density was assumed to be similar to that of air (1.189 kg/m^{3}) which is typical for studies of passive scalar contaminants while the temperature of the cough was assumed to be 30^{o}C, consistent with findings such as Bjorn (2002); reflecting the characteristics of airborne particles that are less than 1µm in size e.g. droplet nuclei that tend to be suspended in air (Morawska, 2006 and Jiang et al. 2009). The use of the passive scalar approach to model airborne contaminants through CFD-based studies has been validated but shown to have limitations (Hathaway et al. 2011; Mao and Celik 2010). Within the 1 µm maximum size of passive scalar contaminants, Dreiling (2008) showed that the sizes airborne viruses (e.g. measles, smallpox and influenza) are between 0.003 and 0.06 µm, while airborne bacteria (e.g. tuberculosis and anthrax) are between 0.4 and 5 µm.

Although the cough event was used in all instances, this was with the knowledge (Loudon and Roberts, 1967 and 1968) that talking for five minutes could emit (from the mouth) as much bio-aerosols as a single cough. As such, the implications of using the cough model are beneficial for evaluating the instantaneous effect of forcefully emitted contaminants or the time-varying equivalent of the slower emission via talking. The density of the meshes varied with each study, typically dependent on whether a stack was used and the size of openings

adopted, as were the number of iterations required to achieve convergence. The subtle differences in the CFD investigations for the separate studies are overviewed in each respective Chapter.

For each ward space, mesh-dependence pilot studies used coarse, medium and fine mesh in order to optimise computational resources without compromising accuracy or reliability of results. The adopted numbers of cells (mesh density) used for simulation of the three wards are reported on a case by case basis, and in some instances, the use of smaller openings (e.g. in winter) required the addition of more meshes to achieve converged and acceptable results. The criterion for a converged simulation exercise was based on 0.1% error margin which is the recommended cut-off value by the software developers (CHAM, 2011).

5.5.3 Salt-bath experiments

The edge-in centre-out strategy of the ANV system using the ADB ward was constructed using Plexiglas to a scale of 1:20. The bed and the overhead duct were also made of the same material as shown in Fig. 5.3a. The area of stack and the duct as well as the entire ward were all internal dimensions, neglecting the thickness of the Plexiglas. Neglecting the effects of radiation, two heat sources were considered independently, using only 50W for convective heat per source. Each heat source (being a solution of brine) was released from a fabricated nozzle based on the design similar to that used in similar experiments such as those of Hunt and Linden (2001). The nozzles were fitted with a mesh 200μm in size permitting virtual origin calculations and creating a turbulent plume. The scaled model was inverted and immersed (Fig. 5.3b) in a large Perspex water tank (Fig. 5.3c) measuring 2 x 2 x 2m, with a clear distance of approximately 300mm between the base of the model and surface of water.

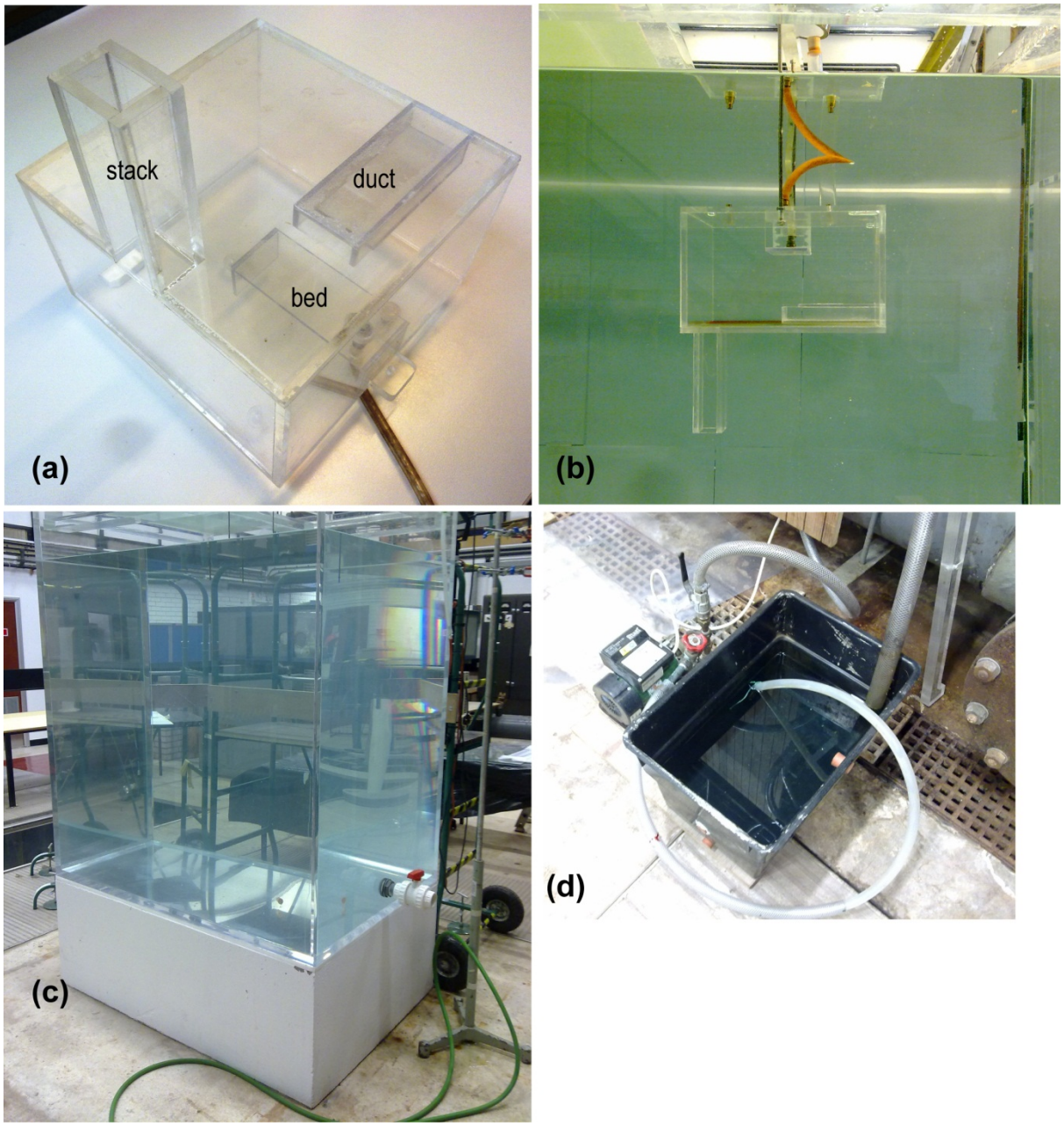

Figure 5:3: Experimental set up showing (a) scaled model (b) inverted and immersed model (c) water tank (d) brine container

Brine was to be mixed in a plastic container on the floor (Fig. 5.3d) from where it would trickle into the nozzles via plastic tube at flow rates controlled by a flow meter and an Anton Parr portable density meter (DMA 35). All sources were assumed to be point sources, including the patient who in reality is laid horizontally on a bed and likely covered by a sheet or blanket. Flow was visualised using hand-held digital cameras fixed into a typical laboratory tripod stand to record the transient flows as static images or video clips for analysis.

5.6 Research strategy and design

The research was classified into five separate studies, each with a distinct focus for a particular natural ventilation system. Study 1 was aimed at single opening and dual opening systems. Study 2, Study 3 and Study 4 were focused on single-cell inlet and stack strategy and the natural personalised ventilation system respectively. Study 4 was a comparative analysis of these systems using a case study of the GOSH single-bed ward while Study 5 was an experimental validation of the novel NPV system. Although Study 1 is a combination of two systems (single opening and dual opening) this was done intentionally to allow a comparison of their differences and to aid understanding of the value of converting current wards with single openings into dual opening systems.

5.6.1 Modelling matrix and ventilation performance metrics

As part of the research strategy, a matrix (Fig. 5.4) was developed to capture the main ventilation issues and system of concern for each Study. This matrix represents the possible permutation that would be done between the ventilation issues and the selected ventilation systems.

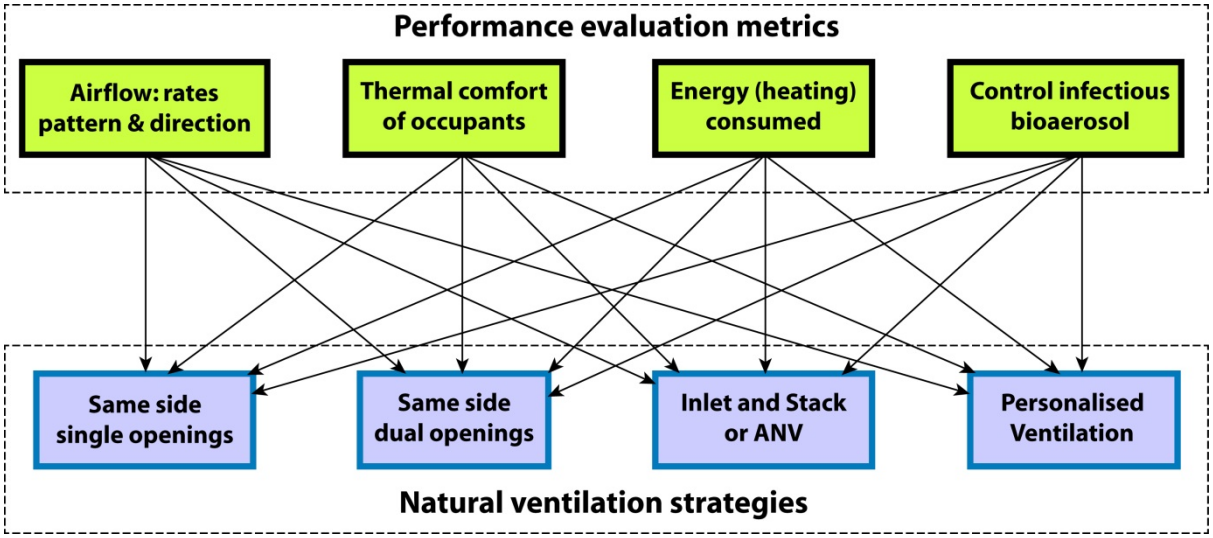

Figure 5:4: Simulation matrix showing relationship between performance metrics and ventilation strategies

The natural ventilation systems investigated in this research will be evaluated based on four performance criteria which are: airflow rates, thermal comfort, heating energy and control of infectious bio-aerosols. In this regard, four ventilation metrics have been identified which are:

local air change index (LACI); mean air change efficiency (MACE); effectiveness of heat removal (EHR) all from Awbi (2003) and Karimipanah (2007, 2008); as well as air turnover time (ATT); and contaminant removal efficiency (CRE) from Zang (2005). These metrics have been explained in Chapter 2. Energy consumption of natural ventilation (i.e. heating needs) however will be assessed using existing benchmarks (CIBSE, 2008) or with findings from similar studies.

5.6.2 The points of interest

In order to apply the identified metrics in the ward designs, and since all the metrics rely on measuring values at specific points, it was necessary to use the concept of points of interest (POIs). These points were usually imaginary points with three dimensional coordinates, selected based on engineering judgement to be representative of potential locations for occupants in a single-bed ward. The POIs were not always the same since different ward designs were used in the various studies carried out. However, as an example, (Fig. 5.5) Points A, B and C are at heights of 1.6m which could be assumed to be the breathing zone of a standing adult. Points D and E are at 1.0m height and could represent a visitor sitting on a chair and a patient lying on the bed, respectively. These points are described graphically in plan with xyz coordinates for the ADB ward in Fig. 5.5a and in 3-dimension in Fig. 5.5b. Similarly, the POIs for the GOSH ward are depicted in Fig. 5.6a and 5.6b. These POIs are used for the ADB ward design. The POIs when used for the GOSH ward are defined in the appropriate chapter, while in the S&A ward, no POIs were used.

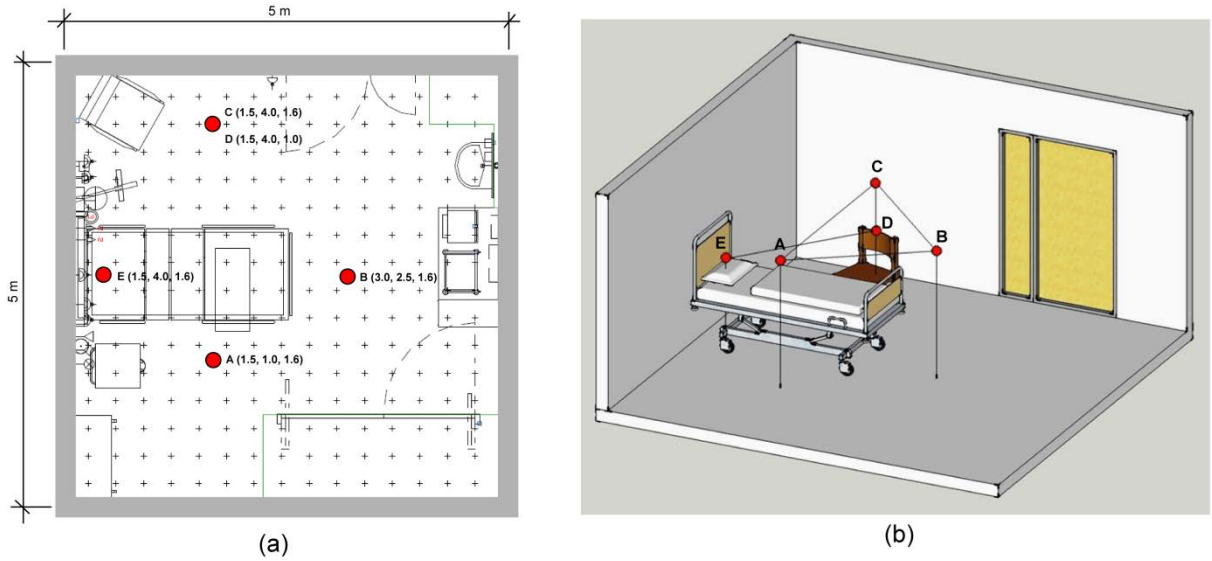

Figure 5:5: Layout of ADB ward showing POIs in (a) Plan and (b) 3-Dimension

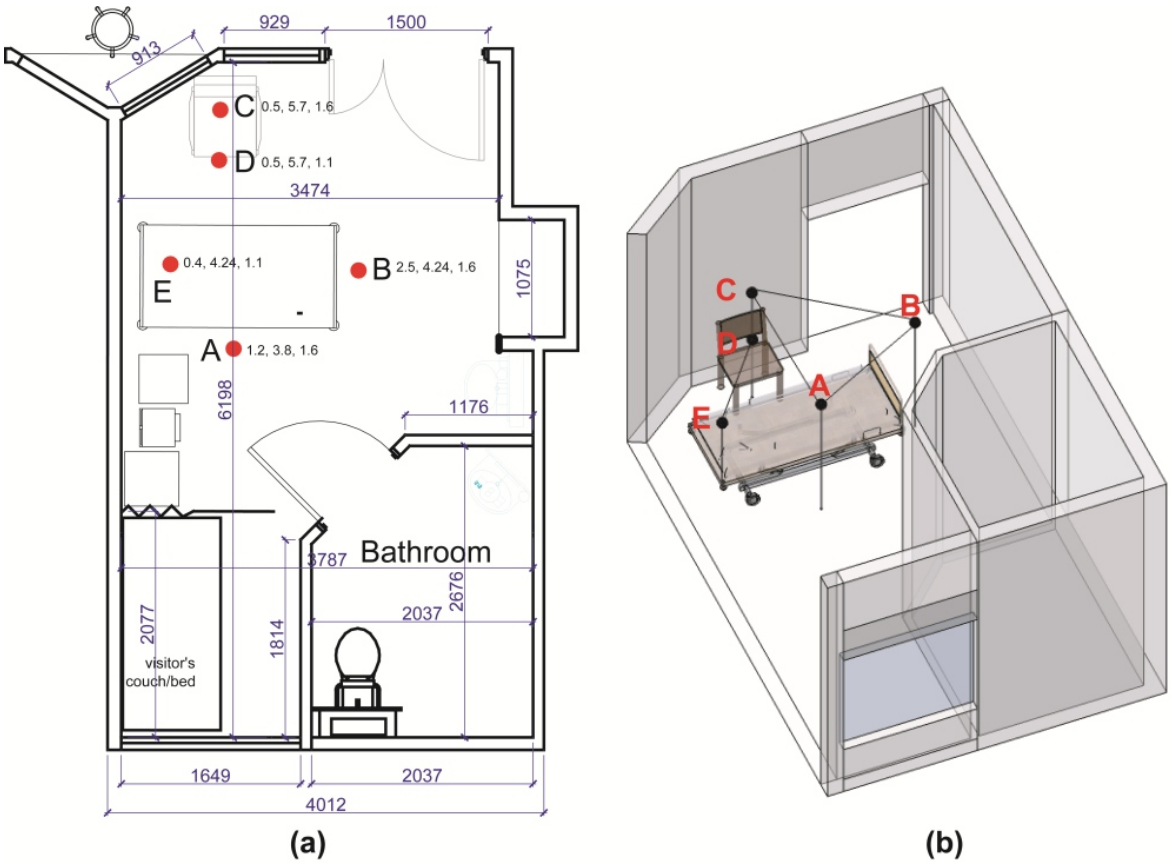

Figure 5:6: Layout of GOSH ward showing POIs in (a) Plan and (b) 3-Dimension

The aim of having POIs is to enable quantitative measurements to be made about the performance of a given ventilation system at specific (absolute) locations of the ward. The POIs are hence an important yardstick through which the various metrics identified previously will be applied, thus giving an objective and comparable overview of the ventilation systems being studied.

5.7 Research design

The various aspects of the research were integrated into a design (Fig. 5.7). This design explains the methods, tools and the phases of modelling in the appropriate sequence. The research process is hinged on the different capabilities of both DTM and CFD tools which are time and space focused, respectively. In the initial stage of each investigation, DTM provides time-varied airflow rates (and in some instances CO_2 concentrations) within a space, based on different systems of natural ventilation. Subsequently, specific points in time are selected for space-varied distributions of air particles (Age of air) or airborne contaminants as well as stratifications of temperature.

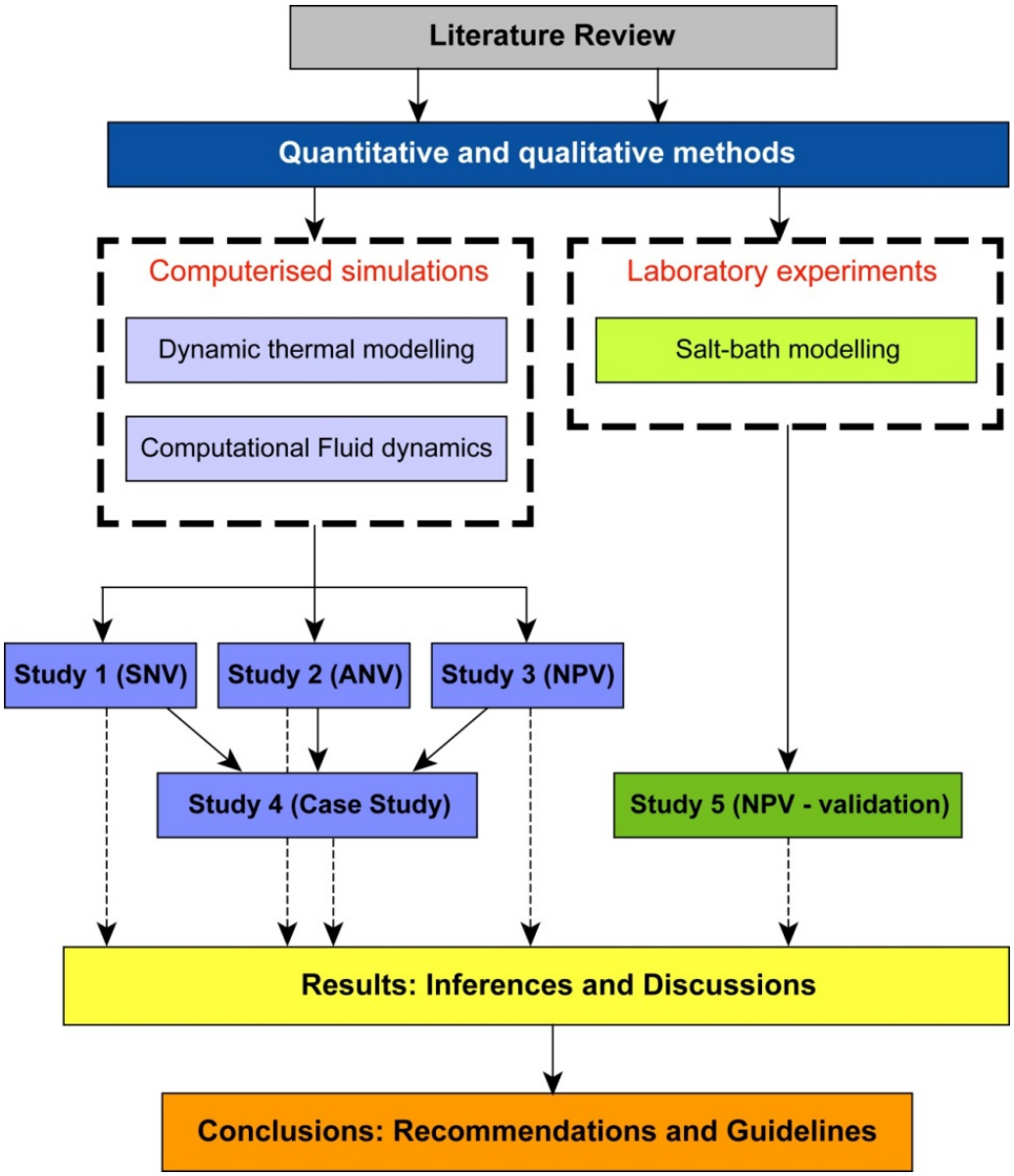

Figure 5:7: The research design: from literature review to conclusions

CHAPTER 6: Study 1 – Same-side systems

6.1 Introduction

Single side natural ventilation systems are often referred to as simple natural ventilation (SNV) systems (Lomas, 2007; Short and Lomas, 2007; Short and Al-Maiyah, 2009). They are essentially ventilation openings located on only one side of a room. Although the single and dual openings are technically two different systems, they share similarity in the single external facade wall upon which the orifices are located. This similarity has bearings on existing facilities which utilise single openings (or windows) and may need to be retrofitted into dual opening systems. This chapter is a simultaneous study of both systems with the aim of providing a relative overview of their performances. This approach will be beneficial for future refurbishment of existing wards.

Dynamic thermal modelling (DTM) and computational fluid dynamics (CFD) were used simultaneously to study the ventilation performances of two single-bed wards: the GOSH ward and the ADB ward. The DTM aspect provide volume (bulk) airflow through the openings over the entire year while CFD was used to study detailed characteristics of airflow in the space at a specific time and occupancy conditions.

6.2 Openings in modern natural ventilation

It is important to consider that in modern studies of natural ventilation, openings are regarded as generic orifices in the building envelope which could be windows or specially designed inlets and outlets. This clarification is important because too often, natural ventilation is viewed as window-based and this definition can be restrictive. Awbi (2003) classifies natural ventilation openings into two major groups: i.e. small openings and large openings. These groups are further sub-divided as follows:

1. Small openings
    a. Trickle ventilators
    b. Flow control ventilators
2. Large openings
    a. Windows
    b. Louvers

In this study, ventilation openings are defined under the louver sub-category of large openings and are explicitly not to be construed as windows, for many reasons. Firstly, the provisions of HTM 55 (windows in healthcare) allow for a maximum window opening area of 100mm for safety reasons, especially in spaces that could be occupied by the elderly, or those who are mentally ill or have learning difficulties (DH 1998). However, if openings are assumed to be specially designed and constructed orifices in which both airflow and safety concerns are taken care of using louvered openings, then this would allow for optimisation of natural ventilation. Secondly, because the multi-purpose nature of traditional windows requires them to provide three primary functions: visualisation, daylighting and airflow, the use of louvers means the airflow aspect can be decoupled, allowing windows to serve only visual and daylight functions. This not only means that windows can be fixed glazed areas, but crucially, louvers (as airflow openings) can be freely located within the facade of buildings without compromising other aspects of indoor environmental quality. Louver blades tend to be made of glass or aluminium and would usually incorporate some capacity to attenuate external noise (Awbi, 2003).

Two types of single-bed ward layouts will be utilised for this study. The first is for the newly designed and constructed single-bed ward of the GOSH in London. It is rectangular in shape with an en-suite bathroom, which was designed to have an auxiliary fan for local exhaust ventilation (LEV) whenever the bathroom is in use. The GOSH design gives an opportunity to evaluate the actual performance of single side openings as obtainable from an existing facility. The second ward type is the ADB single-bed layout which is a standard (and an automatically) generated layout based on health building notes (HBN) space requirements through the AutoCAD interface. This ward design is square in shape and the location of furniture and fittings are rather indicative and not absolute. An overview of the design of both ward types is provided in the following sub-sections.

6.2.1 Overview of the GOSH single-bed ward

The single-bed GOSH ward (Fig. 6.1) is approximately 6.23 x 3.78m for a total floor area of 23.55m^2 (including the en-suite bathroom) with a floor-to-ceiling height of 2.7m and floor-to-soffit height of 3.5m. For the purpose of this study, the floor to soffit height will be used since the extra volume defined and covered by the false ceiling can be advantageous for airflow purposes. For computational purposes therefore, the volume of the GOSH ward is

taken as 82.42m^3. The existing (top-hung) window opening of the GOSH ward is 0.5m in height and 1.65m in width, elevated to a height of 1.9m. This width cannot be increased due to the presence of the bathroom and hence the maximum area of opening is 0.83m^2. For simplicity, it is assumed that the window would be represented by a louver of similar area.

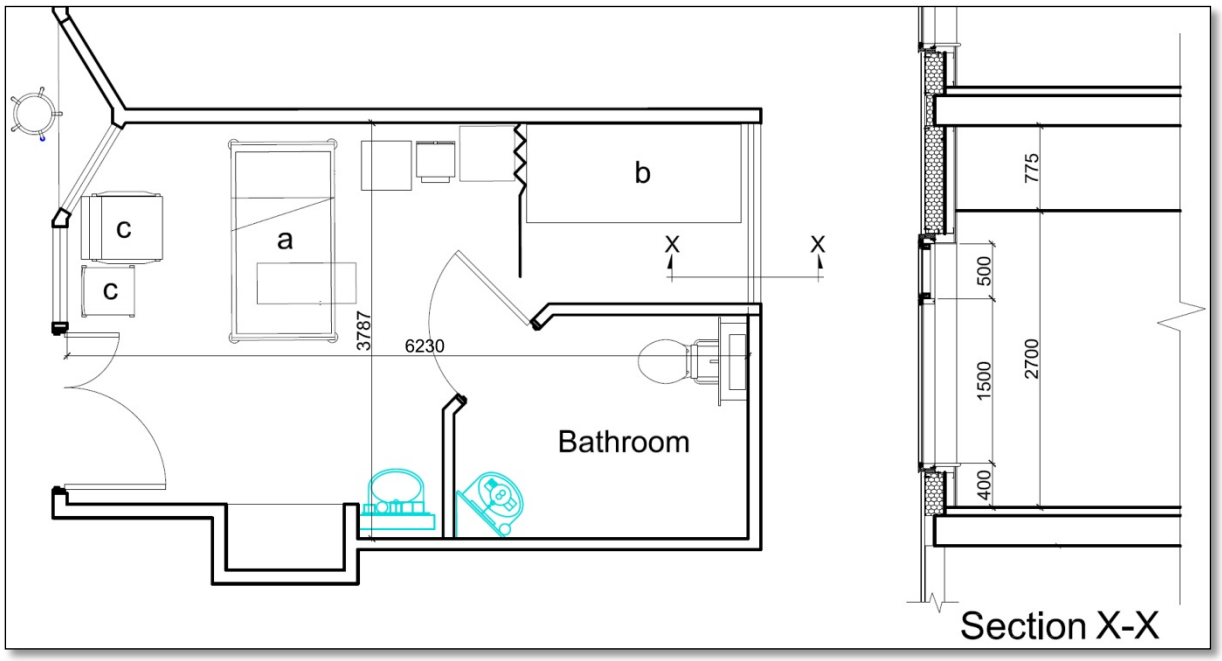

Figure 6:1: Plan and section of GOSH single-bed ward showing (a) patient bed (b) sleeping couch and (c) visitor's chair

Extracting the area of bathroom (5.33 m^2) gives an effective ward floor area of 18.22m^2. The bathroom is currently designed to be ventilated via a mechanical extract fan, but this will be ignored in the modelling. Consequently, natural airflow and required heating will ignore the bathroom interior.

6.2.2 Overview of the ADB single-bed ward

The ADB single-bed ward is a 5 x 5 x 2.7m space designed for single occupancy, giving a total area of 25m^2 and a volume of 67.5m^3. The schematic layout and section (Fig. 6.2) generated by the ADB plug-in for AutoCAD does not include any provisions or suggestions for natural ventilation openings. However, a careful study of the plan suggests that the wall opposite the door is the likely or most viable location for placing openings at least from an architectural point of view. Since this ward type is schematic, the area of openings required needs to be computed using empirical models for example as provided by CIBSE (2005). This exercise is executed in the next subsection.

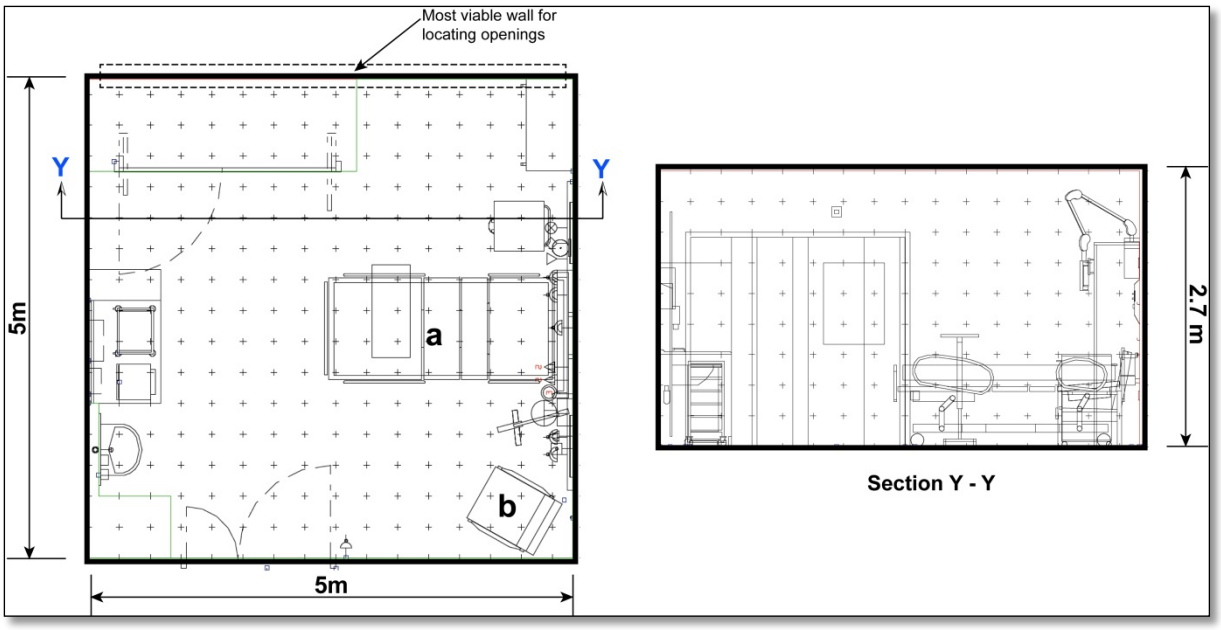

Figure 6:2: Plan and section of ADB single-bed ward showing (a) patient bed (b) visitor's chair

The floor-to-ceiling height is also given as 2.7m, however, it is not clear whether this height is from floor to a false (suspended) ceiling or from floor to an absolute floor or slab. Although, the former is likely to be the case, this study (and subsequent ones) will assume a height of 2.7m.

A simultaneous study of the GOSH ward and ADB has many benefits. Firstly, it allows a performance comparison of an existing design with that of the generic/schematic ADB design. This should provide interesting findings given that they are both of similar floor area, but different in shape and volume. Secondly, the GOSH ward has a single (window) opening which is constrained in width (1.65m) by the presence of a bathroom, whereas for the ADB, an opportunity to design and locate inlets/outlets from scratch is apparent. Thus, when evaluating the performance of dual openings, the GOSH ward would be fitted with a low-level inlet, with the presumption that this could occur as a retrofit measure, while for the ADB ward, dual openings would be designed and located freely along the external wall. Finally, the elongated nature of the GOSH ward as well as its en-suite bathroom makes its internal layout significantly different and interesting for studying age of air (i.e. time taken for fresh air to reach patient bed) as well as the general room air distribution (pattern and direction of airflow). These three core reasons are expected to also play a significant role as far as contaminant dispersal is concerned.

6.2.3 Issues with applying the CIBSE sizing model to wards

The model provided in CIBSE (2005) is provided for sizing single side openings, and depending on the number of openings (single or dual), the coefficient of discharge (*Cd*) is to be adjusted accordingly. This model is given in Eqn. (6.1) where the determinants of the area of opening, *A*, are: the required air flow rate, *Q*; the indoor temperature, T_{int}; outdoor temperature, T_{ext}; height of opening(s), *H*; and force of gravity, *g*.

$$A = \frac{Q}{C_d}\sqrt{\frac{Tint+273}{(T_{int}-T_{ext}) \times gH}} \qquad (6.1)$$

For single openings, a *Cd* value of 0.25 is typical while for dual-openings, a value of 0.6 is assumed (CIBSE, 2005, p. 45). The temperature differential ($T_{int} - T_{ext}$) is assumed to be $1^{o}K$ to account for worse case summer scenario when buoyancy forces are expected to be weak. This would lead to a maximum opening size for summer ventilation which could be reduced in other seasons when outdoor temperature drops, leading to higher temperature differentials. The required flow rate (*Q*) could be taken as 6 ACH based on the guidance of HTM 03-01 (DH, 2007a) which translates to 125 l/s. The height of the single openings, *H*, is the required vertical distance between the base of the opening and the top of the opening, but in the case of dual-openings, *H* becomes the vertical distance between the inlet and outlet determines the required area.

Although natural ventilation openings can be separated from glazed windows, it is still important to consider the size and location of such glazing when sizing and locating airflow openings because provision of daylight will always be important in such clinical spaces. This realisation makes it necessary to restrict the height of airflow openings as much as possible for even if security is assured, there is need to avoid conflict between such ventilation openings and the glazed windows which are traditionally up to 1.2m in height. Therefore, a logical position of a single airflow opening would be below the window sill (i.e. from floor level up to 0.9m height) or anywhere above the window lintel (i.e. from a height 2.0m up to the ceiling). In the case of dual-openings, the air inlet would logically be below the window sill, while the air outlet could be above the lintel, since it is crucial to maximise their height difference for greater airflow to occur.

These variables and positional considerations when applied to the ADB ward for different possible heights (H) are shown in Table 6.1.

Table 6.1: Derived parameters for sizing openings in the ADB single-bed ward

	Height of opening* (H)	Area of opening (From Eqn. 6.1)	Possible dimensions (L x B)
Single opening	0.3	5.0	0.3 x 16
	0.4	4.4	0.4 x 11
	0.5	4.0	0.5 x 8
	0.6	3.6	0.6 x 1.5
Dual Opening	2.7	0.7	0.3 x 2.3
	2.1	0.8	0.3 x 2.6
	1.5	0.9	0.3 x 3.0
	0.9	1.2	0.3 x 4.0

** For single openings, H is absolute vertical height; for dual openings, H is the distance between the two openings (CIBSE, 2005)*

*** For single openings, this ratio is necessary in order to accommodate a realistic size within the 5.0m width of ADB ward (See Fig. 7.2)*

For the CFD investigations, two single opening cases (Case S-GOSH and Case S-ADB) were adopted in addition to two dual opening cases (Case D-GOSH and Case D-ADB). While the maximum area of openings for summer (0.3 x 2.3m) and winter (0.075 x 2.3) are similar, the uniqueness of these individual cases are determined by factors such as elevation above floor level, location along facade and outdoor temperature. The adopted sizes of openings are shown in Table 6.2.

Table 6.2: Adopted CFD sizes and locations for single opening cases and dual opening Cases

	Case S-GOSH	Case S-ADB	Case D-GOSH	Case D-ADB
Size (m)	0.5 x 1.65	0.3 x 2.3	0.5 x 1.65	0.3 x 2.3
Elevation (m)	1.9	2.1	Inlet = 0; outlet = 2.7	Inlet = 0; outlet = 2.7
Facade location	Corner	Corner	Corner	Corner

6.3 Dynamic modelling assumptions

A heating setpoint of 20^{o}C was assumed for all cases. The occupancy pattern for DTM was based on the observed behaviour of healthcare workers and visitors in a typical hospital (Lomas and Ji, 2009). The external walls of each space were assumed to be adiabatic and a number of possible opening fractions were adopted to evaluate the effect of constricted openings on airflow, thermal comfort and contaminant dilution. In cooler periods or during

winter for example, it would be necessary to reduce the size of openings to allow only minimal flow of fresh air that would satisfy basic indoor air quality needs, without excessive heating. In this regard, six opening fractions were selected: 100%, 75%, 50%, 25%, 12.5% and 6.25%. The geographic location of the wards was taken as London, to represent a dense urban setting where buoyancy may be an advantageous driving force over wind.

The opening fractions selected serve three major purposes. Firstly, these opening fractions will enable an evaluation of airflow rates e.g. 60 l/s/patient as suggested by the WHO (Atkinson, et al. 2009) or 6 ACH as required by HTM 03-01 (DH, 2007). Although the 6ACH is arguably designed to be met by mechanical means and while natural ventilation has been shown to be capable of surpassing this rate (Qian et al, 2010); these issues have to be explored within single-bed wards which utilise SNV, especially in temperate climates, under the forces of buoyancy only. Secondly, there is the matter of room air distribution (airflow pattern and direction) and how this affects the dispersal of airborne contaminants, which has to be investigated for both ADB and GOSH wards ventilated by buoyancy-driven airflow regimes under different opening fractions. Thirdly, the smallest of these opening fractions (6.25%, 12.5% and 25%) will shed light on what the acceptable rate of trickle ventilation should be for SNV, an important parameter not defined by existing healthcare ventilation guidelines. Respectively, these opening fractions represent one-quarter, one-eighth and one-sixteenth of the original sizes of the ventilation openings.

6.4 Predictions from dynamic thermal modelling

Three variables related to ventilation are used as metrics for evaluating the predicted performances of the GOSH and ADB ward designs. These are: bulk airflow rates, thermal comfort and heating energy, especially in the winter period. The findings derived from the investigations are detailed below.

6.4.1 Bulk airflow rates

The predictions of volume airflow rates at winter openings (25%; 12.5% and 6.25%) as well as summer openings (100%, 75% and 50%) are reported in this section.

6.4.1.1 Winter ventilation

The mean wind speed in January is 4.08 m/s with maximum and minimum speeds of 9.27 m/s and 1.03 m/s respectively. The DTM predictions indicate that for this month, only the GOSH ward fitted with dual openings can meet the fresh air requirement of WHO (i.e. 60 l/s/patient) at either 25% or 12.5% opening fractions. These represent 1.6% and 0.8% of the floor area respectively. At 25%, the monthly mean flow would be 152.5 l/s (≈ 8 ACH), which exceeds the WHO 60 l/s/patient as well as the HTM 03-01 requirement for 6ACH (Fig. 6.3a). While at 12.5%, the monthly mean flow is 76.5 l/s (3.97 ACH). At the smallest fraction of opening (i.e. 6.25% total openable area or 0.4% of floor area) however, dual openings in the GOSH ward receives a mean monthly flow rate of 37.5 l/s (2 ACH). These airflow rates are for a heating setpoint of 20^{o}C.

By increasing the heating setpoint to 24^{o}C (Fig. 6.3b), the enhanced temperature differential leads to increments in mean flow rates at 25% opening fraction to 169 l/s (+9.8%) while at 12.5% the flow rate is 84.6 l/s (+9.5%). At the 6.25% fraction, the mean flow rate increases to 40.8 l/s (+8.1%). With single opening in the GOSH ward however (Fig.6.3a), the monthly mean flow rates for a setpoint of 20^{o}C at 25%, 12.5% and 6.25% are 31.5 l/s (1.64 ACH), 16.4 l/s (0.85 ACH) and 8.3 l/s (0.45 ACH) respectively. Compared to dual openings, increasing the heating setpoint to 24^{o}C (Fig.6.3b), brings minimal increments in airflow rates of: +2.17%; + 0.61% and +0.0% for the GOSH ward at the three decreasing opening fractions.

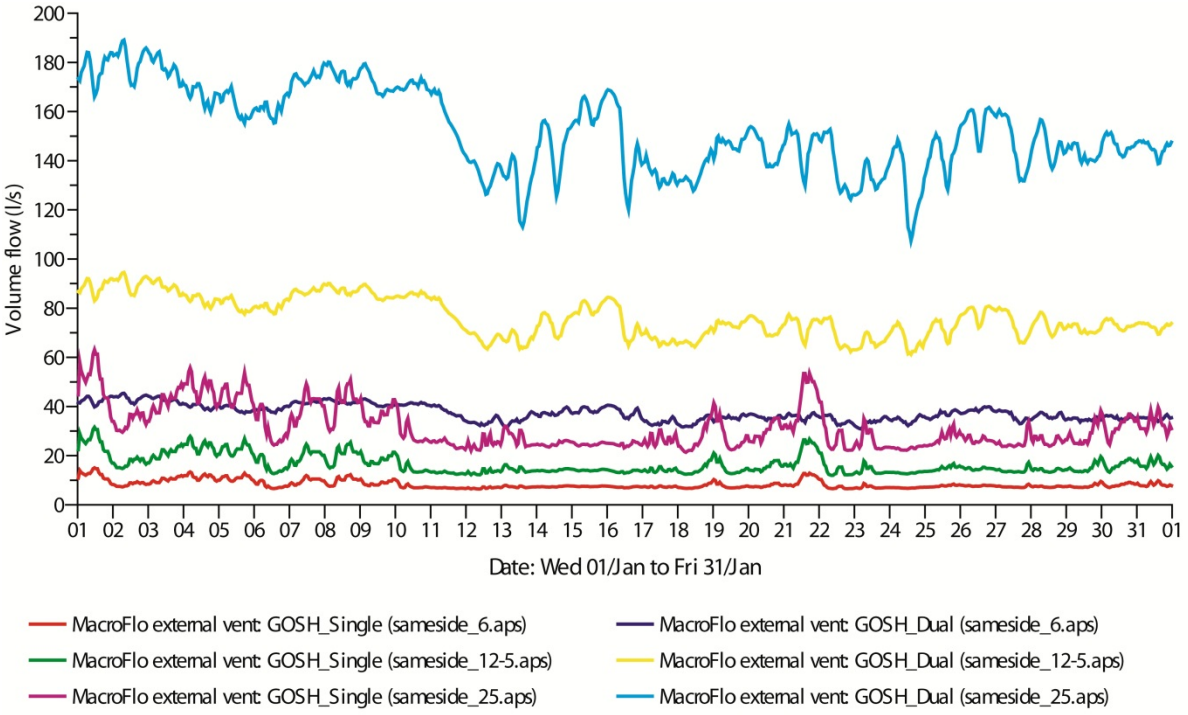

(a)

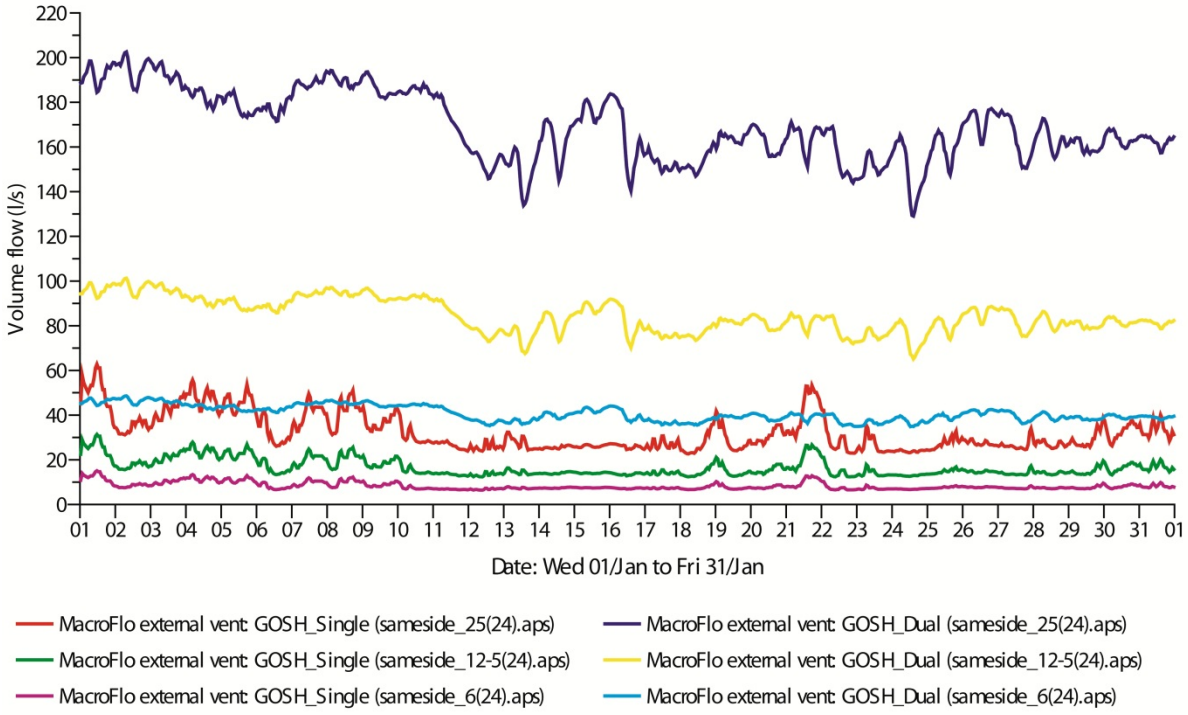

(b)

Figure 6:3: Variation in airflow for the GOSH Ward with single and dual openings at three winter opening fractions for heating setpoints of (a) 20°C and (b) 24°C

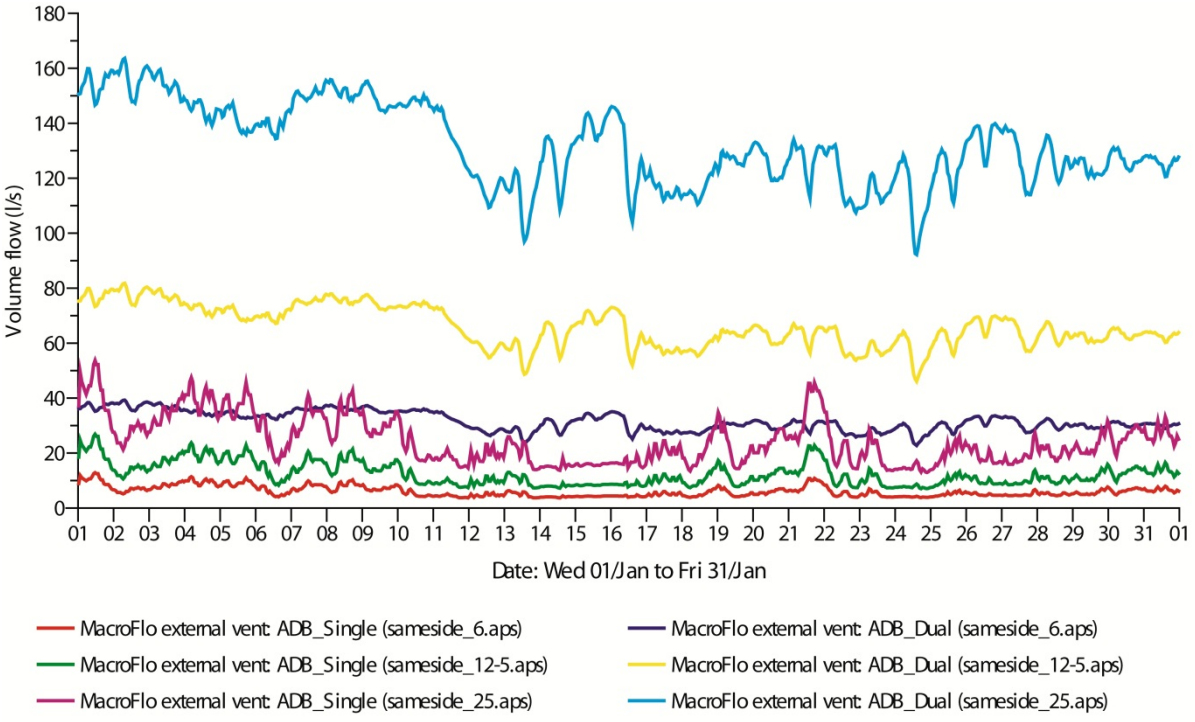

(a)

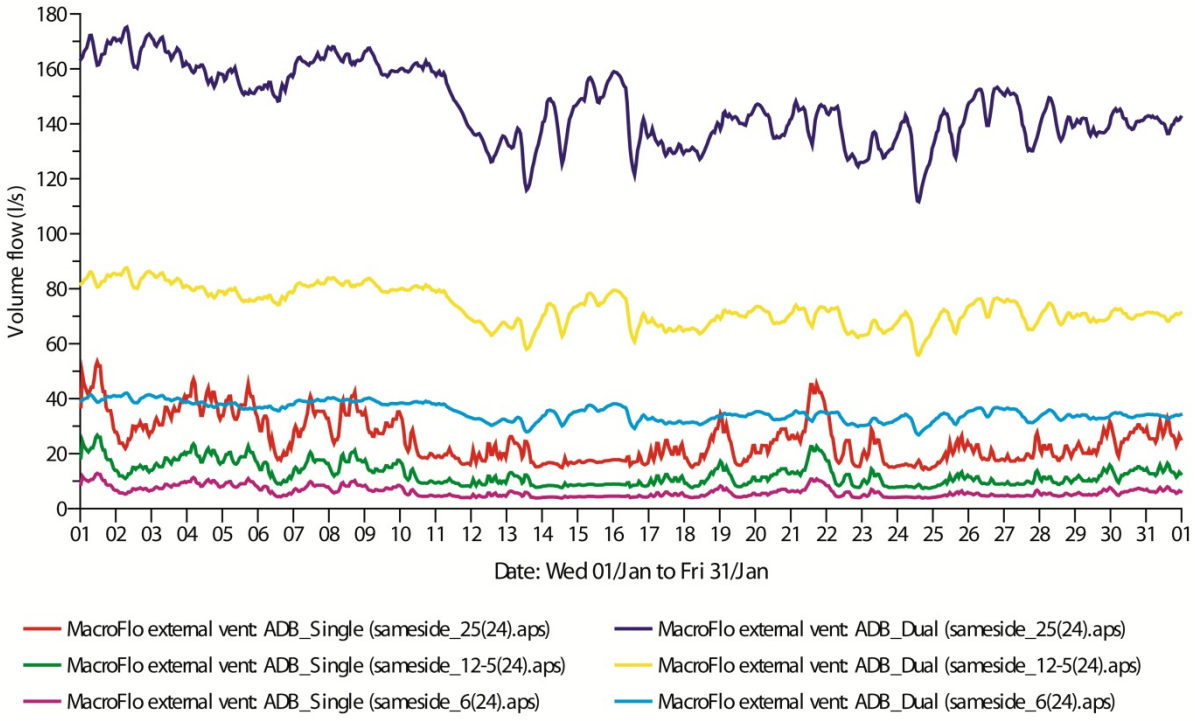

(b)

Figure 6:4: Variation in airflow for the ADB ward with single and dual openings at three winter opening fractions for heating setpoints of (a) 20°C and (b) 24°C

For the ADB ward the 25%, 12.5% and 6.25% opening fractions represent 1.4%, 0.72% and 0.32% of the floor area. Using a heating setpoint of 20^{o}C (Fig. 6.4a), the mean January airflow rates into the dual openings at 25%, 12.5% and 6.25% are respectively, in the order of: 132 l/s; 66 l/s and 33 l/s. Increasing the heating setpoint to 24^{o}C (Fig. 6.4b) leads to increments of volume flow by +9.83%; +9.96% and +9.84% for the same openable areas, respectively. Using single openings in the ADB ward (Fig. 6.4a), the mean January airflow rates are predicted to be 24.4 l/s (1.17 ACH); 12.3 l/s (0.59 ACH); and 6.3 l/s (0.29 ACH). In the ADB ward, the increase in airflow rate when heating setpoint changes to 24^{o}C (Fig. 6.4b) was estimated to be +2.01%, +1.60% and 0.0%. In other words, at the smallest opening fraction, there is no change in ventilation rates even with a higher temperature differential. This was also observed for the GOSH ward too.

In the other winter months of December and February (*Appendix C*), the pattern of wind speeds is not too dissimilar with mean speeds of 4.57 m/s and 5.47 m/s respectively (*Appendix Cd*). This is except for two distinct periods in February: between 10th and 14th when the velocity of wind is rather steady at 9.8 m/s and between 19th and 28th when it steadies at about 5 m/s (*Appendix Cc*). In these specific periods of February, the volume flows into both GOSH and ADB wards (at 25% opening) reveal noticeable fluctuations only in dual openings, apparently due to the sensitivity of dual openings to changes/differentials in temperature. Volume flows into single openings on the other hand, are more responsive to wind speeds; hence the steadiness in the volume flow rates, mimicking the external wind speeds. The unique relationship between wind velocity, buoyancy forces and airflow rates in single and dual opening SNV systems is however much more complicated than is immediately apparent and this issue is discussed in more detailed in Section 6.42.

6.4.1.2 Summer ventilation

The predicted volume flows for summer are studied under 50%, 75% and 100% opening fractions. These are, respectively, the equivalent of 2.4%, 5.0% and 6.6% of the floor area of the GOSH ward; or 2.8%, 4.2% and 6.0% of the floor area in the case of the ADB ward. These areas of openings were selected as being representative of likely operational conditions in summer when vents will not normally be constricted.

Using July as an example month (mid-summer) the mean relative monthly flows are predicted in absolute and relative rates for both GOSH and ADB ward spaces fitted with dual and single openings. With dual openings, the mean (absolute) monthly volume flow at full opening (100%) are 299 l/s (GOSH) and 239.2 l/s (ADB). At three-quarter opening (75%), the airflow rates are 232 l/s (GOSH) and 182 l/s (ADB) while at half-opening (50%), the airflow rates are 164.9 l/s (GOSH) and 125.5 l/s (ADB). With single openings, the airflow rates are predicted to reduce by 62.6% (at 100% opening); by 63.2% (at 75% opening) and by 64.3% (at 50% opening).

.

The predicted fluctuations in monthly flows are depicted in relative rates for both the GOSH (Fig. 6.5) and the ADB (Fig. 6.6) ward spaces. In both ward types, 6 ACH would be unachievable using single openings at 50% opening. On the other hand, with single openings at three-quarters fractions (75%), the maximum airflow into GOSH and ADB wards are 8.73 ACH and 6.79 ACH respectively, while at full (100%) fractions, maximum flow rates are 11.64 ACH and 9.06 ACH respectively. However, the mean relative monthly flow rates into both ward types fitted with single openings fall below 6 ACH, even at 75% and 100% opening fractions. For the GOSH ward, the mean relative ventilation rate in July would be 4.26 ACH (75%) and 5.63 ACH (100%) while in the ADB ward, the rates of airflow in July are 3.22 ACH (75%) and 4.29 ACH (100%).

In the airflow results of both the GOSH ward (Fig. 6.5) and the ADB ward (Fig. 6.6), it can be observed that the fluctuations in airflow are quite pronounced in dual openings which are subjected to the fluctuations in driving forces (wind, outdoor temperature and indoor heat sources). With single openings, there are less pronounced fluctuations in predicted volume flow and this is indicative of the self-regulating mechanism of such openings, which can be attributed to conflict in flow directions, since one opening operates as both an inlet and outlet at the same time. In addition to the smaller areas of opening, this conflict in flow direction is conceivably responsible for the weak ventilation rates and the build-up of internal heat resulting from single openings. Further insight on this can be obtained in the CFD section of this study. A detailed summary of the minimum, maximum and mean January and July airflow rates is provided (Table 6.3) for the opening fractions of winter and summer respectively.

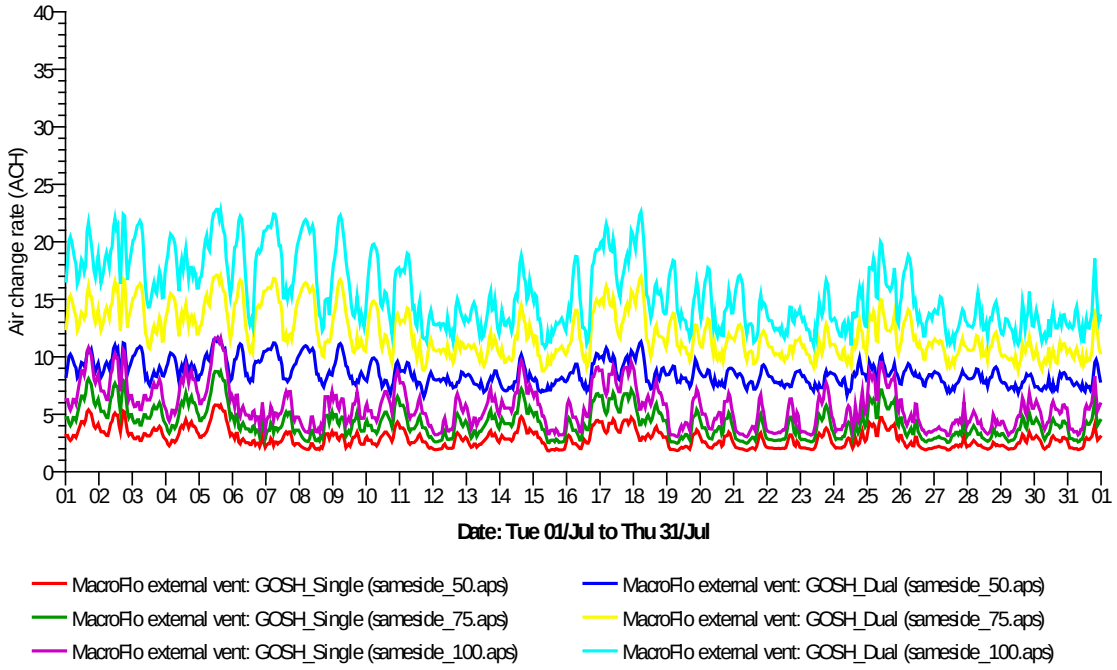

Figure 6:5: Variation in airflow for the GOSH ward with single and dual openings at three summer opening fractions

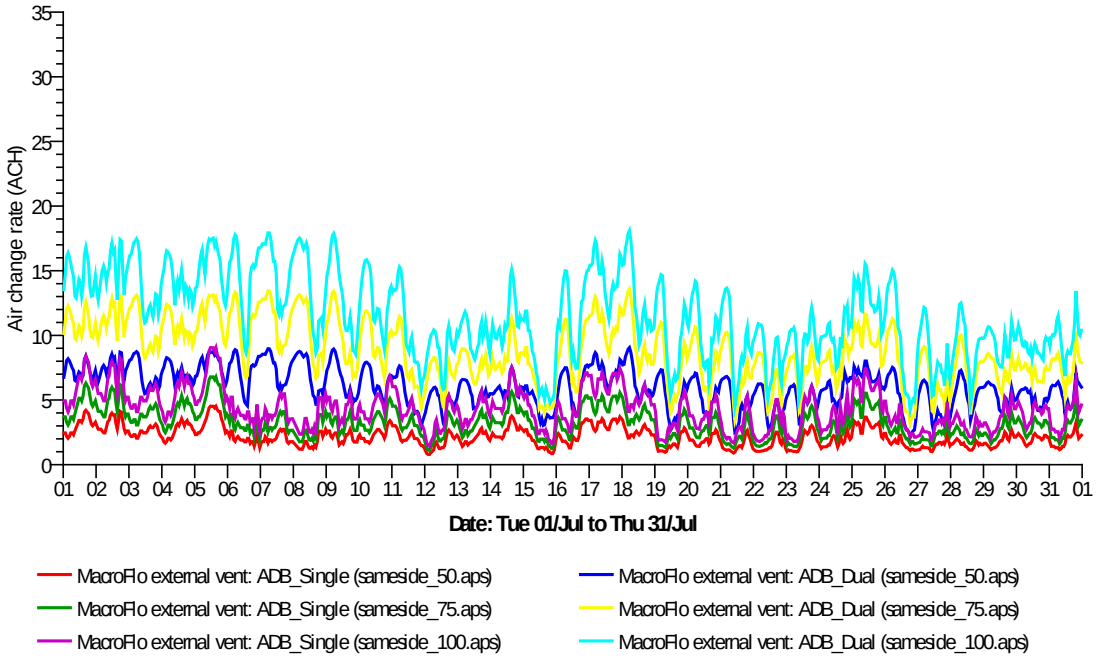

Figure 6:6: Variation in airflow for the ADB ward with single and dual openings at three summer opening fractions

Table 6.3: Summary of minimum, maximum and mean January and July volume flows (L/s)

				Min. Val.	Min. Time	Max. Val.	Max. Time	Mean
20°C heating setpoint	**January**	**6.25%**	*GOSH_Single*	6.4	09:30,12/Jan	15.1	11:30,01/Jan	8.3
			GOSH_Dual	30.9	04:30,23/Jan	45.4	07:30,02/Jan	37.5
			ADB_Single	3.8	23:30,11/Jan	13.4	11:30,01/Jan	6.3
			ADB_Dual	23.7	14:30,24/Jan	40.9	07:30,02/Jan	33
		12.5%	*GOSH_Single*	12	08:30,22/Jan	31.5	11:30,01/Jan	16.4
			GOSH_Dual	61.2	14:30,24/Jan	94.6	07:30,02/Jan	76.5
			ADB_Single	7	17:30,24/Jan	26.9	11:30,01/Jan	12.3
			ADB_Dual	46.1	14:30,24/Jan	81.8	07:30,02/Jan	66
		25%	*GOSH_Single*	21.3	05:30,18/Jan	63.1	11:30,01/Jan	31.5
			GOSH_Dual	107.4	14:30,24/Jan	189.1	07:30,02/Jan	152.5
			ADB_Single	12.9	21:30,24/Jan	53.7	11:30,01/Jan	24.4
			ADB_Dual	92.2	14:30,24/Jan	163.6	07:30,02/Jan	132.1
24°C heating setpoint	**January**	**6.25%**	*GOSH_Single*	6.4	09:30,12/Jan	15.1	11:30,01/Jan	8.3
			GOSH_Dual	34.8	12:30,24/Jan	48.6	07:30,02/Jan	40.8
			ADB_Single	4	17:30,24/Jan	13.3	11:30,01/Jan	6.3
			ADB_Dual	27.9	14:30,24/Jan	43.8	07:30,02/Jan	36.6
		12.5%	*GOSH_Single*	12.4	09:30,12/Jan	31.4	11:30,01/Jan	16.5
			GOSH_Dual	65.2	14:30,24/Jan	101.3	07:30,02/Jan	84.6
			ADB_Single	7.3	17:30,24/Jan	26.7	11:30,01/Jan	12.5
			ADB_Dual	55.8	14:30,24/Jan	87.6	07:30,02/Jan	73.3
		25%	*GOSH_Single*	22.7	05:30,18/Jan	62.7	11:30,01/Jan	32.2
			GOSH_Dual	129.1	14:30,24/Jan	202.5	07:30,02/Jan	169.2
			ADB_Single	14.3	21:30,24/Jan	53.4	11:30,01/Jan	24.9
			ADB_Dual	111.7	14:30,24/Jan	175.2	07:30,02/Jan	146.5
	July	**50%**	*GOSH_Single*	35	11:30,15/Jul	111.8	11:30,05/Jul	55.8
			GOSH_Dual	125.2	17:30,11/Jul	223.4	13:30,05/Jul	164.9
			ADB_Single	16.5	03:30,12/Jul	94.3	11:30,05/Jul	44.8
			ADB_Dual	44.2	18:30,26/Jul	188.6	05:30,18/Jul	125.5
		75%	*GOSH_Single*	47.6	09:30,21/Jul	168	11:30,05/Jul	82
			GOSH_Dual	168.5	07:30,15/Jul	329.4	12:30,05/Jul	232
			ADB_Single	22.7	03:30,12/Jul	141.5	11:30,05/Jul	67.1
			ADB_Dual	66.6	18:30,26/Jul	282.9	05:30,18/Jul	182.3
		100%	*GOSH_Single*	58.4	09:30,21/Jul	224.1	11:30,05/Jul	108.3
			GOSH_Dual	207.9	08:30,15/Jul	439.4	12:30,05/Jul	299.1
			ADB_Single	29.4	03:30,12/Jul	188.7	11:30,05/Jul	89.5
			ADB_Dual	88.5	18:30,26/Jul	377.3	05:30,18/Jul	239.2

6.4.2 The peculiar behaviour of airflow in dual opening SNV systems

Previous research (Allocca, et al., 2003 and Chen, 2004) have described the 'ambiguity' in the behaviour of airflow into same side dual openings. They observed that at low wind speeds (< 4m/s) buoyancy forces dominate wind forces in determining airflow into a space whereas from velocities above 4 m/s, wind forces dominate as the driving force. To explore and

validate this observation, an independent and hypothetical study was carried out via DTM (Appendix D). Four conceptual SNV wards with exact internal loads, schedules and boundary conditions were created with differences being as follows:

1. single opening (buoyancy driven only)
2. single openings (wind + buoyancy driven)
3. dual opening (buoyancy driven only)
4. dual openings (wind + buoyancy driven)

Although it is unrealistic for SNV to operate without influence of wind forces (no matter how low the velocity), for the purpose of the hypothetical study, such openings (Case 1 and Case 3) were assumed to be wind-neutral. The aim of this hypothetical study is to enable the results of Case 2 and Case 4 (impact of wind) to be appreciated with adequate focus and establish the particular speeds at which wind begins to dominate buoyancy. The findings from actual GOSH and ADB wards and recommendations made to designers can therefore be understood better.

The predicted results for volume flow through such openings show that this ambiguity is, firstly, applicable only to dual openings, as single openings will always be influenced by wind forces. Secondly, the results have indeed validated the peculiarity for dual openings where at wind speeds (0 – 7 m/s), both wind and buoyancy forces oppose each other and buoyancy forces dominate wind forces at such speeds in determining airflow. Subsequently, results then confirm that at higher speeds (≥ 7 m/s), wind forces clearly dominate buoyancy forces as reported in Allocca et al. (2003) although in their study, wind began to predominate from speeds of 3 m/s[3].

Since heating energy has a relationship with airflow rates (as well as heat losses through envelope) it was observed that the predicted heating energy for a ward in London during the winter months becomes a function of wind speeds above whereby in January *[Appendix D: Fig. (a) and Fig. (b)]* for example, the effect of wind is negligible due to mean wind velocity being 4.1 m/s. However in the month of February when wind speeds above 7 m/s are

[3] In fact, there studies show that at speeds ≥ 3 m/s, there is reversal in flow directions in same side dual openings, when air supply is from the upper opening and exits via the lower opening. This is as opposed to buoyancy-dominated flows when and fresh air comes in from lower openings and exits at the top.

experienced *[Appendix D: Fig. (c) and Fig. (d)]* the dominance of wind speed becomes apparent particularly between 10th and 14th February. Understanding this ambiguity (or limitation) in wind effects for SNV systems is important not only for sizing such systems, but crucially in appreciating their expected airflow performances.

6.4.3 Thermal comfort

Previously, the impact of various fractions of openings was investigated where it was found that in winter particularly, two heating (20°C and 24°C) setpoints will have little impact on the mean airflow rates with smaller opening fractions (6.25% and 12.5%) using single openings. Significant differences in volume flow are noticeable using the 25% opening fraction. With dual openings however, differences in airflow rates are clearer, even with the smaller opening fractions. This section explores the ramifications of using either single or dual openings on indoor thermal comfort. Primarily, this will be done through the adoption of three metrics: predicted mean vote (PMV); dry-resultant temperature (DRT); and percentage dissatisfied (PD). The predictions from DTM have are presented below using January and July as representative months for winter and summer periods respectively.

Thermal comfort in winter

Using a heating setpoint of 20°C, the mean January PMV for single openings at 6.25% fraction is +1.81 for GOSH ward and +0.74 [4] for the ADB ward (Fig. 6.7a). The corresponding DRT are 30.92°C and 24.96°C and hence, the projected number of dissatisfied occupants would be 63% for GOSH and only 25% for ADB. These differences in thermal comfort conditions have interesting correlations with airflow rates and room volume. Although due to the size of its relatively larger openings, the GOSH was predicted (Table 6.3) to deliver a mean airflow rate of 15.1 l/s as opposed to 13.4 l/s for the ADB ward, the apparently warmer GOSH ward has a smaller effective floor area (18.22m^2, minus the bathroom) than the ADB (25m^2) without an en-suite bathroom. As described in the assumptions and boundary conditions for the DTM simulations (Table 5.2; Section 5.5.1), the effective heat load is 20.6W/m^2 for the GOSH ward and 15 W/m^2 for the ADB ward.

[4] *PMV scale: (+3 = hot); (+2 = warm); (+1 = slightly warm); (0 = neutral); (-1 = slightly cool); (-2 = cool); (-3 = cold).*

The scenario for a heating setpoint of 24^{o}C is not too dissimilar (Fig. 6.7b). A summary of the absolute minimum, maximum and mean PMV and DRT values (Table 6.4) show details of the predicted differences.

Using dual openings for the same 6.25% fraction in January however, produces completely different outcomes. It was predicted earlier (Table 6.4) that airflow into the GOSH and ADB wards would be 45.4 l/s and 40.9 l/s respectively and this increased ventilation rate will succeed in lowering the mean PMV (and DRT) to +0.08 (20.8^{o}C) for GOSH and -0.21 (20.2^{o}C) for ADB. However, the peak PMV and DRT values predicted for these spaces in January are +0.89 (25.83^{o}C) for GOSH and +0.09 (20.65^{o}C) for ADB. A much smaller percentage of occupants will express dissatisfaction with the thermal comfort conditions with dual openings at 6.25%. The GOSH ward will have PD of 6.48% while the ADB ward will have PD of 5.97%.

Doubling the effective area of openings to 12.5% has ramifications for PMV and DRT but again, this is dependent on the heating setpoint used (Fig. 6.8a and Fig. 6.8b) as summarised in Table 6.5. In this case, mean PMV and DRT are predicted to be +0.81 (25.56^{o}C) and +0.14 (21.91^{o}C) for GOSH and ADB wards respectively. The consequences for further increment in area of openings to 25% are also summarised in Table 6.6 and graphically depicted in Fig. 6.8c for a heating setpoint of 20^{o}C and in Fig. 6.8d for heating setpoint of 24^{o}C.

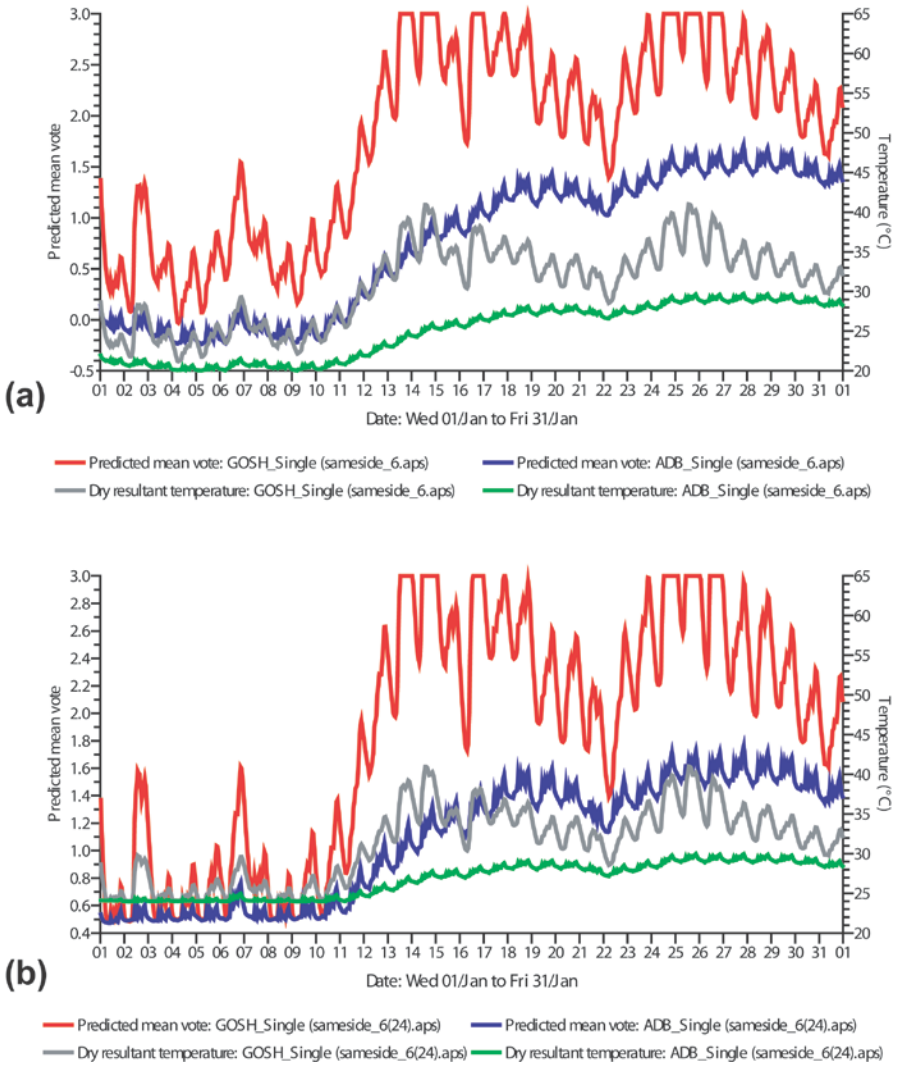

Figure 6:7: Predicted PMV for the GOSH ward with single and dual openings at three winter opening fractions for heating setpoints of (a) 20°C and (b) 24°C

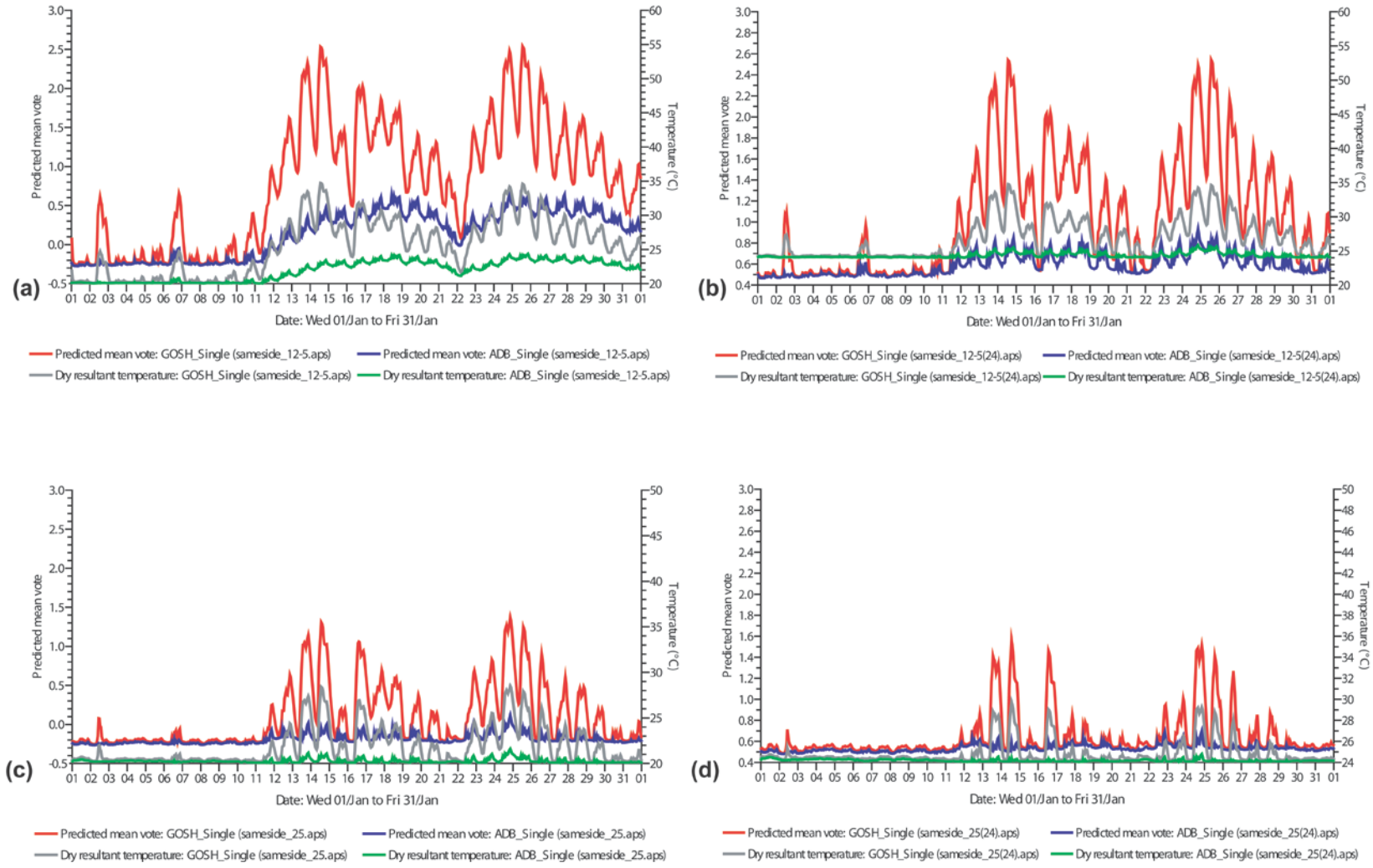

Figure 6:8: Predicted PMV for the ADB ward with single and dual openings at three winter opening fractions for heating setpoints of (a) 20°C and (b) 24°C

Table 6.4: Minimum, maximum and mean PMV values for January for Single and Dual Openings at 6.25% opening fraction

		Var. Name	Min. Val.	Min. Time	Max. Val.	Max. Time	Mean
Single 6.25% opening	PMV	GOSH_Single (20)	-0.03	06:30,04/Jan	3.00	12:30,13/Jan	1.81
		ADB_Single (20)	-0.24	05:30,05/Jan	1.71	20:30,27/Jan	0.74
		GOSH_Single (24)	0.48	05:30,02/Jan	3.00	12:30,13/Jan	1.86
		ADB_Single (24)	0.47	08:30,01/Jan	1.76	20:30,27/Jan	1.08
	DRT	GOSH_Single (20)	21.2	06:30,04/Jan	40.98	13:30,25/Jan	30.92
		ADB_Single (20)	20.04	05:30,09/Jan	29.71	20:30,27/Jan	24.96
		GOSH_Single (24)	24.01	05:30,02/Jan	40.98	13:30,25/Jan	31.21
		ADB_Single (24)	23.98	05:30,02/Jan	29.97	20:30,25/Jan	26.76
Dual 6.25% opening	PMV	GOSH_Dual (20)	-0.27	07:30,01/Jan	0.89	20:30,24/Jan	-0.08
		ADB_Dual (20)	-0.26	03:30,01/Jan	-0.09	20:30,24/Jan	-0.21
		GOSH_Dual (24)	0.48	07:30,01/Jan	1.24	13:30,13/Jan	0.56
		ADB_Dual (24)	0.49	03:30,01/Jan	0.59	20:30,22/Jan	0.53
	DRT	GOSH_Dual (20)	20	04:30,13/Jan	25.83	15:30,13/Jan	20.81
		ADB_Dual (20)	20.08	04:30,23/Jan	20.65	20:30,24/Jan	20.19
		GOSH_Dual (24)	24.03	20:30,29/Jan	27.84	13:30,13/Jan	24.32
		ADB_Dual (24)	24.12	03:30,23/Jan	24.42	07:30,02/Jan	24.24

Table 6.5: Minimum, maximum and mean PMV values for January for Single and Dual Openings at 12.5% opening fraction

		Var. Name	Min. Val.	Min. Time	Max. Val.	Max. Time	Mean
Single 12.5% opening	PMV	GOSH_Single (20)	-0.26	05:30,02/Jan	2.54	13:30,25/Jan	0.81
		ADB_Single (20)	-0.27	07:30,01/Jan	0.65	20:30,24/Jan	0.14
		GOSH_Single (24)	0.47	05:30,02/Jan	2.54	13:30,25/Jan	1.05
		ADB_Single (24)	0.47	07:30,01/Jan	0.93	20:30,24/Jan	0.59
	DRT	GOSH_Single (20)	20.1	05:30,02/Jan	34.72	13:30,14/Jan	25.56
		ADB_Single (20)	20.02	05:30,10/Jan	24.34	20:30,25/Jan	21.91
		GOSH_Single (24)	24.09	05:30,11/Jan	34.75	13:30,14/Jan	26.89
		ADB_Single (24)	24.01	05:30,11/Jan	25.85	20:30,24/Jan	24.36
Dual 12.5% opening	PMV	GOSH_Dual (20)	-0.22	05:30,06/Jan	0.36	13:30,13/Jan	-0.17
		ADB_Dual (20)	-0.22	14:30,14/Jan	-0.15	10:30,12/Jan	-0.19
		GOSH_Dual (24)	0.53	17:30,24/Jan	0.72	13:30,24/Jan	0.58
		ADB_Dual (24)	0.54	14:30,14/Jan	0.61	10:30,12/Jan	0.58
	DRT	GOSH_Dual (20)	20.12	19:30,27/Jan	23.21	13:30,13/Jan	20.43
		ADB_Dual (20)	20.2	03:30,23/Jan	20.76	07:30,02/Jan	20.42
		GOSH_Dual (24)	24.19	18:30,24/Jan	25.27	10:30,02/Jan	24.51
		ADB_Dual (24)	24.3	15:30,24/Jan	24.97	07:30,02/Jan	24.58

Table 6.6: Minimum, maximum and mean PMV values for January for Single and Dual Openings at 25% opening fraction

		Var. Name	Min. Val.	Min. Time	Max. Val.	Max. Time	Mean
Single 25% opening	PMV	GOSH_Single (20)	-0.26	05:30,02/Jan	1.37	20:30,24/Jan	0.09
		ADB_Single (20)	-0.26	05:30,02/Jan	0.11	20:30,24/Jan	-0.19
		GOSH_Single (24)	0.49	05:30,02/Jan	1.56	13:30,14/Jan	0.65
		ADB_Single (24)	0.48	05:30,02/Jan	0.7	20:30,24/Jan	0.53
	DRT	GOSH_Single (20)	20.2	05:30,11/Jan	28.49	20:30,24/Jan	21.83
		ADB_Single (20)	20.05	05:30,18/Jan	21.6	20:30,24/Jan	20.27
		GOSH_Single (24)	24.17	05:30,18/Jan	29.75	13:30,14/Jan	24.83
		ADB_Single (24)	24.05	05:30,18/Jan	24.79	20:30,24/Jan	24.19
Dual 25% opening	PMV	GOSH_Dual (20)	-0.2	16:30,24/Jan	0.03	10:30,02/Jan	-0.11
		ADB_Dual (20)	-0.19	16:30,24/Jan	-0.03	07:30,02/Jan	-0.11
		GOSH_Dual (24)	0.59	16:30,24/Jan	0.88	09:30,02/Jan	0.71
		ADB_Dual (24)	0.6	15:30,24/Jan	0.81	07:30,02/Jan	0.7
	DRT	GOSH_Dual (20)	20.31	18:30,24/Jan	21.95	09:30,02/Jan	20.87
		ADB_Dual (20)	20.39	15:30,24/Jan	21.64	07:30,02/Jan	20.91
		GOSH_Dual (24)	24.54	15:30,24/Jan	26.39	09:30,02/Jan	25.23
		ADB_Dual (24)	24.65	15:30,24/Jan	26.07	07:30,02/Jan	25.25

Unlike for predicted volume flow (Section 6.4.1) where at the smaller opening fractions (6.25% and 12.5%) there was negligible differences in the mean ventilation rates (Table 6.3) at 20^{o}C and 24^{o}C heating setpoints (for single openings of both GOSH and ADB wards), for thermal comfort however, the impact is more noticeable, if not significant. For the mean PMV of ADB wards in particular, the PMV for single opening at 6.25% opening fraction is 0.74 (above neutral, less than warm) at 20^{o}C heating setpoint whereas it is 1.08 (above warm) at 24^{o}C heating setpoint (Table 6.4). In other words, for single openings at 6.25% opening fraction, mean DRT will be 24.96^{o}C at 20^{o}C heating setpoint but rises up to 26.76^{o}C using 24^{o}C heating setpoint. This difference of 1.8^{o}C is indeed significant especially given that at both heating setpoints the mean airflow rates are the same at 6.3 l/s (Table 6.3).

It is beneficial to also review the performance of the three winter opening fractions applicable to winter, in terms of the distribution of number of days in January when different ranges of dry-bulb temperature will be achieved. Using nine temperature ranges from 20^{o}C to 28^{o}C, an interesting pattern is apparent (Table 6.7). It is predicted that the single openings are generally, better able to spread temperature over the entire range in January, especially at the lower 20^{o}C heating setpoint.

Dual openings are prone to having fewer ranges of temperature, especially with larger opening fractions. At an opening fraction of 6.25% for example, dual openings in the ADB

ward at 20°C heating setpoint have all 31 days of the month between 20 and 21°C. On the other hand, at an opening fraction of 25%, approximately 20 days fall into the 20-21°C range, while for 11 days, the ADB ward will experience temperatures between 21 and 22°C. The higher effective heat load (per m^2) of the GOSH ward appears to contribute to the wider spread in temperature ranges, relative to the ADB ward.

Table 6.7: Distribution of number of days in January during which specific DRT ranges will be experienced

			Temperature (DRT) ranges: distribution of days in January								
		Location	**20 - 21**	**21 - 22**	**22 - 23**	**23 - 24**	**24 - 25**	**25 - 26**	**26 - 27**	**27 - 28**	**> 28**
6.25% opening	**20oC**	***GOSH_Single***	***0.0***	***0.5***	***1.0***	***2.8***	***2.1***	***2.0***	***0.8***	***0.9***	***21.0***
		GOSH_Dual	***23.2***	***3.6***	***1.6***	***1.1***	***0.6***	***0.9***	***0.0***	***0.0***	***0.0***
		ADB_Single	***8.4***	***2.7***	***0.7***	***0.8***	***0.9***	***1.8***	***1.8***	***5.5***	***8.4***
		ADB_Dual	***31.0***	***0.0***	***0.0***	***0.0***	***0.0***	***0.0***	***0.0***	***0.0***	***0.0***
	24oC	GOSH_Single	0.0	0.0	0.0	0.0	5.0	2.5	1.3	0.8	21.5
		GOSH_Dual	0.0	0.0	0.0	0.0	28.8	0.7	1.0	0.5	0.0
		ADB_Single	0.0	0.0	0.0	0.7	10.5	1.2	1.1	4.4	13.0
		ADB_Dual	0.0	0.0	0.0	0.0	31.0	0.0	0.0	0.0	0.0
12.5% opening	**20oC**	***GOSH_Single***	***7.9***	***1.3***	***0.8***	***1.3***	***2.4***	***2.4***	***2.5***	***3.0***	***9.4***
		GOSH_Dual	***29.2***	***1.3***	***0.4***	***0.1***	***0.0***	***0.0***	***0.0***	***0.0***	***0.0***
		ADB_Single	***11.4***	***2.3***	***6.8***	***9.5***	***0.9***	***0.0***	***0.0***	***0.0***	***0.0***
		ADB_Dual	***31.0***	***0.0***	***0.0***	***0.0***	***0.0***	***0.0***	***0.0***	***0.0***	***0.0***
	24oC	GOSH_Single	0.0	0.0	0.0	0.0	12.0	3.1	3.0	3.2	9.8
		GOSH_Dual	0.0	0.0	0.0	0.0	30.7	0.3	0.0	0.0	0.0
		ADB_Single	0.0	0.0	0.0	0.0	28.2	2.8	0.0	0.0	0.0
		ADB_Dual	0.0	0.0	0.0	0.0	31.0	0.0	0.0	0.0	0.0
25% opening	**20oC**	***GOSH_Single***	***17.0***	***3.7***	***3.1***	***2.8***	***1.4***	***0.9***	***1.2***	***0.7***	***0.3***
		GOSH_Dual	***20.2***	***10.8***	***0.0***	***0.0***	***0.0***	***0.0***	***0.0***	***0.0***	***0.0***
		ADB_Single	***30.4***	***0.6***	***0.0***	***0.0***	***0.0***	***0.0***	***0.0***	***0.0***	***0.0***
		ADB_Dual	***19.8***	***11.2***	***0.0***	***0.0***	***0.0***	***0.0***	***0.0***	***0.0***	***0.0***
	24oC	GOSH_Single	0.0	0.0	0.0	0.0	25.7	2.0	0.8	0.9	1.5
		GOSH_Dual	0.0	0.0	0.0	0.0	10.8	19.7	0.5	0.0	0.0
		ADB_Single	0.0	0.0	0.0	0.0	31.0	0.0	0.0	0.0	0.0
		ADB_Dual	0.0	0.0	0.0	0.0	8.8	22.0	0.2	0.0	0.0

It can be deduced that for single openings, using 20°C heating setpoint could lead to approximately 14 days in January when DRTs are less than or equal to 24°C (Table 6.7) and that for the remaining half of the month, the days are somewhat spread across different range of DRTs. There are however as many days when DRT will exceeds 28°C as there are days when DRT are between 20-21°C (i.e. 8.4 days each).

Thermal comfort in summer

The quality of indoor air in summer under three opening fractions (50%, 75% and 100%) were considered by focusing on July as an example (mid-summer) month as well as by overviewing the conditions for June, July and August. Thermal comfort conditions were evaluated using predicted minimum, maximum and mean PMV and DRT values as well as the distribution of days under which specific bands of indoor temperature will be experienced in both GOSH and ADB wards.

The number of days in July when different bands of temperature will be experienced is summarised in Table 6.8 for a range between 20^{o}C and 30^{o}C. It is predicted that the 20-21^{o}C range will have most days for dual openings, but with single openings, the days are more evenly spread across the entire range. The predicted indoor thermal comfort for summer (using July as an example month) suggests that the GOSH ward (Fig. 6.9) would experience more extreme diurnal fluctuations in PMV and DRT values than the ADB ward (Fig. 6.10). Since both ward types share similar occupancy profiles and internal heat loads, the influencing factor for the sharp rise and decline in PMV is likely to be linked to the smaller effective floor area of the GOSH ward (minus bathroom), relative to the ADB ward. The larger area of opening (0.825m^2) of the GOSH ward, which is 16% larger than the ADB openings (0.69m^2) would allow higher ventilation rates than attainable in the ADB ward as observed previously, regardless of the opening fraction. However, as in winter, larger airflow rates do not correspond with better indoor thermal comfort. This is evident from the PMV/DRT values predicted for July as an exemplar month (Table 6.9), or for the entire summer months of June, July and August (Table 6.10).

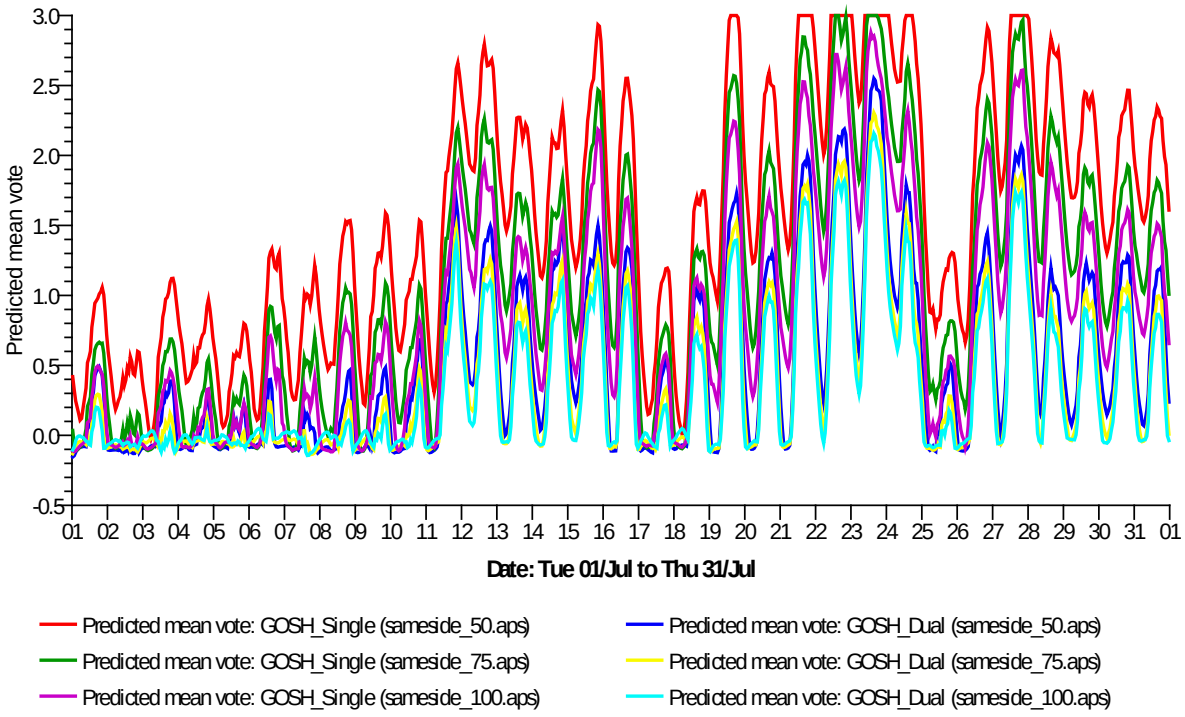

Figure 6:9: Predicted PMV for the GOSH ward with single and dual openings at three summer opening fractions

There is potential for overheating in July, especially in the GOSH ward (Fig. 6.9), where it is predicted that there would not be significant differences in PMV between 50%, 75% and 100% opening fractions in July. For single openings at these fractions, mean PMV values are predicted to be +1.58, +1.12 and +0.87[5] respectively (Table 6.9). So while the peak DRT values are in the order of 41^{o}C, 38^{o}C and 36^{o}C respectively, the number of days in which higher temperatures (>30^{o}C) will be experienced in this ward recede (Table 6.8) from 13.6 days (at 50%) to 8 days (at 75%) and then to 4.9 days (at 100%). With dual openings in the GOSH ward, both PMV and DRT values are predicted to lower mean temperatures by more than 6^{o}C (at 50% fraction) and just above 3^{o}C at 75% and 100% fractions (Table 6.9).

[5] *PMV scale: (+3 = hot); (+2 = warm); (+1 = slightly warm); (0 = neutral); (-1 = slightly cool); (-2 = cool); (-3 = cold).*

Table 6.8: Distribution of number of days in July during which specific DRT ranges will be experienced

		Temperature (DRT) ranges: distribution of days in July										
		20-21	21-22	22-23	23-24	24-25	25-26	26-27	27-28	28-29	29-30	> 30
50%	*GOSH_Single*	0.2	1.0	1.7	2.3	2.1	1.7	2.3	2.5	1.8	1.9	13.6
	GOSH_Dual	10.0	3.5	3.3	2.5	1.7	1.5	2.8	2.2	1.0	0.7	1.9
	ADB_Single	4.9	4.4	2.0	1.7	1.8	4.6	2.8	4.3	2.2	0.8	1.5
	ADB_Dual	13.1	5.0	5.3	3.9	1.4	0.8	0.9	0.4	0.1	0.0	0.0
75%	*GOSH_Single*	3.3	2.6	2.1	1.8	3.1	2.2	1.9	1.9	1.9	2.0	8.1
	GOSH_Dual	13.3	3.7	2.5	1.7	1.8	2.6	2.0	1.0	0.6	0.5	1.3
	ADB_Single	10.0	2.4	1.3	3.9	5.4	3.7	1.8	0.9	0.7	1.0	0.0
	ADB_Dual	16.1	4.8	4.9	2.3	1.2	0.8	0.6	0.5	0.0	0.0	0.0
100%	*GOSH_Single*	6.1	2.3	3.0	2.9	2.3	1.9	1.8	2.1	2.0	1.8	4.9
	GOSH_Dual	13.6	5.0	1.9	1.6	2.6	2.2	1.4	0.7	0.5	0.5	1.0
	ADB_Single	11.3	2.3	3.7	5.5	3.8	1.8	0.7	0.8	1.0	0.2	0.0
	ADB_Dual	16.3	5.6	4.3	1.8	1.3	1.0	0.3	0.4	0.0	0.0	0.0

However, as DTM uses well mixed zone assumptions, individual perceptions of thermal comfort at specific locations may also differ, meaning the impact of opening areas would have to be correlated with airflow rates for a better evaluation of thermal comfort. At 50% fraction for the GOSH ward with single opening for instance, the mean airflow rate in July is 55.8 l/s, while volume flow is up to 82 l/s and 108.3 l/s with 75% and 100% opening fractions – as summarised previously (Table 6.3).

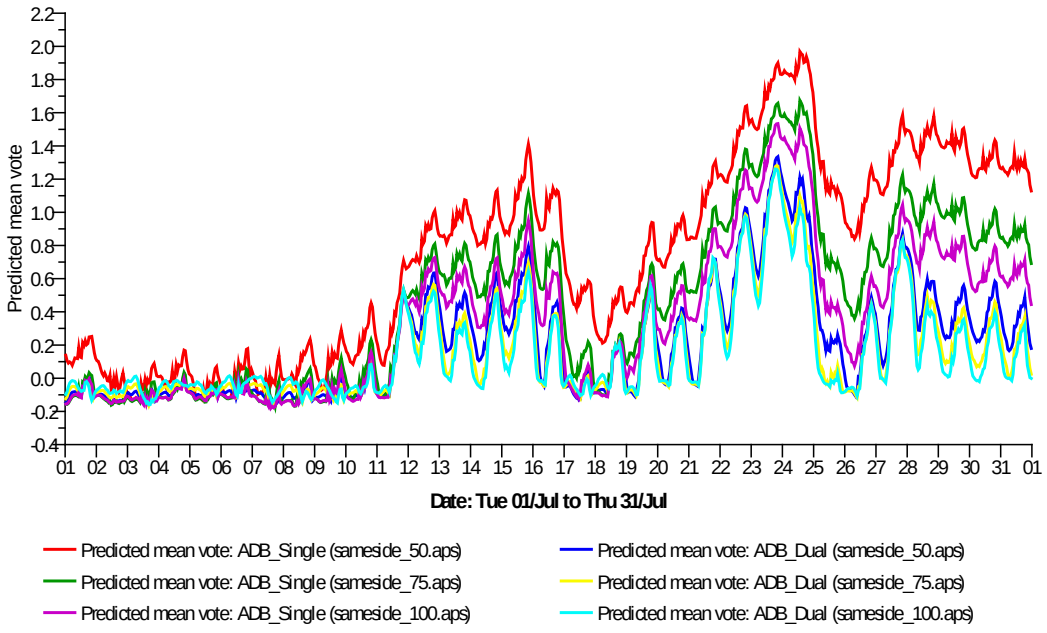

Figure 6:10: Predicted PMV for the ADB ward with single and dual openings at three summer opening fractions

In the ADB ward fitted with a single vent, the lower effective heat load of this space leads to mean PMV and DRT values being not only lower than GOSH ward overall, but they are also much closer in range regardless of the area of opening. For 50%, 75% and 100% fractions, the mean PMV values predicted are +0.74, +0.47 and +0.35 respectively[6], while DRT values will be 24.7^{o}C, 23.3^{o}C and 22.69^{o}C (Table 6.9). The use of dual openings in the ADB ward would produce lower PMV and DRT values. In this case however, at 50% fraction, mean temperatures will drop by about 3^{o}C, half the reduction experienced by dual openings in GOSH ward although the absolute mean temperatures of the ADB ward are much lower.

Table 6.9: Minimum, maximum and mean DRT/PMV values for July at different opening fractions

			Min. Val.	Min. Time	Max. Val.	Max. Time	Mean
DRT	50%	GOSH_Single	20.75	05:30,03/Jul	41.11	13:30,23/Jul	29.35
		GOSH_Dual	20.23	00:30,01/Jul	34.67	15:30,23/Jul	23.67
		ADB_Single	20.19	05:30,06/Jul	31.15	20:30,23/Jul	24.7
		ADB_Dual	20.21	17:30,04/Jul	28.21	20:30,23/Jul	21.98
	75%	GOSH_Single	20.37	04:30,01/Jul	38.12	13:30,23/Jul	26.78
		GOSH_Dual	20.14	05:30,29/Jul	33.41	15:30,23/Jul	23
		ADB_Single	20.14	05:30,08/Jul	29.9	20:30,23/Jul	23.3
		ADB_Dual	20.28	20:30,05/Jul	27.96	19:30,23/Jul	21.72
	100%	GOSH_Single	20.35	05:30,08/Jul	36.32	13:30,23/Jul	25.44
		GOSH_Dual	20.15	05:30,30/Jul	32.65	15:30,23/Jul	22.69
		ADB_Single	20.16	05:30,08/Jul	29.28	19:30,23/Jul	22.69
		ADB_Dual	20.31	15:30,10/Jul	27.85	18:30,23/Jul	21.65
PMV	50%	GOSH_Single	-0.02	05:30,03/Jul	3	14:30,19/Jul	1.58
		GOSH_Dual	-0.15	00:30,01/Jul	2.55	15:30,23/Jul	0.54
		ADB_Single	-0.13	08:30,03/Jul	1.97	13:30,24/Jul	0.74
		ADB_Dual	-0.17	14:30,07/Jul	1.34	20:30,23/Jul	0.22
	75%	GOSH_Single	-0.11	04:30,09/Jul	3	13:30,22/Jul	1.12
		GOSH_Dual	-0.14	17:30,07/Jul	2.3	15:30,23/Jul	0.41
		ADB_Single	-0.17	17:30,07/Jul	1.67	13:30,24/Jul	0.47
		ADB_Dual	-0.17	15:30,07/Jul	1.28	19:30,23/Jul	0.17
	100%	GOSH_Single	-0.12	07:30,08/Jul	2.88	13:30,23/Jul	0.87
		GOSH_Dual	-0.14	15:30,07/Jul	2.16	15:30,23/Jul	0.35
		ADB_Single	-0.18	14:30,07/Jul	1.53	20:30,23/Jul	0.35
		ADB_Dual	-0.16	16:30,03/Jul	1.26	18:30,23/Jul	0.15

[6] *PMV scale: (+3 = hot); (+2 = warm); (+1 = slightly warm); (0 = neutral); (-1 = slightly cool); (-2 = cool); (-3 = cold).*

A summary of the minimum, maximum and mean DRT and PMV values predicted for the entire summer months (June to August) are provided in Table 10.

Table 6.10: Summer (June – Aug) DRT/ PMV ranges and days at different opening fractions

			Min. Val.	Min. Time	Max. Val.	Max. Time	Mean
DRT	50%	GOSH_Single	20.33	05:30,31/Aug	42.82	20:30,08/Jun	29.47
		GOSH_Dual	20.12	05:30,01/Aug	35.87	18:30,08/Jun	23.46
		ADB_Single	20.19	05:30,06/Jul	31.47	20:30,21/Aug	24.91
		ADB_Dual	20.21	17:30,04/Jul	29.43	20:30,08/Jun	21.77
	75%	GOSH_Single	20.36	05:30,05/Jun	39.83	16:30,08/Jun	26.78
		GOSH_Dual	20.13	04:30,10/Aug	34.77	18:30,08/Jun	22.81
		ADB_Single	20.14	05:30,08/Jul	30.3	20:30,08/Jun	23.24
		ADB_Dual	20.26	11:30,14/Aug	29.26	20:30,08/Jun	21.57
	100%	GOSH_Single	20.35	05:30,08/Jul	38.11	16:30,08/Jun	25.34
		GOSH_Dual	20.15	05:30,30/Jul	34.03	18:30,08/Jun	22.52
		ADB_Single	20.16	05:30,08/Jul	29.99	20:30,08/Jun	22.5
		ADB_Dual	20.24	12:30,15/Aug	29.21	19:30,08/Jun	21.53
PMV	50%	GOSH_Single	-0.12	05:30,02/Jun	3.0	10:30,07/Jun	1.6
		GOSH_Dual	-0.17	21:30,21/Jun	2.9	19:30,08/Jun	0.5
		ADB_Single	-0.15	05:30,03/Jun	2.1	20:30,21/Aug	0.8
		ADB_Dual	-0.21	17:30,22/Jun	1.7	20:30,08/Jun	0.2
	75%	GOSH_Single	-0.16	06:30,22/Jun	3.0	12:30,07/Jun	1.1
		GOSH_Dual	-0.19	18:30,22/Jun	2.68	18:30,08/Jun	0.37
		ADB_Single	-0.19	16:30,02/Jun	1.84	20:30,08/Jun	0.45
		ADB_Dual	-0.19	17:30,22/Jun	1.63	20:30,08/Jun	0.13
	100%	GOSH_Single	-0.16	06:30,22/Jun	3	13:30,08/Jun	0.84
		GOSH_Dual	-0.18	20:30,23/Jun	2.53	18:30,08/Jun	0.31
		ADB_Single	-0.21	11:30,22/Jun	1.78	20:30,08/Jun	0.31
		ADB_Dual	-0.17	12:30,13/Jun	1.62	20:30,08/Jun	0.12

6.4.4 Heating energy predictions

In winter season or in any period when heating becomes necessary, the link between airflow rates and the energy required to maintain thermal comfort conditions predicted in the last section will enable an appreciation of the performances of each of the three smaller (winter) opening fractions.

As with airflow rates in winter, the month of January was used to obtain a sample (monthly) heating load for the GOSH ward (Fig. 6.11) and ADB ward (Fig. 6.12). Expectedly, this energy was found to be highest when dual openings are used at 25% opening fraction, although absolute heating power (in kW) are higher for GOSH than for ADB ward. Single

openings will lead to significantly low heating loads, but this is to be expected, considering the lower ventilation rates achieved from single openings.

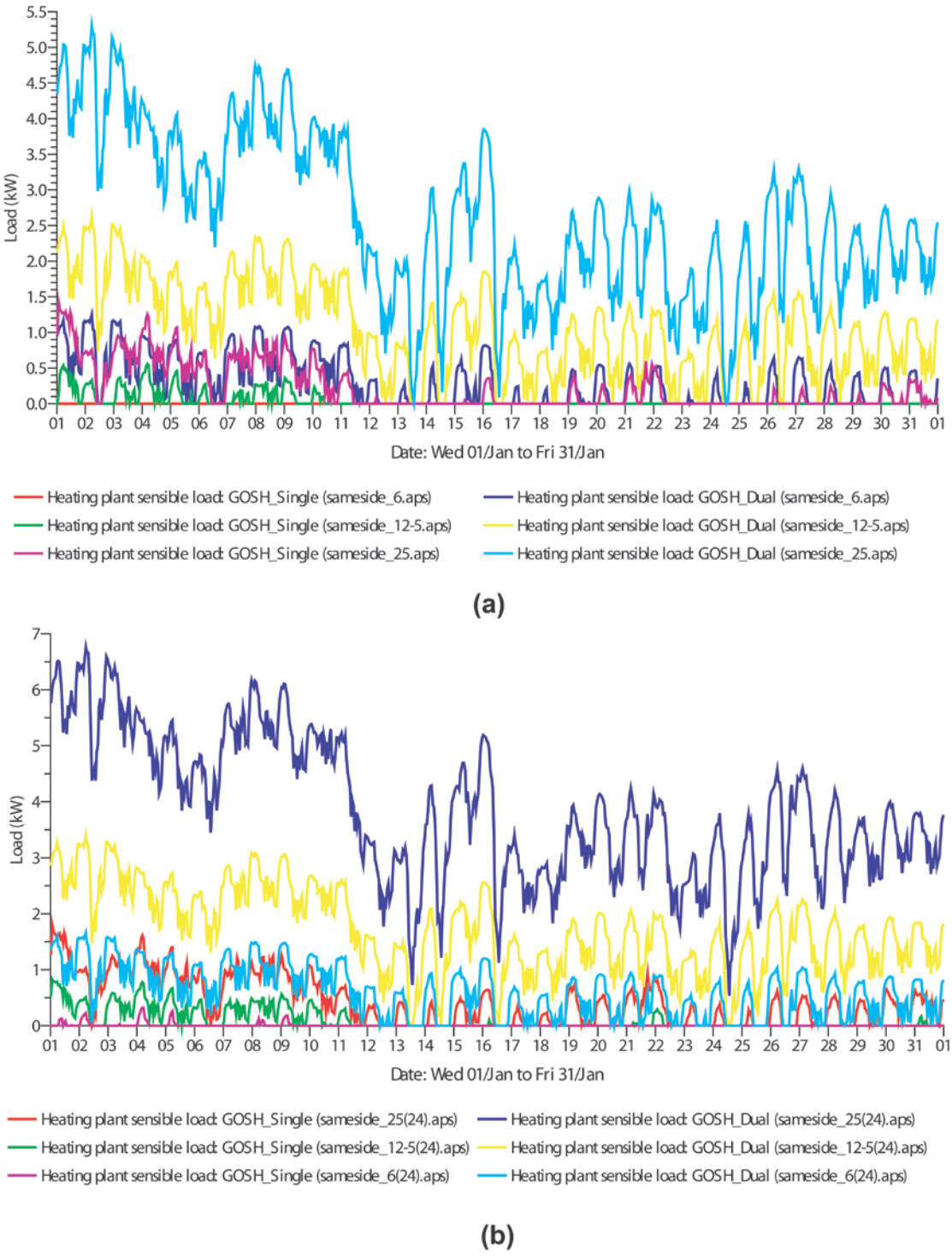

Figure 6:11: Predicted heating power for the GOSH ward with single and dual openings at three winter opening fractions for heating setpoints of (a) 20°C and (b) 24°C

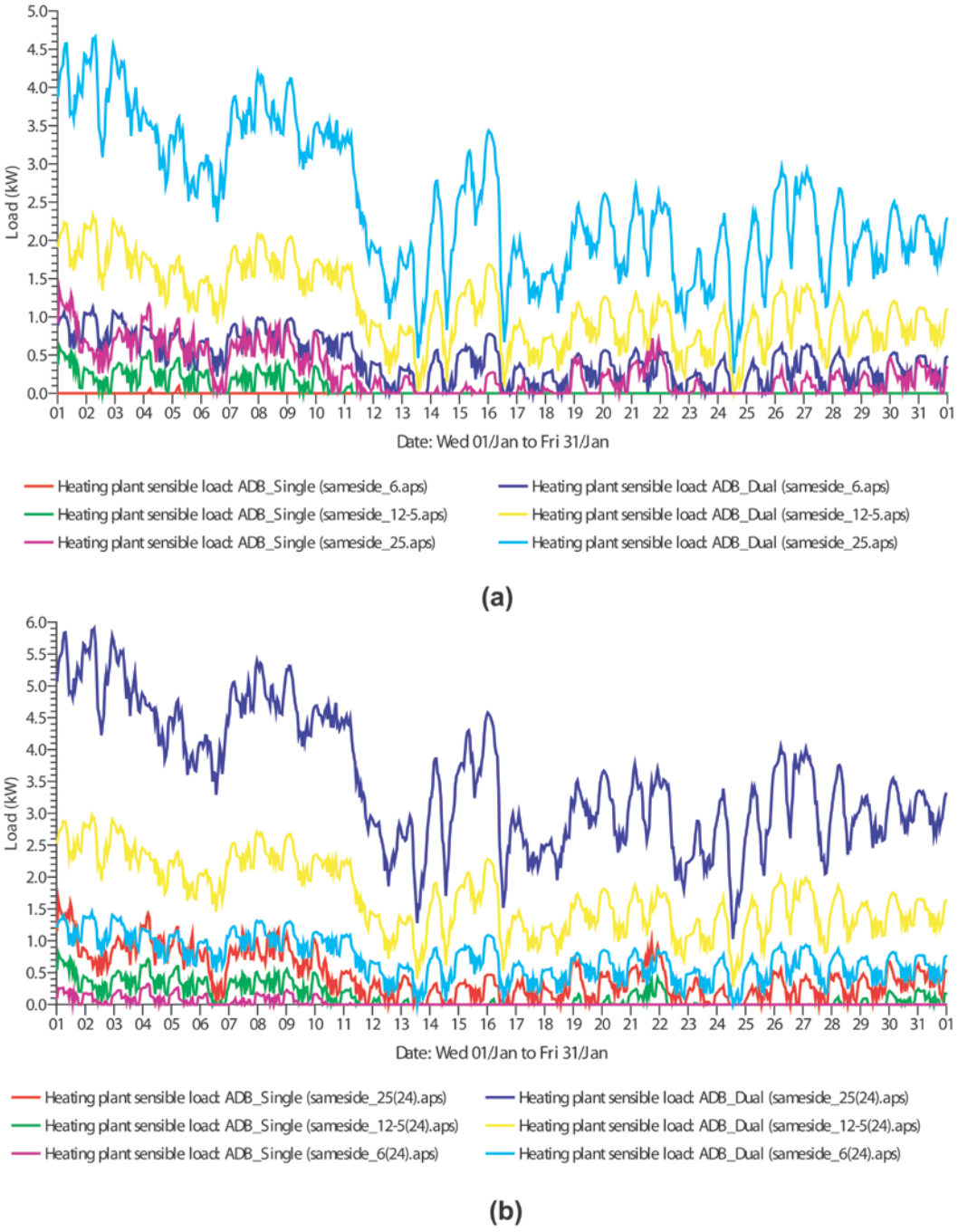

Figure 6:12: Predicted heating power for the ADB ward with single and dual openings at three winter opening fractions for heating setpoints of (a) 20°C and (b) 24°C

The build-up of internal heat that occurs when using single openings was described with the PMV, DRT and PD predictions described earlier and explains why at 6.25% and 12.5% both GOSH and ADB ward spaces would consume negligible energy for heating using single openings (Table 6.11). From the energy perspective, this may appear to be a desirable outcome, but it is doubtful that the spaces will be comfortable for occupants given the 'warm' PMV values and well-spread distribution of days when DRT values exceed 21°C and

approach 30°C especially at 6.25% fraction as suggested earlier (Table 6.6 and Table 6.7). However, if the achievable flow rates at 12.5% are deemed acceptable to meet basic fresh air and odour dilution requirements (mean January flow is 13.3 l/s and 8.1 l/s for GOSH and ADB); then coupled with their respective mean monthly PMV of +1.09 and +0.41, the low annual energy required to heat the spaces (Table 6.11) is more attractive.

Table 6.11: Predicted annual heating energy (MWh) from GOSH and ADB wards at various openings for heating setpoints of 20°C and 24°C

Heating setpoint = 20 deg		6.25% opening fraction				12.5% opening fraction				25% opening fraction			
		GOSH		ADB		GOSH		ADB		GOSH		ADB	
		Single	**Dual**	**Single**	**Dual**	**Single**	**Dual**	**Single**	**Dual**	**Single**	**Dual**	**Single**	**Dual**
	Jan	0.000	0.243	0.001	0.339	0.031	0.786	0.051	0.839	0.171	1.938	0.202	1.840
	Feb	0.000	0.036	0.000	0.098	0.001	0.255	0.002	0.366	0.044	0.862	0.104	0.915
	Mar	0.000	0.004	0.000	0.036	0.000	0.147	0.000	0.255	0.001	0.601	0.012	0.724
	Apr	0.000	0.007	0.000	0.019	0.000	0.100	0.000	0.164	0.006	0.442	0.009	0.533
	May	0.000	0.013	0.000	0.047	0.000	0.159	0.000	0.249	0.013	0.592	0.042	0.698
	Jun	0.000	0.000	0.000	0.000	0.000	0.000	0.000	0.000	0.000	0.047	0.000	0.058
	Jul	0.000	0.000	0.000	0.000	0.000	0.000	0.000	0.000	0.000	0.025	0.000	0.041
	Aug	0.000	0.000	0.000	0.000	0.000	0.000	0.000	0.000	0.000	0.006	0.000	0.010
	Sep	0.000	0.000	0.000	0.000	0.000	0.004	0.000	0.013	0.000	0.090	0.000	0.145
	Oct	0.000	0.000	0.000	0.000	0.000	0.022	0.000	0.049	0.000	0.196	0.000	0.291
	Nov	0.000	0.069	0.000	0.145	0.000	0.348	0.000	0.447	0.030	1.035	0.080	1.076
	Dec	0.000	0.162	0.000	0.270	0.010	0.631	0.028	0.709	0.134	1.643	0.190	1.590
a	**Tp**	**0.000**	**0.533**	**0.001**	**0.954**	**0.042**	**2.452**	**0.081**	**3.090**	**0.399**	**7.477**	**0.639**	**7.920**
b	**%B**	*0.00%*	*12%*	*0.00%*	*21%*	*1.00%*	*56%*	*1.70%*	*67%*	*9.20%*	*172%*	*14%*	*171%*

Heating setpoint = 24 deg		6.25% opening fraction				12.5% opening fraction				25% opening fraction			
		GOSH		ADB		GOSH		ADB		GOSH		ADB	
		Single	**Dual**	**Single**	**Dual**	**Single**	**Dual**	**Single**	**Dual**	**Single**	**Dual**	**Single**	**Dual**
	Jan	0.007	0.489	0.023	0.561	0.076	1.274	0.097	1.248	0.319	2.866	0.329	2.622
	Feb	0.000	0.159	0.000	0.264	0.011	0.607	0.041	0.679	0.167	1.571	0.233	1.508
	Mar	0.000	0.089	0.000	0.197	0.000	0.444	0.000	0.578	0.034	1.302	0.102	1.349
	Apr	0.000	0.058	0.000	0.132	0.001	0.338	0.000	0.448	0.029	1.032	0.062	1.091
	May	0.000	0.095	0.000	0.191	0.000	0.432	0.008	0.557	0.070	1.251	0.149	1.301
	Jun	0.000	0.000	0.000	0.001	0.000	0.047	0.000	0.082	0.000	0.275	0.000	0.347
	Jul	0.000	0.000	0.000	0.001	0.000	0.031	0.000	0.062	0.000	0.199	0.000	0.256
	Aug	0.000	0.000	0.000	0.000	0.000	0.010	0.000	0.028	0.000	0.157	0.000	0.226
	Sep	0.000	0.002	0.000	0.016	0.000	0.095	0.000	0.178	0.003	0.454	0.014	0.563
	Oct	0.000	0.011	0.000	0.051	0.000	0.177	0.000	0.297	0.008	0.692	0.027	0.809
	Nov	0.000	0.215	0.000	0.313	0.003	0.710	0.025	0.781	0.133	1.789	0.205	1.723
	Dec	0.000	0.395	0.003	0.483	0.048	1.101	0.089	1.103	0.291	2.535	0.323	2.342
	Tp	**0.007**	**1.512**	**0.026**	**2.208**	**0.140**	**5.265**	**0.261**	**6.039**	**1.053**	**14.122**	**1.443**	**14.136**
	%B	*0.20%*	*35%*	*0.60%*	*48%*	*3.20%*	*121%*	*5.60%*	*130%*	*24%*	*325%*	*31%*	*306%*

Tp: is total heating energy predicted by dynamic modelling
%B: is percentage of CIBSE benchmark assuming heating takes 44% of total energy ((fossil fuels) which equates to 4.35/9.89 MWh (GOSH) and 4.62/10.5 MWh (ADB)

The CIBSE (2008) benchmark for hospital energy is 9.89MWh for GOSH and 10.5MWh for ADB. Considering, however, that space/air heating are allocated 44% of total energy (DH, 2006), then the adjusted benchmark would be 4.35MWh for GOSH ward and 4.62MWh for ADB ward. For each ward, the proportion of adjusted benchmark (%B) which the total predicted energy (Tp) which each winter strategy requires have been computed and summarised (Table 6.11). Evidently, with 20^{o}C heating setpoint, these adjusted benchmarks will only be exceeded using dual openings at 25% fraction for both GOSH and ADB wards. By implementing a 24^{o}C heating setpoint on the other hand, dual openings cannot be afforded even at 12.5% opening fraction. At this fraction of opening, the adjusted benchmarks will be exceeded by 121% (GOSH) or 130% (ADB). With single openings, it is possible to have 25% openings even with a 24^{o}C heating setpoint as this winter strategy will consume only 24% and 31% of the adjusted CIBSE benchmark for GOSH and ADB wards respectively.

It is noteworthy that at 20^{o}C heating setpoint, the single opening at 25% fraction will consume only 9.4% (GOSH) and 14% (ADB) of the adjusted benchmarks. Relative to the energy requirements of dual opening systems and the obvious implications of a higher (24^{o}C) heating setpoint, the possibility of using the single opening systems with less than 15% of the energy allocated is remarkable. The general pattern of heating energy for these ward designs is such that the ADB ward consumes more energy than the GOSH ward except at 25% opening fraction, when using dual openings consumes more (Table 6.11).

6.5 Predictions from computational fluid dynamics

CFD modelling is able to provide steady-state predictions of airflow movement in a space where the spatial differences in variables such as temperature and airborne contaminants can be viewed in addition to the estimated amount of time a particle has spent in a space. These sections discuss the potential for summer overheating through quantitative and qualitative evaluation of different strategies.

Five points of interests (POIs) were identified for the GOSH and ADB wards. These POIs are similar in relative positions but different in absolute coordinates due to the dissimilarities in room geometry and in location of the bed and visitor's chair in particular. These POIs are given as follows (Table 6.12) and their purpose is to enable a computation of the ventilation

metrics at those specific positions. They have previously been described in 3D by Fig. 5.5 and 5.6.

Table 6.12: Coordinates of the POIs used in this study

GOSH		**ADB**	
POI	**XYZ coordinates**	**POI**	**XYZ coordinates**
A	1.2, 3.8, 1.6	*A*	1.2, 1.5, 1.6
B	2.5, 4.24, 1.6	*B*	2.6, 2.5, 1.6
C	0.5, 5.7, 1.6	*C*	1.2, 4.5. 1.6
D	0.5, 5.7, 1.1	*D*	1.2, 4.5, 1.1
E	0.4, 4.24, 1.1	*E*	0.4, 2.5, 1.1

6.5.1 Thermal comfort and overheating potential

Using single openings in either ward type could lead to indoor thermal discomfort when outdoor temperature is up to 20^{o}C (Fig. 6.13a and Fig. 6.14a). The temperature of the ward spaces using single openings would lead to a build-up of heat due to the mixing of warm outgoing stale air and incoming fresh air. This mixing of stale outgoing air with incoming fresh air is problematic for thermal comfort and this supports the initial DTM predictions (i.e. PMV and PD values) when higher outdoor (e.g. July) temperatures were shown to pose serious risk of overheating. Single openings when used for natural ventilation in summer period will carry the risk of overheating and this may have ramifications for future concerns about resilience of hospitals to climate change as studied by Lomas and Ji (2009).

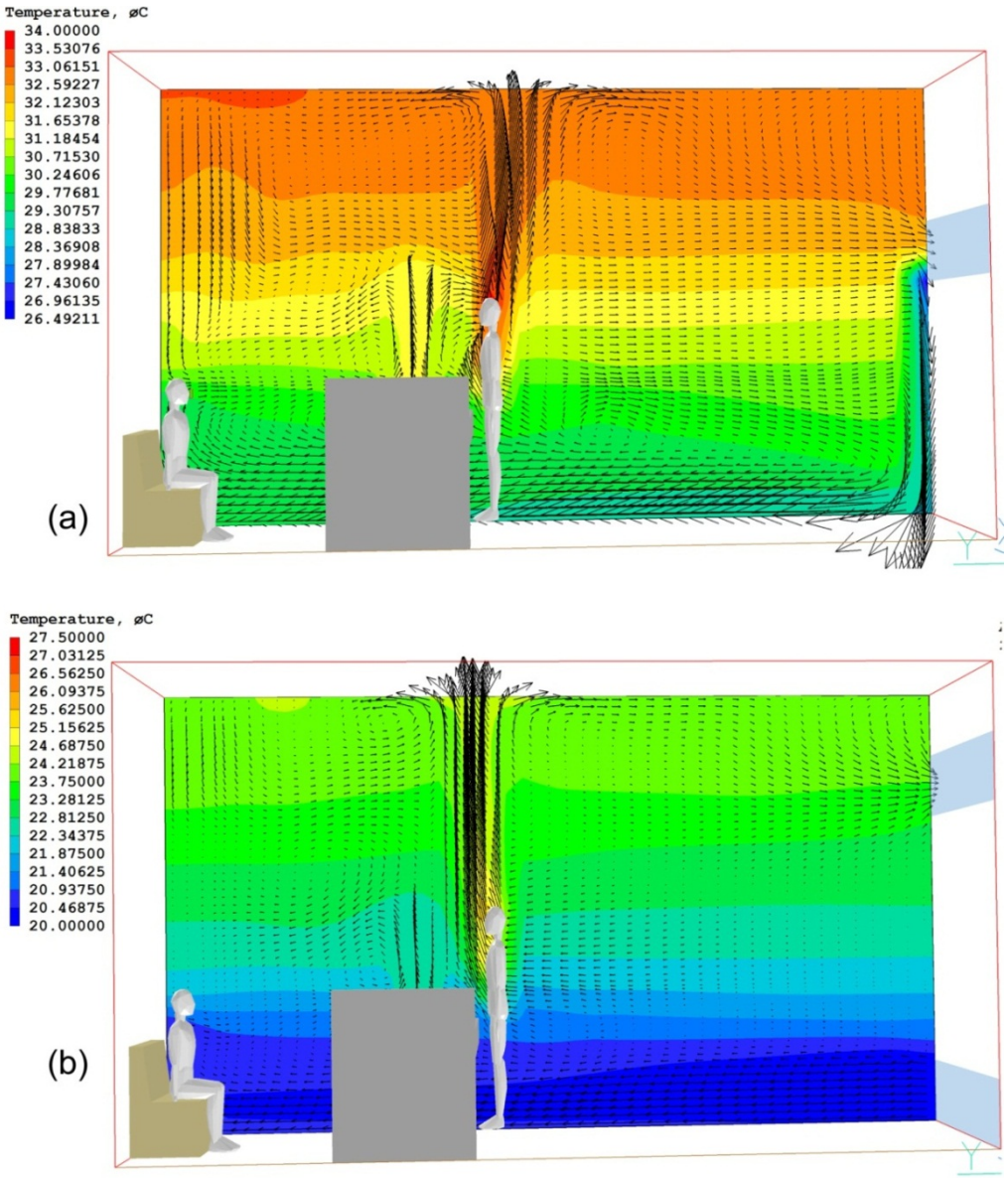

Figure 6:13: Temperature contours for GOSH ward with (a) single and (b) dual openings

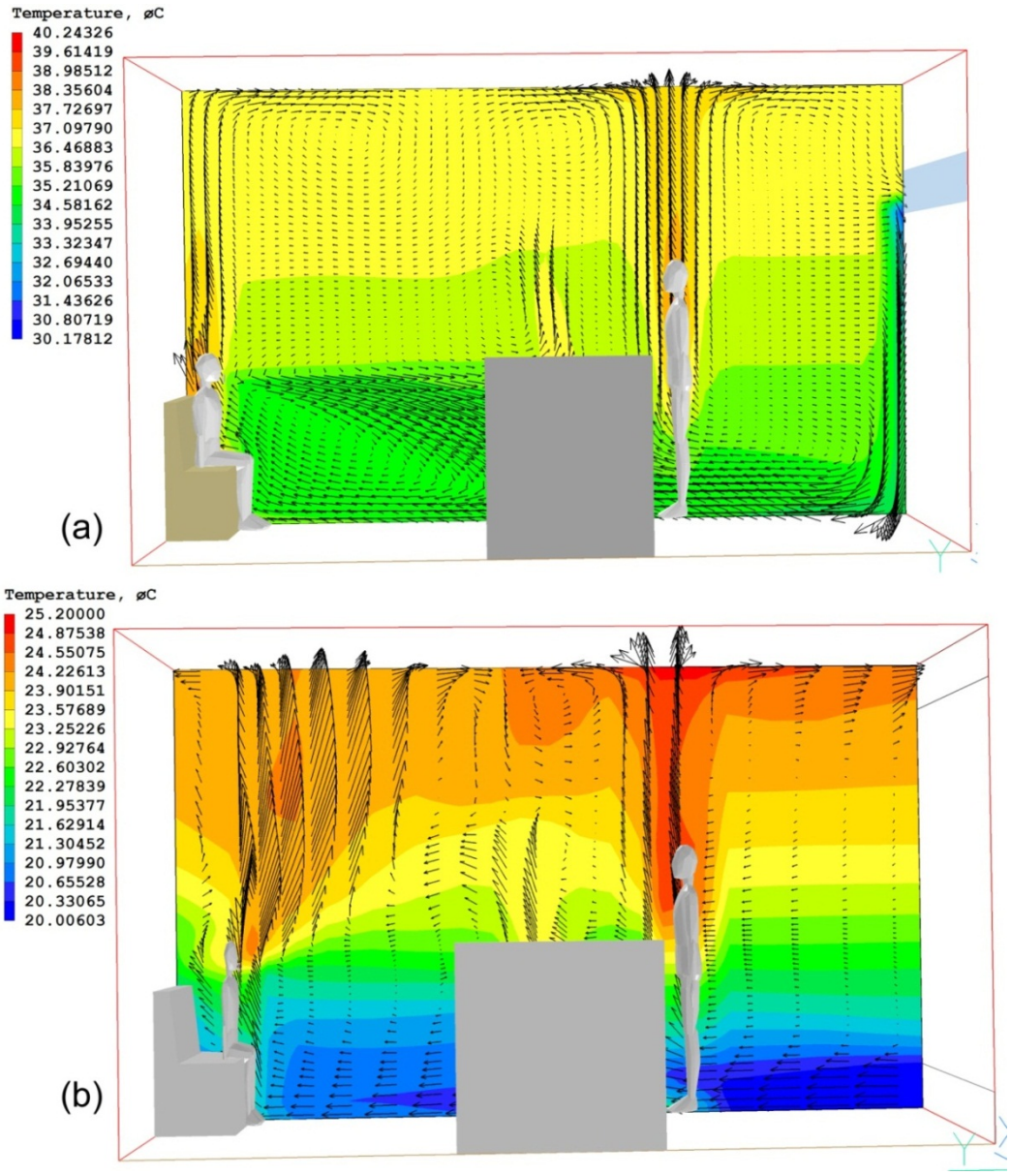

Figure 6:14: Temperature contours for ADB ward with (a) single and (b) dual openings

For single openings which would usually be elevated at some height (e.g. 1.9m in the GOSH ward) when fresh air enters the opening (at the lower/bottom portion of the single opening), three factors work against its freshness. The first is the low ventilation rate as already described by the DTM predictions. The second factor is based on the fact that outgoing air (at the upper portion of the single opening) is able to mix with it, thereby leading to deterioration in its quality (Fig. 6.15a). The third factor is that such air which is still relatively fresher than outgoing air drops to the floor level before it begins to flood the space by traveling towards the opposite end of the room encouraged by heat sources. This is because the air travels a

relatively longer distance than air from a floor level inlet would as occur with dual openings (Fig. 6.15b).

These factors are the primary reasons why the age of air is significantly higher in the single openings of the GOSH ward with incoming air having mean Age of 2092s (Fig. 6.15a) as well as in the ADB wards where the mean Age is 3167s (Fig. 6.16a). It also explains why there is an apparent lower energy need for keeping such spaces warm in winter: i.e. the system allows recirculation of indoor heat due to the entrainment of stale air with fresh air.

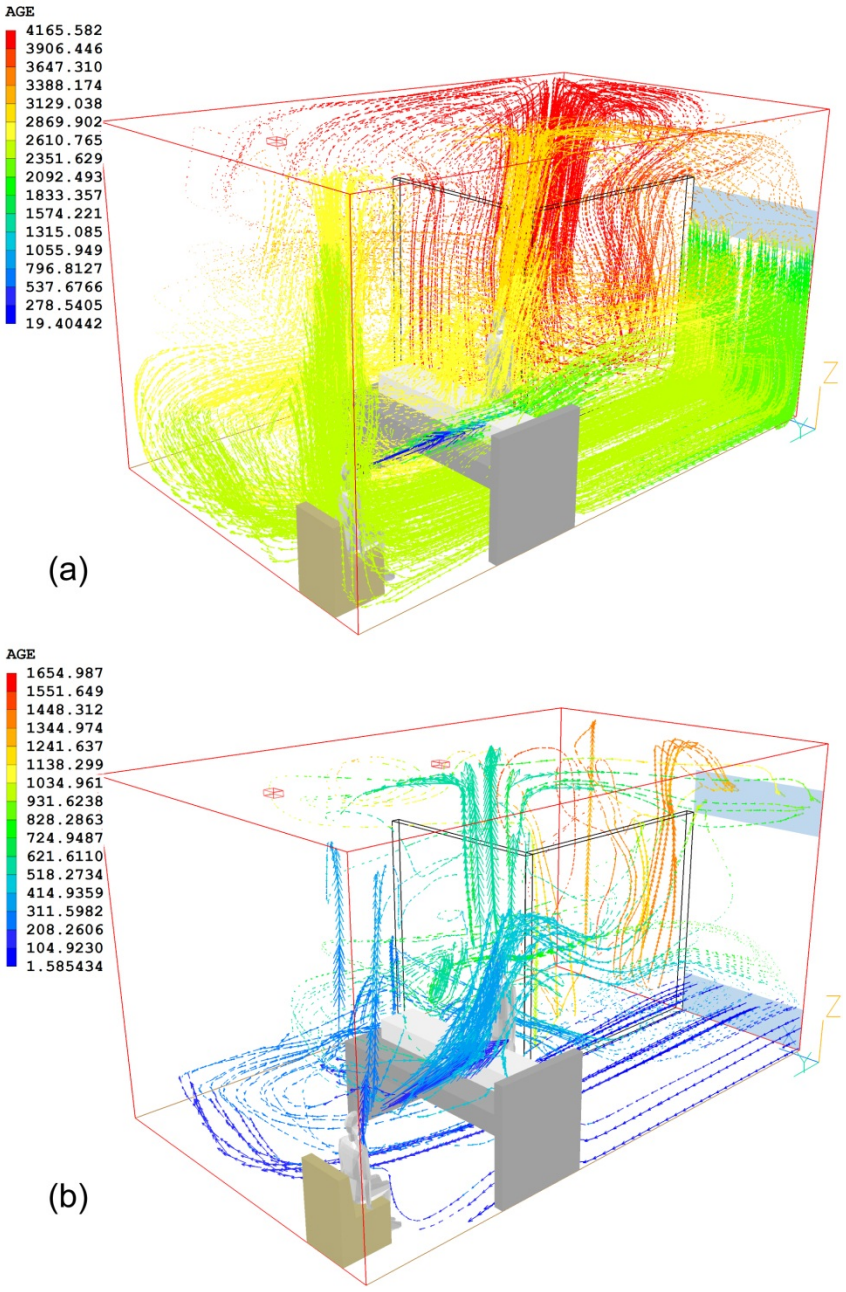

Figure 6:15: The Age of air shown as 3D streamlines for GOSH ward with (a) single and (b) dual openings

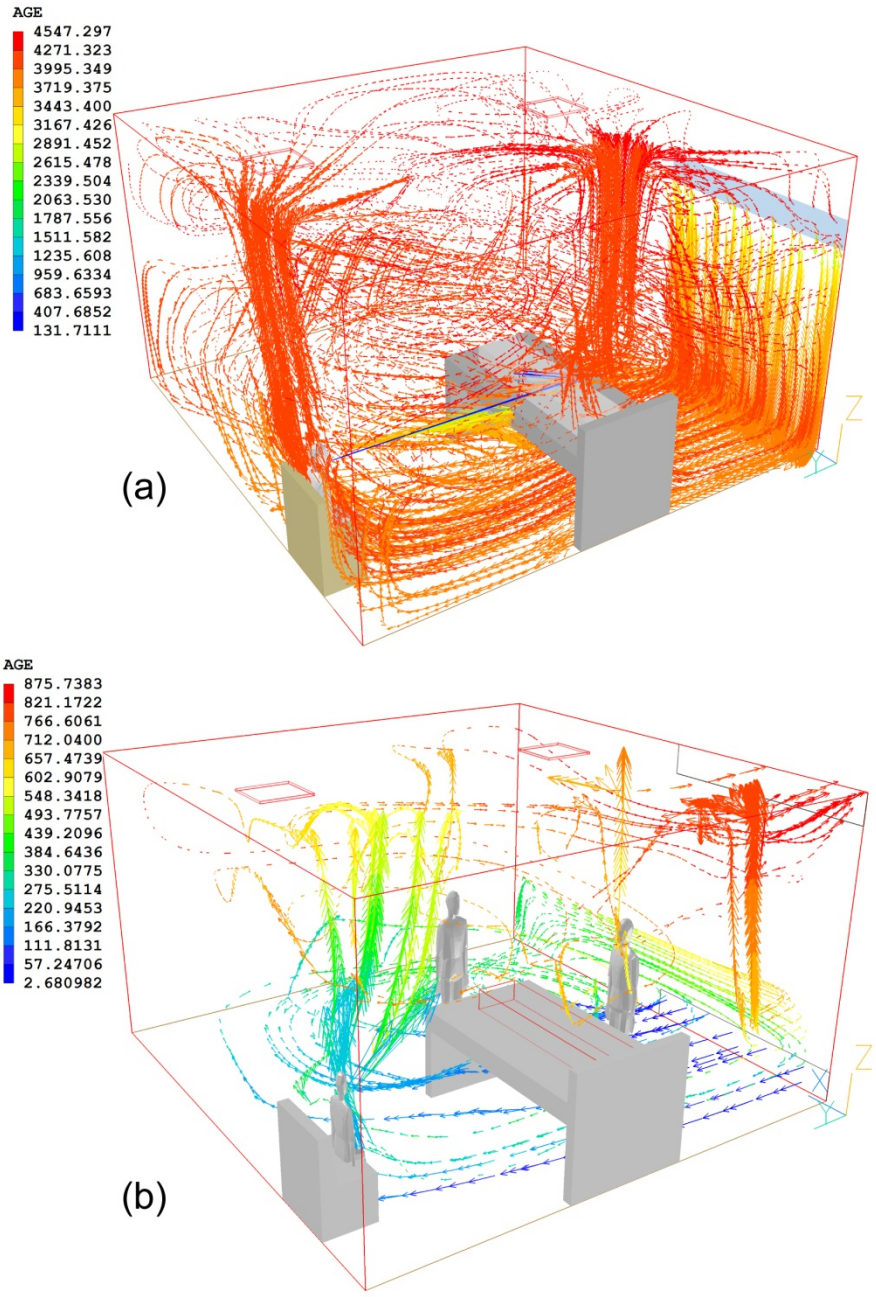

Figure 6:16: The Age of air shown as 3D streamlines for GOSH ward with (a) single and (b) dual openings

The predicted temperatures at the openings and throughout the ward spaces are also dependent on the number of openings used. In the GOSH ward with single opening, the temperature of air the point of entry is 26.4^{o}C (Fig. 6.15a) while for the ADB ward this rises to as high as 30.1^{o}C (Fig. 6.16a).

With dual openings however, the distinction of flow paths into vertically segregated inlet and outlets leads to better indoor thermal conditions for both GOSH ward (Fig 6.13b) and ADB ward (Fig. 6.14b). The benefits of dual opening system can be better appreciated against the backdrop of the relatively better thermal comfort and the significant air flow rates predicted by the DTM simulations.

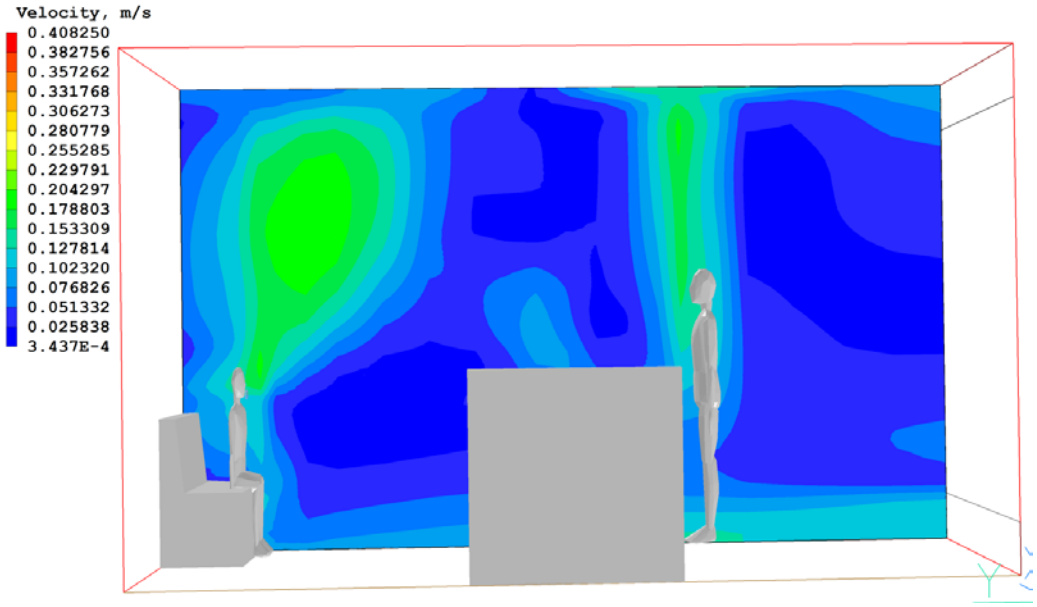

Figure 6:17: Velocity of air in the ADB ward with dual openings

Using dual openings, cooler incoming air from the low-inlets by the floor would flood the space, moving progressively across the floor e.g. at speeds of ≈ 0.17m/s (Fig. 6.17) ageing gradually as it does so (Fig. 6.15b and Fig. 6.16b). Upon meeting a major obstacle (in this case, the opposite wall), the air reverses direction and flows over the layer of incoming fresh air. The presence of occupants and indoor heat sources lead to a gradual rise in the temperature of the air making it increasingly buoyant. Subsequently, the presence of an outlet at a convenient height above the low-level inlet, allows the stale air to be removed from the space. The swift movement of air which floods the floor at the predicted speed when outdoor temperature is 20^{o}C, can still lead to sensations of draught due to the continuous ingress of the air at the predicted velocity. This problem could be pronounced in winter because even if the size of opening is optimised for proper trickle ventilation rates, the combination of speed and low temperature of incoming air could lead to sensations of draught at the floor level. Elevating the inlet to (for example) 1.0m will increase the time taken for air to reach the bed or visitor location. However, there would be penalties for thermal comfort and air quality

(freshness) due to the dual opening to behave more like a single opening as the distance between inlet and outlet reduce (see Fig. 6.18).

The efficiency of the dual opening natural ventilation system is found to be determined by four major variables: (a) the depth of the room; (b) the height/position of the outlet relative to (c) the low level inlet; and (d) the location and magnitude of the heat sources. The first three variables are static while the last one (indoor heat sources) are dynamic in location and in magnitude. Appreciating these variables will be critical for optimised application of this system in the design of naturally ventilated hospital wards. In view of the WHO's guidance which does not recommend single sided openings but in the context of existing modern healthcare facilities in developed countries which cannot dedicate more than one facade for natural ventilation, the dual opening is arguably an underestimated and underutilised system.

6.5.2 Age of air and the distance between inlet and outlet

The elevation of inlets and outlets for dual openings has an effect on the ageing of incoming air but while a reduced elevation of an outlet (e.g. GOSH outlet is only 1.9m high) has insignificant consequences for Age of air, the elevation of an inlet by 1.0m can deteriorate the incoming air. So while the vertical distance between inlet and outlet for the GOSH is smaller (1.9m) than in the ADB ward (2.1m), this fact is not observed to have any significant effect on the entrainment of outgoing stale air with incoming fresh air as would occur when inlets are elevated to a height of 1.0m (Fig. 6.18) for the ADB ward. Outgoing stale air in this context therefore refers to the rising or displaced air which is rising due to buoyancy.

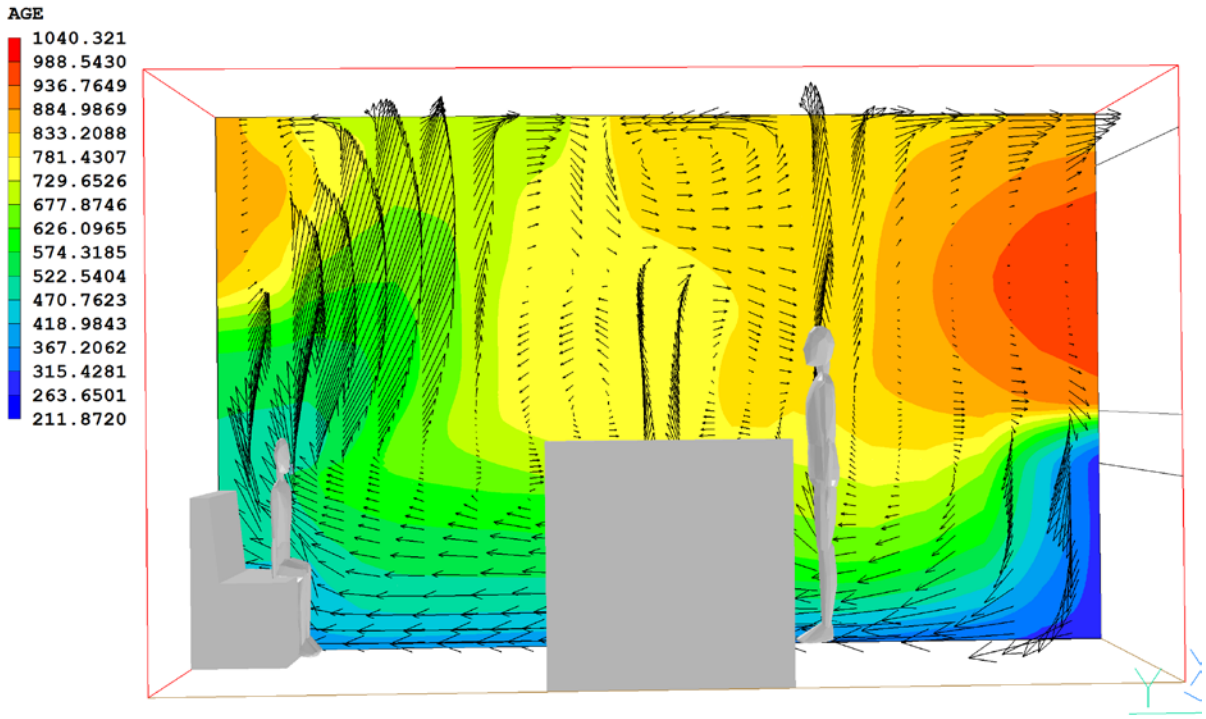

Figure 6:18: Evidence of entrainment of stale air with dual openings when inlet is elevated to 1.0m

It can be deduced that as the vertical height between inlets and outlets is reduced, the airflow characteristics tends to behave similar to single openings. This is illustrated by the results obtained (Fig. 6.19b) when in the GOSH ward fitted with low level inlet (with a height 0.5m located at 0m elevation), the incoming air was relatively fresh with mean Age of 1.6 seconds. The distance from the top of the inlet to the bottom of the outlet in this Case was 1.4m. However, as previously explained for the ADB ward, when this same distance (1.4m) was maintained but the inlet was elevated to 1.0m, there was evidence of entrainment through ageing of fresh air. This entrainment is also as a result of displaced indoor air making its way upward and so technically, is also regarded as stale air on its way to the exhaust.

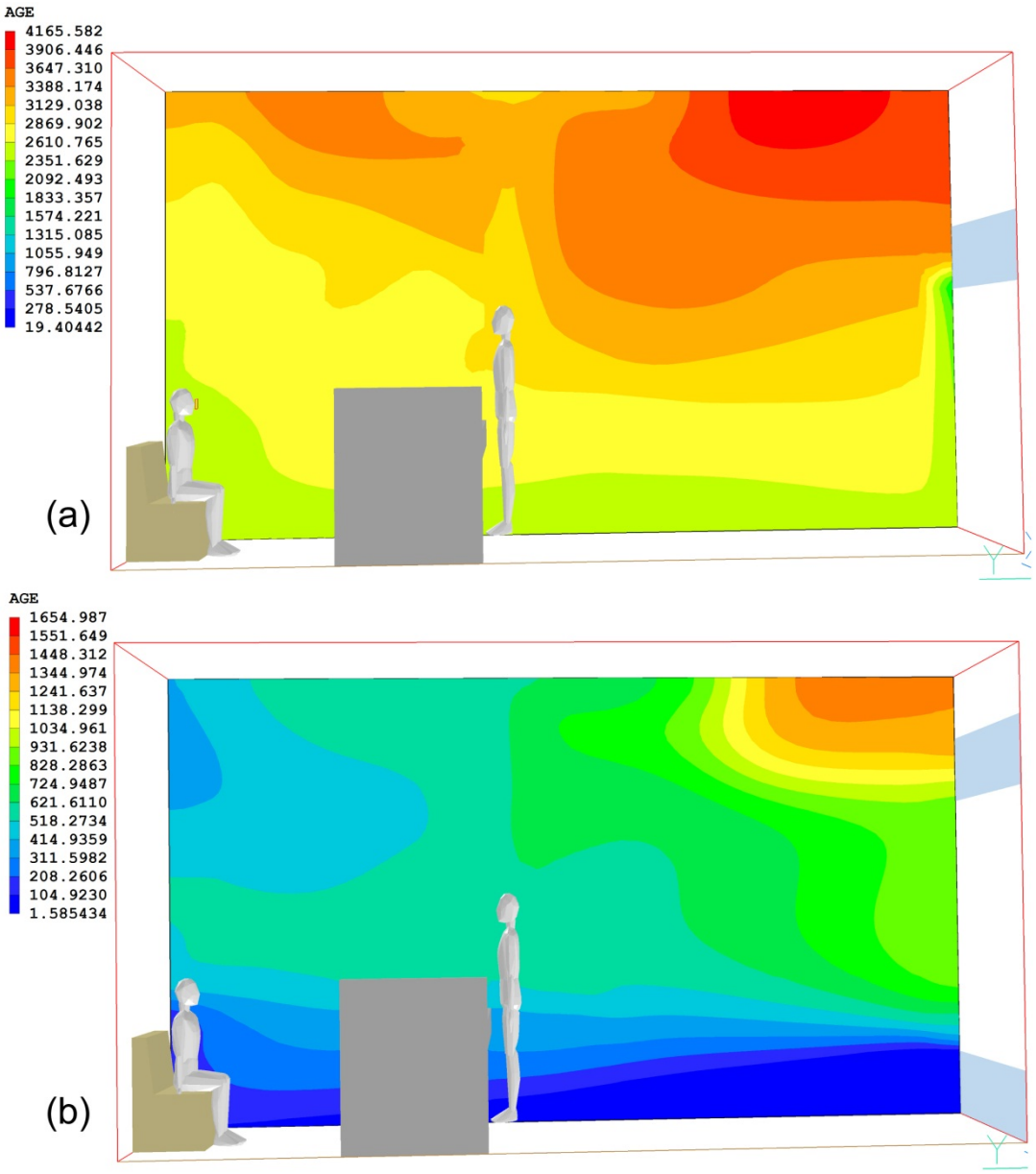

Figure 6:19: Age of air (seconds) for the GOSH ward with (a) single and (b) dual openings

Generally, the Age of air in the ADB ward (Fig. 6.20) is predicted to deteriorate more than would occur in the GOSH ward (Fig. 6.19) regardless of whether single or dual openings are used. This can be attributed to the relatively smaller size of the ADB openings. In the ADB ward, the Age of air at the vicinity of the patient's head is 407s when the inlet was at a height of 0m, but the Age increased to 542s when the inlet was raised to a height of 1.0m.

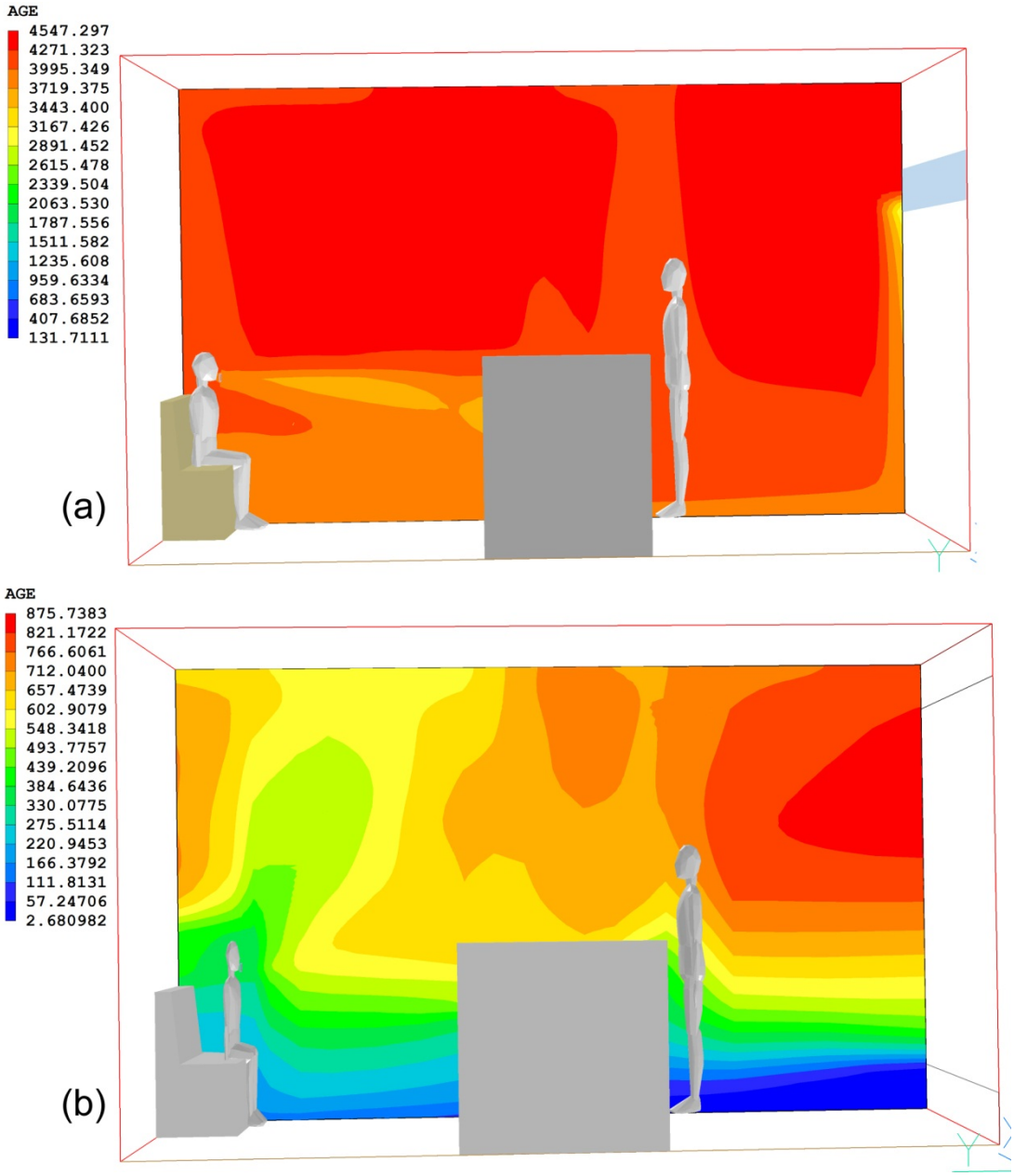

Figure 6:20: Age of air (seconds) for the ADB ward with (a) single and (b) dual openings

In evaluating of Age of air, it needs to be pointed out that the GOSH ward is of rectangular shape and in fact, based on HTM 03-01 (DH, 2007) and WHO (Atkinson, et al. 2009) recommendations, single openings are effective in providing fresh air only to a distance of 3.0m. As such, the relative high Age of air at outlets of dual openings (Fig. 6.19b) can be better appreciated when compared to the much higher Age of air in the single opening (Fig. 6.19a). However, with dual openings there is not much difference between the Age of air at the opposite end of the room for the GOSH ward (Fig. 6. 19b) and the Age of air at similar location in the ADB ward (Fig. 6.20b). The GOSH ward, it should be noted, is of larger

volume than the ADB ward. As shall be explained shortly, the Age of air at the specific POIs are nevertheless lower in the GOSH ward than in the corresponding ADB ward and this is linked to the higher ventilation rates (due to larger area of openings) of the GOSH ward.

With the ADB ward, it is interesting to note that with the inlets at 0m elevation (Fig. 6.20) the mean Age of air at the bed level is 384s (6.4 mins), whereas with the previous case when inlets were elevated to 1.0m (Fig. 6.18), the mean Age of air at the same location was 574s (9.5 mins), a difference of 190s (3 mins). The longer time taken by air in the latter case allows it more time to be pre-heated by indoor sources, which would make it a beneficial strategy for winter applications.

6.5.3 Contaminant dispersal and dilution

The use of single or dual openings expectedly has an effect on contaminant concentrations in the spaces and the differences in size of openings and room volume between the GOSH and ADB wards are also important factors. The primary metric for evaluating concentration of contaminants is contaminant removal efficiency (CRE) which is a ratio of concentration at an outlet to that of a given point, in this case, the POIs (Fig. 6.21). An acceptable or ideal CRE (based on Eqn. 2.3) should be ≥ 1, implying that complete dilution and air change at the specific point has occurred.

The contaminant concentration at the outlets of wards with dual openings are lower than with single openings due to a combination of effective ventilation, in terms actual exhausting, as well as dilution due to higher air change rate. With single openings, the measured concentration for the S-GOSH case is 28.5% while for the S-ADB case it is 25.7% compared to the dual opening scenario when measured concentrations at the outlets for D-GOSH is 13.12% and for D-ADB, it is 8.75%.

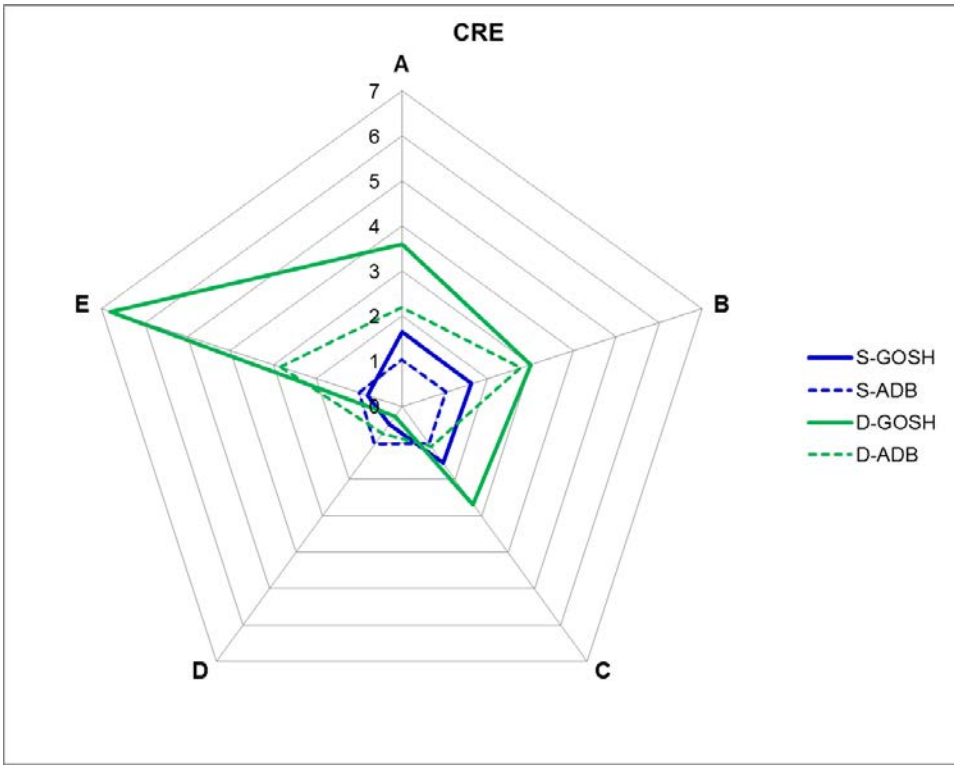

Figure 6:21: Computed CRE of the five POIs for single and dual openings in GOSH and ADB wards

The use of single openings leads to higher (i.e. desirable) CRE at Points A, B, and C for both GOSH and ADB designs, however, the absolute values of CRE in the GOSH ward are higher than those of the ADB. In fact, at these POIs, the CREs of the GOSH are between 34 and 36% better, whereas at POIs D and E, (i.e. where visitor is sitting and at the vicinity of patient's head, respectively) the CREs of the ADB are better by 52.8% and 18% respectively. This difference at Points D and E can be attributed to the shorter distance which fresh air has to travel to get to the visitors chair by the opposite wall in the ADB ward (i.e. 5.0m) as opposed to the situation in the GOSH ward, where the length from opening to visitor's chair is 6.23m. For contaminant dilution therefore, the shorter distance of travel in the ADB ward has thus overcome the disadvantage of having a smaller size of opening than the GOSH ward.

Using dual openings, the GOSH ward achieved better CREs at all POIs except at Point D by the following amounts: Point A (38.9%); Point B (7.3%); Point C (58.7%); and Point E (58.2%). At Point D, the CRE in the ADB ward is better than at the corresponding GOSH point by 63.5%. In terms of pattern of contaminant distribution (Fig. 6.22 and Fig. 6.23), the effect of dilution using dual openings is noticeable from the source location to the window in both GOSH ward (Fig. 6.22b) and ADB ward (Fig. 6.23b).

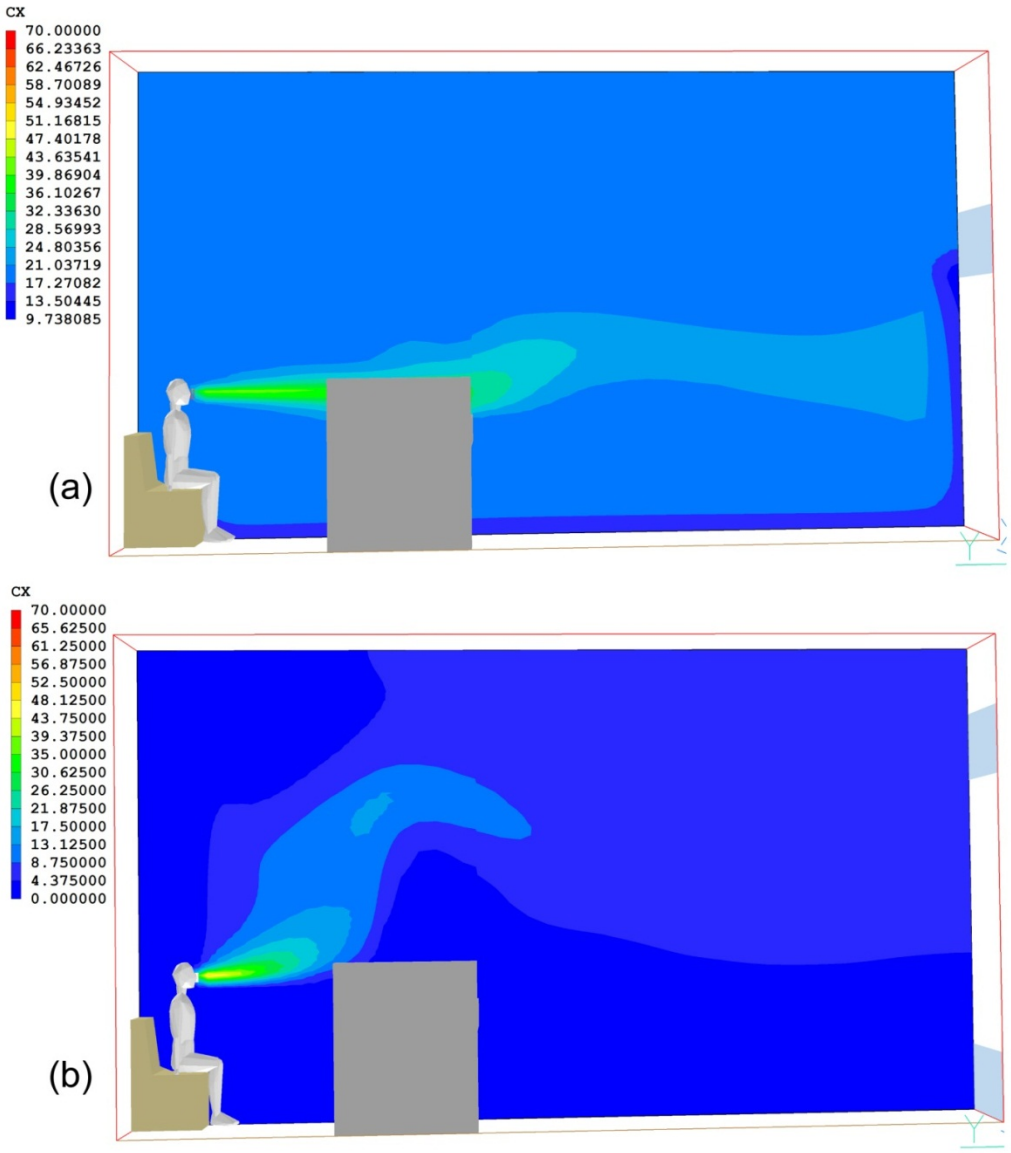

Figure 6:22: Pattern of contaminant distribution from (a) single opening and (b) dual openings of the GOSH ward

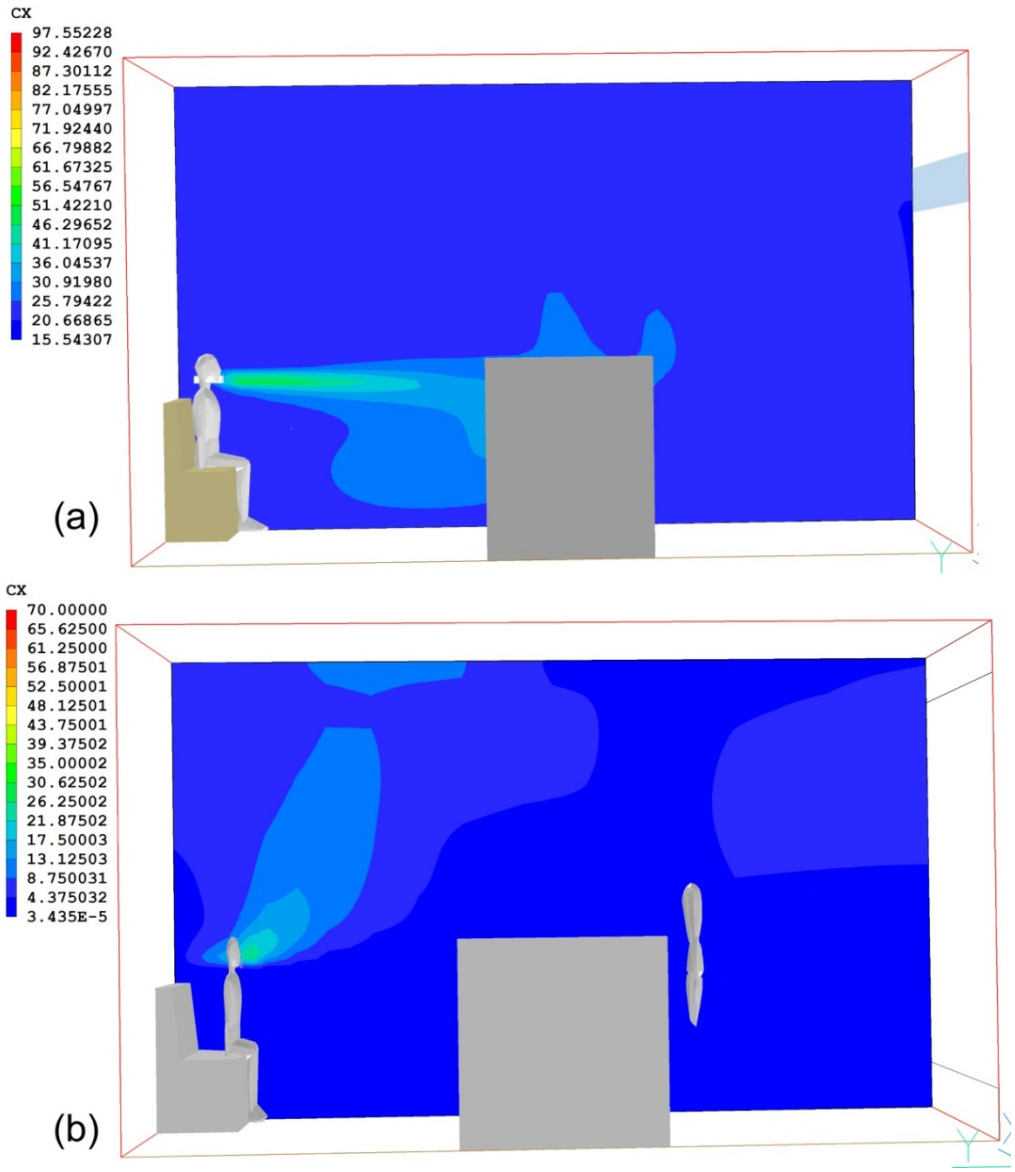

Figure 6:23: Pattern of contaminant distribution from (a) single opening and (b) dual openings of the ADB ward

This predicted reduction in contaminant concentration at the outlets of dual opening cases is supported by many factors. Firstly, the computed absolute and relative ventilation rates (with outdoor temperature of 20^{o}C) for GOSH and ADB wards using single openings are 4.0 ACH and 3.7 ACH respectively whereas with dual openings, the ACH rises to 7.2 for the GOSH and 6.3 for the ADB ward (Fig. 6.24). While this air change rate may appear smaller than rates reported in literature, it should be noted that this is from buoyancy alone, without the influence of wind pressure.

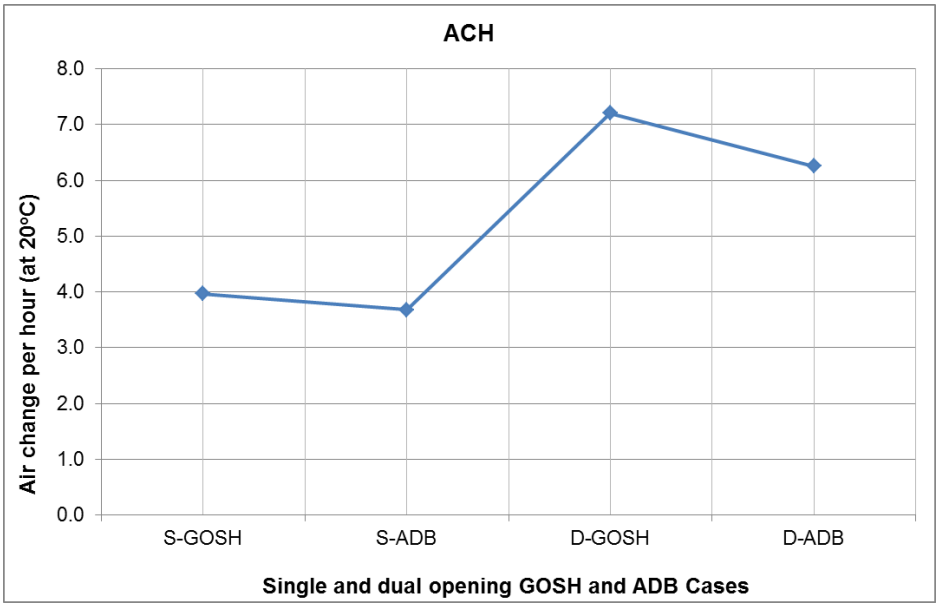

Figure 6:24: CFD Predicted air change rates for all Cases

The second reason for the reduced concentration at outlets has to do with the nominal time constant or air turnover time (ATT, from Eqn. 2.8) which is the total time taken to exhaust pollutants from a space (Fig. 6.25) which for single openings is 908s for the GOSH ward and 978s for the ADB ward. However, with dual openings, this time is reduced to 500s for the GOSH ward and 575s for the ADB ward, leading to a reduction of ≈400s in both cases.

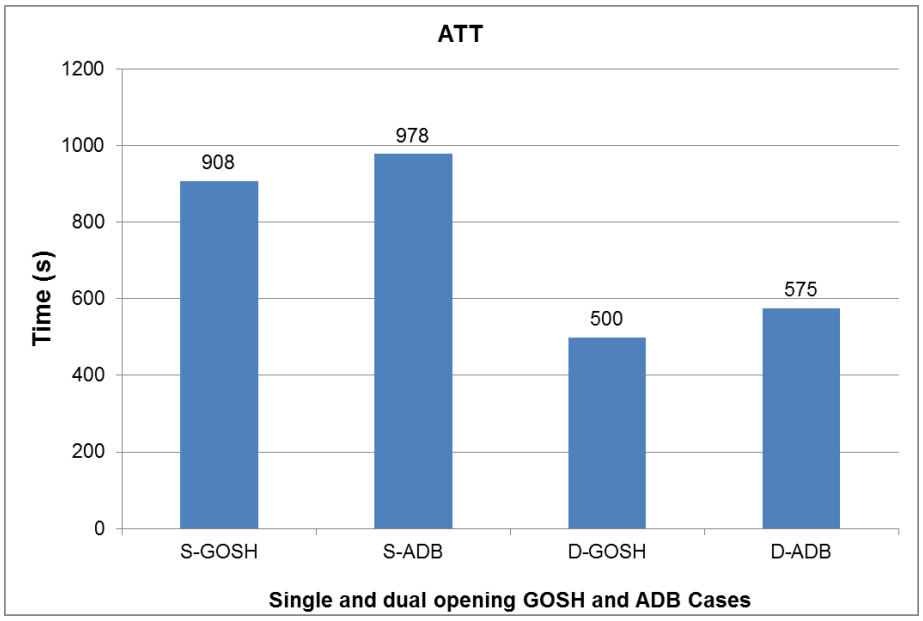

Figure 6:25: Predicted air turnover time for all Cases

It is also important to consider that although the visitor chairs are facing the patient bed and ventilation openings in the same direction in both ward types, the distance from visitor to bed is larger in the ADB than in the GOSH ward. This factor can be critical in the absolute concentrations and/or dilution of emitted contaminants at any point around the patient. Although the cough model has been used in this and subsequent studies, this was done with the knowledge that talking for five minutes can generate as much bio-aerosols as a single cough (Loudon and Roberts 1967; Loudon and Roberts 1968).

6.5.4 Evaluation of ventilation metrics

Apart from CRE, other metrics used in evaluating the performances of the ward designs include: mean air exchange efficiency (MACE) and the effectiveness of heat removal (EHR) both of which deal with the entire volume of a given space (Fig. 6.26). The MACE and EHR of the dual openings are both higher than for single openings in general, but while the EHR of the dual opening of GOSH (165.4%) is slightly better than its ADB counterpart (160%), the opposite is the case for MACE where the GOSH ward has 51.4% efficiency compared to the ADB ward (44.4%).

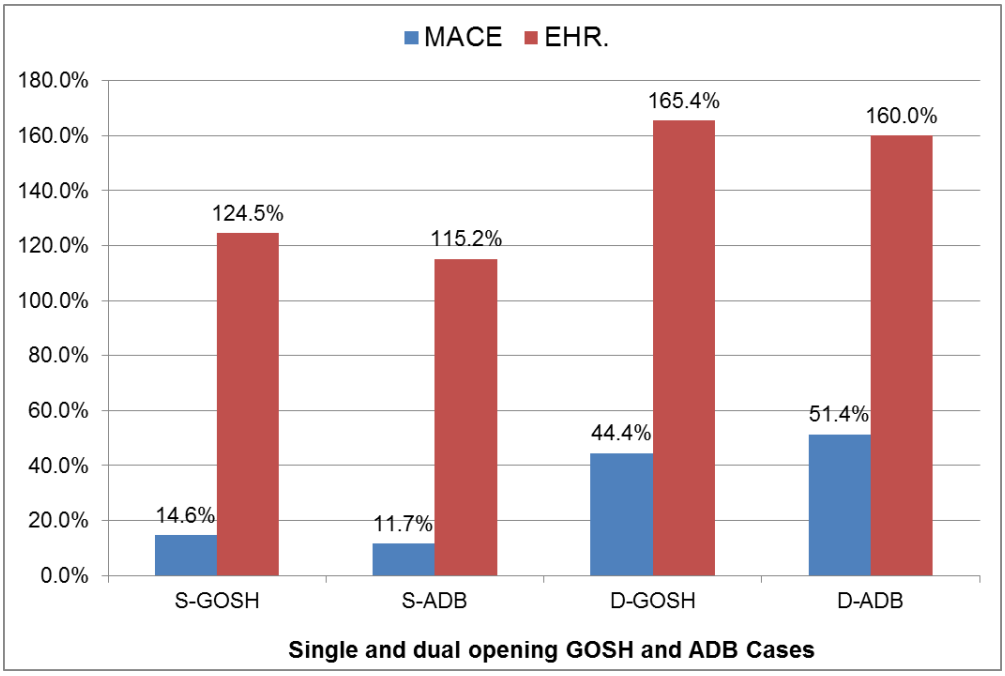

Figure 6:26: Predicted MACE and EHR values for GOSH and ADB wards fitted with single and dual openings

The other metrics are measurable at specific points and include Temperature, Age of air and local air change index (LACI) which is itself derived from Age of air. Each metric (in addition to CRE) explains a different aspect of indoor air quality (Fig. 6.27) and the information they provide about air quality are significantly different.

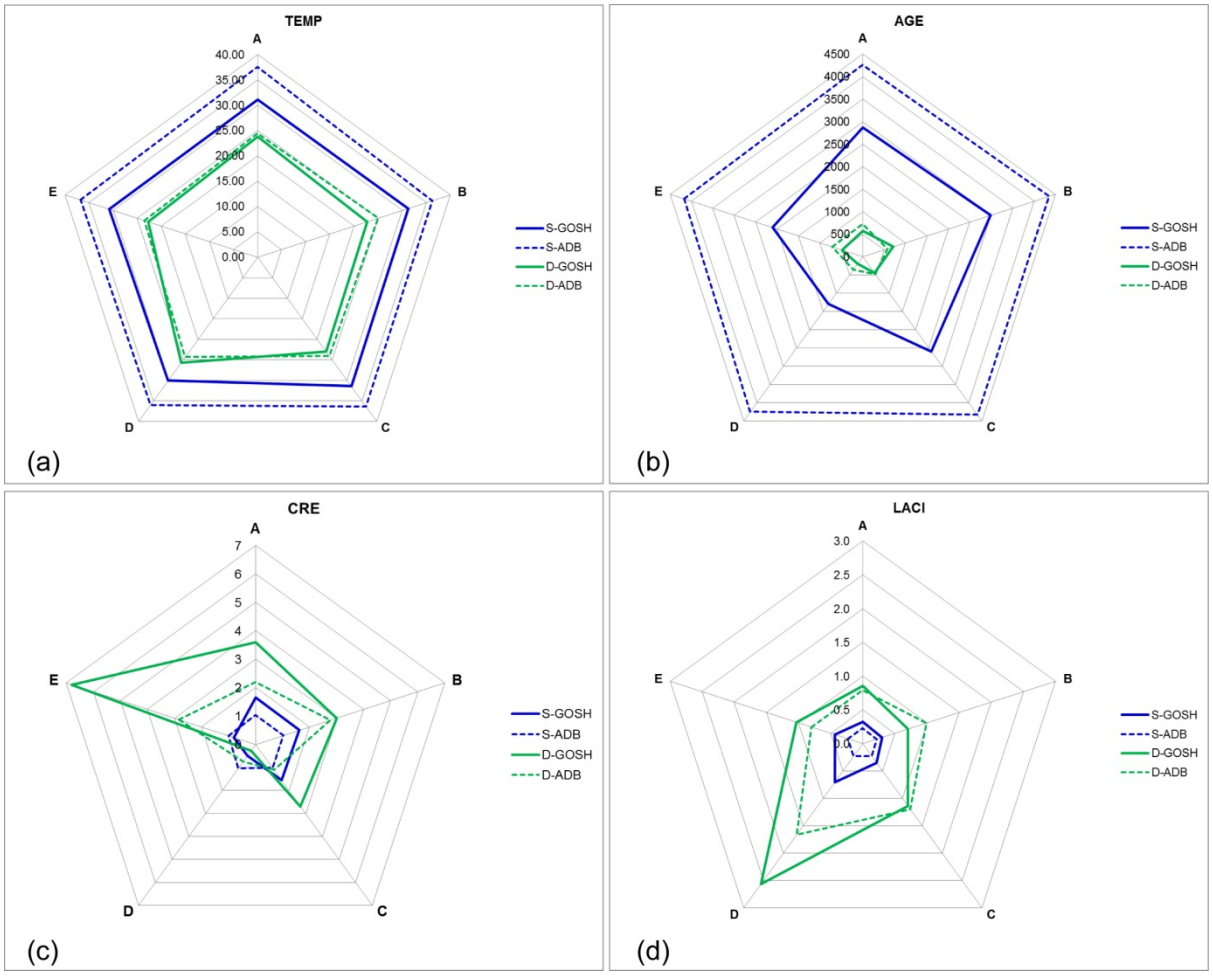

Figure 6:27: CFD results at POIs for (a) Temperature, (b) Age of air, (c) CRE and (d) LACI for the four Cases

Evaluating the performance of the GOSH and ADB ward using these metrics appears complicated due to their fundamental differences in computing the various aspects of indoor air quality at the POIs. It is difficult for instance to use one metric as a measure of how fresh the air is at any given POI. For instance, for CRE and LACI, a higher value is desirable while for Age, a lower value is indicative of the residence time (in seconds) for an air particle in a space. Evaluating temperature itself is probably more difficult due to the subjective nature of thermal comfort of which is a primary determinant. Consequently, the divergent summary of the quality of air at the POIs provided by each metric on its own is inadequate and cannot be

used as a reliable measure of how fresh the air is at a given point. Even the local air change index (LACI) is basically a different way of manipulating Age of air.

6.6 Summary

A combined study of single and dual openings applicable to buoyancy-driven natural ventilation was conducted using two different single-bed ward designs through DTM and CFD simulations. The design of the newly built Great Ormond Street Hospital (GOSH) ward provided an opportunity to investigate the performance of the single openings based on the existing design which had a 1.9m high top-hung window. For the purpose of this study, this opening was assumed to be a louvered vent of the same area. The impact of having a lower opening to function as an inlet was therefore an interesting consideration. For the schematic ADB ward, empirical models were used to size the single and dual openings, which were also investigated for their performances. Studying these rather different designs of single-bed wards together has brought about two advantageous findings.

First, the weaknesses of the single opening system were understood, relative to its closest SNV counterpart, the dual opening system. Secondly, the dual opening was shown to be capable of meeting the ventilation needs of single bed wards from the airflow rates, thermal comfort, heating energy needs and bio-aerosol control perspectives. A simultaneous study of both systems has shown the relative complications in existing metrics used in evaluating the quality of indoor air.

CHAPTER 7: Study 2: Inlet and stack systems

7.1 Introduction

The single-cell inlet and stack natural ventilation system is a composite group of various configurations of air inlets or supply shafts with exhaust stacks. Examples of these configurations are found in the classification by CIBSE (2005, p. 47) under 'Case 6' as well as the advanced natural ventilation (ANV) of Lomas, (2007). In ANV, labyrinths could also be used to channel supply air and this approach has been described in two studies (Short and Al-Maiyah, 2009; Lomas and Ji (2009).

The single-cell inlet and stack system modelled in this study are for two distinct ward designs. The first type is based on the generic ADB ward, where a simple inlet and an exhaust stack are used. The interior layout for this space is exactly the same as for other ADB spaces used in the research, with a floor area of $25m^2$. The second ward type is more sophisticated in its configurations. It has an en-suite bathroom and supply air is delivered through shafts connected to underground labyrinths. This design is obtained from existing studies (Lomas and Ji, 2009; Short and Al-Maiyah, 2009) which describe the architecture and ventilation potential of the edge-in edge-out (EIEO) strategy for single-bed wards. This design shows a three-floor vertical arrangement of shafts and stacks. This ward is similar to the ADB ward in floor area ($25.92m^2$) even though dimensionally, it is more oblong than square (7.2m x 3.6m).

7.2 Need for the investigation

The generic ADB ward is used as a template for investigating the feasibility of buoyancy-driven natural airflows by applying inlet and stack system on the design. It is expected that this can be beneficial as an alternative natural ventilation system in future. The research questions linked to this ward design include the impact that size and location of both inlets and stacks have on airflow within the space. For the second ward type, Lomas and Ji (2009) have already provided a general performance assessment regarding the climatic resilience of the proposed schematic single-bed ward design by Short and Associates (Short and Al-Maiyah, 2009). Their findings from the dynamic thermal modelling (DTM) of the wards which were fitted with ANV included the airflow rates achievable under different future

climatic conditions for various geographic locations. This study has thus provided insights into ventilation efficiency, i.e. the capacity of the ANV to deliver the required airflow rates into this proposed ward, which can always be evaluated against existing guidelines. Although the expected differences in airflow rates due to weak buoyancy forces in summer have been considered by modelling an exhaust fan, other related and important questions remain unanswered. These have been summarised below as part of key goals for investigating the single-cell inlet and stack systems in general.

7.2.1 Purpose of investigation

The specific goals of this investigation include the following.

1. **ADB ward:** The effectiveness of the ventilation design i.e. the actual performance of supplied air in providing comfort, dilution and heating energy consumed over different seasons, needs evaluation. These will be done through DTM primarily by comparing the heights of inlets and the location of stacks in terms of bulk annual airflow and through computational fluid dynamics (CFD) by appraising the pattern of room air distribution and contaminant movement.

2. **ADB and S&A ward:** The ideal size of opening required to maintain minimum trickle rates of ventilation in winter need to be computed and justified. This applies to both the ADB and the S&A ward spaces.

3. **S&A ward**: There are three floors in this schematic design and the heights of supply shafts and exhaust stacks vary per floor. The variations in stack heights are likely to influence flow rates into the three different floors and although this issue was considered by Lomas and Ji, (2009) and it influenced their decision to model the third floor ward (for a different set of objectives). The absolute differences in flow rate relative to the lower wards were not quantified, leaving an interesting gap in knowledge of the performances of these wards. There is thus a need to investigate the extent to which volume flow rates actually vary between the wards on lower floors and those of upper floors, and whether each floor is able to meet 60 l/s/patient as recommended by WHO (Atkinson, et al., 2009) or by the 6 ACH recommended by HTM 03-01 (DH, 2007). This has to be ascertained for assessing ventilation

performance in periods when there is no need for assistance from fans and airflow is dependent on buoyancy forces only. This would be for significant periods of a year.

4. **S&A ward**: There is an absence in literature, of detailed airflow studies using CFD about the patterns and direction expected in the schematic design of the S&A ward. This gap in knowledge is critical for two further reasons.

    a) The presence of an obstacle (bathroom) directly in front of the supply inlets suggests that fresh air flowing via displacement would take longer to reach the patient's bed. The time taken by air particles to reach a point is measured using Age of air, which not only indicates staleness but additionally, as fresh air takes longer to reach a desirable target; its temperature would rise due to indoor heat sources, further deprecating the IAQ.

    b) Since the air inlets are also displaced to different extents horizontally, the path taken by fresh air would vary according to the extent of displacement between the inlet and the edge of the bathroom. This led to a hypothesis that not only would each floor experience different room air distribution but also, the expected deterioration in IAQ would vary according to inlet location, which in turn varies from floor to floor.

This chapter therefore describes the series of investigations executed using DTM and CFD simulations of inlet and stack system as applied to these two unique single-bed ward designs. For the ADB ward type it was important to understand the rates, pattern and direction of airflow achievable from EIEO and EICO strategies. For the S&A ward, CFD investigations were conducted to predict the impact which the bathroom and the effect which the different locations of inlets (per floor) would have on IAQ of the given space; while DTM was executed to investigate airflow and energy variances due to differential stack heights.

7.2.2 General assumptions for the investigations

For the DTM analysis, the site location was taken as Birmingham. With the exception of the facade wall and the adjoining shafts/stacks, all other surfaces were assumed to be adiabatic. The facade wall was of composite brick and concrete construction with a collective U-value

of 0.35 W/m^{2}K. The shaft/stack construction material was assumed to be insulated and monolithic concrete of similar U-value to the facade wall. Two heating setpoints of 18 and 20^{o}C were assumed. Occupancy was scheduled as intermittent with an assumption of 120W gain at peak time from each occupant (sensible heat of 65W and latent heat 55W). Heat gain from lighting accounted for 70W, scheduled to be dimmed between 10:00pm and 06:00am based on deductions from a preceding study by Lomas and Ji (2009) and from expected/logical practices in such facilities. Heat from equipment was assumed to be 75W and constant. The schedule created for constant and intermittent indoor heat sources was created (Fig. 7.1) to mimic the constant operation of equipment and occasional presence of occupants (healthcare workers, visitors) and the use of lighting.

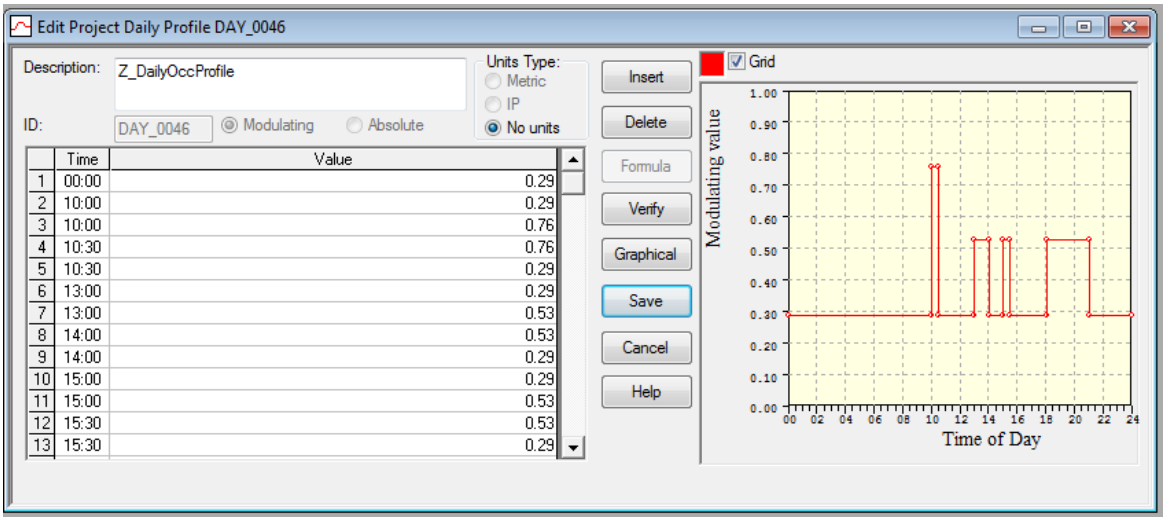

Figure 7:1: Scheduled profile of daily internal heat sources

For the ADB ward, the size of openings (inlets and stacks) was taken as 1.5% of the floor area or 0.375m^2, approximated to 0.4m^2 for convenience. The initial size of inlet was 0.3 x 1.25m which was later reduced in CFD to 0.075 x 1.25, i.e. 25% of the original size for modelling trickle ventilation in winter. Stack size was kept at 0.5 x 0.8m and a height of 3.0m was assumed for the sake of simplicity. The boundary conditions used for CFD simulations have been outlined in Chapter 5 (Methodology). However, the ADB wards typically required 6,000 iterations as opposed to the S&A Ward where 9,000 iterations were needed for convergence to occur. In the DTM, the opening fractions of inlets and outlets that were investigated were 6%, 12.5%, 25%, 50%, 75% and 100%. The lowest three were intended to represent trickle rates in winter while the others were used for summertime cooling. The ADB and the S&A wards were investigated under buoyancy (wind-neutral) conditions. In

particular, for the S&A ward, this replicates the actual proposed design where airflow is from an underground labyrinth.

7.3 Results of the generic ADB ward

7.3.1 Dynamic model: effects of elevation of inlets

Four different combinations of inlet heights and stack locations were created for the dynamic thermal model (Table 7.1), giving rise to four distinct cases of the generic ADB ward.

Table 7.1: Differences in the four ADB ward cases

	Inlet elevation	**Stack location**
Case 1	0.0m	Centre-out
Case 2	2.0m	Centre-out
Case 3	0.0m	Edge-out
Case 4	2.0m	Edge-out

From an initial overview of the predicted airflows from dynamic modelling, it was discovered that differences in stack location (i.e. centre-out or edge-out) do not produce different results. This is due to the well-mixed zone assumption applied for bulk air flow in dynamic models. Any differences in room air distribution are beyond the capabilities of dynamic thermal models. Therefore, for the sake of simplicity, only the results of: Case 1 (Fig. 7.2a) and Case 2 (Fig. 7.2b) will be reported under dynamic modelling sub-section of this Chapter.

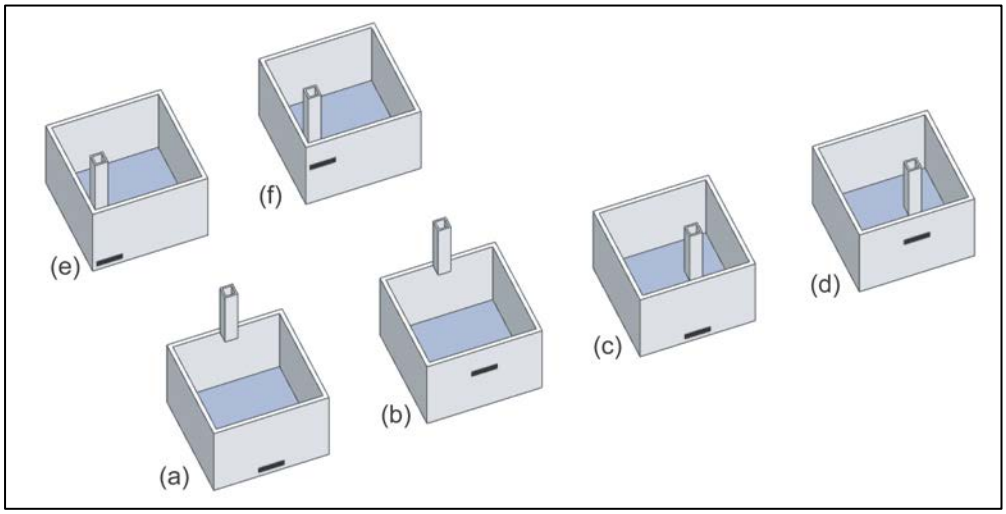

Figure 7:2: Schematic 3D representation of inlet and stack cases showing: (a) Case 1 (b) Case 2 (c) Case 3 (d) Case 4 (e) Case 5 (f) Case 6

The expected differences in pattern and direction of air movement which is likely to occur with the edge-out strategies i.e. Case 3 (Fig. 7.2c) and Case 4 (Fig. 7.2d) are included in the subsection on CFD studies. This would be in addition to new configurations where inlets and stacks are placed at the extreme corners of the ward (Fig. 7.2e and Fig. 7.2f).

7.3.2 Differences in airflow rates: Effect of inlet heights

7.3.2.1 Winter season

For winter, the openings were assumed to be constricted at 6, 12.5 or 25% or their design size for the purpose of determining the most suitable or practical trickle ventilation rate that would not compromise on comfort, air quality and energy. Additionally, it was essential to investigate the comparative differences in energy obtained from heating setpoint of 18^{o}C of HTM 03-01 and from CIBSE's 20^{o}C. Taking January as a representative month for winter period, the predicted results for these heating setpoints were evaluated for 6% opening fraction (Fig. 7.3a), for 12.5% opening fraction (Fig. 7.3b) and for 25% opening fraction (Fig. 7.3c).

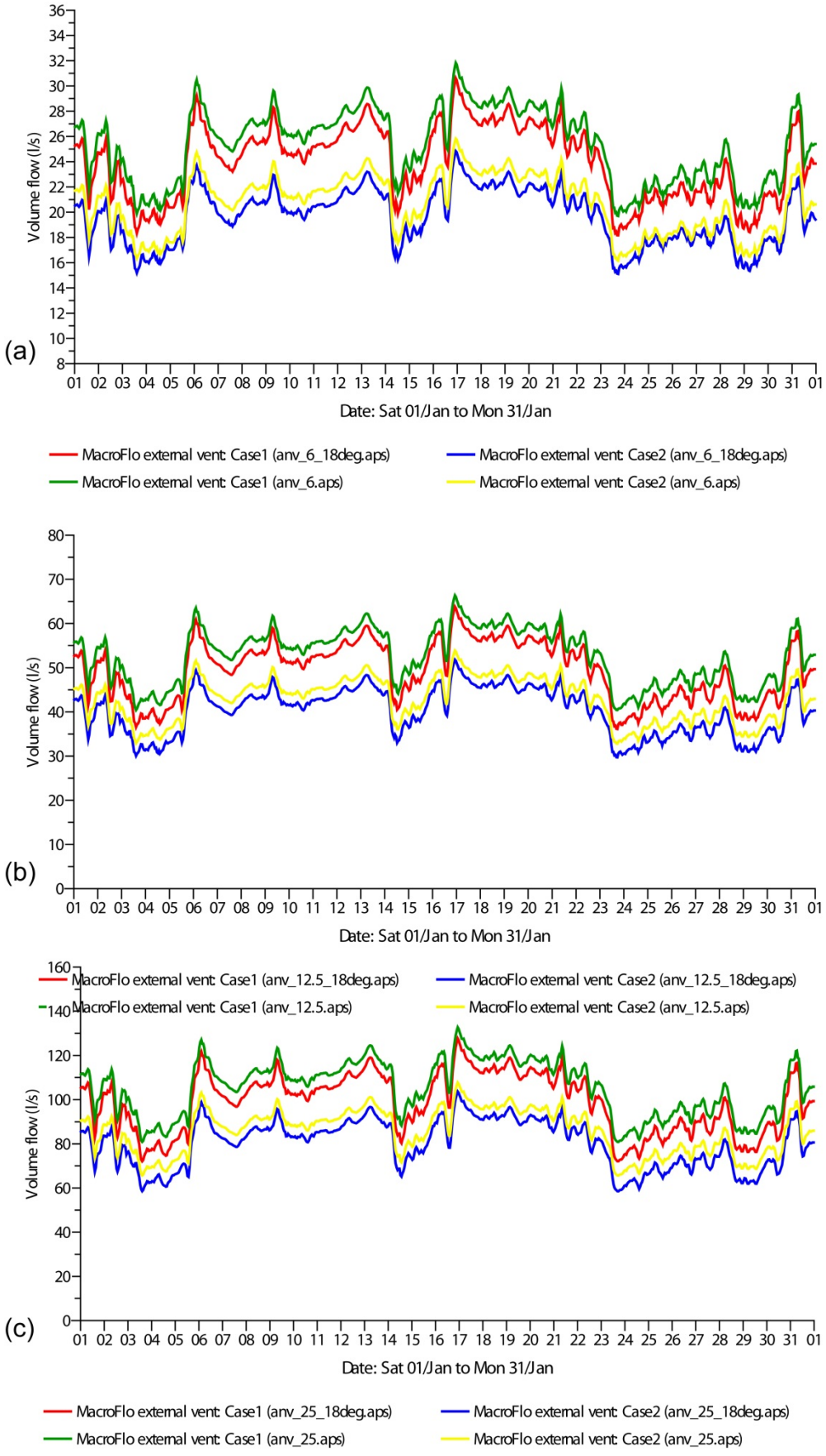

Figure 7:3: Airflow into Case 1 and 2 at 18 and 20°C setpoints for (a) 6% (b) 12.5% (c) 25% opening fractions

Generally, airflow rates in Case 1 are expectedly larger than flows in Case 2 due to the larger height difference between the floor level inlets (height = 0m) and the stack outlet which is 6m from the floor level. However, the magnitude of differences between the mean flows into these wards diminishes in a slightly disproportionate way as the opening fraction reduces from 25% to 6% and as the heating setpoint is reduced from 20 to 18^{o}C. For instance, the mean flow (Fig. 7.4), in Case 1 at 25% and 20^{o}C is 15.2 l/s or ≈ 23% more than the flow in Case 2 at similar conditions. However, the difference between these two cases at the extreme end, where the opening fraction is 6% and heating setpoint is 18^{o}C is 3.1 l/s or ≈21%.

It can, therefore, be deduced that regardless of actual size of constriction, when air inlets are taken from floor level (0.0m) up to lintel level (2.0m); there is likely to be a slight reduction in airflow depending on the heating setpoint. This marginal drop in flow rates when heating setpoints are either 18 or 20^{o}C is in the range of 21 to 23%. It is also found (Fig. 7.4 below) that in winter, the minimal conditions necessary to achieve 60 l/s/patient is with 18^{o}C heating setpoint and at 25% opening fraction.

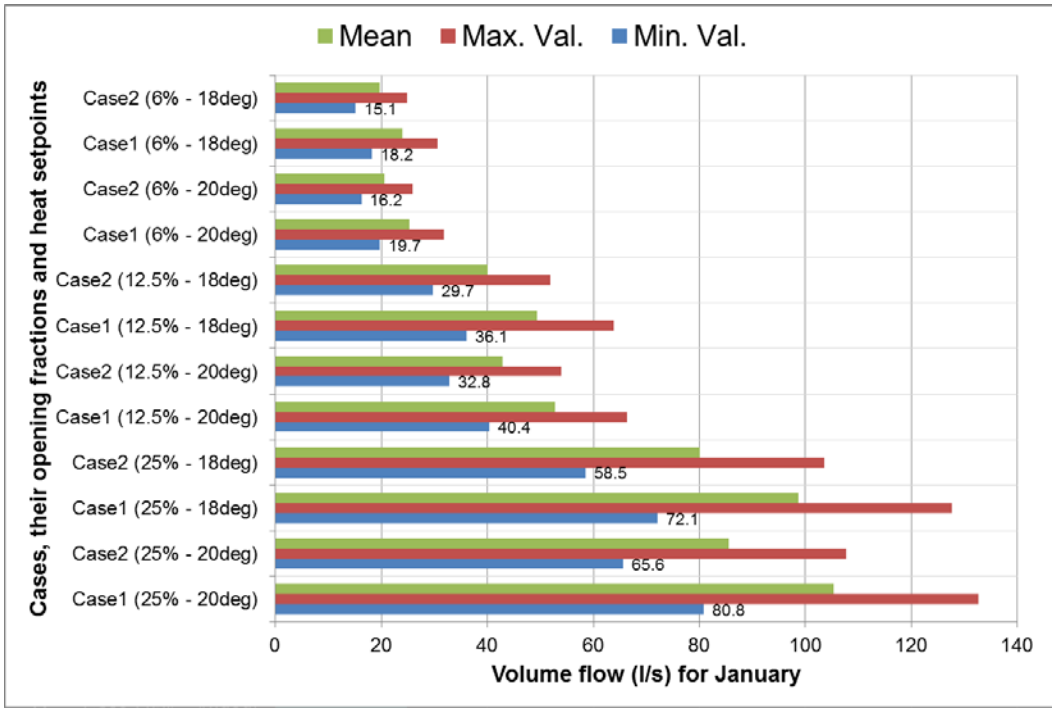

Figure 7:4: Volume flow for three opening fractions and two heating setpoints in January

This deduction can be helpful in determining if the smallest design size for trickle ventilation (e.g. 6%) is adequate to meet healthcare ventilation rates which from the above, is not in the

affirmative. However, this is assuming that the WHO 60 l/s/patient is taken as minimum rate of ventilation even in winter. This is unlikely to be practical because from Fig. 7.3 above, this rate can only be achieved with 25% opening at 18^{o}C heating setpoint. The implication of these two parameters on heating energy and thermal comfort will be discussed in section 7.33.

7.3.2.2 Summer season

August was selected as a representative summer month. The variations in volume flow were predicted to vary significantly between Case 1 and Case 2 (Fig. 7.5). This variation is attributable to the elevation of inlets. The mean difference was found to be as high as 39.5 l/s in favour of Case 1 where inlets are at floor level and at 100% opening fraction. The difference is 29.7 l/s at 75% opening fraction and 19.8 l/s at 50% opening fraction.

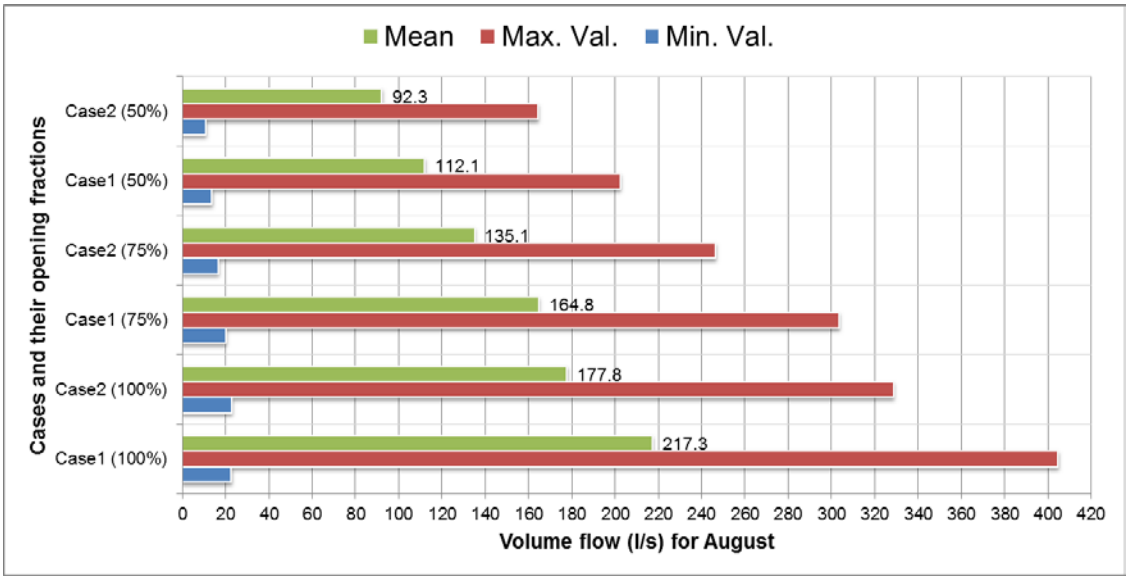

Figure 7:5: Volume flow for two opening fractions and two heating setpoints in August

The ventilation rates predicted for 50, 75 and 100% opening fractions in August (Table 7.2) for Case 1 were as high as 19.14 ACH while for Case 2 they were up to 15.54 ACH.

Table 7.2: Relative ventilation (ACH) for 50, 75 and 100% opening in August

Cases (opening fractions)	Minimum ACH	Maximum ACH	Mean ACH
Case 1 - (50%)	0.65	9.57	5.3
Case 2 - (50%)	0.51	7.77	4.37
Case 1 - (75%)	0.95	14.36	7.79
Case 2 - (75%)	0.79	11.66	6.39
Case 1 - (100%)	1.07	19.14	10.28
Case 2 - (100%)	1.08	15.54	8.41

7.3.3 Differences in thermal comfort

Thermal comfort in these wards is assessed through the predictions for PMV, DRT and PD and for winter, indoor heating is able to keep both values within acceptable ranges. The mean PMV/DRT values for the month of January (Table 7.3 and Fig 7.6) is within the neutral range: -0.19/20.27^{o}C for Case 1; and -0.2/20.21^{o}C for Cases 2 a setpoint of 20^{o}C at 12.5% opening fraction. At 25% opening fraction, the monthly mean PMV/DRT values are -0.14/20.61^{o}C for Case 1 and -0.16/20.48^{o}C for Case 2.

Table 7.3: Minimum, maximum and mean PMV, DRT and PD values for Case 1 and Case 2 in January

	Min. Val.	**Min. Time**	**Max. Val.**	**Max. Time**	**Mean**
Predicted mean vote: Case1 (25%)	-0.19	16:30,30/Jan	-0.07	13:30,06/Jan	-0.14
Predicted mean vote: Case2 (25%)	-0.21	16:30,30/Jan	-0.1	13:30,06/Jan	-0.16
Predicted mean vote: Case1 (12.5%)	-0.23	02:30,12/Jan	-0.11	13:30,24/Jan	-0.19
Predicted mean vote: Case2 (12.5%)	-0.24	02:30,12/Jan	-0.08	13:30,05/Jan	-0.2
Dry resultant temperature: Case1 (25%)	20.24	01:30,24/Jan	21.15	22:30,16/Jan	20.61
Dry resultant temperature: Case2 (25%)	20.18	01:30,24/Jan	20.94	12:30,18/Jan	20.48
Dry resultant temperature: Case1 (12.5%)	20.08	05:30,29/Jan	20.65	13:30,22/Jan	20.27
Dry resultant temperature: Case2 (12.5%)	20.05	05:30,29/Jan	20.8	13:30,22/Jan	20.21
People dissatisfied: Case1 (25%)	5.1	13:30,06/Jan	5.76	16:30,30/Jan	5.41
People dissatisfied: Case2 (25%)	5.19	13:30,06/Jan	5.89	16:30,30/Jan	5.54
People dissatisfied: Case1 (12.5%)	5.24	13:30,24/Jan	6.13	02:30,12/Jan	5.76
People dissatisfied: Case2 (12.5%)	5.13	13:30,05/Jan	6.23	02:30,12/Jan	5.82

The closeness in predicted mean PMV and mean DRT values at both 12.5% and 25% fractions is remarkable (Table 7.3) as even the maximum and minimum values for the entire January share such closeness. This explains why the monthly mean percentage dissatisfied at both fractions is below 6% for both Cases.

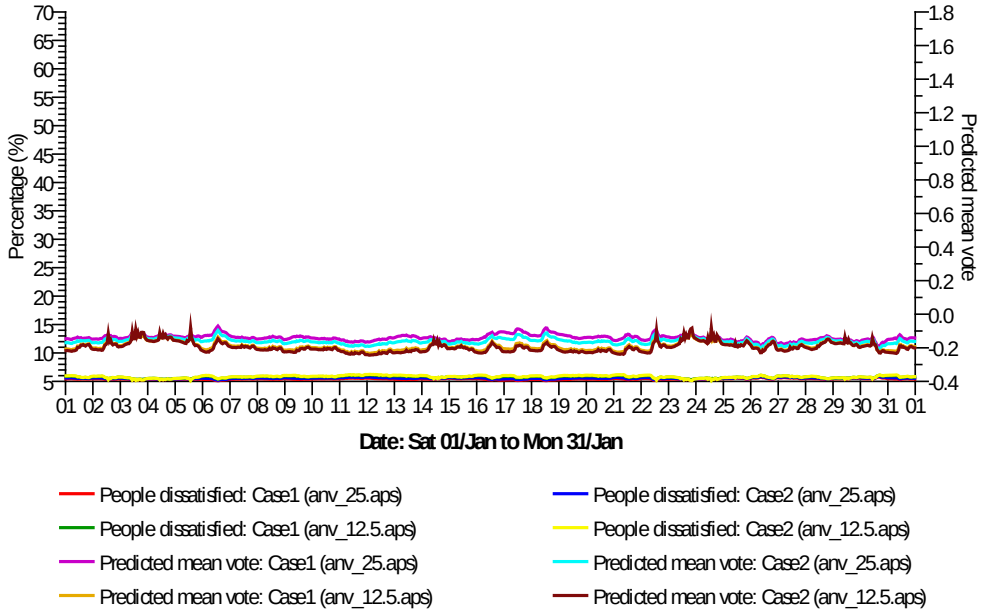

Figure 7:6: PMV and PD values for Case 1 and 2 in mid-January

The comfort scenario in the entire summer months (June, July and August) is also exemplified by the PMV/DRT and PD predictions using the month of August at two opening fractions: 75% and 100%. Like the winter scenario, the mean PMV/DRT values at 75% fraction are within the neutral range: +0.1 (21.28^{o}C) and +0.11 (21.29^{o}C) for Case 1 and Case 2 respectively. At maximum opening fraction (100%) there is a slight reversal in PMV/DRT values: +0.11 (21.32^{o}C) for Case 1 and +0.1 (21.28^{o}C) for Case 2. Similarly, the predicted ratio of people dissatisfied is well below 7% for all Cases, regardless of the opening fraction (Table 7.4).

Table 7.4: Minimum, maximum and mean PMV, DRT and PD values for Case 1 and Case 2 in August

	Min. Val.	Min. Time	Max. Val.	Max. Time	Mean
Predicted mean vote: Case1 (75%)	-0.14	19:30,06/Aug	0.97	19:30,15/Aug	0.1
Predicted mean vote: Case2 (75%)	-0.14	13:30,04/Aug	0.97	19:30,16/Aug	0.11
Predicted mean vote: Case1 (100%)	-0.14	19:30,06/Aug	0.99	19:30,15/Aug	0.11
Predicted mean vote: Case2 (100%)	-0.14	19:30,06/Aug	0.98	19:30,15/Aug	0.1
Dry resultant temperature: Case1 (75%)	20.14	01:30,06/Aug	25.54	19:30,15/Aug	21.28
Dry resultant temperature: Case2 (75%)	20.12	03:30,06/Aug	25.47	19:30,15/Aug	21.29
Dry resultant temperature: Case1 (100%)	20.18	01:30,06/Aug	25.7	18:30,15/Aug	21.32
Dry resultant temperature: Case2 (100%)	20.15	01:30,06/Aug	25.58	18:30,15/Aug	21.28
People dissatisfied: Case1 (75%)	5	07:30,01/Aug	24.99	19:30,15/Aug	6.32
People dissatisfied: Case2 (75%)	5	22:30,28/Aug	24.73	19:30,16/Aug	6.41
People dissatisfied: Case1 (100%)	5	03:30,11/Aug	25.88	19:30,15/Aug	6.26
People dissatisfied: Case2 (100%)	5	23:30,09/Aug	25.21	19:30,15/Aug	6.29

The fluctuations in PMV/DRT and PD values for 100% opening fraction (Fig. 7.7) indicate that it is only for up to four days that PMV is likely to exceed +0.5 and approach +1.0 (warm) at 100% opening. At 75% opening (Fig. 7.8) PMV is likely to exceed 0.6 and approach 1.0 for up to six days.

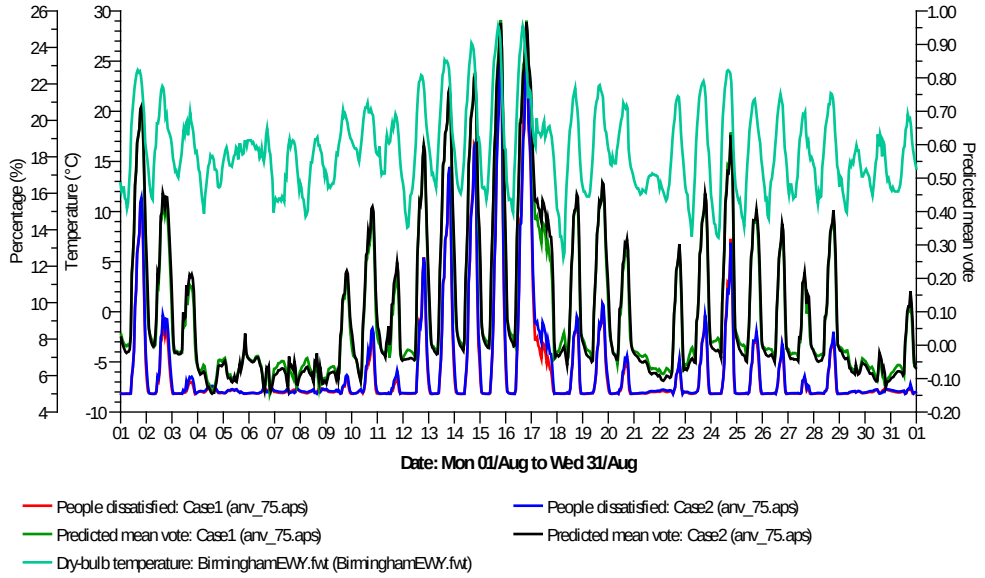

Figure 7:7: PMV and PD values for Case 1 and 2 in mid-August at 75% opening fraction

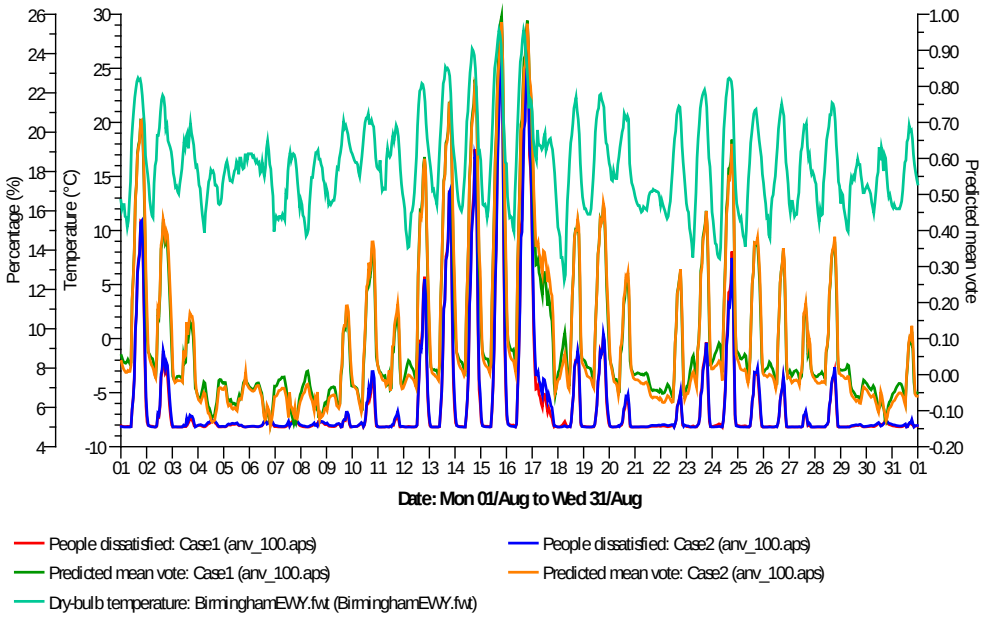

Figure 7:8: PMV and PD values for Case 1 and 2 in mid-August at 100% opening fraction

Additionally, it was found (Fig. 7.8) that at 100 % opening fractions, PD values in August are likely to peak above 24% for three and four days for Case 1 and 2 respectively, while at 75%, PD values are likely to exceed 24% for only two days in both Cases. This arguably suggests that in instances where outdoor temperatures are already high (Fig. 7.9), it may sometimes be better to avoid full openings in summer in order to minimise overheating the wards, which already have high internal gains. In such instances, a fine balance between volume of outdoor air and internal heat gains would have to be struck to achieve thermal comfort.

This scenario provides an argument for automated controls of openings which are linked to real-time sensors or data loggers. Another solution to the overheating potential is the weak differential in temperature between indoors and outdoors. This would directly affect the air change rate that is perceived in absolute terms by occupants in the form of air velocity, which is known to affect the perception and sensation of thermal comfort (Awbi, 2003). This problem is usually overcome by the installation of exhaust fans in ducts, as demonstrated by ANV systems (Lomas and Ji, 2009) but the use of mechanised airflow is outside the scope and interest of this research.

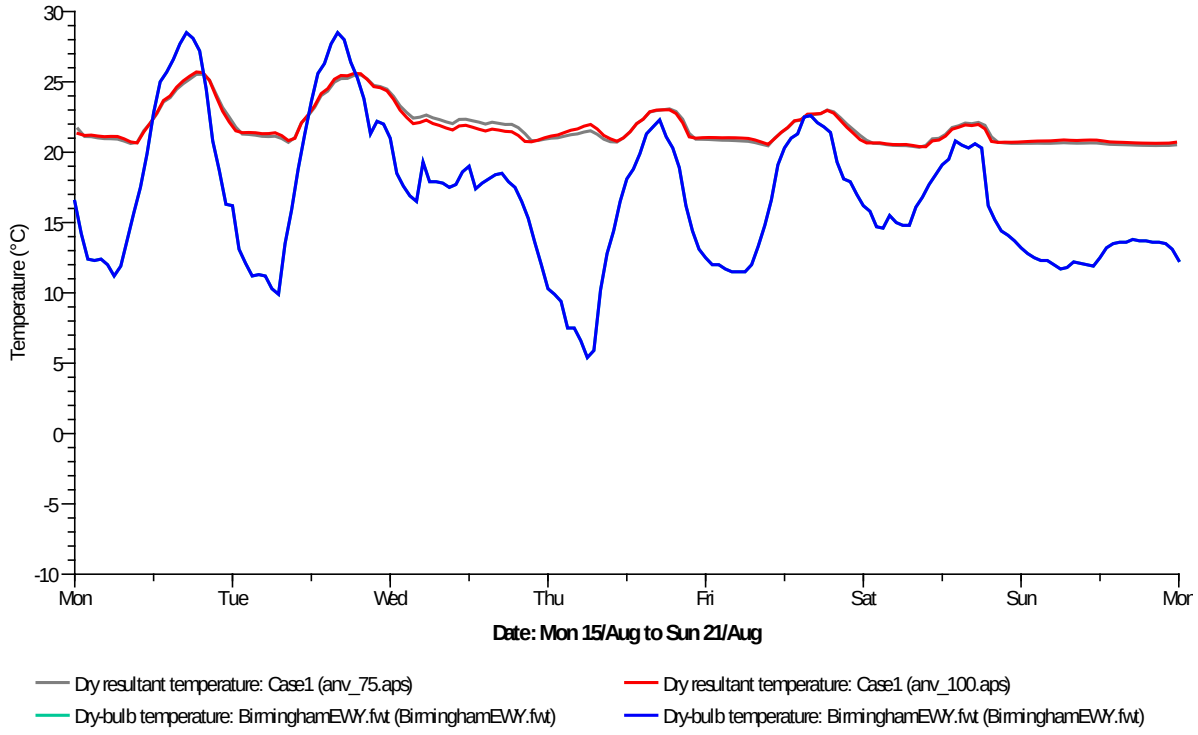

Figure 7:9: Weekly instance of high external temperatures in August leading to potential overheating

7.3.4 Differences in heating (and total) energy

A comparison of the monthly heating energy consumed by each Case under 6%, 12.5% and 25% opening fraction for both 18°C and 20°C heating setpoints is essential. Under these opening fractions and heating conditions, Case 2 (inlet elevation of 2.0m) is found to consume less energy than Case 1 where inlets are at floor level (Fig. 7.10).

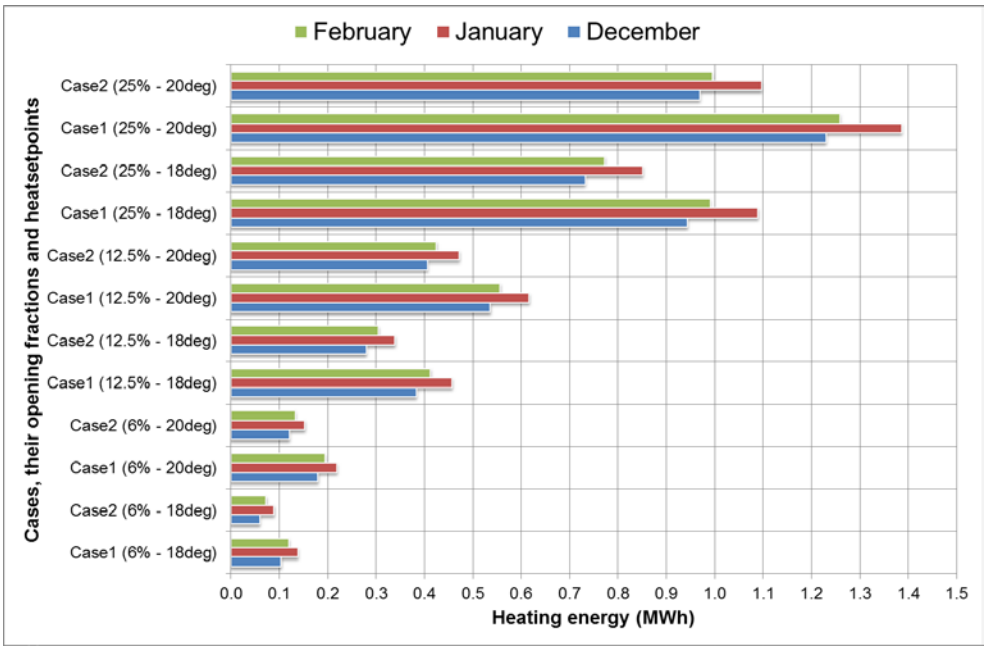

Figure 7:10: Winter heating energy for three opening fractions and two heating setpoints (Dec – Feb)

If the WHO's recommendation of 60 l/s/patient is taken as the minimum absolute rate of ventilation for the entire year, during winter, this volume flow rate can only be achieved with a minimum of 25% opening fraction and the consequent use of 18°C as heating setpoint. With these variables applied, the energy consumed in each winter month i.e. December, January and February would exceed 0.7MWh (Table 7.5).

Table 7.5: Heating load (MWh) for winter opening fractions and two heating setpoints

	6%				**12.5%**				**25%***			
	18°C		**20°C**		**18°C**		**20°C**		**18°C***		**20°C***	
	Case1	*Case2*	*Case1*	*Case2*	*Case1*	*Case2*	*Case1*	*Case2*	*Case1*	*Case2*	*Case1*	*Case2*
Dec	0.103	0.059	0.180	0.120	0.383	0.279	0.536	0.406	0.943	0.732	1.229	0.968
Jan	0.138	0.089	0.219	0.152	0.457	0.339	0.616	0.471	1.089	0.850	1.385	1.096
Feb	0.119	0.073	0.194	0.133	0.412	0.304	0.556	0.424	0.990	0.772	1.258	0.994
Sum	**0.361**	**0.221**	**0.592**	**0.405**	**1.251**	**0.922**	**1.707**	**1.301**	**3.021**	**2.354**	**3.872**	**3.058**

* Under these conditions, 60 l/s/patient will be achieved as recommended by WHO (Atkinson, et al. 2009)

The predicted heating energy for winter months is provided (Table 7.5) in addition to the total annual heating energy (Table 7.6). The annual summation uses 18°C and 20°C (from HTM 03-01) as heating setpoint for both 12.5% and 25% opening fraction. The summed heating energy demanded are compared to the adjusted (CIBSE) benchmark where 44% of total 10.5MWh (or 4.62 MWh) is allocated for space/air heating. It was found that only the use of 25% fraction approached and exceeded this benchmark. With 18°C heating setpoint for example, Case 1 (inlet at 0m) is predicted to require 6.26MWh per annum, equivalent to 136% of the benchmark while in Case 2 (inlet at 2m) the annual energy consumption is 103% of the benchmark. At the 20°C heating setpoint on the other hand, Case 1 requires 187% of the benchmark compared to 144% for Case 2.

Table 7.6: Annual heating energy (MWh) at three opening fractions and two heating setpoints

	Case1	**Case2**	**Case1**	**Case2**	**Case1**	**Case2**	**Case1**	**Case2**	**Case1**	**Case2**	**Case1**	**Case2**
	6.25% (18)	*6.25% (18)*	*6% (20)*	*6% (20)*	*12.5% (18)*	*12.5% (18)*	*12.5% (20)*	*12.5% (20)*	*25% (18)*	*25% (18)*	*25% (20)*	*25% (20)*
Jan	0.14	0.09	0.22	0.15	0.46	0.34	0.62	0.47	1.09	0.85	1.39	1.10
Feb	0.12	0.07	0.19	0.13	0.41	0.30	0.56	0.42	0.99	0.77	1.26	0.99
Mar	0.07	0.03	0.14	0.08	0.35	0.24	0.49	0.37	0.90	0.69	1.19	0.92
Apr	0.04	0.02	0.09	0.05	0.25	0.17	0.39	0.28	0.70	0.53	0.96	0.74
May	0.00	0.00	0.01	0.00	0.06	0.03	0.13	0.08	0.26	0.18	0.45	0.32
Jun	0.00	0.00	0.00	0.00	0.01	0.00	0.03	0.01	0.06	0.04	0.13	0.08
Jul	0.00	0.00	0.00	0.00	0.00	0.00	0.00	0.00	0.01	0.00	0.09	0.04
Aug	0.00	0.00	0.00	0.00	0.00	0.00	0.00	0.00	0.00	0.00	0.05	0.02
Sep	0.00	0.00	0.00	0.00	0.01	0.00	0.04	0.02	0.10	0.06	0.21	0.14
Oct	0.00	0.00	0.02	0.00	0.09	0.05	0.20	0.12	0.37	0.26	0.60	0.45
Nov	0.08	0.04	0.14	0.09	0.31	0.22	0.45	0.34	0.82	0.63	1.08	0.85
Dec	0.10	0.06	0.18	0.12	0.38	0.28	0.54	0.41	0.94	0.73	1.23	0.97
Tp	**0.55**	**0.31**	**1.00**	**0.64**	**2.33**	**1.64**	**3.44**	**2.52**	**6.26**	**4.75**	**8.63**	**6.63**
%B	12%	7%	22%	14%	51%	36%	745%	55%	136%	103%	187%	144%

***Tp** is total heating energy predicted by dynamic modelling*
***%B** is percentage of CIBSE benchmark assuming heating takes 44% of total energy (i.e. 4.62 out of 10.5MWh (fossil fuels)*

There is an apparent advantage in raising the inlets above the floor by up to 2m as this would reduce the annual heating energy required (by 33% at 18°C or by 43% at 20°C). This advantage is more pronounced especially because the difference in airflow rates was predicted to be marginally in favour of inlets at 0m (Fig. 7.13).

7.3.5 Detailed room air distribution in the generic ADB ward

Four stack locations described in Lomas (2007) for inlet and stack or ANV design include: edge-in edge-out (EIEO); edge-in centre-out (EICO); centre-in edge-out (CIEO) and centre-in

centre-out (CICO). For this study, only the EIEO and EICO were tested. This is because by using the simple ADB ward space for computational purposes, the CIEO and CICO strategies differ only in terms of orientation (i.e. they are mirror copies of the other two strategies). Two inlet heights were considered: at floor level (height of 0.0m) and above lintel level (elevation of 2.0m), being a logical architectural design positions especially for existing ward spaces. The inlets and stacks were initially assumed to be located at the centre of walls in the ADB spaces. Subsequently, their positions were changed to align with the corner of the ward so that the impact of having inlets at corners can be evaluated relative to central location of inlets. The scenarios modelled in CFD consisted of eight cases as summarised in Table 7.7 and described in 3D images previously in Fig. 7.2.

Table 7.7: The differences between the Cases modelled in CFD

	Inlet elevation (h)	**Stack location**	**Orientation of openings**	**Outdoor Temp (^{o}C)**
Case 1	0m	Centre-out	Middle of room	20
Case 2	2.0m	Centre-out	Middle of room	20
Case 3	0m	Edge-out	Middle of room	20
Case 4	2.0m	Edge-out	Middle of room	20
Case 5	0m	Edge-out	Corner of room	20
Case 6	2.0m	Edge-out	Corner of room	20
*Case 7**	0m	Edge-out	Middle of room	10
*Case 8**	2.0m	Edge-out	Middle of room	10
** Area of inlet = 0.075m^2 (i.e. 20% of 0.375m^2)*				

7.3.5.1 Air change rates from steady state CFD

Based on the mean volume airflow through the air at inlets, the size of openings and volume of the ADB ward, the computed air changes for each Case were found to be highest (6.3 ACH) when inlets were at floor level (Fig. 7.11). This relative ventilation rate occurred using the edge-out strategy with outdoor temperature of 20^{o}C. If the inlets remain at a height of 0m but stack location was centre-out (Case 1) or when inlets and stack were aligned with the edge of the room (Case 5), the air changes fell to 5.4 and 3.5 respectively. Expectedly, with outdoor temperature of 10^{o}C and 20% opening fraction, the magnitude of drop in air changes

would depend on height of inlets as shown in Case 7 (inlet height = 0m) and Case 8 (inlet height = 2m).

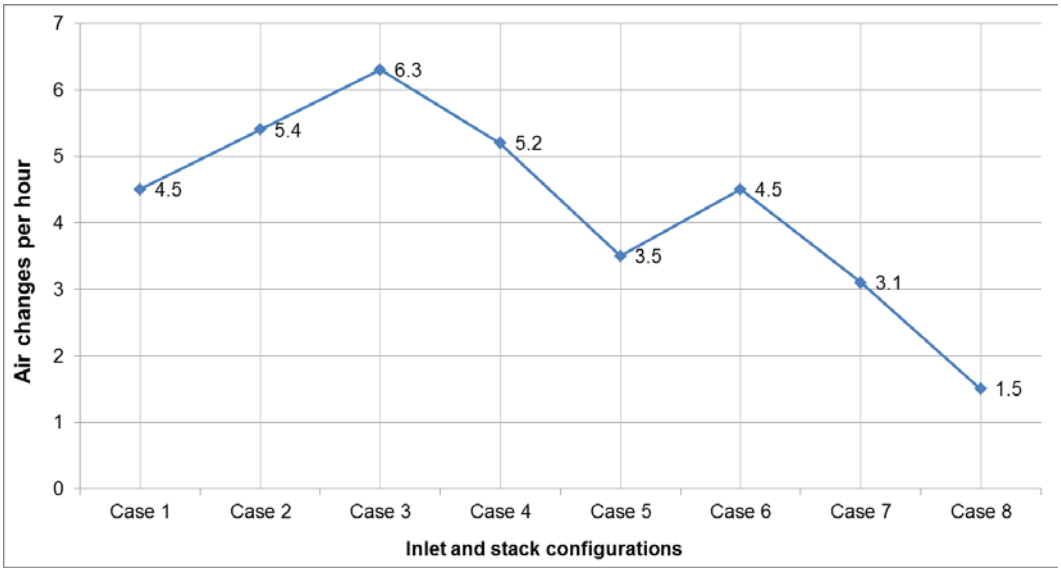

Figure 7:11: Variation in air change rates among the Cases

7.3.5.2 Age of air and room air distribution

The Age of air at the five POIs (Fig. 7.12) was found to be relatively high at points A, B and C in most of the Cases. Conversely, the Age at point D (source location) was found to be the lowest in every Case. This can be explained by the fact that incoming air travels along the floor before it rises upon encountering the opposite wall. Although fresh air is also entrained by heat sources (e.g. occupants), the Age at point B which represents the standing healthcare worker who is 2.5m away from inlet, is still significantly higher than Age at point D (4.5m away from inlet). This indicates that the time it takes for air to rise up to 1.6m (the vertical height of point B) is slower than the time it takes to reach the opposite wall where point D is measured at height of 1.0m.

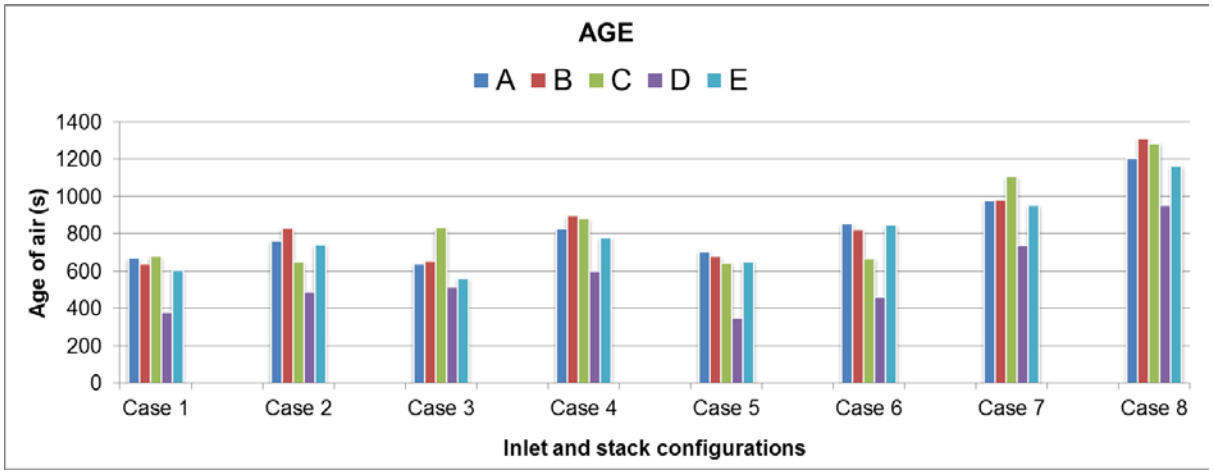

Figure 7:12: Age of air at the POIs for all Cases

In general, it was observed that the Age of air in the raised inlet Cases (i.e. Cases 2, 4, 6 and 8) are higher than their low level inlet equivalents i.e. in Cases 1, 3, 5 and 7 (Fig. 7.12 above). For the first six cases which are similar in outdoor temperature and size of inlet, the behaviour of air in these even number Cases can be explained by the pattern of airflow as shown by 2D contours (Fig. 7.13). In Cases 2, 4 and 6 where air inlets are at a height of 2.0m (Fig. 7. 13b, 7.13d and 7.13f) there is an apparent mixing of stale air in the upper part of the room with incoming fresh air at the raised inlets. This is evident by the relatively high value which Age of air has at the inlets, unlike with the low level inlets (Fig. 7.13a, 7.13c and 7.13e) where Age is almost always zero. This is with the exception of Case 4 (Fig. 7.13d) where the raised inlet is used with edge-out strategy and minimum Age at inlet remains as low as 2s, despite the stack being directly above and on same wall as the inlet. Clearly, the early Ageing of incoming air at the raised inlets will lead to larger Age of air at each of the five POIs as observed previously (Fig. 7.12).

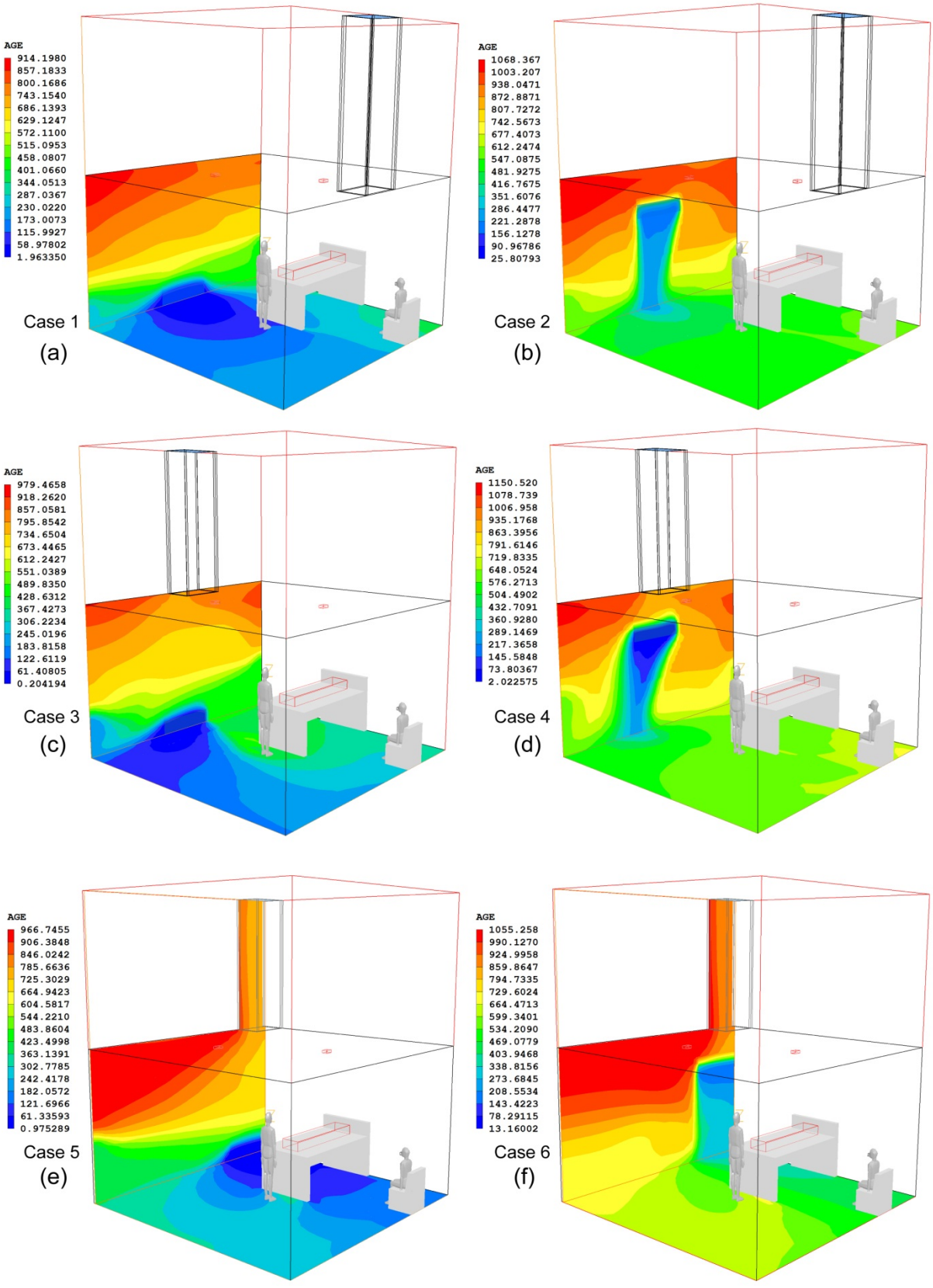

Figure 7:13: Age of incoming air in six non-winter Cases

In winter (outdoor temperature of 10^{o}C) the flow of incoming air in Cases 7 and 8 was observed to follow the right side of the room and towards the wall (Fig. 7.14) even after it descends from a height of 2.0m. This behaviour was observed with Cases 3 (Fig. 7.13c) and Case 4 (Fig. 7.13d), and the logical explanation is that the stack location is determining airflow direction in all four Cases. This is because they share the same *centralised* edge-out strategy. When the stacks were located using the edge-out strategy, but placed in the corner of the ward, as occurs in Cases 5 and 6, this behaviour was not observed.

The restriction of inlets to 20% their design size during winter generally led to larger Age of air at the POIs which is linked to the constriction of fresh air inlets. The Age of air when the inlet is raised to a height of 2.0m (Fig. 7.14b) is significantly higher at the POIs than in Case 7 (Fig. 7.14a).

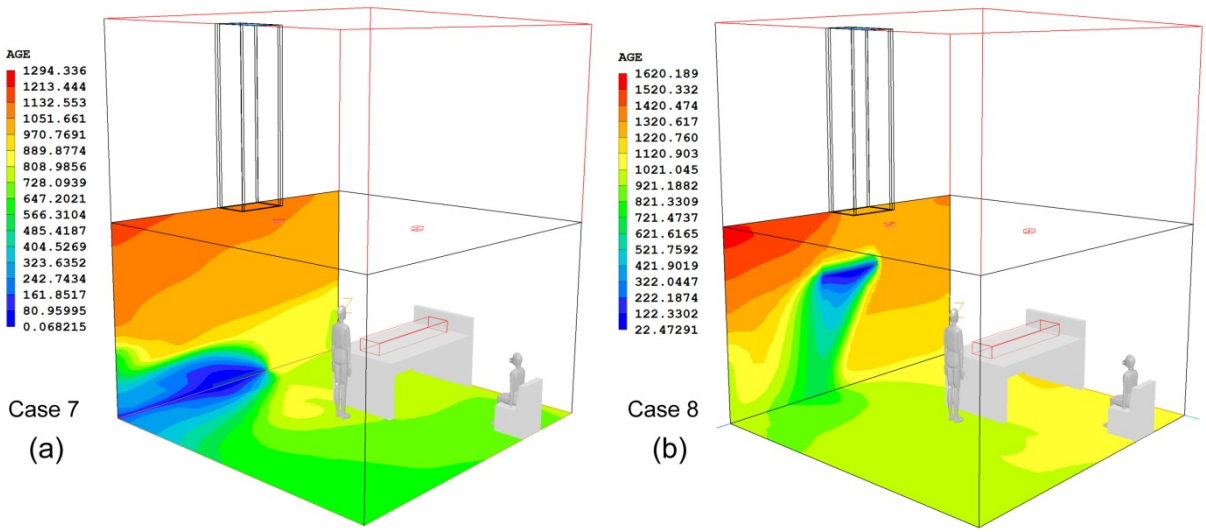

Figure 7:14: Age of incoming air for the two winter Cases

The importance of vertical distance between air inlet and exhaust stack is notable as shown by ageing of incoming air but also of relevance is the pattern of airflow. Streamlines depicting the pattern of airflow in the first six Cases (Fig. 7.15) reveal that air enters, circulates and exhausts each space in unique ways as no two Cases share similar pattern of airflow. However, the flow of air towards the right side of inlets and closer to the wall in edge-out strategy for Cases 3 and 4 (Fig. 7.15c and Fig. 7.15d) is clear.

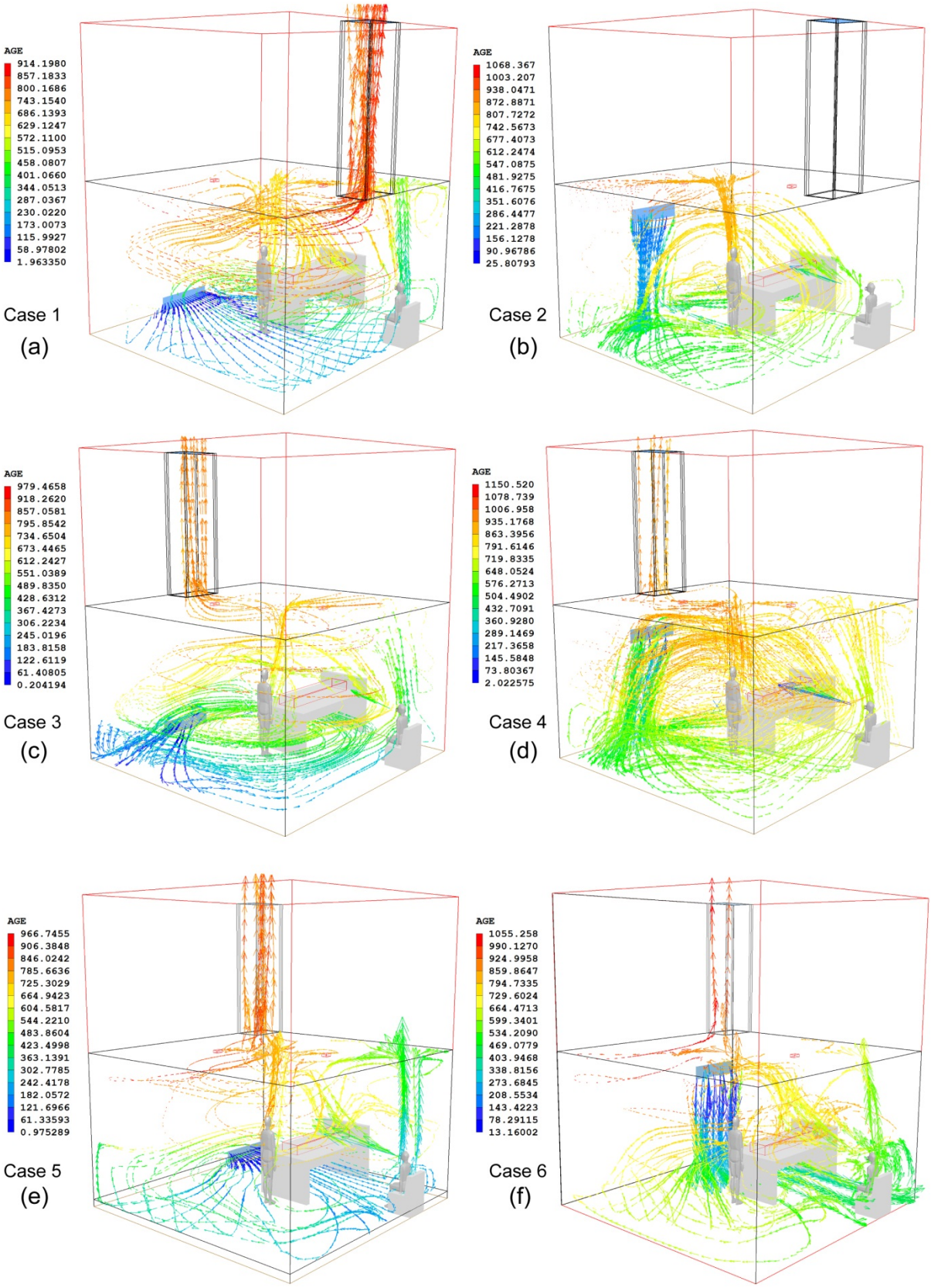

Figure 7:15: 3D streamlines showing pattern of air distribution for the six non-heating cases

The airflow pattern created with smaller openings in winter i.e. Case 7 and 8 as in (Fig. 7.16) which used centralised edge-out strategy, mimics the pattern observed previously in Case 3 and Case 4 in terms of flow along the wall, rightwards of the inlets.

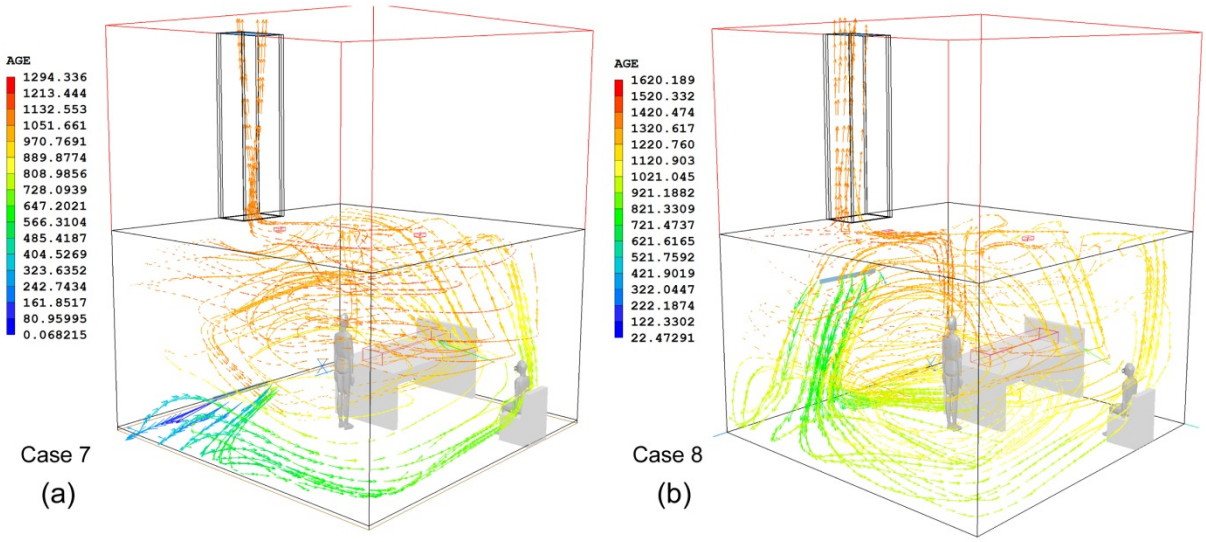

Figure 7:16: 3D streamlines showing pattern of air distribution for two winter cases with inlet heights at (a) 0m (b) 2.0m

7.3.5.3 Ventilation effectiveness

The efficiency of air exchange at each of the POIs, as well as in the overall space, was computed through LACI and MACE respectively. As a higher value of LACI denotes effective ventilation at a specific point with or without the presence of a contaminant, the LACI at point D was found not only to be greater than 1.0 but also higher than all other points in the remaining cases (Fig. 7.17). The LACI of point D was also highest (at 2.94) in Case 5 particularly, where both low level inlet and exhaust stack were located in the corner of the ward. Interestingly, point D represents the source location (from the POIs), which was modelled as the mouth of a seated visitor. This high local air exchange can be explained by the fact that point D (at a height of 1.0m) is actually the first POI to receive fresh cooler air as it floods the floor and approaches the wall which is directly opposite the inlets (this is best depicted in Fig. 7.15a). The other POIs received fresh air after it has begun its backward journey upon encountering the wall and being buoyed by indoor heat sources. In other words, the seated visitor gets the freshest air in the room by virtue of favourable location and low height of POI. As discussed in subsequent sections, this would have consequences in terms of distributing the emitted contaminants generated at this POI to other parts of the room.

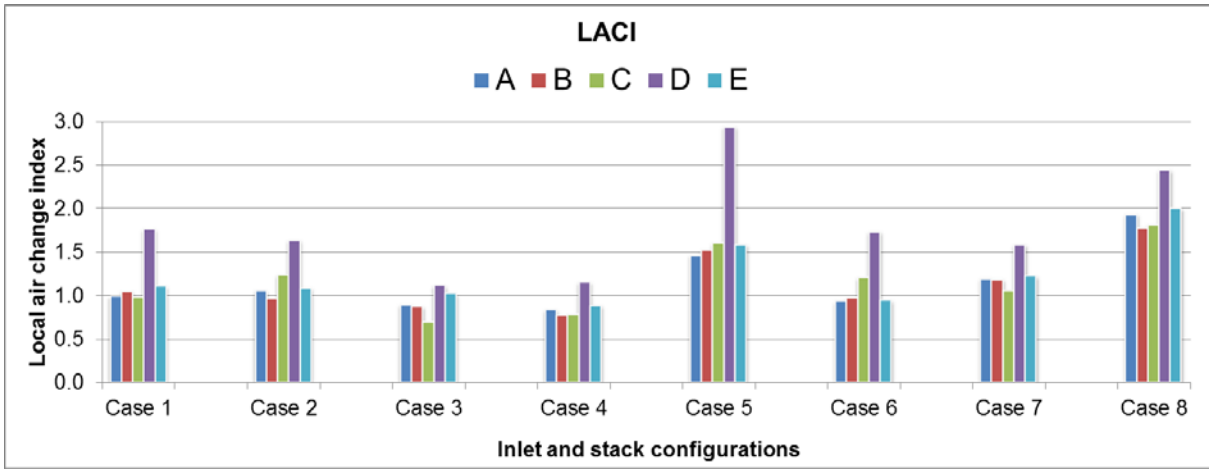

Figure 7:17: LACI for the POIs for all cases

For the entire ward space, however, Case 1 had a higher efficiency of mean (room) air exchange than Case 5 (Fig. 7.18) with MACE values of 136.8% and 134.8% respectively. It was also observed that for Cases 1 to 6 (non-heating scenarios) Case 5 had the best effectiveness of heat removal (Fig. 7.18).

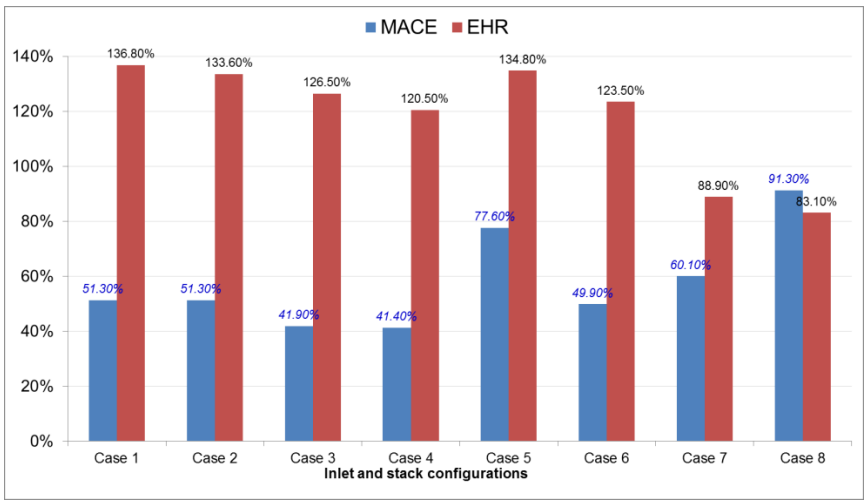

Figure 7:18: MACE and EHR values for all cases

The performance of Case 5 inlet and stack arrangement was therefore relatively better than all other non-winter cases by virture of MACE and EHR results. The temperature distribution in each of the non-winter strategies could be linked to the height of inlet and the manner of airflow into each Case (Fig. 7.19). When inlets were at floor level (i.e. as in Case 1, 3 and 5), the lower parts of the ward up to a height of ≈ 0.5m was flooded with cool air (as seen in by contours in Fig. 7.19a. 7.19c and 7.19e). The air at this lower portion generally retained the outdoor temperature of 20^{o}C.

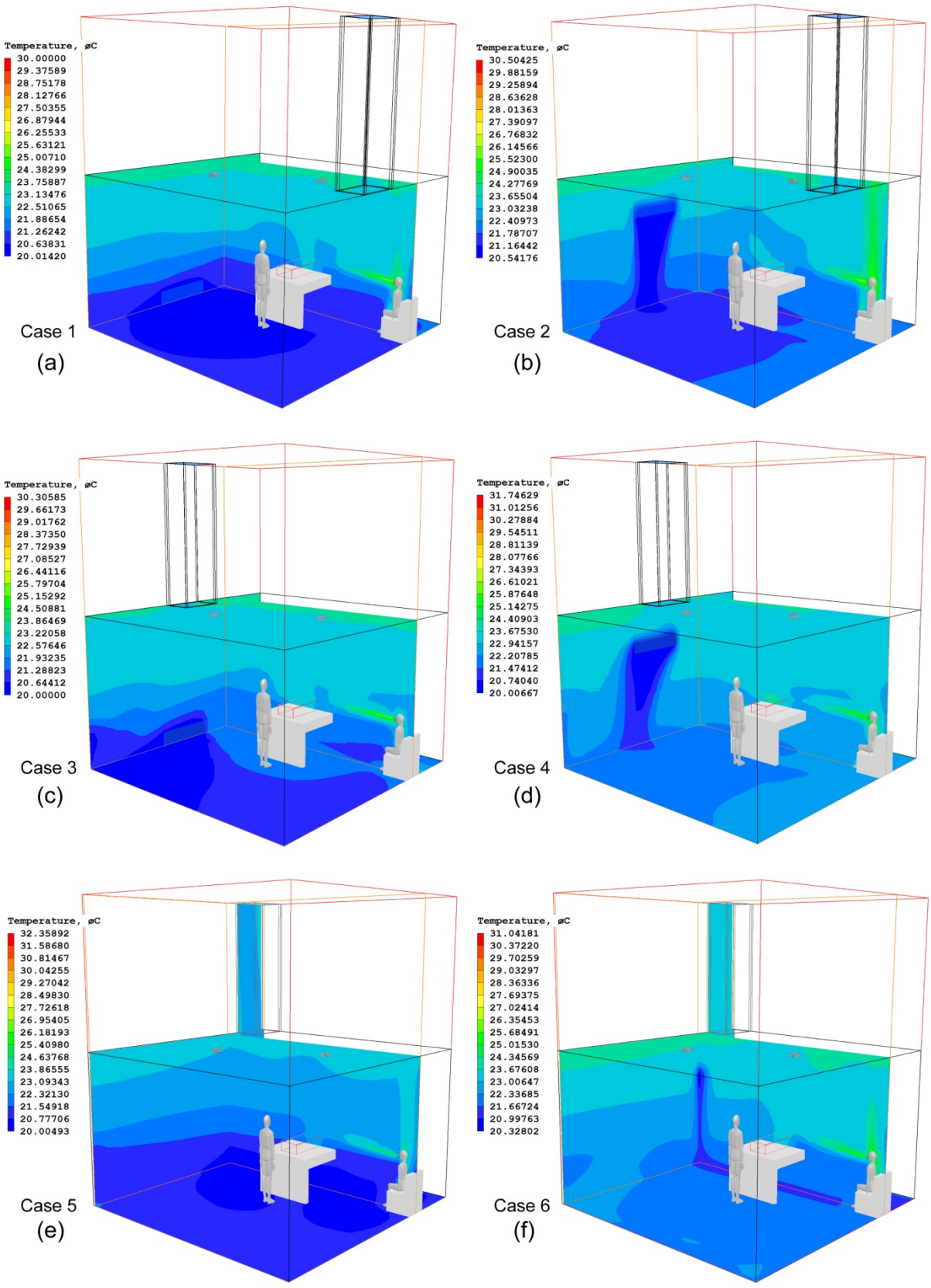

Figure 7:19: Temperature contours for the six non-winter cases

With raised inlets however, by the time the incoming air descends to floor level, the temperature in the middle of the room is already approaching 21^{o}C in Case 2, (Fig 7.19b) or 22.5^{o}C in Cases 4 and 6 (Fig. 7.19d and 7.19f). The EHR values of these raised inlet Cases are higher (Fig 7.18) than their corresponding low level inlet equivalents as expected.

7.3.5.4 Contaminant removal and air turnover

The efficiency with which contaminants are removed from a point is computed using CRE, but for an entire space, ATT gives a measure of how long it would take for a ventilation system to purge airborne contaminants (Zang, 2005). Also known as nominal time, ATT is measured in seconds unlike CRE which is non-dimensional.

A high CRE is desirable and signifies effective contaminant removal at a given point. The CRE of the five POIs in each Case (Fig. 7.20) was calculated and point B emerged as having the best values, especially in Case 5 where both inlet and stack are flush with the corner of the room.

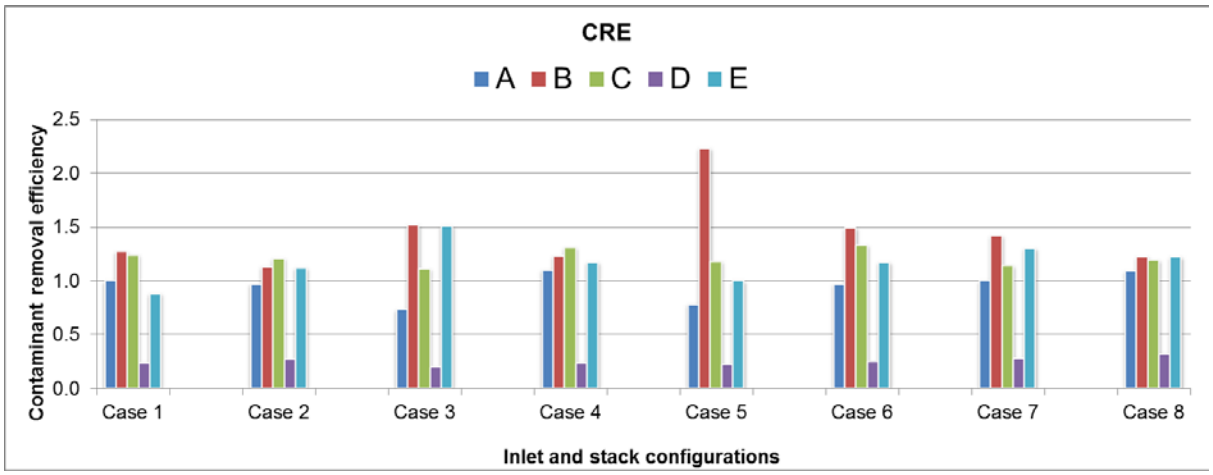

Figure 7:20: CRE values at POIs A to E for all cases

Expectedly, the CRE at source location (point D) is low in each Case (Table 7.8), however this does not detract from the fact that point D experiences the best LACI as found earlier. It is plausible that without the high LACI values at point D (which aids dilution at that point), its CRE values could be even lower.

Table 7.8: Absolute values of CRE at POIs A to E for Cases 1 to 8

	Case 1	Case 2	Case 3	Case 4	Case 5	Case 6	Case 7	Case 8
A	1.00	0.97	0.73	1.1	0.78	0.97	1.00	1.09
B	1.27	1.13	1.52	1.23	2.23	1.49	1.42	1.22
C	1.24	1.21	1.11	1.31	1.18	1.33	1.14	1.19
D	0.24	0.27	0.2	0.24	0.22	0.25	0.28	0.32
E	0.88	1.12	1.51	1.17	1.00	1.17	1.3	1.22

The distribution of the passive scalar contaminants from source to other parts of the room for the non-winter cases (Fig. 7.21) differs in pattern and in the direction of migration. In the edge-out strategy (Fig. 7.21c and 7.21d) the emitted contaminants do not collect over the patient's bed as would occur with centre-out (Fig. 7.21a, 7.21b) or corner edge-out strategies (Fig. 7.21e and 7.21f). The raising of inlets to 2.0m for the centralised stack locations is also observed (Fig. 7.21b, 7.21d) to allow greater distribution of contaminants in much of the space at ≈ 9%.

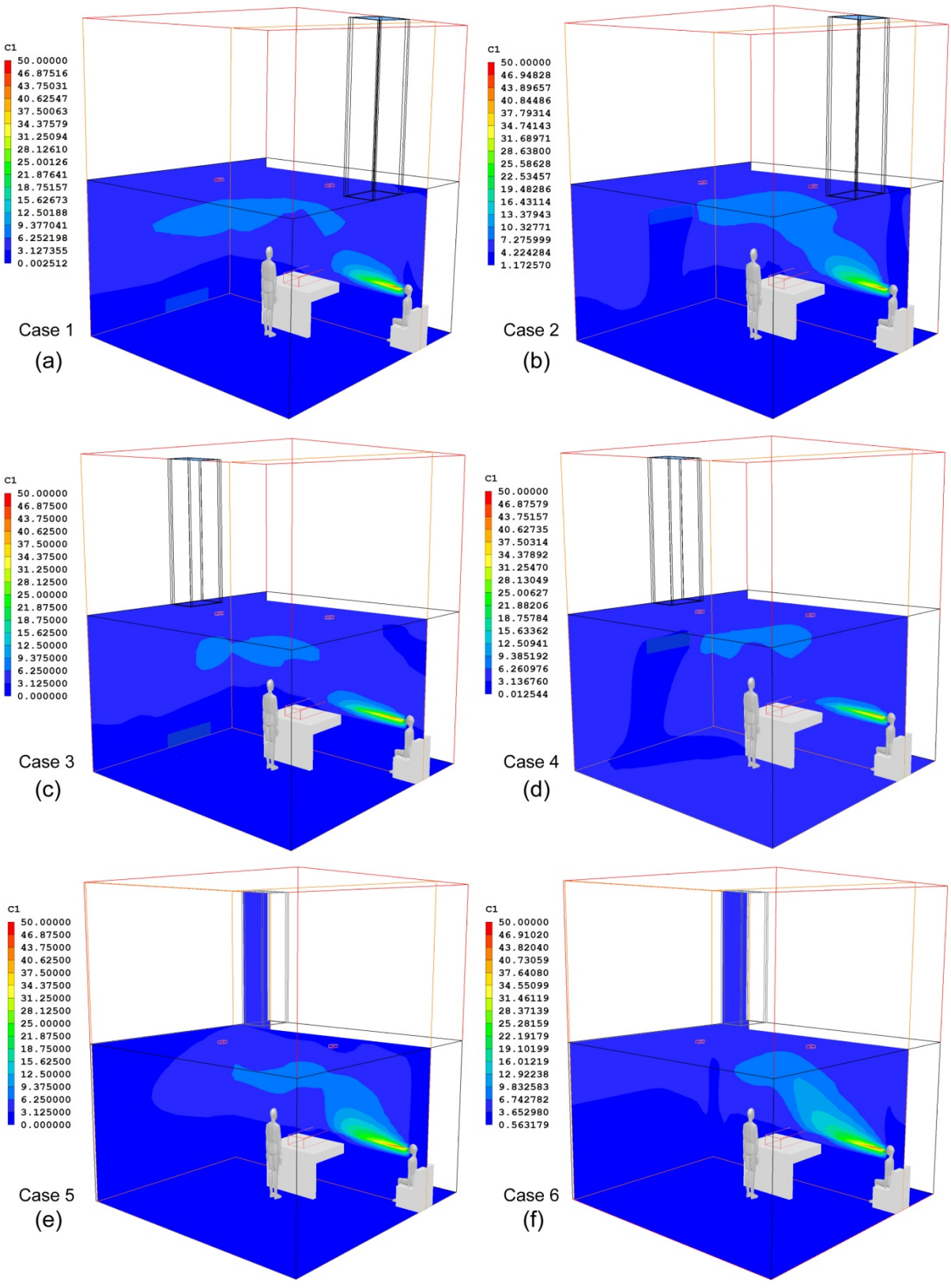

Figure 7:21: Pattern of contaminant dispersal in the non-winter Cases

The air turnover time (ATT) for each Case was computed (Fig. 7.22) to enable an understanding of the overall dilution capacity of each inlet and stack technique and in this regard, a low ATT is desirable, representing a quick turnover time. The ATT for winter Cases (Case 7 and 8) is understandably high, especially in Case 8 when the constricted inlets are raised. However, for all other inlet and stack configurations, Case 5 is seen to have the next highest ATT in which case a low level inlet and a stack both flushed with the corner of ward are used. The perceived benefits of flushing the inlets and stack with the corner of the room as previously implied by MACE and EHR values should hence be reviewed in light of the relatively large ATT for this Case.

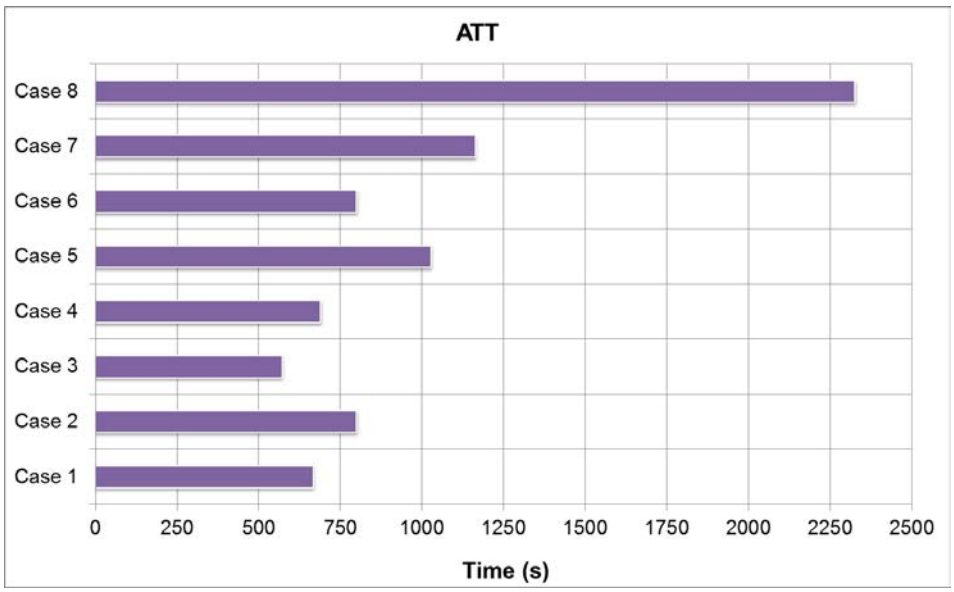

Figure 7:22: Air turnover time for all cases

The lowest ATT was obtained in Case 3 when a low level inlet was used in conjunction with the exhaust stack in an edge-out strategy but centralised position. Generally, the ATT of odd number cases (i.e. those whose inlets are at 0m) were found to be lower than their raised inlet equivalents (i.e. even number cases). It was also observed that in the non-winter scenario, the EIEO strategy when used with low level inlets and having its opening in a corner orientation, the MACE value was superior (77%) just as the ATT value was higher (1052s) than all other EIEO or EICO strategies.

7.4 Results of the schematic S&A ward

DTM and CFD analysis of the schematic S&A ward design (Fig. 7.23) were performed for evaluating the effect of different stack heights on volume flow into each ward as well as for assessment of room air distribution, respectively. The DTM model of this ward design was made to the size and positional specifications of shaft and stacks as contained in Lomas and Ji (2009). The bathroom which was fitted with mechanical extract fan was left as a solid unventilated volume and was hence not included in airflow considerations since it was designed to work with a mechanical extract fan.

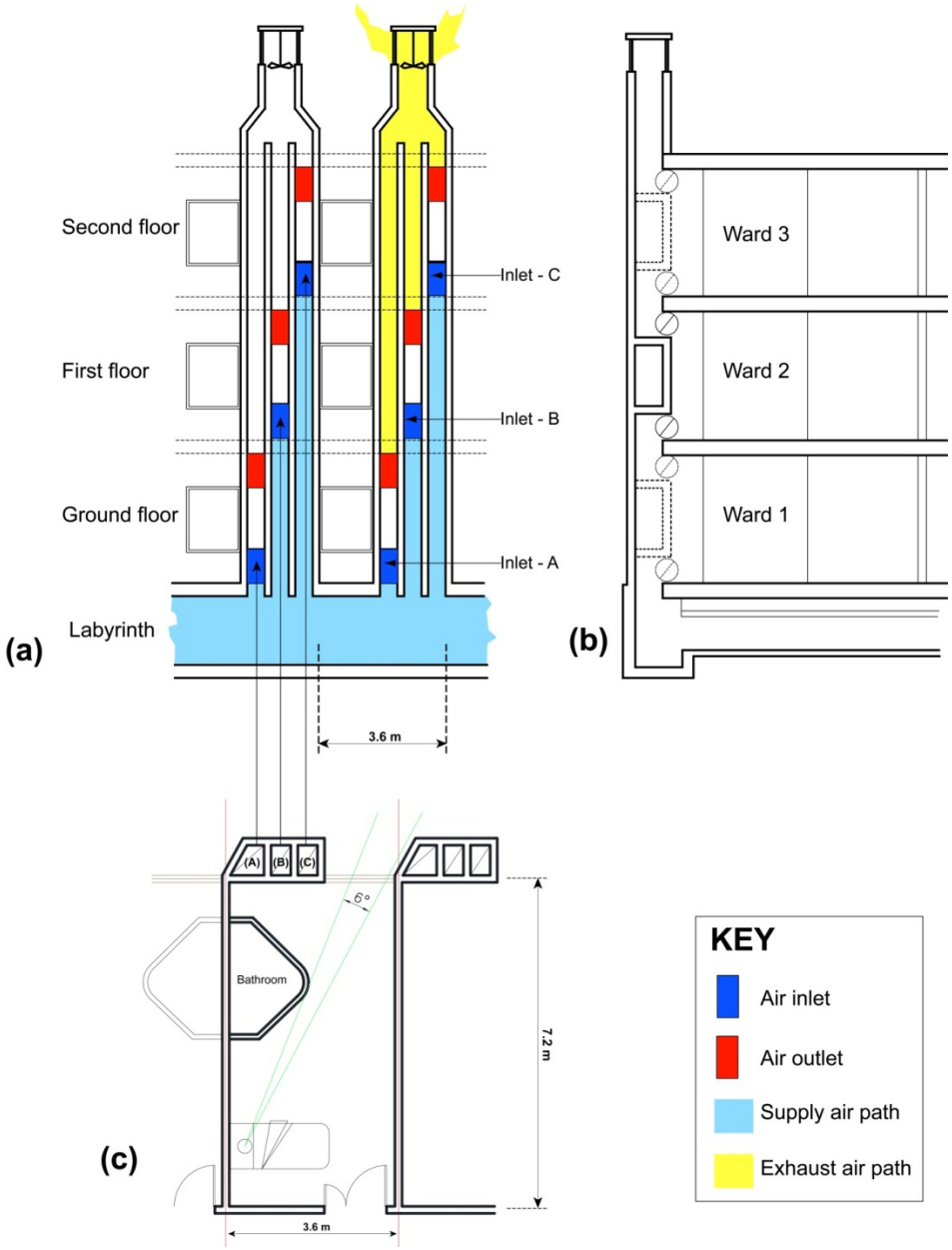

Figure 7:23: Schematic design of the S&A ward showing (a) Facade (b) Section (c) Floor Plan

Source: Lomas and Ji (2009) – adapted and redrawn

7.4.1 Dynamic model: Effect of differential stack heights

The expected differences in performance due to varying height of shafts and stacks for the three ward levels are predicted from dynamic modelling. These differences were considered using: (i) disparity in airflow rates; (ii) concentration of CO_2 which is a surrogate for air quality and ventilation efficiency; and (iii) the extent to which heating energy would vary per floor as a consequence of (i) above. The exhaust fan present in the original design was not modelled, since it falls outside the objectives of this research (i.e. fan-assisted category of natural ventilation strategies).

7.4.2 Differences in airflow rates

7.4.2.1 Winter season

January 17th – 23rd was taken as a representative period for trickle ventilation analysis. The predicted volume flow into these wards (Fig. 7.24) at 12.5% and at 25% opening fractions suggest that Ward 1 (ground floor) would experience higher flow rates than Ward 2 (first floor) and Ward 3 (second floor). The differences in airflow rates increase as the percentage of opening also increase. In fact, under the 12.5% opening regime, the mean flow into Ward 1 is 5.46% higher than flow into Ward 2 which in turn is 3.9% higher than mean flow into Ward 3. The difference in mean flow between Ward 1 and Ward 3 is 9.6%. At 25% opening fraction, however, the differences in mean flow between Ward 1 and 2 almost doubles to 7.2%. Between Ward 2 and Ward 3, the difference is 6.6% at 25% opening fraction and between Ward 1 and Ward 3, it is 14.3% at the same opening fraction.

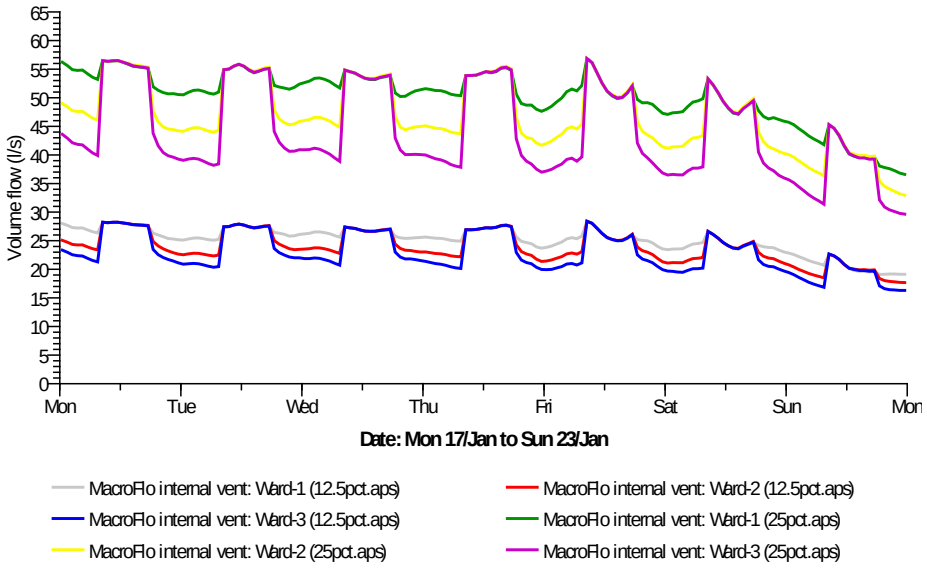

Figure 7:24: Volume flow for mid-January for Wards 1, 2 and 3 at 12.5% and 25% opening fractions

The magnitude of differences in predicted airflow rates is higher with 25% opening than with 12.5% opening as expected. The minimum, maximum and mean airflow rates for the period 17 – 23 January (Fig. 7.25) support this fact. The mean flow at 25% opening is approximately twice the mean flow at 12.5% opening fraction for all the wards. Crucially however, the mean flow rate achieved under the 12.5% regime for all wards is above 20 l/s, which is just a third of the 60 l/s/patient required to meet WHO's recommended flow for naturally ventilated wards.

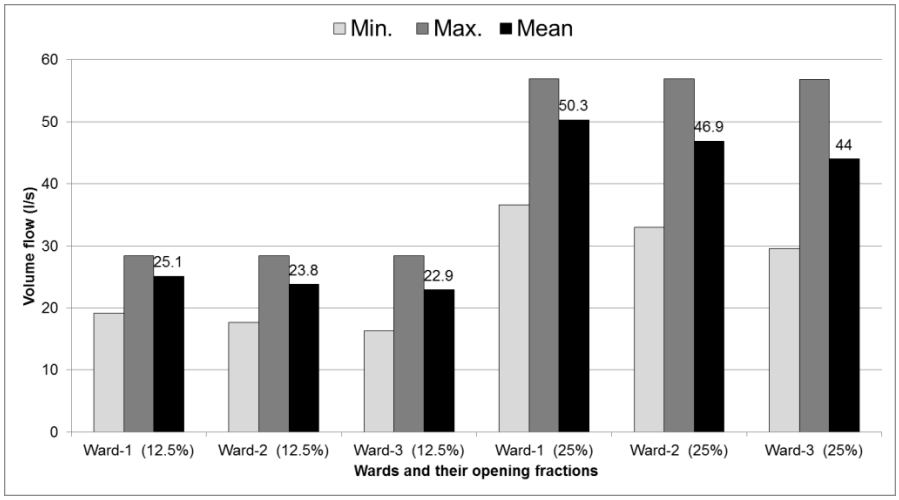

Figure 7:25: Flow rates at 12.5% and 25% opening fractions between 17 and 23 January

Regarding air changes in winter, predicted results for mid-January using 12.5% opening fraction indicate that minimum air change rates experienced by these wards (Fig. 7.26) are 0.59 ACH for Ward 3, 0.67 ACH for Ward 2 and 0.73 ACH for Ward 1. The maximum ACH would be 1.1 for all wards, but at different times; at night (22:30) on 16 January for Ward 1 and in the morning at 08:30 on 21 January for both Wards 2 and 3.

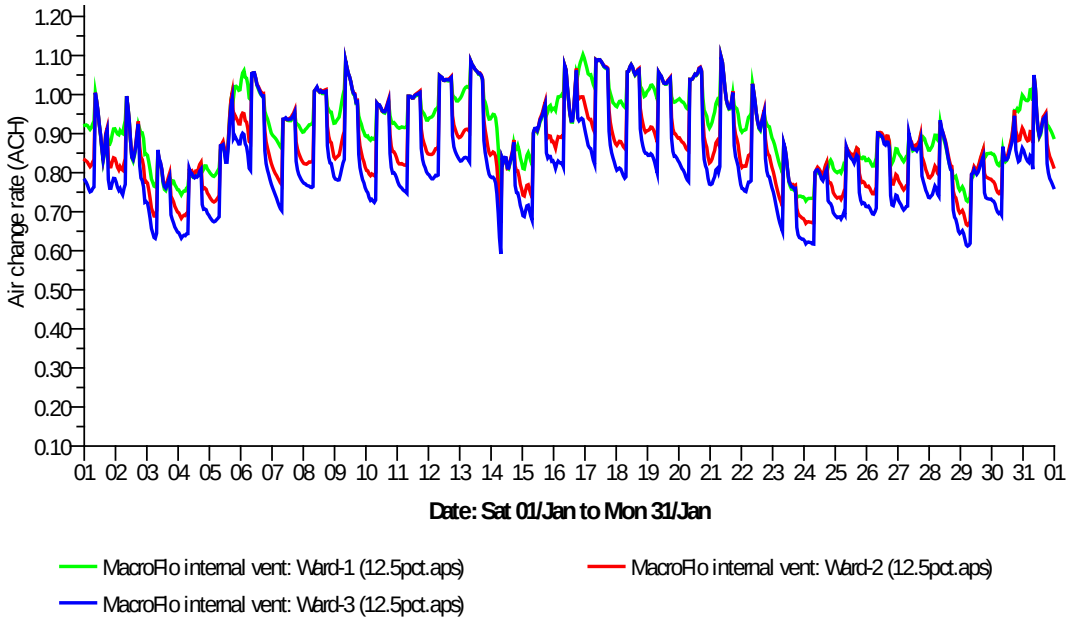

Figure 7:26: Variation in relative ventilation for the three wards at 12.5% opening fraction for January

Using the selected week as a typical period for trickle ventilation in winter at 25% opening fraction, none of these wards was able to meet the WHO requirement of 60 l/s/patient. For instance, in the entire month of January (Fig. 7.27), the mean flow into Ward 1 was 47.1 l/s (1.82 ACH) which was 7.1% higher than flow into Ward 2 with 44 l/s (1.7 ACH). The flow into Ward 1 was also 13.8% higher than flow into Ward 3 with 41.4 l/s (1.6 ACH). Since their design and internal heat load factors are the same, this imbalance in absolute and relative airflow rates was attributed to different heights of stacks between these wards. While Ward 1 had an estimated stack height of 9.2m compared to Ward 3 with 1.3m, the magnitude of difference in ACH between these two wards was only 5.7 l/s or 0.22 ACH at 25% opening fraction.

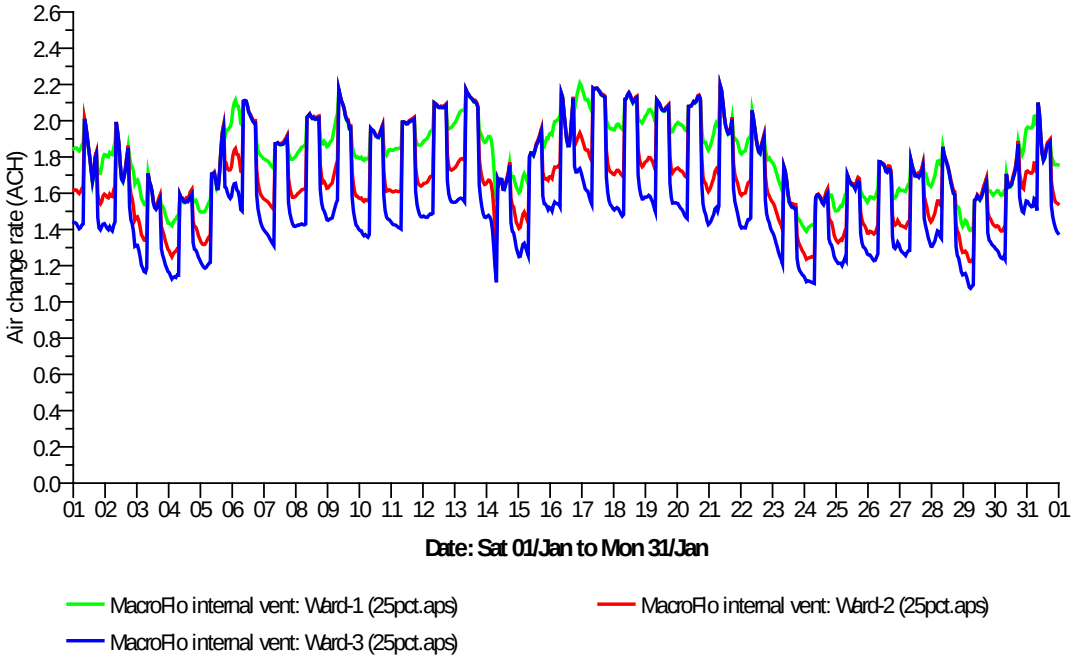

Figure 7:27: Variation in relative ventilation for the three wards at 25% opening fractions for January

7.4.2.2 Summer season

In summer, the absolute flow rates into these wards can be typified by a mid-August week (15 – 21 August) and in this regard 75% and 100% opening fractions were considered. For the given week, each ward would have mean flows above 60 l/s but the diurnal fluctuations (Fig. 7.28) in temperature (minimum of 5.4^{o}C and maximum of 28.5^{o}C) means that flow will drop to as low as 15.9 l/s in Ward 3, but not on the hottest day of the week.

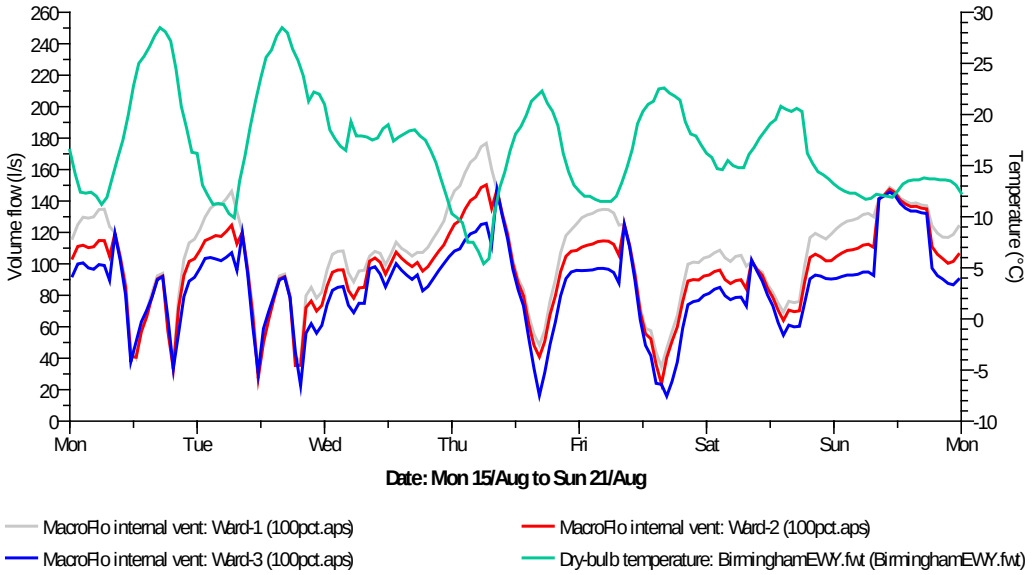

Figure 7:28: Variation in volume flow for all wards at 100% opening fraction in mid-August

When weekly temperatures peak at 28.5°C, this does not coincide with the minimum flow into Ward 2 at 23.7 l/s or the minimum flow into Ward 3 at 30.6 l/s either as summarised in Table 7.9. Since internal heat gain is similar in magnitude and pattern for all wards, this indicates that the height of the stack could be playing a key role in determining the flow rates per ward, regardless of the external temperature. This observation is similar under both 75 and 100% opening fractions.

Table 7.9: Occurrences of minimum, maximum and mean flow into wards at 75% and 100% opening fractions

		Min. Val. (l/s)	Min. Time	Max. Val. (l/s)	Max. Time	Mean (l/s)
100%	Ward-1	30.6	11:30,16/Aug	176.7	06:30,18/Aug	106.3
	Ward-2	23.7	15:30,19/Aug	150.2	06:30,18/Aug	96.1
	Ward-3	15.9	16:30,19/Aug	146.9	08:30,18/Aug	86.2
	DBT for Birmingham (°C)	5.4	06:00,18/Aug	28.5	17:00,15/Aug	16.68
	Var. Name	Min. Val.	Min. Time	Max. Val.	Max. Time	Mean
75%	Ward-1 (75%)	23.3	11:30,16/Aug	132.7	06:30,18/Aug	81.6
	Ward-2 (75%)	19.8	15:30,19/Aug	113.3	06:30,18/Aug	74.1
	Ward-3 (75%)	12.9	16:30,19/Aug	110.1	08:30,18/Aug	67
	DBT for Birmingham (°C)	5.4	06:00,18/Aug	28.5	17:00,15/Aug	16.68

The variations in mean volume flow between the wards during summer (Fig. 7.29) are predicted to be of higher magnitude than variations in winter. For 75% opening fraction, Ward 1 has 10.12% more mean airflow than Ward 2 which in turn surpasses Ward 3 by

10.6%. Mean flow into Ward 1 is 21.8% higher than flow into Ward 3. These differences are similar at 100% opening fraction with notable difference being 23% flow difference between Ward 1 and Ward 3. At both 75% opening fractions the mean flow in each ward would exceed 60 l/s/patient as required by the WHO guidelines, but there would be periods when minimum flows would fall to as low as 12.9 l/s (Ward 3). The minimum flow during this week for Ward 1 is 23.3 l/s. In summer therefore, the impact which differences in stack heights have on airflow is more pronounced than in winter.

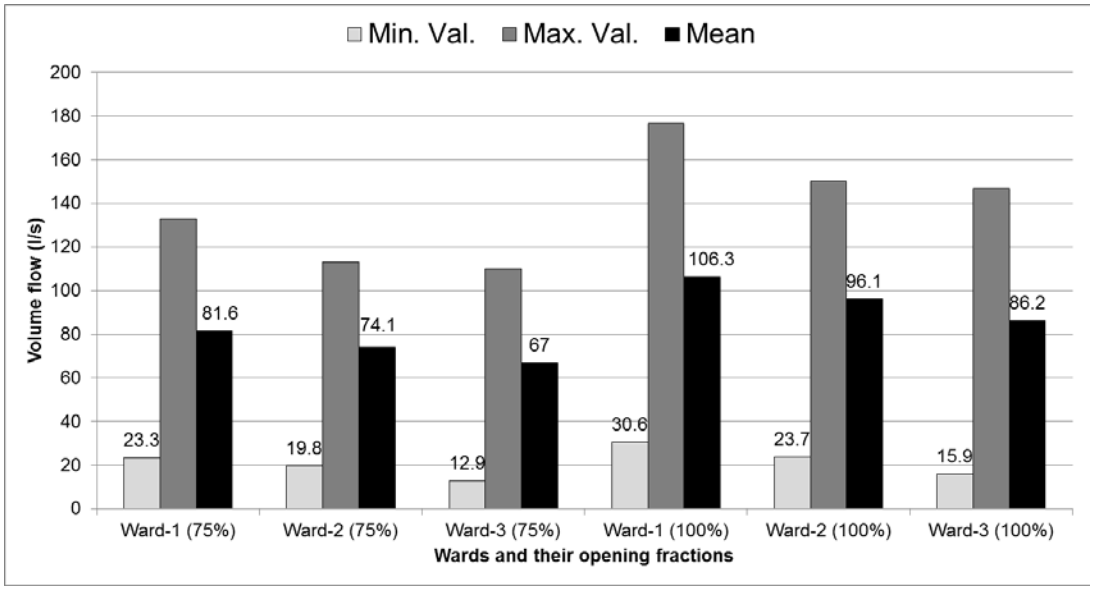

Figure 7:29: Volume flow rates at 75% and 100% opening fraction between 15 and 21 August

For the whole of August, the mean air change rates for Ward 1, Ward 2 and Ward 3 are 4.1, 3.7, 3.3 ACH respectively and the pattern of variation (Fig. 7.30) suggests minimum air changes would dip as low as 0.48 ACH for Ward 3 in particular.

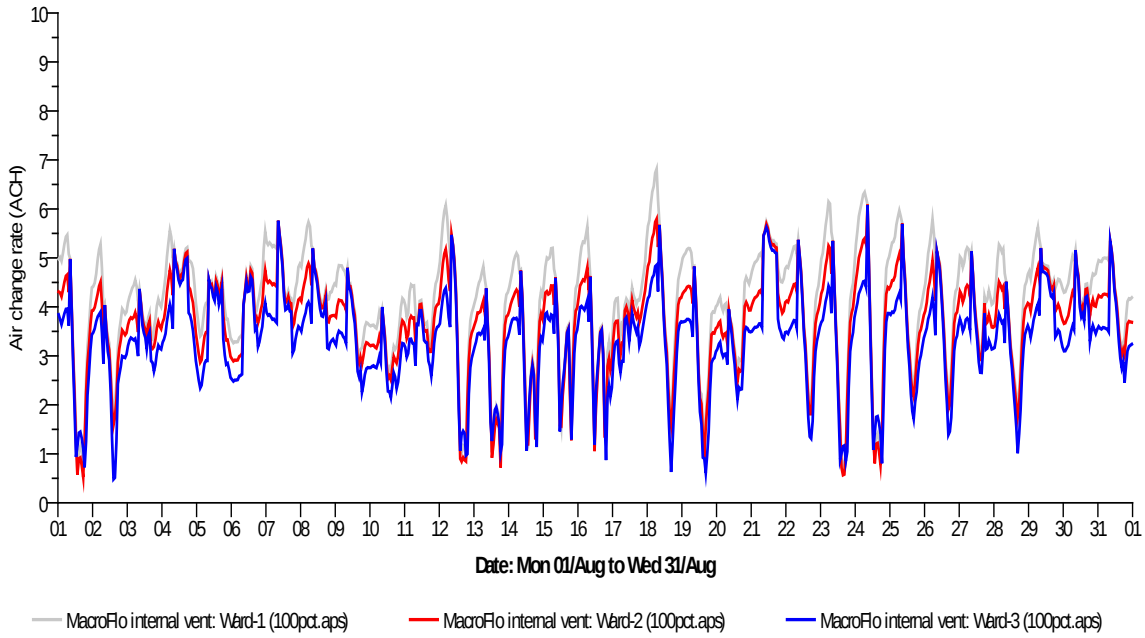

Figure 7:30: Variations in relative ventilation for all wards in August at 100% opening fraction

Another approach used for evaluating ventilation performance in these wards was to use 'fixed ranges' of air change, since no single air change value can be guaranteed with natural ventilation. Throughout the non-winter months starting 1 March and ending 31 November (Fig. 7.31), it was predicted that Ward 1 would experience the most days for air changes ranging from the 5-6 ACH (which is within HTM 03-01 provisions) and up to the maximum > 9 ACH. As from the 4-5 ACH range down to < 1 ACH, Ward 3 experienced the most number of days, especially within the 3-4 ACH range where it had 80 days, about twice as much as Ward 2 with 46 days.

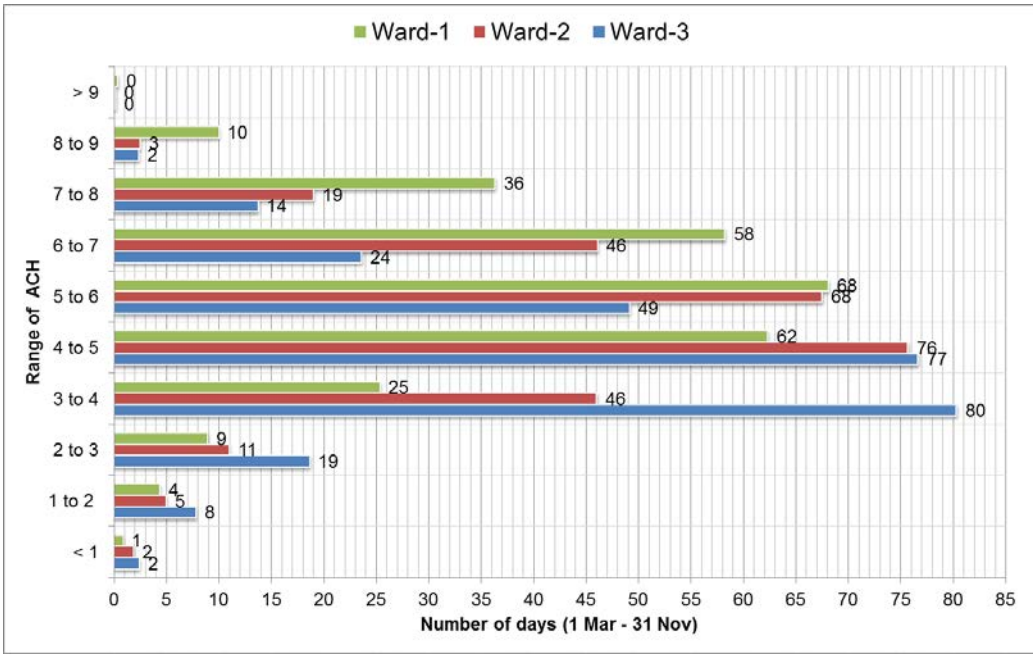

Figure 7:31: Range of ACH for between March and November at 100% opening

A summary of the predicted differences in flow rates between the three wards for the entire months of January (winter) and August (summer) is provided in Table 7.10, with respect to the estimated height of stack for each ward.

Table 7.10: Summary of absolute and relative ventilation rates in January and August

	25% opening (winter)			**100% opening (summer)**	
Ward and stack height*	Mean January airflow (l/s)	Mean January airflow ACH		Mean August airflow (l/s)	Mean August airflow (ACH)
Ward 1 (9.2m)	47.1	1.82		106.2	4.1
Ward 2 (5.3m)	44.0	1.7		96.2	3.71
Ward 3 (1.3m)	41.4	1.6		86.4	3.33
**Approximate height measured from base of outlet to top of highest slab*					

7.4.3 Differences in thermal comfort and indoor CO_2 concentration

7.4.3.1 Winter season

Using PMV and PD to evaluate the expected thermal comfort levels of the three wards, it is predicted that with 18^{o}C (Fig. 7.32) PMV values in winter (17 Jan – 23 Jan) would peak at -0.5 (i.e. 'neutral' but tending towards 'slightly cool') with a weekly mean of -0.31, -0.26 and

-0.21 for Ward 1, 2 and 3 respectively. In general, the predicted PMV values are within neutral range but approach 'slightly cool'. For percentage of people who are likely to be dissatisfied with the thermal environment, the minimum PD values obtained for both 12.5% and 25% opening fractions at both heating setpoints is 5%. However, at 18^{o}C heating setpoint, the maximum PD values for all wards is >13%. At 20^{o}C setpoint however, the maximum PD could be as low as 7-8% at 25% opening fraction.

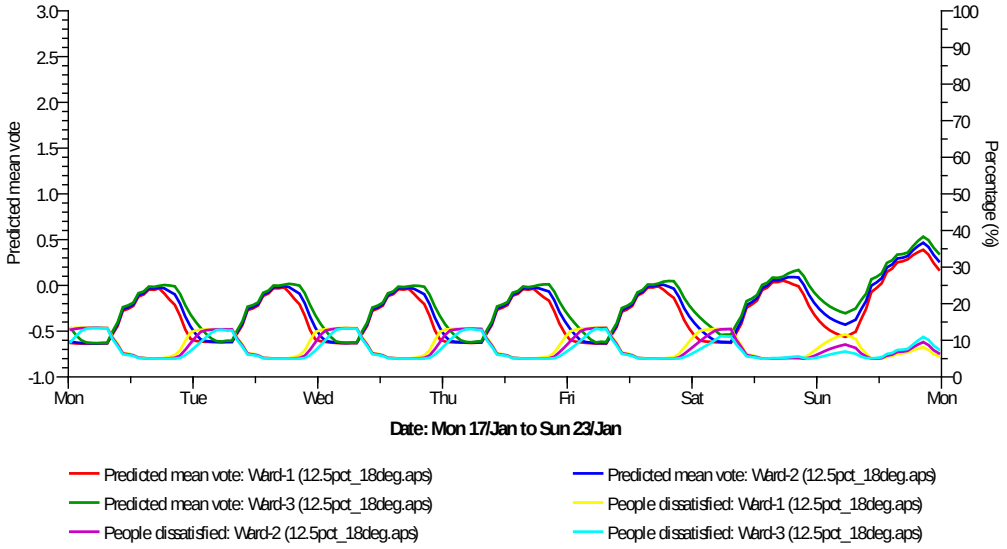

Figure 7:32: Winter PMV and PD values for all wards at 18^{o}C heating setpoint

At 25% opening (Fig. 7.33) and 18^{o}C setpoint, the weekly mean PMV values are -0.38, -0.36 and -0.34 for Wards 1, 2 and 3 respectively which indicates a perception of slightly cooler than PMV values at 12.5% opening fraction. For the entire month of January (Fig. 7.34), the minimum PMV value to be experienced by any ward is -0.63 at a heating setpoint of 18^{o}C, for both 12.5 and 25% opening fractions. This suggests occupants will perceive their thermal environment as being 'slightly cool' since it approaches the -1 value.

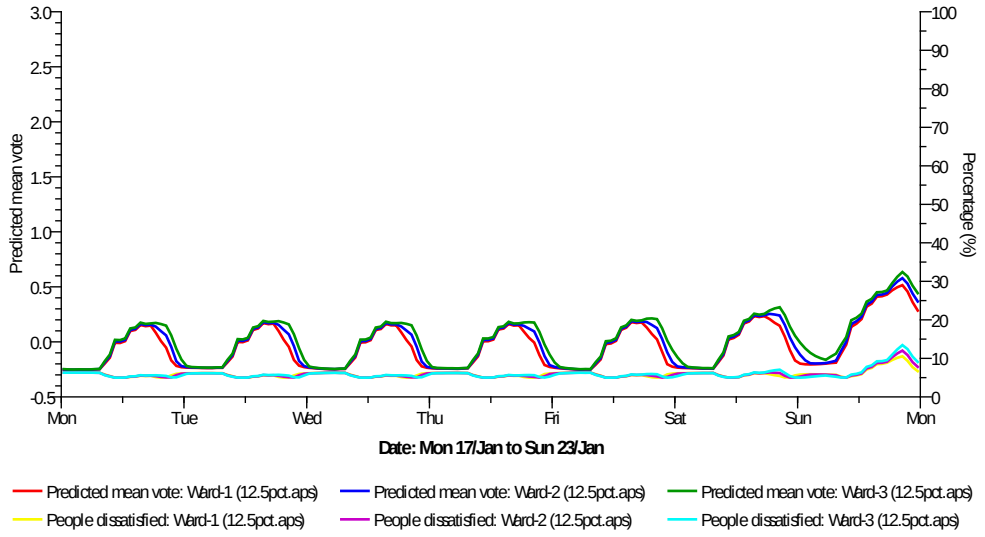

Figure 7:33: Winter PMV and PD values for all wards at 20°C heating setpoint

The maximum PMV for January will occur with the use of 12.5% opening fraction, regardless of which of the two heating setpoints are in operation (Fig. 7.34). In this regard, Ward 3 is predicted to experience higher maximum PMV (i.e. it would be warmer) than Ward 2 which in turn has a higher maximum PMV than Ward 1. These differences in maximum PMV among the wards is obviously linked to the differential volume flow rates, which has been earlier projected to reduce from Ward 1 to Ward 3 due to differences in stack heights. Ward 3 has a +0.17 higher PMV than Ward 1 at both 18 and 20°C setpoints.

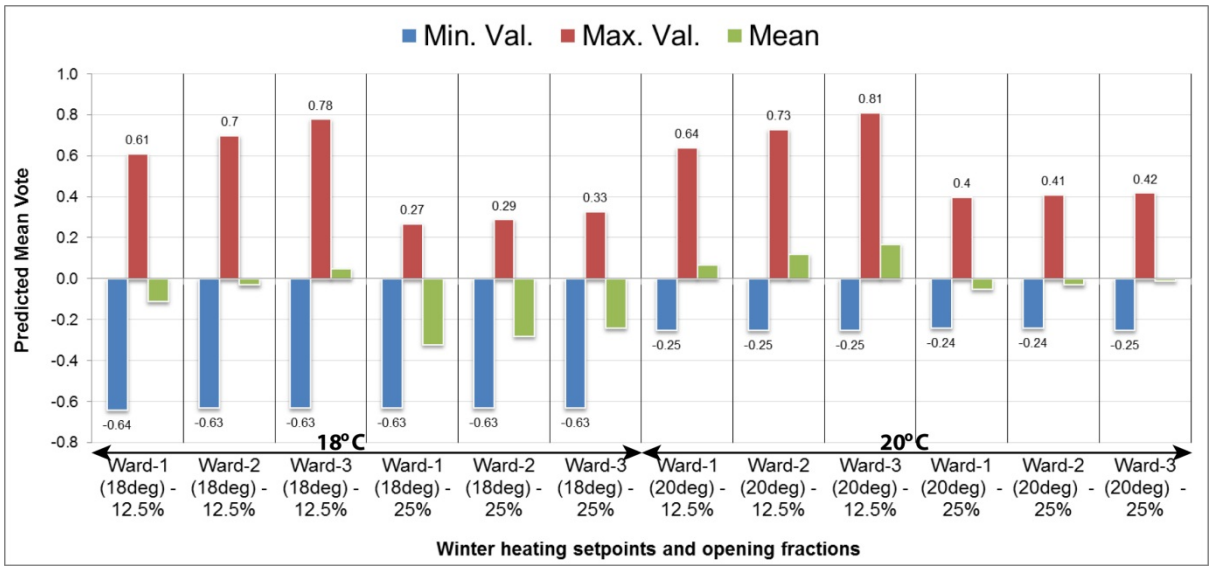

Figure 7:34: Minimum, mean and maximum PMV values for January at two heating setpoints and two opening fractions

7.4.3.2 Summer season

In August, taken as the representative month for summer, the predicted PMV and PD values for the middle of the month (Fig. 7.35) reveals a pattern related to the diurnal swing in outdoor temperatures. PMV values could go as low as -0.11 (Ward 1) to 1.23 (Ward 3) at 100%. For the selected week, minimum PD for all Wards is 5% while the maximum for each space exceeds 30%. This suggests that the ratio of occupants who may express satisfaction with the thermal environments in August is just below 70%.

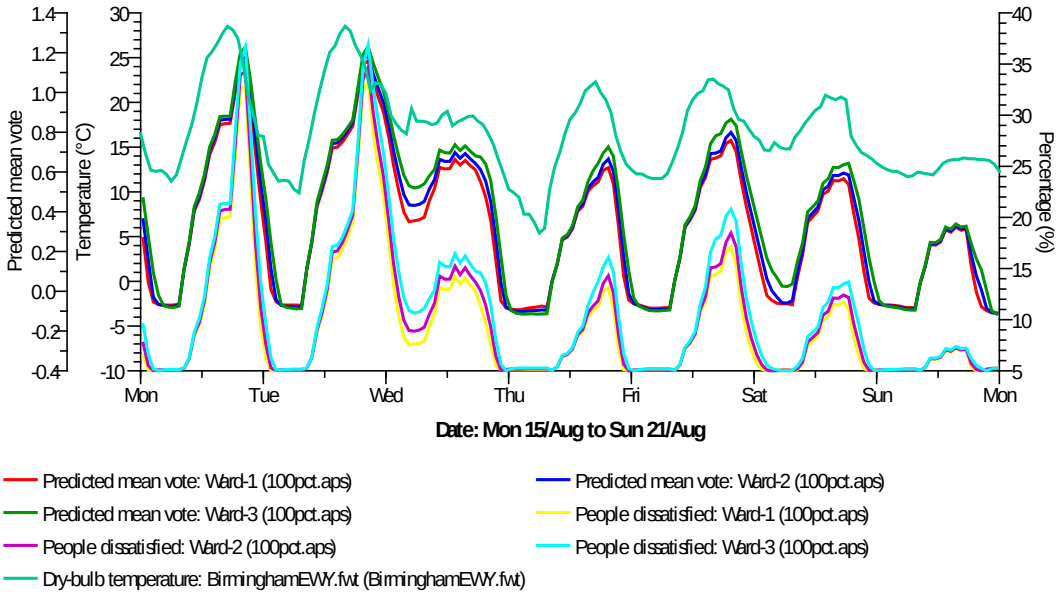

Figure 7:35: PMV and PD values for mid-August at 100% opening fraction

The predicted minimum, mean and maximum PMV for all Wards in August under 75 and 100% opening fractions (Fig. 7.36) indicate that the smaller opening fraction will lead to PMV > +1.2 (i.e. above 'warm' and approaching 'hot') while at 100% opening, the maximum PMV experienced will be just below +1.2 for Ward 1 and 2 and slightly above +1.2 in Ward 3. This indicates the extent to which smaller openings contribute to overheating in these wards during summer when external temperatures are high, as occurs in the month of August (Fig. 7.35) where ambient temperature peaks at 28.5^{o}C.

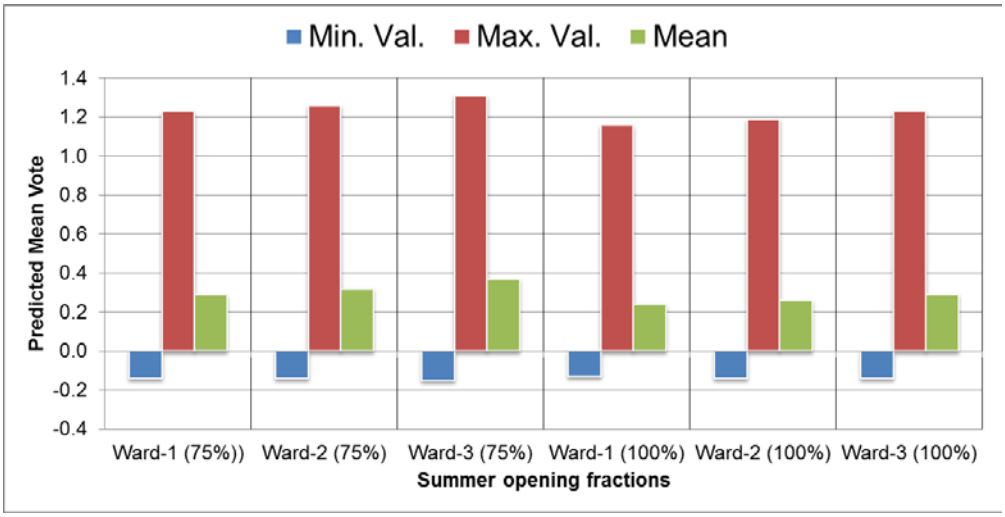

Figure 7:36: Minimum, mean and maximum PMV values for August at two opening fractions

Carbon dioxide (CO_2) is traditionally used as an indicator of human presence in a space. It is also a good indicator of indoor air quality. The implications of the differences in rates of ventilation achievable under each ward can be appreciated in indoor CO_2 concentrations. The difference in mean accumulation of CO_2 during winter (17 – 23 January) is relatively insignificant (Fig. 7.37). During summer (15 – 21 August) however, the mean CO_2 levels in Ward 3 is 36.8% higher than levels in Ward 1, while the levels in Ward 3 is 7.9% higher than in Ward 2 (Fig. 7.38 and Table 7.9).

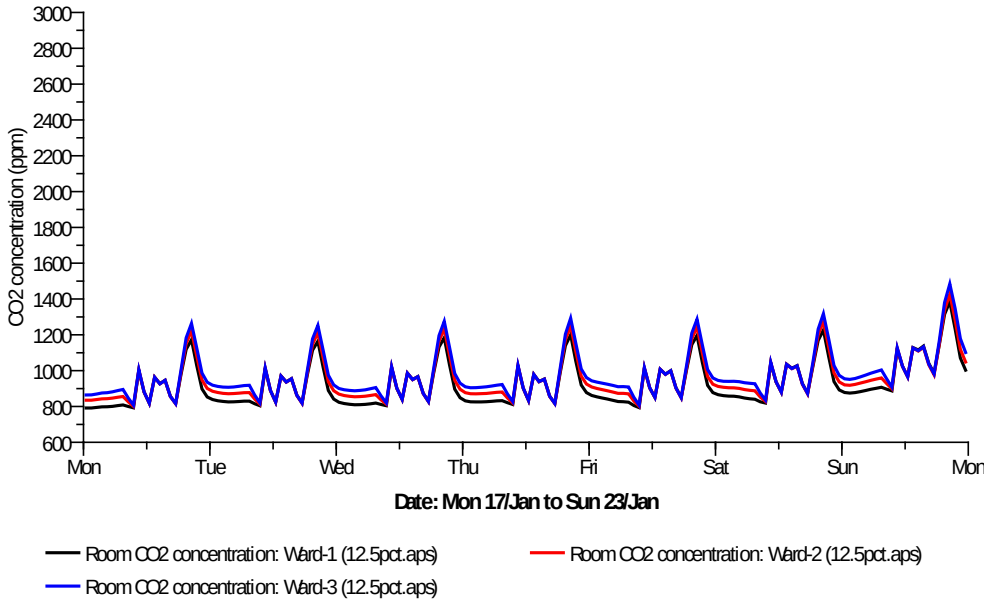

Figure 7:37: Concentration of indoor CO2 at 12.5% opening fraction for the three wards in mid-January

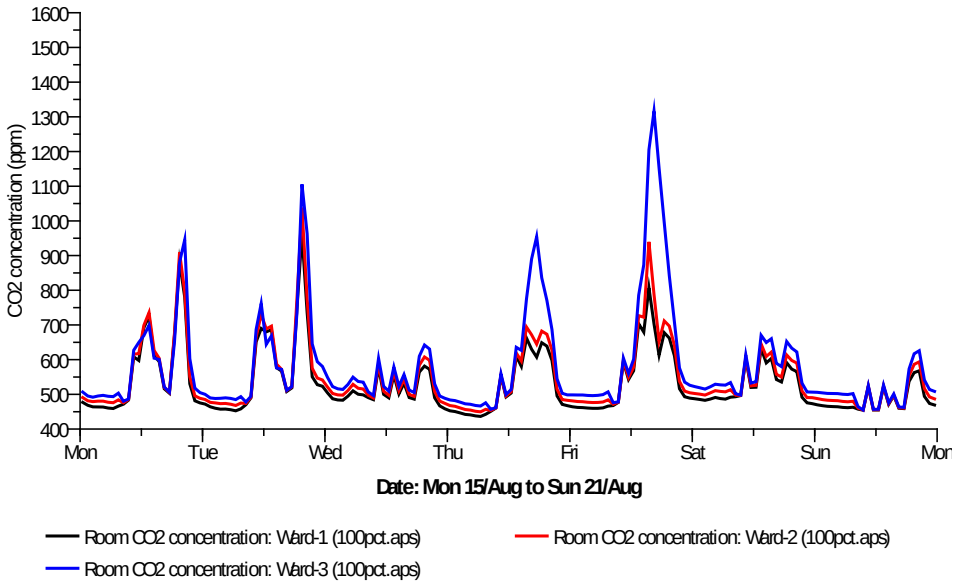

Figure 7:38: Concentration of indoor CO2 at 100% opening fraction for the three wards in mid-August

As predicted by the DTM for the month of August, the indoor concentration of CO_2 in Ward 3 would be as high 1316ppm as opposed to 1038ppm in Ward 2 and 962ppm in Ward 1. However these indoor CO_2 concentrations do not occur at exactly the same time and day except for Wards 2 and 3 (Table 7.11).

Table 7.11: Occurrences of minimum and maximum CO2 concentrations (in ppm) for the wards

	Min. Val.	Min. Time	Max. Val.	Max. Time	Mean
Ward-1	436	06:30,18/Aug	962	19:30,16/Aug	530
Ward-2	450	06:30,18/Aug	1038	19:30,16/Aug	546
Ward-3	455	09:30,21/Aug	1316	16:30,19/Aug	579

Nevertheless, as all wards have similar number and schedule of occupancies, the consequence of the differentials in airflow rates observed earlier becomes apparent. Specifically with regards to Ward 3 which has relatively higher CO_2 levels, the predicted maximum concentrations would be observed at the period when the lowest airflow rate would occur (Fig. 7.39).

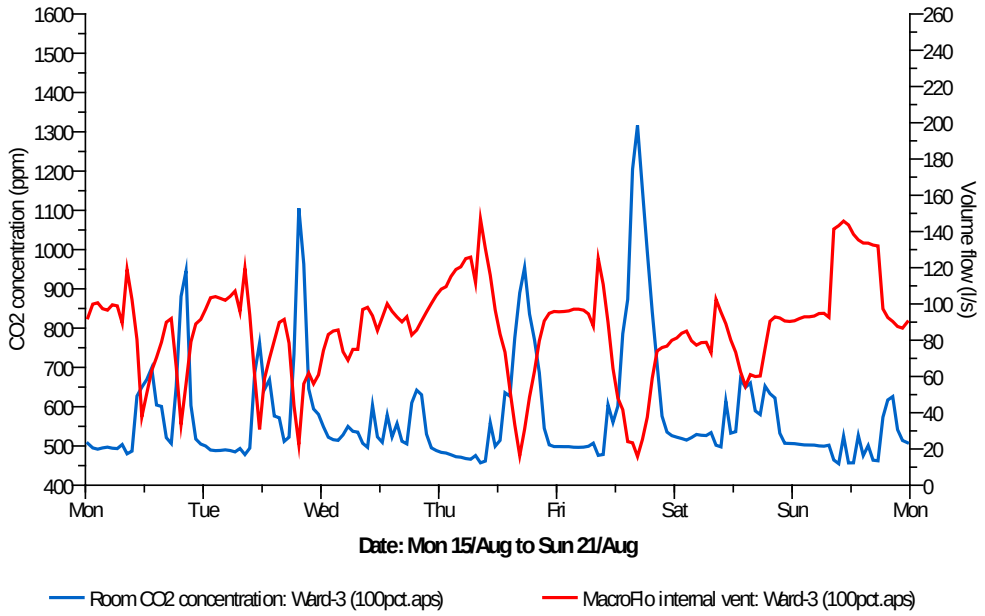

Figure 7:39: Coincidence of rising indoor CO2 levels with falling airflow rates in Ward 3 at 100% opening in August

7.4.4 Differences in heating (and total) energy

The different rates of ventilation predicted for the three wards had consequences in terms of heating energy consumed during winter period. For example, taking the mid-week of January, and at peak periods for 12.5% opening fractions, the heating power required to heat Ward 1 is 0.682 kW which is 56.2% more than the energy used by Ward 3 (i.e. 0.299 kW). With 25% opening fraction however, the difference between these wards is 45.8%. Details of this weekly variation in energy are provided in Table 7.12 where it can be noted that peak consumption in these wards occur on the same day but at different times.

Table 7.12: Energy consumed at 12.5% and 25%

			Max. Val.	Max. Time	Mean
17 – 21 January	12.5%	*Ward-1*	0.682	04:30,17/Jan	0.176
		Ward-2	0.475	04:30,17/Jan	0.1
		Ward-3	0.299	05:30,17/Jan	0.048
	25%	*Ward-1*	1.509	00:30,17/Jan	0.502
		Ward-2	1.154	00:30,17/Jan	0.358
		Ward-3	0.817	00:30,17/Jan	0.236

The pattern of variation in heating that will be experienced within the selected week (Fig. 7.40) can be evaluated against the assumption that some heating would be required outside the winter months (Fig. 7.41) when temperatures may drop. The heating energy scenario for the whole year if 12.5% opening is maintained assumes that as temperatures drop, inlets would be constricted to this particular size to conserve heat while allowing some airflow.

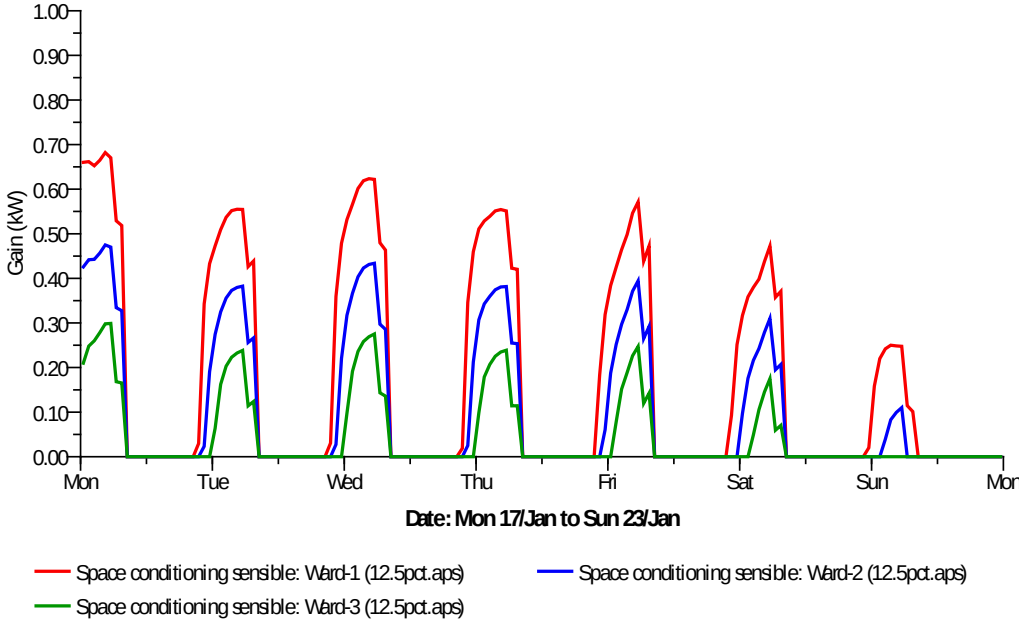

Figure 7:40: Mid-January heat loads at 12.5% opening fraction for the three wards

Based on the assumptions made, it is predicted that only the months of June, July, August and September will remain unheated for all wards. In the month of May, only Ward 1 will require some heating (1.1 MWh) while in October, heating will be needed in Ward 1 (6.3 MWh) and in Ward 2 (0.5 MWh). It can be implied then that the lower volume flow into Ward 3 allows it to require not heating for six months of the year i.e. May to October, (Fig. 7.41), unlike the four months for Ward 1 (June to September) or the five months of Ward 2 (May to September). The trickle ventilation rates predicted for Ward 3 can therefore be used as a benchmark for Ward 1 and Ward 2 so that they can also require no heating for six months. This assumes that the volume flow into Ward 3 meets the health and comfort requirements of occupants.

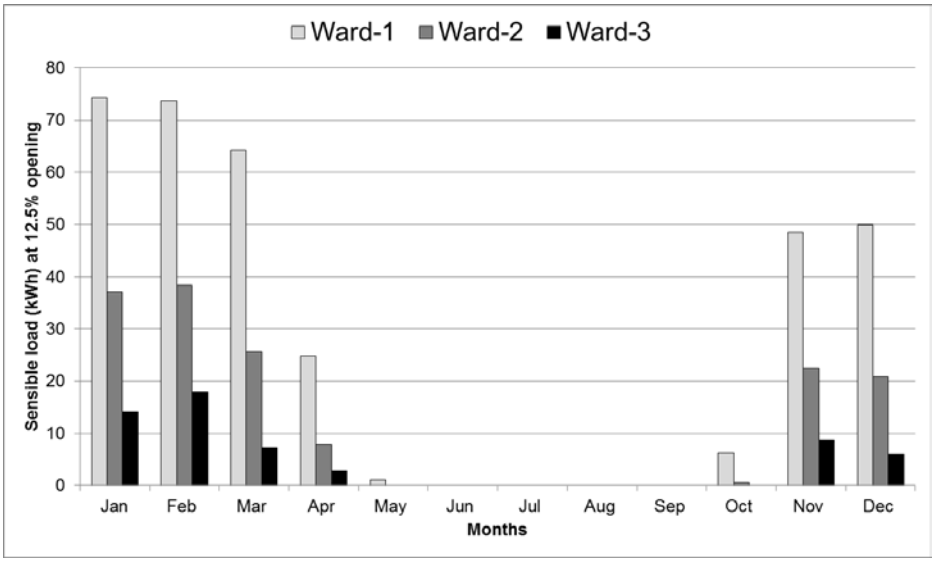

Figure 7:41: Annual energy consumption assuming 12.5% for the entire year

The annual heating energy consumed by each ward (Table 7.11) for airflow at 12.5% and 25% opening fraction throughout the given year at these opening fractions are actually targeted at the cold months not necessarily of winter when openings have to be restricted to reduce heat loss.

The 21.8% differential in flow rates between Ward 1 (ground floor) and Ward 3 (second floor) will lead to more annual heating energy consumed by Ward 1 relative to Ward 3, depending on the heating setpoint. At 18^{o}C heating setpoint, the Ward 1 will consume 92.7% more energy than Ward 3 using 12.5% opening fraction. At 25% opening fraction, the difference is 71%. An increase in the heating setpoint to 20^{o}C will lead to Ward 1 consuming 83.4% more energy than Ward 3 at 12.5% opening fraction while at 25% opening fraction, the magnitude is 63%.

Using the CIBSE (2008) energy benchmark for fossil-thermal sources for category 20 buildings (hospitals), the wards were evaluated under two opening fractions (i.e. 12.5% and 25%). Predicted total annual heating energy values are reported in Table 7.13. The extent to which each strategy exceeds the 4.66MWh adjusted benchmark (space and air heating) is also computed and reported as a percentage of benchmark (%B). It can also be deduced that although 25% is only a doubling of 12.5% as per area of inlet, the total energy consumed at 25% is almost 5 times what would be utilised at 12.5% opening fraction for Ward 1, almost 7 times for Ward 2 and over 10 times for Ward 3. Clearly the pattern of heating energy

consumed at these two fractions is not directly proportional to the differences in area of opening. The main factor responsible for this has to be the differences in airflow rates into each ward as determined by their stack heights.

Table 7.13: Total annual heating energy consumed (MWh) at 12.5% and 25% opening fractions

	12.5%			25%			12.5%			25%		
	18°C						20°C					
	Ward-1	*Ward-2*	*Ward-3*	*Ward-1*	*Ward-2*	*Ward-3*	*Ward-1*	*Ward-2*	*Ward-3*	*Ward-1*	*Ward-2*	*Ward-3*
January	0.030	0.009	0.001	0.175	0.109	0.059	0.074	0.037	0.014	0.275	0.186	0.114
February	0.035	0.015	0.005	0.177	0.112	0.062	0.074	0.038	0.018	0.268	0.184	0.113
March	0.020	0.005	0.001	0.177	0.105	0.052	0.064	0.026	0.007	0.275	0.184	0.109
April	0.006	0.002	0.000	0.100	0.049	0.019	0.025	0.008	0.003	0.185	0.115	0.060
May	0.000	0.000	0.000	0.021	0.006	0.001	0.001	0.000	0.000	0.062	0.031	0.011
June	0.000	0.000	0.000	0.002	0.000	0.000	0.000	0.000	0.000	0.017	0.006	0.001
July	0.000	0.000	0.000	0.000	0.000	0.000	0.000	0.000	0.000	0.000	0.000	0.000
August	0.000	0.000	0.000	0.000	0.000	0.000	0.000	0.000	0.000	0.000	0.000	0.000
September	0.000	0.000	0.000	0.002	0.000	0.000	0.000	0.000	0.000	0.017	0.005	0.001
October	0.000	0.000	0.000	0.035	0.016	0.006	0.006	0.001	0.000	0.087	0.044	0.020
November	0.019	0.005	0.001	0.126	0.075	0.038	0.048	0.022	0.009	0.206	0.136	0.081
December	0.014	0.003	0.001	0.138	0.080	0.039	0.050	0.021	0.006	0.228	0.150	0.088
Total predicted (Tp)[a]	**0.123**	**0.038**	**0.009**	**0.952**	**0.553**	**0.276**	**0.343**	**0.153**	**0.057**	**1.619**	**1.041**	**0.598**
% of benchmark (%B)[b]	**2.7%**	**0.8%**	**0.2%**	**20.7%**	**12.0%**	**6.0%**	**7.5%**	**3.3%**	**1.2%**	**35.2%**	**22.6%**	**13.0%**

[a] *Tp is total heating energy predicted by dynamic modelling*

[b] *%B is percentage of CIBSE benchmark assuming heating takes 44% of total energy which is 4.66MWh out of 10.6MWh (fossil fuels)*

In addition to the energy consumed by each ward for heating, it is also useful to compare the total annual energy (i.e. heating + lighting + equipment) consumed by all three wards. This result (Fig. 7.42) cannot be sorted into individual rooms (wards) due to software constraints. The results demonstrate the total energy consumed according to opening fractions and at 18^{o}C and 20^{o}C heating setpoints. It is observed that using natural gas, the total heating consumed at 25% opening is generally more than twice what is consumed at 12.5% opening. For electricity, the consumption remains largely constant throughout the year.

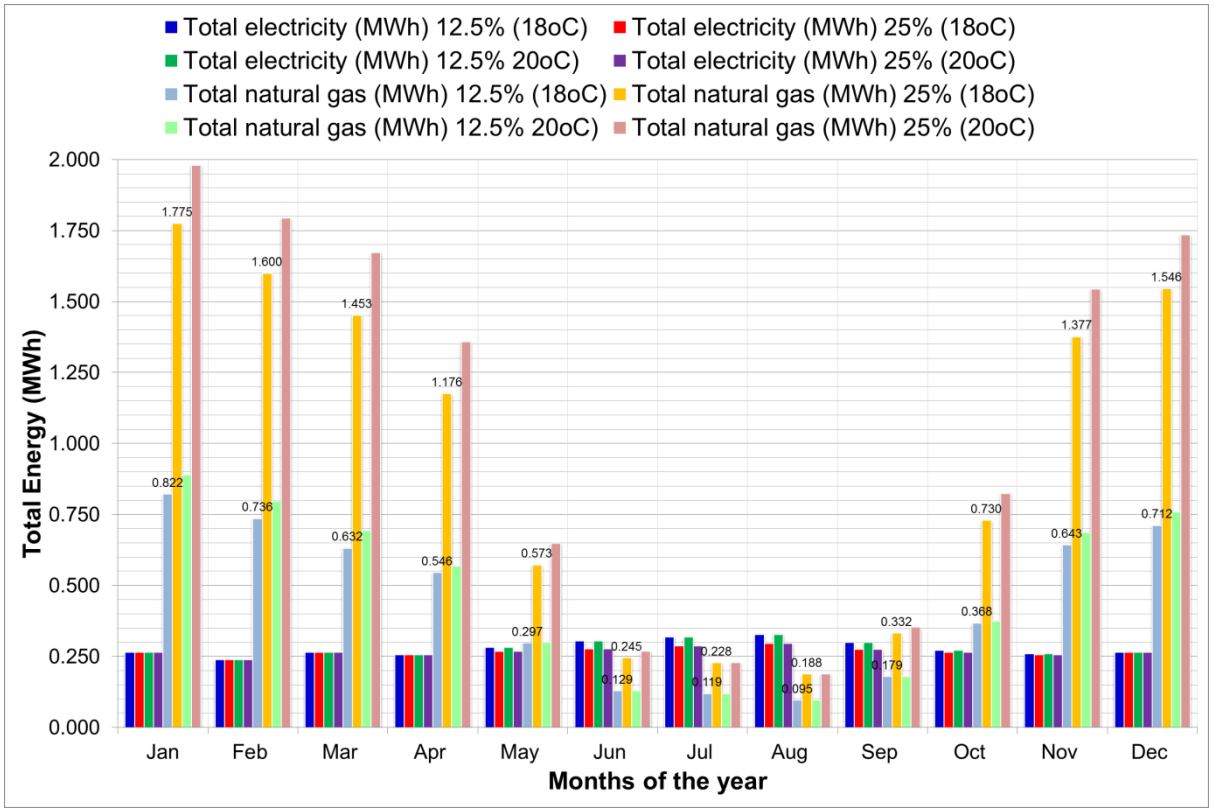

Figure 7:42: Breakdown of Annual total electricity and gas energy usage at two opening fractions and heating setpoints

However, the total energy consumed by Wards 1, 2 and 3 which lie in the same 3.6m structural bay (as depicted earlier by Fig. 7.23) can serve as a schematic (modular) design estimate for each bay of three wards. This can be useful if the bay/module is used to estimate total energy required by an entire wing of single-bed wards.

7.4.5 Detailed room air distribution characteristics

For simplicity of the CFD modelling process, the subterranean labyrinth itself was not modelled, meaning aspects of cooling or air resistance in the supply air were neglected, as this falls outside the scope of research. Rather, the inlets were represented as orifices in each ward's floor which supplied air into an opening on the wall. The actual three storey arrangement of wards was also simplified, such that it is the locations of each stack and each shaft (represented by the horizontally displaced inlets) that defined each floor. The bathroom was a solid block of acceptable geometry and location; and the mechanical extract fan proposed for its interior was not modelled.

The original design of Ward 1 (Fig. 7.43a) was modified by mirroring the bathroom to the opposite side of the room (Fig. 7.43b). This new arrangement is subsequently referred to as Ward 1x. The new bathroom position was estimated to allow similar (i.e. 6^{o}) field of view (FOV) from the bed to the window as obtained in the original design. A doubling of this FOV possible if it was further shifted by 0.6m towards the door.

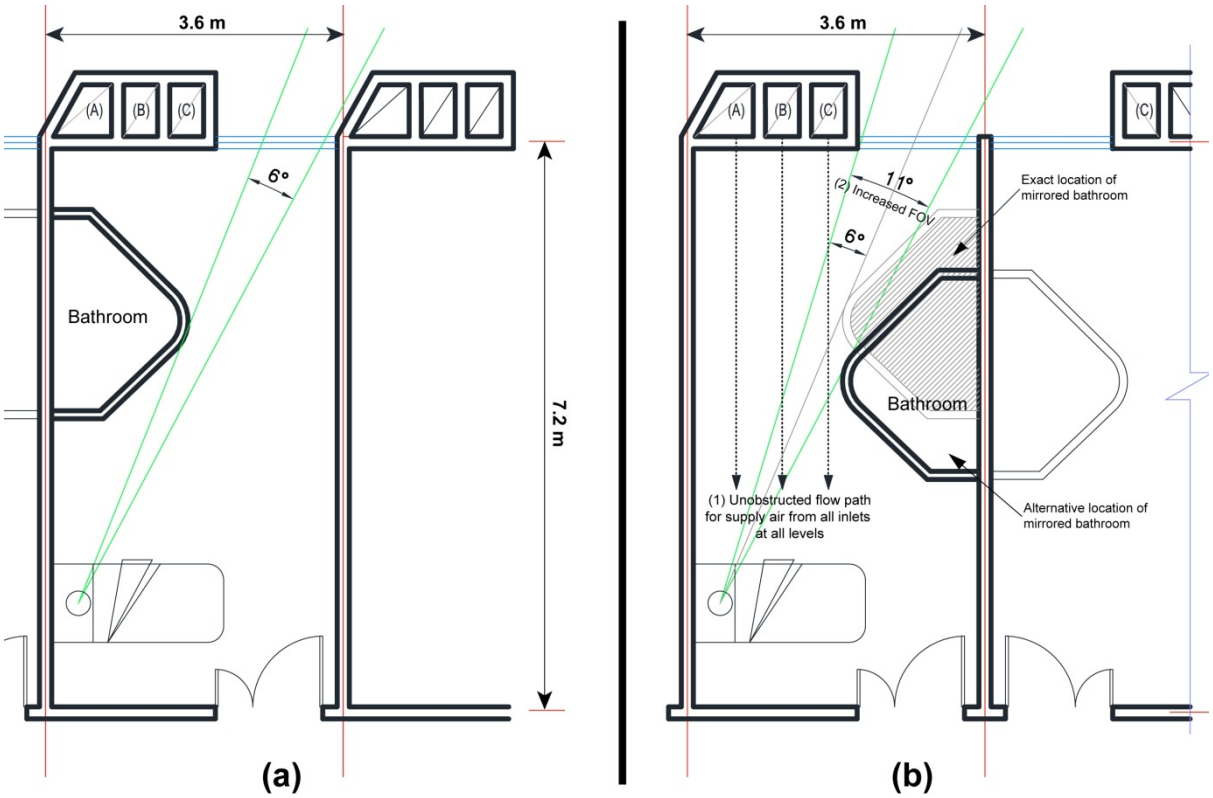

Figure 7:43: Plan of (a) original design of Ward 1 and (b) modified Ward 1x showing actual and alternative position of mirrored bathroom

7.4.5.1 Assumptions and boundary conditions

The heights of stacks for the CFD investigation of these wards were assumed to be the same even though dynamic modelling showed that air flow rate will differ. What was of interest from CFD analysis is how the horizontal location of inlets (A, B and C in Fig 7.43a above) would affect airflow given the presence of an obstacle (bathroom) between them and the patient's bed. Three different wards were modelled in the CFD application PHOENICS (Cham, 2011). The mesh generated for each ward consisted of 18,150 cells for a converged solution using a 0.1% error criterion. A higher mesh density did not produce any significant benefit and consumed more computational time. All other boundary conditions were similar to those used for the ADB simulations include turbulence model (RNG – k-ε) as outlined in Methodology (Chapter 5). For this investigation, no passive contaminant sources were used as the goal was primarily for room air distribution.

7.4.5.2 Age of air and room air distribution

The details of airflow into the four wards were compared using 2D vectors, 2D contours for Age of air and for Temperature as well as 3D streamlines. The initial results from 2D vectors (Fig. 7.44) indicated that as expected, the bathroom obstructs the free movement of air from the inlet to the bed, but the behaviour was different for each Ward. In Ward 1 whose inlet A is the most obstructed, incoming air impinges on the bathroom wall before been forced to change direction, hitting the wall at the left at different angles before proceeding towards the end of the room (Fig. 7.44a).

In Ward 2 the incoming air from inlet B hits the bathroom wall mostly at the slanted surface (Fig. 7.44b), whereas in Ward 3, the air stream only partially hits the bathroom wall. This leads to a situation where one-half of the air stream has unimpeded flow to the bed. The other half hits the bathroom wall before changing direction, where it is also obstructed by its unimpeded half. This behaviour causes a vortex (of stale air) to form at the corner close to the window (Fig. 7.44c).

Essentially, the observed flow characteristics have thus confirmed the initial assumption that the bathroom will block the free flow of air to the bed, and as results show, to different extents. For the purpose of this research these differences in airflow patterns caused by the obstacle have significant implications on the age of air, which is important in measuring the

freshness of indoor air and overall effectiveness of natural ventilation. The plausibility of this argument is demonstrated (Fig. 7.44d) such that the bathroom (i.e. Ward 1x) is mirrored to the other side and the flow of incoming air from the innermost opening (inlet A) has unhindered access to the bed.

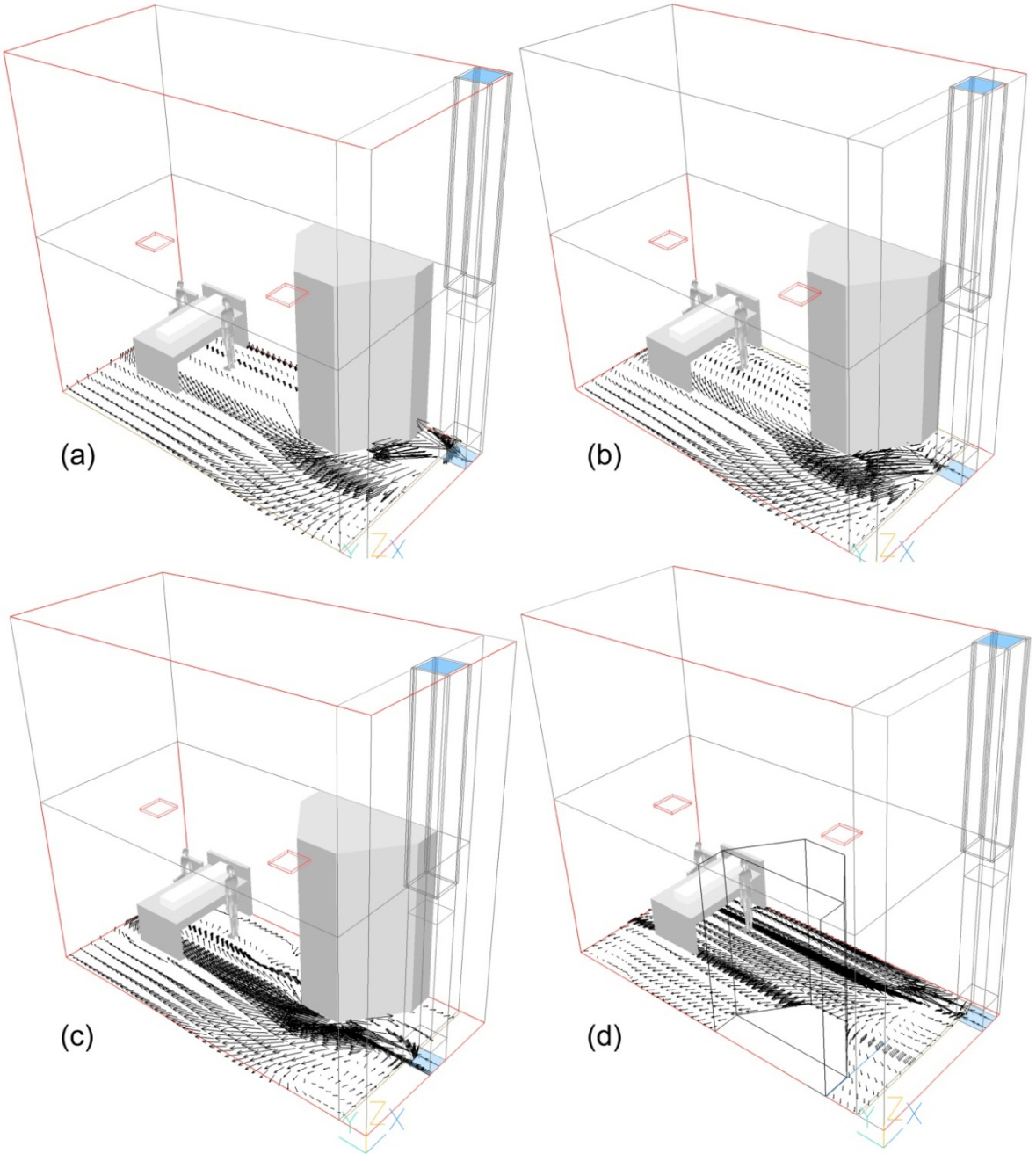

Figure 7:44: 2D vectors for flow direction and pattern through inlets in (a) Ward 1 (b) Ward 2 (c) Ward 3 and (d) Ward 1x

These flow characteristics can also be appreciated from 3D streamlines (Fig. 7.45) which can be appreciated in conjunction with the predicted 2D airflow patterns and direction (Fig. 7.44a-c above). These 2D vector and 3D streamline predictions suggest that two kinds of vortices containing pockets of stale air are created by the laminar supply flow in all cases - but to different extents. The first vortex occurs as a result of supply air bouncing off the walls of the bathroom and thus creating a region of swirl by the window corner (Fig. 7.44c and Fig. 7.45c). The second vortex occurs between the bathroom wall and the patient's bed. This happens after the supply air spreads towards the end of the room, hits the opposite wall and upon its backward flow, bounces of the bathroom wall creating another swirl.

This second vortex may also have been aided by the HCW, whose presence as a heat source would cause air to be entrained in a vertical plume. The 3D streamlines support this deduction. The extent to which the HCW at the given location affects the room air distribution due to entrainment can be subjected to further detailed studies. However, as it would involve a permutation of many potential locations of standing HCWs, embarking on such an exercise falls outside the immediate remits of this study as well as going beyond the scope and objectives of the overall research. Nevertheless it is an issue that is noted for exploration in further research.

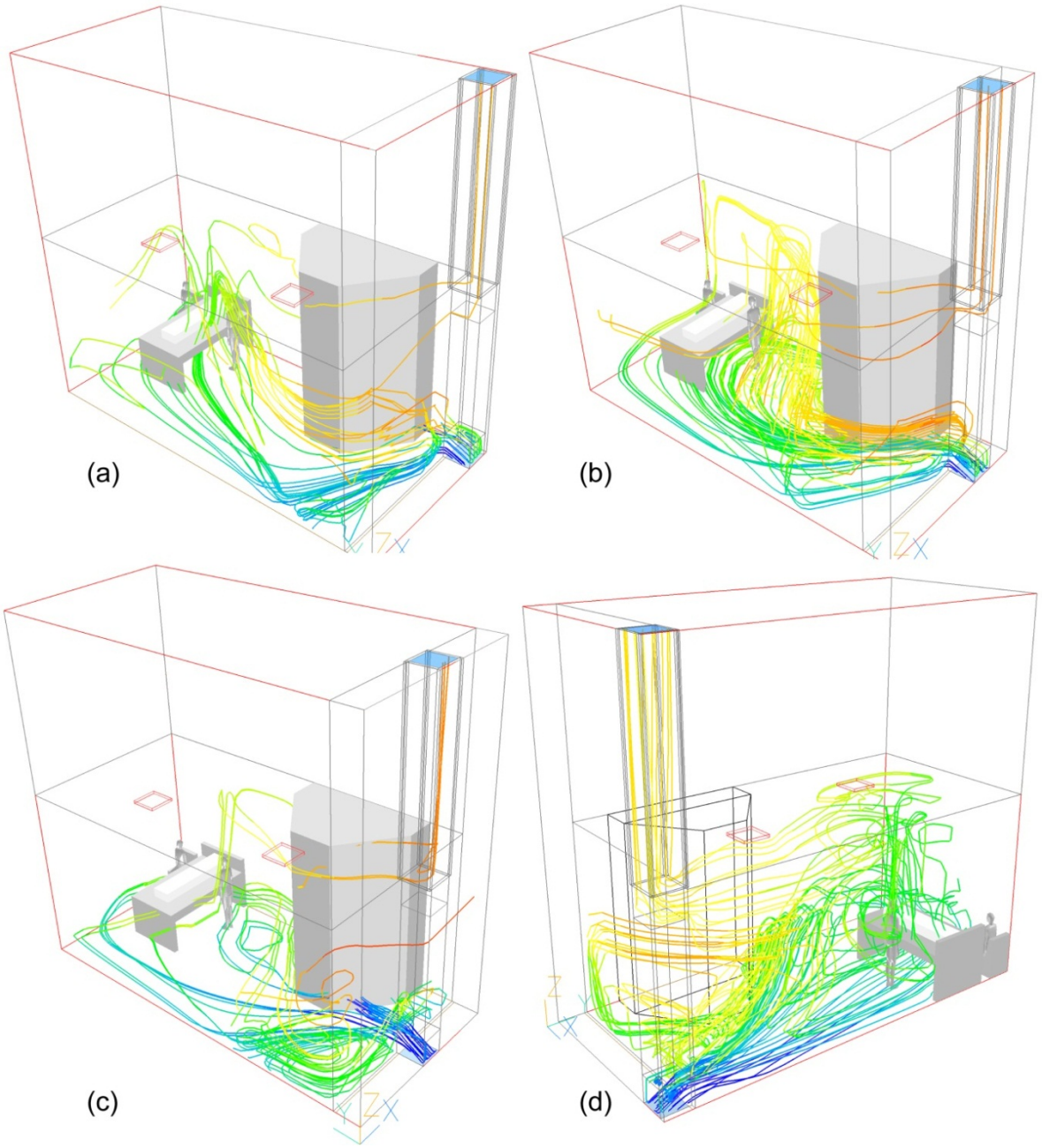

Figure 7:45: 3D streamlines for pattern of airflow in (a) Ward 1 (b) Ward 2 (c) Ward 3 and (d) Ward 1x in reverse angle

7.4.5.3 Age of air

The vortex formed in Ward 3 due to flow out of Inlet C leads to ageing of air at the point where the swirl occurs (Fig. 7.46c). The relocated bathroom in (the modified) Ward 1x also creates a vortex of trapped air as suggested by Fig. 7.44d and 3D streamlines in Fig. 7.45d, however, this does not affect the Age of air as the swirl is isolated and would not occur in the direct path of fresh air (Fig. 7.46d). However for the original cases, (Wards 1, 2 and 3) the presence of a bathroom in the direct line of airflow, the variation in locations of air inlet as well as the formation of vortices both have implications for Age of air. The Ages of air

measured at the top (and middle) of the bed for Ward 1, Ward 2 and Ward 3 are 1276s, 896s and 1042s as shown from 2D contours (Fig. 7.46). With the flipped bathroom (Ward 1x), the Age of air at the bed location is 865s, a difference of 411s (6.85 mins) from Ward 1 and 177s (2.95 mins) for Ward 3. The difference in Age between Ward 2 and the modified Ward 1x is 81s (1.35 mins).

It is of interest to note that in Ward 3 (where half of the incoming fresh air was observed to block the other half) there is a higher Age of air than in Ward 2 whose incoming air from Inlet B is obstructed by the bathroom wall, although this obstruction occurs at a slanted wall angle.

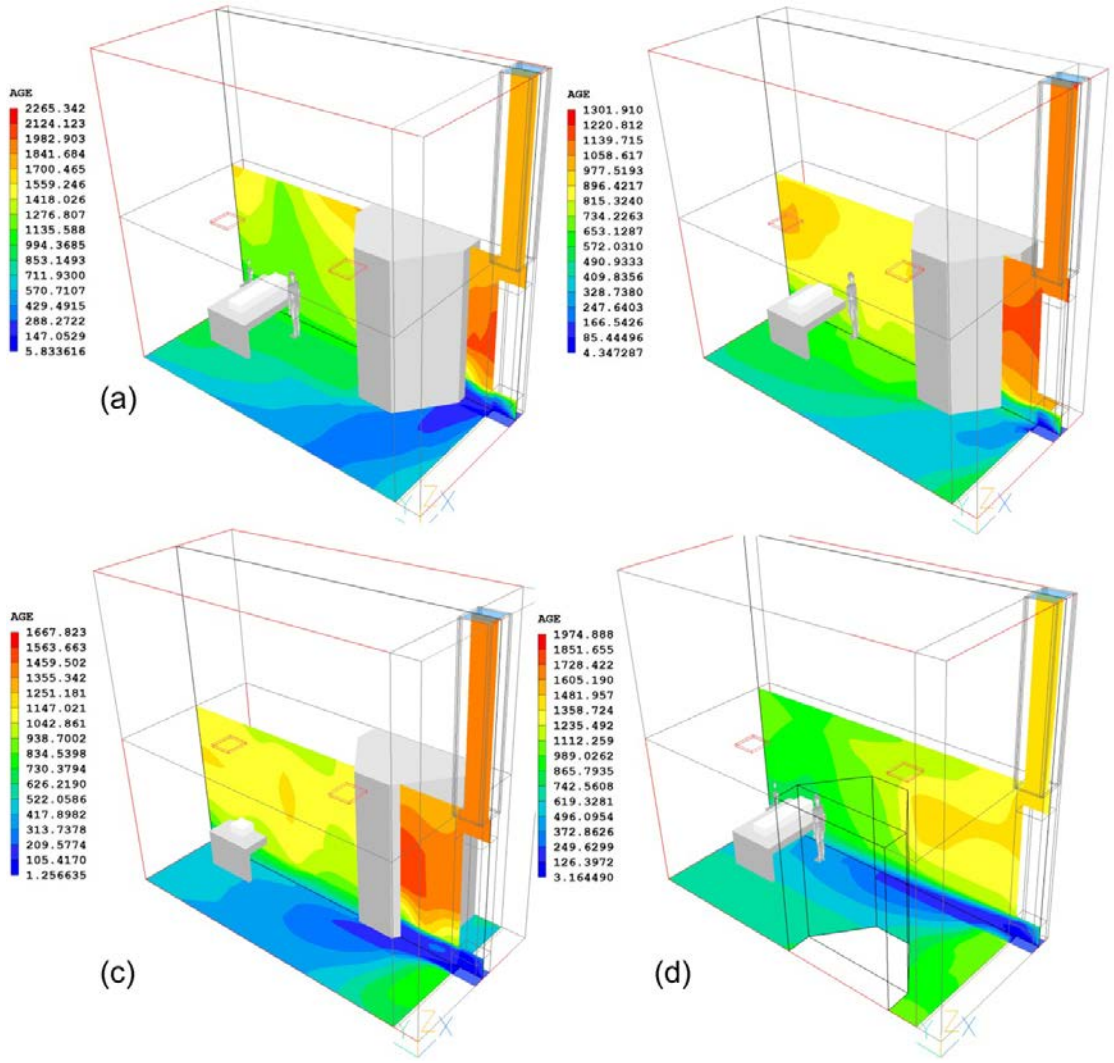

Figure 7:46: Contours for Age of air across (a) Ward 1 (b) Ward 2 (c) Ward 3 and (d) Ward 1x

The gradual ageing of incoming air for Ward 3 in particular is partly due to the bathroom impeding the direct flow of air as occurs in Ward 1 and partly due to do with the swirling of air at the window corner (Fig. 7.46c) as earlier described by 2D vectors. However, whereas Ward 2 has a comparatively similar Age as the case of the flipped bathroom (Ward 1x), it is inferior to Ward 1x in temperature stratification indicated by 2D contours across the room (Fig. 7.47). Airflow into Ward 1x (Fig. 7.47d) which is no longer obstructed by the bathroom will lead to a layered temperature gradient in the vertical direction across the room, which is an expected characteristic of buoyancy driven displacement. In the other cases the temperature gradient is less prominent due to the pattern and ageing of air as implied (Fig. 7.46 above) by Age of air predictions.

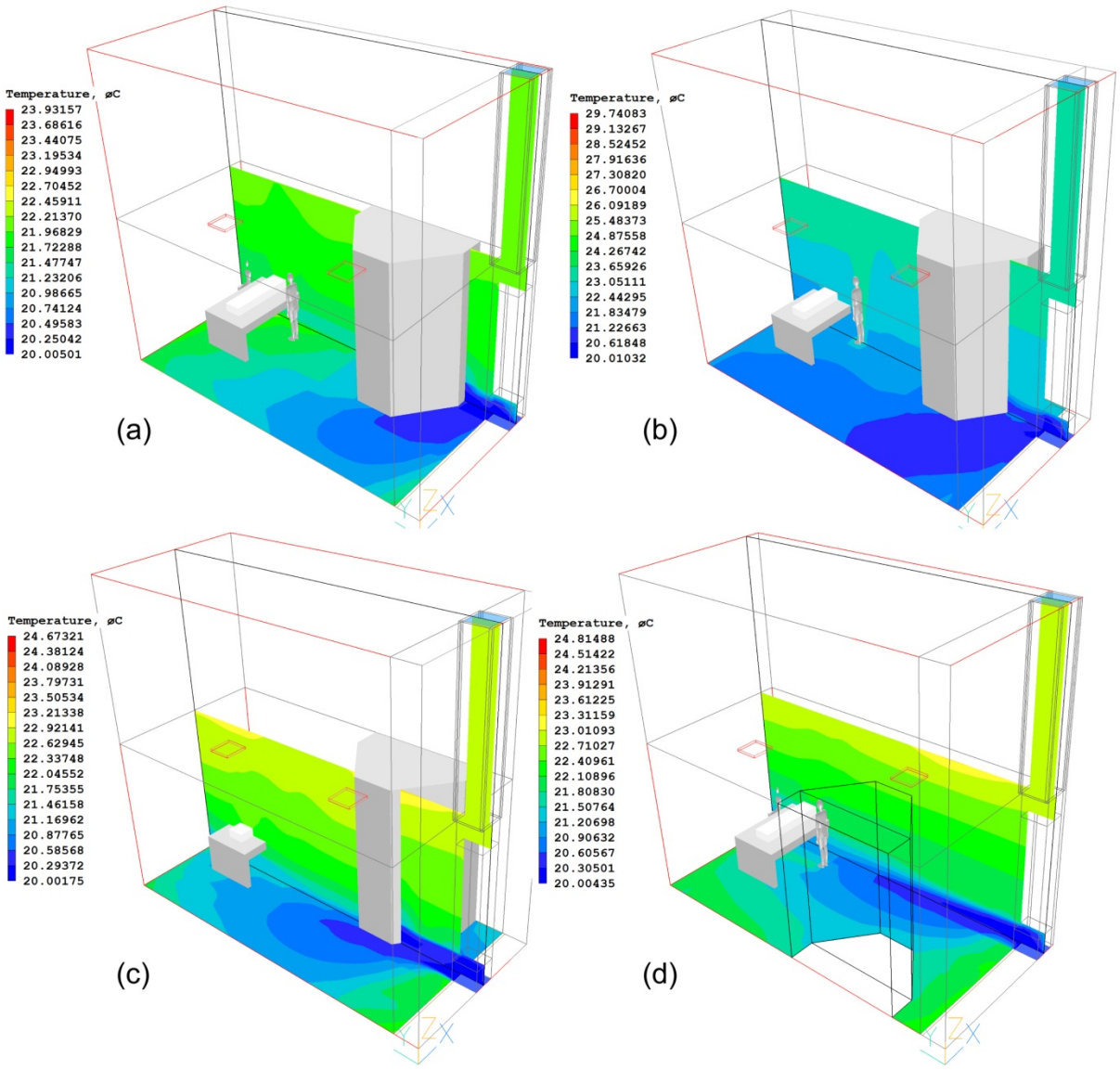

Figure 7:47: Contours for Temperature of air across (a) Ward 1 (b) Ward 2 (c) Ward 3 and (d) Ward 1x

The relocation of bathroom in Ward 1x leads to a 32% (or 6.85 mins) reduction in Age of air at the patient's breathing zone, compared to the original location in the design of Ward 1. The time difference between Ward 1x and Ward 2 is 9% (1.35 mins) and up to 17% (2.95 mins) for Ward 3. These differences in time taken for air to reach the patient's bed have obvious implications for freshness of air. It is generally desirable for fresh air to reach patients as quickly as possible. Based on the original sketch design of the ward, a field of view (FOV) of 6^{o} was created from the patient's bed towards the window. It is essential to demonstrate that this minimum visual access to the window and to daylight is maintained in the modified layout (Ward 1x). The relocated design of the bathroom does not compromise accessibility to daylighting and if the bathroom is slightly shifted (e.g. 0.6m closer to the door), the FOV almost doubles to 11^{o} (Fig. 7.43).

7.5 Summary

The different room air distribution characteristics of two strategies of the single-cell inlet and stack system were investigated in this chapter. The generic ADB single-bed ward was used to demonstrate that inlet height and location of stack have significant impact for buoyancy-dependent ventilation. The predictions from dynamic modelling showed differences in airflow rates between the EIEO and EICO strategies or between low and high-level inlets. The lack of guidance on trickle ventilation rates expected in naturally ventilated wards is an existing shortcoming of both WHO and HTM guidelines. The DTM results obtained from this study can serve as a point of reference for establishing the sizes or fraction of opening fractions for winter ventilation. The heating energy required in winter was also shown to vary significantly depending on the EIEO or EICO strategies adopted as well as on the elevation of inlets. Six different inlet and stack configurations were modelled in CFD where the pattern and direction of airflow which are important for control of pathogenic bio-aerosol were shown to differ significantly based on Age of air, CRE and ATT. These differences were linked to inlet heights and stack location.

These findings are essential for understanding the strengths and weaknesses of each inlet and stack configuration, but these results are only valid for the specific scenarios that were modelled. If either the source of airborne contaminants or the location/orientation of patient's bed change, the potentials and impediments observed are likely to differ as far as occupant

well-being is concerned. These findings demonstrate the ventilation and indoor air quality consequences of locating a stack or raising an inlet. As existing literature is lacking in providing guidance on these issues, the results obtained from these investigations can be beneficial in producing design guidelines for buoyancy-driven ventilation of hospital wards.

The exploratory study (in this chapter) of the potentials, weaknesses and practical implications of buoyancy-driven advanced natural ventilation systems on existing designs of hospital wards accentuate the core objectives of this PhD research. The lessons learnt will be highlighted in Chapter 12 as part of recommendations.

CHAPTER 8: Study 3 - Natural personalised ventilation

8.1 Introduction

It is important for highly susceptible patients in hospitals to be protected from cross-infection due to infectious bio-aerosols in their surroundings as airborne pathogens contribute to hospital acquired infections (HAI). Florence Nightingale was known to promote the principle that without causing any *discomfort*, the air a patient breathed ought to be as *pure* as the *external air*. As simple as this principle sounds, it has three important features: thermal well-being (comfort), air quality (purity) and of course, natural ventilation (external air).

The vulnerability of patients nowadays could arise from suppressed immunity as part of therapeutic procedures or from compromise due to their state of infirmness. A historical overview of patient-centred ventilation has already been covered in Chapters 2 and 3. Since the appearance of the Robbins Aseptic Air Patient Isolation Canopy in the 1970s (as described in Chapter 3, Fig. 3.6), personalised ventilation (PV) has emerged as a modern technique of using clean and conditioned air from a mechanical system usually suspended directly over a patient. This technique ensures that ingress of contaminants into the breathing zone of patients is checked by the downward momentum of supplied air.

The risk to patients that airborne infections pose in single-bed wards could be from other occupants or from medical procedures such as aerosolised medications, as well as from the ingress of contaminated air from contiguous spaces due to poor/failed inter-zonal pressure differences. Apart from HCAI concerns, PV systems also deliver increased comfort to each patient due to the localised control of ventilation including flow rates and temperature of supply air. Despite their benefits however, PV systems are not widely used in hospitals because they have usually been applied only in exceptional cases due to the sophistication and cost of such systems. In addition, there are concerns about reducing the energy consumption of healthcare processes and systems, making use of mechanical PV systems an unattractive option. Coincidentally, the world health organisation (WHO) has recognised the potential for low-energy natural ventilation for airborne infection control as essential to its patient-centred recommended ventilation (i.e. 60 l/s/patient as airflow rates for wards). However, the question of how to meet this recommended airflow rate has remained

unanswered due in part to the fluctuating nature of most natural ventilation systems. There is also the matter of how to ensure that patients benefit directly from such airflow rates if they are to remain safe from airborne pathogens. Supplying 60 l/s efficiently into a ward (or any space for that matter) does not guarantee that it would be effective for aseptic purposes due to problems such as short-circuiting between supply and exhaust points, or due to poor airflow direction and pattern, relative to pollutant sources and sinks.

This chapter describes an innovative natural ventilation system that has potential to provide answers to some of these questions. Natural personalised ventilation (NPV) is a novel system that utilises natural airflow in a simple system comprised of a duct and a stack with the aid of forces of gravity and buoyancy. Different concepts of NPV are presented based on many considerations such as architectural flexibility, expected nature of occupancy and sources of infectious bio-aerosols. The first series of studies of NPV were intended to demonstrate its feasibility using three different architectural configurations while subsequent studies were focused on an optimised design with the intent of exploring effect of stack locations relative to duct inlets (i.e. using edge-in edge-out or edge-in centre-out).

As with other studies done so far, dynamic thermal modelling and computational fluid dynamics are the tools used in the exploratory study of NPV. The metrics used for evaluation include airflow rates, temperature, PMV, Age of air and effectiveness of heat removal. The potential for draught, summer overheating also led to three different external temperature scenarios being considered: 15^{o}C, 20^{o}C and 25^{o}C, for evaluating the effect of temperature differential on both thermal comfort and airflow through the supply ducts.

8.2 Principles and concepts of NPV

The principle of buoyancy-driven natural ventilation hinges on the fact that warmer air rises and cooler air falls. Most buoyancy-driven airflow systems take advantage of this principle to deliver displacement ventilation whereby low-level inlets supply fresh cooler air which ascends upwards, the speed of which depends on factors such as size of openings, the magnitude of internal heat loads and the temperature differentials. With this in mind, NPV was conceived as a system characterised by horizontal duct suspended at the ceiling which does three simple tasks: (a) it collects and directs fresh air coming from an inlet on an external wall; (b) it shields the fresh air from warmer and stale indoor air up to a point in the

space where it; and (c) discharges from an orifice, the fresh cooler air, which then descends into the space below due to gravity and its density, which is relatively higher than the surrounding warmer indoor air. The stale air in the room would then escape via a stack whose point of discharge is significantly higher than the duct in order to create the appropriate neutral pressure line. The architectural engineering concepts used to test this idea and the brief mathematical theories which support it, are explained in the next subsections.

8.2.1 The architectural engineering concepts

Three distinct configurations of NPV ducts were developed (Fig. 8.1) to test its plausibility and eventual performance of the system, taking into cognisance architectural and functional considerations such as shape, length and location. Other considerations taking into account are engineering constraints like shape of duct and the travel distance for air. In the first instance, (Case 1), the computed area of inlet becomes the area of NPV duct, intended to deliver the entire supply air needed by the space directly over the bed as shown in Fig. 8.1a. In the second instance, (Case 2) the computed area of inlet is split into two, the first part of which becomes the area of NPV duct and the second being a low-level supplementary inlet, depicted in Fig. 8.1b. This second case was also designed to be an L-shaped duct, to test the flow characteristics of supply air not driven by mechanical force in a bent duct. In the third design, a short NPV of same area as that of Case 2, is supported by low-level inlet which is this time around split into two distinct openings, separated 2.5 meters apart (Fig. 8.1c).

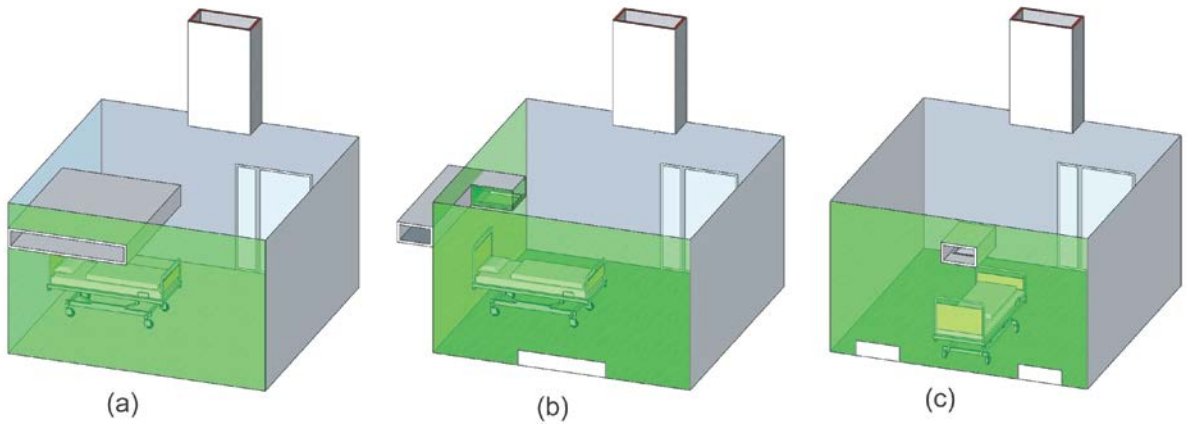

Figure 8:1: Initial design of proposed NPV showing (a) Case 1 (b) Case 2 and (c) Case 3

The three conceptual models of NPV system are subsequently investigated using dynamic thermal modelling (DTM) and computational fluid dynamics (CFD).

8.3 Materials and methods for conceptual investigation

The single-bed ward as specified by the Activity Database, ADB (DH 2010) was modelled as the computational domain in DTM and CFD applications in two separate phases of investigation. The ward dimensions, indoor heat loads and occupancy patterns, other assumptions and boundary conditions applied for this study are similar to those already used for the standard ADB single-bed ward in Chapters 6, 7 and 8. Initially, a temperature differential of 1 Kelvin, representing a worst case summer scenario was used as the basis for sizing the inlets, which were assumed for simplicity to be for single sided natural ventilation. This approach was adopted due to lack of precedence in the design of similar natural ventilated systems. The computed area of opening needed to meet 6 ACH as per HTM 03-01 (DH, 2007) was found to be 0.66m^2 using single side opening sizing model (Equation 9) covered in Chapter 2. A constriction of the cross-sectional area into 0.25m^2 (i.e. 1% of floor area or 0.37% of 0.66m^2) was also done to test the capacity of the systems to meet 6 ACH from smaller opening fractions. This approach mimics the method developed for sizing ANV stacks as demonstrated by Lomas and Ji (2009); whereby the cross sectional area of both inlet/duct and stack is a function of a percentage of the floor area. Finally, one of the conceptual models (Case 2) was adopted and Optimised with an NPV ducts and exhaust stacks sized using 1.5% in this case or 0.375m^2.

The goal of the initial phase of investigation was to ascertain its general plausibility of NPV as a workable concept. This was done with the assumption that like ANV system, airflow into the ward via the NPV system will be based on buoyancy (wind-neutral) designs only. As such, findings focused on ascertaining the airflow rates from the three different cases, and how air flow from the ducts could protect patients from contaminated indoor air. The DTM was used to predict the annual flow rates simplified according to seasons. The CFD simulation provided detailed insights into the metrics of performance such as contaminant removal efficiency, effectiveness of heat removal, age of air and room air distribution (pattern and direction of airflow). These metrics have already been described in Chapters 2 and 3 and applicable ones were measured with respect to the 5 points of interests (POIs) defined in Chapter 5 (Research Methodology).

The goal of the second phase of investigation was to use the Optimised NPV duct and stack system to understand firstly, the expected temperature and concentration of airborne contaminants at the location of fresh air discharge under three different ambient temperatures

(15^{o}C, 20^{o}C and 25^{o}C). Secondly, there was a need to evaluate the effect which two possible stack locations (i.e. edge-out or centre-out) would have on room air distribution. For focus, this second phase of study was conducted using CFD only, as the viability of airflow using NPV concept was the objective of the initial study.

8.4 Bulk airflow results for conceptual investigation

8.4.1 Air changes at 0.66m^2 and 0.25m^{2}openings

The rate of ventilation achievable from each conceptual case at different opening sizes are summarised in Table 8.1. The volumetric flow varies with each case and with opening size under different ranges of air change, and this variation is somewhat random. For instance, in the 6 to 7 ACH range, Case 1 has the most number (59) days at 0.66m^2 opening, whereas Case 2 has the most number of days (20) at 0.25m^2 opening. Similarly, at 0.25m^2, Case 3 has 346 days when it will deliver < 6ACH, comparable to Case 1 with 345 days. The use of air change in ranges (e.g. 6 to 7 ACH) in Table 8.1 was essential because with natural ventilation, fluctuation in flow is certain making it logical to capture ranges rather than fixed rates of ventilation. Although both Cases 2 and 3 have the same cross-sectional area of low-level inlets, the use of two horizontally displaced low openings in Case 3 led to more airflow into the ward than one opening as obtains in Case 2.

Table 8.1: Number of days of occurrence of 6 to 10 air changes at two openings

	NPV Concept	< 6 ACH (Total days)	6 to 7ACH	7 to 8 ACH	8 to 9 ACH	9 to 10 ACH	> 10 ACH (Total days)
0.66m^2	**Case-1**	60 days	59 days	80 days	50 days	17 days	99 days
	Case-2	46 days	49 days	74 days	66 days	26 days	104 days
	Case-3	50 days	53 days	78 days	61 days	22 days	101 days
0.25m^2	**Case-1**	345 days	18 days	3 days	0 days	0 days	0 days
	Case-2	342 days	20 days	3 days	0 days	0 days	0 days
	Case-3	346 days	18 days	2 days	0 days	0 days	0 days

It is clear that when openings are 0.25m^2 in cross-sectional area there will be difficulties achieving more than 7 to 8 ACH into the ward spaces. Rather than use a specific cross-sectional area (0.66m^2 or 0.25m^2) to assess opening fractions, a percentage of these areas (i.e. 100, 50 and 25%) will subsequently be used to assess annual flow into the ward spaces. These percentage fractions can always be converted into an absolute cross-sectional area, and

this approach can help understand the amount of constriction needed to either minimise overheating in summer or to allow trickle ventilation in winter.

8.4.2 Flow into wards at different percentage of openings

Fig. 8.2 reveals the total airflow patterns into the entire ward cases, using the middle week of each season as representative periods of the year, at 25% opening fraction. The variation in volume flow rate is seen to be largely the same at this and other opening fractions as observed in Fig. 8.3 and Fig 8.4 for 50% and 100% opening fractions respectively, with differences being in magnitude of absolute flow rates.

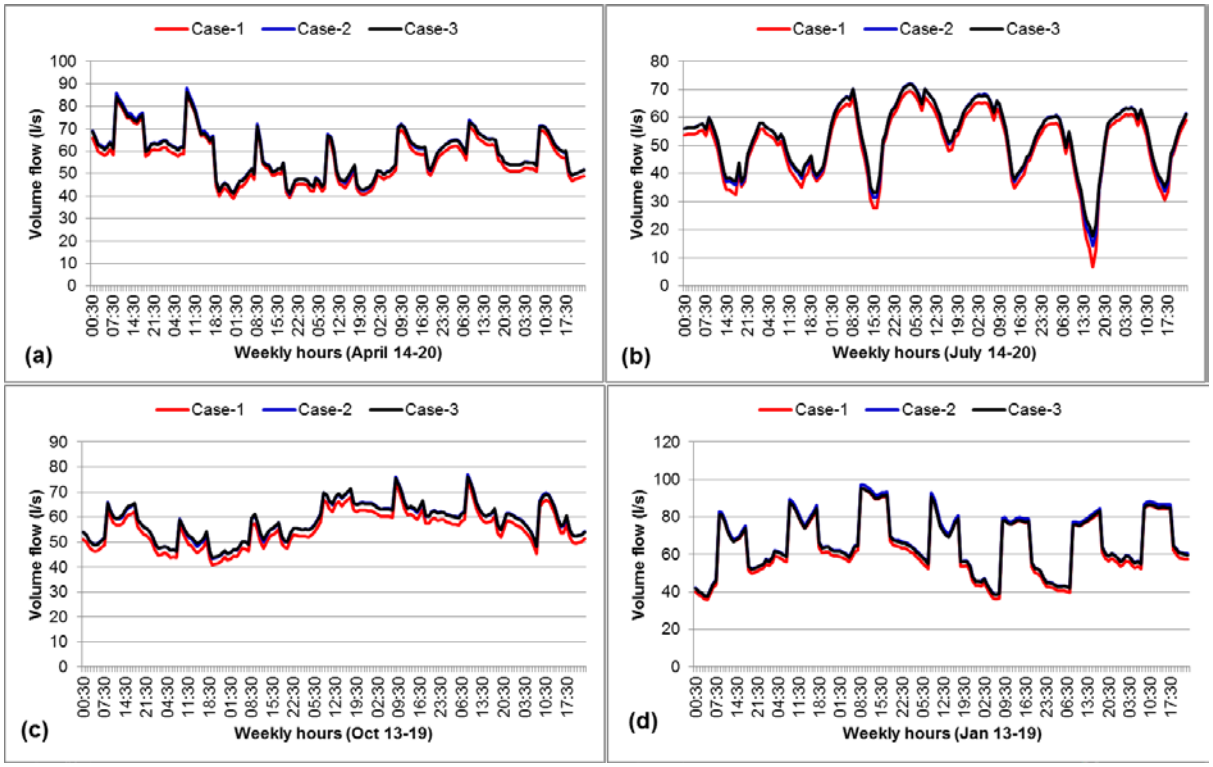

Figure 8:2: Seasonal variation in airflow through entire wards with 25% opening in middle of: (a) Spring (b) Summer (c) Autumn and (d) Winter

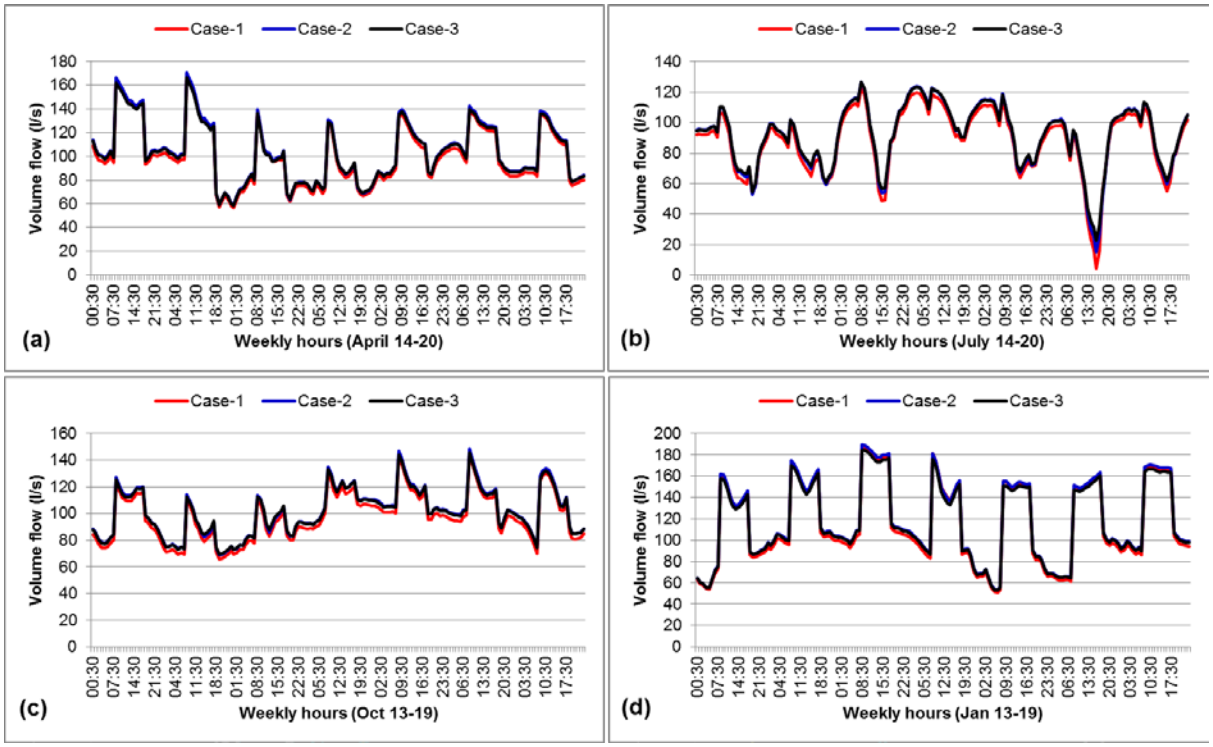

Figure 8:3: Seasonal variation in airflow through entire wards with 50% opening in middle of: (a) Spring (b) Summer (c) Autumn and (d) Winter

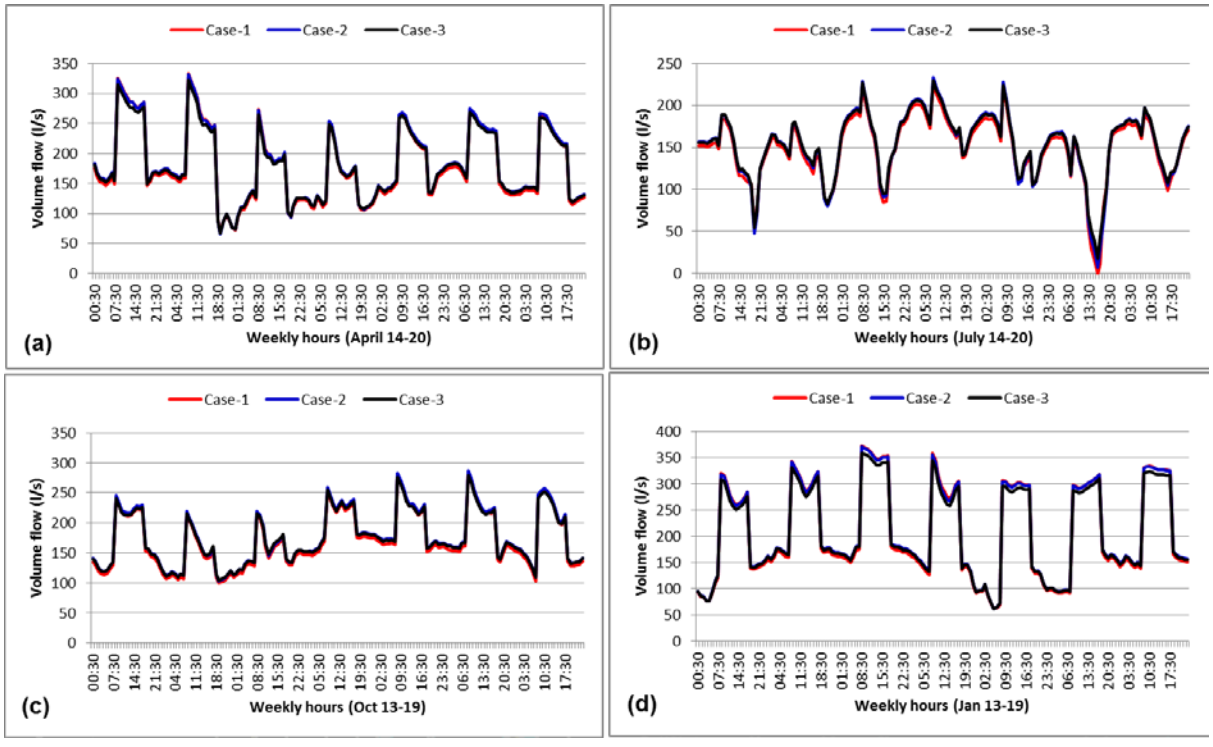

Figure 8:4: Seasonal variation in airflow through entire wards with 100% opening in middle of: (a) Spring (b) Summer (c) Autumn and (d) Winter

8.4.3 Flow through individual NPV ducts

The general pattern of fluctuating airflow into each case is similar for each season at specific opening fractions as seen in previous results, however, it is necessary to review the actual flow into each duct, given that conceptually, they were not sized to be of the same area or location. The seasonal variations expected in airflow through the ducts are shown in Fig. 8.5. This reveals the predicted fluctuations in a typical week, taken at the middle of each season from 0.66m^2 openings: 14-20 April (Spring); 14-20 June (Summer); 13-19 October (Autumn) and 13-19 January (Winter). For clarity and comparison, the results have been structured as total airflows into entire ward (Fig. 8.5a) and total airflow via each NPV duct (Fig. 8.5b), bearing in mind that there is additional airflow into the ward from supplementary low-level inlets in Case 2 and Case 3 concepts. This enables an assessment of performance to be made of airflow rates into each duct relative to total flow into each ward. For simplicity, Case 2 was selected for this detailed study of airflow into ward versus airflow into duct as shown in Figures 8.5 and 8.6.

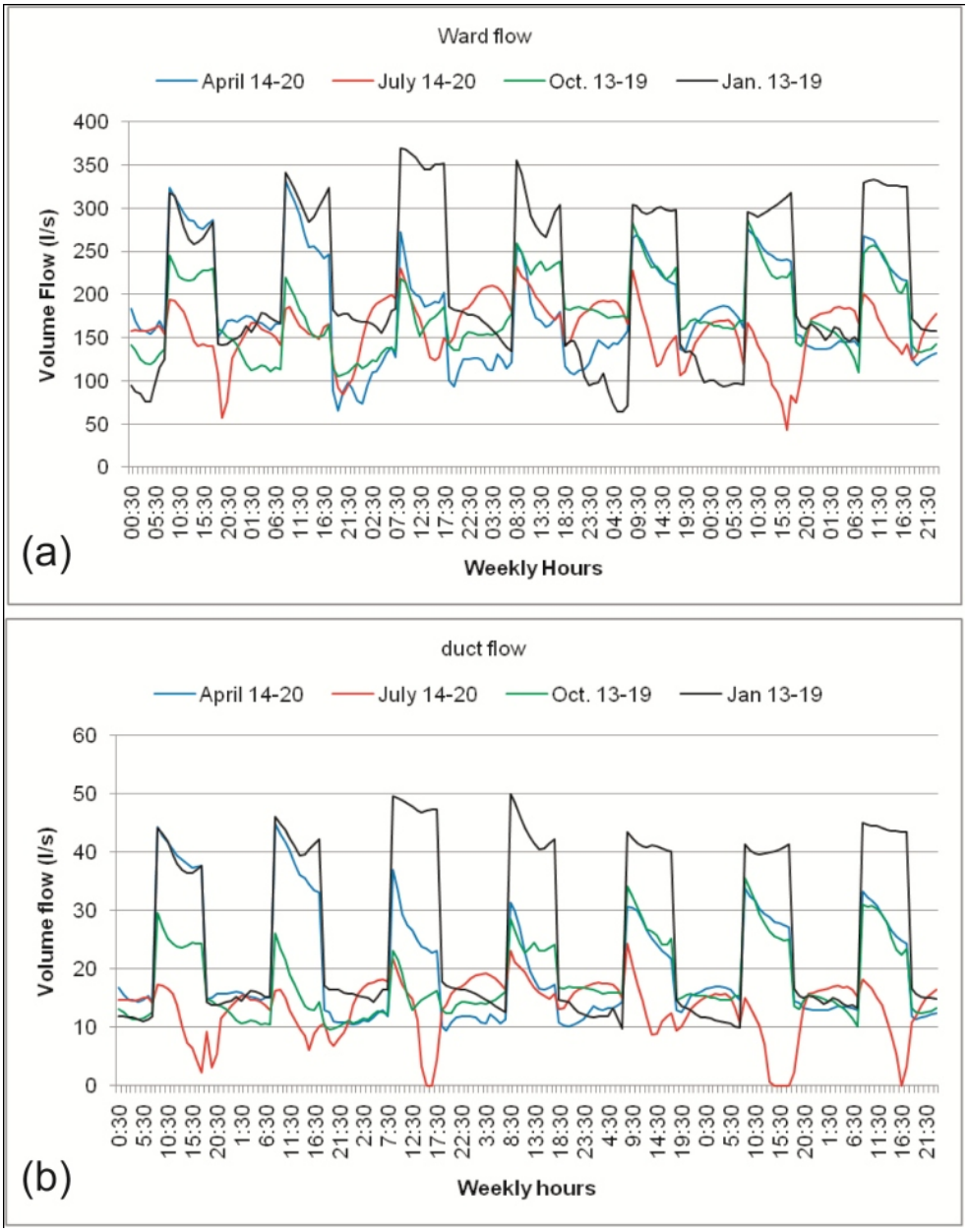

Figure 8:5: Weekly flows for 0.66m^2 opening into (a) ward and (b) duct

For the stack area of 0.25m^2, the predicted total flows in the selected weeks of each season are given in Fig. 8.6. The airflow into Case 2 ward shown in Fig. 8.6a are modest, compared to previous case when stack size of 066m^2 was used. The flows substantially fall below the recommended 60 l/s/patient rate of the WHO when duct sizes are 0.25m^2 as indicated by Fig. 8.6b.

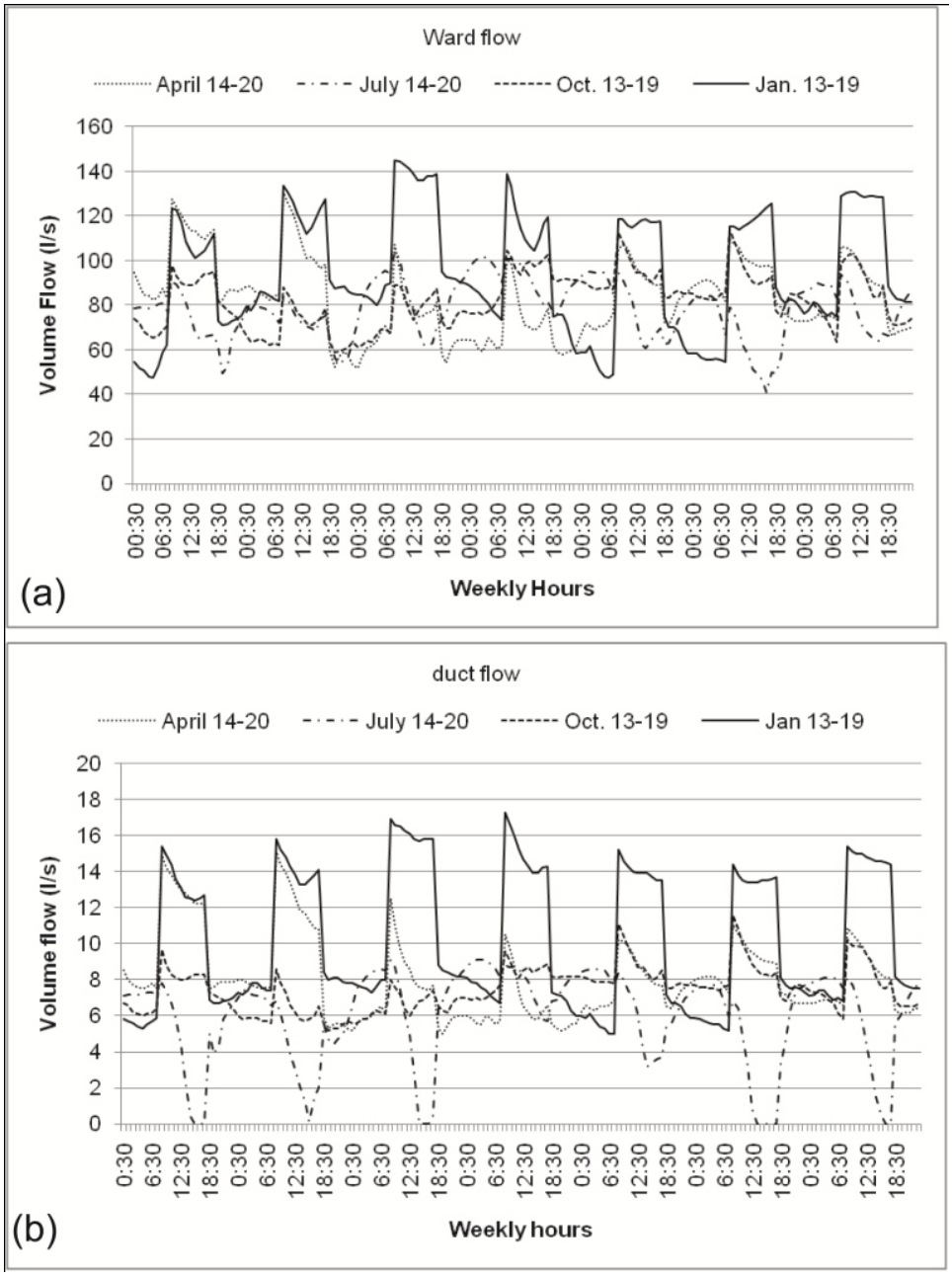

Figure 8:6: Weekly flows for 0.25m^2 opening into (a) ward and (b) duct

A direct comparison of airflow into each duct using mid-July week was made. As could be expected, the flow through NPV ducts is much lower using cross-sectional area of 0.25m^2, as opposed to 0.66m^2 as evident from Fig. 8.7. The significant differences in flow rates between the larger duct in Case 1 and the flow in ducts of Case 2 and 3 at 0.25m^2 (i.e. 38% of original size) is evident.

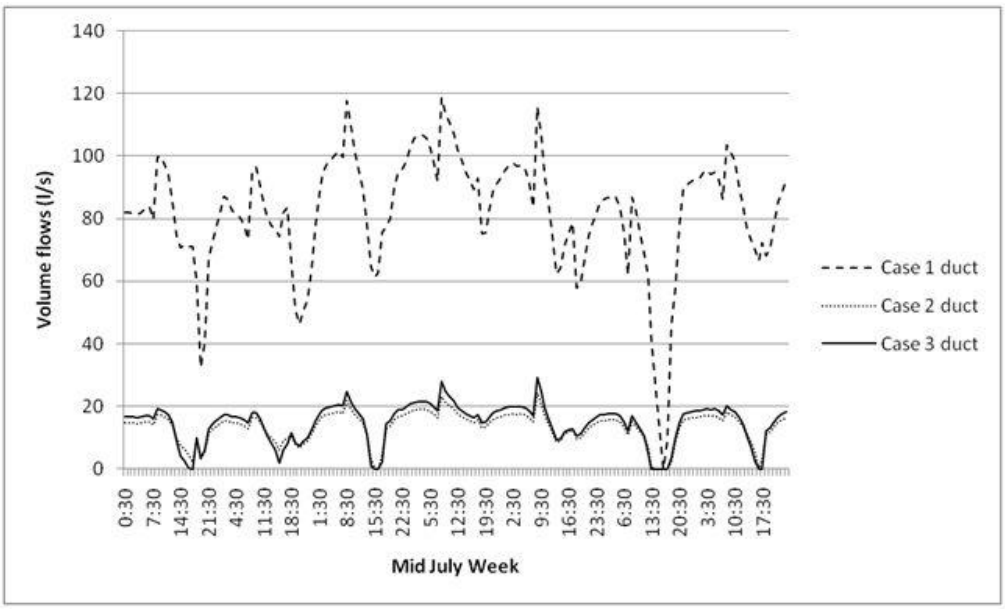

Figure 8:7: Weekly flow of air into ducts of Cases 1, 2 and 3 at 38% opening fraction

Two arguments can be made based on these results, firstly, that an ideal size of stack could lie between 1% of floor area (i.e. 0.25m^2) and 2.6% of floor area (i.e. 0.66m^2). Secondly, the presence of additional low-level inlets (which have greater chance of airflow due to their superior vertical distance to exhaust) deprive the 0.25m^2 duct of more airflow than would have been possible in their absence. However, since for the strict evaluation of NPV as a feasible system, these low level inlets are rather unnecessary. Therefore this deduction serves as the primary rationale for using 1.5% of floor area (0.375m^2) as the cross-sectional area of both stack and duct in the Optimised NPV system – without any low-level inlets.

8.5 CFD results from conceptual investigation

8.5.1 Indoor air quality metrics

The metrics used to evaluate the performance of the three conceptual cases include Age of Air, LACI, MACE, CRE, EHR and ATT as previously defined in Chapter 2. For the points of interest, comparisons of the Cases for these metrics are provided in Fig. 8.8a, Fig. 8.8b and Fig. 8.8c; with exception of MACE, EHR and ATT which relate to an entire space shown in Fig. 8.8d. There is an apparent correlation between Age, LACI, MACE, EHR and ATT and in all instances; Case 2 has the best overall performance, except regarding ATT, where its value of 352s is more than twice the value for Case 1. With regards to removal of contaminants from the space, each Case provides unique values for the selected POIs. The

implication of this is that practical application would depend on what the design goals are or who among the occupants is considered most at risk since CRE varies from point to point for each Case even though source location is constant. The CRE value for point D is similar for all cases, being the actual source location.

The absolute values which the different metrics take are an important criteria but the magnitude of a particular metric determines its interpretation. For example, for Age of air in Fig. 8.8a, a lower Age at a point indicates that the air at that point is relatively young in the space. Similarly, for ATT in Fig. 8.8d, a lower value is preferable, since it signifies the turnover time required for ventilation system to remove pollutants from a space. For all the other metrics in Fig. 8.8, a higher value implies better performance, as exemplified by LACI, CRE and EHR which deal with efficiency of air exchange at a point and the effectiveness of contaminant and heat removal, respectively.

Results shown in Fig. 8.8c suggest that NPV duct in Case 3 is able to provide relatively high CRE at points A, B and E, despite having a lower airflow rate than Case 1 duct (as earlier implied by Fig. 8.7). However, the potential impact of two low-level inlets cannot be discounted. In general, it can be shown from the results that the performance of NPV systems in terms of airflow rates is not proportionate to their effectiveness as per dilution of contaminants. This further supports the need for detailed investigation into an optimised design of NPV system.

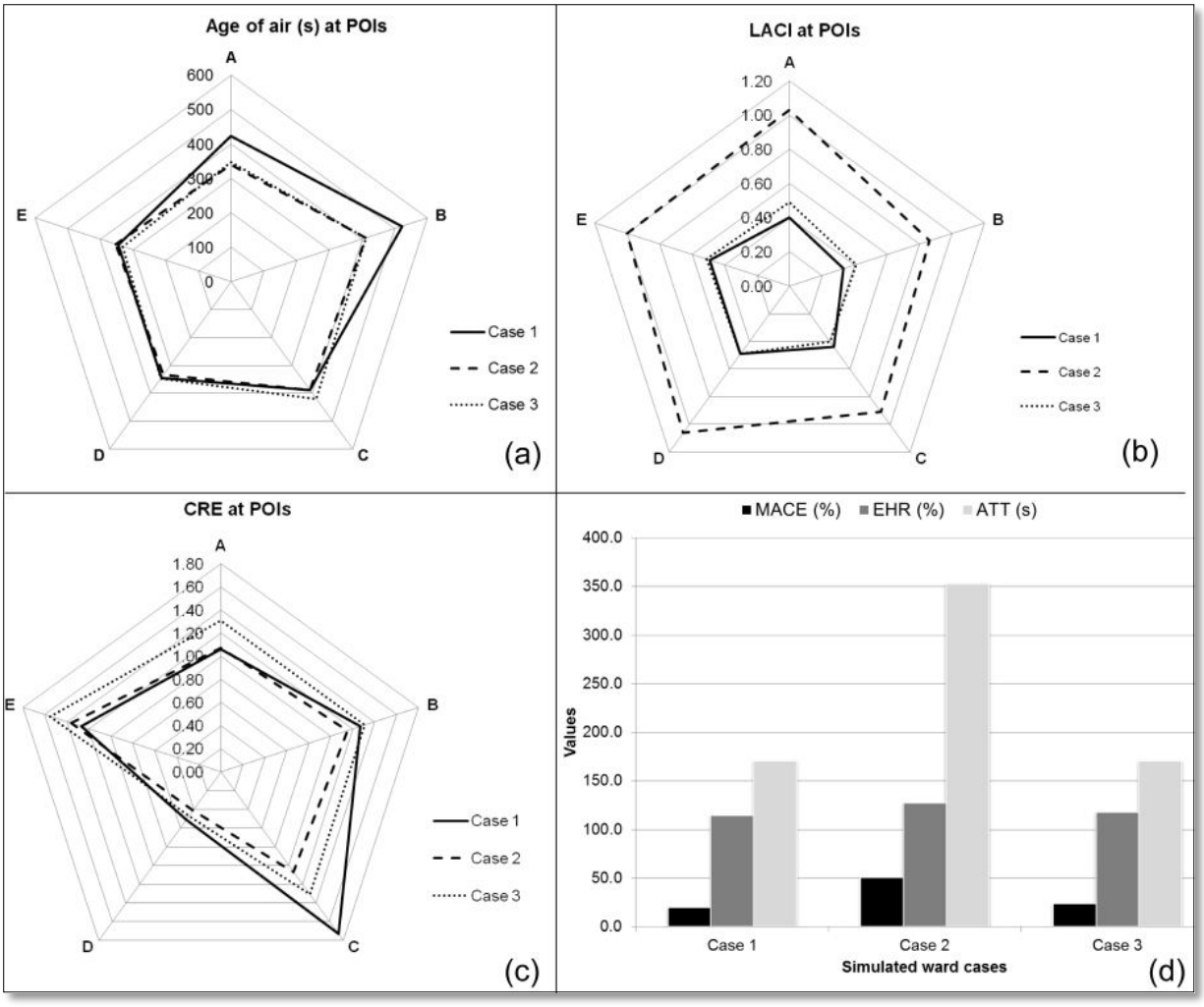

Figure 8:8: Airflow metrics with (a) Age (b) LACI (c) CRE and (d) MACE, EHR and ATT for all Cases

For practical purposes, more detailed studies about airflow direction against the backdrop of clinical needs of a ward could be used to determine how best to utilise NPV for contaminant control. This deduction is supported by the negligible differences in EHR of all Cases which is contrasted by the significant variances in MACE values in Fig. 8.8d. Both metrics deal with the entire volume of space and not specific points. The MACE value of Case 2 (50.4%) for example is more than twice that of Case 1 (19.5%) and Case 3 (23.3%), further complicating the results and their potential benefits.

8.5.2 Room air distribution

The results obtained from both dynamic modelling and CFD so far have been scalar quantities which deal with numbers and the relative significance of their magnitudes. However, because ventilation is in fact a three dimensional matter occurring in space and in

time, the use of airflow contours and 2D/3D vectors can provide qualitative input for better interpretation of results. In the conceptual cases, different room air distributions were observed from CFD results. Streamlines depicting the different directions and patterns of airflow from the three Cases are shown in Fig. 8.9.

Relative to ducts in Cases 2 and 3, the large duct in Case 1 causes an understandably large volume of cooler air, which descends to the bed below due to influences of density and gravity, (Fig. 8.9a) thereby leading to substantial mixing of air over and around the patient's bed. In the conceptual design of NPV system, the conscious decision to allow a 0.5m space between the ceiling and the duct pays dividends in the sense that stale buoyant air collecting at the ceiling is discouraged from mixing with fresh air. In general, all NPV ducts exhibit the capacity to create mixing ventilation purely from buoyancy, which has hitherto the exclusive reserve of mechanical ventilation or wind/fan assisted natural ventilation.

Conversely, the presence of low level inlets and utilisation of smaller ducts in Case 2 and Case 3 meant these designs are unable to provide as much mixing as occurs in Case 1, due to the displacement nature of their supplementary air supply. The typical weekly flows into ducts of Cases 2 and 3 which are lower than for Case 1 duct, (Fig. 8.7) are related to their smaller sizes, leading to a smaller mass of cooler air falling into the space. However, the larger Age of air at the POIs in Case 1 also implies that notwithstanding its greater ventilation rate and mass of air, the substantial mixing occurring is also responsible for partial recirculation of indoor air. This may indeed be desirable since mixing ventilation is known to be suitable for dilution of pollutants, and for creating more uniform thermal environments.

Also observed from CFD results is the fact that descending fresh air does not just 'drop' directly and vertically into the space. Rather, it experiences some amount of displacement in the form of a horizontal throw in the direction of air supply, as shown in Fig. 8.10. This behaviour is a known phenomenon of a jet of cool air entering a warmer space (Koestel, 1955; Awbi, 2003). The approximate throw distance is 0.3m for Case 1 and Case 3 ducts (Fig. 8.10a and Fig. 8.10b respectively) and up to 0.5m for the duct in Case 2 (Fig. 8.10c). Thus, there is need to consider the actual drop zone of a refined and Optimised NPV system for future applications. Although temperature differential, location of inlets/outlets and pressure gradient will determine total flow into the space, it is conceivable that for practical purposes, the preferred drop zone will be determined by the type of control mechanisms to be used for

regulating flow and clinical factors including patient's condition and thermal comfort needs including draught sensation.

In spite of the mixing occurring in Case 1, the mean Age of air at the level of patient's bed is ≈ 305s whereas in Case 2, it is 353s with a comparatively large pocket of stale air (Age = 469s) over its duct. For all cases, the Age of air at the point representing patient's head (Point E) is the lowest with respect to other POIs (see Fig. 8.8a). For indoor temperature, all three Cases display different pattern of indoor heat distribution. In Case 1 (Fig. 8.11a) for instance, the temperature gradient is more evenly distributed over the entire length of patient's bed with a mean value of 23.7^{o}C. In other Cases (Fig. 8.11b and Fig. 8.11c), the momentum of descending jet of fresh air creates, a cooler zone up to the middle of the bed, with mean temperatures of 22.8^{o}C and 22.6^{o}C for Cases 2 and 3 respectively. Additionally, the temperature at the foot of the bed for these two Cases is as high as 24^{o}C. However, the low level inlets of these Cases allow the encroachment of cooler air, rising towards the middle of the room. This fact is responsible for the mean room temperatures of Cases 2 and 3 being 23.2^{o}C and 23.5^{o}C respectively, whereas Case 1 has a higher mean value at 24.2^{o}C, i.e. an approximate rise of 1^{o}C in mean room temperature. The higher values of EHR (which considers heat removal from the entire space) in Cases 2 and 3 spaces corroborate to this observation.

It must however, be pointed out that in reality, preheating of fresh air would more or less be mandatory in winter because dumping of cold air over patients would be undesirable and counter-productive. This aspect (pre-heating) has not been considered but is an opportunity for further research.

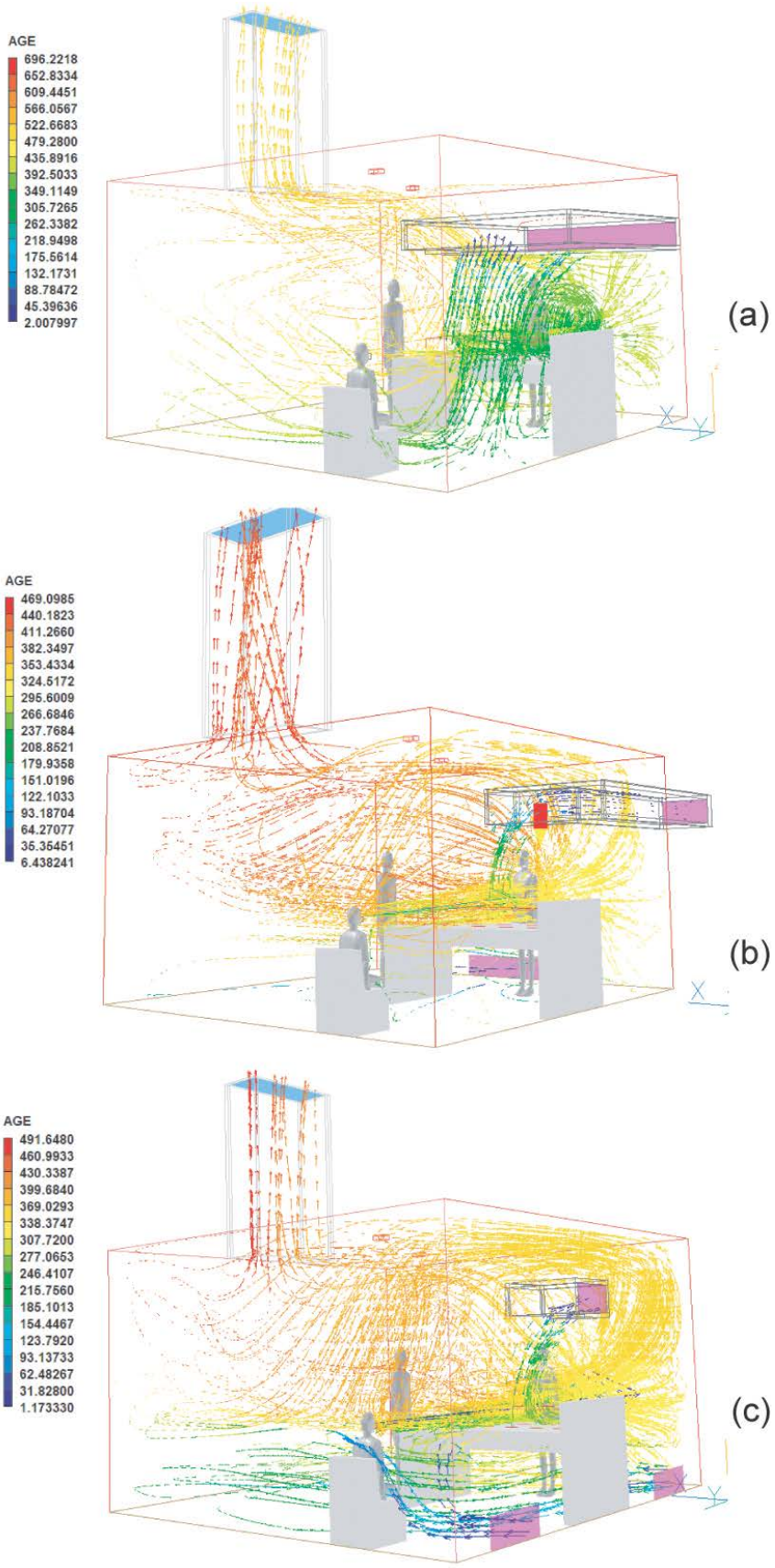

Figure 8:9: Age of air (s) shown as 3D vector streamlines in (a) Cases 1, (b) Case 2 and (c) Case 3

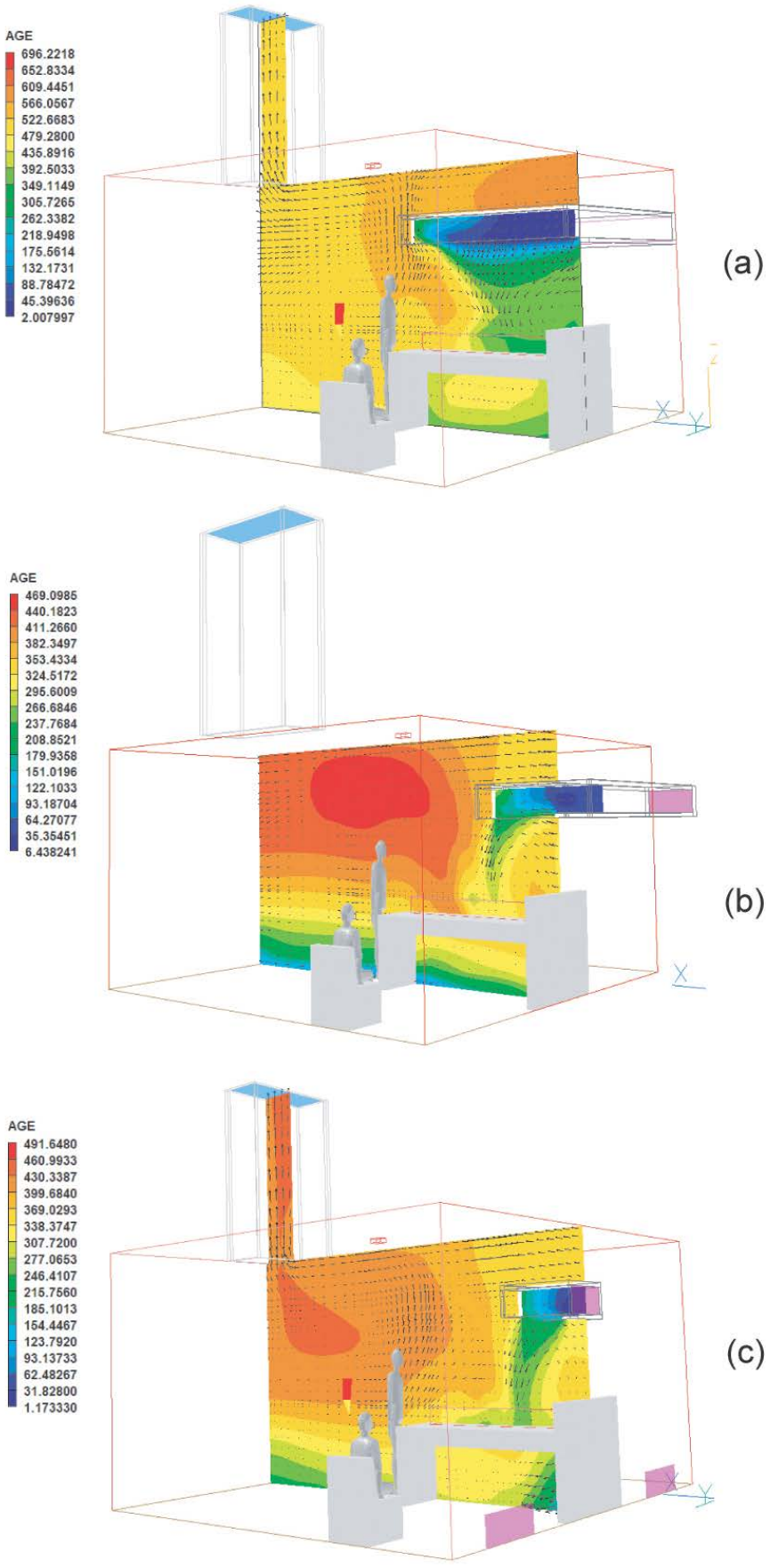

Figure 8:10: Age of air (s) shown as 2D Vectors in (a) Cases 1, (b) Case 2 and (c) Case 3

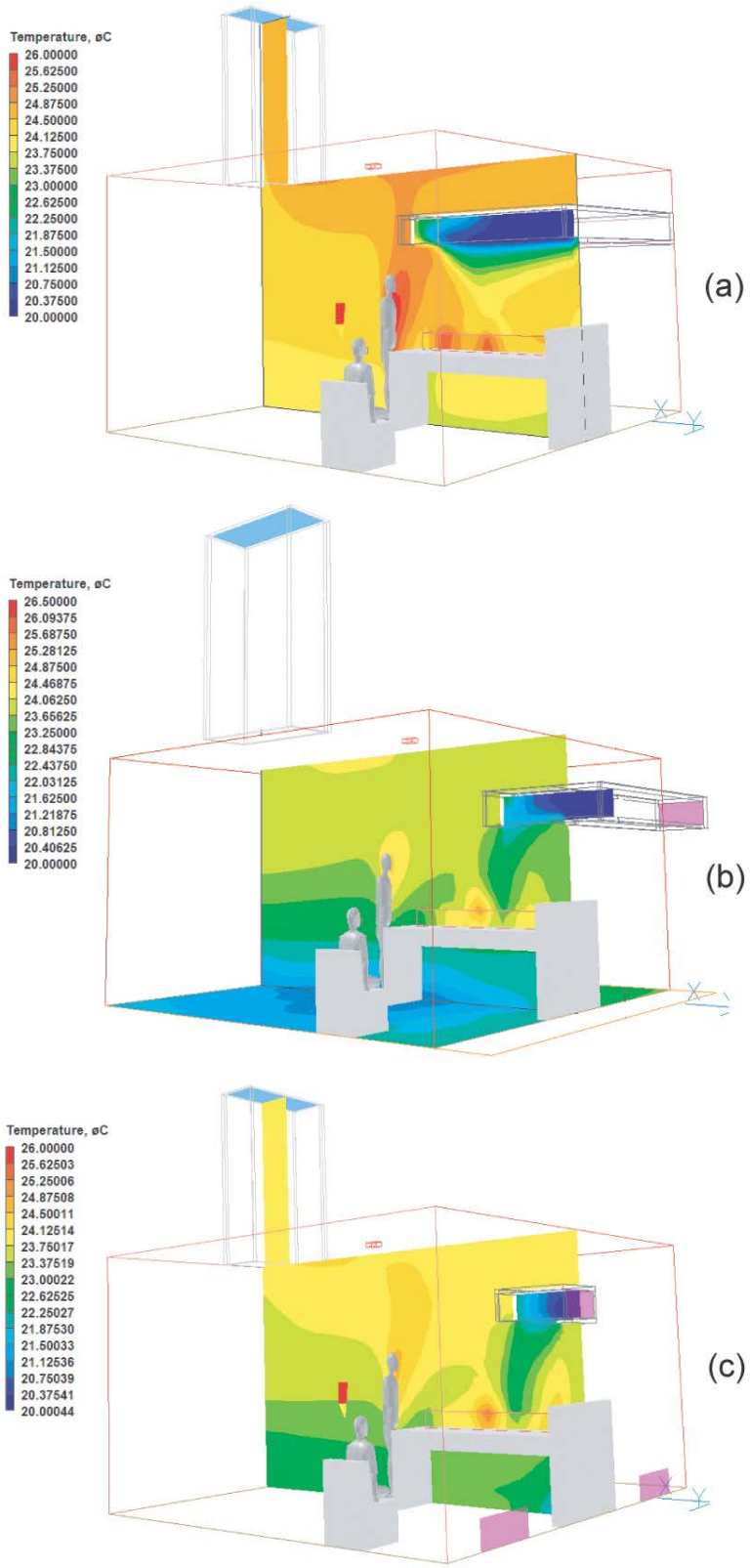

Figure 8:11: Temperature contours in (a) Cases 1, (b) Case 2 and (c) Case 3

8.6 The optimised NPV duct design

For further detailed research on the performance of NPV in a single-bed ward, it was essential to optimise the size of the duct and stack in addition to their specific locations. For the stack in particular it became convenient to adopt the edge-out and centre-out concepts from ANV (Lomas, 2007). The sizes and possible configurations of NPV as adopted for the ADB ward are shown in Fig. 8.12. Due to the observed poor performance of the previous duct size which was 1% of floor area, for the optimised design, the opening was taken as 1.5% of the floor area or 0.375m^2. This was approximated to 0.4m^2 for convenience, giving rise to an inlet 0.4 x 1.0m and an equivalent stack area dimensioned at 0.5 x 0.8m. The duct was located 0.6m from the edge of the wall closest to the patient's headboard. The discharge orifice of the duct was offset backwards by 0.3m, accounting for the expected and observed throw of jet of cooler air unto the warmer space below. The width of supply orifice was 0.4 x 1.0, equal to the cross-sectional area of the duct. The plan, section and 3D view of this design are shown in Fig. 8.12a, Fig. 8.12b and Fig. 8.12c respectively.

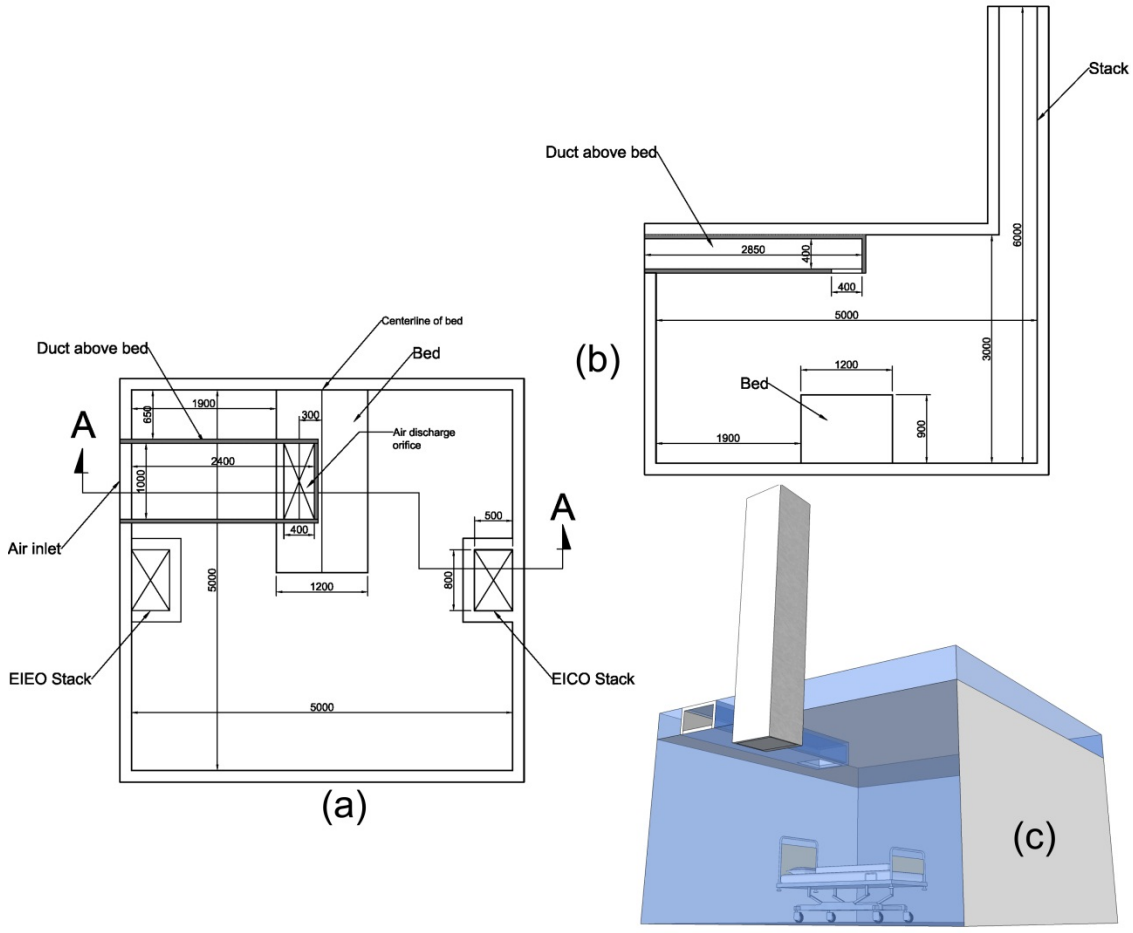

Figure 8:12: Schematic of Optimised NPV in (a) plan view (b) section (c) EIEO in 3D. All dimensions in mm

Similar to the conceptual NPV studies, the height of stack was retained as being equal to floor-ceiling height of 3m. For the ensuing investigation, of which only CFD was utilised, similar boundary conditions to the conceptual study were used, including number of occupants. However, radiated heat from patient was ignored in favour of convective heat which was assumed to be 50W.

Optimisation of NPV has many benefits for this study. First of all, the location of the exhaust could have significant bearing on room air distribution in the ward, with regards to the general pattern of airflow and the specific direction which exhausted air takes. This can impact on the spread of contaminants within the space. Secondly, unlike the initial conceptual studies of NPV which utilised broadly different geometry, sizes and location of ducts, standardisation of these features would enable the effect which different outdoor temperature could have on the IAQ of the ADB ward space. This is particularly critical for understanding how contaminants could move relative to a source (e.g. a seated visitor), at different temperatures and under edge-out or centre-out stack locations. Finally, an optimised system will make it easier to carry out further comparative studies such as experimental validation using a scaled model in a salt-bath tank.

The following subsections summarise the findings that were obtained from an investigation into contaminants, temperature and age of air in the optimised NPV system in the ADB ward. Six unique cases were modelled and their distinctiveness is summarised in Table 8.2.

Table 8.2: Features of optimised NPV Cases

Optimised NPV Case	**Temperature (^{o}C)**	**Stack location**
1	25	Edge-Out (EIEO)
2	25	Centre-Out (EICO)
3	20	Edge-Out (EIEO)
4	20	Centre-Out (EICO)
5	15	Edge-Out (EIEO)
6	15	Centre-Out (EICO)

8.6.1 Ingress of contaminants into patient zone

The boundary conditions and other assumptions used for modelling passive scalar contaminants have already been covered in Chapter 5 (Methodology). To assess the migration of airborne contaminants from the source towards the patient, a horizontal profile of contaminants was plotted (Fig. 8.13) at a constant height of 1.2m, from the headboard to the opposite end of the ward. The results for all six Optimised NPV Cases were compared. Given that each duct now has an offset of 0.6m from the edge (origin 0 in Fig. 8.13) of the wall; it is observed that the lowest mean concentration at the region of fresh air discharge is recorded at ambient temperature of 25^{o}C using centre-out strategy. Conversely, the highest mean concentration is recorded at 20^{o}C but with the edge-out strategy. At 15^{o}C, the concentrations profile from edge-out and centre-out strategies are largely similar in magnitude, and both fall short of the concentration from edge-out at 20^{o}C. This strongly implies that the relationship which outdoor temperatures and exhaust location have on the effectiveness of NPV is not linear but depends on specific combinations of outdoor temperature and stack locations. In general and regardless of the ambient temperature, NPV systems using centre-out strategies will provide lower concentrations, than edge-out strategies.

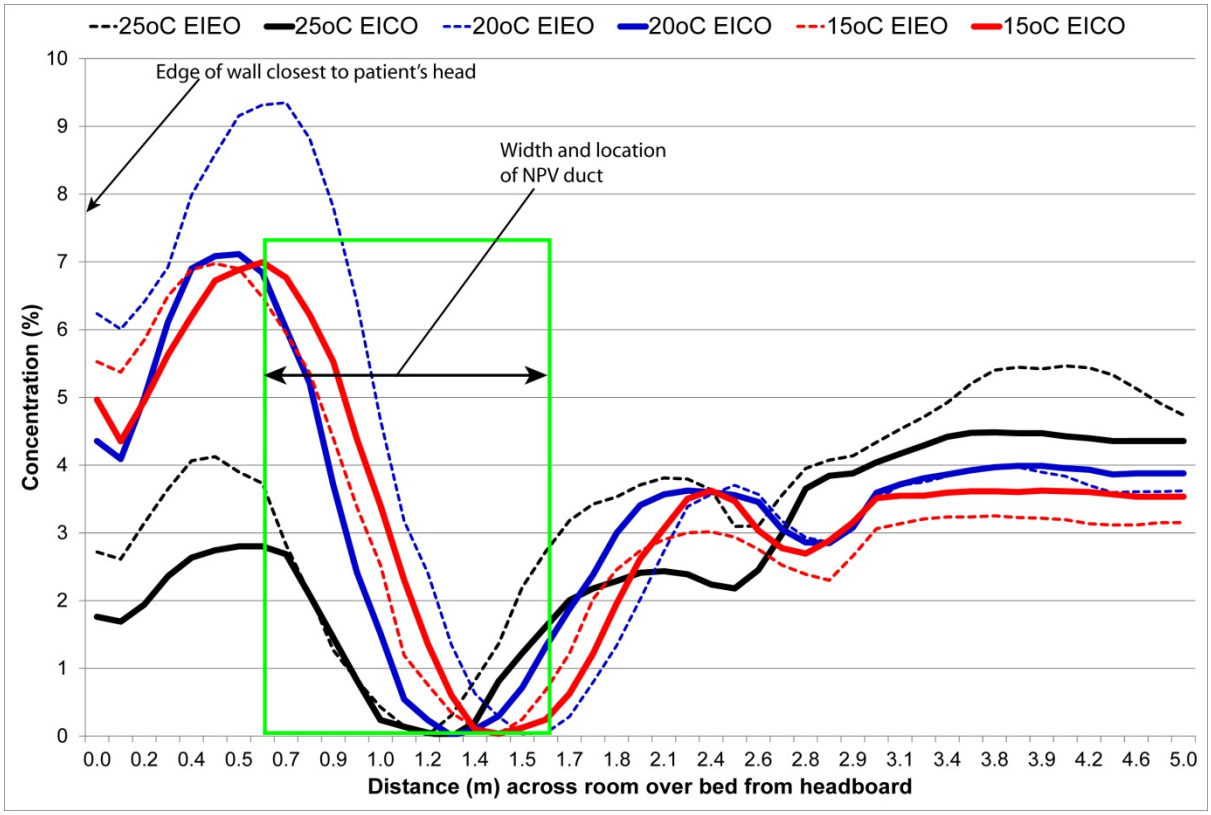

Figure 8:13: Profile of contaminants in six optimised NPV Cases

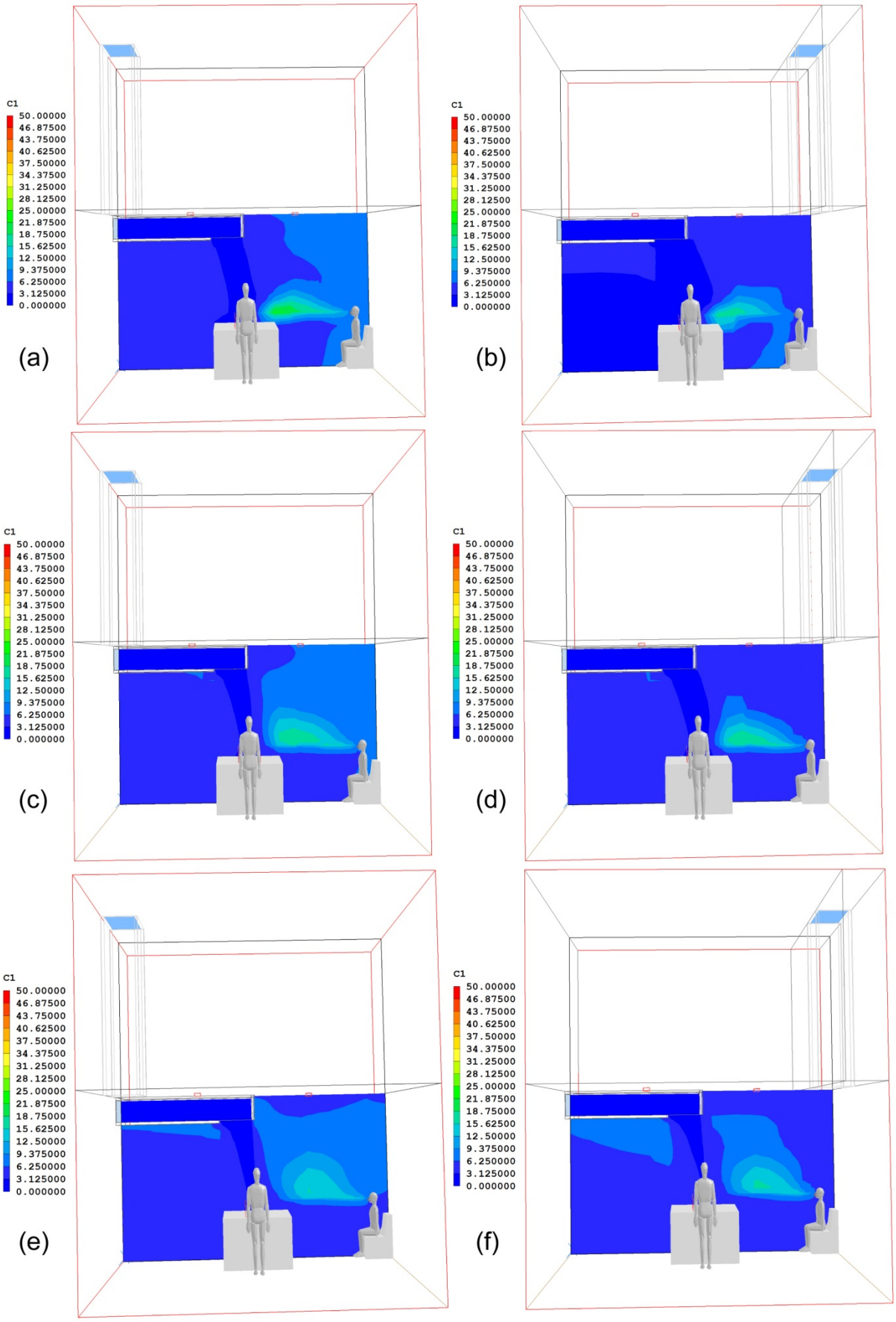

Figure 8:14: Concentration (%) contours at various outdoor temperatures and strategies showing: 25°C for (a) EIEO (b) EICO; at 20°C for (c) EIEO (d) EICO; at 15°C for (e) EIEO and (d) EICO

While the dip in concentration from 0.6m up to 1.8m is clearly attributable to the flow of fresh air from the overhead duct, it is also observed that at lower (15^{o}C) outdoor temperatures, the buoyant nature of emitted contaminants (cough temperature is 30^{o}C) becomes apparent (Fig. 8.14). This is specifically evident for edge-out and centre-out exhaust locations through Fig. 8.14e and Fig. 8.14f respectively. This is supported by the horizontal profile of contaminants in Fig 8.13 and the 2D contours of contours of contaminants in the lateral plane shown in Fig. 8.14. The effectiveness of the centre-out strategy at 25^{o}C is particularly obvious in Fig. 8.14b where the descending jet of uncontaminated fresh air is wider than with other strategies or outdoor temperatures. This explains why the centre-out strategy at 25^{o}C recorded the lowest mean concentration from the horizontal profile shown previously in Fig. 8.13.

8.6.2 Temperature at patient's zone

The differences which the edge-out and centre-out exhaust locations have on indoor temperature around the bed level are evident in Fig. 8.15a and 8.15b respectively. The results shown for outdoor temperature of 20^{o}C is similar for other temperatures, and indicates that the edge-out stack locations will induce a more even spread of cooler air over both sides of the bed. This can be explained by two factors. Firstly, the horizontal throw of the incoming jet of fresh air leads to the availability of cooler air at the visitor side of the bed in both cases.

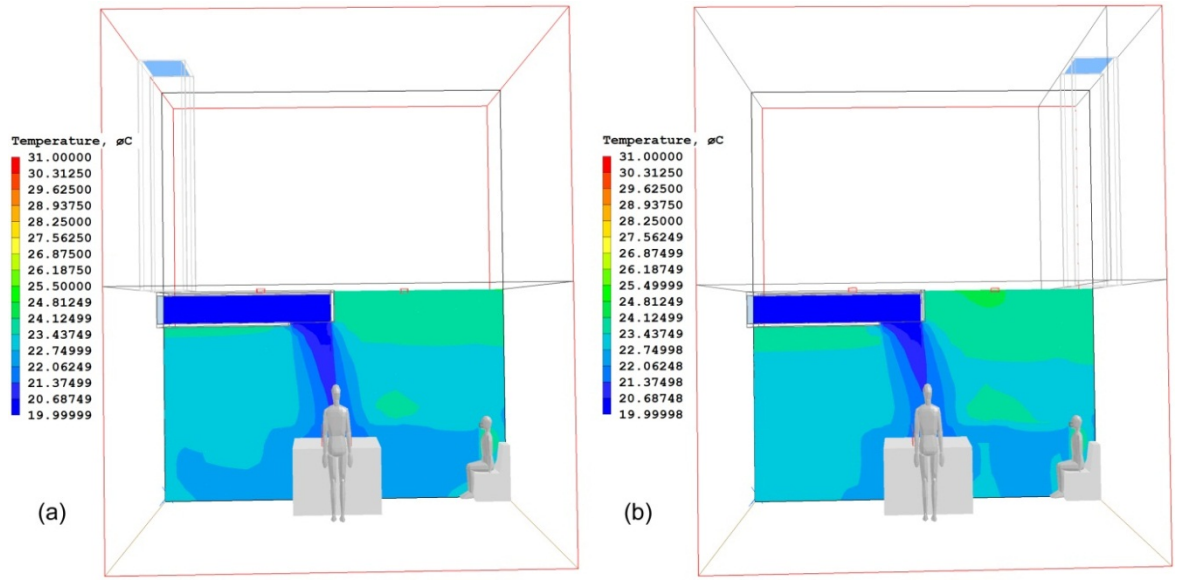

Figure 8:15: The flow of cooler air around bed level for (a) EIEO and (b) EICO strategies, both at 20^{o}C

Secondly, the edge-out exhaust location (8.15a) also encourages a reverse flow as cool air attempts to rise and exhaust from the same edge/wall as it was thrown in. This indicates that exhaust location is a factor in the relative amount of mixing generated by an NPV system.

8.6.3 Age of air and room air distribution

Age of air is an indicator of the mean time spent by air particles at a point in space. While the edge-out strategy appears to be suitable in creating a more even spread or mixing of room air, the centre-out strategy performs better when it comes to Age of air as implied by results in Fig. 8.16. In the centre-out strategy (Fig. 8.16b), the visitor side of the bed which also has the stack experiences fresh air delivered in the same direction as it is required to exhaust from the space. In the edge-out strategy, (Fig. 8.16a) supplied air has to exhaust by making a backward return journey, hence depriving the visitor side of the bed with as much fresh air as previously obtained with centre-out stack.

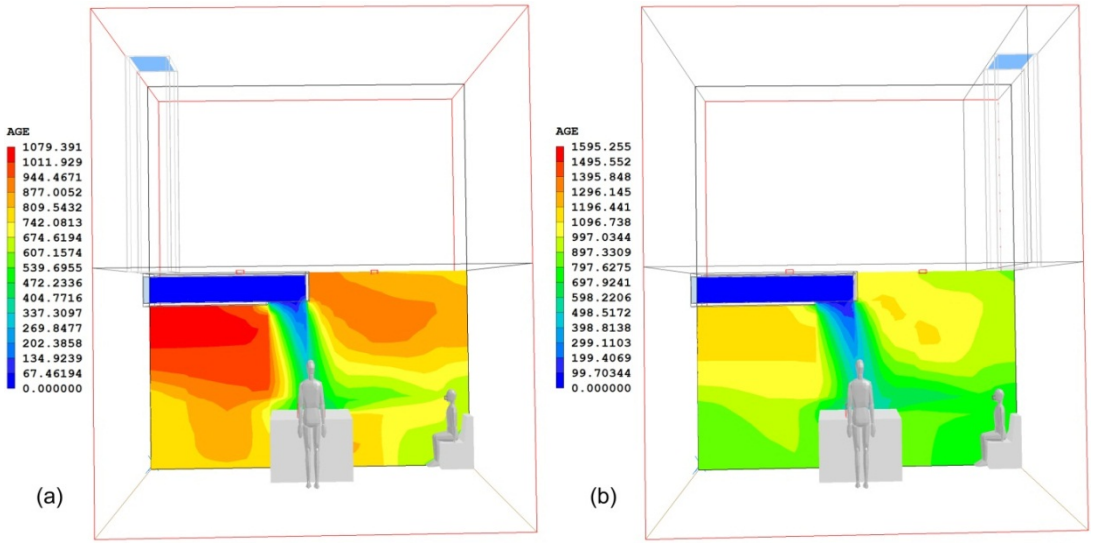

Figure 8:16: The Age of air (s) around bed level for (a) edge-out and (b) centre-out strategies, both at 20^{o}C

The relative differences in mixing occurring due to stack location is evident in Fig. 8.17, where 3D streamlines depict the supply, local eddies and exhausting of air for better mixing in edge-out strategy (Fig. 8.17a) than in centre-out strategy (Fig. 8.17b).

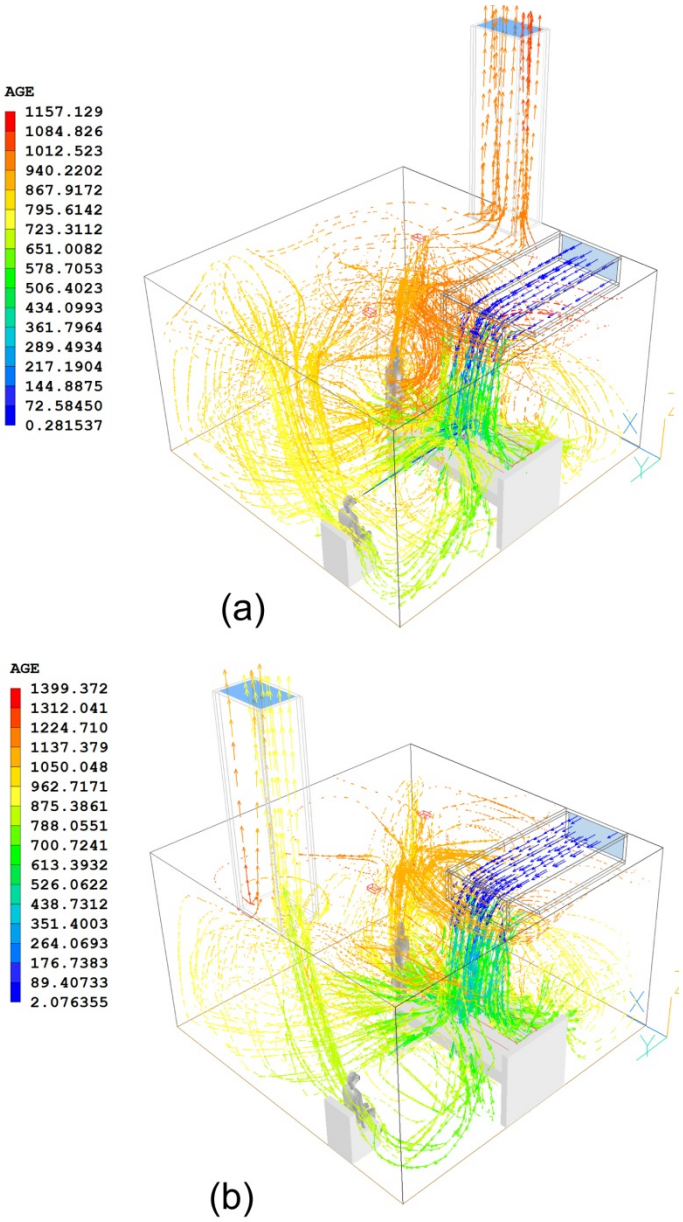

Figure 8:17: Age of air (s) shown as 3D streamlines showing flow pattern, direction and mixing of incoming air for (a) EIEO and (b) EICO

8.6.4 Ceiling space over the NPV duct

Observed in the initial conceptual studies was the fact that a 0.5m space between the ceiling and the top of the duct allows buoyant stale air to collect before exiting via the stack. This reduced the likelihood of fresh air mixing with rising warm stale air, which is able to collect at a higher level than the supply air. This interesting observation was pursued further in the optimised NPV design, where the ceiling height (and hence the stack) was elevated by 0.5m, all other objects remaining as they were. Both the edge-out and centre-out strategies were utilised for this purpose, using 20^{o}C outdoor temperature.

From the results obtained for Age of air when the ceiling is raised (Fig. 8.18), both the edge-out and centre-out strategies would have different patterns of stale air. The collection of stale air with edge-out mimics the scenario when the ceiling was flush with top of the duct (i.e. as in Fig. 8.16a). The maximum Age was however 1182s above the duct and 1260s below the duct, whereas previously with a flush ceiling, the mean Age of air below the duct was 1079s (Fig. 8.18a). Using the centre-out approach with a raised ceiling, the maximum Ages of air over and below the duct were 1401s and 1294s respectively (Fig. 8.18b).

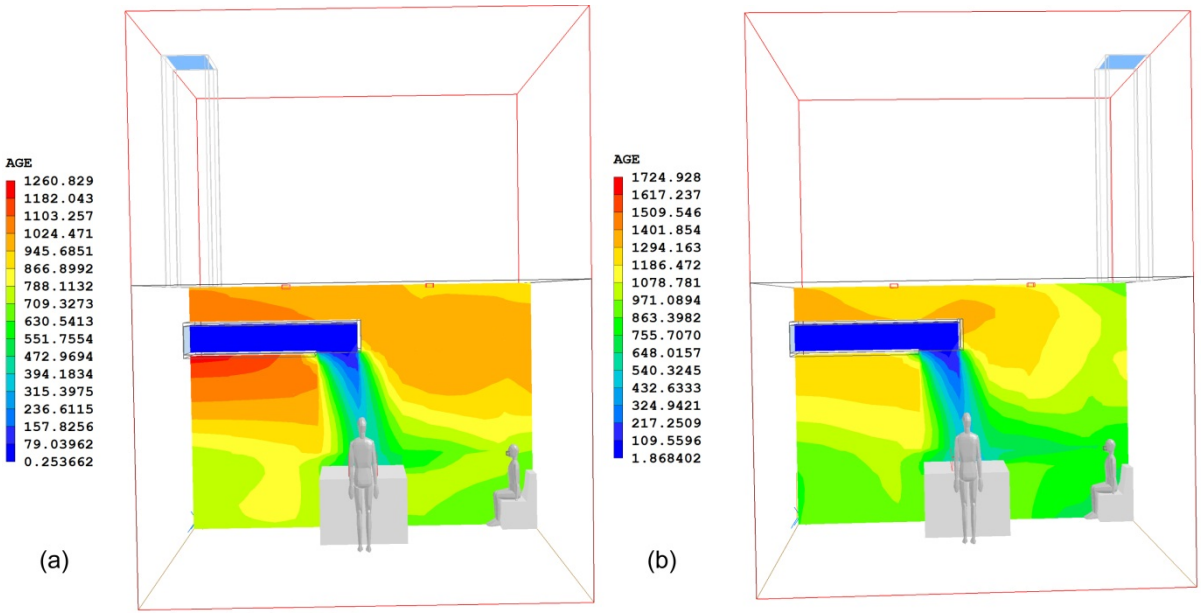

Figure 8:18: Age of air (s) in ward with raised ceiling for (a) EIEO and (b) EICO

However, 3D streamlines (Fig. 8.19) which reveal further evidence of the stagnation occurring above the duct in both strategies also suggest that the mean age of air on all sides of the bed is ≈ 630s when the edge-out strategy is used, as opposed to ≈ 540s obtained using centre-out strategy. More turbulent activity would occur above the duct in edge-out strategy (Fig. 8.19a).

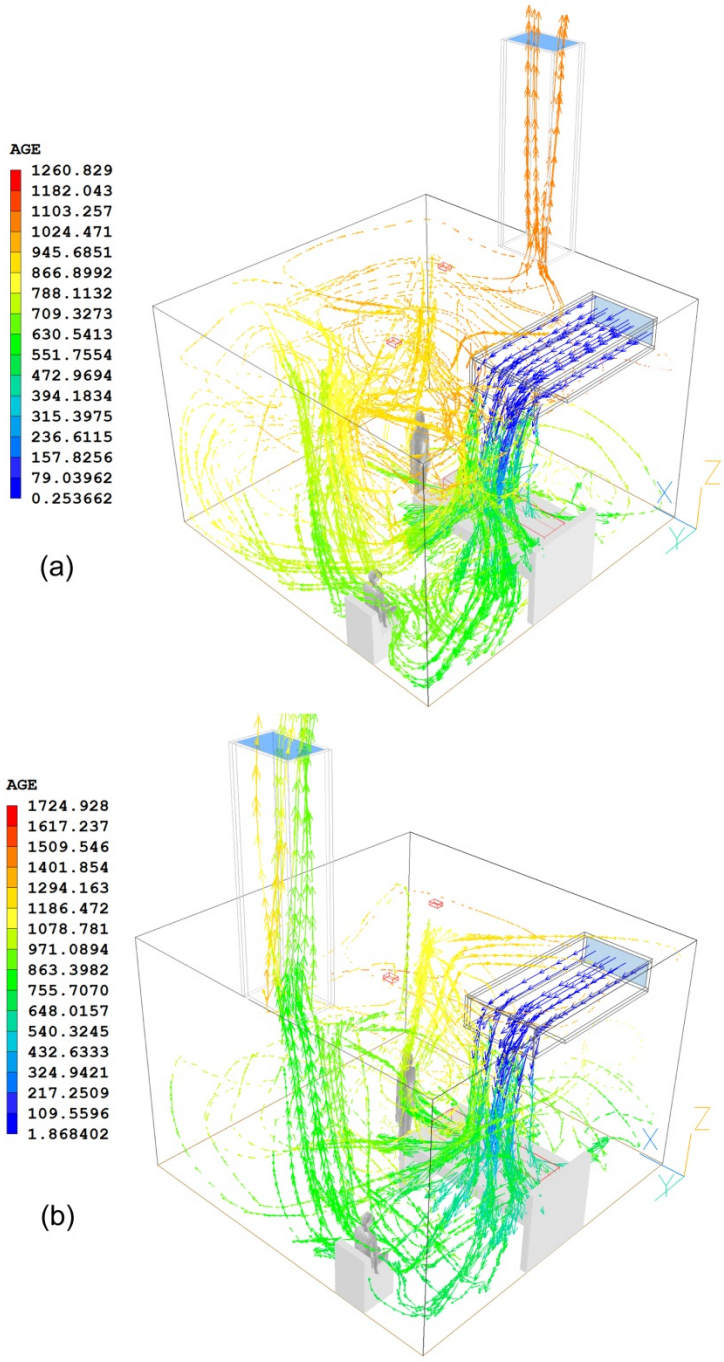

Figure 8:19: Age of air (s) shown as 3D streamlines in ward with raised ceiling showing flow pattern, direction and mixing for (a) EIEO and (b) EICO

Furthermore, results also indicate that raising the ceiling will lead to fairly uniform mixing of airborne contaminants in most of the room with mean concentration of 6.25% with the edge-out strategy (Fig. 8.20a). However, the mean contaminant concentration value obtained with the centre-out strategy in the room would be 12.50%, there would also be a dispersion and collection of contaminants at the base of NPV duct with a mean value of 15.63% (Fig. 8.20b). The raised ceiling is seen to create more mixing of contaminants in the room than previously

occurred with a lower ceiling as depicted earlier in Fig. 8.14d. Thus, the relatively lower Age of air above the duct and at the visitor's location make the centre-out strategy appear interesting from the perspective of fresh air delivery into the space. However, this apparent efficiency of air supply from the centre-out strategy is rather nullified by its relative ineffectiveness of contaminant removal based on the lower mean room concentration obtained using edge-out strategy. The backward return flow which stale air has to make as it exhausts the space clearly gives the edge-out strategy more advantage in terms of enhanced mixing and thus more contaminant dilution.

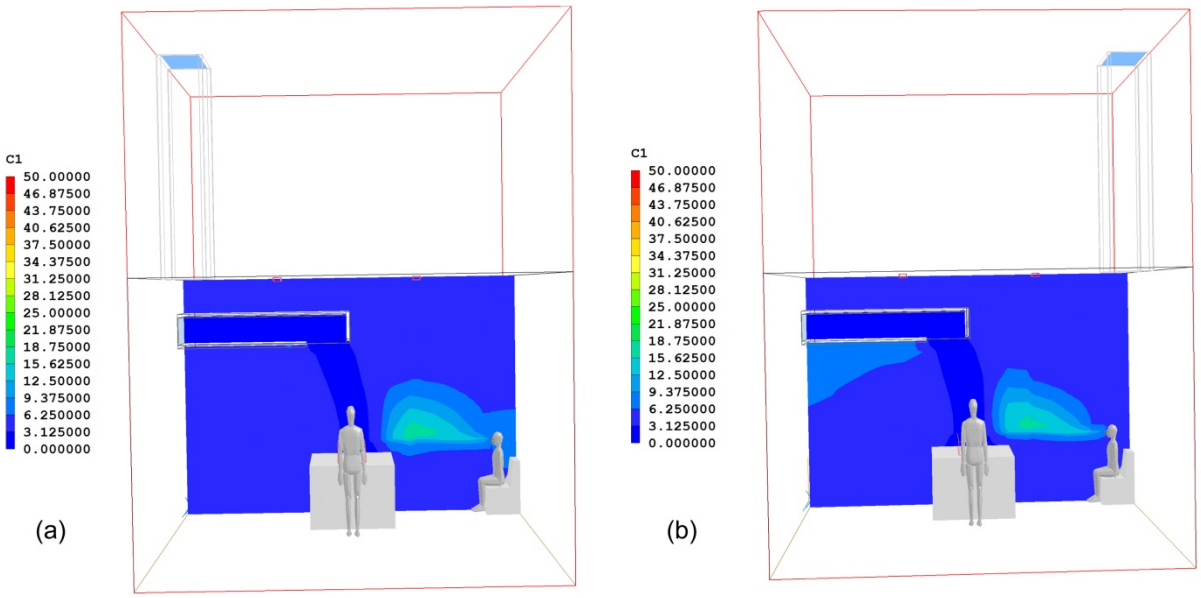

Figure 8:20: Contaminant spread (%) in ward with raised ceiling for (a) EIEO and (b) EICO

8.6.5 The dual orifice NPV duct

The direction of airflow into the duct and to the space below is determined by the horizontal orientation of the duct. While the horizontal throw was accounted for by a 0.3m backward offset of the drop zone, the desirable spread of fresh air sideways, is unfortunately limited by the momentum in the supply or longitudinal direction. This has resulted in lesser fresh air reaching the headboard (or lateral direction) as shown in Fig. 8.21a, and a build-up of contaminants at the same location as depicted in Fig. 8.21b.

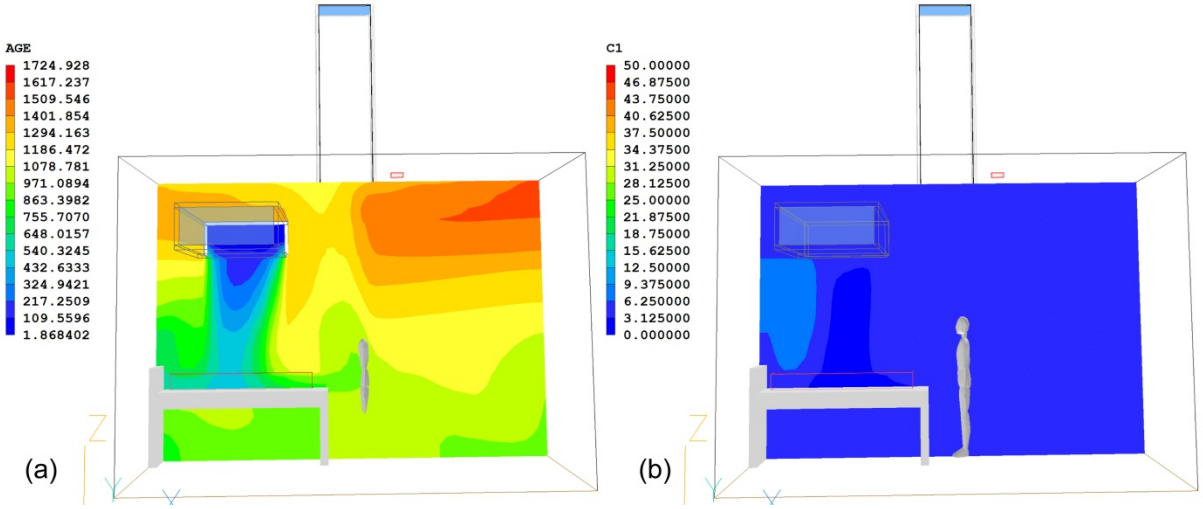

Figure 8:21: Single orifice showing from inlet side: (a) Age of air (s) and (b) contaminant concentration (%) over patient's head

This problem was carefully considered and a potential solution was obtained by splitting the duct vertically mid-way creating two orifices of equal area for supply as shown in Fig. 8.22. The orifice furthest from the headboard was allowed to retain its initial drop zone along the X-axis (in plan). The second orifice was extended forward by 0.3 thus aligning it with the middle of the bed, and creating its opening in the direction of the headboard, at right angles to the supply direction (i.e. along Y-axis in plan view). The expected redirection of air in the Y-axis is expected to work as a result of observed behaviour from the initial Case B concept where an L-shape duct was used. The duct in crooked Case B was able to provide airflow, despite the expected pressure drop that would normally occur when fluid in a conduit changes direction. The design of this dual-orifice is described with a plan view in Fig. 8.22a and a 3D worm's eye view in Fig. 8.22b.

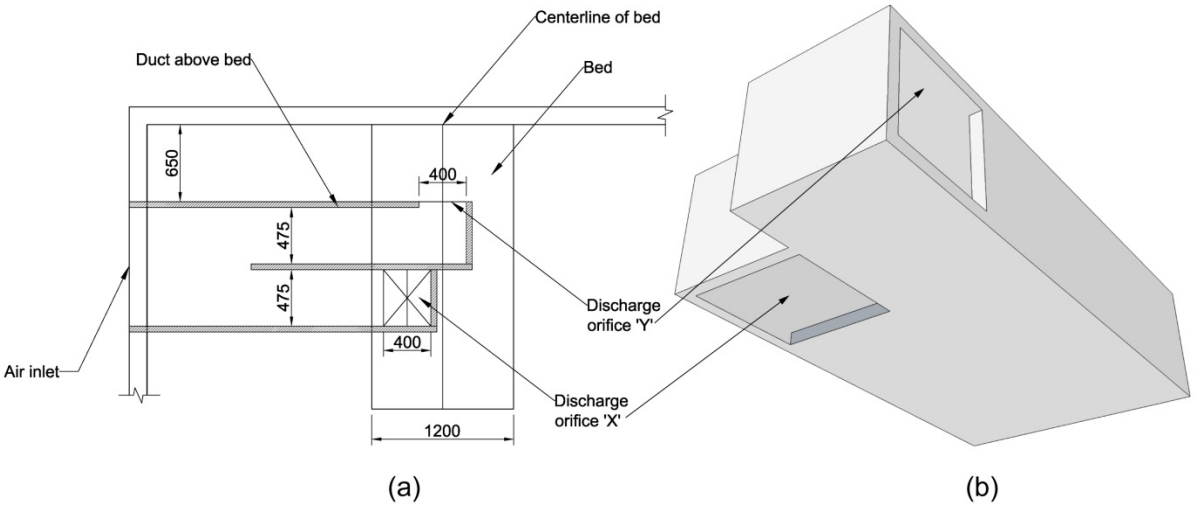

Figure 8:22: The improved design of NPV duct showing the dual-orifice in (a) Plan view (b) 3D worm's eye view

The modified design was then replicated in CFD without changing any other boundary condition. The results obtained are graphically illustrated using 2D contours and vectors in Fig. 8.23.

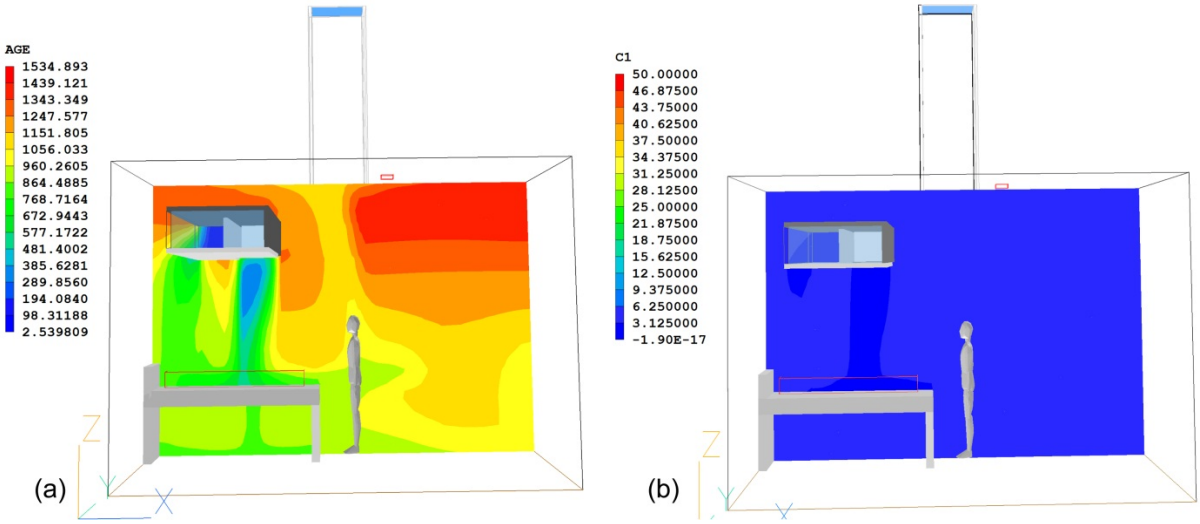

Figure 8:23: Dual orifice showing from inlet side: (a) Age of air (s) and (b) contaminant concentration (%) over patient's head

The results from Fig. 8.23 suggest that there will indeed be flow from both orifices of the same duct, with air falling towards the headboard (Fig. 8.23a) of the patient creating more mixing and leading to lower concentration of contaminants towards the headboard. For the second orifice, the throw of cooler jet of air into the warm space below is also observed, although there is evidence of ageing in the air. This could be attributed to more mixing taking place in that direction, or reduced velocity due to sudden change in direction which air has to make. Detailed studies into these characteristics of the dual orifice could reveal more, but is currently outside the immediate scope of this PhD research, which is more about proof of concept.

2D contours and 3D streamlines (Fig. 8.24) provide further insight into the thermal and room air distribution of the dual-orifice NPV duct. The dual-orifice NPV duct has been able to achieve two different flow directions from a single duct. This feature improves airflow delivery and capacity for enhanced thermal comfort and bio-aerosol performance, in addition to greater flexibility for control.

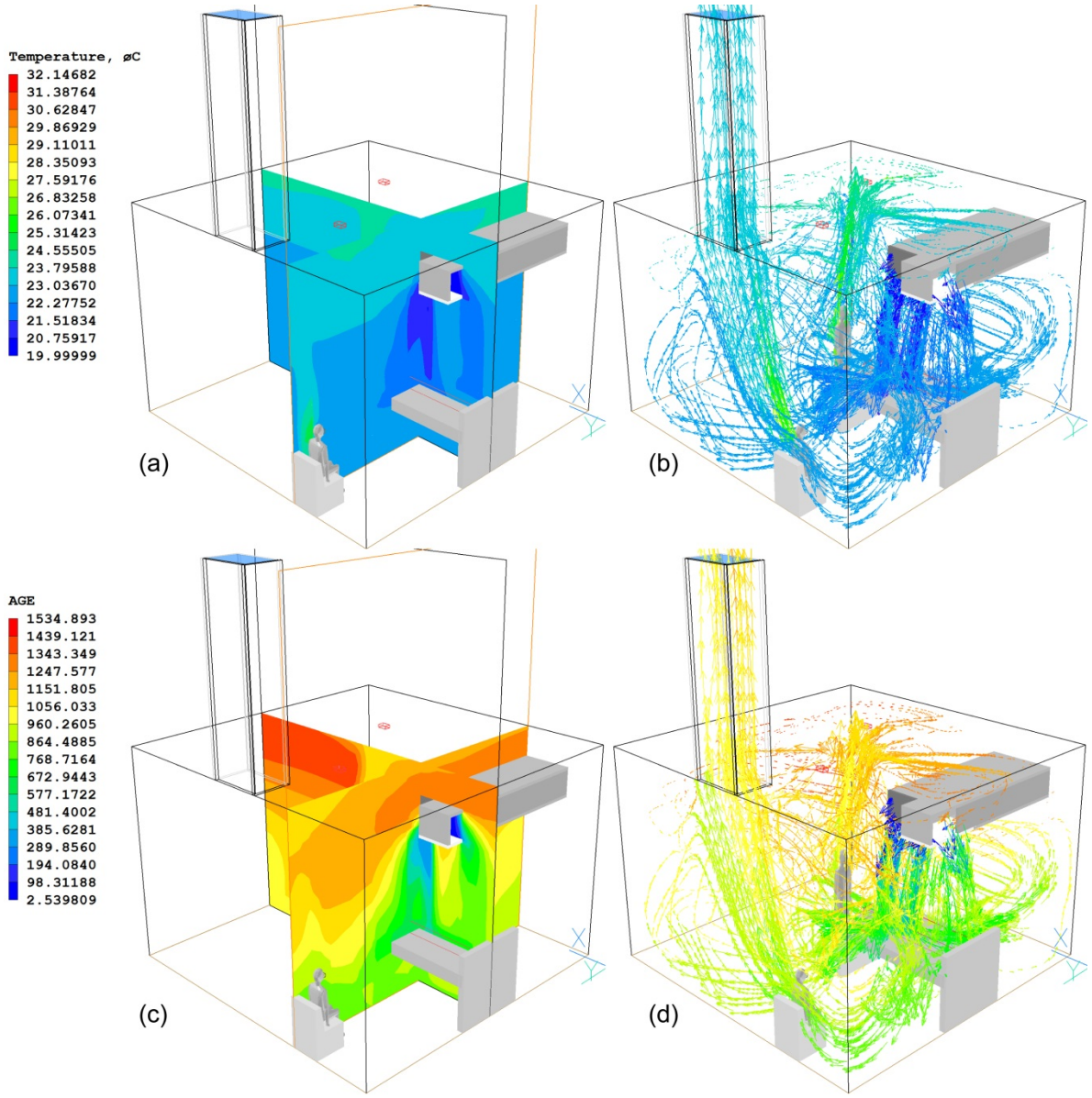

Figure 8:24: Contours and 3D streamlines of temperature (a, b) and Age of air (c,d) for dual-orifice NPV duct

8.7 Summary

The conceptualisation and predictive modelling of a novel buoyancy-driven natural ventilation system was demonstrated as a feasible and potentially practical solution for ventilation of hospital wards. The three initial concepts were significantly different in shape, sizes and location of openings but the results were all encouraging from airflow point of view. The most notable characteristics of these concepts were their capacity to provide mixing ventilation as well as localised delivery of fresh air from an external wall to a target location indoors.

Unlike mixing achieved with forced air in mechanical ventilation, mixing in NPV occurs when dense cooler air flowing from a duct by the ceiling falls to the space under gravity rises upwards due to buoyancy forces, to exit via a stack. Thus, because these mixing and local delivery (i.e. personalisation) characteristics of NPV have hitherto been the exclusive reserve of mechanical ventilation systems, the airborne contaminant control and low energy potential which this system offers makes it unique and attractive. Numerous new studies (Beggs et al, 2008; Eames et al. 2009 and Li et al. 2011) have demonstrated that mixing ventilation should be preferred to displacement ventilation in clinical spaces where dilution of contaminants is essential. This is because the gentle speed of ascent for supply air in displacement ventilation can be overpowered by the emission momentum of a cough or sneeze emitted in a room – making it easy for airborne pathogens to travel far from source and or to get 'trapped' in space within the stratified occupied zone.

The NPV system can contribute to resolving this problem using natural flow of air to achieve mixing, instead of the traditional mechanical approach, primarily for the zero energy required to drive air from outside to the interiors of wards. In the same vein, the NPV can therefore be appreciated as a modern attempt to ensure that the air remains as fresh as the air outside, being one of the guiding principles of Florence Nightingale (Nightingale, 1859). If the NPV system were to be (re)named Nightingale Personalised Ventilation, this would not be out of place in terms of its unique airflow characteristic or the historical significance.

This innovative capacity to deliver fresh air purely from buoyancy-driven natural ventilation and deep into a built space, has potential benefits for protecting immune-compromised or immune-suppressed patients, as observed from the reduced concentration of contaminants in the drop zone, relative to the surrounding space. For each of these cases considered, 60 l/s/patient was achieved, demonstrating that this specific recommendation by the WHO can indeed be achieved from natural ventilation. The initial studies of NPV have been published in a peer-reviewed journal paper with the title: *Natural Personalised Ventilation: A novel approach,* published by the International Journal of Ventilation (December 2011 edition).

Subsequently, the Optimised design of NPV system enabled the effects of stack location and outdoor temperature to be studied in more detail. This was necessary in order to understand the influences which these variables have on IAQ parameters of the ward, of which ingress of contaminants into patient's breathing zone was central. In addition, the design of NPV system

underwent a further design iteration to improve its performance by the introduction of two orifices at the point of discharge. This allowed air to be supplied seemingly from two directions. An integration of aspects of ANV stack locations contained in Lomas (2007) showed that the level of performance of NPV system for airborne contaminant control can be influenced by edge-out or centre-out strategies, as does the use of a raised ceiling above NPV duct.

CHAPTER 9: STUDY 4 - Comparative analysis

9.1 Introduction

The Great Ormond Street Hospital (GOSH) is a children's specialist hospital located in London. Built in the 1930s, the facility has aged and is currently undergoing major redevelopment. The existing wards of GOSH are described as being cramped, inconvenient, out-dated and unsuitable for modern paediatric healthcare delivery, especially of the world-leading standards it has been known for. The increasing demand for its services also means a projected 20% increase in bed spaces is inevitable. As this would have direct consequences for patient visitors' and the new facility is actively pursuing a design that would allow more family participation in the care process. The National Health Service (NHS) Trust has thus embarked on a large scale redevelopment project aimed at delivery of a state-of-the-art facility. One important feature of the redevelopment is the provision of single bed wards which are designed to allow parents to sleep over with their sick children (GOSH, 2011).

The issue of a modernised hospital, increased patient visits and parents sleeping over logically translate to increased occupancy which can have ramifications for comfort, energy and spread of airborne pathogens in light of recent airborne pandemics. It is on record that the DH pursued a policy of restricting hospital access during the last H1N1 pandemic. Although, the new facility has already moved into the construction phase, it is important to evaluate the likely performance of the wards so that learning can take place, for the benefit of similar future projects. In this regard, a workshop was organised by the Health and Care Infrastructure Research and Innovation Centre (HaCIRIC) research group with the design teams and client representative. Among the outcomes of the workshop was an agreement to furnish the research team with the design of the single-bed ward for subsequent studies on natural ventilation and airborne infection. This chapter describes the research work undertaken in this regard as a case study.

The work is structured and presented as a performance evaluation of different natural ventilation systems, all of which have been covered and pre-selected at the literature review stage in Chapter 2. The investigation utilised dynamic thermal modelling and computational fluid dynamics. The results were benchmarked with known standards (e.g. ISO), guidelines

(e.g. HTM, WHO) as well as from findings in contemporary literature (e.g. Qian, et al. 2006; Jiang, et al. 2009).

The primary aim of this case study was to provide a comparative evaluation of four key indicators of performance: ventilation, thermal comfort, energy and control of airborne pathogens, which can be expected from the selected natural ventilation systems. Specifically, the study intends to use buoyancy-driven flow to:

1. determine and evaluate the achievable ventilation rates obtainable from each system in a given year, from buoyancy-driven flow using acceptable techniques of sizing the ventilation openings;

2. establish whether trickle ventilation rates are achievable with buoyancy-driven airflows keeping in mind the provisions of guidelines (60 l/s/patient of the WHO) for effective control of airborne contaminants;

3. demonstrate the performance of natural personalised ventilation (NPV) and an extended concept referred to as ceiling-based natural ventilation (CBNV) regarding their capabilities to meet sub-objectives 1 and 2 above;

4. investigate the performance of each system regarding the migration of airborne contaminants from indoor sources; and

5. demonstrate the benefits of using computational fluid dynamics in addition to dynamic thermal modelling as viable methods for such investigation, which has not been adopted in previous similar studies (Short, et al. 2010; Short and Al-Maiyah, 2009) of hospital ward ventilation.

9.2 The Great Ormond Street Hospital (GOSH)

The single bed ward of the Great Ormond Street Hospital (GOSH) has dimensions of 3.78 x 6.23 x 3.5m (Fig. 9.1a). This gave a floor area of 23.55m^2 and room volume of 82.42m^3. The existing window design used as Base Case (Case 1) is a high-level (1.9m) fenestration measuring 1.65m wide x 0.5m below is a fixed glazing of same width for visual and

daylighting purposes. Two visitor chairs were available, one of which (position Vc in Fig. 9.1a) served as one potential source of contaminant (cough) for this study. A second potential source was assumed to come from the sleeping couch (position Sc in Fig. 9.1a) provided for an overnight visitor. In line with the philosophy of parent participation in care (GOSH, 2011) the principle of family participation in the care process was demonstrated in actual design by the existence of the sleeping couch. The floor plan and interior of the GOSH ward are shown in Fig. 9.1a and Fig. 9.1b respectively.

Crucial to the purposes of this study, was the capacity to measure contaminant levels at points which are important to patient well-being. In this regard, 12 Points of Interests (POIs) which formed and imaginary Volume of Interest (VOI) identified in Fig. 9.1a (and enlarged in Fig. 9.1c and Fig. 9.1d) are central because they represent the area in space closest to the patient's upper body and breathing zone. For each ventilation system, the absolute values of contaminants in the POIs and VOI would be measured and compared to other systems. Two other POIs (points 13 and 14 in Fig. 9.1a) respectively represent the likely position of a standing healthcare worker (HCW) and a second visitor on another chair. Two axial profiles (axis A-B and axis C-D in Fig. 9.1a) are also identified for measuring concentrations at specific heights. The longitudinal profile A-B cut across the length of the ward (at height of 1.5) from the external wall to the location of Vc. This profile was deemed representative for measuring the concentrations of contaminants in the breathing zone of sitting co-occupants. Another (transverse) profile C-D cut through the width of the ward at height of 1.8m along the side of bed where HCW is likely to stand, which was to be used in evaluating the concentrations of contaminants around the head of a standing co-occupant.

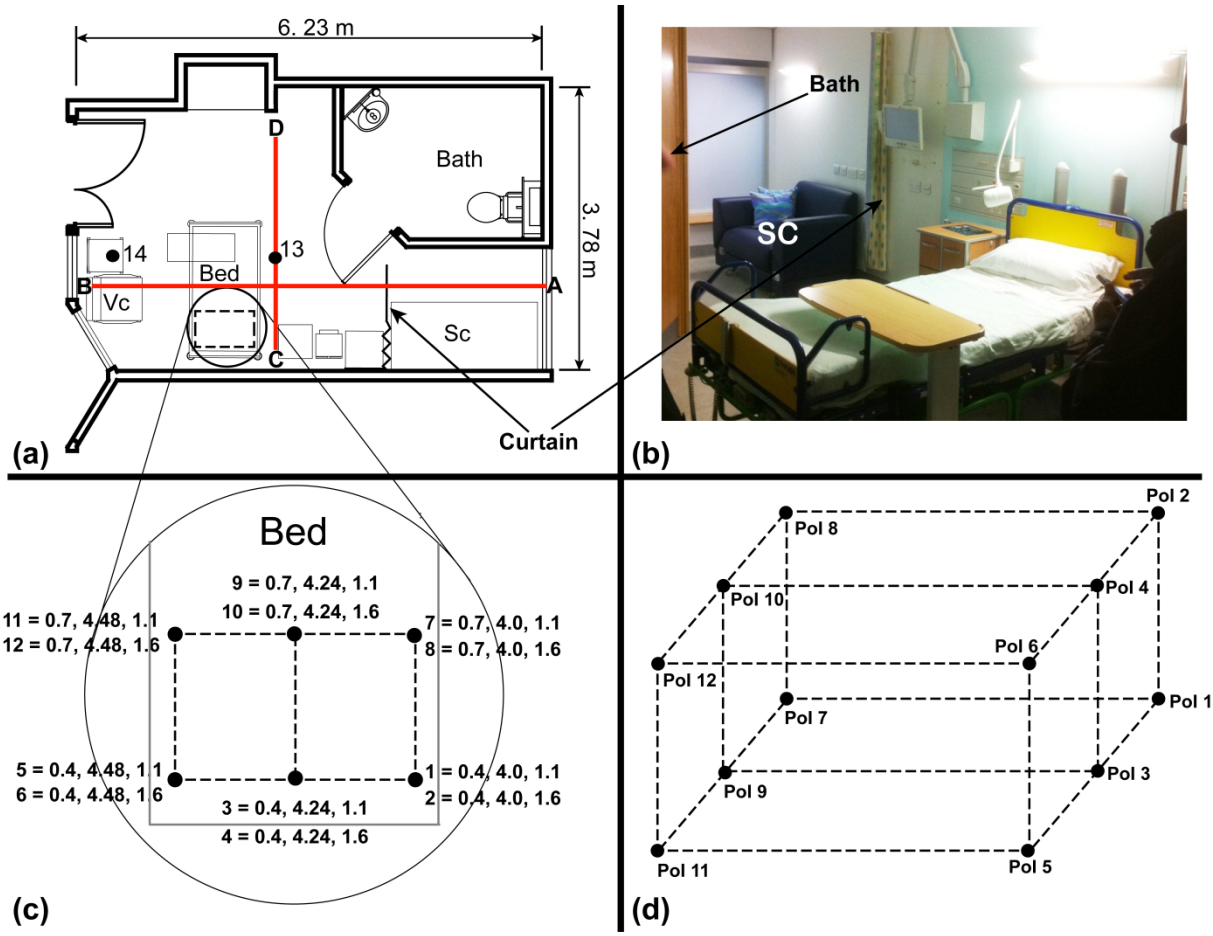

Figure 9:1: The GOSH ward in (a) floor plan (b) interior of mock-up (c) details of POIs in plan (d) details of POIs in 3D

9.2.1 The ventilation systems

The first system comprises the as-built design, which utilises a 1.9m high single top-hung window. This design serves as a Base Case (Case 1) upon which performances of other systems will be relatively measured using the identified metrics and benchmarks. The width of existing window is 1.65 and the height was 0.5m. This case is graphically represented in 3D in Fig. 9.2a.

The second system (Case 2) is made of single-sided, dual-openings sized according to CIBSE's guide on natural ventilation (CIBSE, 2007). Inputs for Case 2 model were derived from Eqn. 9 (Chapter 2) with variables given the following values: C_d = 0.6; H = 2.5m (measured from centres of both openings); g = 9.81 m/s^2; and ΔT = 1 (for a worse case temperature differential scenario). The required area of opening was computed as 0.78m^2. The presence of design constraints due to existing fixed glazing meant the openings could be no

wider than 1.65m. The final size of openings was therefore made 0.47 x 1.65m. A 3D conceptual representation of this scheme is shown in Fig. 9.2b where the fixed glazing is between the two openings which are shaded in solid black.

The third system (Case 3) comprises of inlet and stack ventilation specifically the Edge-In-Edge-Out strategy defined in Lomas (2007) whose stacks are sized using 1.5% of floor area using techniques elaborated in Lomas and Ji (2009) and is represented conceptually in 3D by Fig. 9.2c. Using the model in Eqn 13 from Chapter 2, the following inputs where used: F = 1.5% of floor area or 0.015; and n = 1.65, W = 3.78. The area of exhaust stack (*As)* was calculated as 0.35m^2, which was used to determine the area of inlet as well. Exhaust stacks were dimensionally sized to be 0.5 x 0.7m. The height of stacks was for simplicity, made equal to 3.5m which is the floor-to-ceiling height. The inlet itself was sized as 0.21 x 1.65m, again working with the design constraints offered by width of existing fixed glazing.

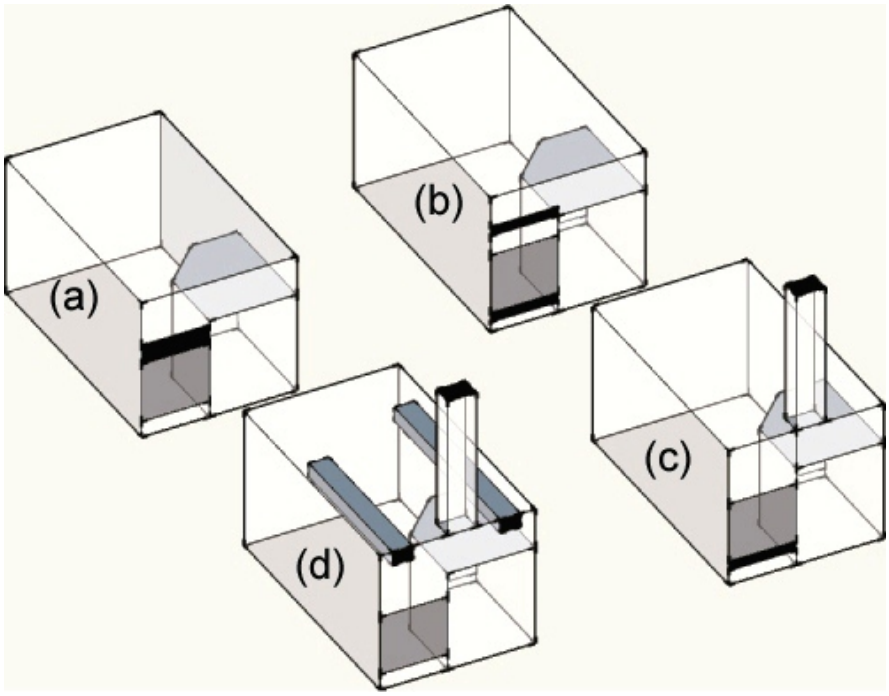

Figure 9:2: GOSH ventilation strategies with openings depicted in solid black showing (a) Case 1: window (b) Case 2: dual-opening (c) Case 3: inlet and stack (d) Case 4: ceiling-based natural ventilation

The fourth system (Case 4) comprises of two elevated (ceiling-based) ducts, one of which functions as a natural personalised ventilation duct (NPV) systems that was developed as part of this research (Adamu et al. 2011b) which delivers fresh air directly over the patient, while the second duct is designed to provide supplementary air into a remote part of the room

without any personalisation. The NPV duct and supplementary duct have both been classified as Ceiling-Based Natural Ventilation (CBNV) and are represented in Fig, 9.2d. The NPV duct was shortened by 0.3m. This was intended to align the issuing jet of cold air with the patient's bed. This phenomenon was also observed in a separate study of the NPV (Adamu, et al. 2011b). Without this backward offset of the orifice, the descending cooler air could be thrown much further away from desired location over patient. The second duct in the CBNV system providing supplementary air had its opening displaced 0.9m longer than the NPV duct. The stack height was the same as in Case 3 (i.e. 3.5m) bearing in mind that the neutral pressure level (NPL) would lie somewhere between the ceiling level inlets and the tip of the exhaust stack, and that this vertical distance ought to be maximised to encourage airflow. These cases are also schematically presented as cross-sections in Fig. 9.3.

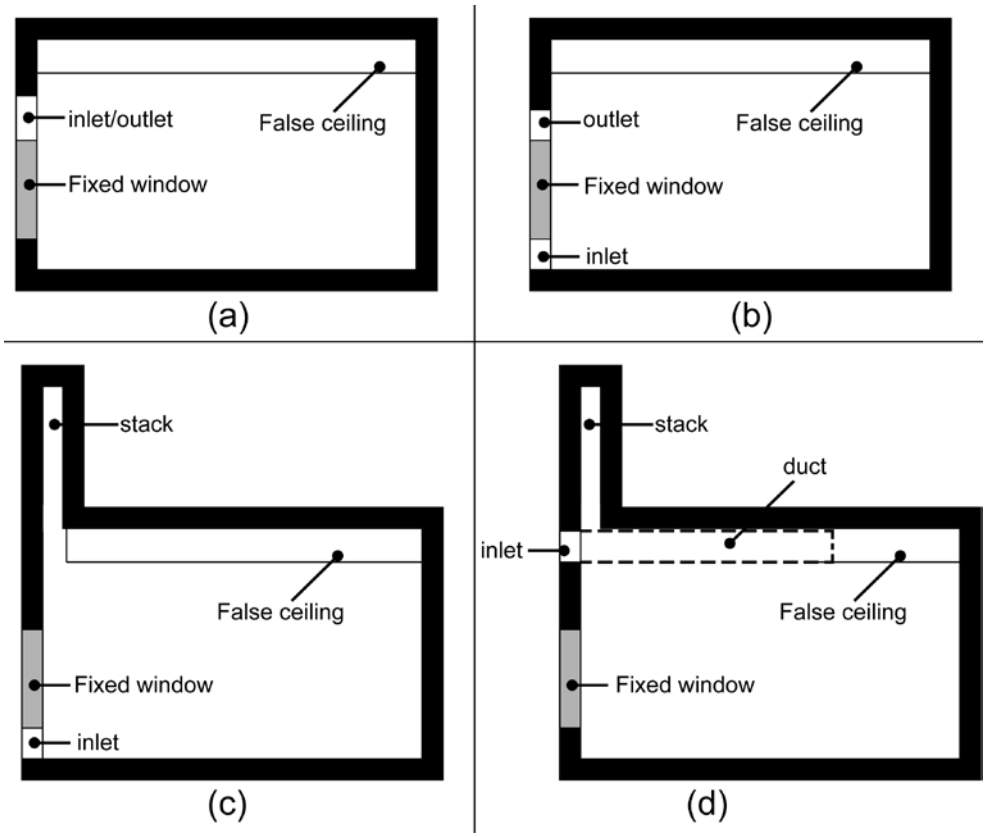

Figure 9:3: Schematic cross-sections showing (a) Case 1 (b) Case 2 (c) Case 3 (d) Case 4

9.3 Materials and methods

9.3.1 Performance metrics and benchmarks

Airflow rates achieved for each ventilation system in this study, will be evaluated according to provisions of three guidelines: HTM 03-01 (6ACH), the WHO (60 l/s/patient) and EN ISO 7730 (47 l/s); and two research findings on effective use of ventilation for dilution of airborne contaminants – 8 ACH from Qian et al. (2006) and 3000m^3/hr from Jiang, et al. (2009)Thermal comfort will be evaluated using PMV ranges acceptable for Class I buildings i.e. EN ISO 7730 (Olesen, 2007) with temperature referenced to 18 – 28^{o}C range allowable in the Health Building Notes (HBN) and HTM 03-01. This is in addition to predicted percentage dissatisfied (PPD) and predicted percentage dissatisfied due to draught (PD). Energy used for heating would be cross-referenced with the benchmarks developed by CIBSE for Category 20 buildings which are: 90kW.h/m^2 for electricity sources and 420kW.h/m^2 for fossil-thermal sources (CIBSE, 2008). Using the CIBSE-approved RICS method for gross internal floor area of the GOSH ward (23.55m^2), the equivalent energy consumption targets are 2.12MWh for electricity and 9.89MWh for fossil-thermal.

For protection of exposed occupants from airborne contaminants in a ventilated room, two similar metrics will be used. The first is personal exposure index (PEI) as described in many studies (e.g. Brohus and Nielsen, 1996; and Nielsen, et al. 2007b). This metric is also referred to as contaminant removal efficiency (CRE) defined in Cheong and Phua, (2006)[7]. PEI and CRE are both computed as the ratio of the steady state concentration of contaminant at the point of exhaust (C_R), to the concentration at a (breathing) point (C_{exp}) shown previously in Chapter 2 as Eqn. (2.3) and revisited below as Eqn. (9.1).

$$PEI\ (CRE) = \frac{C_R}{C_{exp}} \qquad (9.1)$$

A higher value of PEI or CRE indicates greater efficiency, and depending on the effectiveness of the ventilation system in actual removal of contaminants at the point of exhaust, it is not uncommon to have values significantly higher than 1.0. Although PEI and CRE are mathematically the same, in this study, PEI will be attributed to the actual breathing points of co-occupants, while CRE will be used for the POIs and VOI defined earlier.

[7] Both PEI and CRE are also equivalent to air quality index, AQI in Zang, (2005)

In this investigation, PEI will be calculated for assumed standing healthcare worker (POI 13) and another sitting visitor (POI 14). The source of contaminant is assumed to be a visitor who is assumed in one instance to be sitting down on a visitors chair (Vc) or lying down on the sleeping couch (Sc) both depicted in Fig. 9.1a above. Although passive scalars have limitations (Hathaway, et al. 2011; Mao and Celik, 2010), they offer an opportunity to study the effects of ventilation on completely aerosolised contaminants as can be expected of droplet nuclei which for this study are assumed to < 2μm in size and negligible in mass (i.e. same density as air).

9.3.2 Base case and general assumptions

The GOSH ward was modelled in DTS (IES, 2011) and PHOENICS CFD (CHAM, 2011) applications. As with many studies of the indoor built environment utilising computer modelling, it is often essential to simplify certain features of spaces, usually due to software constraints or because impact of such parameters are negligible to the overall outcome. The chamfered corner of the en-suite bathroom were for instance, ignored. Similarly, the presence of an extract fan in the bathroom was also overlooked as the study aims for airflow driven purely by buoyancy forces. In order to account for airflow in the entire geometry however, vents were created at the base and ceiling of the bathroom to allow ventilation of that space.

The investigation was done in two phases with initial phase focusing on airflow, comfort and energy performances, and second phase focusing entirely on the behaviour of airborne contaminants under buoyant airflow. In the first phase, occupancy was considered using three people: patient, healthcare worker and sitting visitor while in the second phase similar number of occupants were used, but with additional studies using patient and a sleep-over visitor. Each typical occupant was assumed to emit 90W of heat while the patient was allocated 50W, assuming the patient was partially covering with a blanket. The variation in internal heat from varying number of occupants and how this may influence buoyant airflow in the GOSH ward can be appreciated in Table 9.1 which shows the heat gain density during the day and at night, as well as the total load for both scenarios.

The total miscellaneous internal heat loads differ in these base cases as outlined in Table 9.1. In the CFD model, lighting (70W) was split into convection/radiation ratio of 20:80 according

to CIBSE (2006) guide for fluorescent bulbs encased in prismatic luminaires, giving a ceiling wattage of 7W and a floor radiated wattage of 56W.

Table 9.1: Inputs used to define CFD model cases

Contaminant Source	Sitting visitor (daytime)				Sleeping visitor (night time)			
	Case 1A	**Case 2A**	**Case 3A**	**Case 4A**	**Case 1B**	**Case 2B**	**Case 3B**	**Case 4B**
POIs	14				12			
Total heat (W)	300				210			
Total heat (W/m2)	12.73 W/m^2				8.9 W/m^2			
Area of Inlet (m^2)	0.82	0.45	0.35	0.35	0.82	0.45	0.35	0.35

In Phase Two of the investigation, two fundamental scenarios were developed based on source of airborne contamination. In one scenario, a daytime visitor sitting on a chair (position Vc in Fig. 9.1a) is the source of contaminants, while in the second scenario, an overnight visitor lying on a couch (position Sc in Fig. 9.1a) is the source. The differences in these scenarios are captured in Table 2 above.

A passive scalar contaminant of generic nature and of dimensionless value with initial concentration of 100% was emitted from the mouth of a male person. The average mouth opening area of a male person was shown by Gupta et al., (2009) to be 4.0 ± 0.95 cm^2; hence an area of 0.0049m^2 was used to inject the contaminant. Due to constraints inherent in the CFD application, no downward tilt of the mouth was modelled, thus the orifice was perpendicular to the vertical axis. The cough was discharged using a mass flow rate of 0.005kg/s at temperature of 30^{o}C (Bjorn, 2002). According to Cox and Wathes, (1995) a density of 1.1 g/cm^3 is widely used for computational applications.

9.3.3 Dynamic thermal model

Bulk airflow through the different ventilation systems were executed using IES (IES, 2011) for Phase 1 of the studies only, since the software is incapable of modelling contaminant transport. The building envelope was also assumed to be largely adiabatic with the exception of the external wall hosting the fixed glazed area and the ventilation openings. This wall was assumed to be constructed of 100mm brickwork and concrete in two plies, encasing

Styrofoam insulation of 58.5mm thickness. The wall was finished with 15mm gypsum-based plaster giving a total U-value for the composite assembly of 0.35 W/m^{2}K. Occupancy was assumed to comprise of three people using the space intermittently. At peak time, the total heat from each person was 120W, as would be applied in the CFD equivalent model. Lighting and equipment were responsible for an additional 70 and 75W respectively and a schedule of operation from 10:00pm to 06:00am was created for the lights to be off. All equipment was assumed to be always on, to account for use of critical medical devices.

For temperature control, two heating setpoints were created at 18^{o}C and at 20^{o}C, but only the results for the latter were eventually of reported. To account for control and variability in vent opening, several opening fractions ranging from 5% to 100% were created and simulated. However, for winter period (December – February) the 25% opening fraction was deemed of interest due to its overall performance in meeting the minimum required rates of existing guidelines for majority of the Cases, as well as for determining what the trickle ventilation rates should be for low-energy and thermal comfort to be achieved. In the non-winter months (March – November) two sets of opening fractions are reported: 60% and 100%, with respect to their capacity to deliver acceptable thermal comfort and to minimise overheating potential especially in summer season.

9.3.4 Computational fluid dynamics model

The CFD model was meshed after pilot studies for different grid resolutions in PHOENICS (Cham, 2011). A total of 45,000 cells from a 30 x 50 x 30 grid were established for the Case 1 and Case 2 but for Cases 3 and Case 4, the total cells were 90,000 with an increase of 30 extra cells in the vertical axis to account for the presence of stacks. As with the DTM model, all surfaces were assumed to be adiabatic with the exception of the fixed glazed area, whose temperature would be determined by the working temperature of ambient air. This was mostly 28^{o}C representing summer conditions and intended test the resilience and performance of each system in a period when buoyancy-driven flows are sluggish, but studies for lower temperature were also performed. The turbulence model used was the RNG k-ε model (Yakhot and Orszag, 1986) applied with the Boussinesq approximation for buoyancy. Convergence was attained after 5,000 iterations for Case 1 and Case 2 and after 6,000 and 7000 iterations for Case 3 and Case 4. For the airborne contaminant studies, it was necessary for converged solutions, to increase the iterations to 6,500 for Cases 1 and 2 as well as up to

8,000 and 9,000 iterations for Cases 3 and 4 respectively. In all instances, a 0.1% error margin was applied for acceptable and converged solutions.

9.4 Phase 1: Airflow rates, comfort and energy

For the first phase covering airflow rates, thermal comfort and energy consumption, the results obtained from DTM and CFD simulations are provided in the following subsections.

9.4.1 Bulk airflow

Analysis of the bulk air flow during the winter period has been simplified using January as a representative month. For each case, the fluctuating pattern of airflow for this month are shown in Fig. 9.4a while a summary of the minimum, maximum and mean flow rates are shown in Fig. 9.4b. From both figures, it is observed that Case 1 (window) has the least flow rates. For winter, predictions for airflow rates which have been obtained at 25% opening fraction (based on previous findings in these research) in order to provide sufficient ventilation at minimal energy.

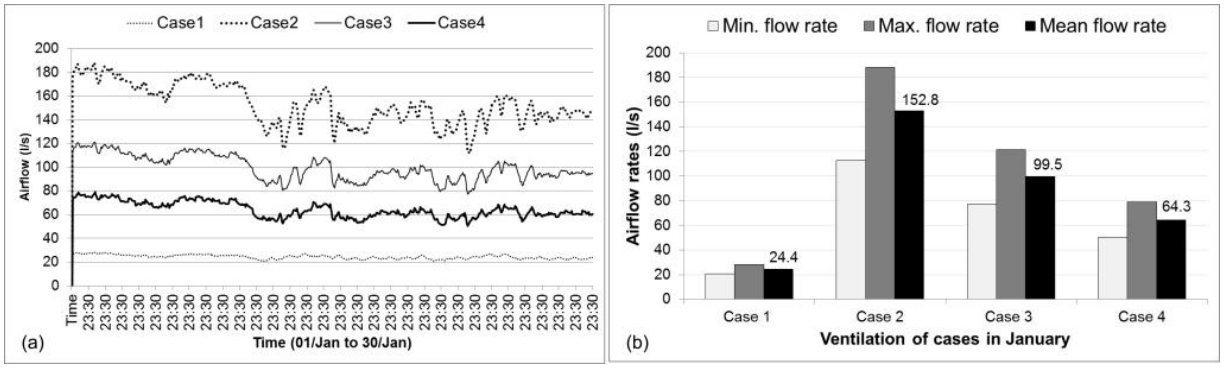

Figure 9:4: Airflow at 25% opening in January showing (a) monthly flows and (b) minimum, maximum and mean flow rates

At 12.5% opening fraction, the pattern of flow in the entire month is largely similar (Fig. 9.5a) and the airflow rates are also halved, in terms of minimum, maximum and mean flow rates (Fig. 9.5b).

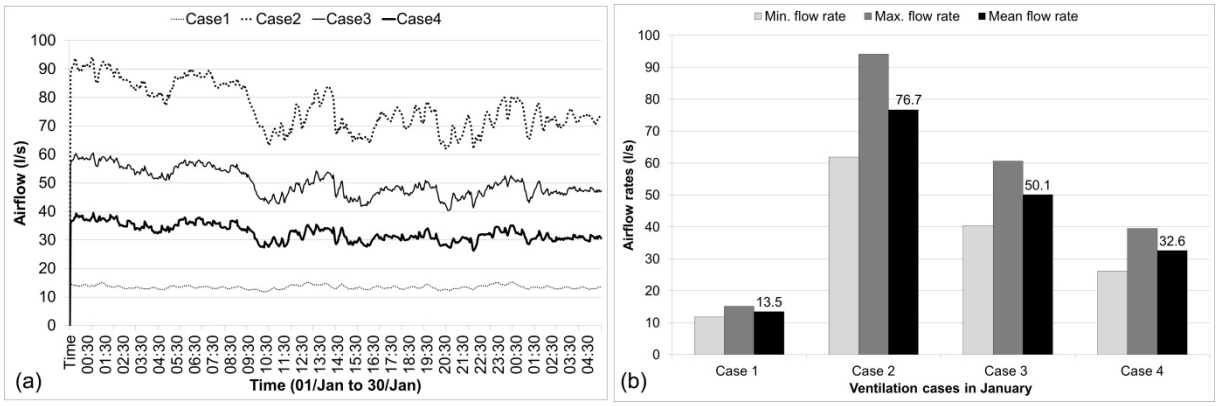

Figure 9:5: Airflow at 12.5% opening in January showing (a) monthly flows and (b) minimum, maximum and mean flow rates

Of the non-winter months (March-November), the summer period presents the most challenging and interesting case due to potential for buoyancy forces to fall as a result of small temperature differentials. This is in addition to the potential for overheating to occur due to solar gain from high external temperatures. As pointed out in Gan (2000), indoor temperatures and therefore thermal comfort not only depend on outdoor temperatures and internal heat gains, but air velocity also has an effect on the sensation of comfort. If the month of July is taken as representative of the summer period, each system is able to provide airflow at varying levels of minimum, maximum and mean rates as summarised in Fig. 9.6. Generally, the proportionate pattern of flow for each case is not dissimilar to the January (winter) situation and thus, in increasing order of performance, they are ranked as Case 1, Case 4, Case 3 and Case 2.

It is instructive from these results of winter and summer that Case 2 (single side) which was more or less dismissed from being useful in dealing with airborne contaminants (Atkinson, et al. 2009), happens to produce the highest ventilation rate amongst the four selected systems. Its predicted flow rates peak at 437.5 l/s (22.73 ACH), with a mean of 289.5 l/s (15.03 ACH) and a minimum flow rate of 162.2 l/s (8.43 ACH). Although subsequent studies will reveal how exactly these flow rates perform for migration of airborne pathogens, evidence from literature review strongly imply that greater airflow rates are always beneficial. To give a better perspective of the airflow achievable, the maximum airflow rate from dual-openings at 100% opening fraction is 5.7 times greater than the maximum flow rate using single opening (Case 1) which produces 76.9 l/s or 3.99 ACH in the same month.

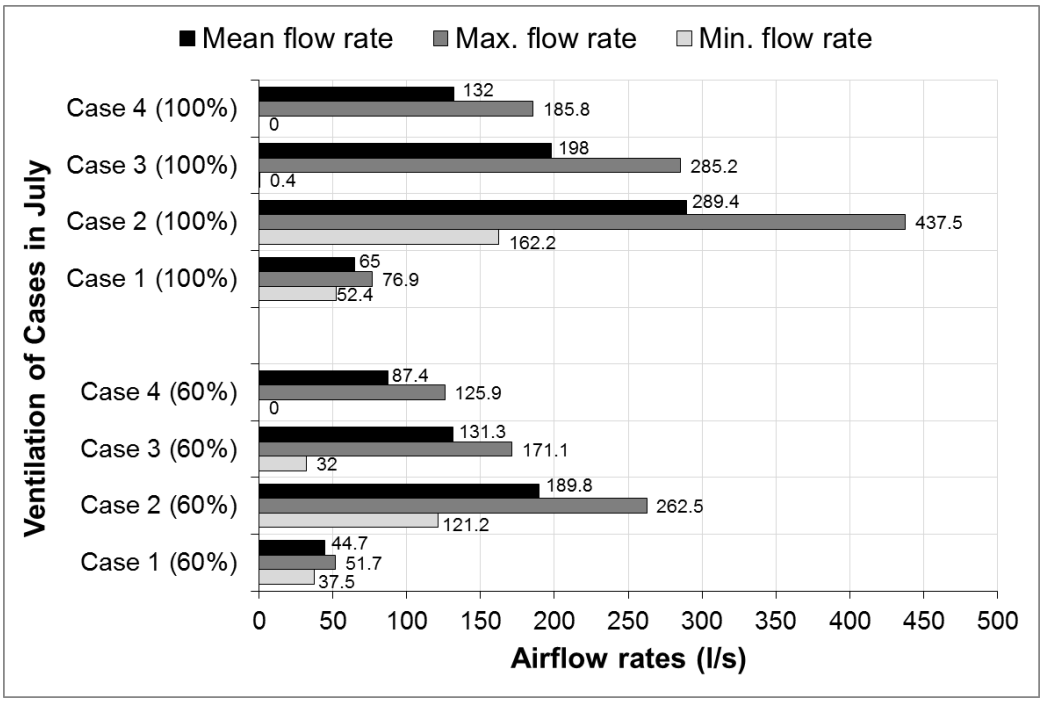

Figure 9:6: Airflow rates for all cases in July through 100% and 60% opening fraction

The fluctuations expected in July shown in Fig. 9.7 reveal that substantial rise and fall could occur depending on time of day in all cases except for Case 1 (windows), in which the flow pattern remains stable in the range 52.4 l/s to 76.9 l/s.

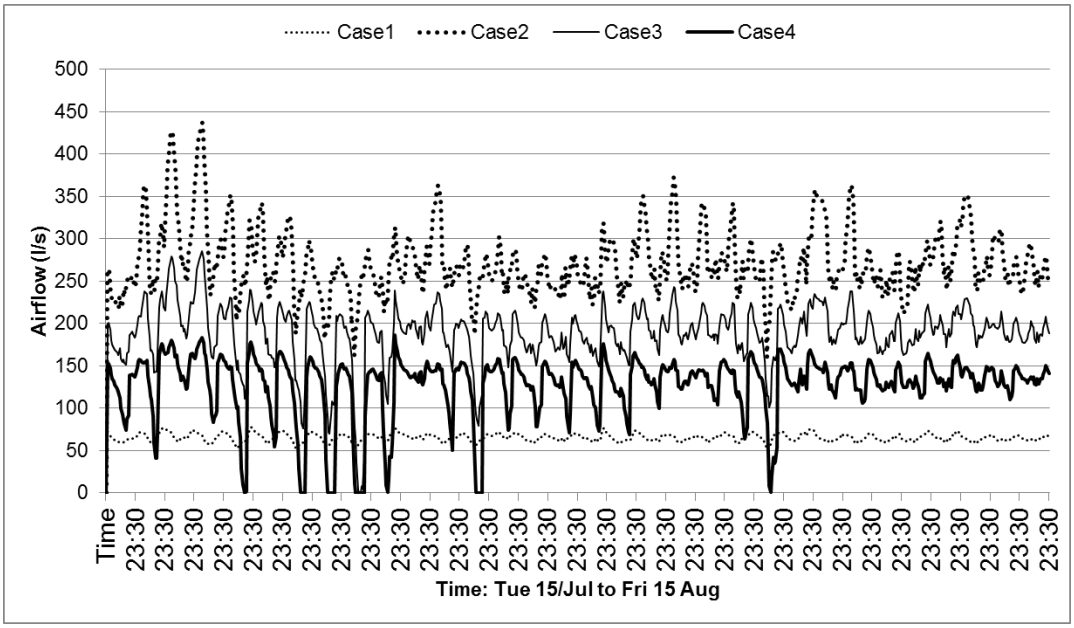

Figure 9:7: Fluctuating pattern of airflow for each strategy at 100% opening fraction in July.

More details of airflow rate performances for each system are contained in Table 9.2 where the airflow rates in all four cases are compared at 100% and at 60% opening fractions.

Table 9.2: Predicted airflow rates in July in ACH and L/s for each case at 100% and 60%

		100%				60%		
		Min. Val.	**Max. Val.**	**Mean**		**Min. Val.**	**Max. Val.**	**Mean**
ACH	Case 1	2.72	3.99	3.38		1.95	2.68	2.32
	Case 2	8.43	22.73	15.03		6.3	13.64	9.86
	Case 3	0.02	14.81	10.29		1.66	8.89	6.82
	Case 4	0	9.66	6.86		0	6.54	4.54
L/s	Case 1	52.4	76.9	65		37.5	51.7	44.7
	Case 2	162.2	437.5	289.4		121.2	262.5	189.8
	Case 3	0.4	285.2	198		32	171.1	131.3
	Case 4	0	185.8	132		0	125.9	87.4

By aggregating flow for the two winter and non-winter categories (i.e. December to February and from March to November), the airflow performances of each of the four natural ventilation systems are presented and evaluated against established benchmarks and guidelines in Table 9.3.

Table 9.3: Performance evaluation of mean airflow rates in different seasons

		Case1 (window)	Case 2 (dual-opening)	Case3 (inlet/stack)	Case4 (CBNV)
100% Mar – Nov	**Mean ACH**	**3.63**	**20.1**	**13.43**	**8.83**
	Meets HTM's 6 ACH?	*No*	*Yes*	*Yes*	*Yes*
	Exceeds 8 ACH (Qian et al, 2006)?	*No*	*Yes*	*Yes*	*Yes*
	Mean flow rate (l/s/patient)	**69.9**	**387**	**258.6**	**170**
	Meets WHO's 60 l/s/patient?	*Yes*	*Yes*	*Yes*	*Yes*
	Meets HTM-03-01 10 l/s (odour)	*Yes*	*Yes*	*Yes*	*Yes*
	Meets EN ISO 7730 47 l/s?	*Yes*	*Yes*	*Yes*	*Yes*
	Mean flow rate (m^3/hr)	**251.64**	**1393.2**	**930.96**	**612**
	Meets 3000m^3/hr (Jiang, et al. 2009)	*No*	*No*	*No*	*No*
60% Mar – Nov	**Mean ACH**	**2.41**	**12.42**	**8.35**	**5.53**
	Meets HTM's 6 ACH?	*No*	*Yes*	*Yes*	*No*
	Exceeds 8 ACH (Qian et al, 2006)	*No*	*Yes*	*Yes*	*No*
	Mean flow rate (l/s/patient)	**46.3**	**239**	**160.8**	**106.4**
	Meets WHO's 60 l/s/patient?	*No*	*Yes*	*Yes*	*Yes*
	Meets HTM-03-01 10 l/s (odour)	*Yes*	*Yes*	*Yes*	*Yes*
	Meets EN ISO 7730 47 l/s?	*No**	*Yes*	*Yes*	*Yes*
25% Dec - Feb	**Mean flow rate (l/s)**	**23.77**	**142.50**	**93.10**	**60.30**
	Meets WHO's 60 l/s/patient	*No*	*Yes*	*Yes*	*Yes*
	Meets EN ISO 7730 47 l/s?	*No*	*Yes*	*Yes*	*Yes*
	Meets HTM-03-01 10 l/s (odour)	*Yes*	*Yes*	*Yes*	*Yes*

*Marginally falls short of 47 l/s.

9.4.2 Thermal comfort and overheating potential

Using PMV and PPD, results for thermal comfort in winter and summer are presented using a heating setpoint of 20^{o}C, which is just above the 18^{o}C minimum temperature allowed by guidelines. From Fig. 9.8, both the performances for each system in winter are shown using January as a representative month. Bearing in mind that these results are for 25% opening fraction, PMV for all cases appear to be around the neutral point (0) with the exception of Case 1 (window). For PPD, predicted results imply that in Case 1, there will be 5 days of the month when up to and over 50% of occupants would be dissatisfied with the thermal environment.

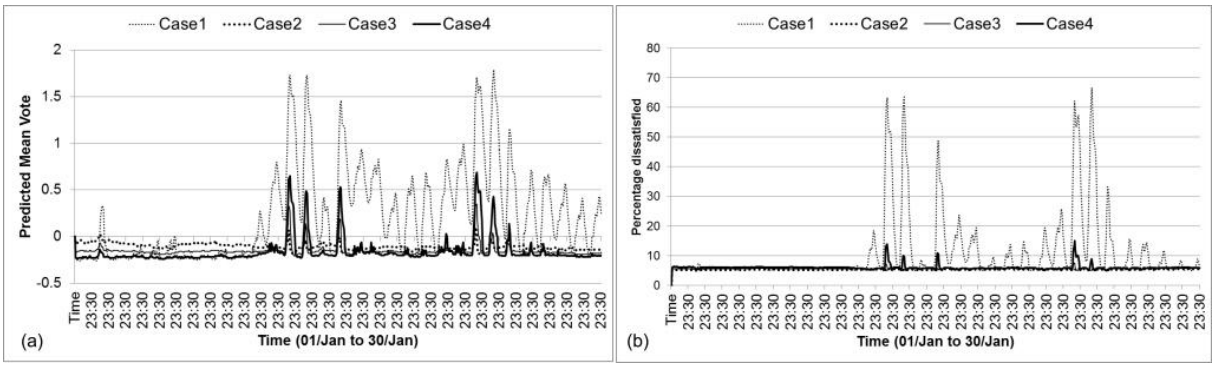

Figure 9:8: Opening fraction at 25% with 20°C setpoint for (a) PMV and (b) PPD

In summer the PMV comfort ranges expected in each system have been summarised for 100% opening fraction in Fig. 9.9a and for 60% opening fraction in Fig. 9.9b. It is apparent from predicted results that Case 1 has more days when PMV exceeds 1.0 (slightly warm) at both 100 and 60% opening fractions. Specifically, Case 1 will also experience 15 days when PMV will exceed +2.0 (hot) at 100% opening fraction; or 36 days at 60% opening fraction.

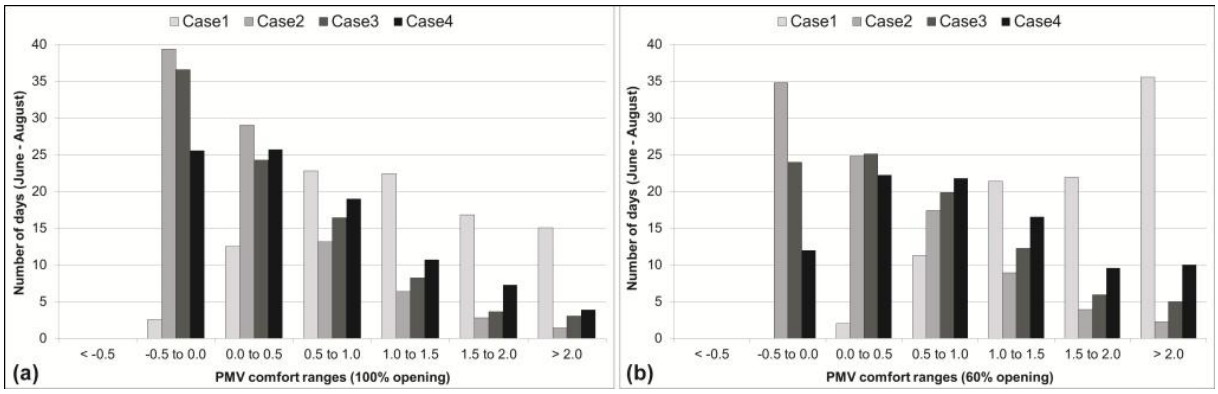

Figure 9:9: PMV comfort ranges at 100% and 60% openings for July to August

Since PMV has been shown to over-predict neutral temperature levels, and because HTM and HBN both require a dry-bulb temperature range between 18 and 28°C, the results for March to November should be evaluated with respect to temperature. For the predicted results, it should be borne in mind that a heating setpoint of 20°C was utilised for DTM analysis. In Fig. 9.10, the predicted temperatures are shown for 100% opening fraction (Fig. 9.10a) and for 60% opening fraction (Fig. 9.10b) when summer overheating is a risk. As with PMV results, Case 1 performs poorly, relative to other Cases, with just 42 days experiencing 20-21°C temperatures when openings are at 60% of their maximum size. At this opening fraction, Case 1 also experiences 91 days of >28°C temperatures, three times higher than other cases. At

100%, Case 4 has the maximum number of days in the 20-21^{o}C range (155 days). This could be attributed to the mixing behaviour observed for the NPV duct in Adamu et al. (2011b) unlike other cases which depend on displacement. At 60% Case 2 would have the most days (143 days) closely followed by Case 4 (135 days). The pattern of temperature ranges shown in Fig. 9.10 strongly suggest that each system is peculiarly better in certain temperature ranges. However, at 60% opening fraction, Case 1 has a more proportionate number of days across the different temperature ranges with exception of 20-21^{o}C and for >28^{o}C.

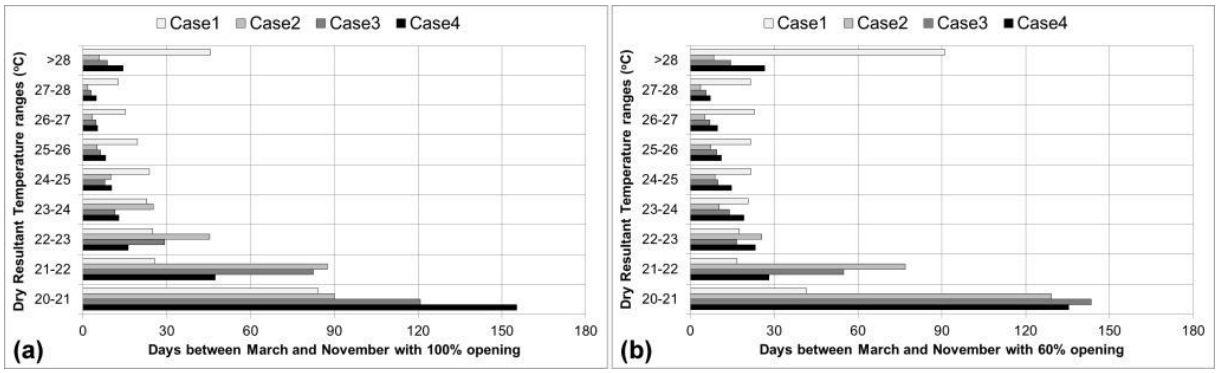

Figure 9:10: Indoor temperature ranges in non-winter months at (a) 100% and (b) 60% opening

For the entire winter months, Fig. 9.11a is a summary of predicted PMV hours, using EN ISO standard ranges (-0.2<PMV<+0.2) as a benchmark for comfort. The number of hours when these hours will be achieved in the non-winter months are summarised in Fig. 9.11b.

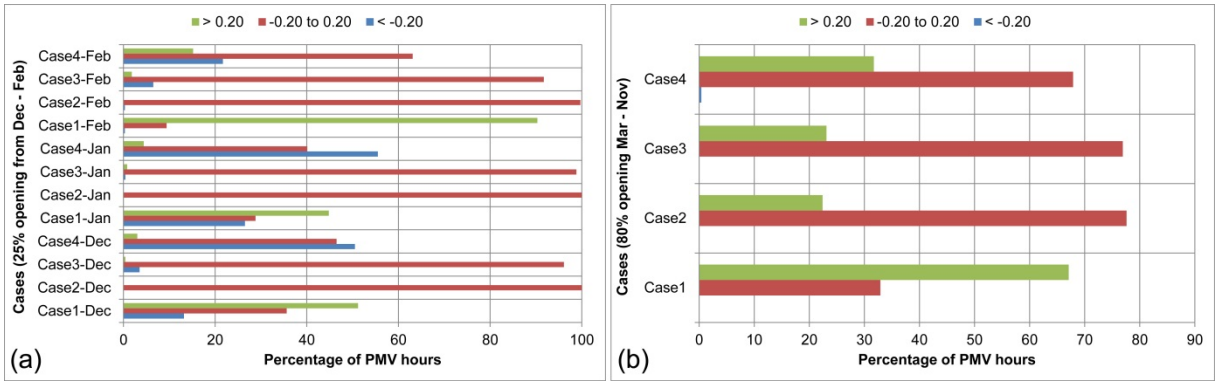

Figure 9:11: Thermal comfort results using PMV for (a) winter months and (b) non-winter months

The location and size of the window in Case 1 has already been shown to lead to discomfort, as predicted by dynamic thermal model even at 25% opening fraction during winter. This system has been compared with other systems using CFD to explore the potential for

overheating in the peak of summer when outdoor temperatures can reach and exceed 28°C. For Case 1 whose mean July flow rates are 44.7 l/s and 65 l/s at 60% and 100% opening fractions respectively, there is restriction in airflow due to entrainment of stale air with incoming fresh air at the same vent. While this conflict in airflow is the plausible cause of lowest energy consumption by this system, it is also a basis of discomfort to be experienced as predicted by the dynamic thermal model. Evidence of this conflict and ensuing discomfort are shown through CFD contours for temperature in Fig. 9.12a and contours for Age of air superimposed over 2D airflow vectors in Fig. 9.12b. The contours for Age specifically demonstrate that the incoming air will be relatively stale due to the mixing which occurs with outgoing air at the same vent. This therefore leads to a gradual build-up of heat for Case 1 system, which can reach a maximum of 40°C from top of window opening up to the ceiling. This is also the approximate temperature of the rising plume of warm air over the visitor, while the mean temperature for the entire space is 39°C.

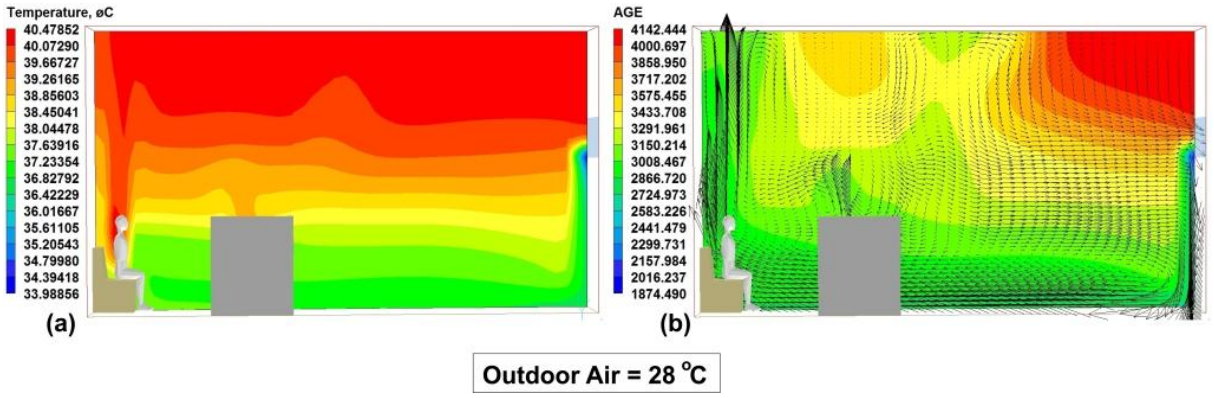

Figure 9:12: Summer CFD results for Case 1 showing (a) indoor temperature (b) Age and 2D flow vectors

From Fig. 9.12b, the mean Age of fresh air at the lowest part of the vent is already 1874s while the approximate mean Age of outgoing air is 4000s. At the level of the patient's bed and head of visitor, the mean Age of air is ≈ 3008s, while the temperature approaches 38°C, which is 10°C higher than outdoor levels. These results illustrate the staleness and high temperature of indoor air and help to explain the poor performance of windows used for ventilating similar spaces in summer. As applied in the existing redevelopment of the GOSH facility, these results strongly imply that the single window opening will not meet the comfort requirements of occupants when outdoor temperatures approach or exceed 28°C. Streamlines revealing Age of air in 3D (Fig. 9.13) show how fresh air not only mixes with outgoing stale

air, but it also takes significant time descending to the floor and creeping towards the bed location, both phenomenon contribute to the high Age of air at patient/visitor locations.

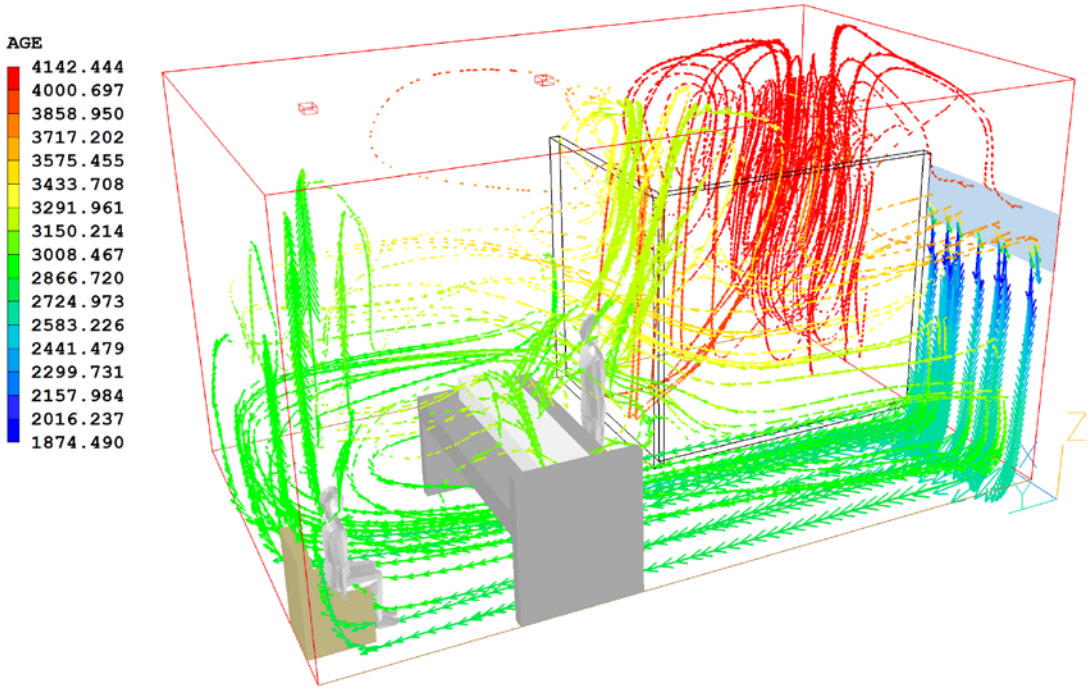

Figure 9:13: 3D streamlines for Age of air using single window strategy at 28^{o}C outdoor temperature

By contrast, in Case 2 (dual-opening), the distinction in airflow inlet and outlets leads to marked difference in performance when the outdoor temperature is 28^{o}C. In this case, the inevitable build-up of internal heat leads to maximum room temperature of ≈ 32^{o}C at the ceiling level (Fig. 9.14a), but critically, this is also about 8^{o}C lower than what was obtained using single windows in Case 1. Importantly, the Age of air at the raised outlet is ≈1254s, while it is close to 0s at the inlet (Fig. 10.14b). At the occupied levels, the temperature at the plume directly above head of visitor is 31^{o}C and the strata extending across the top of bed, the temperature is ≈ 29^{o}C, representing a rise of 1^{o}C and 2^{o}C above outdoor levels at these locations. The freshness of air at these levels also improves relative to Case 1 with Age of air being ≈ 419s, a seven-fold reduction relative to Age of air in Case 1, implying quality of air would increase by up to seven times using this system.

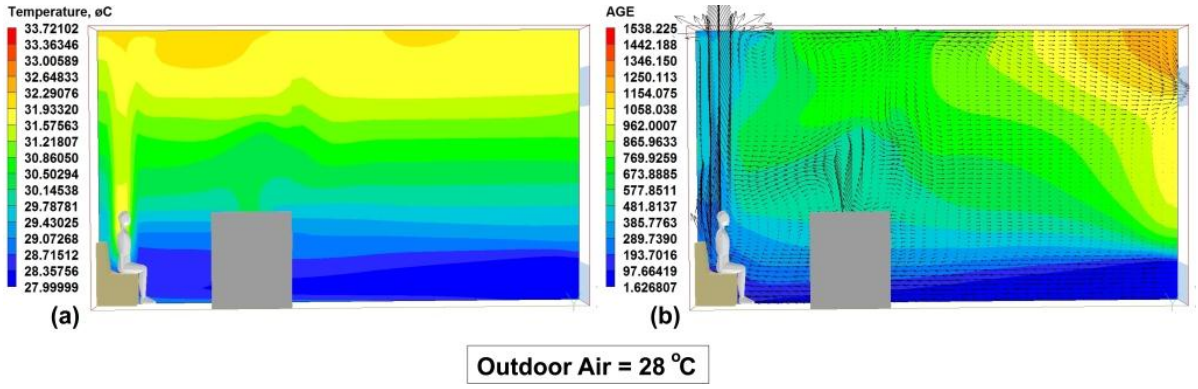

Figure 9:14: Summer CFD results for Case 2 showing (a) indoor temperature (b) Age and 2D flow vectors

The CFD results are not surprising since the DTM predictions implied that dual-openings can have up to 22.73 ACH (437.5 l/s) in July. The practical implications of having dual-openings based on these results would come in the form of refurbishing existing wards which currently have single openings. However, by creating a second vent at ceiling level as found in a dedicated study of this system (Chapter 7), the vertical distance between two openings is a determinant of airflow rates, the best performance coming from floor level inlet and ceiling level outlet, as applied in this case study. These CFD results are therefore further evidence of the airflow characteristics of the dual-opening system. The airflow rates predicted by the dynamic model and the airflow direction and Age of air revealed by 2D vectors and 3D streamlines could prove crucial in controlling/diluting airborne contaminants to be tackled in Phase 2 of this case study. The pattern of airflow with respect to Age of air is shown using 3D streamlines in Fig. 9.15 which also gives a better overview of airflow direction.

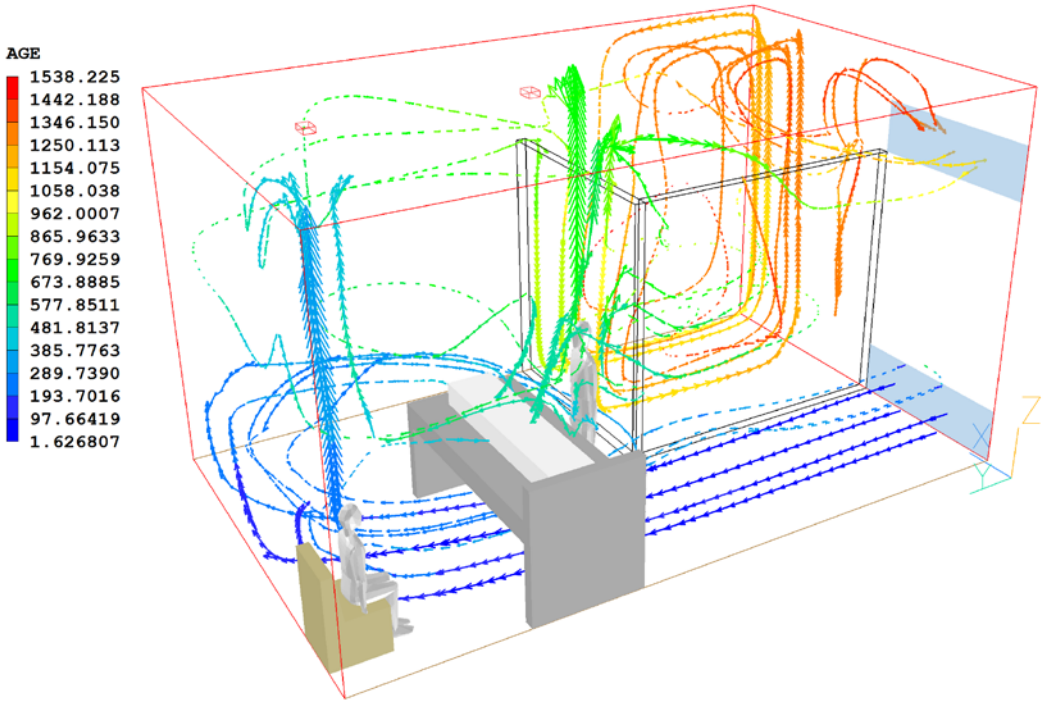

Figure 9:15: 3D streamlines for Age of air using dual-opening strategy at 28^{o}C outdoor temperature

In the simplified ANV system which characterises the inlet and stack system of Case 3, the temperature at the visitor's head and at the bed level is ≈ 29^{o}C which is a 1^{o}C rise above outdoor temperature, while the mean temperature of the plume over visitor is 31^{o}C (Fig. 9.16a). This represents a rise of 1^{o}C above ambient temperature and as with dual-opening system of Case 2; the maximum temperature in the room is 32^{o}C at ceiling level. Similar to Case 2 regarding air quality, the Age at inlet is 0 seconds (Fig. 9.16b) and 29s at the layer over bed. The difference in air quality is thus significantly improved over Cases 1 and 2 systems.

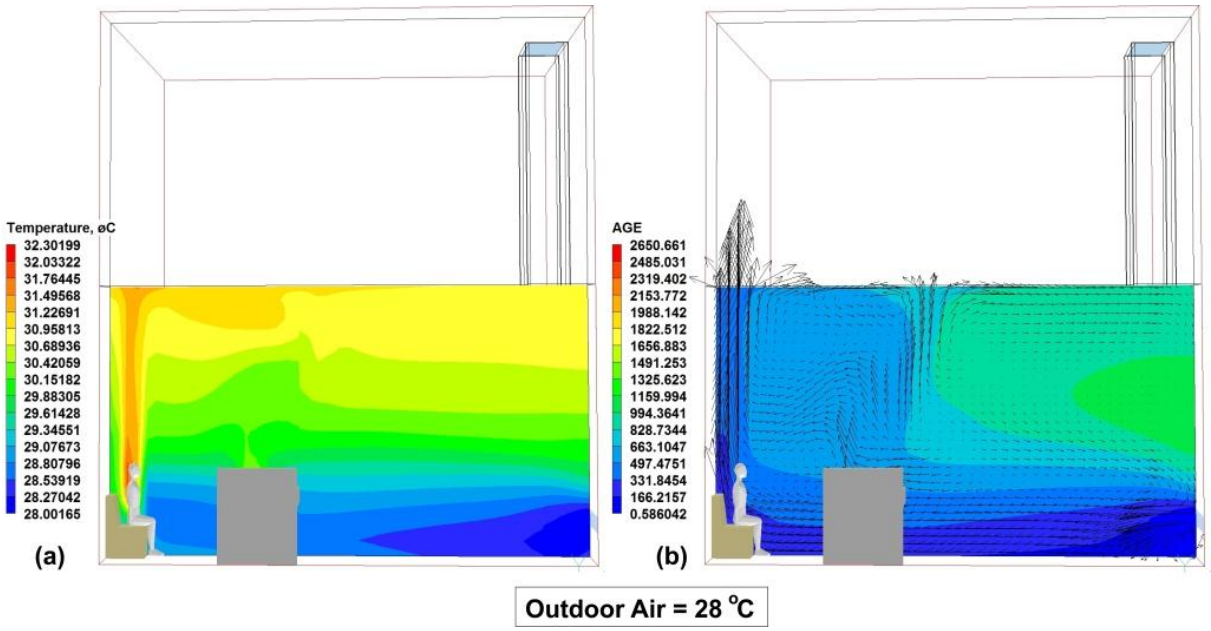

Figure 9:16: Summer CFD results for Case 3 showing (a) indoor temperature (b) Age and 2D flow vectors

The flow direction of air represented in 2D vectors superimposed over Age of air contours in Fig. 9.16b are supported by a 3D representation of airflow from the low-level inlet and out through the stack in Fig. 9.17.

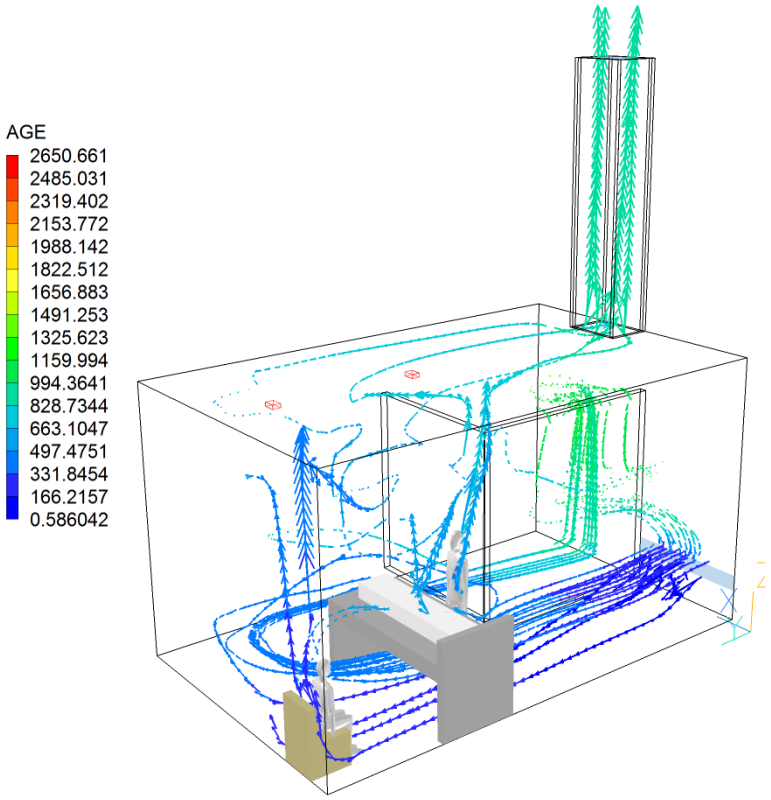

Figure 9:17: 3D streamlines for Age of air using inlet and stack strategy at 28°C outdoor temperature

The first striking characteristics of Case 4 (CBNV) which has air supply from two ceiling-mounted ducts is the apparent uniformity in room temperature and Age of air, represented by a lack of distinct stratification of these variables as shown in Fig. 9.18. There is an obvious absence of the usual plume of hot rising air over the visitor (Fig. 9.18a) which characterises most displacement strategies. Like the inlet and stack system of Case 3, the mean temperature in the ward is ≈ 29^{o}C for this CBNV system, a 1^{o}C rise above external temperature. Directly over the bed, the mean Age of air coming out of the NPV duct is 0s at the orifice of discharge but the Age approaches 744s at the bed level (Fig. 9.18b).

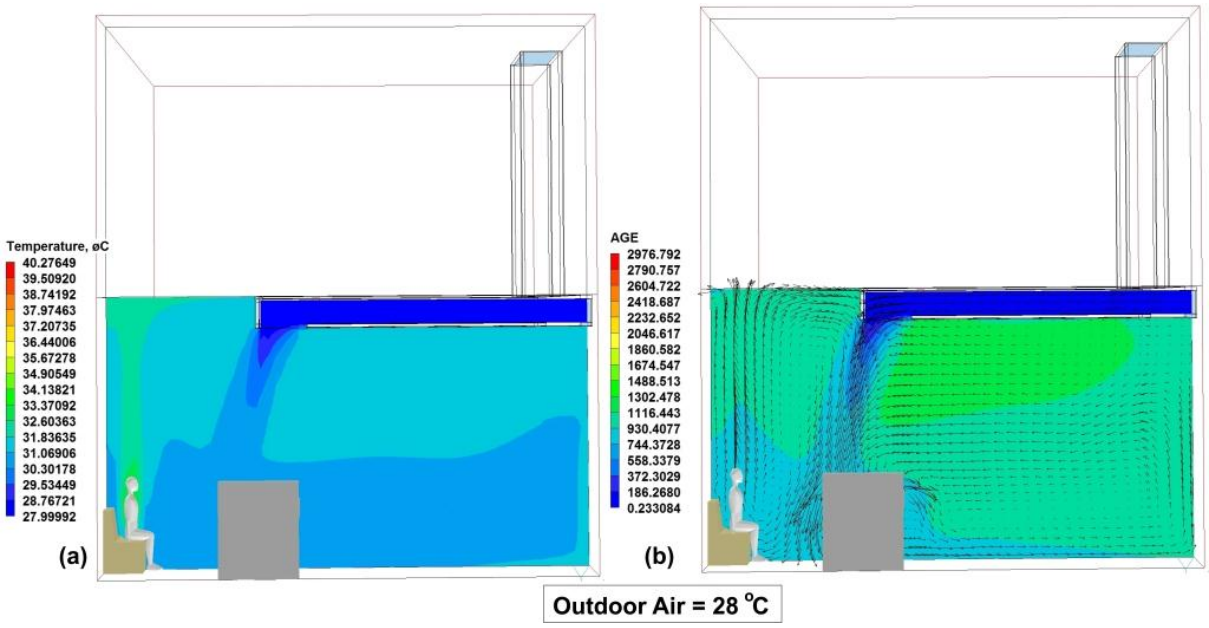

Figure 9:18: Summer CFD results for Case 4 showing (a) indoor temperature (b) Age and 2D flow vectors

The second remarkable feature of this system is the near total mixing occurring in the entire space, as the descending cooler air is forced to rise again, creating mild local turbulence as indicated by 3D streamlines in Fig. 9.19. These results support the dynamic model predictions, where this system not only delivers better PMV and PPD than Cases 2 and 3, but also consumes less heating energy in winter. It remains to be explored in Phase 2, whether this mixing and turbulence has benefits for dilution of contaminants.

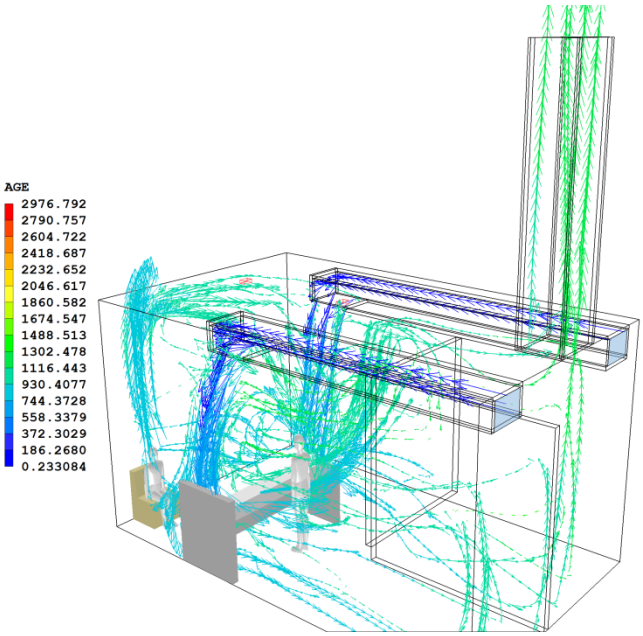

Figure 9:19: 3D streamlines for Age of air using CBNV strategy at 28^{o}C outdoor temperature

Additional studies conducted on this novel natural ventilation system investigated performance at other temperatures and as shown in Fig. 9.20, when outdoor temperature is 19^{o}C, the largely uniform indoor temperature is in the order of 22^{o}C. Airflow into the ward is captured using slices across both NPV and supplementary air duct. The cascading of cooler air over both sides of the patient's bed and the spreading of descended air at the floor level in all directions is also observed using a slice at the z-axis.

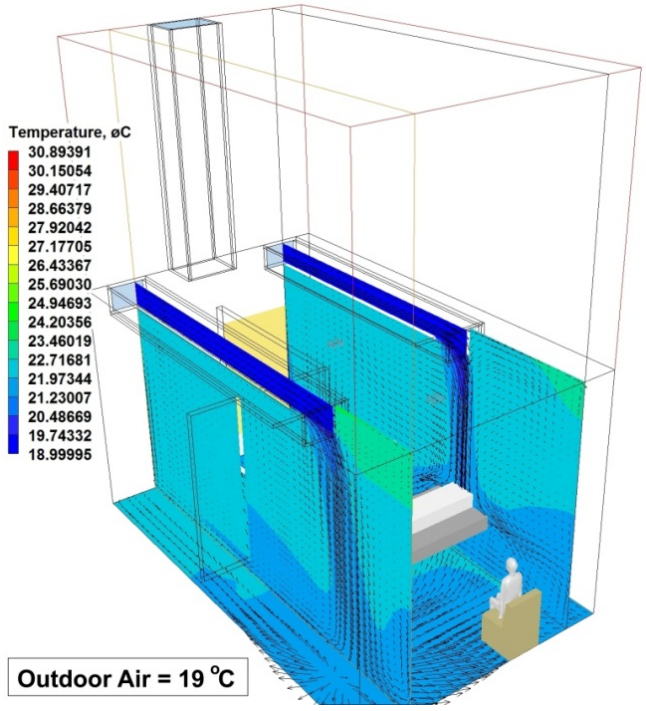

Figure 9:20: Airflow through CBNV ducts showing 2D vectors and temperature contours at 19^{o}C outdoor temperature

9.4.3 Energy consumption

The heating power and energy consumed for heating in winter in each case is evaluated when openings are opened to 25% of their actual size. Starting with January as a representative month, Fig. 9.21 summarises the fluctuating pattern of energy consumed (Fig. 9.21a) as well as the classification of a range of energy required for the heating setpoint of 20^{o}C (Fig. 9.21b). The maximum heating power required by Case 1 system is 1.5kW, representing the lowest among all systems. This is not surprising considering that outgoing stale and warmer air is entrained into fresh incoming air as implied by CFD results. This leads to a recirculation of heat within the room, hence its relatively low heating requirements. However, as observed in the predicted PMV results earlier, this comes with penalties in thermal comfort, where PMV values are higher for most of January.

For other systems, the heating power varies significantly with Case 2 (dual-opening) having the greatest heating load as expected, due to its significant rates of ventilation. In January, the dual-opening system requires up to 5kW of heating load (Fig 9.21a), over 4 times the load required by the single opening (window) system of Case 1. However, this peak load value occurs for only four days of this month, for most other days, the heating load will fluctuate between a minimum of 0.5kW and 4.5kW. For inlet and stack system, there would be 13 days when it is predicted that heating load will range between 1 and 2kW (Fig. 9.21b) with a peak load of 3.5kW needed for 1 only day. For Case 4, the CBNV system has a maximum load of 2.5kW for 1 day only, and for 20 days of January, 0.5kW of heating load is required (Fig. 9.21b).

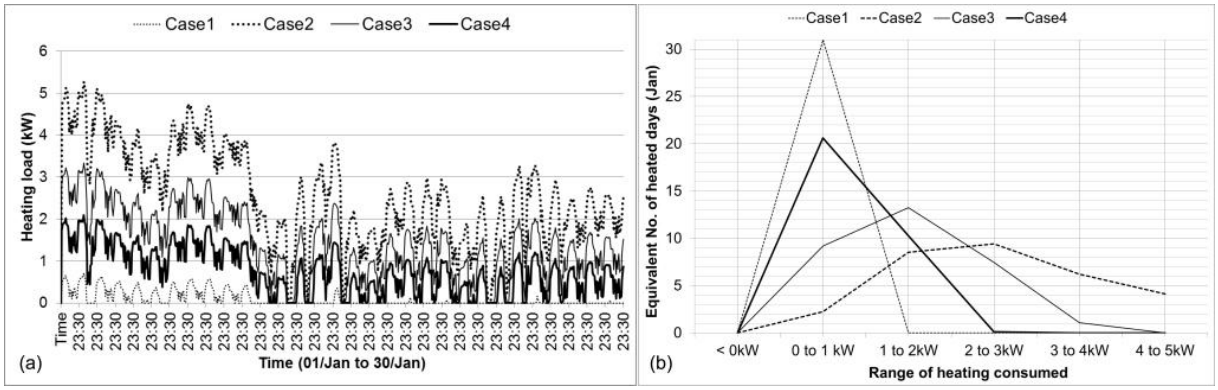

Figure 9:21: Heating energy in January showing (a) fluctuating patterns and (b) energy ranges and required number of days

For the entire winter months (December to February) the cases were compared regarding total heating energy required for each month and for the entire period as shown in Table 9.4, where they have also been ranked.

Table 9.4: Performance ranking for total winter heating energy (MWh)

	Case1	**Case2**	**Case3**	**Case4**
December	0.028	1.6473	0.9143	0.4436
January	0.069	1.9334	1.1045	0.5709
February	0.0008	0.8501	0.4104	0.149
Total (MWh)	**0.0978**	**4.4308**	**2.4292**	**1.1635**
Rank	**1**	**4**	**3**	**2**

It is plausible that since the predicted results for heating energy from the DTS model can be viewed in terms of minimum, maximum values, as well as the estimated times when these values will be reached, this can serve as a feedback or input for further CFD modelling of room heaters. This would be valuable because most fast and reliable CFD simulations are for steady state conditions with fixed outdoor temperatures, therefore, representing only an instant 'snapshot' of a dynamic process. However, selecting the appropriate external temperature and the expected heat to be consumed under such, can not only lead to efficient sizing of room heaters (heating capacity), but optimising the shape and location of such heating devices can be evaluated relative to air inlets and expected airflow rates. For instance, in January when dry bulb temperature is 3.75^{o}C, Table 9.5 shows the different heating required for each case in minimum, maximum and mean values as well as in Watts per square meter and the times when each value will be approached.

Table 9.5: Heating load at 25% opening for January

Variable	**Min. Value**	**Min. Time**	**Max. Value**	**Max. Time**	**Mean Value**	**Watts per m^2**
Case1	0 kW	10:30,02/Jan	0.708 kW	05:30,02/Jan	**0.093**	**0.0039**
Case2	0 kW	12:30,13/Jan	5.279 kW	05:30,02/Jan	**2.599**	**0.11**
Case3	0 kW	10:30,13/Jan	3.341 kW	05:30,02/Jan	**1.485**	**0.063**
Case4	0 kW	10:30,12/Jan	2.096 kW	05:30,02/Jan	**0.767**	**0.033**
Dry-bulb temp.	- 3.6^{o}C	07:00,02/Jan	11.9 ^{o}C	15:00,24/Jan	**3.75**	

A summary of the monthly totals in the energy consumed by each system at 12.5%, 25%, 35% and at 80% are shown in Table 9.6, including annual totals. The relatively high heating required to deal with the significant airflow rates in Case 2 is obvious, since it exceeds CIBSE's 90 kWh/m^2 benchmark. This is for the equivalent value of 2.12 MWh for the given ward area of 23.55m^2 which occurs even when the dual-openings are constricted to 12.5% of their maximum size. Maximum annual consumption is predicted to occur in Case 2 where 32.753 MWh is needed at 80% opening fraction. At 12.5% and 25% opening fraction, Case 1 and Case 4 fall below this energy benchmark

An attempt at equalising the energy demanded by each system was done by aggregating the predicted consumption of different opening fractions over a year is show in Fig. 9.22[8].

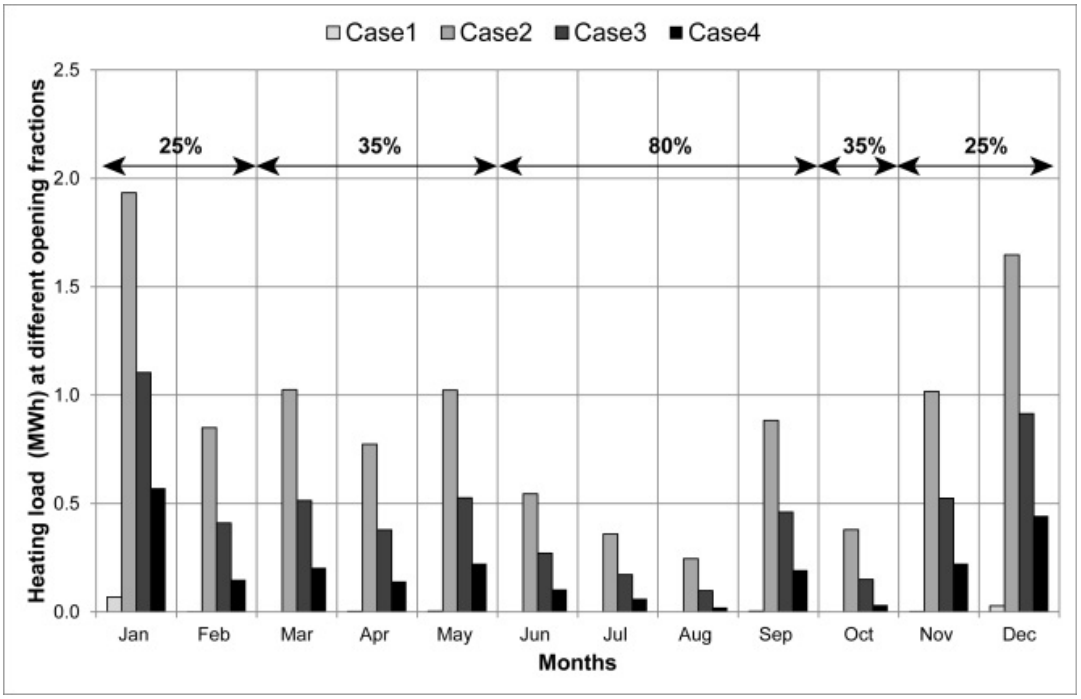

Figure 9:22: Monthly heating loads at different opening fractions

[8] The findings of this comparative study (up to this point), where published as: Adamu, et al. (2012) Available at: http://dx.doi.org/10.1016/j.buildenv.2012.03.011

Table 9.6: Monthly and annual heating plant sensible load (MWh) for selected opening fractions

	80% opening				35% opening				25% opening				12.5% opening			
	Case1	**Case2**	**Case3**	**Case4**	**Case1**	**Case2**	**Case3**	**Case4**	**Case1**	**Case2**	**Case3**	**Case4**	**Case1**	**Case2**	**Case3**	**Case4**
Jan 01-31	0.748	7.050	4.436	2.714	0.165	2.863	1.707	0.953	0.069	1.933	1.105	0.571	0.002	0.782	0.373	0.136
Feb 01-28	0.233	3.644	2.229	1.282	0.015	1.357	0.731	0.331	0.001	0.850	0.410	0.149	0.000	0.250	0.075	0.008
Mar 01-31	0.133	2.985	1.768	0.961	0.000	1.025	0.514	0.204	0.000	0.610	0.268	0.071	0.000	0.152	0.024	0.000
Apr 01-30	0.092	2.316	1.355	0.722	0.003	0.774	0.379	0.141	0.000	0.453	0.189	0.049	0.000	0.104	0.020	0.001
May 01-31	0.154	2.943	1.751	0.961	0.003	1.023	0.527	0.223	0.000	0.620	0.284	0.094	0.000	0.170	0.043	0.001
Jun 01-30	0.000	0.545	0.272	0.104	0.000	0.123	0.036	0.001	0.000	0.051	0.007	0.000	0.000	0.000	0.000	0.000
Jul 01-31	0.000	0.359	0.173	0.062	0.000	0.074	0.017	0.000	0.000	0.027	0.001	0.000	0.000	0.000	0.000	0.000
Aug 01-31	0.000	0.245	0.098	0.021	0.000	0.029	0.003	0.000	0.000	0.006	0.000	0.000	0.000	0.000	0.000	0.000
Sep 01-30	0.003	0.883	0.461	0.193	0.000	0.219	0.069	0.008	0.000	0.096	0.018	0.000	0.000	0.004	0.000	0.000
Oct 01-31	0.016	1.399	0.751	0.344	0.000	0.379	0.151	0.033	0.000	0.193	0.055	0.004	0.000	0.021	0.000	0.000
Nov 01-30	0.322	4.212	2.580	1.501	0.031	1.588	0.883	0.435	0.002	1.017	0.525	0.223	0.000	0.341	0.126	0.018
Dec 01-31	0.601	6.171	3.866	2.340	0.099	2.470	1.449	0.780	0.028	1.647	0.914	0.444	0.000	0.629	0.272	0.076
Annual total	**2.301**	**32.753**	**19.740**	**11.205**	**0.315**	**11.923**	**6.465**	**3.108**	**0.100**	**7.504**	**3.777**	**1.605**	**0.002**	**2.454**	**0.935**	**0.240**

9.5 Phase 2: Airborne contaminants

With respect to the two potential sources of infectious bio-aerosols (i.e. daytime visitor and over-night sleeper), the results obtained from CFD investigation of contaminant dispersal are discussed. Some of the results are evaluated based on the defined points of interest (POIs) which create the imaginary volume of interest (VOIs) as described in Fig. 9.1c and 9.1d. Other results are evaluated based on the longitudinal axis, A-B and the transverse axis C-D also shown in Fig. 9.1a; using contour slices of contaminants and Age of air, for both sources.

9.5.1 Concentrations at Points of Interests (POIs)

Case 1 (Window Cases): Daytime Visitor (Case 1A) vs. Overnight Sleeper (Case 1B)

When two scenarios for daytime and overnight sources are compared, the concentrations at the POIs are more even, averaging at 20.26% when the overnight sleeper (who is closer to the air inlet) is the source of contaminant, (Fig. 9.23) in Case 1A. This is opposed to Case 1B, when the visitor is the source. In the second scenario, the concentrations at POIs fluctuate such that at the odd number POIs which are closer to the bed (measured at 1.1m), the values are significantly higher than concentrations at even number POIs (measured at 1.6m), averaging at 25.10%.

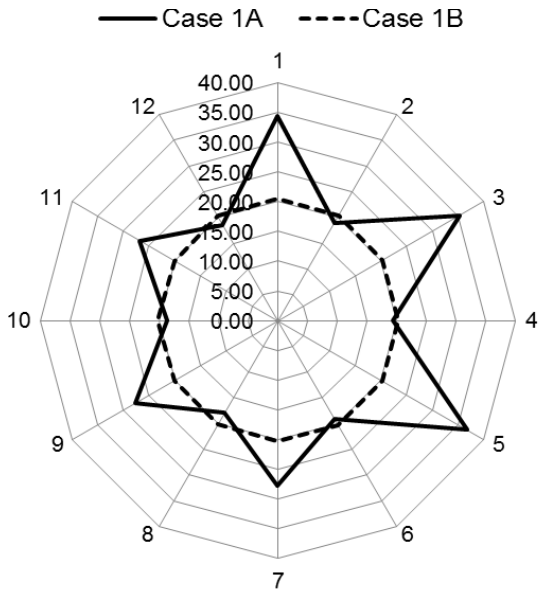

Figure 9:23: Concentrations for Case 1 when source is visitor (1A) and sleeper (1B)

These results from the window (Case 1) system have been separated from other systems due to the difference in scale whereby the results of concentration obtained from the window case are significantly higher than what is obtained in Cases 2, 3 and 4, making a combined graph difficult to read.

Cases 2, 3 and 4: Daytime Visitor vs. Overnight Sleeper

For the other cases, Fig. 9.24 compares how each system performs with respect to time emission and location of source. When the daytime visitor is the source, remarkable differences are observed. From results shown in Fig. 9.24a, the dual-opening (Case 2A) system actually has lowest concentrations at most of the POIs with the exception of points 4, 5 and 6. The mean concentration over the entire imaginary volume of interest (VOI) defined by all POIs is 3.68% for this system. With the ANV system in Case 3A, the concentrations at POIs are also high at points 4, 5 and 6, as well as being highest at points 9, 10 and 11, with a mean of 4.91%. Case 4A on the other is unique in the sense that it has a roughly even concentration at most POIs, with a minimum of 3.73% and a maximum of 4.84%. The mean concentration over the VOI is 4.43%.

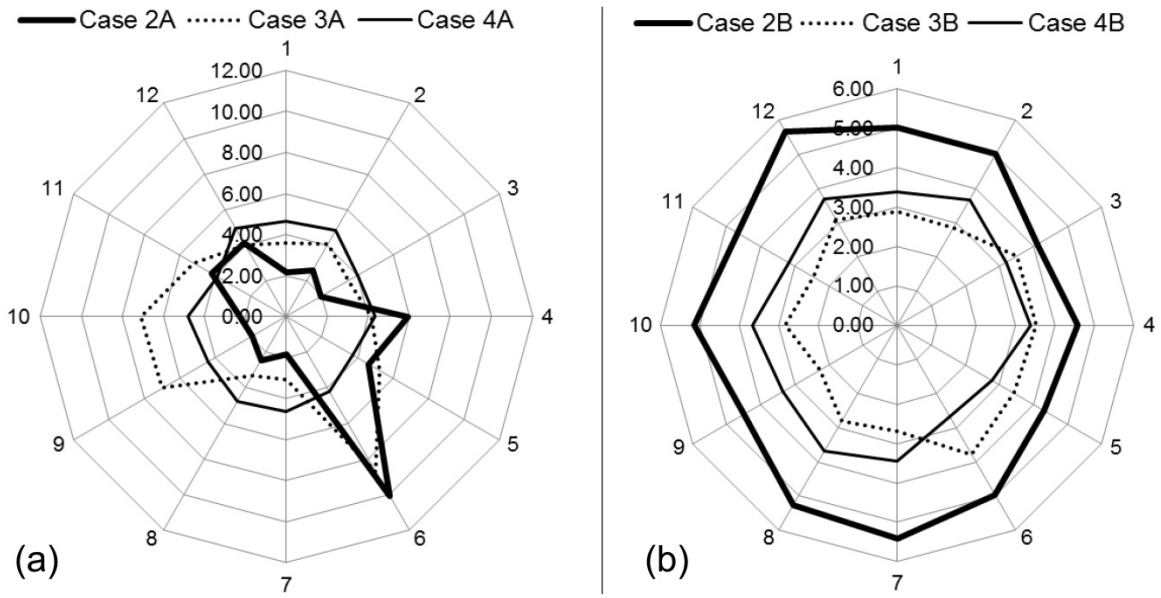

Figure 9:24: Concentrations for other cases when source is (a) Visitor and (b) Overnight sleeper

For the scenario of overnight sleeper, the concentrations at all POIs appear to be approximately of uniform magnitude, without any fluctuations (Fig. 9.24b). This could be attributed to significant dilution taking place by the time the contaminants have reached the POIs. However, the dual-opening system in this scenario performs poorest resulting from the

high concentrations relative to other systems, with a mean concentration of 4.89%. In this scenario, the ANV performs best, (mean concentration of 3.01%) with the exception of concentrations at POIs 3, 4, 5 and 6. The performance of the CBNV becomes apparent, specifically due to the presence of a dedicated (NPV) duct over the bed. The CBNV produces lower values at points 3, 4, 5 and 6 than for the ANV, with a mean concentration of 3.34%.

9.5.2 Concentration across entire ward space

Source: Daytime visitor

The emitted cough behaves differently in all four cases when viewed from source (sitting visitor) towards the external wall as identified in Fig. 1a as profile A-B. In Case 1A, (Fig. 9.25a) the cough appears to have unhindered drift across the patient's bed although concentrations diminish with distance. From contours of concentrations in Fig. 9.24a and from measurements at POIs 1, 3 and 5 which are lowest and closest to the bed (Fig. 9.24a), concentrations are >35%. In Case 2A where two segregated openings are used, Fig. 9.25b indicates that buoyant plume rising from the patient's body causes a gentle uplift in the contaminants as the emission approaches the bed.

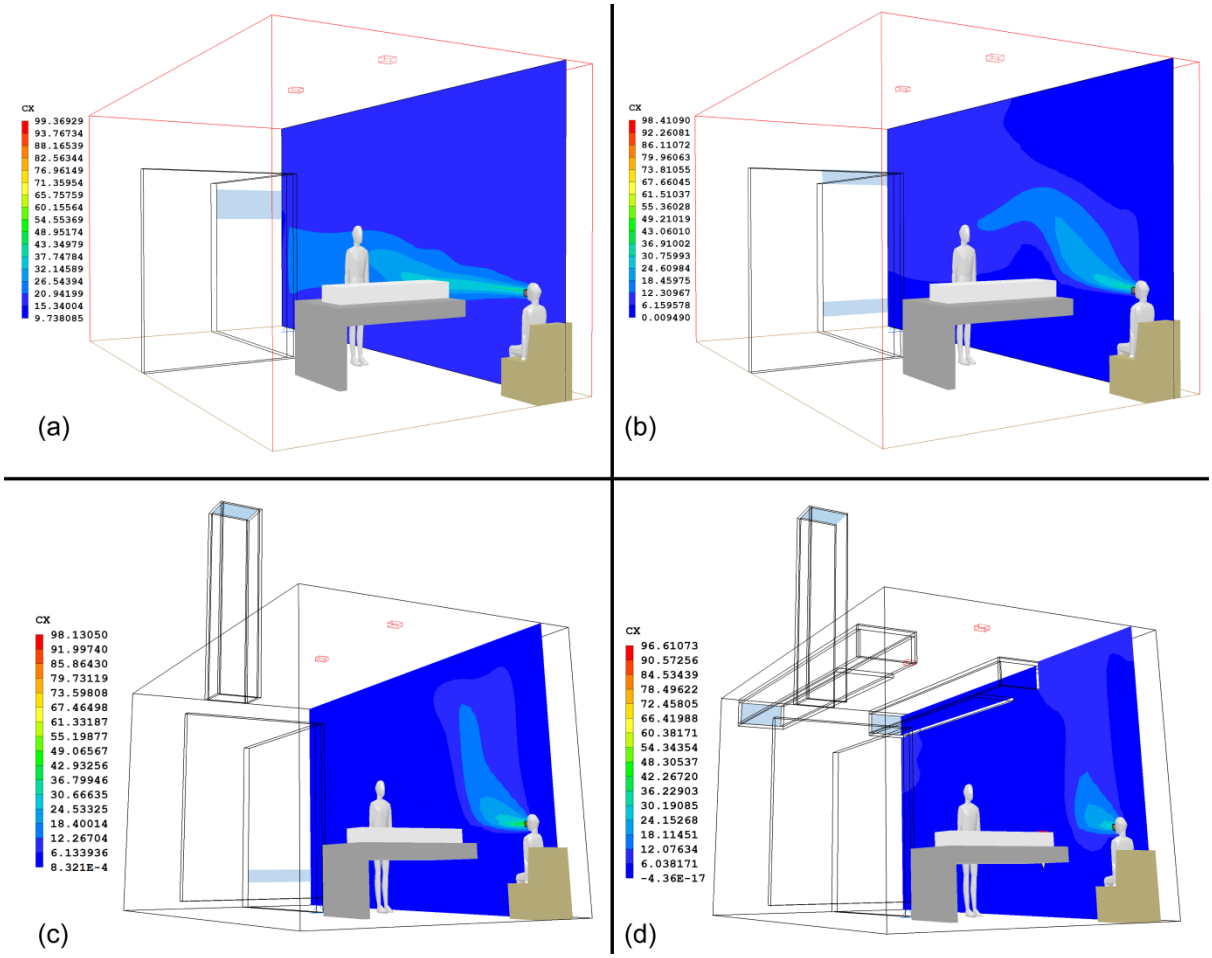

Figure 9:25: Contaminant contours from source across bed in (a) Base Case A (b) Case 1A (c) Case 2A and (d) Case 3A

The presence of an exhaust stack encourages a more pronounced uplift of contaminants towards the ceiling as shown in Case 3A (Fig. 9.25c) and Case 4A (Fig. 9.25d).

Regarding the concentration profile across the entire length of ward (axis A-B) Fig. 9.26 summarises the differences in each system. In fact, all cases with the exception of the window-based design (Case 1A) display a dip in concentration profile around the bed (whose edge is 3.75m from the external wall as seen in Fig. 9.26a. However, the role of downward air supply which causes mixing in Case 4A leads to much lower concentrations at the bed location as supported by Fig. 9.26d, where the concentration approaches a value of zero compared to Case 4A where the minimum dip is approximately 3%.

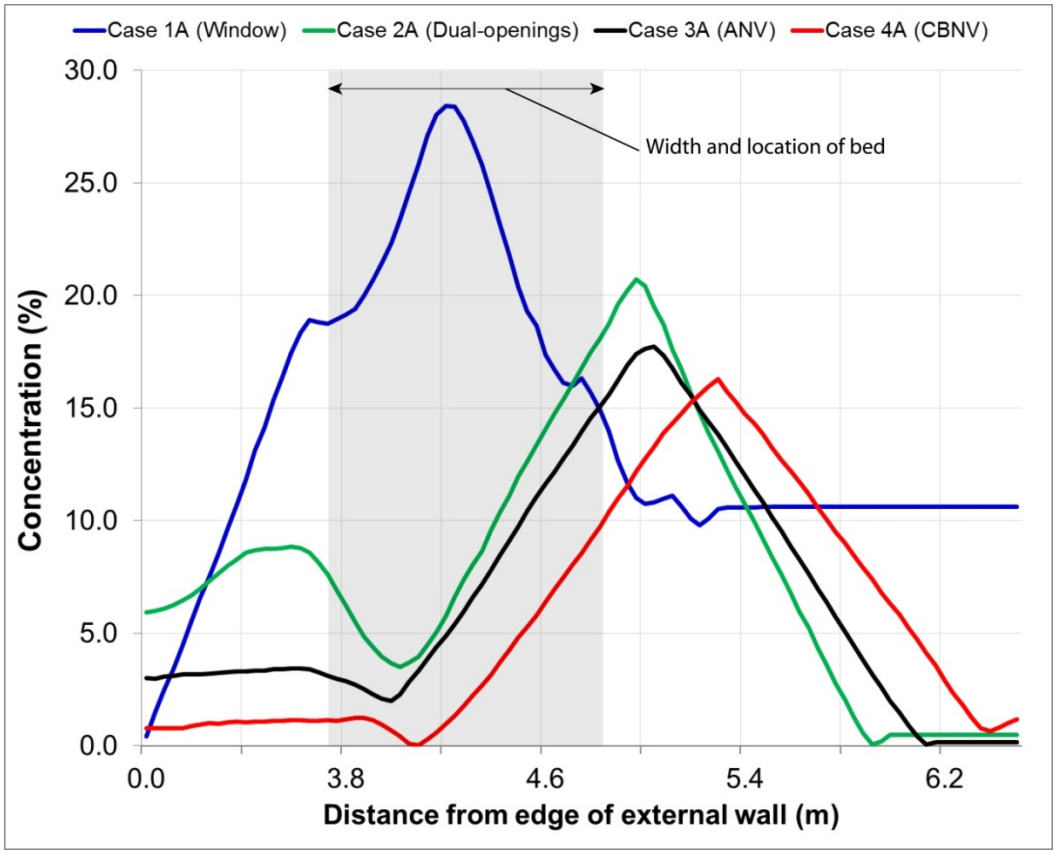

Figure 9:26: Contaminant profile across bed (shaded portion) from source (point 6.23) to external wall (point 0) for (a) Case 1A (b) Case 2A (c) Case 3A and (d) Case 4A.

In addition to CFD contours of contaminants, 2D airflow vectors across the length of ward (Fig. 9.27) indicate that in Case 1A, buoyancy influences the emitted airborne contaminants but in a subdued manner and only after a distance of about 3 meters; as seen in the mostly uninterrupted movement from source across the patient's bed (Fig. 9.27a). This is in contrast to Case 2A which differs from Case 1A by having segregated inlet and outlet and where buoyancy plays a dominant role as indicated by airflow vectors (Fig. 9.27b). In Case 4A the airflow vectors suggest that momentum of buoyancy is overpowered by the descending cooler air, which also counters the flow of contaminants towards the patient (Fig. 9.27d). The contours for Age of air in Fig. 9.27 also reveal influence of displacement to different extents in Figs. 9.27a, 9.27b and 9.27c and the mixing occurring in Fig. 9.27d for the window, dual-opening, ANV and CBNV systems respectively.

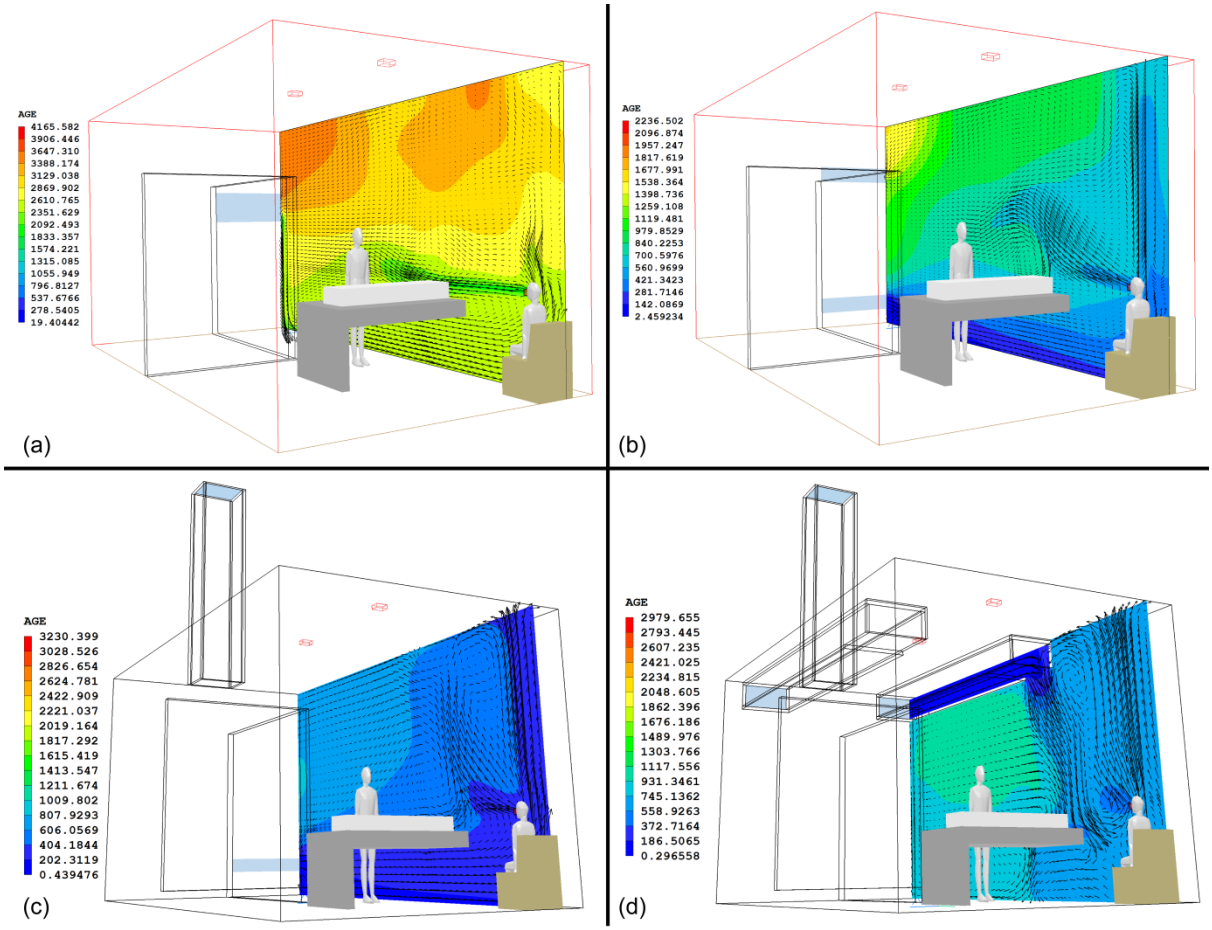

Figure 9:27: Airflow vectors over contours for Age of air across room length for (a) Case 1A (b) Case 2A (c) Case 3A and (d) Case 4A

The characteristics of airflow vectors across the shorter dimension (width) of the ward space (axis C-D in Fig. 9.1a) are revealed in Fig. 9.28. The results support the impact of buoyant plume over patient's body and particularly the mixing which occurs in Case 3A (Fig. 9.28d). There is however a noticeable drift of the descending cooler air towards the wall behind patient's head where impact of a rising plume of warmer air is minimal.

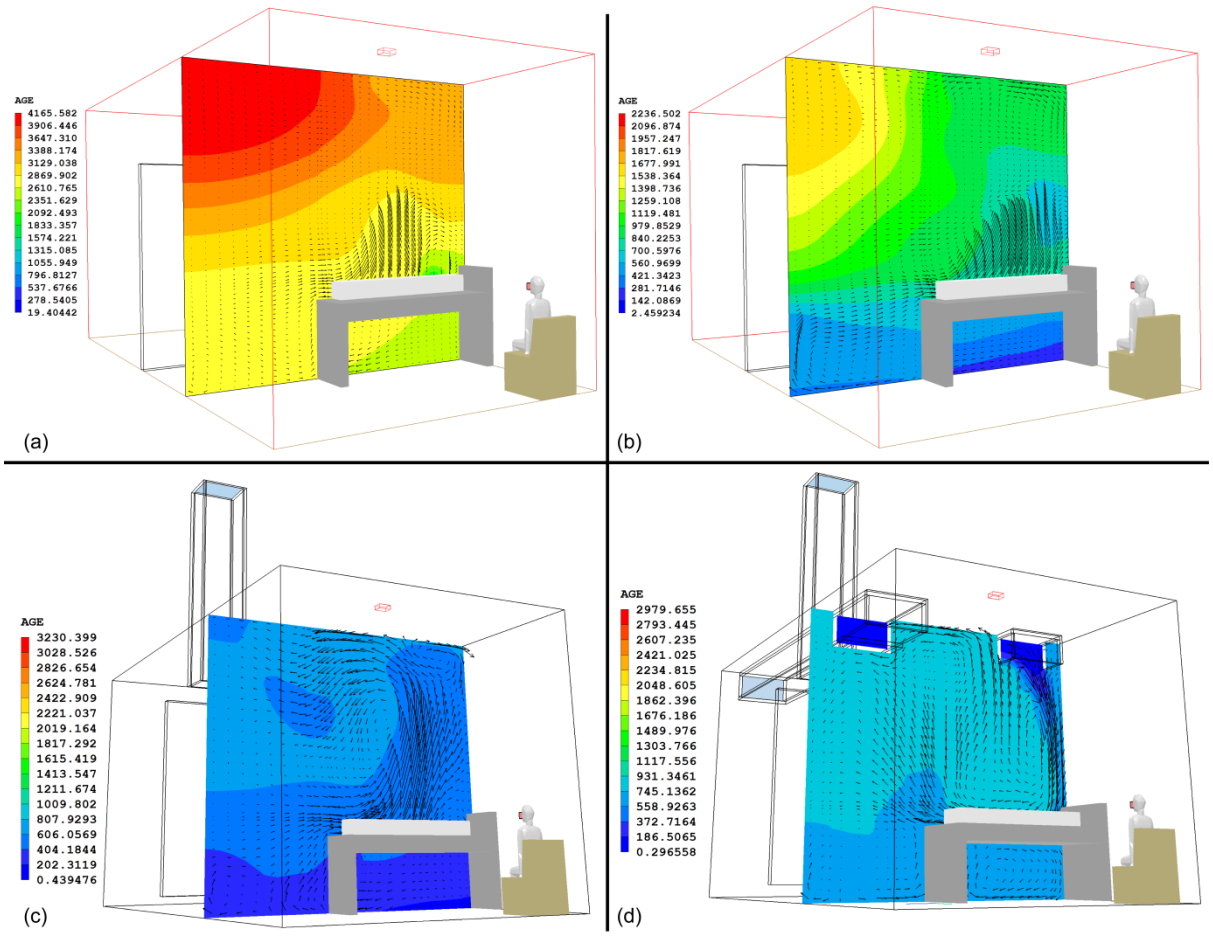

Figure 9:28: Airflow vectors over contours for Age of air across room width for (a) Base Case A (b) Case 1A (c) Case 2A and (d) Case 3A

The contaminant profile across the width is measured at height of 1.8m for each case is shown in Fig. 9.29. It is observed that at 1.0m distance from the bed's head (where the HCW is standing), there is significant drop in concentration for all cases. However, Fig. 9.29d showed that concentrations after this location will be much lower (even approaching zero) than in other cases. This is attributable to mixing and to the presence of the second duct which provides supplementary air into an area that would have otherwise been remote and cut off from direct path of fresh air as applicable to other cases.

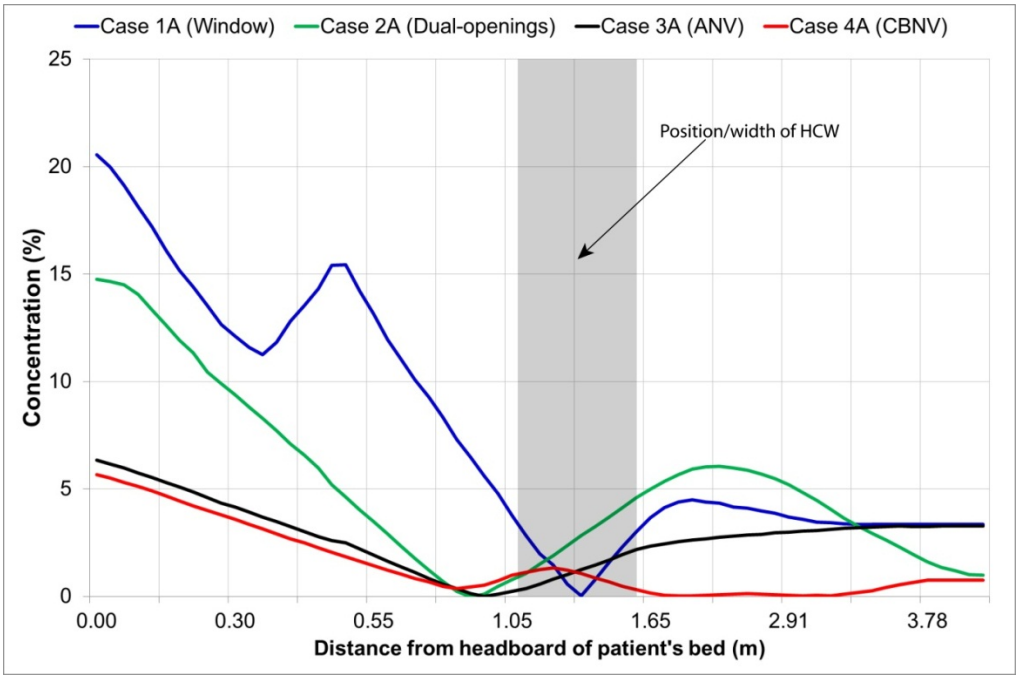

Figure 9:29: Contaminant profile across width of ward on x-axis from headboard (0) to opposite wall (3.78) for (a) Case 1A (b) Case 2A (c) Case 3A and (d) Case 4A.

Source: Overnight Sleeper

When the overnight sleeper becomes the source of airborne pathogens, the pattern of contaminant concentration in all four systems differ significantly (Fig. 9.30). The general behaviour of emitted contaminants is the migration towards the patient's bed; but each system offers different levels of mixing with indoor air. There is for example a build-up of concentration around the sleeping couch for the single opening (window) system (Fig. 9.30a), which is much less in the dual-opening (Fig. 9.30b). The ANV system (Fig. 9.30c) and the CBNV system (Fig. 9.30d) however are able to provide greater dilution in the entire space, minimising the build-up of concentration even around the couch where the emission occurred. The better dilution capacity of the CBNV relative to ANV is also evident.

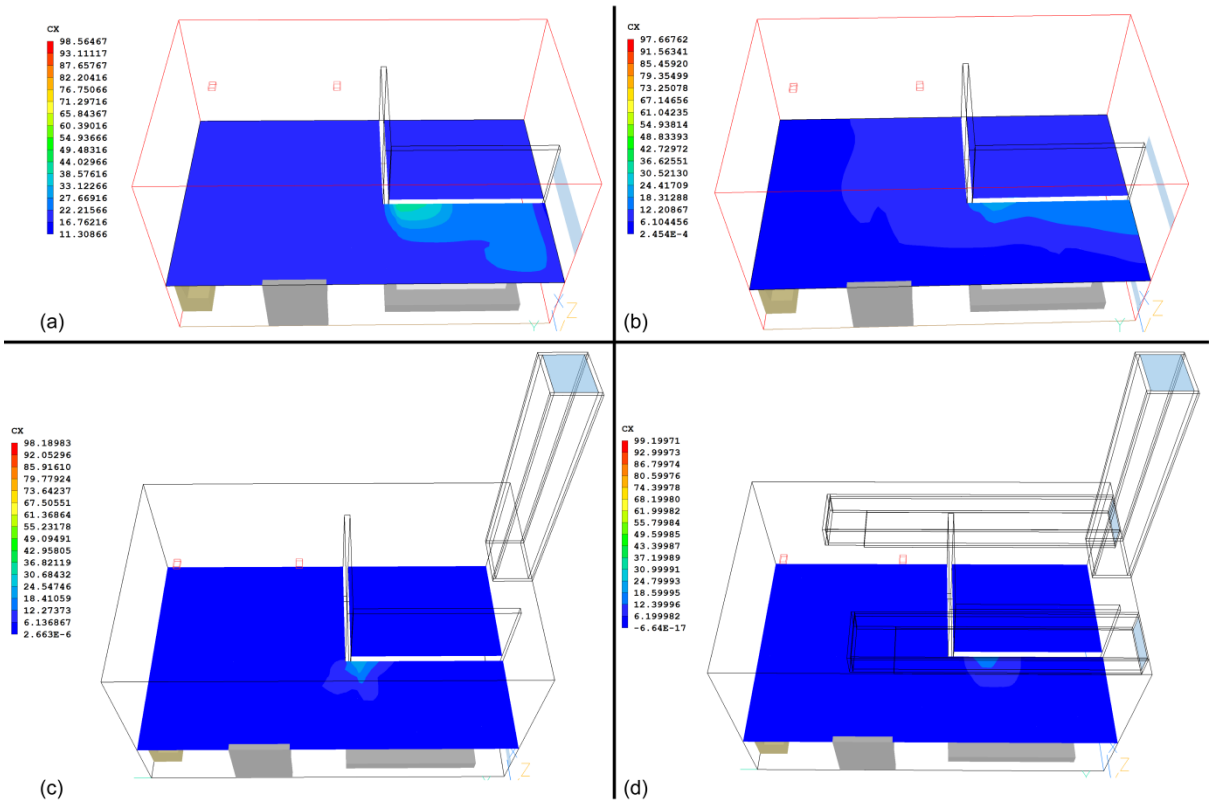

Figure 9:30: Concentration contours due to emission from overnight sleeper in (a) Case 1B (b) Case 2B (c) Case 3B (d) Case 4B

Across the length of the room from the external wall towards the bed (axis A-B in Fig. 9.1a), Fig 9.31 shows different characteristics from each ventilation system. In this scenario, only dual-opening and CBNV systems are able to significantly lower concentrations around the bed location.

The overall efficiency of each system in removing or diluting airborne pathogens is computed using contaminant removal efficiency (CRE) at the 12 identified POIs in Fig. 9.32. In the first scenario when the daytime visitor is the source, (Fig. 9.32a) the exceptionally better performance of dual-openings (Case 2A) is apparent with CRE values approaching 2.0 in many of the POIs except at some locations (points 4, 5 and 6). This is in agreement with the absolute concentrations previously recorded in Fig. 9.23. Conversely, with the overnight sleeper (Fig. 9.32b), it is the CBNV that produces the best overall efficiency. The single opening system in this scenario produces the poorest level of efficiency with minimum and maximum CRE values being 1.12 and 1.13, for the given POIs.

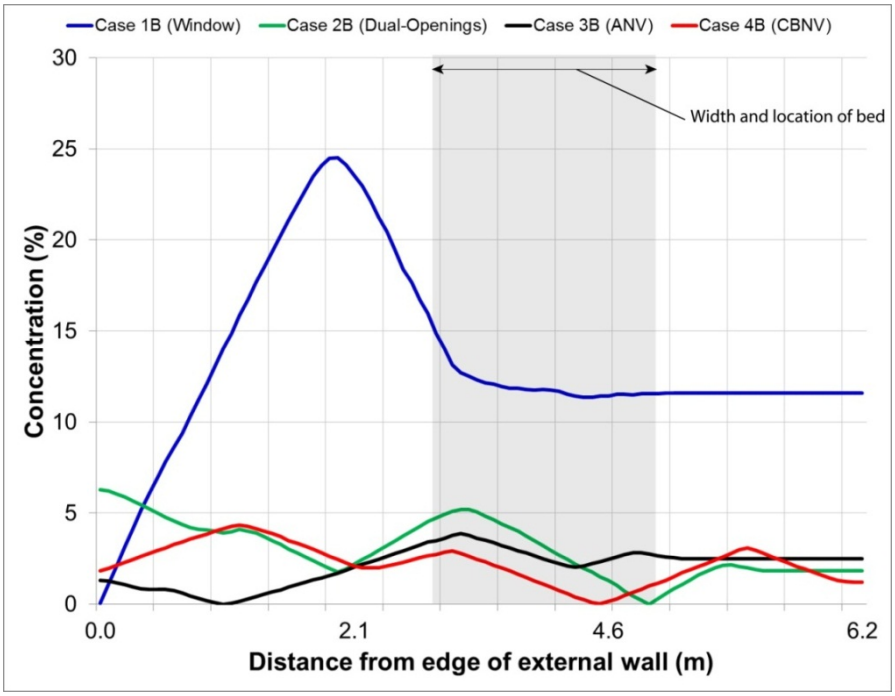

Figure 9:31: Concentration profile due to emission from overnight sleeper in (a) Case 1B (b) Case 2B (c) Case 3B (d) Case 4B. The dotted lines represent location of emission.

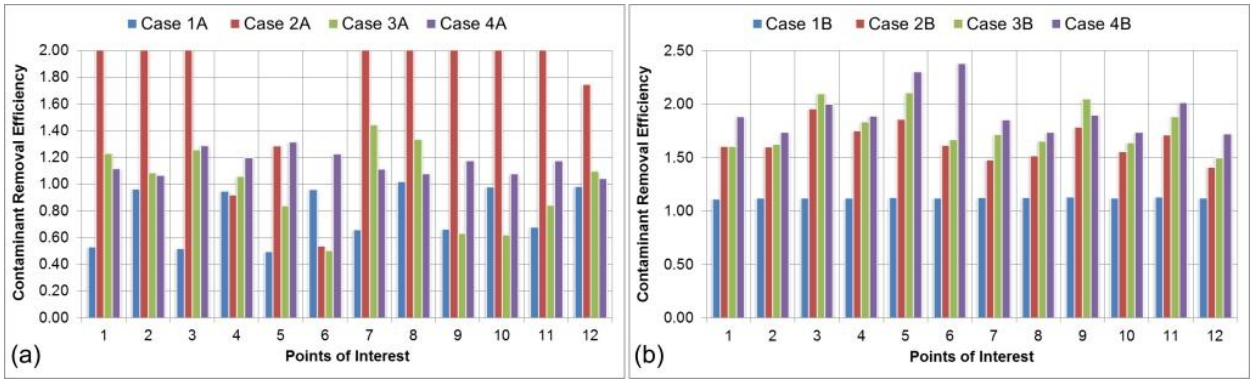

Figure 9:32: CRE values at the POIs based on two source locations for (a) daytime visitor (b) overnight sleeper

9.6 Summary

Four natural ventilation systems were investigated with respect to their capacity to deliver adequate airflow rates, provide acceptable thermal comfort and the energy required in heating the GOSH ward. This is in addition to their capacity to achieve acceptable control of indoor airborne contaminants.

An understanding of the relatively poor performance in terms of airflow rates, thermal comfort and control of airborne contaminant for the as-built window system is gained against the backdrop of three other systems. The use of single vent leads to less heating energy due to entrainment of warm stale air with cold fresh air, but this has obvious comfort and air quality ramifications. The relatively impressive performance of the dual-opening system is worthy of note as its significant airflow rates are able to dilute contaminants, but this is at a cost of higher heating energy in winter.

However, this system has obvious potentials in non-winter periods, and should be exploited. A detailed argument on the way forward for this and other system will be made under Chapter 11 (Discussions). Appropriate recommendations will be provided in Chapter 12, including suggestions for refurbishing existing wards especially regarding dual-openings. The dual-opening system will be limited to wards in low-rise buildings due to potential for cross-flow of contaminated air in multi-floor spaces as observed in Alloca et al. (2003). This shortcoming is eliminated by the use of exhaust stacks for removing stale air using stacks (as applied in Case 3) which is the ANV. The performance of the CBNV system is significant in the sense that it is able to deliver relatively modest airflow rates through mixing, which encourages thermal comfort, such as absence of distinct plume of warmer air over occupants. This system is also able to reduce contaminant concentrations at key locations (POIs).

CHAPTER 10: Study 5 – Experimental validation

10.1 Introduction

The NPV system introduced in Chapter 9, the findings of which have been published in Adamu et al. (2011b), has so far been studied using dynamic modelling and steady state computational fluid dynamics. Both methods are based on classic numerical models and are widely applied in research and industry (Chen, 2009; Li et al. 2011). While these techniques have independently shown that the NPV is feasible and beneficial, its validation through experiments becomes imperative for three main reasons. Firstly, it is traditional in CFD-based studies for experimental validation to be done either at the full building or scaled level. Second, due to the novelty involved in the NPV as a new system it is always helpful to corroborate the flow behaviour using an experimental method. Finally, although dynamic bulk airflow modelling does provide predictions of transient flow, use of an experimental 'real-time' modelling can only increase confidence in the performance of the proposed system. This is especially because the transient DTM predictions have the inherent weakness of assuming that each zone is well mixed, which as the CFD predictions have shown, cannot be totally relied upon for studying airflow in clinical spaces. This chapter describes the laboratory experiments performed on a scaled model of the standardised ADB single-bed ward fitted with the NPV components. The purpose of the series of experiments was primarily to obtain data and information regarding the transient nature of airflow in this system.

10.2 Experimental procedure

The materials and experimental setup have already been described under the research methodology (Chapter 5). The mathematical equations which describe the salt bath model, the actual procedure followed and the observed behaviour of fluid flow are described in the next sub-sections.

The buoyancy of brine plume B_m, is calculated using Eqn. (10.1):

$$B_m = F_{o,m} g'_m = F_{o,m} g \frac{\Delta \rho_m}{\rho_m} \qquad (10.1)$$

Where: B_m is the buoyancy of brine plume; $F_{o,m}$ is the flow rate of brine in model; g'_m is reduced gravity for model; and ρ_m is density at model scale.

To calculate the approximate interface height to be observed within the scaled model, the following relationship is used.

$$\frac{A_m^*}{H_m^2} = C_{mt}{}^{\frac{3}{2}} \sqrt{\frac{\left(\frac{h_m}{H_m}\right)^2}{1-\left(\frac{h_m}{H_m}\right)}} \qquad (10.2)$$

where A_m is the effective area of opening; H_m is the height between inlet and outlet, C_{mt} is Morton's constant (Morton, et al. 1956) and can be assumed to be 0.158.
The buoyancy of the plume can then be calculated through Eqn. (10.3).

$$B = \sqrt{\frac{\left(g'_f C_m\right)^3}{h_f^{-5}}} \qquad (10.3)$$

Where the thermal expansion coefficient (α) and the specific heat capacity (*C)* of water are given, Eqn. (10.3) can be rewritten as follows:

$$B = \frac{W\, g\alpha}{\rho_f C} \qquad (10.4)$$

The actual size of the ward was scaled to 1:20 and then fabricated using Plexiglas (Fig. 10.1).

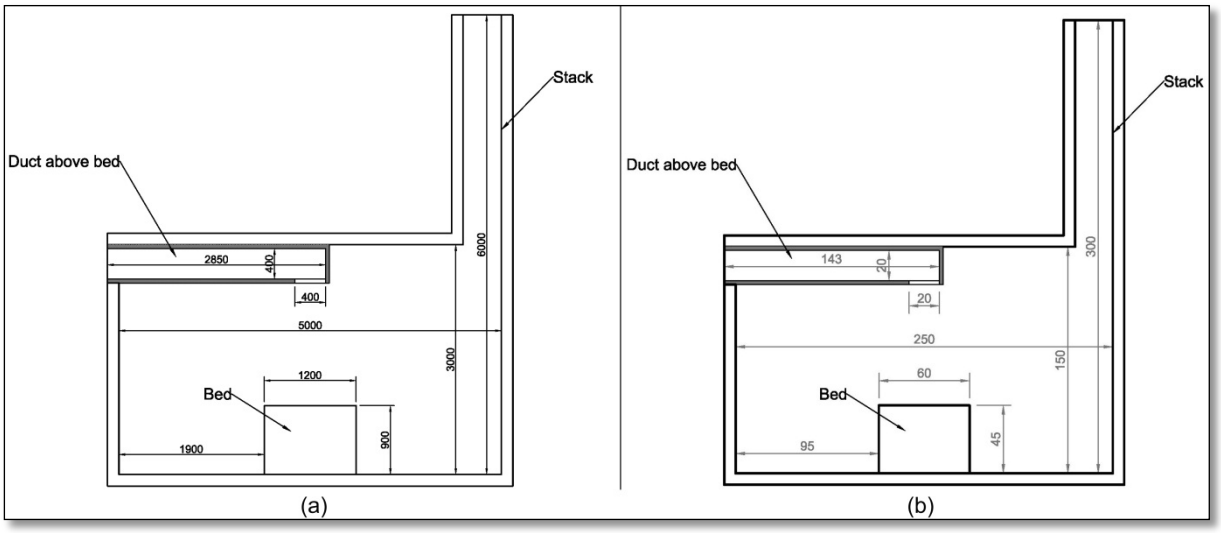

Figure 10:1: Dimensions of (a) ward at scale 1:1 and (b) the Plexiglas model at scale 1:20

A brine solution (water + salt) was prepared according to a calculated density which equates it to a heat source of 50W. Blue coloured food dye was then added to give the brine

pigmentation necessary for visualisation. The brine was stored in a large plastic container on the floor from where it was pumped into a header tank which had a built-in overflow pipe to ensure a constant head. This fed into an analogue flow meter that allowed for control of brine flow as it pours into the nozzles in the submerged Plexiglas model.

Water and salt were mixed together to form the required density as calculated above. The brine was pumped into a header tank which had an overflow pipe to ensure a constant head. This fed into an analogue flow meter which allowed for control of the flow before going into the Perspex model. The Perspex model was suspended several inches below the surface of the water within the tank, with brine building up at the bottom of the tank. The brine was calibrated to flow at a rate of 210 cm^3/min. Up to five different runs of the experiment were executed in order to measure density of brine at the stack and to capture still and video footage from different angles. The location of heat source (nozzle) was changed in two runs to evaluate any differences in flow behaviour. In particular, the heat source at the bed was used as an instance for comparing with the equivalent CFD model.

10.3 Observed flow behaviour

The flow characteristics of the brine were recorded using a digital camera in phases (Fig. 10.2). Brine leaving the nozzle was turbulent such that the plume began entraining straight away. It usually took approximately three seconds for the brine to be visible at the ceiling of the model (Fig. 10.2a) from the moment it exits the nozzle. Upon reaching the ceiling, the brine steadily increased in thickness (Fig. 10.2b) and was observed to spread out horizontally until it completely covers the entire ceiling, descending gradually towards the floor (Fig. 10.2c). After approximately 2 minutes and 20 seconds, the horizontal layer of brine stopped descending, creating the steady interface height (Fig. 10.2d) which was measured as being 13cm from the bottom of the model (i.e. from the floor of the ward). This height would be equivalent to 2.6m in the real model (Fig. 10.1) which has a height of 3.0m.

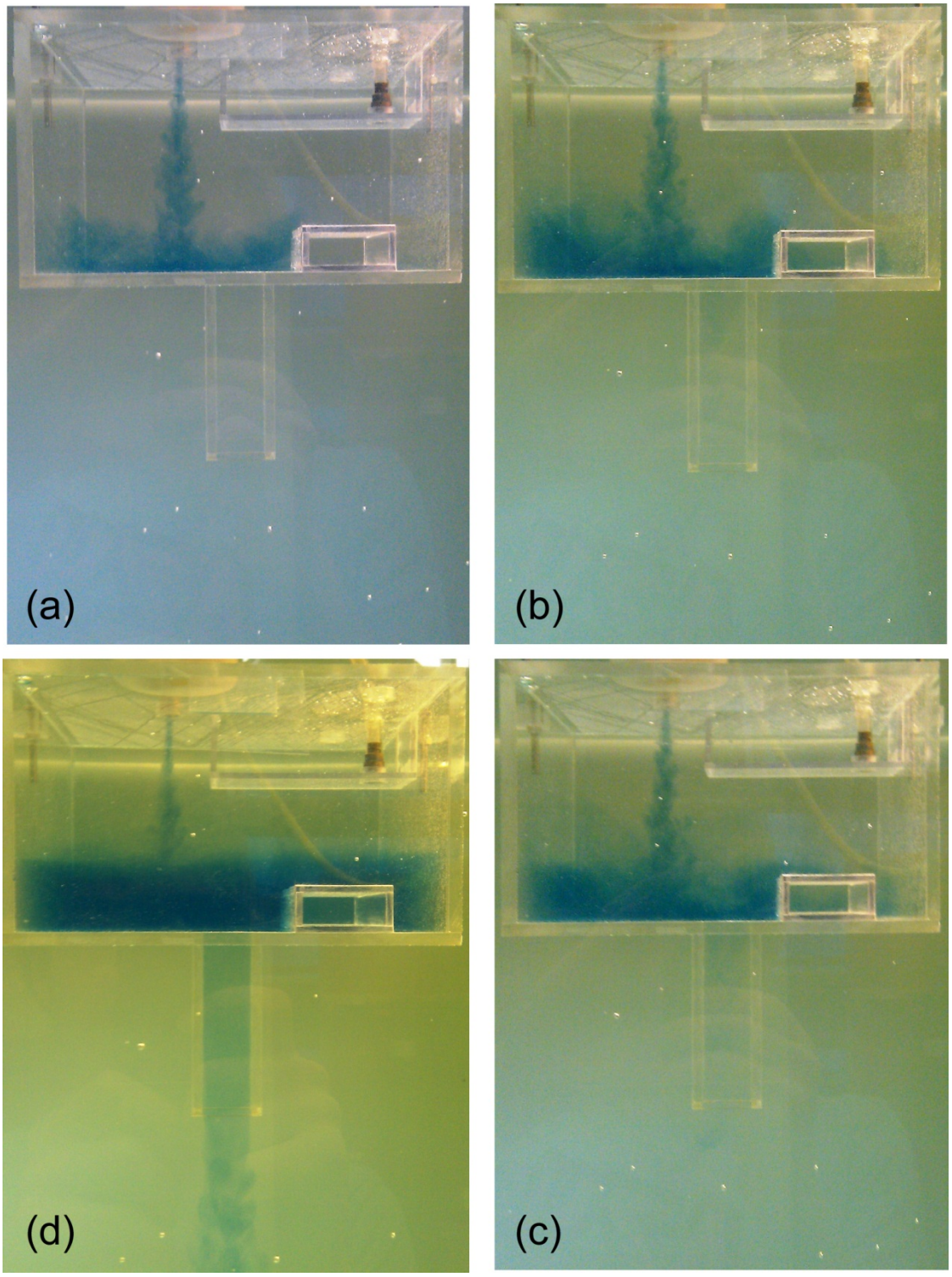

Figure 10:2: Four pre-steady state phases of plume development shown in clockwise direction from (a) initialisation to (d) attainment of maximum interface height. All views looking through the NPV duct which remains free of brine.

Steady state was achieved after the 2.5 minutes period, during which some brine begins to mix with the lower layer of the interface (Fig. 10.3). This is evidence of the mixing characteristics of the NPV system observed previously in Chapter 8. From this stage onwards,

the interface layer remains clearly distinguished, even though the lower portion continues to maintain a lighter shade of the brine solution. The occupied zone is evidently receiving some of the heat (brine) from the upper strata of the interface but the primary difference created by the interface layers remained visible throughout the transient flow period.

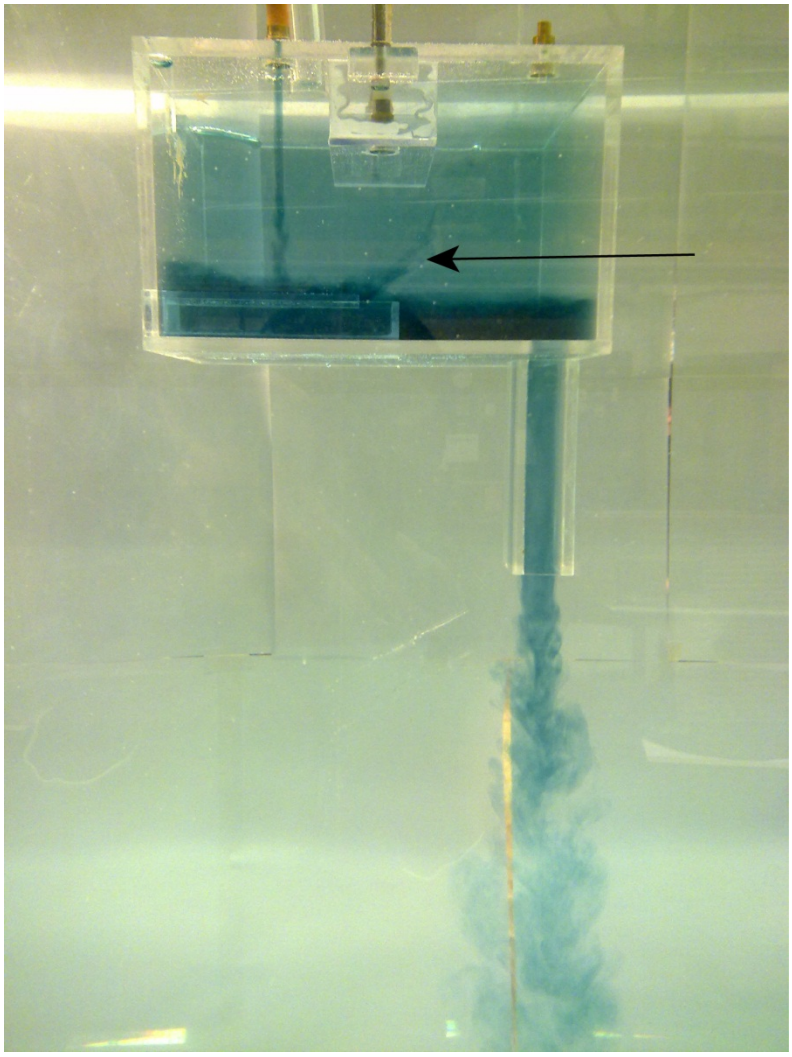

Figure 10:3: The scaled model at steady state (arrow indicates flow of fresh air from the duct)

The horizontal throw of incoming fresh air is also observed in the scaled model at the inverted (up-side down) orientation as depicted by the arrows in Fig. 10.3 and Fig. 10.4. At steady state, the density of brine was measured by collecting several samples using a pipette. The densities were measured at the stack using a pipette from three samples and found to be 1.008 g/cm^3, 1.004 g/cm^3 and 1.006 g/cm^3, giving a mean density of 1.006 g/cm^3. This density will be compared with the effectiveness of heat removal (EHR) obtained from CFD predictions.

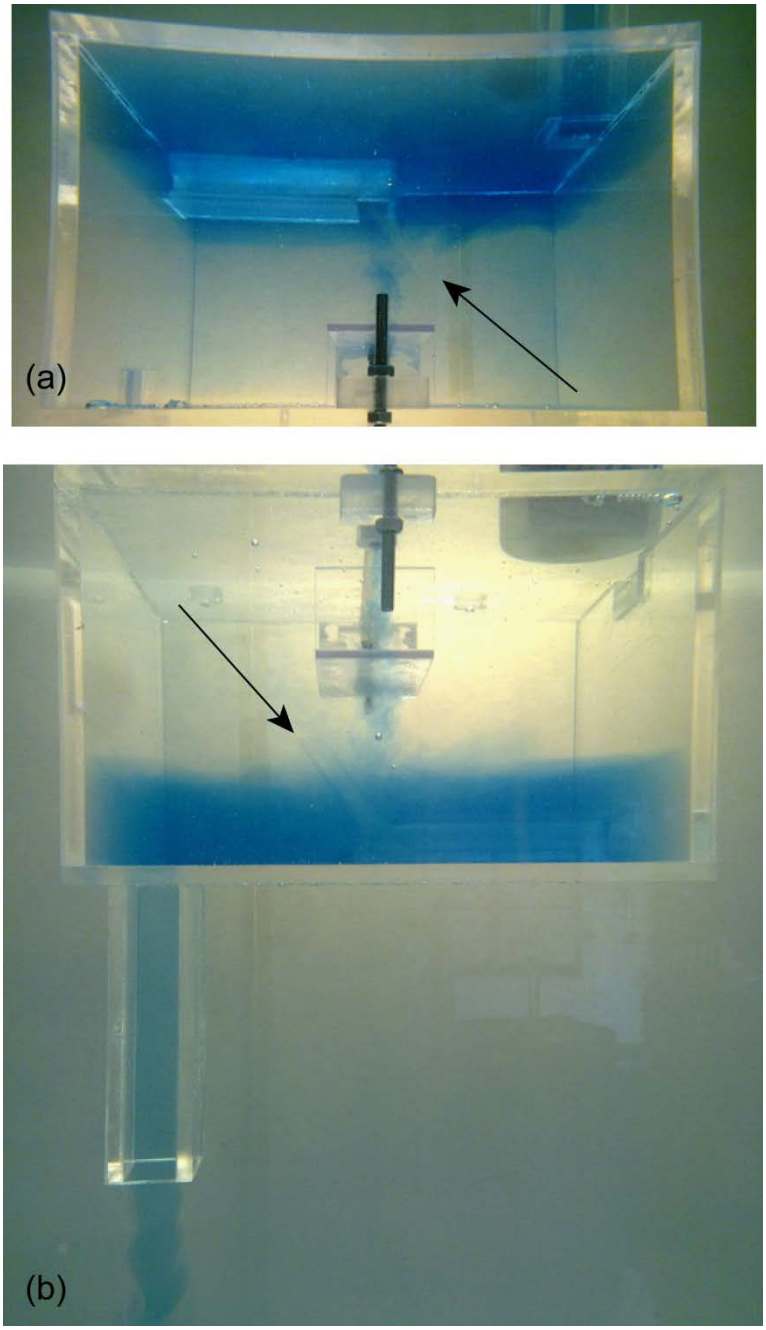

Figure 10:4: Horizontal throw of ambient water into the model shown from (a) inverted model (b) actual orientation of model in the water tank

10.4 Comparison with CFD predictions

10.4.1 Interface height and formation of local eddies

The interface height at steady state in the salt-bath model was measured and found to be 13cm (i.e. equal to 2.6m in full scale) measured from the floor. This was compared with the interface height of the CFD model by simple graphic overlay (Fig. 10.5). The correlation was found to be reasonable.

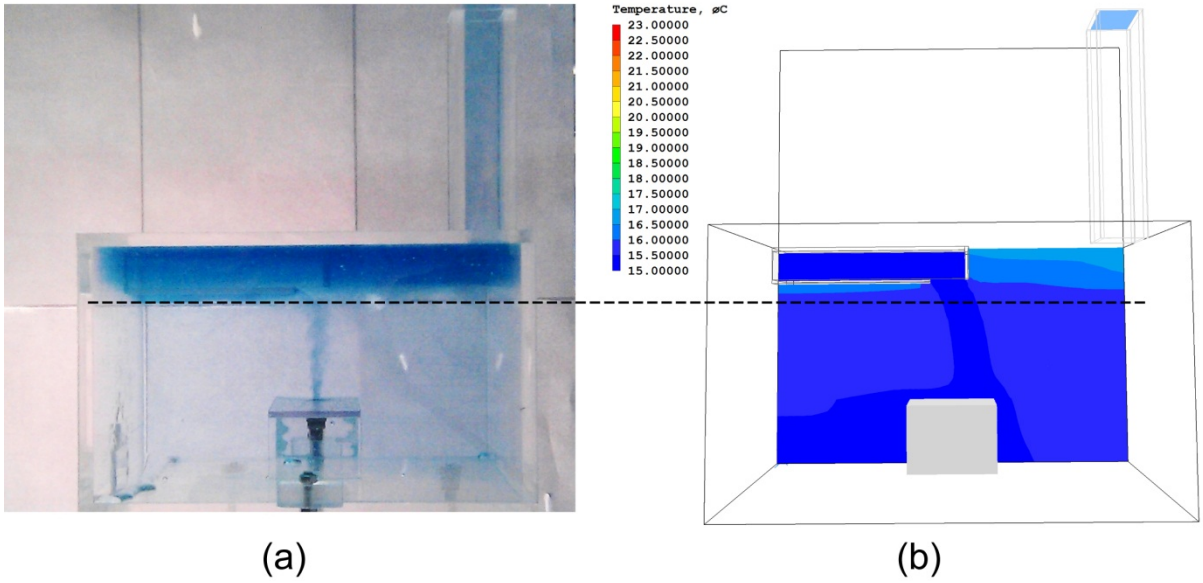

Figure 10:5: The interface layer in (a) Salt-bath model and (b) CFD equivalent

Another similarity observed in both salt-bath and CFD models was the entrapment of fluid at the bottom of the duct (Fig. 10.6). Although this was an unexpected finding, it serves to confirm the relative accuracy in flow predictions in both models.

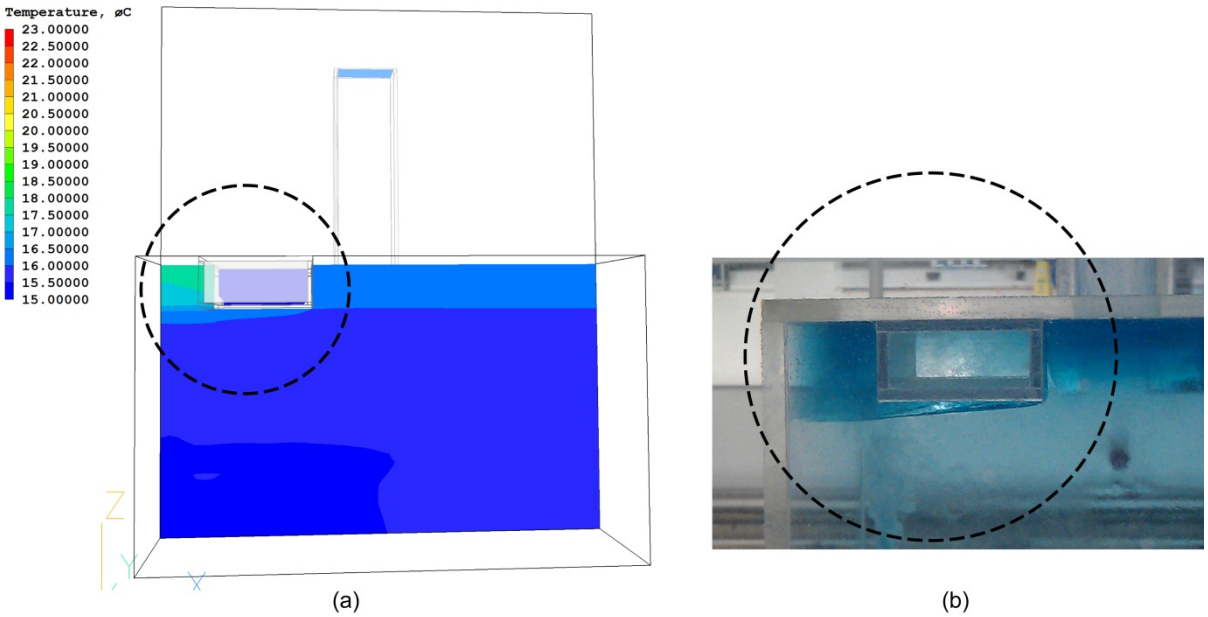

Figure 10:6: Formation of eddies around duct in (a) CFD and (b) Salt-bath model

10.4.2 Density of brine and effectiveness of heat removal

The density of brine at exhaust stack and at source point in the scaled model can be compared with the temperature at similar points in the CFD. The ratio of temperature at the exhaust point to the ratio at source point is analogous to the effectiveness of heat removal (EHR). The mean density at the exhaust stack (1.006 g/cm^3) to the source density (1.158 g/cm^3) was computed as 0.87 (87%). The equivalent of brine density in the CFD model is temperature which was measured at the stack and found to be 16.9^{o}C whereas at the source, the temperature was calculated to be 18.6^{o}C, giving a ratio of 0.91 (91%). The EHR in the salt-bath is therefore found to be ≈ 4.4% lower than in the CFD model, but this difference can be regarded as marginal.

10.5 Summary

The salt-bath experiment was aimed at two sub-objectives. Firstly, it allowed for the visualisation of transient flow of fluid in the scaled model and secondly, it was an opportunity to validate the performance of the NPV system as a whole. The 1:20 scaled model was fabricated using Plexiglas which was then immersed in a large water tank. Brine solution was introduced using nozzles that represented a human heat source. The observed flow of fluid in the scaled model was captured using a digital camera at regular intervals and the concentrations of brine at the source and at the point of exhaust were measured and computed

against equivalent CFD temperatures. These were found to be closely matched with an approximate difference of 4.4%.

There was also similarity in the interface height for both models as well as in the formation of eddy flows beneath the duct. These results support the feasibility of the NPV as a feasible system of providing patients with improved proximity to fresh air. Although airborne contaminant dispersal was not included in this experimental work, the dedicated study (Chapter 9) using CFD indicated that the NPV system can provide benefits to hospital wards. These benefits are primarily through the provision of cleaner air around the patient's bed, in the overall dilution of room air through via mixing and in the relatively low heating energy required in winter.

CHAPTER 11: Discussion of results

11.1 Introduction

DTM and steady state CFD modelling are fundamentally different in the nature of their predictions. Given the same ward space or geometry, DTM predictions are focused on time, meaning results obtained are one dimensional and quantitative only. For example, temperature or PMV predictions are typically shown as graphs where the values and their variation are time dependent. This is not a wholly accurate approach, but is an inherent feature (and weakness) of empirical models which use the well-mixed zone assumption. On the other hand, steady state CFD predictions as used in this study provide two and three-dimensional results which indicate the variation in the values of variables (e.g. temperature contours) to represent spatial distribution. Steady state CFD predictions are however valid only for a specified period and boundary conditions, and the use of passive scalar contaminants as surrogate for airborne pathogens which are less than 1μm is not without its criticisms and shortcomings.

In addition, while it is common practice in winter for fresh air to be preheated, this aspect was implicitly considered by the heating setpoints in the DTM aspect of the studies (and this may be interpreted as either space or air heating) but preheating was not considered in the CFD aspect. In fact, no winter modelling was carried out using CFD. Finally, although studies have shown the effect of urban heat islands (UHI) and its effect on thermal comfort of naturally ventilated indoor spaces in in cities like London (Oikonomou, et al 2012; Demanuele, et al. 2012 and Kolokotroni et al. 2006), this aspect has been ignored for the purpose of this research. All these limitations require, therefore that the results for both DTM and steady-state CFD to be considered carefully and in their right context.

Existing guidelines, standards and relevant findings from contemporary literature serve as the basis for cross-referencing and discussing the findings from this study, however, as most of these documents focus on the quantitative features of ventilation (i.e. absolute or relative flow rates), the lack of qualitative guidance presents a knowledge gap in itself. A ventilation system should simultaneously aim for efficient (quantitative) and effective (qualitative) performance. In terms of efficiency of natural ventilation of hospital wards, the rates of 6 ACH (DH, 2007a) and 60 l/s/patient (Atkinson, et al, 2009) are formalised guidelines backed

by health-related institutions, while 8 ACH (Qian, et al. 2006) and the 'safe dilution' rate of 83 l/s (Jiang, et al. 2009) are from general literature. The performance of selected natural ventilation systems was therefore evaluated using DTM predictions against these figures.

There are other quantitative metrics such as LACI, MACE, EHR, CRE and ATT which can only be obtained from CFD. Unfortunately, there are no known precedents of the application of these metrics within contemporary literature for natural ventilation of hospital wards, making it difficult to put the predicted results in their proper perspective. The only metric that has some element of healthcare-related application is CRE which was applied by Nielsen et al (2007b) as personal exposure index (PEI) but this was not actually a hospital ward study. Pentelic, et al. (2009), on the other hand, investigated the performance of personalised ventilation and used the distance from source of emission to the flow region of the PV system in addition to the probability of infection to from tuberculosis and influenza A virus. However, there research was not in a hospital environment and the PV system used was mechanical.

In addition, the qualitative aspects of an effective ventilation system which deal with room air distribution, is not easily 'measured' due to the nature of the vectors involved. The closest qualitative indication of desirable airflow pattern and direction for hospitals is found in CDC (2005) where the mechanical ventilation of a negative pressure airborne infection isolation room (AIIR) is described. In other words, there are no known studies of (buoyancy-driven) natural ventilation of hospital wards in which performance was evaluated using pattern and direction of airflow.

11.2 Performance of same side systems

The performance of single openings (whether louvered or windows) as investigated in this research demonstrates (through DTM) the potential for overheating to occur in the entire space and (through CFD) at localised points. This problem is less pronounced with dual openings. However, while single openings are fully under the influence of wind forces, regardless of velocity, dual opening systems are sensitive to wind speeds as velocities below 6 – 7 m/s have minimal effect on airflow rates. At such low speeds, dual openings are more

sensitive to internal heat loads or buoyancy effect. This is in agreement with findings from previous research (Allocca, et al. 2003; Chen 2004).

11.2.1 Single openings

Single openings tend to have lower air changes relative to dual openings and other natural ventilation systems. Incoming air mixes with stale outgoing air and this inevitably leads to pollution of fresh air by re-circulated air, which may contain airborne contaminants. The airflow performance of this system is very sensitive to by heating setpoints. The following discussions focus on the performance of single openings at 20^{o}C and at 24^{o}C heating setpoints.

In winter (with 20^{o}C heating setpoint), the mean monthly flow rate (January) using the 6.25% opening fraction leads to 6.3 l/s in the ADB ward and 8.3 l/s for the GOSH ward. By doubling this fraction to 12.5%, the ADB and GOSH ventilation rates are 12.3 l/s and 16.4 l/s respectively. Using a 25% opening fractions leads to 24.4 l/s for the ADB ward and 31.5 l/s for the GOSH ward. The predicted heating energy at 6.25% is negligible.

The 12.5% fraction (applied to both GOSH and ADB wards) at 20^{o}C heating setpoint is able to deliver 10 l/s required to meet odour dilution requirements of HTM 03-01 (DH, 2007a). Although the total annual energy required for heating the spaces even at this fraction is only 1% of the CIBSE benchmark for GOSH ward, the ADB ward consumes nearly double or 1.7% of the equivalent benchmark. The heating energy predicted to be consumed at 25% fraction is 9.2% of the benchmark for GOSH ward and 14% for ADB ward. In other words, doubling the area of single openings has a proportionate effect on both airflow rate and heating energy.

The scenario with heating setpoint of 24^{o}C is rather peculiar. At the smallest opening, the mean airflow rates are very similar to the rates at 20^{o}C with very marginal differences even in the absolute minimum and maximum values. The differences become more pronounced as the size of openings increase progressively from 6.25% to 25%. Consequently, the annual heating energy for this heating setpoint is as follows: at 6.25% fraction it is 0.2% of the benchmark for GOSH ward and 0.6% of the benchmark for ADB ward. Increasing the openings to 12.5% means GOSH will consume 3.2% while ADB ward will consume 5.6% of the benchmark. Finally, at 25% opening, the GOSH ward will consume 24% of the benchmark compared to 31% for the ADB ward.

In summer, the mean July airflow rates with 50%, 75% and 100% fractions for GOSH ward are 55.8 l/s, 82 l/s and 108 l/s, while for the ADB ward, they are: 44.8 l/s; 67 l/s and 89.5 l/s. Therefore unlike in winter, the difference is area of vents has more influence during summer in the air exchange process between outdoors and indoors.

The mean January PMV for single openings at 6.25% fraction is +1.81 (above warm) for GOSH ward and +0.74 (above slightly warm) for the ADB ward with corresponding DRT of 30.92^{o}C and 24.96^{o}C respectively. The projected number of dissatisfied occupants would be higher in the GOSH ward (63%) compared to only 25% for ADB ward. These differences in thermal comfort conditions are for heating setpoint of 20^{o}C and are correlated with the predicted airflow rates and room volume. At the largest (25%) winter opening fraction, mean DRT in the ward spaces will reduce to 21.83^{o}C and 20.27^{o}C for GOSH and ADB wards respectively, using a heating setpoint of 20^{o}C. Increasing the setpoint to 24^{o}C leads to mean DRT values of 24.83^{o}C (GOSH) and 24.19^{o}C (ADB) but in the case of the GOSH the maximum DRT will approach 29.75^{o}C, compared to just 24.79^{o}C for the ADB.

Table 11.1: SWOT analysis of the single opening system

Strength	**Weakness**
• Utilises less heating energy than other systems for the same opening fraction • Simple to construct/implement • Can deliver sufficient rates (i.e.10 l/s) for dilution (based on HTM 03-01) at 12.5% opening fraction. • Can meet thermal comfort needs at 25% opening fraction	• Thermal comfort in winter may not be desirable at 6.25% in the GOSH ward. • Recirculates stale and contaminated air • Falls short of 60 l/s/patient or 6 ACH • When used as windows, also has to provide daylight and vista to outdoors • Requires pre-heating of supply air in winter
Opportunities	**Threats**
• Automation of this system may lead to better indoor environmental quality. • Can be re-modelled to work with a second inlet at a lower or higher level, depending on design and practical circumstances.	• Hazard of cross infection of co-occupants by airborne pathogens.

11.2.2 Dual openings

In winter, the air change rates achievable with dual openings at 25% opening fraction varies with the heating setpoint. With a setpoint of 20^{o}C the mean January flow rate is 152 l/s and 132 l/s for the GOSH and ADB wards respectively. At 24^{o}C setpoint however, the flow rate increases to 169 l/s and 146 l/s for GOSH ward and ADB ward respectively. Like with single openings, as the openings become smaller approaching 6.25% the differences between airflow rates under 20^{o}C and 24^{o}C become less noticeable. The predicted heating energy compared with the CIBSE benchmark indicates that at the largest fraction (25%) operating a 20^{o}C heating setpoint will lead to the GOSH ward consuming 172% of the allocated energy target while at 24^{o}C, this will be by 325%. Clearly, operating 25% opening fraction in winter is not an attractive proposition. On the contrary, halving this opening fraction to 12.5% will lead to consumption of just 56% of the benchmark (GOSH) or 67% (ADB) – with a 20^{o}C heating setpoint, that is. If the setpoint were increased to 24^{o}C, a 12.5% opening fraction will consume 121% of the benchmark for GOSH ward or 130% for the ADB ward. Given that the achievable airflow rates at 20^{o}C for 12.5% fraction of opening (i.e. 76.5 l/s for GOSH ward and 66 l/s for ADB ward), there is a strong case for adopting 12.5% opening fraction for winter ventilation using dual openings. This is because these airflow rates are above the WHO recommended standards for naturally ventilated wards even if they fall short of 6 ACH as recommended by HTM 03-01. In summer, it was also predicted that dual openings at 50%, 75% and 100% will respectively, deliver up to 164.9 l/s, 232 l/s and 299 l/s (for GOSH ward) or 125.5 l/s, 182 l/s and 239 l/s (for ADB ward).

For thermal comfort using the smallest opening fraction (6.25%), the mean January PMV and DRT values with dual openings were predicted be +0.08 (20.8^{o}C) for GOSH and -0.21 (20.2^{o}C) for ADB which (for PMV) are within the 'neutral' scale of comfort, although peak values are in the order of +0.89 (25.83^{o}C) for GOSH and +0.09 (20.65^{o}C) for ADB. When area of openings are doubled to 12.5% the PMV and DRT predicted are +0.81 (25.56^{o}C) and +0.14 (21.91^{o}C) for GOSH and ADB wards respectively. At the higher setpoint of 24^{o}C, the tendency for overheating was apparent even with dual openings. Mean DRT for GOSH and ADB wards are 25.23^{o}C and 25.25^{o}C.

In the dual opening SNV system, a low level inlet can lead to sensation of draught due to the speed at which the incoming air floods the floor. Raising the inlet by up to 1.0m was shown to increase the time (Age of air) taken for the air to reach its desired location, during which its temperature would rise. This would be a useful strategy in winter, when low temperatures and air velocity could aggravate the sensation of draught, but this technique has some associated problems.

Firstly, deliberate ageing of air defeats the essential need to get the air as quickly and as possible to the patient. Secondly, the longer the incoming air takes (Age) to get to the patient, the more likely it is to be contaminated. As shown by recent findings (Li, et al. 2011, Beggs, et al. 2008 and Qian, et al. 2006), displacement systems have limitations in controlling airborne pathogens within clinical spaces because the emitted contaminants remain trapped in the occupied zone. Therefore, any time delay in the displacement of fresh air from inlet to occupant locations will likely increase the chance of pre-contamination of the supply air.

The pattern and direction of airflow using dual opening is restricted by the single side external facade wall upon which the openings are located, however, the CFD predictions indicate that when the vertical distance between inlets and outlets are maximised in both ADB and GOSH wards, the concentration of contaminants at the outlets of these wards are 8.75% and 13.12% respectively. This indicates that relatively better dilution has occurred compared with the single opening when concentrations at outlets were 25.7% and 28.5% for the ADB and the GOSH ward respectively.

These results demonstrate the significant potential of the dual opening system, which is relatively better than having a single opening. As such, although the WHO does not recommend use of any single side ventilation systems (single or dual), cross ventilation using opposite walls and courtyards (Atkinson, et al. 2009) will not be practical in modern hospitals of developed countries. This is evident from layouts of modern hospitals which use deep plans (Short and Al-Maiyah, 2009) and rely on single (window) openings for natural ventilation of perimeter spaces. Nevertheless, these results strongly imply that at least for existing facilities, conversion of the SNV systems to dual openings will bring improved rates of ventilation and acceptable thermal comfort. When 6.25% opening fractions are used in winter, the mean flow rates are above 30 l/s and the energy needed to heat the spaces will be significantly less than CIBSE’s threshold values.

The height between inlet and outlet of dual opening has been known to be critical in determining airflow rate. This study has demonstrated that the closer the inlet is to the outlet, the greater the likelihood of stale outgoing air being entrained into fresh incoming air, thereby reducing the quality of indoor air.

Table 11.2: SWOT analysis of the dual opening system

Strength	**Weakness**
• Can provide airflow rates in excess of 60 l/s/patient • Can be retrofitted unto existing perimeter wards • Does not have to provide daylighting or vista to outdoors	• Will require proper simultaneous control of inlets and outlets work • Winter heating can be significant if trickle ventilation opening size is not controlled • Requires pre-heating of supply air in winter • Cannot recover heat lost through raised outlets
Opportunities	**Threats**
• Retrofit can occur on ward by ward basis	• Malfunctioning of one opening eliminates the benefits of entire system • Draughts and discomfort in extreme outdoor temperatures

11.2.3 Control strategies for SNV systems

Based on the predicted performances of SNV systems, an important consideration for future application should be the control strategy used in their operation. Three obvious options are: fully manual control, completely automated control or an automated control system with manual overrides. As implied by the prediction of their airflow and contaminant dilution performances, various opening fractions will be suitable for different scenarios such as the required ventilation rate or the heating energy from specific heating setpoints (e.g. 20^{o}C vs. 24^{o}C). For single orifice SNV systems, automation of their operation will bring advantages through instant reaction to indoor parameters, e.g. from sensors of CO_2, whose concentration acts as a surrogate for passive airborne contaminants and/or as an indicator of dilution levels.

Dual openings SNV systems (by definition and by function) must be used in tandem; otherwise the system will most likely not function as desired. Meaning for example, if manual operation is selected for dual opening SNV systems, the opening mechanism for both

inlet and outlet should be linked and not independent. Simultaneous control of such openings via automation will bring benefits for airflow rates of airborne pollutants like CO_2 which as describe earlier, can serve as a substitute for pathogenic passive airborne contaminants.

For both single and dual opening SNV systems occupant behaviour must be considered in the design and operation of such systems. An advantage of natural ventilation is the ability of occupants to interact with the airflow needs. However, in a clinical setting where airborne contaminants are of concern or where strict control of heating energy is desirable, it is doubtful whether occupants in such settings should be given full control of the natural ventilation system. As no guideline currently exists for restriction of opening fractions based on energy and contaminant control, this presents an interesting opportunity for future work, as implied by recent findings by (Gilkeson, et al. 2013) who investigated the relationship between window openings, heating energy and risk of airborne contaminants in Nightingale wards.

This position is strengthened by emerging research (Gilkeson, et al. 2013) which provides evidence that in a nightingale ward, closing of windows to reduce heating energy leads to quadrupling of the risks of airborne infection. Hence, getting the right balance between airflow/dilution requirements and heating energy consequences will be important for SNV systems.

11.3 Performance of inlet and stack systems

As noted in Lomas and Ji (2009), the inlet and stack natural ventilation system (as applied in their study of ANV in a single-bed ward) can be retrofitted unto the facades of existing facilities. This further emphasised the need to understand the implications of flow components specifically heights of inlets as well as stack locations. Clearly, some strategies like edge-in centre out may be impractical for retrofit because of challenges of inserting a stack in the interior space of a hospital ward.

In assessing the potential winter performance of the ADB ward using basic inlet and stack system, two extremes of opening sizes and heating setpoint are used. At the minimum end of the extreme, a 6% opening fraction is used with 18^{o}C heating setpoint while at the other end, a 25% opening fraction is used with 20^{o}C heating setpoint. In between these sizes and heating

setpoints lies 12.5% opening fraction at both 18°C and 20°C heating setpoints. The DTM predictions of flow into the ADB inlet and stack system suggested that for the month of January, up to 18.2 l/s mean flow will be achieved using a floor based inlet, (Case 1) whereas raising the inlet by 2.0m (Case 2) leads to a mean monthly flow of 15.1 l/s, in both cases, opening sizes are at 6% of the designed area and heating setpoint is at 18°C. This was the smallest opening fraction and lowest heating setpoint used in evaluating the ADB ward and based on HTM 03-01 requirements of 10 l/s, (and 18-28°C temperature range) this flow rate is deemed acceptable for dilution of odours (DH, 2007a). The maximum opening size and heating setpoint used for the winter month of January is 25% at 20°C heating setpoint during which Case 1 would provide a mean monthly flow rate of 80.8 l/s while for Case 2, the mean flow rate reduces to 65.6 l/s.

If it is assumed that either of the two extremes (opening size and heating setpoint) would be adopted whenever heating is required at any time of the year, the annual energy consumed for Case 1 and Case 2 would be 0.55 MWh and 0.31 MWh at the minimum end of the extreme for Case 1 and 2 respectively. This is below adjusted CIBSE (2008) benchmark for hospital wards 4.62 MWh for fossil fuel sources. At the maximum end of the extreme, the annual heating energy would be 8.63 MWh and 6.63 MWh for Case 1 and 2 respectively. This consumption exceeds CIBSE's adjusted benchmark by 187% and by 144% respectively. So whereas the maximum winter opening size assumed for the inlet and stack system for the ADB ward will meet the WHO (Atkinson, et al. 2009) requirement of 60 l/s/patient, this will come at a significant energy cost. This further emphasises the shortcoming of the WHO guidelines which have not indicated the ventilation rates suitable for winter period and/or the heating energy that may accompany natural ventilation in temperate climates.

Dynamic modelling predicted that raising the inlets above the floor by up to 2m would reduce the annual heating energy required (by 33% at 18°C or by 43% at 20°C) for only a marginal reduction in airflow rates obtainable when inlets were at 0m. This reduced heating energy is explained by CFD modelling which reveals that with raised inlets, fresh air takes longer time to descend into the room. This delay helps in warming the air as it approaches the inner (occupied) portions of the room. Similar behaviour was previously found in SNV dual openings.

For the ADB ward, as long as the opening fractions are not up to 25%, the heating energy being consumed in excess of CIBSE benchmark (4.62 MWh) regardless of the heating setpoint. These opening fractions (i.e. 6.25% and 12.5%) used with 18^{o}C or 20^{o}C heating setpoint can therefore potentially be considered as evidence-based design parameters for trickle ventilation rates for the inlet and stack system, as used in ADB wards.

The air changes that were predicted for the ADB ward imply that for periods when no heating is required (e.g. in summer), up to 217 l/s (19 ACH) can be obtained with a floor level inlet, while an elevated inlet (2.0m high) will be able to produce 178 l/s (15.5 ACH). These flow rates are in agreement with Qian, et al (2010) and far exceed the 6 ACH required by HTM 03-01 (DH, 2007a) or the 60 l/s/person suggested by the WHO (Atkinson, et al. 2009).

However, it has been predicted that for the ADB ward, raising the inlets to a height of 2.0m will lead to higher mean Age of air than when they are at floor level. Also when inlets are located flush with the corner of the wall and at 0m elevation, there is relative better LACI, MACE and EHR than when they were when located in the middle of the wall with elevation of 2.0m. The best ATT was also recorded with low level corner inlet. Using the edge-out strategy will lead to better dilution of contaminants. With the centre-out or corner edge out, the contaminants would collect over the patient's bed. As there are no known CFD studies of hospital wards fitted with inlet and stack systems, it is difficult to evaluate these results using precedents in contemporary literature.

CFD was used to predict the characteristics of airflow in a schematic ward design produced by Short and Associates (Short and Al-Maiyah, 2009) and studied by Lomas and Ji (2009). The design of this ward is pioneering in its use of vertical alignment of shafts and stacks for ventilating the same space, as well as for the use of labyrinths and triple shaft/stacks for servicing three different floors. However, this investigation has demonstrated that the differences in stack heights will have impacts on the ventilation efficiency as per absolute airflow rates into each ward. The differences between airflow rates into the ground floor ward (Ward 1) and first floor ward (Ward 2) is in the order of 10%. Similar difference in magnitude is predicted between airflow into the first floor and into the second floor ward (Ward 3). These differences conform to the stack equations (Lomas and Ji, 2009). The total difference between airflow rates into the ground floor ward and the flow rates into the highest (second) floor is 21.8%. These differences also manifest in energy required for heating where

Ward 1 is estimated to consume more energy than Ward 3 by a minimum of 63% (at 20^{o}C heating setpoint and with 25% opening fraction); or by as much as 92.7% when heating setpoint of 18^{o}C is used with 12.5% opening fraction.

Additionally, the effectiveness of ventilation (room air distribution) for the three ward levels is not the same taking into account the differences in Age of air and temperature resulting from inlet locations relative to the obstacle (bathroom). Relocating the bathroom (mirrored location across the room) leads to a reduction in the average time it takes for air particles to reach the patient's breathing zone from the inlet. This is will have benefits in delivering fresh air to patients quickly (reduction by 411s) and effectively (elimination of stale zones due to formation of vortexes).

The findings related to the proposed S&A ward layout are expected to generate interest in further detailed exploration of the proposed schematic ward design since there is a clear link to practical benefits. Importantly, the observed marked differences in airflow characteristics and IAQ due to simple relocation of the en-suite bathroom, underscores the importance of designers appreciating both the architectural and the ventilation engineering significance of design options right from the schematic stage. It is imperative that those who design a clinical space like wards and those tasked with ventilating such spaces are courageous to ask the 'what if' types of questions. It is also necessary to clarify that location of bathrooms in ward spaces during the architectural design process does take into account several important factors including adjacency to patient (i.e. bathroom being same wall as patient). This is to allow handrails to be installed and used for patient mobility. As such, the enhanced ventilation performance achieved due to the relocation of the bathroom (as carried out in this research) needs to be considered carefully within a wider context of multiple design criteria and constraints.

Such questions can be asked and answered through the iterative fine tuning of the relationship between the room air distribution and the architecture of the space because evidently, one can significantly influence (and be influenced) by the other, as this study has demonstrated. Designers would also need to understand (as Nightingale did centuries ago) that it is people (patients) who actually need air, and not the space. It is unlikely that an empty ward would require ventilation and therefore the underlying goal should be to get fresh and unadulterated air as quickly as possible to the designed locations of occupants, (e.g. a patient on a bed).

Such occupant-centred approach to ventilation will allow the best use of design resources (e.g. time/effort), construction resources (creation of walls/shafts) and natural resources (i.e. fresh air).

If this sort of philosophy can be adopted at the schematic design stage and requisite changes/improvements are made based on simulation evidence, then costly or undesirable outcomes at later stages can be minimised or avoided. Significant benefits can be realised if ineffective design decisions are identified early enough, but improving such ventilation design decisions requires the capacity to firstly understand the space and how or why it works, and secondly to be bold and creative in manipulating it without compromising function or aesthetics. This would require even greater collaboration at the schematic design phase; for it is doubtful that one group of professionals (architects or engineers) will have sufficient in-depth skills or know-how to manage both the architectural or ventilation engineering aspects of healthcare ventilation.

Table 11.3: SWOT analysis of the single-cell inlet and stack system

Strength	**Weakness**
• Can achieve 60 l/s/patient • Up to 49 l/s trickle ventilation rate possible • Provides proper segregation of inlets and outlets	• Differential stack heights in multi-floors lead to disparities in airflow rates and heating energy • Presence of obstacles along flow path of fresh air will lower IAQ • Requires pre-heating of supply air in winter (but this can easily be integrated via labyrinth pre-conditioning system)
Opportunities	**Threats**
• Can be retrofitted unto existing facades • Possible to integrate heat recovery in stacks • The ANV openings in the second floor of the S&A ward can be reduced to 90% of the size of the third floor ward. The first floor can be reduced to 80% of the maximum flow in the third floor.	• None foreseeable • Bathroom in original schematic S&A wards leads to poorer IAQ • Differential in stack heights leads to less airflow for highest ward

11.4 Performance of natural personalised ventilation

The NPV has been shown to be a novel system of getting fresh air directly to patients, protecting them from surrounding contaminated air. The mixing it creates in the entire space is also beneficial for overall control of airborne pathogens since it leads to better dilution than obtainable from displacement technique. The preference of mixing to displacement ventilation in clinical spaces is a relatively new finding (Beggs, et al. 2008; Atkinson, et al. 2009; Li, et al. 2011). This makes the NPV a timely innovation.

Since the NPV system has no equivalent in buoyancy-driven natural ventilation (whether for clinical or other purposes), assessing its performance is difficult, however, it has been shown to be capable of delivering more than 60 l/s/patient or 6 ACH, depending on the external climatic conditions and the internal heat loads. Furthermore, when compared with other systems using the single-bed ward design of the new Great Ormond Street Hospital, the NPV system was found to have modest heating energy demands. To put its performance in perspective, the mean January flow rate for the NPV (used as CBNV) is 32.6 l/s (at 12.5% opening fraction) which is above the HTM 03-01 rate for dilution but below the WHO rate per patient. However, at 25% opening fraction, the mean January flow rate into the CBNV system is 64.3 l/s. The equivalent mean January flow rate for inlet and stack system in the GOSH ward is 50.1 l/s and 99.5 l/s at 12.5% and 25% opening fractions respectively.

For heating energy in the GOSH ward, the CBNV system will consume 1.1635 MWh of heating energy from December to February, whereas the inlet and stack system consumes 2.4292 MWh of heating energy, with 25% opening. This is 52% less energy for the same period. The annual heating energy consumed will be 1.65MWh for CBNV and 3.777 MWh for the inlet and stack system. At 12.5% opening fraction, the annual energy consumed by the CBNV system is 0.24 MWh while the inlet and stack will require 0.935 MWh. To put these figures in their proper perspective, the comparative CIBSE benchmark for fossil fuel used for space and air heating for this ward space is 4.62MWh.

Furthermore, results indicate that raising the ceiling (i.e. allowing a space of 0.5m between the top of the duct and the ceiling) will lead to fairly uniform mixing of airborne contaminants in most of the room. The raised ceiling is seen to create more mixing of contaminants in the room than previously occurred with a lower ceiling, however, raising the

ceiling also traps more stale air at the upper level, but the mean age using the edge-out strategy is lower than with centre-out strategy. However, having such a ceiling space above the NPV duct could have consequences which could be detrimental to infection control.

It has been known that skin particles of various sizes are carriers of staphylococci (MRSA) and although the natural tendency of such particles is to settle on floors, draughts and air currents when doors are opened have been known to influence such particles to become airborne and settle at elevated surfaces (Hambraeus, et al. 1978, Rutula, et al. 1983). Similar air movement are inherent features of the NPV system which creates a mixing regime. It is also known that after bed-making, MRSA particles can remain in the air for up to 15 minutes (Shiomori, et al. 2002) further complicating the potential sources of particles for deposition on surfaces. In addition, the DNA of Norovirus has been found on horizontal surfaces which are elevated five feet above levels where hands could reach or contaminate, indicating the role of aerosolisation of this pathogen (Cheesborough, 2000). So although this research does not consider these semi-airborne contaminants of particles, the potential problem due to their settling and the associated difficulties that may arise with cleaning the top surfaces of the NPV ducts in wards arguably outweighs the observed mixing benefits. Further studies on the creation of a ceiling space and the migration of MRSA-laden particles will be required for more definitive conclusions.

This supports the feasibility of retrofitting existing facilities with NPV and stack along the facade wall. Modifying the NPV duct to deliver fresh air through two adjacent orifices further improves the quality of air around the breathing zone of the patient. The air would be less contaminated and the relative temperature of the location indicates thermal comfort could be enhanced giving the right outdoor weather condition.

Table 11.4: SWOT analysis of the NPV system

Strength	Weakness
• Local protection against airborne pathogens • Mixing enables dilution and better comfort • Modest energy consumption (relative to SNV/ANV) • Can be retrofitted unto facade • Can meet 60 l/s/patient flow rate	• Will require cooling of supply air • Dropping of supply air dependent on temperature differential • Will require detailed performance modelling • Requires pre-heating of supply air in winter
Opportunities	**Threats**
• Enhanced/direct occupant control of airflow • Applicable to multi-bed wards/other spaces • Can be further optimised to include wind • Can be improved to recover waste heat	• Draughts and discomfort in extreme outdoor temperatures. • Suspension of duct below ceiling space can allow particulates settle on surface

11.5 The comparative case study

The performances of four architecturally distinct natural ventilation systems were evaluated with respect to airflow capacity, thermal comfort and summer overheating as well as potential energy consumption in winter. Systems such as dual opening (Case 2) and inlet and stack (Case 3) provide distinctly segregated flow paths for incoming and outgoing air (as shown previously by CFD Age of air and flow vector results). Although this is desirable for dilution, it comes with energy penalties. Whereas the mean January airflow rates for Cases 2 and 3 are substantial at 152.8 l/s (≈ 7.9 ACH) and 99.5 l/s (≈ 5.2 ACH) respectively; in terms of heating energy, Case 2 was ranked last (at number 4), while Case 3 was ranked second to last in Table 1. Case 4 appears to be a good compromise among the cases due to its modest airflow (mean January flow is 64.3 l/s (≈ 3.3 ACH) and its position is number 2 in the energy ranking (Table 2). The performance of Case 4 in terms of comfort and energy is attributable to its mixing behaviour, despite its relatively modest airflow rates.

In general, the methods used in sizing openings were based on an empirical model in Case 2 and a rule of thumb in Case 3 and Case 4, however, while using the rule of thumb (percentage of floor area) has been tested and validated in previous studies of ANV systems similar to

Case 3 (Lomas and Ji, 2009; Lomas, 2007); using the same sizing technique for the CBNV is probably inappropriate. Apart from similarity in exhaust stacks, Case 4 differs significantly because the CBNV functions with elevated and horizontal supply ducts and a neutral pressure line which is reduced by the elevated ducts. A technique for determining the appropriate size of ducts is therefore required. This is possible, using trial and error by systematically increasing the percentage of floor area from current 1.5% upwards until a size which delivers equivalent flow rate as Case 3 is achieved.

It should be pointed out stated that although Case 3 produces mean flows of 5.2 ACH in winter (January), this is arguably an over ventilation with significant heating required. Similarly in summer, the CBNV of Case 4 produces mean flows of 132 l/s (6.9 ACH) and 87.4 l/s (4.5 ACH) at 100% and 60% opening fractions respectively. This flow rate may appear acceptable, using the 6 ACH benchmark of HTM 03-01 but it has been argued severally (Gammage, 1996; Lomas and Ji, 2009)) and inferred from a specific enquiry made directly to ASHRAE (Hammerling, 2009) that this benchmark rate is rather ambiguous in origin, even if it enjoys an apparent consensus amongst researchers and practitioners. The CBNV is uniquely unable to produce any flow for 222 hours of the year, equivalent to about nine days between July and August. This is probably due to its incapacity to cope with weak temperature differentials, further emphasising the need to reconsider its component sizing methods. Although Case 1 (as-built) was computed to produce zero flows as well for 1721 hours (71 days) in the same summer months, this is not attributable to weak temperature differentials only. The use of a single opening (for inflow and outflow of air) leading to conflict in flow directions or entrainment cannot be ruled out as suggested by CFD results (Fig. 8).

11.6 Experimental validation of the NPV system

Flow through the NPV system was validated using salt-bath experiment, providing results that compared favourably with the equivalent CFD models both quantitatively and qualitatively. The qualitative aspect was of unique significance because the inadequacies of steady state CFD modelling were resolved by transient flow visualisation. The use of salt-bath as an experimental was influenced by readily-available resources and expertise in the host department.

The results obtained after several runs of the experiments were captured using digital (still and video) imaging through which the system was analysed for its qualitative features. Due to technical constraints, only one heat source could be modelled at a time in the salt-bath model. The observed behaviour of fluid flow was found to be in agreement with CFD prediction in terms of interface height and formation of eddies underneath the NPV duct. Measured concentration of brine at the stack was compared with original density of the pumped solution. The ratio was found to be within reasonable agreement with (≈ 4.4% lower than) the CFD equivalent model prediction of temperature at the stack and at the source.

CHAPTER 12: Conclusions and recommendations

12.1 Conclusions

The aim of this research was to study the feasibility of various natural ventilation systems and their impacts on indoor air quality, thermal comfort and energy performance of healthcare facilities, for the overall wellbeing of occupants. Four distinct natural ventilation systems, which were selected based on evidence of their current use or future potential, were explored using specific performance criteria to determine their viability in single bed hospital wards. These systems were: single side single opening; single side dual opening; single-cell inlet and stack including advanced natural ventilation (ANV); and natural personalised ventilation (NPV). Three distinct geometries of single bed wards were modelled using dynamic thermal modelling (DTM) and computational fluid dynamics (CFD). For NPV in particular, salt-bath experiments were also performed to support the predictions made regarding the feasibility of buoyancy-driven airflow. The four systems were investigated in terms of their capacity to deliver adequate airflow rates (including trickle ventilation in winter); optimum thermal comfort; control of airborne contaminants and heating energy in cold periods. With respect to the findings derived from the review of literature and the various independent modelling studies, the following conclusions linked to specific research objectives were drawn. These conclusions form the core contributions of this thesis to the body of existing knowledge and are stated within the context of the limitations of the research summarised in the next section.

12.2 Focus, scope and limitations of research

The research has focused on natural ventilation through three existing systems while proposing a new system. These systems have been modelled using single bed hospital wards using DTM, CFD and salt-bath experiments. The choice of hospital ward layouts was informed by provisions of guidance including: the schematic design from Activity Database (i.e. ADB ward); the contemporary research from Short and Associates (i.e. S&A ward); as well as contemporary practice from Great Ormond Street Hospital (i.e. GOSH ward). Due to the exploratory nature of the research and need to emphasise the potentials of natural airflow, mechanical exhaust ventilation as commonly found in en-suite bathrooms of traditional wards was intentionally ignored. In current practice, the design of such exhaust ventilation is

factored into the overall airflow regime of an entire ward. Although an exhaust fan would function for brief periods when a bathroom is occupied, its operation could have consequences such as: inducing the flow of external air through natural ventilation openings; infiltration; circulation of indoor air; as well as the overall pressure balance in such wards. It is therefore important that the results of this research are viewed with the unique scope of purely natural airflow in mind.

The choice and use of passive scalar contaminants as surrogates for airborne pathogens for the CFD aspect of this study also mean the results which relate to dispersal of airborne contaminants be considered carefully. The use of passive scalar contaminants is limited to those pathogens which are not bigger than 1µm and which tend to remain in perpetual floatation, such as droplet nuclei. Airborne particulates whose size and density allow them settle on surfaces and become re-suspended due to external forces are therefore not covered by the results of this research. Other aspects that were not considered include: the impact of urban heat island (UHI); pre-heating of supply air, summer cooling (e.g. via underground labyrinths) and heat recovery as used through mechanical ventilation with heat recovery (MVHR).

12.3 Conclusions for Objective 1:

Objective 1: *To investigate the contemporary issues which influence natural ventilation systems and strategies, airborne infection control and overall indoor air quality (IAQ) of healthcare buildings with the goal of defining the areas of emphasis for the study based on contemporary research/practice and to identify knowledge gaps for potential exploitation.*

The conclusions drawn for the first objective are outlined as follows.

- **Quantitative parameters:** The current guidelines and standards are largely dependent on specifying airflow rates. This has been shown to be inadequate to meet the needs of hospital wards where airborne pathogens are a hazard. The use of absolute ventilation rates were found to be more effective especially when linked to patients e.g. 60 l/s/patient (Atkinson, et al. 2009) or the 83.3 l/s ‘safe dilution rate’ (Jiang, et al. 2009).

- **Qualitative performance:** The review of literature identified the lack of guidance or implementation of qualitative performance for naturally ventilated hospital wards. Although room air distribution (pattern and direction of airflow) has been known to be important for controlling airborne pathogens, this has mostly been applied to mechanically ventilated spaces only.

- **Displacement ventilation** as used in natural ventilation systems is argued in some emerging literature to be unsuitable for dealing with emission of airborne contaminants. Contemporary findings have demonstrated that emitted airborne contaminants can get trapped in the occupied zone of indoor spaces which are ventilated using displacement techniques. This issue led to the research question about the reliability of buoyancy-driven displacement ventilation techniques through natural ventilation for airborne contaminant control in hospital wards. A possible solution was identified in this research by the development of a new buoyancy-driven natural ventilation system (i.e. natural personalised ventilation, NPV) as part of a wider concept for ceiling-based natural ventilation (CBNV) systems.

- **Windows** are the dominant natural ventilation system in hospitals. In wards, there is little evidence to show that they have been sized empirically for optimum airflow or optimised to deal with airborne contaminants. Windows in hospital wards are also constrained by HTM 55 to have a maximum openable area of 100mm. The performance of windows in meeting the contemporary natural ventilation needs of single-bed wards is therefore an area of concern.

- **Segregation of inlets and outlets** in natural ventilation is important in providing acceptable air quality and specifically for dealing with airborne contaminants. This requirement rules out single-openings regardless of whether they are dedicated vents or traditional windows – unless such vents are designed to work in tandem with exhaust fans located in en-suite bathrooms.

- **Personalisation of ventilation** can play a valuable role in protecting patients susceptible to airborne infections carried by visitors and healthcare workers in

hospital wards. Existing personalised ventilation systems have been based on mechanical ventilation.

- **In multi-floor layouts of hospital wards,** it may not be desirable to have dual openings which are aligned directly above each other, since the high-level outlets of lower floors could exhaust stale/contaminated air which could flow into low-level inlets of higher floors.

- **Computer-based simulations** including dynamic thermal simulation and computational fluid dynamics have become viable research and industry methods of investigating airflow in built environments, including healthcare spaces. However, experimental work is also encouraged for validation.

12.4 Conclusions for Objective 2:

Objective 2: *To assess the performance and potential of existing, emerging or innovative natural ventilation systems in single-bed wards of hospitals to simultaneously meet the needs for: (a) effective room air distribution in terms of airflow rates, pattern and direction; (b) thermal comfort of occupants; (c) airborne contaminant removal or dilution; and (d) energy consumed for heating in winter periods.*

The conclusions drawn for the second objective are outlined as follows, and these constitute the core contribution of this thesis to existing body of knowledge bearing in mind the focus, scope and limitations outlined in Section 12.2.

1. **Single opening system:** The single opening is a common system of natural ventilation whose continuous use in hospital ward ventilation has been encouraged by two factors: the restrictions in openable area (100mm) as well as by the traditional design approach of using windows for airflow, lighting and visual communication with the exterior. This research has drawn the following conclusions for single openings.
   a) The airflow rates achievable by single openings as sized and applied in this study range from 24.4 l/s to 31.5 l/s when used at 25% of the maximum possible size during winter period at 20^{o}C heating setpoint. Increasing the heating setpoint to 24^{o}C has negligible impact in driving more airflow into the ward. In summer, the airflow rates

achieved with single openings at their maximum size could be between 89.5 l/s and 108 l/s. However, while in absolute terms these airflow rates appear to meet the dilution requirements of such wards, the effectiveness of ventilation could be compromised as outlined in the next conclusions.

b) This system encourages the recirculation of indoor air, making it useful for retaining indoor heat that would otherwise have escaped, but also rather unsuitable for control of airborne pathogens. This could be an important disadvantage in future due to warmer climates and airborne pandemics.

c) It is feasible and logical for single opening systems to be transformed into dual opening systems, whereby current glazed openings are supported by low-level (louvered) inlets.

2. **Dual opening system:** This has been shown to have capacity for achieving relatively high airflow rates resulting in the removal of contaminants at upper level outlets. However, this system is unable to provide instant dilution of contaminants emitted at the occupied zone, as observed in the trajectory of a cough. The following conclusions were subsequently drawn.

    a) When the dual opening was studied and compared with the single opening, the difference in performance is superior regarding volume of airflow involved in the air exchange process. In winter, operating a 20^{o}C heating setpoint would lead to flow rates of up to 132 l/s and 152 l/s while in summer the absolute flow rates ranged between 239 l/s and 299 l/s. The relative increase in flow rates depend on the size of the openings, the distance between the openings and the impact of driving forces such as temperature differentials and wind speeds. However, this leads to the next conclusion.

    b) There is a danger of draught at floor levels when inlets are at 0m elevation but such draught /thermal discomfort may be alleviated by increasing the elevation of the inlets by up to 1.0m. Although such elevation would increase the likelihood of entrainment of outgoing air with fresh air, this height forces the supply air to take a longer time (up to 190s in the ADB ward) to reach the occupied zones which allows more time for outdoor winter air to be warmed by indoor sources).

However, the chances of cross-contamination of such elevated fresh air supply by airborne pathogens may also increase.

c) The relatively high airflow rates achievable by dual openings has potential to require significant energy for heating in winter, but this problem can be alleviated by using trickle ventilation rates at between 6% to 12.5% of the original area of opening.

d) Given the appropriate (designed) size of inlets and outlets, the efficiency (air flow rates) and effectiveness (air quality) of the dual opening system depends on the relative elevation or distance between the inlets and the outlets. A reduced elevation of an outlet (e.g. the GOSH outlet is only 1.9m high) has insignificant consequences for freshness of air, but elevating the inlet by 1.0m can deteriorate the quality (age of air, temperature and airborne pollutants) of incoming air. Therefore, in retrofitting or new designs, it would be better to minimise the elevation of inlets.

e) A height difference of 1.4m between inlet and outlet was found to be adequate to ensure segregation of airflow - as long as inlets are at floor level (0m elevation). For the types of (single-bed) wards investigated, these dimensions are optimum and recommended.

f) When adopted into the design of the Great Ormond Street Hospital ward, the dual opening was demonstrated to be a better natural ventilation option than the current single opening system being used in terms of airflow rates and overall indoor air quality.

g) When free stream air speeds are low (e.g. between 0 and 7 m/s) buoyancy forces dominate as the driving force into dual opening SNV systems of wards, such as those described in the study. At higher speeds, wind forces dominate buoyancy.

3. **The inlet and stack system (ADB)**:

a) The inlet and stack system used in the ADB ward design is capable of meeting 10 l/s odour dilution rate in winter, with heating energy below the regulatory

benchmark. It can also exceed 60 l/s/patient in summer, with potential overheating occurring in two to four days of a summer month (August).

b) In non-winter scenarios, the edge-in, edge-out (EIEO) strategy used with low level inlets and having all openings in a corner orientation were found to have better mean air change efficiency (MACE) value (77%) as well as higher air turnover time (ATT) value of 1052s than all other EIEO or EICO strategies. This was the most effective configuration of inlet and stack design, based on the characteristics of the ADB ward studied.

c) Qualitatively, it was found that using the central EIEO strategy, emitted airborne contaminants do not accumulate over the patient's bed as would occur with central edge-in, centre-out (EICO) or with cornered EIEO strategies. Elevating the inlets to 2.0m for the centralised EIEO or EICO strategies would encourage/increase the distribution of contaminants in the space by as much as 9%.

4. **The inlet and stack system (ANV)**: The ventilation performance of the S&A wards in terms of airflow rates, room air distribution and energy consumption were shown to have significant variations based on their elevation as follows.

a) The difference in airflow rates is in the order of approximately 10% from one floor to the next, with the lower floors e.g. Ward 1 (first floor) having more airflow due to the stack being longer than the stack of Ward 2 (second floor). Similar difference in airflow rates occurs between Ward 2 and Ward 3 (third floor). This difference is also linked to the cross-sectional area of stacks as well as to the height of each floor (3.6m).

b) The heating energy required also varies according to floor level. The lowest floor (Ward 1 on first floor) is estimated to consume more energy than the highest floor (Ward 3) by a minimum of 63% (at 20^{o}C heating setpoint and with 25% opening fraction); or by as much as 92.7% with a heating setpoint of 18^{o}C and 12.5% opening fraction.

c) The nature of some en-suite ward design means some necessary features (e.g. a bathroom) could obstruct the free flow of air. As incoming air circumvents these impediments, it leads to time-dependent deterioration in the quality of fresh air in terms of temperature and age. Relocating the bathroom leads to a reduction in the average time it takes for air particles to reach the patient's breathing zone from the inlet. This is will have benefits in delivering fresh air to patients quickly, reducing the time taken by up to 411s (i.e. reduction of time by 32% for the worst case). This also has implications for ventilation effectiveness due to the elimination of stale zones created by the formation of vortexes. The temperature stratification without a bathroom is also found to be more uniform, with less pockets of stale air.

5. **The natural personalised ventilation (NPV) system**: The NPV system is a feasible technique of protecting patients from airborne pathogens. The flow characteristics predicted by CFD have been validated using scaled salt-bath experiments. Relative to other systems studied, it provides five advantages as follows.

    a) The system can deliver airflow rates which meet the WHO 60 l/s/patient requirement in summer.
    b) The system creates mixing ventilation in the space through buoyancy alone, thereby eliminating the drawbacks of existing natural displacement ventilation which other researchers have found to be incapable of controlling airborne pathogens.
    c) The creation of a ceiling space (e.g. an open plenum) above the NPV duct was found to create an enhanced mixing regime compared to when the ceiling was flush with the top of the NPV duct. When the ceiling is raised by an additional 0.5m, the mean room concentration of contaminants was 6.25% with the edge-out (EIEO) whereas with a centre-out (EICO) strategy the mean room concentration was 12.50%. The EIEO strategy is therefore preferable for design situations where airborne contaminants are of concern and having a high floor-to-ceiling height would be helpful.
    d) The system could be used without personalisation in the form of CBNV, which could deliver fresh air to remote or isolated parts of a ward space.

e) The NPV could also be integrated with SNV using low level inlets for supplementary supply of air. This would not invalidate the flow regime, since the NPV exhaust stack is always likely to be higher than all inlets.

6. **The ceiling-based natural ventilation (CBNV) system** was developed as a derivative of the NPV and was found to be a suitable approach for providing fresh air to remote parts of a ward, as demonstrated in the GOSH case study. The fundamental difference between the CBNV and NPV is a matter of supply point and personalisation of fresh air. The following conclusions were drawn from application of the CBNV in the GOSH ward.
    a) It is possible (and desirable) to fit a ward with NPV duct for personalisation of air delivery and protection of patients from airborne contaminants, as well as a secondary (CBNV) duct for supplementary room ventilation.
    b) The quantitative performance of CBNV is similar to NPV in terms of airflow rates.
    c) Qualitatively, using CBNV (i.e. multiple ducts) is likely to lead to better mixing than using NPV alone. This is regardless of whether NPV system is supported by low-level inlets for supplementary air supply.

12.5 Conclusions for Objective 3: (Recommendations)

Objective 3: *To extract the outcomes from objectives (1) and (2) to develop recommendations for future guidelines on design and operation of natural ventilation of single-bed ward spaces.*

As part of the objectives of this research, some recommendations are proposed for future guidelines. These recommendations are aimed at providing modelling-based performance advice to building designers and facility managers including infection control experts who form part of healthcare facility design teams. The recommendations provided here are primarily for single-bed wards intended to be ventilated naturally using buoyancy as the driving force. The recommendations for using natural ventilation in hospitals have been categorised according to the systems investigated. These recommendations are also sub-categorised according to issues such as design and operation, performance modelling and provisions for future guidelines. The conclusions drawn for the third objective are outlined as follows.

12.4.1 Recommendations for simple natural ventilation (SNV) for wards

1. **Design of dual openings:**

   The following recommendations are made for the purpose of designing dual openings in single bed hospital wards.

   a. In refurbishment of existing wards having single (window) openings sized according to empirical models, inlets should consider room depth[9], the relative location of inlets and outlets and the magnitude and position of heat sources. A room depth of 6.25m (GOSH ward) was found to be feasible, just as a room depth of 5.0m (ADB ward). However, in this study, the area of ventilation openings in the GOSH ward were larger by ≈ 20%. Furthermore, the floor area of the GOSH ward is smaller than the ADB ward by ≈ 6% (bathroom inclusive) or by 27% without the bathrooms.

   b. Evidence from literature and this research indicates that designers should not rely on or expect wind to drive airflow if wind speeds are low (between 4 m/s and 7 m/s). Sizing dual openings based on purely analytical methods could incorrectly assume that airflow rates will be higher than expected. Dynamic thermal modelling will give a more accurate picture of when wind can be expected to dominate buoyancy. This point was found to be 7 m/s, much higher than suggested by literature (4 m/s). Other factors, such as internal heat load (W/m^2), wind direction and building orientation may have played a role in these discrepancies, so these need further detailed investigation with sensitivity analyses of their impacts (causal or co-relational).

   c. Dual openings should be designed according to the CIBSE (2005) model, but this by itself does not guarantee optimum performance. For standardised layouts of wards, CFD modelling is useful for studying the impact of the location of openings on room air distribution. This includes issues such as vertical distance between inlet and outlet and the implications of an elevated inlet, which has interesting energy-saving consequences.

[9] The WHO (Atkinson, et al. 2009) and DH (2007) guidance on SNV systems (windows) recommend a maximum effective depth of 2.5m, but evidence suggests this limitation applies only to single-openings (traditional windows), not dedicated dual-openings as used in this research. There is in fact, lack of quantitative and qualitative guidance on the feasibility of dual-openings in both the WHO and DH guidelines as well as in CIBSE.

d. **Design of dual openings:** Evidence from literature[10] suggests that when wind overcomes buoyancy forces at free wind speeds starting from 4 m/s, it is likely to lead to a reversal in intended flow direction (i.e. supply would be from top opening and extract is from bottom opening). This needs to be considered carefully, especially since there could be consequences in terms of pattern and direction which can affect contaminant dilution and extraction.

2. **Operation of dual openings:** Wards fitted with dual openings should have a single control such that both openings (inlet and outlet) are always adjusted simultaneously. This is regardless of whether such control is automated or manual. The rationale for this is to avoid healthcare workers or occupants misusing the system out of ignorance. Having only one of the two orifices opened at a time would defeat the essence of the design.

12.4.2 Recommendations for inlet and stack and ANV

1. **Design of inlet and stack**: For the configurations of wards used in this research where source (visitor) location is adjacent to the patient, it was found that the ventilation strategy worked best when the low level inlets and stack were flushed with the corner of the room (towards the bed). This technique was found to provide better air quality to the patient than centrally located inlets.

2. **Design of ANV exhaust stacks**: With the aid of the stack equation, the sizing of ANV stacks should ideally begin with the stack of the highest floor (Ward 3) whose flow rate and consequent heating energy should be based on specific minimum requirements (e.g. the 60 l/s/patient requirement). Assuming the stack sized for the highest floor (Ward 3) is capable of meeting minimum airflow rates, the next lower floor (i.e. Ward 2) will have approximately 10% more airflow due to its longer stack – assuming they are of same cross sectional area. As such, starting with the highest floor and in a descending order, the absolute area of inlets could be decreased by a suitable fraction. This will ensure the equalization of airflow rates into all wards. An alternative approach would be to reduce the cross-sectional area of the stacks (using the stack equation), in a descending order.

[10] Allocca, et al. (2003)

This way, the topmost ward will retain the original computed cross sectional area while the stacks of the middle and lowest wards are reduced appropriately.

3. **Operation of ANV supply shafts**: It is possible that occasionally, the stacks cannot be sized to factor the expected difference in airflow rates as discussed above (e.g. due to constraints of standardised stack sections or the need to simply construction). In this case, a control algorithm can be put in place such that the air in the supply shafts of lower floors are regulated appropriately in order to achieve airflow rates which meet the required ventilation rates. This rate (e.g. when determined by guidelines) can be designed for the highest floor with the shortest stack and working downwards. Without such operational measures in place, the heating energy of lower floors will greatly exceed the minimum requirement. This excessive difference in heating energy has been shown to be as much as 63% at 20^{o}C heating setpoint and with 25% opening fraction, or up to 92.7% with a heating setpoint of 18^{o}C at 12.5% opening fraction.

12.4.3 Recommendations for Natural Personalised Ventilation (NPV)

- **Design of NPV**: The design of the NPV system should consider the 'drop' zone of fresh air; since there would always be a horizontal throw in the supply direction as long as supply air is cooler than indoor air. Design of the system should also include supplementary (or optional) low level inlets to augment the supply of fresh air into the space.
- **Operation of NPV**: To avoid draught or discomfort, the design of the NPV system would require greater control systems from occupants since fresh air is being delivered much closer to the patient than would occur in other systems. This can be achieved by using diffusers at the supply end of the duct which would be controlled by airflow regulators.
- **Contemporary research impact:** The natural personalised ventilation (NPV) system has been discussed in Chapter 5 of the draft version of the upcoming revised edition of CIBSE Guide A: Environmental Design (CIBSE, 2012). This is evidence of research impact in terms of guidelines. It is possible that guidelines suggested from the findings of SNV and ANV systems will also feature in similar guidelines especially in any revision of the WHO guideline on natural ventilation for infection control (Atkinson, et al. 2009).

- **Preheating of outdoor air:** Pre-heating of air through the NPV will be necessary when outdoor temperatures are lower than acceptable. In this regard, it will be necessary for the room heating system to be integrated with the ventilation system. This aspect was not considered in this work.

12.4.4 General recommendations

- **Limit the use of single openings:** In the context of the natural ventilation systems investigated in this research, the single opening has benefits, limitations and potential. Its uniqueness in design, though useful in retaining indoor heat in winter, adequate ventilation rates and room air distribution as may be compromised, sometimes leading to overheating. It should be used carefully where necessary and existing systems can be refurbished to work with new low level inlets, thereby converting it to dual openings.
- **Implementation of dual openings:** Dual openings are suitable for adoption in new or existing single bed wards if other natural ventilation systems (e.g. ANV) are not a feasible option. This could mean that existing windows usually constrained by their statutory 100mm maximum opening - as outlined in HTM 55 (DH 1998) will serve as outlets, while new inlets are fitted at low levels.
- **Vertical distance in dual openings:** The vertical distance between inlets and outlets is critical in determining ventilation efficiency (airflow rates) as well as effectiveness of air circulation. With an outlet which is 0.3m high raised to an elevation of 2.7m, placing the inlet 1.0m above the floor will lead to entrainment of room air into the fresh air of the raised inlet.
- **Architectural layouts:** Architectural designs which encourage pockets of stagnant air (e.g. a spaces/obstacles located along the path of fresh air) should be avoided or justified. This can be done by using CFD to study room air distribution of wards.

12.4.4.1 Performance modelling

- **Performance criteria:** Designers may often be required to demonstrate that performance criteria (quantitative and qualitative) have been met in the design of hospital wards, especially when energy and airborne contaminants are an issue. The simultaneous investigation of airflow performance of hospital wards using DTM and

CFD provides a method for performance-based design of hospital wards. These tools are not only useful for evaluating performance, but are beneficial for exploring innovative concepts in natural ventilation. In situations where a combination of factors such as availability of resources, expertise as well as complicated ward designs make it conceivable, scaled (water-based) experiments can be used to support the flow characteristics of natural ventilation systems.

12.4.4.2 Provisions of guidelines (e.g. HTM 03-01 and WHO Guidelines)

Current guidelines and standards are prescriptive-based as evident in their emphasis on airflow rates. What is equally important is room air distribution and freshness of air as determined by location of inlets and outlets, which combine to determine the age of air at key locations. Performance-based guidelines can be based on the following principles.

a) **Occupancy-centred ventilation:** People are the eventual targets of ventilation and not the spaces they inhabit. Designers of hospital wards should be encouraged to have this concept as a central theme.
b) **Minimum (absolute) airflow rates:** There should be a specified range of acceptable rate of ventilation in absolute terms as opposed to the use of relative ventilation rates.
c) **Maximum age of air at specific POIs:** The age of air at specific locations in a ward is currently not used as an airflow parameter and may be worth considering along with airflow rates. This may take the form of specific (maximum) age of air at patient locations, determined by xyz coordinates. Age of air can be predicted using CFD or smoke tests. The former is a cheaper and quicker option.
d) **Pattern and direction of airflow:** It would be useful to provide qualitative guidance on the techniques that can achieve desirable room air distribution, including the segregation of openings. The pattern of displaced incoming fresh air can determine the re-distribution of emitted contaminants but this pattern also depends on the specific locations of inlets and outlets relative to potential sources (e.g. seated visitors).
e) **Natural ventilation components**: Examples of natural ventilation components (e.g. louvered inlets and outlets) should be provided including empirical guidance on how they should be sized.
f) **Method of verification of performance:** It would be useful for designers of hospital wards to demonstrate acceptable ventilation performance through modelling.

Performance criteria should include absolute airflow rates, thermal comfort, heating energy and control of passive scalar airborne pathogens.

12.5 Feasibility of natural ventilation in single-bed wards

Based on the findings from this study, in light of its scope and limitations, it is concluded that natural ventilation is not only feasible for single-bed ward spaces but that there are opportunities for further research/innovation in this under-utilised and underestimated system.

12.5.1 The viability of natural ventilation systems

The viability of a specific ventilation system (SNV, ANV or NPV) for any given hospital ward would depend on its overall purpose, occupancy type and the expected air quality challenges. Clearly, single-bed wards would be designed and allocated to serve different types of patients whose needs will vary. Where airborne infection is not perceived as an immediate concern, SNV and ANV will suit most purposes, whereas NPV will be advantageous to instances where patient health is threatened by contaminated indoor sources. The choice of appropriate natural ventilation system is one which should be made by a multidisciplinary team which includes all stakeholders ranging from infection control officers, architects, engineers, facility managers and client representatives. The multidisciplinary nature of ventilation and indoor air quality is what would make key findings of this research relevant as a basis for understanding the potentials and limitations of performance in the ventilation systems studied.

The effective use of any natural ventilation system is likely to include a careful assessment and necessary implementation of automation of control system which links airflow rates, contaminant dilution and thermal comfort levels. This (automation) aspect was not explored in this research because real-time detection of airborne contaminants is complex and the technology is still in its infancy. Nevertheless, it is plausible that CO_2 (and its simpler automated detection and consequent dilution) can be used as a surrogate for more harmful airborne pollutants.

The contributions to knowledge made in this thesis can be extended to other clinical and non-clinical spaces which are suitable for natural ventilation including treatment rooms, office spaces and waiting areas.

12.5.2 The future role of naturally ventilated single bed wards

In a future energy-conscious healthcare environment, single bed wards can serve as a cross between air infection and isolation rooms (AIIRs) and general hospital wards, albeit with limited exposure to co-patients. However, this is assuming the valid concerns about the social, emotional and psychological implications of isolating patients are alleviated as implied by studies such as Florey, et al. (2009) and Abad et al. (2010). Some of these concerns may be addressed by for example, the Cruciform ward layout (Fig. 12.1) as proposed by Nightingale Associates (Paradise, 2011). This design already implemented in the new Peterborough City Hospital (Nightingale Associates, 2010), proposes collapsible partitions that separate four patients (into distinct zones) within a shared multi-bed ward.

Figure 12:1: Typical layout of the Cruciform four-bed ward (Source: Paradise (2011)

While, this design has advantages such as being compact, multi-occupant and providing privacy or semi-isolation for each patient, for the purposes of natural ventilation, it is likely to be challenged in three ways. Firstly, the partitioning of the bed areas could disrupt natural displacement ventilation. This disruption may prevent proper room air distribution and dilution. It could even lead to localised pockets of stale air, if the partitions are ceiling-high. Secondly, because the proposed SNV systems (single openings) are located in waiting/sitting areas (Fig. 12.1), any *visitor carrying an airborne disease (e.g. influenza) could unknowingly help in distributing infectious droplet nuclei amongst vulnerable patients*. Thirdly, the Cruciform ward layout still has to deal with the problem of limited access to external facade like many other existing four-bed ward designs. This could make the use of single-opening SNV systems limited in impact, if better IAQ is desirable (as suggested by results from this

study). It must be noted that there is potential for an exhaust fan in the en-suite bathroom to induce different airflow regimes (and hence different outcomes) which depart from those implied by these three challenges. However, because such use of mechanical fans tends to be occasional (typically when the bathroom is in use, lasting minutes - not hours), the three areas of concern discussed above require consideration.

Nevertheless, the Cruciform layout has some interesting potentials. Using SNV systems in this design *could* mean that displaced fresh air is not compelled to pass through (or over) any particular patient's bed as it reaches remote corners. If this happens to be the case, it would be helpful in *minimising risk of cross-infection from one patient to another*[11]. For future new builds which adopt the Cruciform layout, ANV strategies particularly the Centre-In strategy (Lomas and Ji, 2009) should be considered for delivering fresh air to those beds which are far from the external facade. In fact, it may be possible to have a Centre-In-Edge-In strategy, where two points of fresh air supply are designed to work with one stack (Edge-Out or Centre-Out). There is also an opportunity to investigate the NPV system for such a ward design.

As implied by literature and this study which focused on single bed wards, the absence of shared contaminated air amongst co-patients means the sources of infectious airborne pathogens will be largely limited to visitors and healthcare workers. This risk can be reduced by careful design (sizing and placement) of natural ventilation systems.

12.6 Recommendations for further research

The aspects of buoyancy-drive natural ventilation that can be pursued following this research include the following.

- The challenge of using dual openings (whether as new design or retrofit measure) may be overcome by staggering the location of inlets and outlets to break the vertical alignment in their positioning. Such arrangements may reduce or eliminate the cross-contamination of air between the floors, where air being exhausted from outlets of lower floors is sucked into the inlets of upper floors as already observed in Alloca, (2003). This concept can be explored further using CFD studies.

[11] This issue (as well as the three challenges discussed) would require in-depth study and there is no evident yet that the Cruciform has been investigated in terms of the behaviour of natural airflow within the layout.

- The stagnant pocket of air closer to the patient's bed observed in the S&A ward could also have been caused by the standing HCW, whose presence as a heat source, would cause air to be entrained in a vertical plume. The 3D streamlines support this deduction. The extent to which the HCW at the given location affects the room air distribution due to entrainment can be subjected to further detailed studies. However, as it would involve a permutation of many possible locations, embarking on such an exercise falls outside the immediate remits of this study and the context, scope and objectives of the overall research. Nevertheless, it is an issue that could be explored in further studies.

- The S&A ward needs to be further evaluated with respect to distribution of airborne contaminants in the space. Based on findings from other studies in this thesis, it is expected that the significant variation in age of air brought about by different inlet locations and the presence of an en-suite bathroom can impact on dilution of contaminants. This aspect of distribution of airborne contaminants requires further detailed consideration, even though as has been demonstrated, reflecting the bathroom to a mirror location on the opposite wall largely eliminates the age of air and vortex problem.

- The differences in air flow rates brought about by differences in stack heights of the S&A ward are likely to have an impact on room air distribution. Although the room air distribution aspect were studied in this research using CFD, for simplicity and time constraints, it was assumed that the wards were on the same floor and results were valid only to the extent that they relate to the location of inlets and the presence of the obstructing bathroom. A detailed CFD study where each ward is elevated to its real height would allow further evaluation on performance to be done, such as the differential in airflow rates predicted by DTM due to differences in stack heights.

- Most heat recovery systems are based on mechanical ventilation with heat recovery (MVHR). However, it is possible that both ANV and NPV systems can be researched further with the aim of achieving passive heat recovery. The potential for this lies in the presence of an exhaust stack where such recovery may take place. Heat recovery would be difficult but not impossible for SNV systems.

- There is a need to explore how the mean monthly DTS energy loads can aid the sizing of room heaters which can be studied in detail using CFD models. However, locating such heaters requires careful consideration as their positions can affect comfort and efficiency of heating and it may emerge from further CFD studies that optimum placement could lead to even better comfort and lower energy than suggested by DTS simulations. It is also possible to monetise the equivalent consumption of energy from both electricity and gas sources under each system as this can aid designers and clients in making informed decisions about cost implications of proposed design alternatives.

- The NPV-CBNV system can be further studied for potential integration with air disinfection systems such as with upper-room ultraviolet germicidal irradiation (UVGI). As shown by Noakes, et al. (2006a), mixing ventilation is necessary for this aseptic technique to work. Therefore, since the NPV-CBNV can provide mixing ventilation through a zero to low energy technique (buoyancy-driven flow), then investigating of the viability of the NPV-CBNV concept with UVGI is a plausible extension of this research. It is worth noting that Noakes, et al. (2006a) developed a technique where CFD was used to model and optimise the performance of a UVGI system. As such, further studies could build upon this, by using CFD as a research tool for modelling UVGI with focus on naturally ventilated hospital wards.

- The use of NPV can be extended for existing multi-bed wards, where refurbishment using individual ducts over patient beds can enhance the quality of air at those locations, in addition to minimising the ingress of polluted air from the surrounding spaces. It is also important to consider adoption of NPV principles for supplying fresh air into other healthcare spaces, for example treatment rooms, emergency rooms and consulting offices, even if personalisation is unnecessary. This could lead to a generic approach of using ceiling-based ducts for better natural ventilation. The influence of wind is also a matter that needs to be considered since if harnessed carefully, it can improve ventilation rates. Another aspect that needs considering is the possible use of sub-ground level labyrinths for controlled supply of preheated air or pre-cooled air using passive downdraught evaporative cooling, into NPV ducts. This could lead to a system that is beneficial for use in climatic conditions when outdoor air is too warm for indoor ventilation purposes.

APPENDIX A: Paper 1 (International Journal of ventilation)

Natural Personalised Ventilation - A Novel Approach

Z.A. Adamu, M.J. Cook and A.D.F. Price

School of Civil and Building Engineering, Loughborough University, LE11 3TU, UK

Abstract

The need to protect susceptible patients from cross-infection resulting from airborne pathogens is essential in hospitals, especially when patient immunity is either suppressed due to medical procedures or compromised by ailment. Personalised ventilation (PV) is a method of creating a local zone of high air quality around such patients. However, contemporary PV techniques are based on mechanical ventilation, which adds to the energy burden of healthcare buildings. In single-bed wards, a potential source of infection could be other occupants such as visitors and healthcare workers. Threats may also come from airborne pathogens migrating from adjacent zones, especially if the single-bed wards in question are not positively pressurised. While the World Health Organisation (WHO) has issued guidelines on using natural ventilation to control infectious bio-aerosols in hospital wards (with flow rates of up to 60 L/s.patient), how to achieve this rate without high energy and carbon costs, remains unanswered. The objective of the research reported here is to demonstrate a novel approach of using low-energy, buoyancy-driven natural airflow for personalised ventilation of single-bed hospital wards. The investigation has been carried out by undertaking dynamic thermal simulations (DTS) and computational fluid dynamics (CFD) simulations. Findings indicate that, given appropriate design, it is possible to achieve personal protection for vulnerable patients using a natural mode of ventilation alone. Co-occupants could also benefit from the mixing characteristics offered by the proposed system, which does not occur in typical buoyancy-driven displacement ventilation.

Key words: natural personalised ventilation, buoyancy, single-bed ward, dynamic thermal simulation, computational fluid dynamics.

1. Background

The importance of clean air around patients has been aptly captured by Florence Nightingale, who promoted the first rule of nursing as being to "keep the air within as pure as the air without". In her *'Notes on Nursing'* she further emphasised the need to ensure that, without chilling a patient, the air he breathed had to be as pure as the external air (Nightingale, 1859). More recent attempts at hospital ventilation which focused on patients can be found (Luciano, 1977) including the Trexler Life Island Unit, made of plastic sheets, which did not get acceptance in the United Kingdom (UK) primarily because it was *'so very different from established methods'* (White, 1981). Other types of patient-centred ventilation solutions did not use physical barriers. They were essentially ventilation 'canopies' over each patient in a multi-bed ward. Examples of this approach are the Robbins Aseptic Air Patient Isolation Canopy (Luciano, 1977) which was developed in the United States; as well as the Sterair Patient Isolator (White, 1981) whose canopy delivered HEPA-filtered air over a patient.

Gradually, the benefits of patient-centred ventilation saw the emergence of personalised ventilation (PV) as distinct airflow systems. PV has been defined by Melikov (2004) as a system which delivers cooler and cleaner air directly to or over an occupant in such a manner that allows them to customise the flow characteristics (temperature, flow rate, direction) according to their needs. PV systems have developed as a ventilation technique which works independently of any supplementary/additional room ventilation system and, in hospitals, it is common for them to be used for aseptic purposes.

Current developments in personalised ventilation systems are still in the research and experimental stage where many concepts have been developed. Notable studies from the last decade include Melikov et al (2002) and Melikov et al. (2003). Innovative approaches include the use of PV systems as parts of objects including: hospital beds (Nielsen, et al., 2007 and 2008); pillows (Nielsen, 2009) and chairs (Niu, et al., 2007). These studies also assessed risk to occupants from contaminants generated in such spaces using pollutant exposure models. So far, all PV systems have been

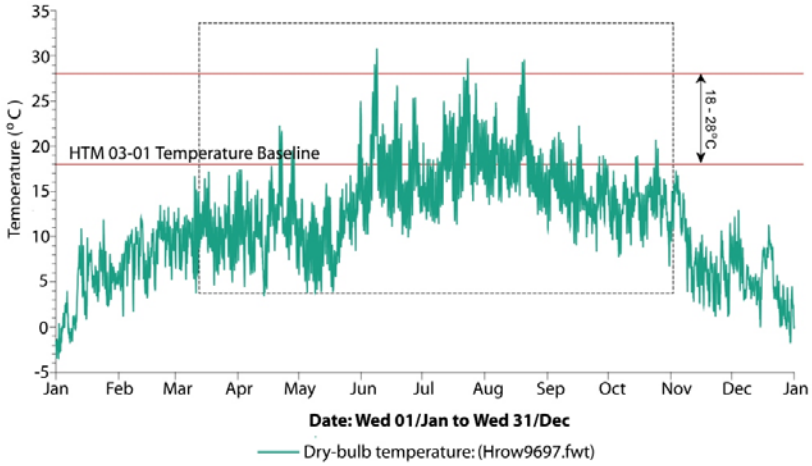

Figure 1. Annual external temperature fluctuations for London (Test Reference Year (TRY) data).

mechanical, adding to energy and carbon concerns as outlined by the UK Department of Health (DoH, 2006) where space conditioning accounted for over 40% of energy consumed in typical UK hospitals. There is hence a need to pursue more energy efficient options for PV and, crucially, no evidence currently exists in literature suggesting that natural ventilation has been exploited for PV purposes.

1.1. Objectives and Justification of Study

The aim of this study is to demonstrate the feasibility of using buoyancy as a driving force for natural personalised ventilation (NPV) in a novel way which delivers fresh air to patients in hospital wards. The case for using natural ventilation in ward ventilation within the UK comes from two main sources. Firstly, empirical evidence from weather studies indicate that for up to 8 months of the year, external thermal conditions in the UK favour the use of natural ventilation as shown in Figure 1 for the city of London

This figure uses HTM 03-01 range of 18-28°C internal ward temperature (DoH, 2007). Secondly, the WHO has produced guidelines (Atkinson, et al., 2009) for utilising natural ventilation for infection control of healthcare buildings in which an absolute rate of 60 L/s.patient was 'strongly recommended' for general patient wards. As PV systems are designed to achieve such prioritisation of airflow directly over occupants, this study demonstrates how PV systems can work with natural ventilation to meet required airflow rates. Although room temperature will be considered, comfort is not part of current research objectives.

2. Methods

Two methods are used in this investigation: dynamic thermal simulation (DTS) and computational fluid dynamics (CFD). The DTS investigations were used to assess annual bulk airflow patterns in the context of seasonal variations, and current guidelines on ward ventilation rates. The CFD studies predicted detailed room air distribution, effectiveness of heat removal, thermal stratification and contaminant dilution or removal efficiency. In both DTS and CFD studies, no control of the thermal environment was modelled as the goal was to evaluate the capacity of the proposed system to bring in fresh air. A single-bed ward, sized according to the specifications of the Activity Database, ADB (DoH 2010) guideline, was modelled using both DTS and CFD programs. The ward dimensions were 5 m x 5 m and a height of 3 m. Three architecturally distinct concepts of delivering air over patients were conceived to exploit the buoyancy effects for supply air which, due to density differences, would fall into the space from a ceiling duct, before rising again upon being heated to escape via a stack. These concepts are illustrated in Figure 2. Figure 2a shows the entire supply from a wide duct (Case 1), while Figure 2b (Case 2) and Figure 2c (Case 3) show smaller supply ducts supported with variations of low-level inlets for supplementary ventilation.

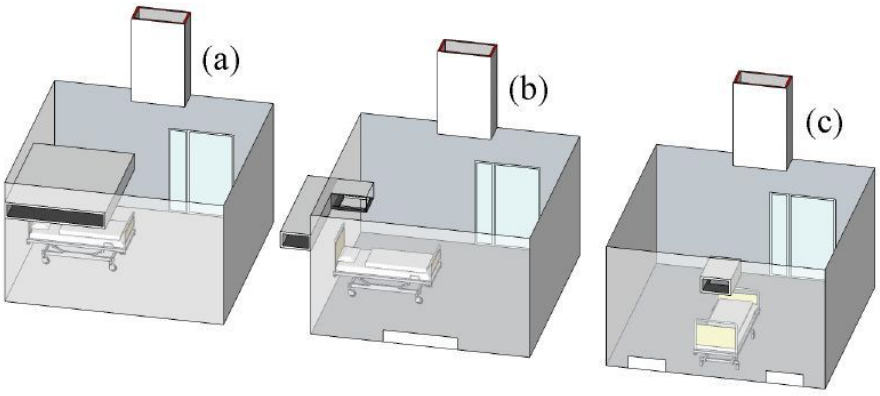

Figure 2. Three conceptual design cases for proposed NPV.

The ducts in all cases serve to prevent entrainment of stale air with incoming fresh air which is released at the desired location. The openings were sized according to CIBSE's guidance for single-sided ventilation, using a temperature differential of 1 K (CIBSE, 2005). This gave an opening area of 0.66 m^2 for 6 ac/h based on ventilation provisions of HTM 03-01 (DoH, 2007). For simplicity the stack heights were 3 m with cross-sectional area sized according to methods outlined in Lomas and Ji (2009). Based on floor area of the model wards, the computed cross-sectional area of stack was found to be to 0.25 m^2.

2.1 DTS Inputs and Assumptions

The wall constructions for the wards comprised 100 mm outer-leaf brickwork, 58.5 mm Styrofoam insulation, 100 m medium concrete blocks and 15 mm gypsum plaster finish, giving a U-value of 0.35 W/m^2K. The roofs were made of 150 mm cast concrete, glass fibre quilt and bituminous felt with tiles, having a CIBSE U-value of 0.25 W/m^2K while floors were 130 mm concrete with 3.06 W/m^2K. Low pressure ducts were assumed to be made of insulated sheet metal with CIBSE U-Value of 0.65 W/m^2K. The occupancy schedule assumed one patient to be always present and two healthcare workers whose presence was scheduled intermittently. Occupants accounted for 380 W of peak internal heat sources while lighting and equipment contributed 70 W and 75 W respectively.

2.2 CFD Boundary Conditions

CFD simulations were carried out using a commercial package Phoenics, (Cham, 2009) using 52,920 cells to achieve converged results. Heat gains for occupants were purely convective and similar to assumptions made in the DTS models. The assumed breathing points of each occupant were represented using points of interest (POIs) shown graphically and with coordinates (in plan and 3D) in Figures 3a and 3b respectively. The convection-to-radiation split for the lighting was 20:80 (CIBSE, 2006). All other surfaces were assumed to be adiabatic. The RNG k-ε turbulence model (Yakhot and Orszag, 1986) was applied with the Boussinesq approximation for buoyancy. The external air temperature was assumed to be 20 °C. A passive scalar contaminant source (C1) was emitted from an orifice of 0.0025 m^2 located at the sitting visitor's mouth and based on Xie et al (2007), the speed of coughing was taken to be 10 m/s with a mass flow rate of 0.03 kg/s. The temperature of cough was taken as 32 °C with density of particles similar to that of air, consistent with the observed behaviour of passive contaminants such as droplet nuclei (Morawska, 2006; Jiang et al., 2009). The limitations and validity of using passive scalars for bio-aerosol modelling of respiratory diseases using CFD can be found in Hathaway et al. (2011) and in Mao and Celik (2010). From these references, pathogenic particles less than 2 µm in size are known to be fully airborne with negligible mass. Therefore, it was assumed in this work that passive scalars could be used for modelling bio-aerosols.

3. Ventilation Performance Metrics

3.1 Contaminant Removal Efficiency

The first metric applied to this study is contaminant removal efficiency, CRE (Zang, 2005). A passive

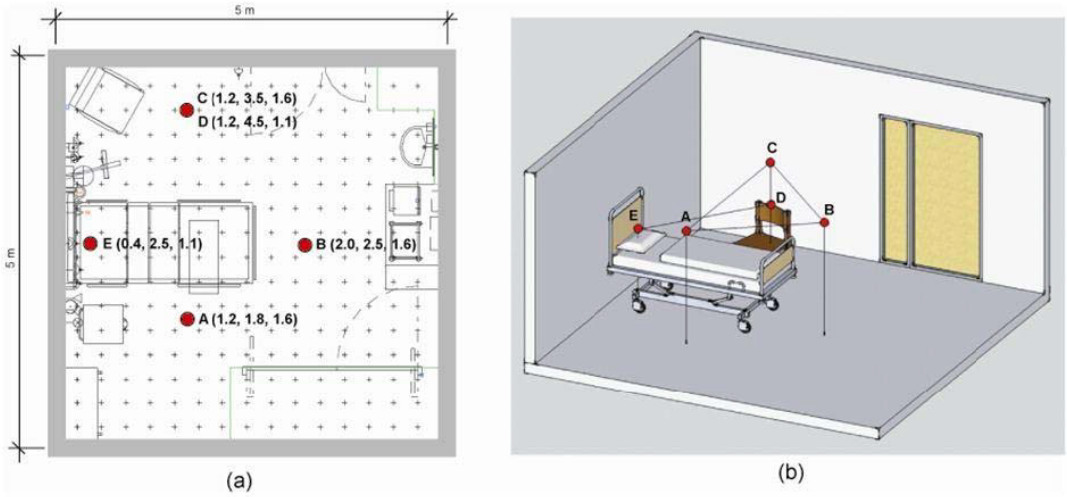

Figure 3. The points of interest (POIs).

scalar airborne contaminant (C1) representing a generic bio-aerosol was assumed to be emitted from a sitting visitor's mouth (POI = E). The initial non-dimensional concentration of 1.0 was assigned to C1. CRE was estimated using the model described in Equation (1):

$$\mathrm{CRE} = \frac{C_e}{C_p} \tag{1}$$

where
C_e is contaminant concentration at outlet
C_p is contaminant concentration at specific POI.

An ideal CRE would be equivalent to 1.0. Three other metrics were used to evaluate the performance of each ventilation technique. These are local air change index, (LACI), mean air exchange efficiency (MACE) and effectiveness of heat removal (EHR), all derived by Awbi (2003).

These metrics have also been demonstrated and applied in Karimipanah et al., (2007 and 2008). LACI is calculated from the ratio of mean age of air in the room to the mean age of air at the POIs. The nominal time or air turnover time τ_n is essential in calculating LACI accurately and it is calculated from Equation (2):

$$\mathrm{LACI} = \frac{\tau_n}{2\overline{\tau}_p} \tag{2}$$

where
$\overline{\tau}_p$ is age at particular point (in this case at POI).

MACE is derived according to Karimipanah, et al. (2007) as shown in Equation (3):

$$\mathrm{MACE} = \frac{\tau_n}{2\overline{\tau}_i} \times 100\ [\%] \tag{3}$$

where $\overline{\tau}_i$ = local age of air at a point in space (e.g. POI). EHR is derived as follows in Equation (4):

$$\mathrm{EHR} = \frac{T_e}{T_m} \tag{4}$$

In this case, T_e is temperature at exhaust; and T_m is mean room temperature. Air turnover time (ATT) is a time constant of a ventilation system's capacity to remove a contaminant from a well-mixed space (Zhang, 2005). The model is given by Equation (5) and is also referred to as the nominal time. The ATT of a ventilation system is measured in seconds and should not be construed as CRE, which deals specifically with efficiency (of contaminant removal) and is non-dimensional.

$$\mathrm{ATT} = \frac{V}{Q} \tag{5}$$

where
V is volume (m^3) and
Q is flow rate (m^3/s).

Specifically, the inverse of ATT is air turnover rate (Q/V) which is not employed as a metric in this study.

Table 1. Number of days of occurrence of 6 to 10 air changes per hour at two openings.

		< 6 ac/h	6 to 7ac/h	7 to 8 ac/h	8 to 9 ac/h	9 to 10 ac/h	> 10 ac/h
$0.66m^2$	**Case-1**	60 days	59 days	80 days	50 days	17 days	99 days
	Case-2	46 days	49 days	74 days	66 days	26 days	104 days
	Case-3	50 days	53 days	78 days	61 days	22 days	101 days
$0.25m^2$	**Case-1**	345 days	18 days	3 days	0 days	0 days	0 days
	Case-2	342 days	20 days	3 days	0 days	0 days	0 days
	Case-3	346 days	18 days	2 days	0 days	0 days	0 days

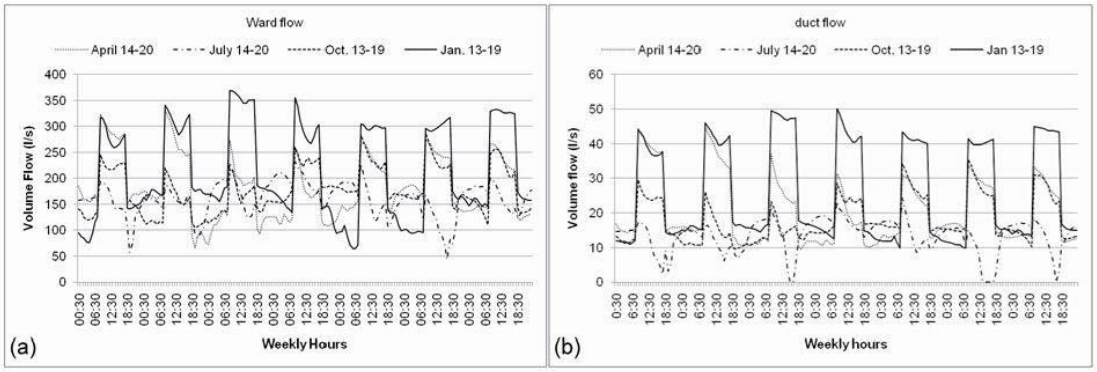

Figure 4. Weekly flows for 0.66 m^2 opening into (a) ward and (b) duct.

4. Results and Discussion

4.1 Bulk Airflow Characteristics

Ventilation rates of 60 L/s.patient and 6 ac/h were used as a basis for assessing all cases. Table 1 summarises the number of days for which specific ranges of air change rates were achieved for each case. The predicted variation in bulk airflow pattern over four different weeks in each ward is shown in Figure 4a for Case 2 when areas of openings are 0.66 m^2. This shows volumetric flow in a typical week in the middle of the four seasons (April 14-20 for spring; June 14–20 for summer; October 13–19 for autumn and January 13–19 for winter). Figures 5a and 5b are for the scenario when stack cross-sectional area is 0.25 m^2 giving insight into the capacity for NPV to meet the required airflow rates.

Other Cases (1 and 3) were also computed for similar weeks but are not reported, as the pattern is largely similar. Notably, (from Table 1 and Figure 4a) the three NPV concepts are all robust enough to meet the 6 ac/h requirement.

With respect to the WHO recommended flow of 60 L/s,patient (which the NPV strives to meet) actual flows through the duct of Case 2 are shown in Figure 4b. Although the flows generally fall short of 60 L/s.patient and fluctuations due to seasonal variations do occur, this result demonstrates the potential for the NPV to deliver the minimum design flow rate. Similarly, total flows into the ward when cross-sectional stack area is 0.25 m^2 are shown in Figure 5a while actual flows through the NPV duct for same stack size are given in Figure 5b

Whereas the direct flow through the NPV duct is significantly lower when stacks are 0.25 m^2 compared to when they were 0.66 m^2; with proper design and manipulation it is possible to enhance the performance of the NPV system to meet the optimum flow rate. For instance, when effects of wind or fan-assisted modes of natural ventilation (both not considered in this study) are incorporated, the potential of NPV becomes more apparent. Indeed, if 60 L/s.patient must be maintained in summer, fan assistance may be necessary in situations when temperature differentials are small,

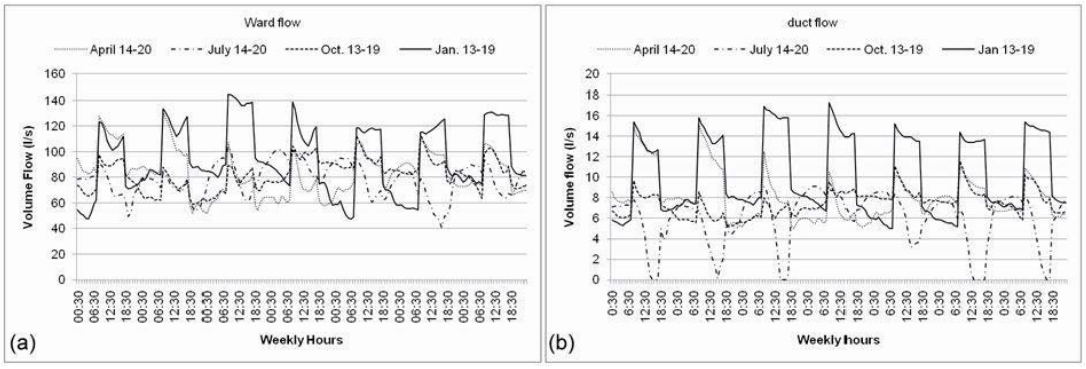

Figure 5. Weekly flows for 0.25m^2 opening into (a) ward and (b) duct.

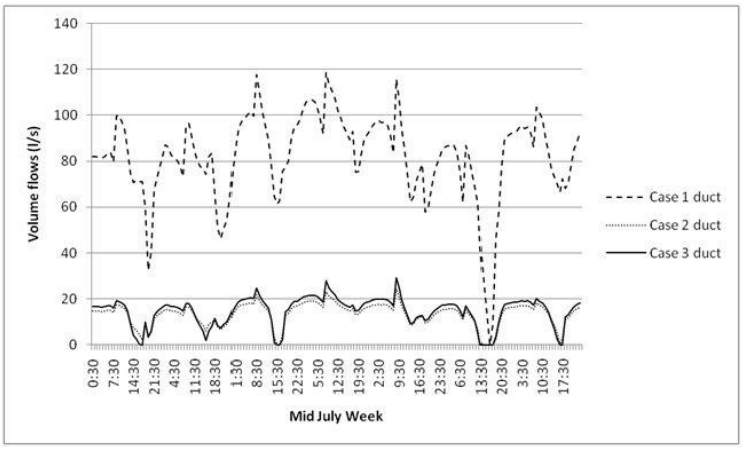

Figure 6. Weekly flow of air into ducts of Cases 1, 2 and 3.

and buoyancy-induced flows are sluggish. Even then, the potential for overheating has to be considered too. A comparison of the flow through the NPV ducts for cases 1, 2 and 3 are shown in Figure 6 for a mid-July week. Clearly, the large duct of the NPV in Case 1 outperforms the smaller ducts in Cases 2 and 3. The optimum duct size that would deliver sufficient flow rates for the patient as well as background ventilation for the ward, lies somewhere between Case 1 and Case 3 and this presents an interesting theme for further research.

4.2 CFD Output: The Ventilation Metrics

The CFD investigation sought to capture the fresh air distribution in the NPV cases and to evaluate the performances of the cases using metrics mentioned earlier (LACI, MACE, EHR and ATT). The values of these metrics for Cases 1, 2 and 3 are given in Figure 7. The ATT for Case 1 is 170.45 s while that of Cases 2 and 3 are 352.66 s and 170.44 s respectively. It is noticed that while there is a correlation between the Age, LACI, MACE, EHR and ATT (where Case 2 records the best set of values as shown in Figures 7a, 7b and 7d respectively), the same is not true for contaminant removal. With respect to efficiency of contaminant removal, there is no generalised way of providing a performance evaluation. This indicates that contaminant removal requirements in a ward would depend on who is most at risk, as each Case is largely unique for the POIs. Notably though, the CRE values at point D (source location) are similar for each case.

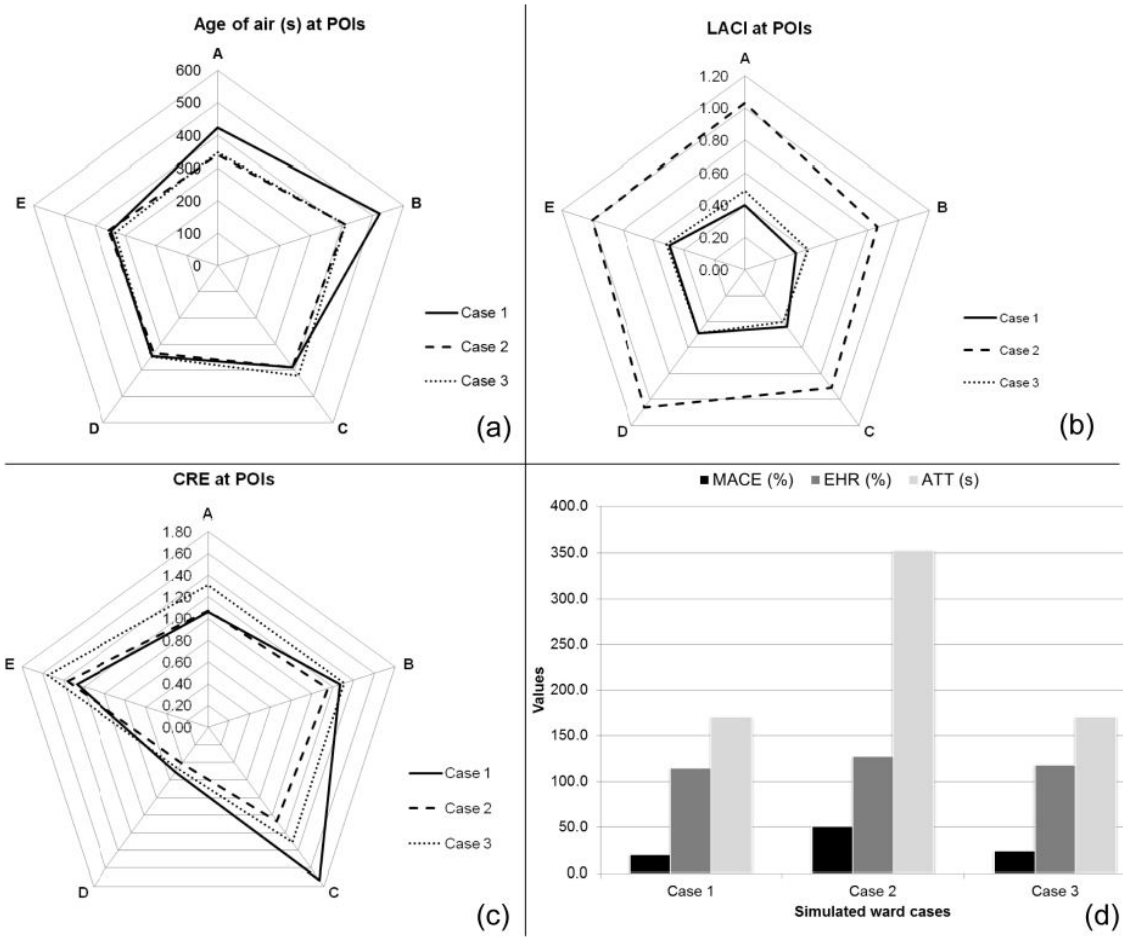

Figure 7. Airflow metrics with (a) Age (b) LACI (c) CRE and (d) MACE, EHR and ATT for all Cases.

When interpreting Figure 7, it should be noted that for some of these metrics, a lower value is ideal e.g. for Age and ATT which deal with time; whereas for LACI, CRE, MACE and EHR, higher values are desirable. Figure 7c suggests that flow through the NPV duct of Case 1 performs well as identified by CRE at POIs B and C; the NPV duct in Case 3 performs well in CRE at POIs A, B and E, and to some extent at point C. Compared with previous results, it is obvious that the performance of an NPV system in delivering the airflow rates is not directly proportional to its effectiveness in dilution or removal of contaminants from a space. Careful studies of the clinical needs of each ward space should determine which strategy is best. Figure 7d reveals the MACE, EHR and ATT performances of each strategy. It can be observed that while there is marginal difference in EHR values (percentages) the differences in MACE are significant. The MACE for case 2 is 50.4% which is about twice the MACE of Cases 1 and 2 which are 19.5% and 23.3% respectively.

4.3 CFD Output: Room Air Distribution

In Case 1, the large downward flow of air, caused by the large size of opening and temperature difference, creates substantial mixing around the bed area (see Figure 8). It should be noted that the top of the inlet duct was located at 0.5 m below the ceiling which separates the incoming air from stale buoyant air accumulating at the ceiling level.

The presence of low level inlets and a raised higher NPV inlet in Cases 2 and 3 do not appear to provide as much mixing as Case 1 around the patient's bed area. This is indicated by the typical weekly airflow patterns for each season as indicated in Figure 6.

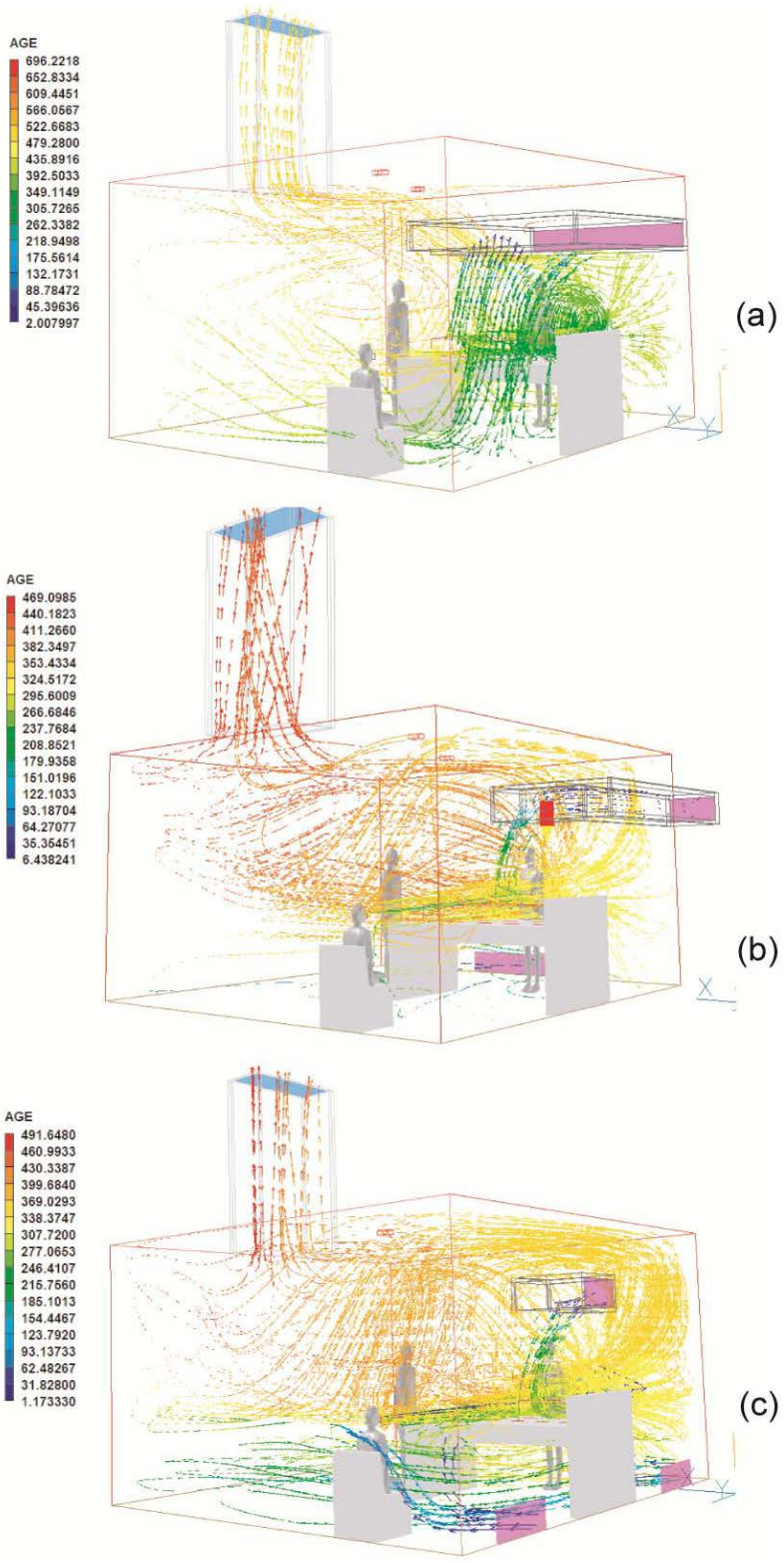

Figure 8. 3D vector streamlines in (a) Case 1, (b) Case 2 and (c) Case 3.

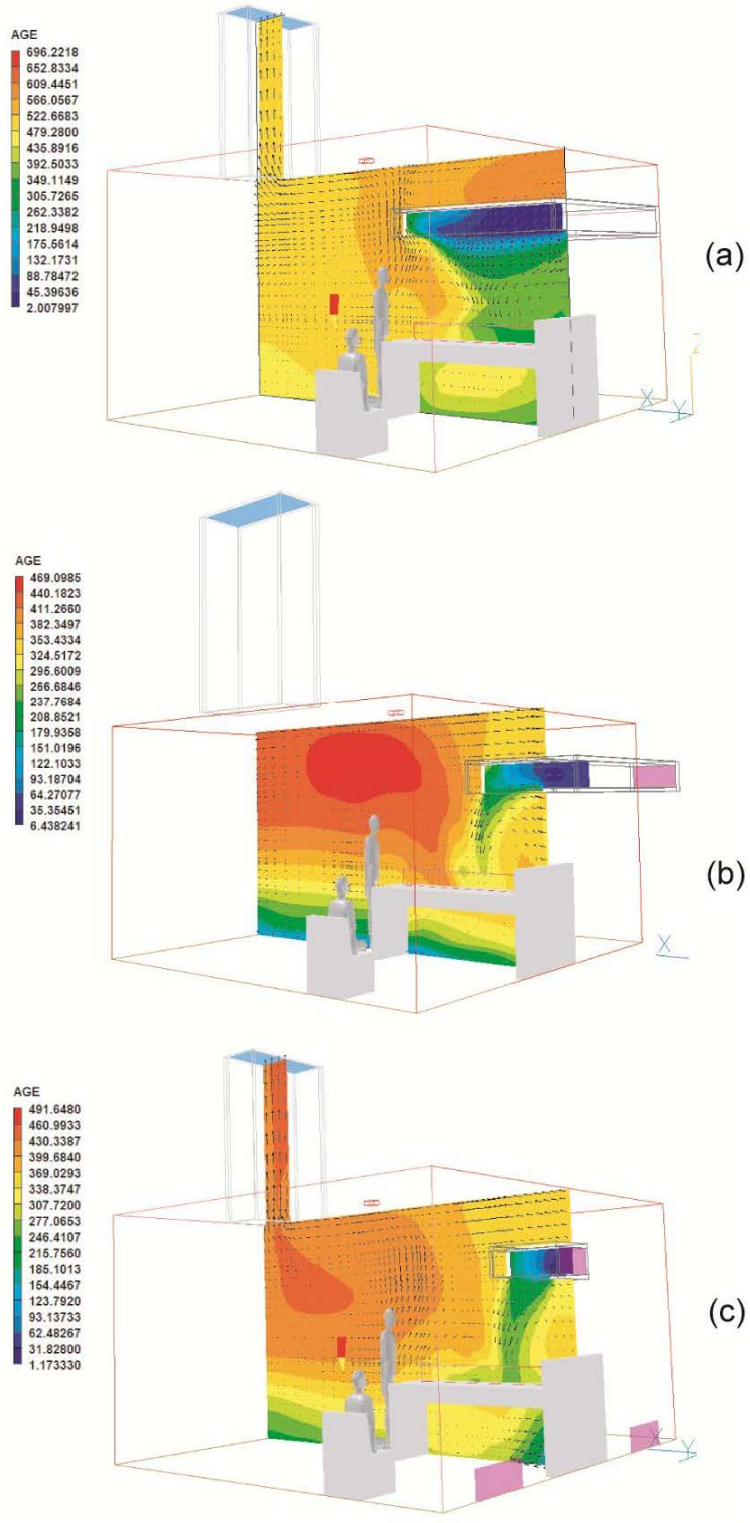

Figure 9. Age of air and 2D Vectors in (a) Case 1, (b) Case 2 and (c) Case 3.

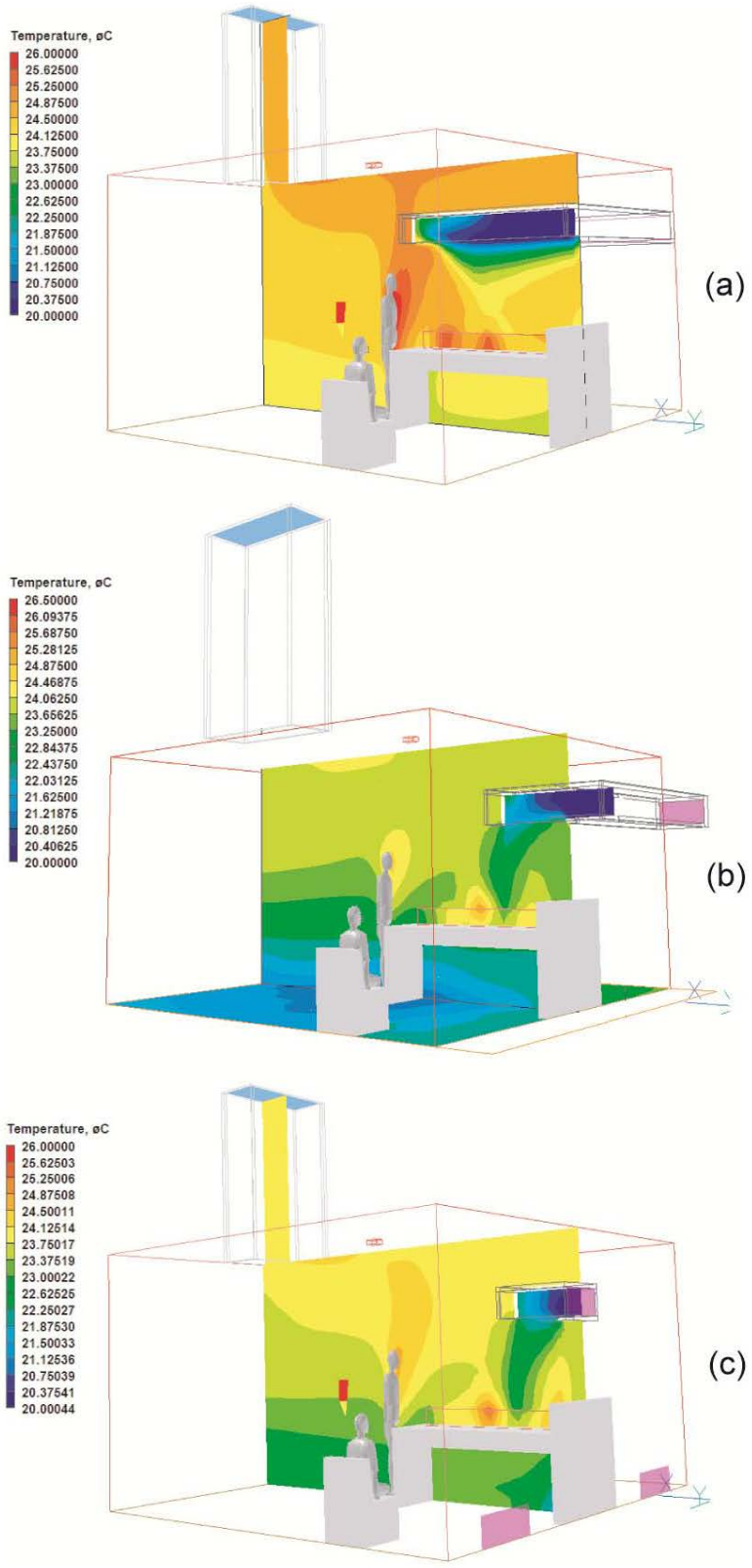

Figure 10. Temperature contours in (a) Case 1, (b) Case 2 and (c) Case 3.

The significant difference can be attributed to the smaller mass of air descending from the NPV inlet in both Cases 2 and 3. However, this behaviour contrasts with the age of air at POIs shown in Figure 7 where Case 1 has relatively higher age of air values than Cases 2 and 3. The behaviour of air through the different NPV ducts is depicted by streamline vectors which indicate the pattern and direction of air from inlets to outlets as shown in Figures 8a, 8b and 8c.

The age of air observed above the duct in Case 1 supports this mixing behaviour (Figure 9a). In all Cases, but most prominently in Cases 2 and 3, the fresh air does not just descend into the space, but a horizontal 'throw' from incoming jet of air is observed for about 0.3 m in Cases 1 and 3 and up to a distance of about 0.5 m in Case 2 (Figures 9a, 9b and 9c). This throw distance of a cooler incoming jet of air has been described by Koestel (1955) and in Awbi (2003).

The throw distance can be used to determine the exact location of fresh air delivery (e.g. the upper portion or midsection of a lying patient) although an adjustable system could be more practical. In Case 1, the significance of the large duct area is evident, where the mean age of air at bed level is about 305 s compared to Case 2 where it is up to 353 s. A large pocket of relatively stale air (469 s) collects at the ceiling level in Case 2. The age of air at POI-E (patient's head) is found to be lowest in all cases (Figure 7a).

The thermal distribution obtained from the three Cases (Figure 10) also exhibits different behaviour for each strategy. At the bed level, there is a more even temperature distribution over the patient in Case 1 (~23.7 °C), compared with Cases 2 and 3. In the latter cases, the momentum of the incoming air generates a cool zone in the centre of the bed (about 22.8 °C for Case 2 and about 22.6 °C for Case 3) relative to the head and foot of the bed where the temperature is about 24 °C.

In Cases 2 and 3 however, cooler air rising from low inlets encroaches the foot of the bed, and with respective mean room temperatures being 23.2 °C and 23.5 °C compared to Case 1 where the mean is 24.2 °C; this signifies the importance of having the low level inlets, which is absent in Case 1. It can be deduced that low level inlets contribute to cooling and heat removal (EHR values for Cases 2 and 3 are higher than Case 1).

Conclusions

Three conceptual cases were investigated to demonstrate a novel approach for delivering fresh air directly to patients in hospital wards. DTS and CFD modelling indicated that all three concepts are feasible and could be useable without extra heating for up to 8 months in a year (early March to end of October) in an urban setting such as London. This is using the 18 – 28 °C thermal range (of HTM 03-01) as shown earlier in Figure 1. However, detailed comfort studies will be required under several climatic conditions as well as the use of heating setpoints. All concepts are able to create more mixing than is obtainable in a basic (bottom-to-top) displacement strategy. Mixing has already been shown to be a desirable feature of ward ventilation for bio-aerosol control (Beggs et al., 2008) and in this case, mixing occurs due to the falling of cooler air and its subsequent rise upon being heated by internal sources. Case 1, in which the supply inlet is large and directly over the patient, has significant potential for prioritising patient ventilation over that of co-occupants. This could be especially beneficial for immune-compromised or immune-suppressed patients. Cases 2 and 3 demonstrate the benefits of having supplementary airflow from floor level inlets. Overall, the study shows that direct delivery of cooler air into the breathing zone of the patient with warmer air in the surrounding area (usually desirable in PV systems) can be achieved using natural ventilation powered by buoyancy forces. These concepts present a novel approach to meeting fresh air and contaminant dilution requirement of hospital wards. Using an NPV strategy in wards can help 'keep the air within as pure as the air without' (Nightingale, 1859) as well as lowering the energy requirements of hospital ward ventilation. There are however opportunities for further refinement of the NPV technique.

Future work will include experimental validation of the NPV technique using brine in water. There is also need for further studies in terms of: thermal comfort performance for each strategy; patient interaction in adjusting flow rates to their needs; potential for hybrid modes/heat recovery and fan assisted flows as well as the impact of wind. As with all natural ventilation systems in the UK, over-heating in summer where outdoor temperatures could approach 30 °C, as well as determining appropriate trickle ventilation rates for winter are also opportunities for further research. The possibility to utilise the NPV system for retrofitting multi-bed wards is also being considered as

personalised airflow for each bed area could improve individual comfort and alleviate airborne cross-infection amongst co-patients. Finally, integrating NPV systems with advanced natural ventilation (ANV) methods (Lomas, 2007) is likely to be a realistic way forward and worth developing.

Acknowledgements

The authors are grateful to Engineering and Physical Sciences Research Council (EPSRC) and the Health and Care Infrastructure Research and Innovation Centre (HaCIRIC), both of the UK, for supporting this research.

References

Atkinson J, Chartier Y, Pessoa-Silva CL, Jensen P, Li Y and Seto W-H. (ed.): (2009) "Natural Ventilation for Infection Control in Health-Care Settings". WHO Guideline, WX 167.

Awbi HB: (2003) "Ventilation of Buildings" 2nd Ed. ISBN 0415270553, Taylor & Francis (E&FN Spon).

Beggs CB, Kerr KG, Noakes CJ, Hathway EA and Sleigh PA: (2008). "The ventilation of multiple-bed hospital wards: Review and analysis". *Am J Infect Control.* **36**, (4), pp250-259.

Cham: (2009). Cham Phoenics version 2009, available from: Cham Co. Ltd. http://www.cham.co.uk/.

CIBSE: (2005) "Natural ventilation in non-domestic buildings", CIBSE Applications Manual AM10. (2nd Ed.), The Chartered Institution of Building Services Engineers Publications.

CIBSE: (2006) "Guide A: Environmental Design" The Chartered Institution of Building Services Engineers, London.

DoH: (2006) "Health Technical Memorandum 07-02: EnCO2de-, Making Energy Work in Healthcare, Environment and Sustainability" Department of Health Estates and Facilities Division, The Stationary Office, ISBN: 0-11-322731-0.

DoH: (2007) "Department of Health: Heating and ventilation systems; Health Technical Memorandum 03-01: Specialised ventilation for healthcare premises" 2007, TSO (The Stationery Office). Also available at: www.tsoshop.co.uk.

DoH: (2010) "Activity Database, Space for Health: Information for healthcare premises professionals". Available at: https://spaceforhealth.nhs.uk/

Hathway EA, Noakes CJ, Sleigh PA and Fletcher LA: (2011) "CFD simulation of airborne pathogen transport due to human activities", *Building and Environment*, **46**, (12), pp2500-2511.

IES: (2010) "Integrated Environment Solutions, IES VE Software Version 6.2.0.3", www.iesve.com.

Jiang Y, Zhao B, Li X, Yang X, Zhang Z and Zhang Y: (2009) "Investigating a safe ventilation rate for the prevention of indoor SARS transmission: An attempt based on simulation approach", *Building Simulation*, **2**, (4), pp281-289.

Karimipanah T, Awbi HB, and Moshfegh B: (2008) "The Air Distribution Index as an Indicator for Energy Consumption and Performance of Ventilation Systems", *Journal of the Human-Environment System*, **11**, (2), pp77-84.

Karimipanah T, Awbi HB, Sandberg M and Blomqvist C: (2007). "Investigation of air quality, comfort parameters and effectiveness for two floor-level air supply systems in classrooms", *Build Environ.*, **42**, pp647-655.

Koestel A: (1955) "Paths of horizontally projected heated and chilled air jets", *Trans. ASHAF*, **61**, pp231-232.

Lomas KJ and Ji Y: (2009). "Resilience of naturally ventilated buildings to climate change: Advanced natural ventilation and hospital wards", *Energy Build.*, **41**, pp629-653.

Lomas KJ: (2007). "Architectural design of an advanced naturally ventilated building form", *Energy Build.*, **39**, pp166–181.

Luciano JR: (1977). "Air Contamination in Hospitals", Plenum Press. New York.

Melikov A, Cermak R, and Mayer M: (2002) "Personalized ventilation: evaluation of different air terminal devices". *Energy Build.*, **34**, pp829–836.

Melikov AK, Cermak R, Kovar O, and Forejt L: (2003). "Impact of airflow interaction on inhaled air quality and transport of contaminant in rooms with personalised and total volume ventilation". In *Proc. Healthy Buildings 2003,* Singapore, **2**, pp592–597.

Melikov A; (2004). "Personalized ventilation". *Indoor Air*, **14** (Suppl. 7), pp157–167.

Mao S and Celik IB: (2010). "Modelling of indoor airflow and dispersion of aerosols using immersed boundary and random flow generation methods", *Computers & Fluids*, **39**, (8), pp1275-1283.

Morawska L: (2006). "Droplet fate in indoor environments, or can we prevent the spread of infection?" *Indoor Air*, **16,** pp 335-347.

Nielsen PV, Jiang H, and Polak M: (2007) "Bed with integrated personalized ventilation for minimizing cross infection". In *Proc. Roomvent 2007, 10th Int. Conf. Air Distribution in Rooms*, Helsinki, Finland, 13–15 June, **3**, pp387–396.

Nielsen PV, Polak M, Jiang H, Li Y and Qian H: (2008) "Protection against cross infection in hospital beds with integrated personalized ventilation". In *Proc. Indoor Air 2008, 11th Int. Conf. on Indoor Air Quality and Climate*, Copenhagen, Denmark, 17–22 August.

Nielsen PV: (2009). "Control of airborne infectious diseases in ventilated spaces". *J. R. Soc. Interface*, **6**, S747–S755.

Nightingale F: (1859) "Notes on Nursing: What It Is, and What It Is Not". Available at http://www.gutenberg.org/.

Niu J, Gao N, Phoebe M, and Zuo H: (2007). "Experimental study on a chair-based personalized ventilation system", *Build Environ.* **42**, pp913–925.

White PAF: (1981) "Protective Air Enclosures in Health Buildings" Macmillan Press Ltd. London.

Xie X, Li Y, Chwang ATY, Ho PL and Seto WH: (2007) "How far droplets can move in indoor environments–revisiting the Wells evaporation–falling curve" *Indoor Air*, **17**, pp211–225.

Yakhot V and Orszag SA: (1986) "Renormalization group analysis of turbulence" *J Sci Comput.* **1**, pp3–51.

Zang Y: (2005) "Indoor Air Quality Engineering" CRC Press, New York.

APPENDIX B: Paper 2 (Building and Environment)

Building and Environment 56 (2012) 211–222

Contents lists available at SciVerse ScienceDirect

Building and Environment

journal homepage: www.elsevier.com/locate/buildenv

Performance evaluation of natural ventilation strategies for hospital wards – A case study of Great Ormond Street Hospital

Z.A. Adamu*, A.D.F. Price, M.J. Cook

School of Civil and Building Engineering, Loughborough University, Loughborough, LE11 3TU, United Kingdom

ARTICLE INFO

Article history:
Received 8 December 2011
Received in revised form
24 February 2012
Accepted 12 March 2012

Keywords:
Buoyancy-driven airflow
Hospital ward
Thermal comfort
Energy consumption
Dynamic thermal modelling
Ceiling-based natural ventilation

ABSTRACT

Natural ventilation is attractive due to its potential lower energy consumed by healthcare environments but maintaining steady/adequate airflow rates and thermal comfort is challenging in temperate countries. Although many contemporary hospitals use traditional windows for natural ventilation, there are alternative strategies that are largely under-utilised probably due to lack of knowledge of their ventilation performances. Each alternative has design implications and airflow characteristics – both of which affect thermal comfort and heating energy. This study evaluates the performance of buoyancy-driven airflows through four selected natural ventilation strategies suitable for single-bed hospital wards. These strategies are: single window opening, same side dual-opening, inlet and stack as well as ceiling-based natural ventilation (CBNV), a new concept. These strategies have been explored via dynamic thermal simulation and computational fluid dynamics, using a new ward of the Great Ormond Street Hospital (GOSH) London as a case study. Results reveal that 25% trickle ventilation opening fraction is required to achieve required airflow rates and acceptable thermal comfort in winter, and with exception of window-based design, other strategies minimise summer overheating to different extents. The CBNV concept uniquely shields fresh air and delivers it to isolated parts of wards or directly over patients (i.e. personalisation). This provides higher air quality at such locations and creates mixing which aids comfort and dilution. The findings demonstrate how quantitative data from simulations can be used by designers to meet qualitative or sensory design objectives like airflow direction and thermal comfort with respect to the energy consumed in space and time.

1. Introduction

1.1. Natural ventilation in hospitals

A major advantage of natural ventilation in healthcare facilities is the significant ventilation rates (18–24 ACH) that can be achieved for wards which can be a bonus if airborne infection is a risk [1]. In their study of a Hong Kong hospital, Qian et al. [1] showed that up to 69 ACH was possible given the right environmental conditions and that when carefully integrated with exhaust fans, such hybrid systems can eliminate the unreliability of driving forces like wind or problems associated with pressure breakdown due to activities like opening of doors. The apparent need in countries like the UK, to refurbish existing stock of hospital buildings with low-energy ventilation solutions in a manner that permits their resilience to a warming climate makes natural ventilation a logical alternative [2]. Studies on achieving low-energy hospital ventilation in the UK [3] have therefore been undertaken to demonstrate how shaft and stack-based strategies as used in advanced natural ventilation [4] could be considered for wide-scale adoption –including for refurbishing of existing hospital stock. ANV has benefits of relying not on winds but on buoyancy forces [4]. Other stack-based approaches that could have potential for ventilation of hospital facilities include solar chimneys [5] although there is no strong evidence of its application in healthcare. These alternative ventilation strategies are not yet in the mainstream as design options but they have lower carbon and operational costs compared to mechanical ventilation [4,5]. The choice of a natural ventilation strategy for refurbishment will be constrained by the logistic of constant usage [6] and patient susceptibility to noise [2]. One strategy that has not featured as a refurbishment option in contemporary literature is same side dual-opening, which though may be restricted to low-rise facilities [7] could be better than existing single (window) openings.

As for room air distribution, displacement ventilation which is a feature of buoyancy-driven natural ventilation has advantages over mixing ventilation in healthcare settings as long as bio-aerosols are

* Corresponding author. Tel.: +44 755 231 2811; fax: +44 1509 223 981.
E-mail address: z.a.adamu@lboro.ac.uk (Z.A. Adamu).

0360-1323/$ – see front matter © 2012 Elsevier Ltd. All rights reserved.
doi:10.1016/j.buildenv.2012.03.011

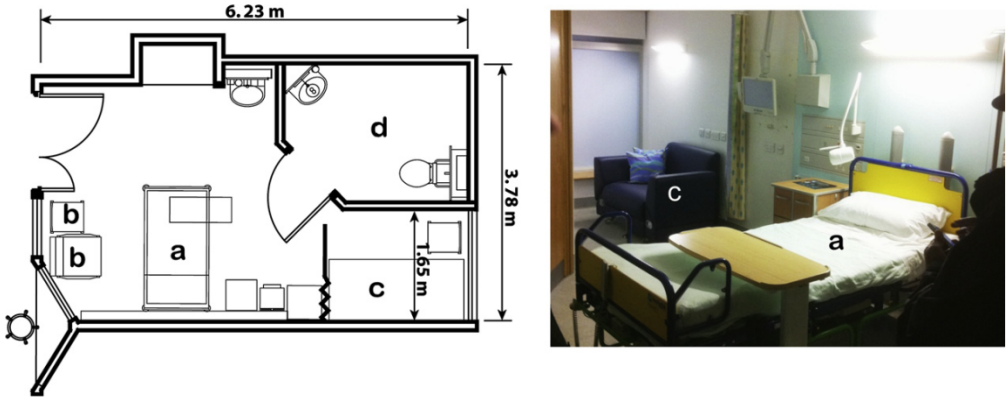

Fig. 1. The GOSH ward showing (a) patient bed (b) visitor chair (c) visitor sleeping couch/bed (d) bathroom.

not of concern in a particular space earlier shown by Beggs et al., 2008 [8] and more recently in Li et al. (2011) [9]. In particular, displacement is not recommended for ward ventilation whether in single or multi-patient spaces since it is adjudged as incapable of protecting healthcare workers, patients or their visitors [11]. This deduction brings with it some implications on the displacement strategies already in use or emerging/recommended for hospital wards, such the buoyancy-driven ANV [3]. However, a new approach to buoyancy-induced natural ventilation which is capable of providing not only mixing but personalised delivery of fresh air over patients has been demonstrated [10] through the use of ceiling mounted supply ducts with exhaust air escaping via stacks. These findings and their implications hence make it necessary to evaluate the performance of selected (and fundamentally different) natural ventilation strategies in terms of their airflow rates/room air distribution patterns, thermal comfort as well as energy potential.

There are currently many different modelling approaches used in predicting building ventilation including analytical models, empirical models, multizone models, zonal models, models, experimental models and computational fluid dynamics (CFD) models [11]. The use of CFD in particular has risen steadily since 2002, especially within the research community, where it has become a major tool for airflow investigations. The wide applicability, acceptability of CFD as a ventilation modelling tool is however tied to its concurrent use with theoretical and experimental models as verification and validation of available codes become increasingly important [12]. This study intends to use

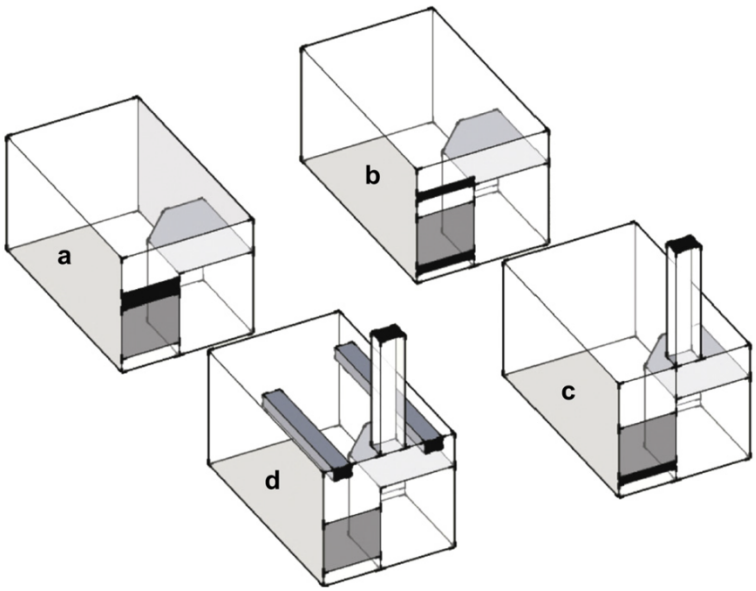

Fig. 2. Four strategies with openings shown in solid black for (a) single window (b) Dual-opening (c) inlet and stack (d) Ceiling-based strategy.

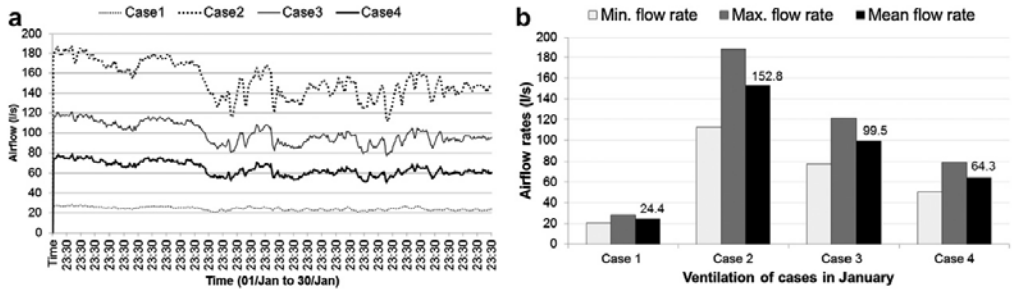

Fig. 3. Airflow via 25% opening in January showing (a) Monthly flows and (b) Minimum, maximum and mean flow rates.

(zonal) dynamic thermal model (DTM) as well as CFD modelling as methods of airflow investigation.

The UK's Department of Health technical memorandum (HTM 03-01) allows natural ventilation as an acceptable method of ventilation of hospital spaces but is silent on how this can be achieved, especially with respect to the six air changes per hour (ACH) [13] which was specified as minimum rate for wards. This rate has been suspected as being 'arbitrary' due to lack of evidence-based performance studies [14,15]. The World Health Organisation (WHO) on the other hand has documented a specific guideline for natural ventilation of hospitals, in which it strongly recommends the rate of 60 l/s/patient [16]. However, there is no specific guidance on how this rate can be accomplished with acceptable climatic conditions or for that matter, what the rates should be during winter when trickle ventilation needs to be maintained. It has also been established that for hospital wards, airflow rates need to be deployed with engineered patterns as well as directions of airflow for effective ventilation of hospital wards [17]. Besides, achieving this rate steadily with natural ventilation is challenging because, unlike mechanical ventilation, the driving forces (i.e. wind and buoyancy) tend to fluctuate depending on climatic factors as well as occupancy and miscellaneous internal heat loads.

There is, therefore, a need for evidence-based investigations to support these provisions for the benefit of practitioners. In this regard, dynamic thermal simulation (DTS) and computational fluid dynamics (CFD) modelling techniques can simultaneously provide annual bulk airflow and detail room air distribution characteristics, respectively.

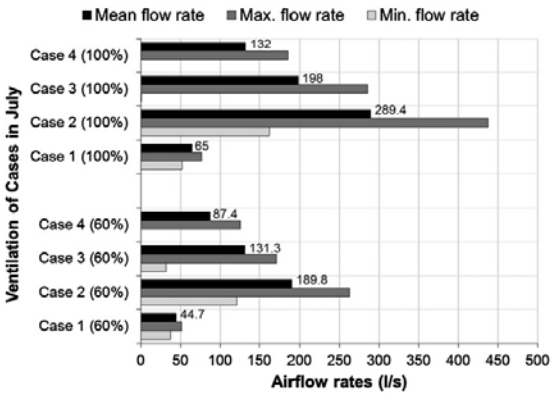

Fig. 4. Airflow rates for all cases in July through 100% and 60% opening fraction.

1.2. Objectives and justifications

The primary aim of this work is to provide a comparative evaluation of the ventilation, thermal comfort and energy performances that can be expected from four selected natural ventilation strategies applicable to hospital wards. The natural ventilation will focus on bouyancy-driven flows only, which can be valuable for facilities located in urban locations where wind forces are unreliable or minimal. The study specifically intends to: (a) determine and evaluate airflow and energy performance of different configurations of natural ventilation openings with respect to their sizes and locations; (b) establish if and how regular, as well as trickle ventilation rates, can be achieved with buoyancy-induced airflows keeping the WHO's natural ventilation requirement of 60 l/s/patient in perspective; (c) present a concept called ceiling-based natural ventilation and its benefits regarding airflow and energy and finally (d) to demonstrate benefits of a two-pronged approach for studying the airflow, comfort and energy performance of natural ventilation using dynamic thermal simulation and computational fluid dynamics. The research findings should empower designers with sufficient knowledge needed to make informed decisions with respect to low-energy hospital ventilation, especially considering that over 40% of a typical UK hospital's energy goes into space conditioning [18].

1.3. The natural ventilation concepts

The Great Ormond Street Hospital (GOSH) has a single occupant wards one of which was adopted as a case study to achieve the stated objectives. The dimensions of the GOSH ward are 3.78 m × 6.23 m with ceiling height of 3.5 m, giving a floor area of 23.55 m^2 and a volume of 82.42 m^3. The existing window is 1.65 m wide and 0.5 m high and is situated 1.9 m above a fixed glazing of same width. The plan and section of the GOSH ward are shown in Fig. 1.

Table 1
Performance evaluation of mean airflow rates.

		Case1	Case2	Case3	Case4
25% Dec–Feb	Mean flow rate (l/s)	23.77	142.50	93.10	60.30
	Meets EN ISO 7730 47 l/s?	No	Yes	Yes	Yes
	Meets WHO's 60 l/s/patient	No	Yes	Yes	Yes
100% Mar–Nov	Mean ACH	3.63	20.1	13.43	8.83
	Meets HTM's 6 ACH?	No	Yes	Yes	Yes
	Mean flow rate (l/s/patient)	69.9	387	258.6	170
	Meets WHO's 60 l/s/patient?	Yes	Yes	Yes	Yes
60% Mar–Nov	Mean ACH	2.41	12.42	8.35	5.53
	Meets HTM's 6 ACH?	No	Yes	Yes	No
	Mean flow rate (l/s/patient)	46.3	239	160.8	106.4
	Meets WHO's 60 l/s/patient?	No	Yes	Yes	Yes

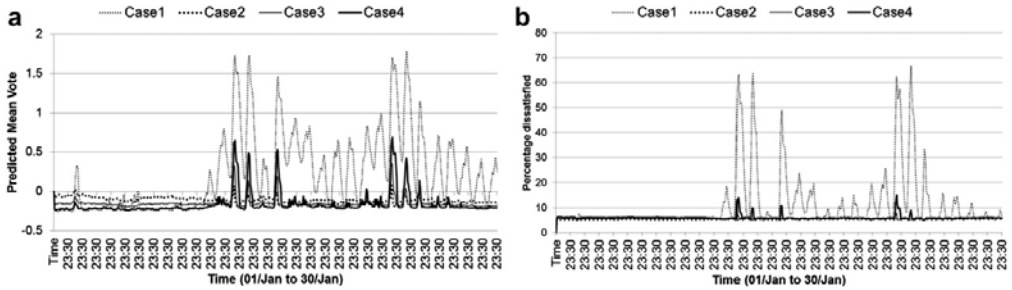

Fig. 5. Opening fraction at 25% with 20 °C setpoint for (a) PMV and (b) PPD.

The following subsections describe the various strategies investigated with the above ward design. Although there is an en-suite bathroom which has an extract fan that works occasionally, the operation of this fan is not modelled in terms of its impact on airflow or energy. This is because the goal of this study is to demonstrate the feasibility of buoyancy-driven flows into the main ward space only.

1.3.1. The (as-built) single window concept

Case 1 model, which serves as the base case for this investigation, was derived directly from the as-built design of the GOSH ward with minor modifications. It utilises a 1.9 m high-level top-hung window on the exterior wall just above a fixed glazed area (Fig. 2a). Although CIBSE [19] provides guidance on sizing single vent buoyancy-driven openings using Eq. (1), there was no evidence that this model was applied in sizing the window of the existing ward. It is presented here nevertheless for the benefit of designers:

$$A = Q/C_d\sqrt{(T_{int}+273)/(T_{int}-T_{ext})gH} \quad (1)$$

where A = area of opening (m^2); Q = required ventilation rate (m^3/s); C_d = discharge coefficient; T_{int} = internal temperature (K); T_{ext} = external temperature (K); g = gravitational force per unit mass ($m\ s^{-2}$) and H = height of opening. In the application of this model for single vent, C_d typically takes a value of 0.25 [19]. In Fig. 2a, the window opening is shown in shaded black, above the fixed glazed area.

1.4. Same side dual-opening

Case 2 of this study was conceived as two openings of same area, separated vertically. The areas of inlets and outlets for dual-opening vents were also obtained from Eq. (1), from [19]. In this instance, the value of C_d is typically 0.6 and H becomes the height *between* the two openings. It is evident from Eqn. (1) that the required flow rate, Q, the temperature differential ΔT i.e. $T_{int} - T_{ext}$ and the vertical distance between the two openings H, will all affect the size of opening, A. In this study, C_d and g were taken as 0.6 and 9.81 m/s^2 respectively, while ΔT was assumed to be 1. Computed area of opening was found to be 0.78 m^2 when the vertical distance, H, between the openings is maximised to 2.5 m, measured from their centres. Due to width of existing glazed area (1.65 m) being a constraint (see Fig. 1) in determining width of opening, the dimensional sizes applied in the model were therefore 0.47 m × 1.65 m. The schematic of this case is represented in Fig. 2b showing the fixed glazing between the two openings.

1.4.1. Inlet and stack concept

Case 3 concept comprises a low-level inlet and exhaust stack and can be regarded as a type of advanced natural ventilation (ANV), as presented in [4]. In this study, the inlet and stack strategy is analogous to edge-in, edge-out ANV strategy because both openings are on the external wall. The stack sizes were based on the estimation techniques given by Lomas and Ji [15] where the free opening area is assumed to be a fraction, F, of the gross floor area. Typical values of F range from 0.5 to 1.5% and the computed area should not be less than the area of the supply inlets so that flow is not restricted. Furthermore, the authors indicated that even though the value of F may appear small, it is the length of shaft which then becomes a primary determining factor in the stack performance. The process used to derive the cross-sectional area of a stack (As) when a given space of width W, has a depth $n.W$ (where n is the aspect ratio or depth/width) is given by [15] as shown in Eq. (2).

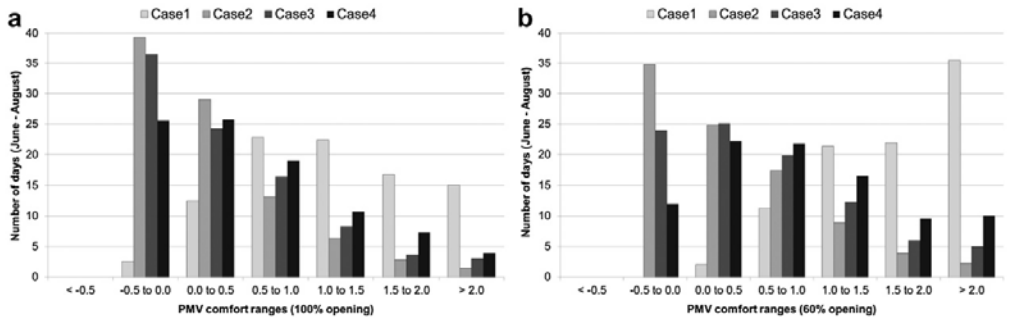

Fig. 6. PMV comfort ranges at 100% and 60% openings for July to August.

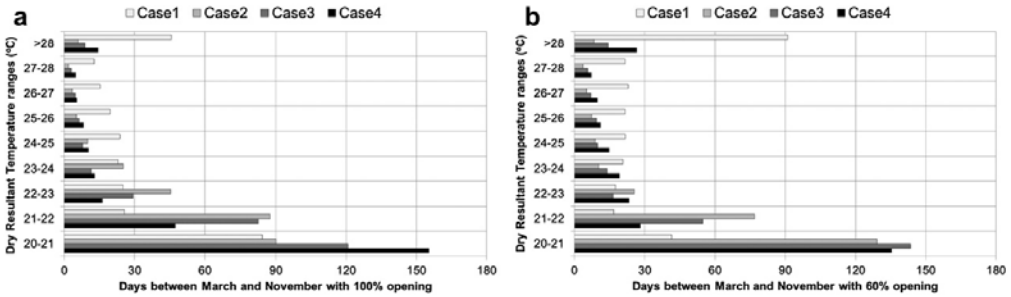

Fig. 7. Indoor temperature ranges in non-winter months at (a) 100% and (b) 60% opening.

$$As = FnW^2\ \left(m^2\right) \tag{2}$$

In this study, F is assumed to be 1.5% of floor area (or 0.015) and $n = 1.65$, and $W = 3.78$. As was then computed to be 0.35 m^2. The exhaust stacks were then translated into dimensional size of 0.5 m × 0.7 m; and for simplicity, the stack height was assumed to be equal to floor height (i.e. 3.5 m). The area of stack therefore determined the size of air inlets, which for Case 3 was a low-level inlet sized at 0.21 m × 1.65 m. The conceptual design of Case 3 is shown in Fig. 2c.

1.4.2. Ceiling-based natural ventilation concept

Case 4, which is the ceiling-based natural ventilation strategy, is based on conceptual principles that depend on two main factors. The first is the density of cooler air falling into the warmer surrounding; while the second is the behaviour of non-isothermal jet including its flow velocity in a duct as well as drop distance of the air [20]. Assuming that the indoor air is at a higher temperature than outdoor air, the denser cooler would travel along the duct and then drop down before rising again. Subsequently, the air gets heated due to convective and radiated heat from miscellaneous internal sources (lighting, people and equipment) before it escapes into the stack whose pressure boundary is much higher than the duct inlet (Fig. 2d). The use of ceiling-based ducts to convey fresh air under buoyancy has already been demonstrated in previous work by Adamu et al. [12], as a novel way of achieving natural personalised ventilation (NPV). The NPV was shown to be natural ventilation equivalent of mechanised PV systems as defined in [21], however, as conceived for this study, the NPV concept can be applied for isolated spaces even if personalised delivery of air to patients is not the goal. Ceiling-based natural ventilation is, therefore, a superior nomenclature which encompasses the essential concept and in this study because one duct serves NPV purposes while the other provides supplementary fresh air to isolated spaces. The height of the stack relative to the duct inlets determines the neutral pressure line (NPL) which in addition to temperature differential determines the pressure difference needed to induce buoyant flow of air. The openings in Case 4 had same size as Case 3 (0.35 m^2) which was shared equally by the two ducts giving each an area of 0.175 m^2. This translated into 0.5 m × 0.35 m in absolute dimensions. Stack size in this case remained similar to Case 3 in cross-sectional area, height and location.

2. Materials and methods

2.1. Performance metrics

Three categories of performance metrics are used in this study. For ventilation, the 6 ACH of HTM 03-01 [13] and the 60 l/s/patient of the WHO's guideline on natural ventilation for hospitals [16] are used in addition to EN ISO 7730 recommendation [22] of 2 l/s/m^2 dilution rates for Class I buildings, which for the given floor area of 23.55 m^2, equates into ≈ 47 l/s. For thermal comfort, the predicted mean vote (PMV) ranges specified for Class I buildings under the EN ISO 7730 standard [22] is applied in addition to ISO's PMV and PPD indices [23] by cross-referencing these metrics with two heat set-points used in the DTS simulation (i.e. 18 and 25 °C). The PMV ranges for this Class in [22] are defined as $-0.2 < PMV < +0.2$. For energy performance, the CIBSE energy benchmarks for Category 20 buildings (hospitals) of 90 kWh/m^2 (electricity typical) and 420 kW h/m^2 (fossil-thermal) are used with floor areas according to RICS gross internal area [24]. Hence, given a total floor area of 23.55 m^2 (for the selected ward) each strategy has to aim for

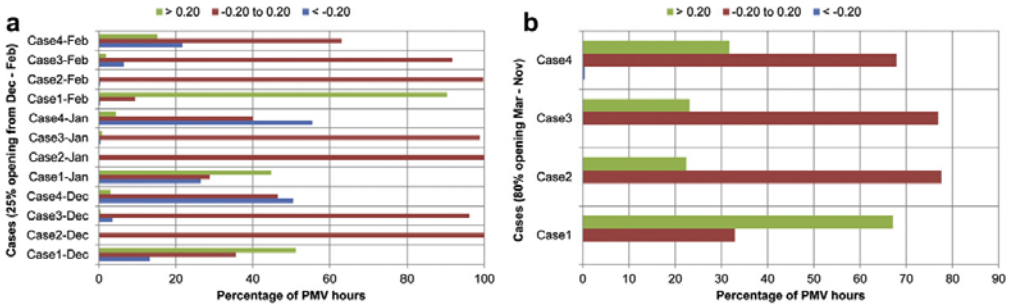

Fig. 8. Thermal comfort results using PMV for (a) winter months and (b) Non-winter months.

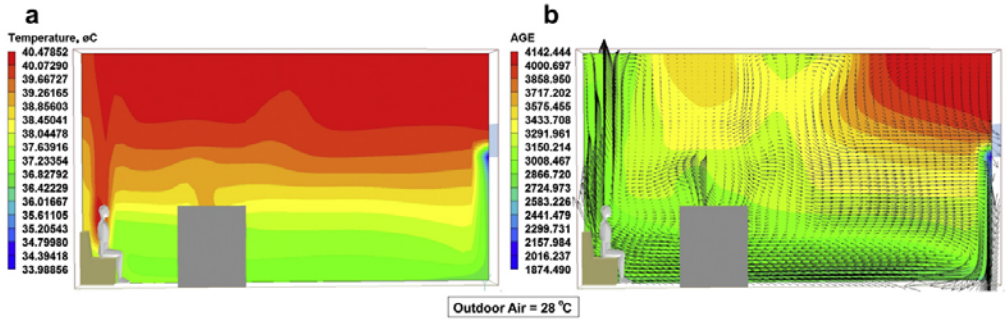

Fig. 9. Summer CFD results for Case 1 showing (a) Indoor temperature (b) Age and 2D flow vectors.

2.12 MWh if electricity is to be used or 9.89 MWh if fossil-thermal source of energy is to be used.

2.2. Base case and general assumptions

For the CFD input, the chamfered edges of the bathroom (Fig. 1) were neglected due to software constraints. The mechanical extract operating in the bathroom was also omitted as the study aims at evaluating buoyancy-driven flows only. However, openings were made in the bathroom to allow air move in (low-level inlet) and out (high-level outlet); but only for Cases 2, 3 and 4. Three occupants were considered: a lying (covered) patient emitting 50 W; a standing healthcare worker (HCW) and a sitting visitor, both emitting 90 W each. Lighting produced 70 W and, assuming it was made of fluorescent lamps enclosed in prismatic luminaires [25], the convection-to-radiation ratio of 20:80 becomes applicable. Hence, two luminaires emitted 7 W each while the floor radiated 56 W. For the CBNV, due to the observed expected throw of cooler incoming jet of air [12,20,26], the first duct over the patient had its canopy shortened backward (using engineering judgement) by 0.3 m from the assumed centre of the patient. This offset was expected to enable the jet of air to drop directly over the patient in the longitudinal direction of airflow. The second duct had its canopy extended 0.6 m further along the longitudinal direction creating a displacement of 0.9 m between the two CBNV duct supply points. An absolute floor-to-ceiling height of 3.5 m was used in all cases.

2.3. Dynamic thermal simulation model

DTS investigation was performed using IES [27]. With the exception of external wall, other surfaces were assumed to be adiabatic, similar to the conditions to be applied to the CFD models. The external wall construction was made of two plies of 100 mm brickwork and medium concrete, sandwiching 58.5 mm Styrofoam insulation, and finished with 15 mm gypsum plaster for a combined U-value of 0.35 W/m^{2}K. The intermittent occupancy had three people at peak times accounting for a total of 230 W. Equipment and lighting contributed 75 W and 70 W respectively, with the former scheduled to be off from 10:00pm to 06:00pm daily. Two heat setpoints (18 °C and the second at 20 °C) were considered while no cooling was considered even in summer. The air inlets and outlets were modelled at different opening factions but, for this study, 25% opening fraction for winter months as well as 60% and 100% for summer period are reported. For winter, the goal was to assess opening fractions for adequate trickle ventilation (with respect to occupant comfort and heating energy) for all four strategies, whereas for summer the objective was to measure comfort and potential for overheating with openings fractions at 60% and 100%.

2.4. CFD model

CFD modelling was performed using a commercial package PHOENICS [28]. With the exception of fixed glazing, all other surfaces were assumed to be adiabatic. After a series of pilot simulations to establish sufficient mesh, each case model comprised 45,000 cells (a grid of 30 × 50 × 30 cells) although in Case 3 and 4, the z-axis grid was increased to 60 cells to account for the stacks within the computational domain. The Boussinesq buoyancy approximation was applied to the standard RNG k–ε turbulence model of Yakhot and Orszag [29]. Satisfactory convergence was achieved using criteria of 0.1% error and this was

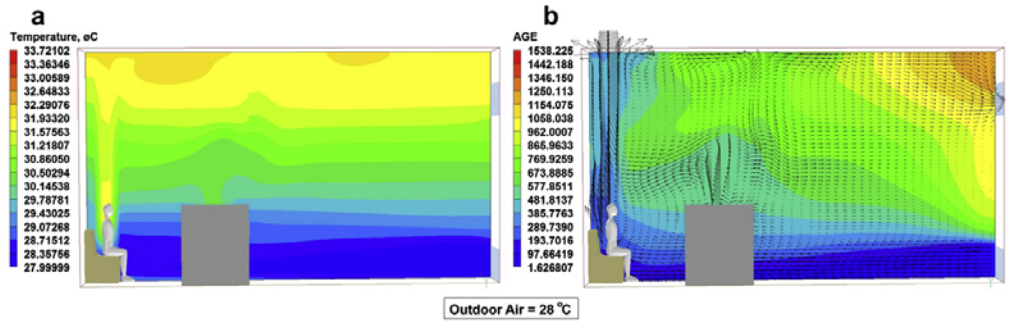

Fig. 10. Summer CFD results for Case 2 showing (a) Indoor temperature (b) Age and 2D flow vectors.

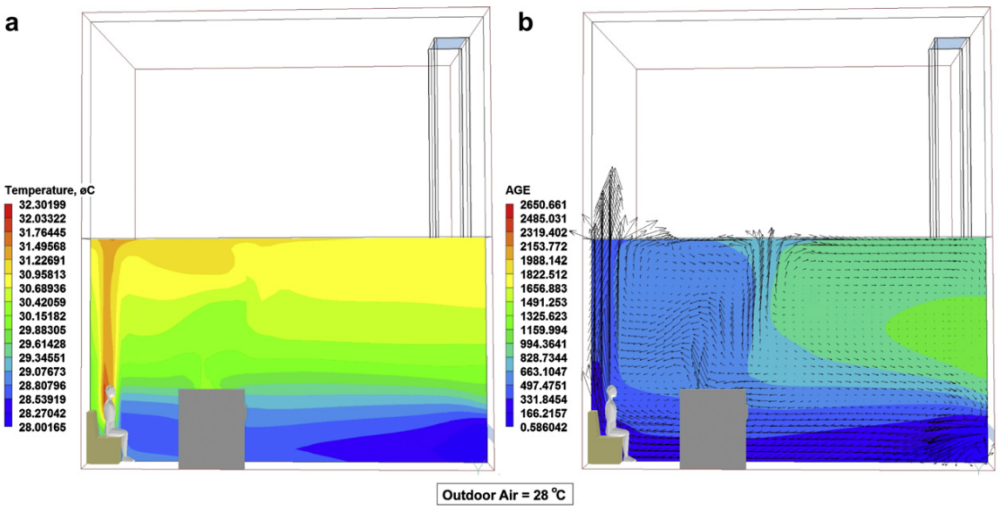

Fig. 11. Summer CFD results for Case 3 showing (a) Indoor temperature (b) Age and 2D flow vectors.

attained after 5000 iterations for Case 1 and 2; and after 6000 and 7000 iterations for Cases 3 and 4 respectively.

3. Results and discussions

The results from both DTS and CFD investigations are discussed below under airflow, comfort and energy sub-headings.

3.1. Airflow rates

Using January as a sample winter month, all cases exhibit marked differences in airflow regimes as shown in Fig. 3. The monthly flow patterns via each strategy is shown in Fig. 3a, while minimum, maximum and mean airflow rates regime for each case is shown in Fig. 3b.

To rank their performances in airflow capacity, Case 1 produces the least flow rates, followed by Cases 4, 3 and Case 2. While it is proper to evaluate these flow rates with respect to either HTM 03-01 [13] or WHO's 60 l/s/patient [16], this ought to be done against backdrop of draught potential in January. In this regard, Case 2 presents the highest risk of draught, followed by Cases 3, 4 and 1.

The month of July was used for assessing the airflow rates in summer period (Fig. 4) when openings are either fully open at 100% or constricted to 60% of their maximum size. The observed pattern of airflow performance mimics the winter (January) situation where in increasing order, their performances are ranked: Case 1, Case 4, Case 3 and Case 2. Fig. 4 shows the difference between airflow through openings at 100% and 60% fractions in which Case 2 performs better in both instances. Again, airflow rates into Case 1

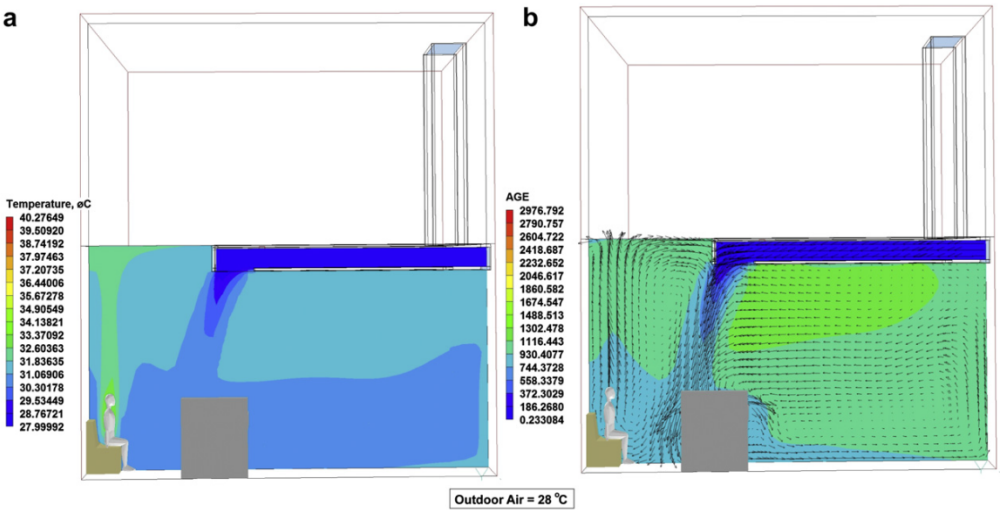

Fig. 12. Summer CFD results for Case 4 showing (a) Indoor temperature (b) Age and 2D flow vectors.

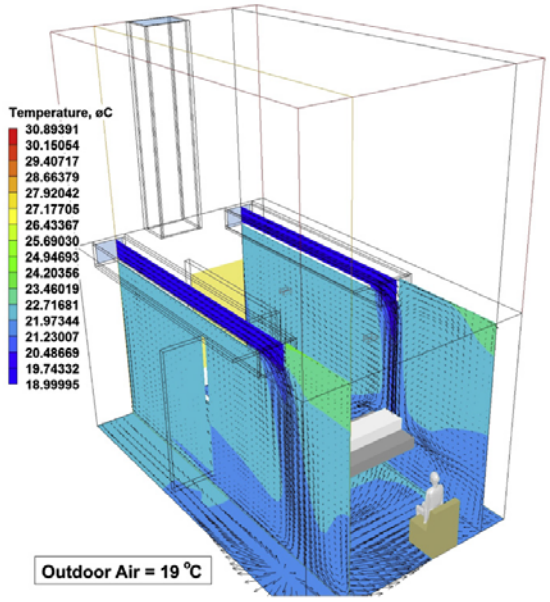

Fig. 13. Airflow vectors through both CBNV ducts.

are seen to fall significantly below those of other cases as observed from mean values for the month.

Table 1 is a summary of how each strategy has performed using recommendations of HTM 03-01, the WHO and EN ISO 7730.

Notably, the (as-built) window-based strategy of Case 1 is unable to meet any of the airflow rates required by HTM 03-01, WHO or EN ISO 7730, except when openings are at 100% between March and November. Conversely, the CBNV meets the required flow rates for all the standards except at 60% opening between March and November for HTM 03-01, but even then 5.53 ACH is just marginally short of 6 ACH.

3.2. Thermal comfort

The performance of each strategy regarding thermal comfort was evaluated using predicted mean vote (PMV), predicted percentage dissatisfied (PPD) as well as dry resultant temperature, all of which were obtained from DTS results. PMV is rated using a scale (ranging from +3 to −3) in which: +3 = hot; +2 = warm; +1 = slightly warm; 0 = neutral; −1 = slightly cool; −2 = cool and −3 = cold [23]. The potential for overheating was appraised from CFD results using an assumption of 28 °C outdoor temperature.

With a heat setpoint of 25 °C in January, the PMV values (Fig. 5a) are within acceptable range for all Cases with values generally around the ideal value of zero. This is with the exception of: Case 1, where for substantial number of days, PMV values exceed 0.5 and approach 1.5 (i.e. between slightly warm and warm); and Case 4 where PMV approaches 0.5 for 5 days. These comfort readings are supported by the predicted percentage of people who would be dissatisfied with their thermal environment (Fig. 5b), where it is observed that Case 1 would have up to 60% dissatisfied occupants on specific days.

For comfort in summer, the PMV values (Fig. 6a) and PPD values (Fig. 6b) taken for the entire summer period (July to August) indicate that both 100% and 60% opening fractions produce different patterns of indoor comfort ranges. Again, for both opening fractions, Case 1 has more days when both PMV and PPD values exceed 1.0 (slightly warm); but with over 15 days when PMV is in the 1.5 and 2.0 range.

Fig. 7, shows that during the non-winter months of March to November, the ventilation strategies would perform in terms of internal dry resultant temperatures ranges if openings were left at 100% (Fig. 7a) or when openings are constricted to 60% their original size (Fig. 7b). Noticeably, at 60% opening fraction (Fig. 7b), Case 1 performs relatively poorly with just 42 days falling within 21–22 °C range. Consequently this case also has the most days (91) when temperatures would exceed 28 °C which is three times as many days when other cases experience >28 °C temperatures.

At 100%, Case 4 (CBNV) performs exceptionally better in keeping temperatures between 20 and 21 °C during the non-winter months. This can be attributed to mixing behaviour previously observed for the NPV system in [12], as opposed to the displacement behaviour of the other three cases.

With regards to EN ISO 7730 standard [22], Fig. 8 is an indication of the percentage of hours where the given PMV ranges would be achieved in winter (Fig. 8a) and other months (Fig. 8b).

3.2.1. Overheating potential

The size and location of the single opening of Case 1 has been shown to cause discomfort in winter at 25% opening fraction. While this can is attributable to the low airflow rates in winter. During summer, when temperatures can exceed 28 °C, this ventilation strategy is also problematic. Firstly, airflow would be restricted due to entrainment of stale air with incoming fresh air, leading to conflict in airflow direction and hence reduction in flow rates (mean July flow rates are 65 l/s and 44.7 l/s at 100 and 60% fractions

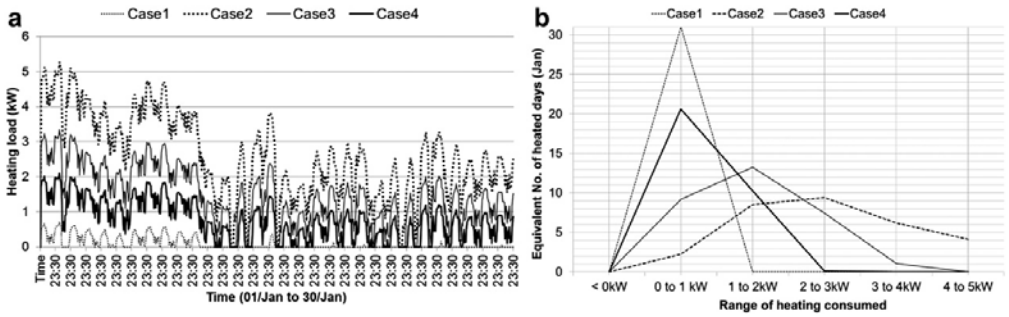

Fig. 14. Equivalent number of heating days (January).

Table 2
Performance ranking based on total energy (MWh) consumed in winter.

	Case1	Case2	Case3	Case4
December	0.028	1.6473	0.9143	0.4436
January	0.069	1.9334	1.1045	0.5709
February	0.0008	0.8501	0.4104	0.149
Total (MWh)	0.0978	4.4308	2.4292	1.1635
Rank	1	4	3	2

respectively). At 28 °C in summer specifically, this conflict is evident from high indoor temperature as suggested by CFD contours in Fig. 9a. Also, the Age of air and 2D flow vectors from CFD results in Fig. 9b indicate that indoor air will be quite stale. Secondly, because already warm stale air which ought to exit the room is forced to mix with incoming fresh air, this leads to overall build-up of internal heat. This build-up of heat helps to explain the apparent low winter energy consumption of Case 1 which scored number 1 in the energy rankings. It is also observed from Fig. 9a that internal temperatures could rise to as high as 40 °C (from top of window towards ceiling) when outdoor air is 28 °C, and the mean Age (Fig. 8b) of fresh air at lower portion of opening is 1874 s while Age of outgoing air is about 4000 s. The mean temperature at the bed and sitting visitor's head in this Case is ≈38 °C (Fig. 9a), a rise of 10 °C above outdoor air temperatures. This is a plausible explanation of why overheating does occur in summer when single openings are used in such spaces. The mean Age of air (Fig. 9b) at the bed level and visitor's head is also significantly high at ≈3008 s, an indication of staleness of air at these locations. The rising plume of hot air over visitor approaches 40 °C.

For Case 2, where there is clear distinction in flow airflow paths (Fig. 10), the room temperature builds up when outdoor air is 28 °C (Fig. 10a) is not as severe as in Case 1. The maximum indoor temperature is ≈32 °C towards the ceiling while the Age of air at outlet is ≈1254 s, and almost 0 s at inlet (Fig. 10b). Also, it is noticed that mean temperature around bed level (and head of sitting visitor) is ≈30 °C (a rise of 2 °C above outdoor air temperature). This is also the mean temperature of rising plume of hot air over the visitor. Also, unlike Case 1, the mean Age at these occupant locations is ≈419 s. The maximum room temperature in Case 2 is up to 8 °C lower than what obtained in Case 1, which emphasises the benefits of having segregated openings.

In Case 3, the mean temperature at the bed level and at visitors head location (Fig. 11a) is ≈29 °C representing a rise of just 1 °C above outdoor air temperature at that location, ignoring the rising plume of hot air (31 °C) over visitor. The maximum room temperature is 32 °C towards the ceiling. The Age of air is 0 s at inlet (Fig. 11b) and about 29 s at the bed level. These represent significant differences compared to Case 1 and 2.

For Case 4, when outdoor air is 28 °C, the CBNV offers more uniformity in both the mean temperature and Age of air in the space. There is a distinct lack of rising plume of hot air over the visitor, suggesting better comfort than in other cases and maximum room temperature is about 32 °C. Like in Case 3, at the patient's bed level the temperature is also ≈29 °C (Fig. 12a) i.e. 1 °C above outdoor air temperature. The absence stratification of indoor air temperature or Age of air unlike previous cases and this can be attributed to the mixing of room air due to drop and subsequent rise of incoming cooler air as shown by 2D vectors in Fig. 12b. This mixing characteristics clearly has comfort benefits, and further (planned) studies should reveal how this affects dilution of airborne contaminants.

Fig. 13 shows the predicted flow behaviour of both CBNV ducts using temperature and 2D flow vectors at outdoor temperature of 19 °C. The mixing offered by both ducts is evident even though the slice planes are in two dimensions, however, from the pattern of vectors on the floor (z-axis) planes which indicate distribution of cooler air in all directions is evidence of mixing characteristics offered by CBNV.

3.3. Heating load and energy consumption

January was also used as a sample winter month in which 25% opening fraction of openings can be used to evaluate heating energy patterns and to estimate the total heating required for each case. Fig. 13 describes the pattern of heating load using January as an exemplar winter month for all cases, where Fig. 13b suggests that Case 1 would have the least heating load, with required power peaking at 1.5 kW. While this represents the lowest heating load of all four cases, this comes with a comfort penalty as evident from PMV values (Fig. 5a) which are high for about two-thirds of the month.

From Fig. 14, it can be seen that at the same (25%) opening fraction in January, the heating load/power that would be imposed on the Cases differ (Fig. 14a). Case 2 in particular would experience the most heating load in January with values approaching 5 kW, although this peak value would be for just four days, while for most other days, the load would fluctuate between 0.5 and 4.5 kW (Fig. 14b). Case 3 at 25% opening fraction would result in up to 13 days where the space has to cope with between 1 and 2 kW of heating load (Fig. 14b) but a maximum load of 3.5 kW would be required for 1 day only. Finally, while the heating power in Case 4 would actually approach 2.5 kW (for 1 day only) and this strategy would require up to 20 equivalent days of heating in January using 0.5 kW of power only (Fig. 14b).

Summarily, the cases were compared and ranked in terms of total monthly energy (in MWh) expected to be consumed for heating the entire winter months of December to January. Table 2 shows the results for each cases as well as their performance ranking.

The DTS modelling results can produce mean energy requirement from each strategy, which can become an input for CFD modelling of room heaters – and subsequently a potential source for customised sizing of room heating equipment. With 25% opening fraction in the month of January for instance, the mean heating requirements for all cases are shown in Table 3, when mean dry-bulb temperature is 3.75 °C.

For energy benchmarking of each Case, CIBSE's benchmark for hospitals i.e. Category 20 buildings [24] are used for evaluating

Table 3
Heating load at 25% opening for January.

Variable	Min. value	Min. time	Max. value	Max. time	Mean value	Watts per m^2
Case1	0 kW	10:30, 02/Jan	0.708 kW	05:30, 02/Jan	0.093	0.0039
Case2	0 kW	12:30, 13/Jan	5.279 kW	05:30, 02/Jan	2.599	0.11
Case3	0 kW	10:30, 13/Jan	3.341 kW	05:30, 02/Jan	1.485	0.063
Case4	0 kW	10:30, 12/Jan	2.096 kW	05:30, 02/Jan	0.767	0.033
Dry-bulb temperature	−3.6 °C	07:00, 02/Jan	11.9 °C	15:00, 24/Jan	3.75	

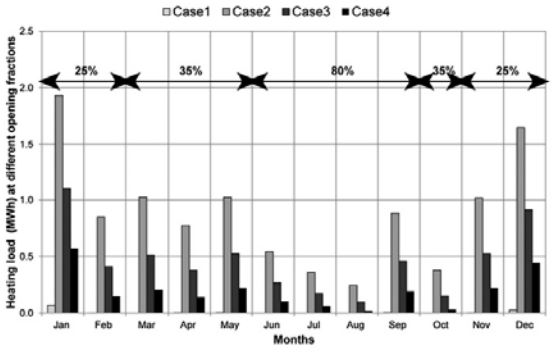

Fig. 15. Monthly heating loads at different opening fractions.

performance of each strategy. Appendix 1 (Table 4) provides a summary of monthly energy consumed using 80%, 35%, 25% and 12.4% opening fractions, as well as the annual summations. From the given table, the poor energy performance of Case 2 which allows significant flow rates is obvious because it goes over CIBSE's 90 kWh/m^2 benchmark [24] i.e. equivalent to 2.12 MWh for the 23.55 m^2 of ward space, even at 12.5% opening fraction. Only Case 1 and Case 4 fall below this benchmark at 12.5% and 25% opening fractions. Although, as discussed earlier, Case 1 (the as-built strategy which has a single opening) consumes significantly less energy even at 35% and 80% opening fractions, the CFD results show evidence of recirculation of outgoing air and hence re-heating of incoming fresh air indicating the consequent comfort penalties that will definitely ensue. Further work being planned on the impact of this recirculation on dispersal of airborne contaminants (and cross-infection) is expected to further shed light on the behaviour of this and other strategies.

A composite graph that combines different opening fractions and their consequent heating loads in attempt to normalise monthly consumptions is provided in Fig. 15. Added into monthly totals over a whole year, the energy consumed by each strategy would fall below the 90 kWh/m^2 benchmark. As no single Case consumes up to or above this electricity benchmark monthly or annually, the case for fossil-thermal (i.e. 420 kWh/m^2) was not considered for evaluation. From Appendix 1, the maximum to be consumed annually would be 32.753 MWh using 80% opening fraction in Case 2.

4. Conclusions

The performances of four architecturally distinct natural ventilation strategies were evaluated with respect to airflow capacity, thermal comfort and summer overheating as well as potential heating energy consumption in winter.

Strategies such as Case 2, Case 3 and Case 4 provide distinctly segregated flow paths for incoming and outgoing air (as shown previously by CFD Age of air and flow vector results). Although this segregation of flow openings is desirable for meeting high air change rates and dilution, it comes with energy penalties. Whereas the mean January airflow rates for Cases 2 and 3 are substantial at 152.8 l/s (≈7.9 ACH) and 99.5 l/s (≈5.2 ACH) respectively; in terms of heating energy, Case 2 was ranked last (at number 4), while Case 3 was ranked second to last in Table 1. Case 4 appears to be a good compromise among the cases due to its modest airflow (mean January flow is 64.3 l/s (≈3.3 ACH)) and its position is number 2 in the energy ranking (Table 2). The performance of Case 4 (CBNV) in terms of comfort and energy is attributable to its mixing behaviour, achieved regardless of its relatively modest airflow rates. Such mixing characteristics of the CBNV have previously being the exclusive reserve of mechanised ventilation systems, so it is encouraging that a low-energy (buoyancy-driven) natural ventilation alternative is feasible. The distinct difference in airflow rates performance is summarised in Table 1 where Case 4 meets all the minimum requirements of HTM 03-01, the WHO and EN ISO 7730; whereas Case 1 (window-based) fails to meet all, except for 6 ACH (HTM 03-01) and that is only if openings are left at 100% between March and November. The significant variations in airflow rates demonstrated by these four distinct strategies point to need for ventilation standards to be more comprehensive in suggesting established design strategies which can achieve the prescribed flow rates, for the benefit of designers and facility managers. It is inadequate to specify airflow rates without suggesting how they might be achieved. Subsequently, there is need for developing performance-based natural ventilation codes, which would encourage further research into more creative ways of using natural ventilation (other than windows) for hospitals and similar buildings.

Interestingly, HTM 03-01 (Section 2.6, p. 8) implies that single-sided natural ventilation is effective only to a depth of 3 m. However, the as-built reality of the new Great Ormond Street Hospital ward is that it utilises this strategy (i.e. the 1.9 m high window) in its single-bed wards which was modelled as Case 1 in this study. The creation of a lower inlet (i.e. converting it to same side dual-opening as in Case 2) will result in significant improvements in airflow rates. This would be a relatively cheaper and easier option than inlet and stack or CBNV, should refurbishment be considered for this or similar facilities. In fact, the airflow potentials of Case 2 is limited only by its significant winter energy demands, which can be countered with appropriate sizing and control mechanisms; or with heat recovery via bathroom exhausting. However, the WHO on the other hand, does not encourage the use of dual-openings for airborne contaminant control in multi-floor facilities due to dangers of cross flow from outlets of lower floor to inlets of higher floors [20]. But for facilities whose wards are not multi-floor, dual-openings remains a viable option especially for retrofitting purposes. It is probably second-best option to cross-ventilation in terms of airflow, but most modern facilities especially in urban locations are unable to have openings on two separate walls due to architectural and/or operational constraints.

The patterns and direction of airflow shown by CFD results indicate that alternative strategies (Cases 2, 3 and 4) are indeed better in many regards than Case 1. These results collectively help to explain the poor performance of single window openings when used for natural ventilation. Additionally, the DTS results have shown potential to assist designers in evidence-based sizing of heating equipment using mean monthly energy consumption, for whatever ventilation strategy is chosen. This approach has benefits especially at the schematic design stage when far reaching decisions are made about building configuration.

In general, the methods used in sizing openings were based on an empirical model in Case 2 and a rule of thumb in Case 3 and Case 4, however, while using the rule of thumb (percentage of floor area) has been tested and validated in previous studies of ANV systems similar to Case 3 [4,15]; using the same sizing technique for the CBNV is probably inappropriate. Apart from similarity in exhaust stacks, Case 4 differs significantly because the CBNV functions with elevated and horizontal supply ducts and a neutral pressure line which is reduced by the elevated ducts. A technique for

determining the appropriate size of ducts is therefore required and is under consideration. This is possible, for example by using trial and error to systematically increasing the percentage of floor area from current 1.5% upwards until a size which delivers equivalent flow rate as Case 3 is achieved. The mixing property of Case 4 is a feature that has hitherto been the exclusive reserve of mechanical ventilation. This mixing is evidently pronounced by falling and rising of CFD airflow vectors, through the absence of temperature strata (common in displacement ventilation); as well as through the minimisation of rising plume of hot air over occupants. This mixing characteristic can be exploited further as it has obvious thermal comfort benefits, which manifests in more uniform room temperature. Expectedly, this has contributed to the low heating energy required in Case 4.

Case 2 (same side dual-openings) produced the highest flow rates, leading to substantial heating energy requirements as well as potential for draught at the floor level, but these can be overcome by better automation and control of openings. The tool used for the dynamic simulation is unfortunately limited in not allowing airflow rates to be used as regulating sensors. Using CO_2 as an indicator for acceptable indoor air quality by such applications is a weakness because high airflow rates can be required in clinical environments for health and safety reasons, regardless of the presence of occupants. It should also be pointed out that although Case 3 (inlet and stack) produces mean flows of 5.2 ACH in winter (January), this is arguably an over-ventilation with significant heating required to achieve acceptable thermal comfort.

In summer, the CBNV of Case 4 produces mean flows of 132 l/s (6.9 ACH) and 87.4 l/s (4.5 ACH) at 100% and 60% opening fractions respectively. This flow rates may appear acceptable, using the 6ACH benchmark of HTM 03-01 [13] but it has been argued severally [14,15]; and inferred from a specific enquiry made directly to ASHRAE [30] that this benchmark rate is rather ambiguous in origin, even if it enjoys an apparent consensus amongst researchers and practitioners. Additionally, the absolute (and personalised) flow rates of 60 l/s/patient recommended by the WHO could be a better metric if the rates per patient can be scientifically justified. This is because since it ties ventilation to occupancy (patients) and not room volume (ACH) therein lies the potential for NPV [12] and CBNV systems. Both concepts can induce the movement of fresh outdoor air towards each patient as defined by Melikov [21] for personalised ventilation – but using buoyancy only, thus at zero energy (or low energy, if fans are to provide occasional assistance).

The CBNV is uniquely unable to produce any flow for 222 h of the year (i.e. about 9 days), between July and August. This is probably due to its incapacity to cope with weak temperature differentials between interior and exterior, further emphasising the need to standardise its component sizing methods. This also makes a case for hybrid modes in certain times of the year when fan-assistance at either the supply duct or exhaust stack is necessary to enhance airflow. Although Case 1 (window-base) was computed to produce zero flows as well for 1721 h (71 days) in the same summer months, this is not attributable to weak temperature differentials only. The use of a single opening (for inflow and outflow of air) leading to conflict in flow directions or entrainment is the most plausible explanation as suggested by CFD results (Fig. 8). Importantly, the use of distinct inlets and outlets in natural ventilation (as represented by Case 2, 3 and 4) clearly has potential to minimise overheating which as occurs in Case 1 can be for up to three months.

5. Future work

Further to this work, there is a need to explore how the mean monthly DTS energy loads can aid the sizing of room heaters which can be studied in detailed through CFD models. However, locating such heaters requires careful consideration as their positions can affect comfort and efficiency of heating and it may emerge from further CFD studies that optimum placement could lead to even better comfort and lower energy than suggested by DTS simulations. It is also possible to monetise the equivalent consumption of energy from both electricity and gas sources under each strategy as this can aid designers and clients in making informed decisions about cost implications of proposed design alternatives. However, as evident from this study, savings in energy need to be cross-referenced with equivalent performance in delivering adequate airflow rates and acceptable thermal comfort. The CBNV in particular presents a unique challenge in the design and location of heating system at the fresh air supply points, without which cold drafts over occupants are almost a certainty. The performance of CBNV is currently being validated through salt-bath experiments of the NPV Case 1 and Case 2 duct configurations, previously demonstrated [12] in Adamu et al. (2011). Such experiments have the potential to offer visualisation of transient flow across the NPV duct as well as understanding the real-time nature of mixing which occurs within the ventilated space. There is also a need to model the performance of heat-recovery ventilator fitted within the bathroom from where unwanted air is channelled first before being exhausted e.g. through the stacks.

Finally, there is also a need to assess the performance of these four selected strategies with respect to control of infectious bio-aerosols in same or similar ward spaces. This aspect was not considered in the present study due to several reasons. First, there is need for focus and for the systematic classification of findings according to airflow rates, energy and comfort. Second, the control of bio-aerosols is a unique subject of special interest in its own right given contemporary concerns about airborne pandemics in hospitals (e.g. SARS, H1N1) as well as drug-resistant strains of diseases like Methicillin-resistant *Staphylococcus aureus* (MRSA) and Tuberculosis (DRTB). Third, because the potential source of airborne pathogens can vary: from a sitting visitor (position 'b' in Fig. 1); to a sleeping visitor (position 'c' in Fig. 1); or even a standing healthcare worker (who is often mobile). These three locations represent extensive variability of pollutant source which require a dedicated study. Concurrent (and independent) research is therefore exploring these issues.

With reference to the findings from this study, it is expected that in future work, weights could be assigned to each of four major parameters (airflow, thermal comfort, energy and bio-aersosol control) so that the performance of each ventilation strategy can be translated into alternative solutions, whereby designers, facility operators and infection control experts can elect or rank the aspect of ventilation that matters most to the client or clinical space in question. That way, objective selection of a ventilation strategy can not only be done – based on evidence, but can also be explained especially if the quantitative and qualitative metrics are encoded into an expert system.

Acknowledgements

The authors are grateful to: Engineering and Physical Sciences Research Council (EPSRC) of the UK; the Innovative Manufacturing Research Centre (IMRC); the Health and Care Infrastructure Research and Innovation Centre (HaCIRIC) as well as Llewelyn Davies Yeang Architects and the Department of Health/Great Ormond Street Hospital (GOSH) for supporting this research.

Appendix 1

Table 4
Monthly and annual heating plant sensible load (MWh) for selected opening fractions.

	80% opening				35% opening				25% opening				12.5% opening			
	Case1	Case2	Case3	Case4	Case1	Case2	Case3	Case4	Case1	Case2	Case3	Case4	Case1	Case2	Case3	Case4
Jan 01–31	0.748	7.050	4.436	2.714	0.165	2.863	1.707	0.953	0.069	1.933	1.105	0.571	0.002	0.782	0.373	0.136
Feb 01–28	0.233	3.644	2.229	1.282	0.015	1.357	0.731	0.331	0.001	0.850	0.410	0.149	0.000	0.250	0.075	0.008
Mar 01–31	0.133	2.985	1.768	0.961	0.000	1.025	0.514	0.204	0.000	0.610	0.268	0.071	0.000	0.152	0.024	0.000
Apr 01–30	0.092	2.316	1.355	0.722	0.003	0.774	0.379	0.141	0.000	0.453	0.189	0.049	0.000	0.104	0.020	0.001
May 01–31	0.154	2.943	1.751	0.961	0.003	1.023	0.527	0.223	0.000	0.620	0.284	0.094	0.000	0.170	0.043	0.001
Jun 01–30	0.000	0.545	0.272	0.104	0.000	0.123	0.036	0.001	0.000	0.051	0.007	0.000	0.000	0.000	0.000	0.000
Jul 01–31	0.000	0.359	0.173	0.062	0.000	0.074	0.017	0.000	0.000	0.027	0.001	0.000	0.000	0.000	0.000	0.000
Aug 01–31	0.000	0.245	0.098	0.021	0.000	0.029	0.003	0.000	0.000	0.006	0.000	0.000	0.000	0.000	0.000	0.000
Sep 01–30	0.003	0.883	0.461	0.193	0.000	0.219	0.069	0.008	0.000	0.096	0.018	0.000	0.000	0.004	0.000	0.000
Oct 01–31	0.016	1.399	0.751	0.344	0.000	0.379	0.151	0.033	0.000	0.193	0.055	0.004	0.000	0.021	0.000	0.000
Nov 01–30	0.322	4.212	2.580	1.501	0.031	1.588	0.883	0.435	0.002	1.017	0.525	0.223	0.000	0.341	0.126	0.018
Dec 01–31	0.601	6.171	3.866	2.340	0.099	2.470	1.449	0.780	0.028	1.647	0.914	0.444	0.000	0.629	0.272	0.076
Annual total	2.301	32.753	19.740	11.205	0.315	11.923	6.465	3.108	0.100	7.504	3.777	1.605	0.002	2.454	0.935	0.240

References

[1] Qian H, Li Y, Seto WH, Ching P, Ching WH, Sun HQ. Natural ventilation for reducing airborne infection in hospital. Building Environ 2010;45:559–65.
[2] Lomas KJ, Giridharan R. Thermal comfort standards, measured internal temperatures and thermal resilience to climate change of free-running buildings: a case-study of hospital wards. Building Environ. Available online (22 Dec. 2011) at: http://dx.doi.org/10.1016/j.buildenv.2011.12.006; 2011.
[3] Short CA, Al-Maiyah S. Design strategy for low-energy ventilation and cooling of hospitals. Building Res Inf 2009;37(3):264–92.
[4] Lomas KJ. Architectural design of an advanced naturally ventilated building form. Energy Build 2007;39:166–81.
[5] Khanal R, Lei C. Solar chimney – a passive strategy for natural ventilation. Energy Build 2011;43(8):1811–9.
[6] NHS, Quality and performance, report to trust board, University Hospitals of Leicester, Trust Board report, 2010; 47.
[7] Allocca C, Chen Q, Glicksman LR. Design analysis of single-sided natural ventilation. Energy Build 2003;35:785–95.
[8] Beggs CB, Kerr KG, Noakes CJ, Hathway EA, Sleigh PA. The ventilation of multiple-bed hospital wards: review and analysis. Am J Infect Control 2008; 36(4):250–9.
[9] Li Y, Nielsen PV, Sandberg M. Displacement ventilation in hospital environments. Ashrae J 2011;53(6):86–8.
[10] Adamu ZA, Cook MJ, Price ADF. Natural personalised ventilation: a novel approach. Int J Ventilation 2011;10(3):263–75.
[11] Chen Q. Ventilation performance prediction for buildings: a method overview and recent applications. Building Environ 2009;44(4):848–58.
[12] Li Y, Nielsen PV. CFD and ventilation research. Indoor Air 2011;21(6):442–53.
[13] DoH, Department of Health. Heating and ventilation systems; health technical memorandum 03-01: specialised ventilation for healthcare premises. TSO (The Stationery Office). Also available at: www.tsoshop.co.uk; 2007 [accessed Feb. 2011].
[14] Gammage RB. Controlling aerial transmission of Aspergillosis, Legionellosis and drug-resistant Tuberculosis. In: Maroni M, editor. Ventilation and indoor air quality in hospitals. Dordrecht: Kluwer Academic Publishers; 1996. p. 71–84.
[15] Lomas KJ, Ji Y. Resilience of naturally ventilated buildings to climate change: advanced natural ventilation and hospital wards. Energy Build 2009;41: 629–53.
[16] Atkinson J, Chartier Y, Pessoa-Silva CL, Jensen P, Li Y, Seto W-H, editors. Natural ventilation for infection control in health-care settings. WHO Guideline; 2009. p. WX167.
[17] Li Y, Leung MKH, Seto WH, Yeun PL, Leung J, Kwan JK, et al. Factors affecting ventilation effectiveness in SARS wards. Hong Kong Med J 2008; 14:33–6.
[18] DoH. Health technical memorandum 07-02: EnCO2de-, making energy work in healthcare, environment and sustainability. Department of Health Estates and Facilities Division, The Stationary Office, ISBN 0-11-322731-0; 2006.
[19] CIBSE. Natural ventilation in non-domestic buildings, CIBSE applications manual AM10. 2nd ed. Chartered Institution of Building Services Engineers Publications, ISBN 1903287561; 2005.
[20] Awbi HB. Ventilation of buildings. 2nd ed. Abingdon: Taylor and Francis (E&FN Spon), ISBN 0415270553; 2003.
[21] Melikov A. Personalized ventilation. Indoor Air 2004;14:157–67.
[22] Olesen BW. The philosophy behind EN 15251: indoor environmental criteria for design and calculation of energy performance of buildings. Energy Build 2007;39:740–9.
[23] ISO. Moderate thermal environments: determination of the PMV and PPD indices and specification of the conditions for thermal comfort. ISO 7730; 1994. 12–15.
[24] CIBSE. Energy benchmarks, technical memorandum 46;, ISBN 9781903287958; 2008.
[25] CIBSE. Guide A: environmental design. London: The Chartered Institution of Building Services Engineers; 2006.
[26] Koestel A. Paths of horizontally projected heated and chilled air jets. Trans ASHAF 1955;61:231–2.
[27] IES. Integrated Environment Solutions. IES VE software version 6.2.0.3, www.iesve.com; 2011.
[28] Cham. Phoenics version. Cham Co. Ltd. Available from: http://www.cham.co.uk/; 2009.
[29] Yakhot V, Orszag SA. Renormalization group analysis of turbulence. J Scientific Comput 1986;1:3–51.
[30] Hammerling S. shammerling@ashrae.org. Subject: ASHRAE/ASHE 170-2008. [Email] Message to Z.A.Adamu@lboro.ac.uk. Personal communication; Sent Tuesday, 3rd November 2009, 20:00; (Steve Hammerling, Assistant Manager of research & technical Services, ASHRAE, USA).

APPENDIX C: Wind speeds and air flow rates in winter (Dec – Feb)

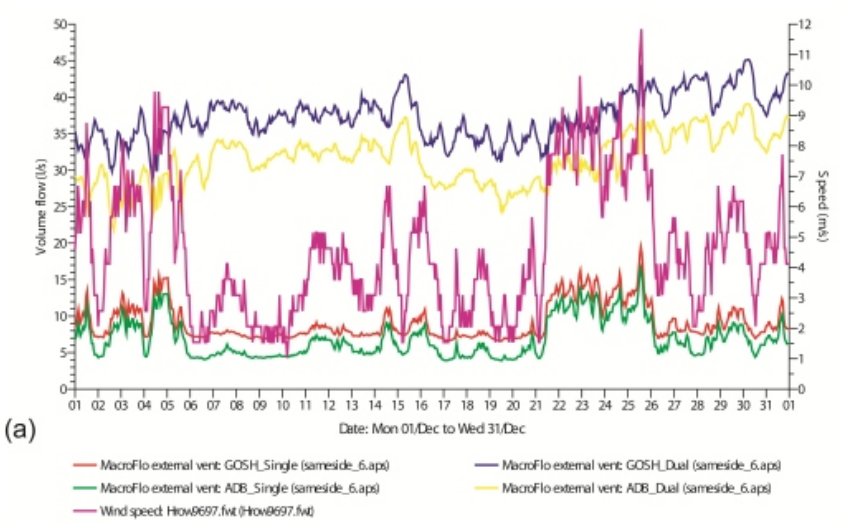

(a)

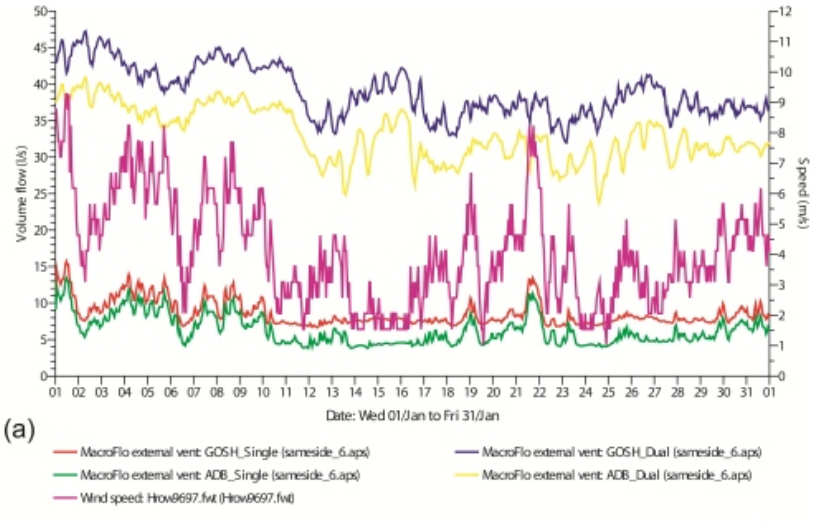

(a)

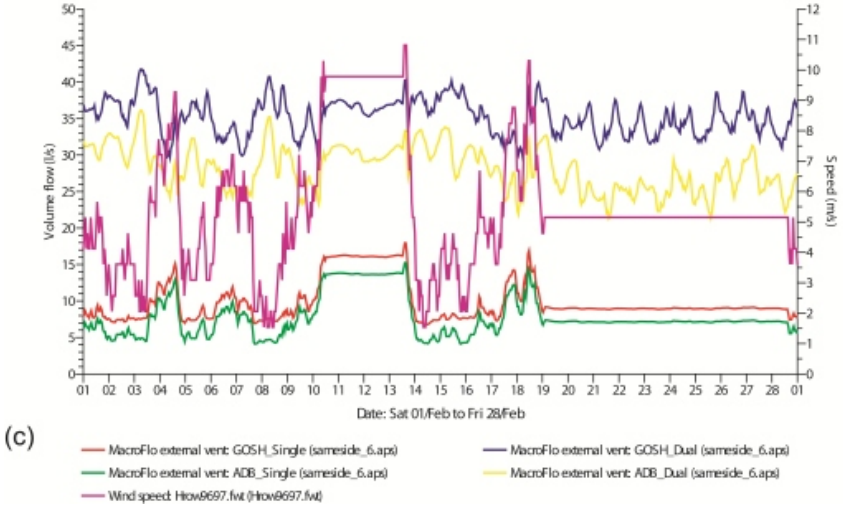

(c)

(d)

Openings at 25% fraction	DECEMBER	Min. Val.	Min. Time	Max. Val.	Max. Time	Mean
	Wind speed: Hrow9697.fwt	1.03	05:00,10/Dec	11.84	14:00,25/Dec	4.57
	MacroFlo external vent: GOSH_Single	20.6	11:30,19/Dec	78.9	13:30,25/Dec	33.9
	MacroFlo external vent: GOSH_Dual	96.9	15:30,02/Dec	180.6	05:30,30/Dec	145.3
	MacroFlo external vent: ADB_Single	12.7	01:30,17/Dec	66.6	13:30,25/Dec	26.9
	MacroFlo external vent: ADB_Dual	84.1	16:30,02/Dec	156.3	05:30,30/Dec	125.7
	JANUARY	Min. Val.	Min. Time	Max. Val.	Max. Time	Mean
	Wind speed: Hrow9697.fwt	1.03	14:00,19/Jan	9.27	11:00,01/Jan	4.08
	MacroFlo external vent: GOSH_Single	21.3	05:30,18/Jan	63.1	11:30,01/Jan	31.5
	MacroFlo external vent: GOSH_Dual	107.4	14:30,24/Jan	189.1	07:30,02/Jan	152.5
	MacroFlo external vent: ADB_Single	12.9	21:30,24/Jan	53.7	11:30,01/Jan	24.4
	MacroFlo external vent: ADB_Dual	92.2	14:30,24/Jan	163.6	07:30,02/Jan	132.1
	FEBRUARY	Min. Val.	Min. Time	Max. Val.	Max. Time	Mean
	Wind speed: Hrow9697.fwt	1.54	02:00,08/Feb	10.81	14:00,13/Feb	5.47
	MacroFlo external vent: GOSH_Single	21.4	17:30,07/Feb	72.7	14:30,13/Feb	37.9
	MacroFlo external vent: GOSH_Dual	95	14:30,21/Feb	167.1	06:30,03/Feb	129.3
	MacroFlo external vent: ADB_Single	13.5	17:30,07/Feb	61.3	14:30,13/Feb	31.1
	MacroFlo external vent: ADB_Dual	79.2	15:30,21/Feb	144.5	06:30,03/Feb	111.4

APPENDIX D: Hypothetical comparison of driving forces in SNV systems

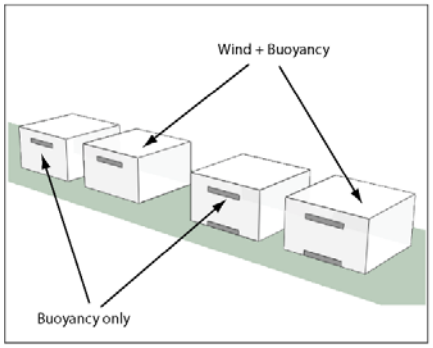

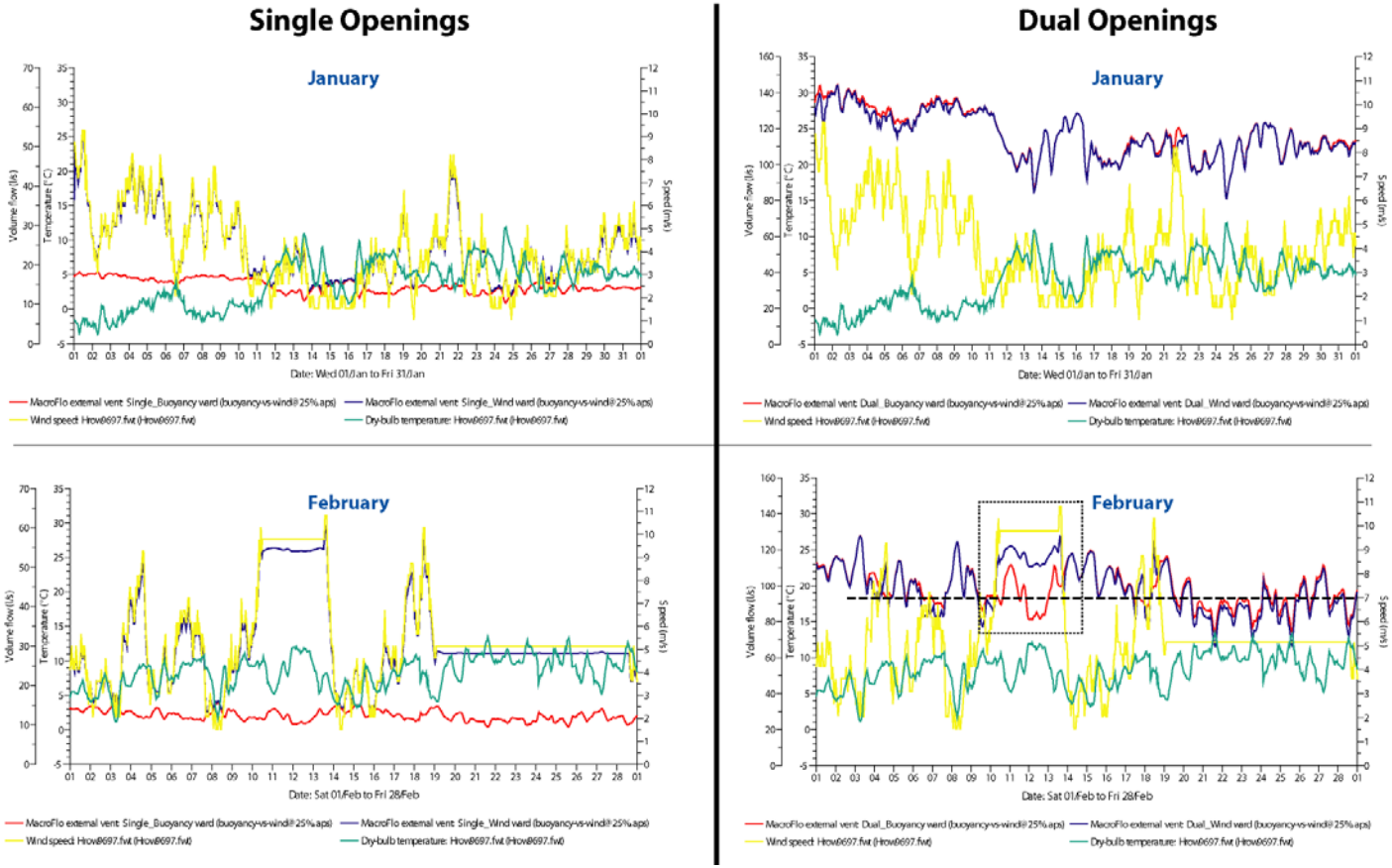

REFERENCES

Abad C., Fearday A and Safdar N. (2010) Adverse effects of isolation in hospitalized patients: a systemic review. Journal of Infect Control; **76**: pp. 97-102.

Adamu, Z.A. Price, A.D.F and Cook, M.J. (2011a) Same-sided ventilation strategies for healthcare buildings, ROOMVENT 2011, *12th International Conference on Air Distribution in Rooms*, (Paper No. 134), June 19 -22, Trondheim, Norway.

Adamu Z.A, Cook M.J, Price A.D.F. (2011b). Natural Personalised Ventilation: A novel approach, International Journal of Ventilation, 10(**3**): pp. 263-275.

Allard F. ed. (1998) Natural ventilation in buildings — a design handbook. London, James & James.

Allocca, C., Chen, Q. and Glicksman, L.R. (2003) Design analysis of same-sided natural ventilation. Energy and Buildings, **35**, pp. 785–795.

ANA – Ann Nobel Architects. (2003) Reduction of Hospital Acquired Infection by Design: NHS Estates Research and Development Project B(**01**)06. July 2003.

Andersson, P.A, Hambraeus A., Zettersten, U., Ljungqvist, B,, Neikter, K. and Ransjö, U. (1983) A comparison between tracer gas and tracer particle techniques in evaluating the efficiency of ventilation in operating theatres, The Journal of Hygiene, 1983; **91**: pp. 509–519.

Appleby, P. (1989) Displacement ventilation: a design guide. Building Services, CIBSE Journal, pp. 63-69.

ASHRAE (2008) ASHRAE/ASHE Standard: Ventilation of Health Care Facilities – ANSI/ASHRAE/ASHE Standard 170-2008. ISSN 1041-2336. American Society for Heating, Refrigeration and Air-conditioning Engineers, Atlanta, Georgia.

ASHRAE (2004) Ventilation for Acceptable Indoor Air Quality. ANSI/ASHRAE 62.1-2004. American Society for Heating, Refrigeration and Air-conditioning Engineers, Atlanta, Georgia.

Atkinson, J., Chartier, Y., Pessoa-Silva, C.L., Jensen, P., Li, Y. and Seto, W-H. (ed.) (2009) Natural Ventilation for Infection Control in Health-Care Settings. WHO Guideline. WX 167.

Attia, S., Gratia, E., De Herde, A., and. Hensen, J.L.M. (2012) Simulation-based decision support tool for early stages of zero-energy building design, Energy and Buildings, Available online 10 February 2012: http://dx.doi.org/10.1016/j.enbuild.2012.01.028.

Awbi H.B. (2003) Ventilation of Buildings, Second Edition, 2003, ISBN 0415270553, Taylor and Francis (E&FN Spon).

Axley J. (1998) Introduction to the design of natural ventilation systems using loop equations. In: Ventilation technologies in urban areas, Proceedings of the 19th AIVC Conference, Oslo, Norway, 28–30 September: pp. 47–56.

Baker, N.V. and Standeven, M.A. (1996) Thermal comfort in free-running buildings Energy and Buildings, 23 (**3**) pp. 175 - 182.

Baker, N.V. & Standeven, M.A. (1995) A behavioural approach to thermal comfort assessment in naturally ventilated buildings. Proceedings CIBSE National Conference, Eastbourne, pp 76-84.

Barlow, S. and Fiala, D. (2007) Occupant comfort in UK offices - How adaptive comfort theories might influence future low energy office refurbishment strategies Energy and Buildings, Vol. 39 (**7**), pp. 837-846

Beggs, C.B., Kerr, K.G., Noakes, C.J., Hathway, E.A and Sleigh, P.A. (2008) The ventilation of multiple-bed hospital wards: Review and analysis. American Journal of Infection Control, 36 (**4**). pp. 250-259.

Best et al., E.L. Best, W.N. Fawley, P. Parnell and M.H. Wilcox (2010) The potential for airborne dispersal of Clostridium difficile from symptomatic patients. Clinical Infectious Diseases, 50 , pp. 1450–1457.

Bjorn E. (2002) *Dispersal of exhaled air in stratified surroundings-CFD studies*. Proceedings of the ROOMVENT2002, Copenhagen, Denmark, 2002, pp. 285–88.

Bolashikov, Z. D. & Melikov, A. K. (2009) Methods for air cleaning and protection of building occupants from airborne pathogens. Building and Environment. Vol. 44; pp. 1378–1385.

Brohus, H., and P.V. Nielsen (1996) Personal exposure in displacement ventilated rooms. Indoor Air: International Journal of Indoor Air Quality and Climate 6(**3**): pp. 157-67.

Carbon Trust UK (2007) Hospitals: Healthy budgets through energy efficiency. Available online at: www.carbontrust.com/media/39216/ctv024_hospitals.pdf; Accessed 28 Jan 2013.

Centre for Disease Control and Prevention (CDC) (2005) Guidelines for preventing transmission of Mycobacterium tuberculosis in health-care settings, 2005, Morbidity and Mortality Weekly Report (MMWR) 2005; 54:RRe17.

Cepeda, J.A., Whitehouse ,T., Cooper, B., Hails, J., Jones, K., Kwaku, F., (2005) Isolation of patients in single rooms or cohorts to reduce spread of MRSA in intensive-care units: prospective two-centre study, Lancet, 365 (9456): pp. 295–304.

CHAM (2011) Cham Phoenics version 2009, available from: Cham Co. Ltd. Wimbledon, United Kingdom, http://www.cham.co.uk/

Cheesbrough J.S., Green J., Gallimore C.I, Wright P.A. and Brown D.W. (2000) Widespread environmental contamination with Norwalk-like viruses (NLV) detected in a prolonged hotel outbreak of gastroenteritis, Epidemiol Infect; 125(**1**): pp. 93-98.

Chen, Q. (2009) Ventilation performance prediction for buildings: a method overview and recent applications, Building and Environment, 44 (**4**) (2009), pp. 848 – 858.

Chen, Q. and Glicksman, L. (2001) Application of Computational Fluid Dynamics for Indoor Air Quality Studies. In: Spengler J.D., Samet J.M. and McCarthy J.F. eds. Indoor Air Quality Handbook. New York: McGraw-Hill; 2001.

Cheng V.C., Tai, J.W., Wong, L.M., Chan, J.F., Li, I.W. and To K.K. (2010) Prevention of nosocomial transmission of swine-origin pandemic influenza virus A/H1N1 by infection control bundle. Journal of Hospital Infection, 74: pp. 300–302.

Cheong, K.W.D. and Phua, S.Y. (2006) Development of ventilation design strategy for effective removal of pollutant in the isolation room of a hospital, Building and Environment, 41, pp. 1161 -1170.

CIBSE (2012) Guide A: Environmental Design, The Chartered Institution of Building Services Engineers: London (in press) and based on personal communication with Prof. Malcolm Cook on his contribution to the revised version of the document.

CIBSE (2008) Energy Benchmarks, Technical Memorandum 46, 2008: ISBN 9781903287958.

CIBSE (2006) Guide A: Environmental Design, The Chartered Institution of Building Services Engineers, 2006: London.

CIBSE (2005) Natural ventilation in non-domestic buildings, CIBSE Applications Manual AM10. Second Edition, 2005, Chartered Institution of Building Services Engineers Publications, ISBN 1903287561.

CIBSE (2002) Chartered Institute of Building Services Engineers, Heating, CIBSE Guide B1.

Clark R.P. and de Calcina-Goff M.L. (2009) Some aspects of the airborne transmission of infection, Journal of the Royal Society Interface, 6, S767–S782, doi:10.1098/rsif.2009.0236.focus.

Cook, M.J., Ji, Y. and Hunt, R., (2008) CFD modelling of natural ventilation: combined wind and buoyancy forces, International Journal of Ventilation, 1(**3**), pp 169-179.

Cook, M.J., Ji, Y. and Hanby, V.I., (2006) CFD modelling of natural displacement ventilation in an enclosure connected to an atrium, Building and Environment, 42(**3**), pp. 1158-1172.

Cook, M. J., Ji, Y., and Hunt, G. R. (2003) CFD Modelling of Natural Ventilation: Combined Wind and Buoyancy Forces, International Journal of Ventilation, Vol. 1, No. 3, pp. 169-179.

Cook, M. J. (1998) An evaluation of Computational Fluid Dynamics for modelling buoyancy-driven displacement ventilation, PhD Thesis, De Montfort University.

Cousin, G. (2009) Researching learning in higher education- An introduction to contemporary methods and approaches, New York, NY: Routledge.

Cox, C.S. and Wathes, C.M. (1995) Bioaerosols Handbook, Lewis Publishers, Boca Raton, Florida; pp 17.

Crawley, D.B., Hand, J.W., Kummert, M. and Griffith, B.T. (2008) Contrasting the capabilities of building energy performance simulation programs Building and Environment, 43 (**4**) , pp. 661-673.

Crawley D.B., Pedersen C.O., Lawrie L.K., Winkelmann F.C. (2000) Energy plus: Energy simulation program, ASHRAE Journal, 42 (**4**), pp. 49-56.

Dascalaki, E., Santamouris, M., Argiriou, A., Helmis, C., Asimakopoulos, D.N., Papadopoulos, K., and Soilemes, A. (1995) Predicting single sided natural ventilation rates in buildings, Solar Energy, Vol. 55, No. 5, pp 327 – 341.

de Dear, R.J. , and Brager, G.S. (1998) Towards an adaptive model of thermal comfort and preference, ASHRAE Transactions, 104 (**1**), pp. 145 – 167

de Dear, R. J. & Auliciems, A. (1985) Validation of the predicted mean vote model of thermal comfort in six Australian field studies. ASHRAE Transactions, 91(**2**), pp. 452-468.

Demanuele, C., Mavrogianni, A., Davies, M.,Kolokotroni, M., Rajapaksha, I. (2012) Using localised weather files to assess overheating in naturally ventilated offices within London's urban heat island, Building Services Engineering Research and Technology 33 (**4**), pp. 351-369

DH (2010) Activity Database (ADB): The briefing, design and commissioning tool for both new-build and refurbishment of healthcare buildings, Space for Health: Information for healthcare premises professionals, available at: https://spaceforhealth.nhs.uk/.

DH (2007a) Department of Health: Heating and ventilation systems; Health Technical Memorandum 03-01: Specialised ventilation for healthcare premises. Part A: Design and validation, TSO (The Stationery Office); also available at www.tsoshop.co.uk.

DH (2007b) Department of Health: Heating and ventilation systems; Health Technical Memorandum 03-01: Specialised ventilation for healthcare premises. Part B: Operational management and performance verification. TSO (The Stationery Office); also available at www.tsoshop.co.uk/.

DH (2006) Health Technical Memorandum 07-02: EnCO2de: Making Energy Work in Healthcare, Environment and Sustainability, Department of Health Estates and Facilities Division, The Stationary Office, ISBN: 0-11-322731-0.

DH (1998) Health Technical Memorandum HTM 55 (Building Components) Windows, NHS Estates, (2nd edition) ISBN 011 322009 X; London: The Stationery Office.

Dols, W. S. and Walton, G. N. (2000) CONTAMW 2.0 user manual: Multizone airflow and contaminant transport analysis software Gaithersburg, MD: National Institute of Standards and Technology.

Dowdeswell, B., Erskine, J., and Heasman, M., Hospital ward configuration. Determinants influencing single room provision, A Report for NHS Estates, England by the EU Health Property Network (EuHPN), 2004.

Dreiling, J.B.(2008) An evaluation of ultraviolet germicidal irradiation (UVGI) technology in health care facilities, Master thesis, Kansas State University, Manhattan, Kansas, 2008.

Eames I., Tang J.W., Li Y. and Wilson P. (2009a) Airborne transmission of disease in hospitals, Journal of the Royal Society Interface, 6, S697–S702: doi:10.1098/rsif.2009.0407.focus.

Eames I., Tang J.W., Li Y. and Wilson P. (2009b) Airborne transmission of disease in hospitals, Journal of the Royal Society Interface 6, S697–S702, doi:10.1098/rsif.2009.0407.focus).

Escombe, A. R., Moore, D.A.J., Gilman, R.H., Navincopa, M., Ticona, E., Mitchell, B., Noakes. C., Martinez, C., Sheen, P., Ramirez, R., Quino, W., Gonzalez, A., Friedland, J.S. and Evans, C.A. (2009). Upper-room ultraviolet light and negative air ionisation to prevent tuberculosis. PLOS Medicine, Vol. 6, No. 3; pp 312-323.

Escombe A.R., Oeser C.C. and Gilman R.H. (2007) Natural ventilation for the prevention of airborne contagion, PLoS Medicine.2007;4:e68.

ESRU (1997) The ESP-r system for building energy simulation, Energy System Research Unit, University of Strathclyde.

Etheridge, D. and Sandberg, M. (1996) Building Ventilation: Theory and Measurement: John Wiley & Sons Ltd.

Fanger, P. O. (1967) Calculation of thermal comfort: Introduction of a basic comfort equation. ASHRAE Transactions, 73(**2**), III4.1-III4.20.

Finlayson, E. U., Gadgil, A. J., Thatcher, T. L. and Sextro, R. G. (2004) Pollutant dispersion in a large indoor space. Part 2: Computational fluid dynamics predictions and comparison with a scale model experiment for isothermal flow, Indoor Air, 14(**4**) pp. 272-283.

Fisk, W., Commentary on predictive models of control strategies involved in containing indoor airborne infections, Indoor Air, 2008, 16: pp. 469–481.

Fitzgerald, S.D. and Woods, A.W. (2008) The influence of stacks on flow patterns and stratification associated with natural ventilation, Building and Environment, 43 (**10**) pp. 1719 – 1733.

Florey, L., Flynn, R. and Isles, C. (2009) Patient preferences for single rooms or shared accommodation in a district general hospital. Scott Medical Journal, 54 (**2**): pp. 5-8.

Flow3D (2012). Available at: www.flow3d.com/

Friberg B., Friberg s., Burman L. G:, Lundholm R. and Ostensson R. (1996) Inefficiency of upward displacement operating theatre ventilation, Journal of Hospital Infection, **33**, 263-272.

Gammage, R.B. (1996) Controlling aerial transmission of Aspergillosis, Legionellosis and Drug-Resistant Tuberculosis, in: Maroni, M (ed.) Ventilation and Indoor Air Quality in Hospitals, Kluwer Academic Publishers, Dordrecht, pp. 71-84.

Gan, G. (2000) Effective depth of fresh air distribution in rooms with same-sided natural ventilation, Energy and Buildings, Volume 31, Issue 1, pp. 65 – 73.

Gilkeson, C. A., Camargo-Valero, M. A., Pickin, L. E., and Noakes, C. J. (2013) Measurement of Ventilation and Airborne Infection Risk in Large Naturally Ventilated Hospital Wards, Building and Environment, doi: 10.1016/j.buildenv.2013.03.006.

Gladstone, C. and Woods, A.W. (2001) On buoyancy-driven natural ventilation of a room with a heated floor, Journal of Fluid Mechanics. 441, pp. 293-314.

Glanville, R. (2009). Interview with Dr. Rosemary Glanville, Head of Medical Architecture Unit (MARU), London Southbanks University, (LSU), London. December 2nd 2009 at MARU Office, LSU.

GOSH (2011) The Great Ormond Street Hospital – 'Why we need to redevelop'. Also available at: http://www.gosh.org/gen/redevelopment/ Accessed on 16 Nov. 2011.

Gupta, J., Lin, C.-H., and Chen, Q. (2009) Flow dynamics and characterization of a cough, Indoor Air, 19, pp. 517-525.

Halawa, E., and van Hoof, J. (2012) The adaptive approach to thermal comfort: A critical overview, Energy and Buildings, Vol. 51, pp. 101 – 110

Hambraeus, A., Bengtsson, S. and Laurell, G (1978) Bacterial contamination in a modern operating suite. 3. Importance of floor contamination as a source of airborne bacteria Journal of Hygiene, Vol. 80; pp. 169 – 174.

Hammerling, S., shammerling@ashrae.org. (2009). Subject: ASHRAE/ASHE 170-2008. [Email] Message to Z.A.Adamu@lboro.ac.uk. Personal communication; Sent Tuesday, 3rd November 2009, 20:00; (Steve Hammerling, Assistant Manager of Research & Technical Services, ASHRAE, USA).

Hathway, E.A., Noakes, C.J., Sleigh P.A. and Fletcher, L.A. (2011) CFD simulation of airborne pathogen transport due to human activities, Building and Environment, Vol. 46 (**12**) pp. 2500-2511.

Heiselberg, P., and Li, Zhigang (2009) Buoyancy Driven Natural Ventilation through Horizontal Openings, International Journal of Ventilation, Vol. 8, No. 3, pp. 219-231.

Heiselberg, Per. (2008) Characteristics of natural and hybrid ventilation systems; in Awbi, H.B (2008) Ventilation Systems: Design and Performance, Taylor and Francis. Abingdon.

Heisleberg, Per (2002). (ed.) Principles of Hybrid Ventilation. Hybrid Ventilation Center, Aalborg University, Aalborg, Denmark.

Heiselberg, P., Svidt, K. and Nielsen, P.V. (2001) Characteristics of airflow from open windows, Building and Environment, Volume 36, Issue 7, August 2001, pp. 859 – 869.

Hens, H. (2012) Applied building physics: Boundary conditions, building performance and material properties; Wilhelm Ernst and Sons/John Wiley: Darmstadt, ISBN 978-3-433-02962-6.

Hohmann, U. (2006) Quantitative Methods in Education Research. Available at: http://www.edu.plymouth.ac.uk/resined/Quantitative/quanthme.htm; Accessed 22 August 2011.

Hu, B., J. Freihaut, C. Gomes, W. Bahnfleth, and B. Thran. (2005) Literature Review and Parametric Study: Indoor Particle Re-suspension by Human Activity. Proceedings of Indoor Air 2005, 10th International Conference on Indoor Air Quality and Climate, pp. 1541-1545.

Hunt, G.R., and Syrios, K. (2004) Roof-Mounted Ventilation Towers – Design Criteria for Enhanced Buoyancy-Driven Ventilation, International Journal of Ventilation, Vol. 3, No. 3, pp. 193-208.

Hunt, G.R., Cooper, P. and Linden, P.F. (2001) Thermal stratification produced by plumes and jets in enclosed spaces, Building and Environment, 36(**7**), pp. 871 – 882.

IES (2011) IES VE software version 6.2.0.3, Integrated Environment Solutions, Available at: www.iesve.com.

ISO (1994) Moderate thermal environments: Determination of the PMV and PPD indices and specification of the conditions for thermal comfort, ISO 7730, 1994-12-15.

Jiang, Y., Zhao, B., Li, X., Yang, X., Zhang, Z. and Zhang, Y. (2009) Investigating a safe ventilation rate for the prevention of indoor SARS transmission: An attempt based on simulation approach, Building Simulation, Volume 2, No. 4, pp. 281-289.

Jiang, Y., Alloca, C., and Chen, Q. (2004) Validation of CFD simulations for natural ventilation. International Journal of Ventilation 2(4) pp 359-370.

Jiang, Y. and Chen, Q. (2003) Buoyancy-driven same-sided natural ventilation in buildings with large openings, International Journal of Heat and Mass Transfer, Volume: 46, Issue: 6, pp. 973-988.

Kaye, N.B., Flynn, M.R., Cook, M.J. and Ji, Y. (2010) The role of diffusion on the interface thickness in a ventilated filling box, J. Fluid Mech. vol. 652, pp. 195–205.

Karimipanah, T., Awbi, H.B., and Moshfegh, B. (2008) The Air Distribution Index as an Indicator for Energy Consumption and Performance of Ventilation Systems, Journal of the Human-Environment System, 11 (**2**) pp. 77-84.

Karimipanah, T., Awbi, H.B., Sandberg, M. and Blomqvist, C. (2007) Investigation of air quality, comfort parameters and effectiveness for two floor-level air supply systems in classrooms, Building and Environment, 42 pp. 647-655.

Karimipanah, T. and Awbi, H.B. (2002) Theoretical and experimental investigation of impinging jet ventilation and comparison with wall displacement ventilation, Building and Environment Vol. 37, pp. 1329 – 1342.

Khan, T. A., Higuchi, H., Marr, D. R. and Glauser, M. N. (2004) Unsteady flow measurements of human micro environment using time-resolved particle image velocimetry, Proceedings of Room Vent 2004, Coimbra, Portugal.

Klein, S.A. (1976) TRNSYS, a transient simulation program, ASHRAE Transactions, 82 (1976), pp. 623 – 631.

Koestel A (1955) Paths of horizontally projected heated and chilled air jets, Transactions of ASHAF, 61 pp. 231-232.

Kolokotroni M., Giannitsaris I., Watkins R. (2006) The effect of the London urban heat island on building summer cooling demand and night ventilation strategies, Solar Energy, 80 (4) , pp. 383-392.

Kubica, G. (1996) Exposure risk/prevention of aerial transmission of tuberculosis; in Gamage R. B. and Berven, B.A. (1996) Indoor Air and Human Health, Lewis Publishers, CRC Press Inc. (2nd Edition).

Lagus, P.L., and Persily, A. (1985) A review of tracer gas techniques for measuring airflows in buildings ASHRAE Transactions Part 2, 91.

Larsen, T. and Heiselberg, P. (2008) Same-sided natural ventilation driven by wind pressure and temperature difference, Energy and Buildings, Vol 40, No. 6.pp. 1031-1040.

LBNL (1982) DOE-2 Engineering Manual Version, 2.1C, Lawrence Berkeley National Laboratory, Berkeley, CA (1982).

Lawson, B., and Phiri, M. (2004) The Benefits of single rooms' provision and their impact on Staff and patient health outcomes within the NHS in England, Interim Study Report for NHS Estates, 2004.

Leonard J. J, and McQuitty J. B, (1985) Criteria for control of cold ventilation air jets, ASAE Paper No. 85-4014.

Levy, F. (1996) Indoor air quality problems in hospitals, In: Maroni, M (ed.), Ventilation and indoor air quality in hospitals, pp. 19-28.

Li, Y. and Nielsen, P.V. (2011) CFD and ventilation research, Indoor Air, 21 (**6**), pp. 442 – 453.

Li, Y., Nielsen, P.V., and Sandberg, M. (2011) Displacement Ventilation in Hospital Environments. ASHRAE Journal, 53(**6**), pp. 86-88.

Li Y., Leung, M.K.H., Seto, W.H., Yeun, P.L., Leung, J., Kwan, J.K. and Yu, S.C.T. (2008) Factors Affecting Ventilation Effectiveness in SARS wards, Hong Kong Medical Journal, 14(**1**), Supplement 1; Feb. 2008.

Li, Y., Leung, G.M., Tang, J.W., Yang, X., Chao, C.Y. H., Lin, J.Z., Lu, J.W., Nielsen, P.V., Niu, J., Qian, H., Sleigh, A.C., Su, H.-J. J., Sundell, J., Wong, T.W. and Yuen, P.L. (2007) Role of ventilation in airborne transmission of infectious agents in the built environment – a multidisciplinary systematic review. Indoor Air, 17(**1**), pp. 2–18.

Li, Y., Huang, X., Yu, I.T.S., Wong, T.W. and Qian, H. (2005) Role of air distribution in SARS transmission during the largest nosocomial outbreak in Hong Kong, Indoor Air, 152: pp. 83–95.

Lin, Y.J.P. and Linden, P.F. (2002) Buoyancy-driven ventilation between two chambers J. Fluid Mech., 463, pp. 293 – 312.

Liddament, M.W. (1996) A Guide to Energy Efficient Ventilation. Oscar Faber / AIVC, Warwick.

Linden, P.F., (1999) The fluid mechanics of natural ventilation, Annual Review of Fluid Mechanics, 31, pp. 201-238.

Linden, P. F., Lane-Serff, G. F. & Smeed, D. A. (1990) Emptying filling boxes: The fluid mechanics of natural ventilation, Journal of Fluid Mechanics, 212, pp. 309–335.

Lomas, K.J. and Giridharan, R. (2012) Thermal comfort standards, measured internal temperatures and thermal resilience to climate change of free-running buildings: A case-study of hospital wards, Building and Environment, 55, pp. 57-72.

Lomas, K.J. and Ji, Y. (2009) Resilience of naturally ventilated buildings to climate change: Advanced natural ventilation and hospital wards, Energy and Buildings. Vol. 41; pp. 629-653.

Lomas, K.J. (2007) Architectural design of an advanced naturally ventilated building form. Energy and Buildings, Vol. 39, pp. 166 – 181.

Lomas, K.J., Eppel, H., Martin C.J. and Bloomfield D.P. (1997) Empirical validation of building energy simulation programs, Energy and Buildings, 26 (**3**), pp. 253-275.

Loudon, R.G. and Roberts, R.M. (1968) Singing and the dissemination of tuberculosis. American Review of Respiratory Disease, Vol. 98, pp. 297-300.

Loudon, R.G. and Roberts, R.M. (1967) Droplet expulsion from the respiratory tract. American Review of Respiratory Disease, Vol. 95, pp. 435-442.

Luciano, J.R. (1977) Air Contamination in Hospitals, Plenum Press, New York.

Mao, S. and Celik, I.B. (2010) Modelling of indoor airflow and dispersion of aerosols using immersed boundary and random flow generation methods, Computers & Fluids, 39 (**8**), pp. 1275-1283.

McGilligan, C., Natarajan, S., and Nikolopoulou, M. (2011) Adaptive Comfort Degree-Days: A metric to compare adaptive comfort standards and estimate changes in energy consumption for future UK climates, Energy and Buildings, Vol. 43, Issue 10, October 2011, Pages 2767 – 2778

Melikov A. (2004) Personalized ventilation, Indoor Air, 14: pp. 157–167.

Melikov, A.K., Cermak, R., Kovar, O. and Forejt, L. (2003) Impact of airflow interaction on inhaled air quality and transport of contaminant in rooms with personalised and total volume ventilation, In: Proceedings of Healthy Buildings 2003, Singapore 2, pp. 592–597.

Melikov, A., Cermak, R. and Mayer, M. (2002) Personalized ventilation: evaluation of different air terminal devices, Energy and Buildings, 34, pp. 829–836.

Mendez, C., San Jose, J.F., Villafruela, J.M. and Castro, F. (2008) Optimisation of a hospital room by means of CFD for more efficient ventilation, Energy and Buildings, 40, pp. 849-854.

Montero, J.I., Anton, A., Kamaruddin, R. and Bailey, B.J. (2001) Analysis of thermally driven ventilation in tunnel greenhouses using small scale models, J. Agric. Eng. Res., 79 (**2**) pp. 213 – 222.

Morawska, L. (2006) Droplet fate in indoor environments, or can we prevent the spread of infection? Indoor Air, Volume 16, pp. 335-347.

Morton, B.R., Taylor, G.I. and Turner, J.S. (1956) Turbulent gravitational convection from maintained and instantaneous sources, Proceedings of the Royal Society A, 234: pp. 1-23

NHS (2010) Quality and performance, report to trust board, University Hospitals of Leicester, Trust Board report, 2010; 47.

NHS (2007) NHS Confederation: Taking the Temperature: Towards an NHS Response to Global Warming, NHS Confederation Publ., London.

NHS Estates (1994) Hospital Technical Memorandum (HTM) 2025, Ventilation of healthcare premises.

Nicol, J.F. (2011) Adaptive comfort, Editorial, Building Research & Information, 39 (2) (2011), pp. 105 – 107

Nielsen, P.V. (2009) Control of airborne infectious diseases in ventilated spaces, Journal of the Royal Society Interface, Vol.6, No. Suppl. 6.

Nielsen, P.V., Polak, M., Jiang, H., Li, Y. and Qian, H. (2008) Protection against cross infection in hospital beds with integrated personalized ventilation, In Proceedings of Indoor Air 2008, 11th International Conference on Indoor Air Quality and Climate, Copenhagen, Denmark, 17–22 August 2008.

Nielsen, P.V., Jiang, H. and Polak, M. (2007a) Bed with integrated personalized ventilation for minimizing cross infection, In Poceedings of Roomvent 2007, 10th International Conference of Air Distribution in Rooms, Helsinki, Finland, 13-15 June 2007, Vol. 3, pp. 387 – 396.

Nielsen, P. V., Hyldgard, C-E., Melikov, A., Andersen, H. and Soennichsen, M. (2007b) Personal exposure between people in a room ventilated by textile terminals with and without personalized ventilation, HVAC and R Research, Vol. 13, No. 4, 2007, pp. 635-644.

Nightingale Associates (2010) Peterborough City Hospital Opens. Nightingale Associates, available online at: http://www.nightingaleassociates.com/news10-1312.html, Accessed December 2012.

Nightingale, F. (1859) Notes on Nursing: What it is, and what it is not, Release Date: May 26, 2004, Available at http://www.gutenberg.org/cache/epub/12439/pg12439.html Accessed 28 Jan. 2011.

Niu, J., Gao, N., Phoebe, M., and Zuo, H. (2007) Experimental study on a chair-based personalized ventilation system, Building and Environment, 42, pp. 913–925.

Noakes, C. J., Sleigh, P. A., Fletcher, L. A. and Beggs, C. B. (2006a) Use of CFD modelling to optimise the design of upper-room UVGI disinfection systems for ventilated rooms, Indoor and Built Environment, Vol. 15; pp. 347–356.

Noakes, C.J., Beggs, C.B., Sleigh, P.A. and Kerr, K.G. (2006b) Modelling the transmission of airborne infections in enclosed spaces, Epidemiology and Infection, 134 (**05**). pp. 1082 - 1091.

NPHT – Nuffield Provincial Hospitals Trust (1955) Studies in the functions and design of hospitals, the report of an investigation sponsored by the Nuffield Provincial Hospitals Trust and the University of Bristol. Oxford University Press. London.

Oikonomou, E., Davies, M., Mavrogianni, A., Biddulph, P., Wilkinson P. and Kolokotroni M (2012) Modelling the relative importance of the urban heat island and the thermal quality of dwellings for overheating in London, Building and Environment, 57, pp. 223-238.

Olesen, B.W. (2007) The philosophy behind EN 15251: Indoor environmental criteria for design and calculation of energy performance of buildings. Energy and Buildings, 39: pp. 740-9

Oseland, N. A. (1996) Thermal comfort in naturally ventilated versus air-conditioned offices. In S. Yoshizawa, K. Kimura, K. Ikeda, S. Tanabe, & T. Iwata (Eds.), Indoor Air '96: The 7th International Conference on Indoor Air Quality and Climate, Vol. 1, pp. 215-220.

Oseland, N. (1995) Predicted and reported thermal sensation in climate chambers, offices and homes, Energy and Buildings, 23, pp. 105-115.

Özcan, S.E., Vranken, E., Malcot, W.V. and Berckmans, D. (2005) Determination of the Airflow Pattern in a Mechanically Ventilated Room with a Temperature-based Sensor, Biosystems Engineering, Vol. 90, No. 2, pp. 193-201.

Pantelic, J., Sze-To, G.N., Tham, K.W., Chao, C.Y.H. and Khoo, Y.C.M. (2009) Personalized ventilation as a control measure for airborne transmissible disease spread., Journal of the Royal Society Interface 6, S715–S726.

Paradise, C. (2011) Innovative patient accommodation, International Academy for Design and Health 7th World Congress & Exhibition, Boston, USA, Available online at: http://www.designandhealth.com/uploaded/documents/Awards-and-events/WCDH2011/Presentations/Friday/Session-8/CarolineParadise.pdf, accessed 5 Jan. 2013

Policy+. Splendid isolation? The pros and cons of single occupancy rooms for the NHS. Issue 17 April 2009.

Prior, J., Littler, J. and Adlard, M. (1983) Development of multi-tracer gas techniques for observing air movement in buildings, Air Infiltration Review, 4 (3).

Qian, H., Li, Y., Seto, W.H., Ching, P., Ching, W.H. and Sun, H.Q. (2010) Natural ventilation for reducing airborne infection in hospitals. Building and Environment, Vol 45, pp. 559 – 565.

Qian, H., Li, Y., Nielsen, P. V., Hyldgaard, C. E., Wong, T. W. and Chwang, A. T. Y. (2006) Dispersion of exhaled droplet nuclei in a two-bed hospital ward with three different ventilation systems, Indoor Air; 16, pp. 111–128.

Qian, H., Nielsen, P.V., Li, Y. and Hyldgaard, C.E. (2004) Airflow and contaminant distribution in hospital wards. In: Proceedings of the second international conference on building environment and public health, Shenzhen, China, 6–10 December 2004. pp. 355–64.

Randall, J.M. and Battams, V.A. (1979) Stability criteria for airflow patterns in livestock buildings, Journal of Agricultural Engineering Research 24(**4**), pp. 361–374.

Riley, R. L., Knight, M., and Middlebrook, G. (1976) Ultraviolet susceptibility of BCG and Virulent Tubercle Bacilli, American Review of Respiratory Diseases, 113: pp. 413–418.

Roberts, K., Hathway, A., Fletcher, L.A., Beggs, C.B., Elliott, M.W. and Sleigh P.A. (2006) Bioaerosol production on a respiratory ward, Indoor and Built Environment, Vol. 15; pp. 35-40.

Roulet, C-A. and Vandaele L. (1991) Air flow patterns within buildings measurement techniques, Technical Note 34, Air Infiltration and Ventilation Centre, Coventry, Great Britain.

Rudnick, S.N. and Milton, D.K. (2003) Risk of indoor airborne infection transmission estimated from carbon dioxide concentration. Indoor Air, 2003, 13(**3**), pp. 237-245.

Rutula, W.A., Katz, E.B.S., Robert, J., Sherertz, T, and Sarubbi, F.A. (1983) Environmental study of a methicillin-resistant Staphylococcus aureus epidemic in a burn unit, Journal of Clinical Microbiology, Vol. 18; pp. 683–688.

Rydock, J.P. and Eian, P.K. (2004) Containment testing of isolation rooms, Journal of Hospital Infection, 57, pp. 228–232.

Schild, P.G. (2006) Ventilation performance indicators and targets, In: Santamouris, M. and Wouters, P. (2006). (ed). Building ventilation: state of the art, INIVE/AIVC. Earthscan, UK.

Schiller, G. E. (1990) A comparison of measured and predicted comfort in office buildings. ASHRAE Transactions, 96(**1**), pp. 609-622.

Seckar, S.C., Tham, K.W. and Cheong, D.(2002) Ventilation Characteristics of an Air-conditioned Office Building in Singapore, Building and Environment. Vol. 37. pp. 241-255.

Seppanen, O. and Tarvainen, K. (1996) Design criteria of ventilation for hospitals; In: Maroni, M (ed.), Ventilation and indoor air quality in hospitals, Kluwer Academic Publishers, The Netherlands, pp. 71-84.

Shiomori, T., Miyamoto, H., Makishima, K., Yoshida, M., Fujiyoshi, T., Udaka, T., Inaba, T. and Hiraki, N. (2002) Evaluation of bed making-related airborne and surface methicillin-resistant Staphylococcus aureus contamination, Journal of Hospital Infection, Vol. 50, pp. 30 – 35.

Short, C.A., Cook, M.J., Cropper, P.C. and Al-Maiyah, S. (2010) Low-energy refurbishment strategies for health buildings, Journal of building performance simulation, 3:3, pp. 197-216.

Short, C.A. and Al-Maiyah, S. (2009) Design strategy for low-energy ventilation and cooling of hospitals, Building Research and Information, 37(**3**), pp. 264-292.

Short, C.A., Cook, M.J. and Lomas, K.J. (2009) Delivery and performance of a low-energy ventilation and cooling strategy, Building Research and Information, 37(**1**), 1-30.

Short, C.A. and Lomas, K.J. (2007) Exploiting a hybrid environmental design strategy in a US continental climate, Building Research and Information, 35(**2**) pp. 119-143.

Sparks, L.E. (2001) Indoor Air Quality Modelling, In: Spengler JD, Samet JM, McCarthy JF, eds. Indoor Air Quality Handbook. New York: McGraw-Hill.

Sparks, L. E. (1988) Indoor Air Quality Model Version 1.0, Documentation, EPA -600/8-88-097a (NTIS PB89-133607), Research Triangle Park, NC.

Spengler, J.D. and Chen, Q. (2000) Indoor air quality factors in designing a healthy building. Annual Review of Energy and the Environment. 25, pp. 567–601.

Tang J.W., Noakes C.J., Nielsen P.V., Eames I., Nicolle A., Li, Y., and Settles, G.S. (2011) Observing and quantifying airflows in the infection control of aerosol- and airborne-transmitted diseases: an overview of approaches. Journal of Hospital Infection 77, pp. 213–222.

Tang, J.W. and Settles, G. S. (2008) Coughing and aerosols, New England Journal of Medicine, Vol. 359.

Tang, J.W., Li, Y., Eames, I., Chan, P.K.S. and Ridgway, G.L. (2006) Factors involved in the aerosol transmission of infection and control of ventilation in healthcare premises. Journal of Hospital Infection 64(**2**), pp. 100-114.

Tang, J.W., Eames, I., Li, Y., Taha, Y.A., Wilson, P., Bellingan, G., Ward, K.N. and Breuer, J. (2005) Door-opening motion can potentially lead to a transient breakdown in negative-pressure isolation conditions: the importance of vorticity and buoyancy airflows. Journal of Hospital Infection. 61(**4**), pp. 283-286.

Thatcher, T. L., Wilson, D. J., Wood, E. E., Craig, M. J. and Sextro, R. G. (2004) Pollutant dispersion in a large indoor space: Part 1 – Scaled experiments using a water-filled model with occupants and furniture, Indoor Air, 14 (**4**) pp. 258-271.

Thomas, J., Mage, D., Wallace, L., and Ott, W. (1984) A sensitivity analysis of the enhanced Simulation of Human Air Pollution Exposure (SHAPE) model, Environmental Monitoring Systems Laboratory, U.S. Environmental Protection Agency, Research Triangle Park, NC, NTIS No. PB 85-201101/AS (1984)

Trexler, P.C. (1975) Microbial isolators for use in the hospital. Biomedical Engineering. Vol. 10. pp 63-67.

Ulrich, R., Quan, X., Zimring, C., Anjali, J. and Choudhary, R (2004) The Role of the Physical Environment in the Hospital of the 21st Century: A Once-in-a-Lifetime Opportunity, The Center for Health Design.

van de Glind, I., de Roode, S. and Goossensen, A. (2007) Do patients in hospitals benefit from single rooms? A literature review, Health Policy, 84 (**2-3**): pp. 153-161.

Versteeg, H.K. and Malalasekera, W. (2007) Computational fluid dynamics: The finite element method, Prentice-Hall: Harlow, England.

Vietri, J.N., et al. The effect of moving to a new hospital facility on the prevalence of methicillin-resistant Staphyloccocus aureus, American Journal of Infection Control, 2004, 32 (5).

Vortex (2012) www.reading.ac.uk/~kcsawbi/Vortex.html

Walker, C.E. (2006) Methodology for the evaluation of natural ventilation in buildings using a reduced-scale air model. PhD dissertation, MIT.

Wells, W.F. (1955) Airborne Contagion and Air Hygiene: an Ecological Study of Droplet Infection, Cambridge, MA, Harvard University Press.

White, P.A.F. (1981) Protective Air Enclosures in Health Buildings, The Macmillan Press Ltd, London.

Whyte, W., Shaw, B.H. and Freeman, M.A.R. (1974) An evaluation of a partial-walled laminar-flow operating room. Journal of Hygiene, 73, pp. 61–76.

Xie, X., Li, Y., Chwang, A. T. Y., Ho, P. L. and Seto, W. H. (2007) How far droplets can move in indoor environments – revisiting the Wells evaporation–falling curve, Indoor Air, 17, pp. 211–225.

Xing, H., Hatton, A. and Awbi, H.B. (2001) A study of the air quality in the breathing zone in a room with displacement ventilation. *Building and Environment*, Vol. 36, pp 809 – 820.

Yakhot, V. and Orszag, S.A. (1986) Renormalization group analysis of turbulence, Journal of Scientific Computing, 1 pp. 3–51.

Yam, R., Yuen, P.L., Yung, R., Choi, P. (2011) Rethinking hospital general ward ventilation design using computational fluid dynamics, Journal of Hospital infection, 77, pp 31-36.

Yang, T., Buswell, R.A. and Cook, M.J. (2011) Exploring rapid prototyping techniques for validating numerical models of naturally ventilated buildings, Proceedings of Building Simulation 2011:12th Conference of International Building Performance Simulation Association, Sydney, 14-16 November.

Yang, T., Wright, N.G., Etheridge, D.W. and Quinn, A.D. (2006) A Comparison of CFD and Full-scale Measurements for Analysis of Natural Ventilation, International Journal of Ventilation, 4(**4**), pp. 337-348.

Yang C., Demokritou, P., Chen Q., Spengler J. (2001) Experimental Validation of a Computational Fluid Dynamics Model for IAQ applications in Ice Rink Arenas. Journal of Indoor Air and Climate, Vol. 11, p. 120.

Zanetti, P. (1990) Air Pollution Modelling: Theories, Computational Methods and Available Software, Van Nostrand Reinhold. New York.

Zang, Y (2005) Indoor Air Quality Engineering, CRC Press, New York.

Zhang, Q., Strom, J. and Morsing, S. (1996) Jet drop models for control of air jet trajectories in ventilated livestock buildings; In: Proceedings of Roomvent 1996, Fifth International Conference on Air Distribution in Rooms (Murakami S, ed), Yokohama, Japan, pp. 305–316.

Zhang, G.Q., Strom, J.S. and Morsing, S. (1992) Wall inlets for winter ventilation control. ASAE Paper No. 92-4531.

Zhao, B., Yang, C., Chen, C., Feng, C., Yang, X., Sun, L., Gong, W., and Yu, L. (2009) How many airborne particles emitted from a nurse will reach the breathing zone/body surface of the patient in ISO Class-5 single-bed hospital protective environments? – A numerical analysis, Aerosol Science and Technology, Vol. 43: pp. 990-1005.